1229220

[00816504]

SGW-50280
Revision 0

Conceptual Site Models for the 200-DV-1 Operable Unit Waste Sites in the S Complex Area, Central Plateau, Hanford, Washington

Prepared for the U.S. Department of Energy
Assistant Secretary for Environmental Management

Contractor for the U.S. Department of Energy
under Contract DE-AC06-08RL14788

CH2MHILL
Plateau Remediation Company
P.O. Box 1600
Richland, Washington 99352

RECEIVED
MAR 23 2015
EDMC

200-DV-1

Approved for Public Release;
Further Dissemination Unlimited

306

SGW-50280
Revision 0

Conceptual Site Models for the 200-DV-1 Operable Unit Waste Sites in the S Complex Area, Central Plateau, Hanford, Washington

Document Type: RPT

B. A. Williams
CH2M HILL Plateau Remediation Company

V. J. Rohay
CH2M HILL Plateau Remediation Company

Date Published
November 2014

Prepared for the U.S. Department of Energy
Assistant Secretary for Environmental Management

Contractor for the U.S. Department of Energy
under Contract DE-AC06-08RL14788

CH2MHILL
Plateau Remediation Company
P.O. Box 1600
Richland, Washington 99352

APPROVED
By Lee Ann Snyder at 8:39 am, Dec 02, 2014

Release Approval | Date

Approved for Public Release;
Further Dissemination Unlimited

TRADEMARK DISCLAIMER

Reference herein to any specific commercial product, process, or service by tradename, trademark, manufacturer, or otherwise, does not necessarily constitute or imply its endorsement, recommendation, or favoring by the United States Government or any agency thereof or its contractors or subcontractors.

This report has been reproduced from the best available copy.

Printed in the United States of America

Executive Summary

This report offers detailed conceptual site models for the distribution of five key groundwater contaminants—technetium-99 (Tc-99), nitrate, chromium, iodine-129 (I-129), and uranium—associated with waste sites in the 200-DV-1 Operable Unit (OU) near Waste Management Area S-SX in the 200 West Area of the Hanford Site. This area, which includes waste sites and S-SX Tank Farms, is referred to in this report as the S Complex Area.

For ease of discussion, the 200-DV-1 waste sites in the S Complex Area are grouped into two geographic subregions (Figure ES-1):

- **Subregion 1** – 216-S-9 and 216-S-23 Cribs (including the S Tank Farm)
- **Subregion 2** – 216-S-21 and 216-S-25 Cribs (including the SX Tank Farm)

For these two groups of waste sites, the extent of the associated subregion is defined as the area within 100 m (328 ft) of the waste sites. With the exception of the 216-S-23 and 216-S-25 Cribs, other waste sites within the area that are sources of vadose zone and/or groundwater contamination are not included in the discussions of these conceptual site models, (e.g., 216-S-1 and 216-S-2 Cribs).

The conceptual site models of the nature and extent of residual contamination in the vadose zone rely primarily on data from borehole gamma logging, groundwater monitoring, and on inferential evidence from soil electrical resistivity surveys. There are no sediment analytical data available near or within these four waste sites. There is some sediment analytical data from boreholes and direct push samples from within the S-SX Tank Farm. These data and the geophysical logging within the tank farms do not adequately define the vertical extent of contamination in the vadose zone for the S Complex Area.

The conceptual site models (CSM) developed for the S Complex Area waste sites suggest that breakthrough to groundwater may have occurred in at least three of the sites. Limited lateral spreading evidence implies that most of the effluent disposed penetrated fairly deeply beneath the sites. Estimates of remaining waste (by percent) still within the vadose zone beneath three of the cribs are 20 percent for 216-S-25 Crib, 33 percent for 216-S-21 Crib, and 77 percent for 216-S-23 Crib. Calculations suggest that almost all of the waste

disposed to the 216-S-9 Crib remain in the vadose zone. The CSMs illustrate the primary hydrogeologic intervals that caused lateral liquid waste spreading within the vadose zone beneath the waste sites.

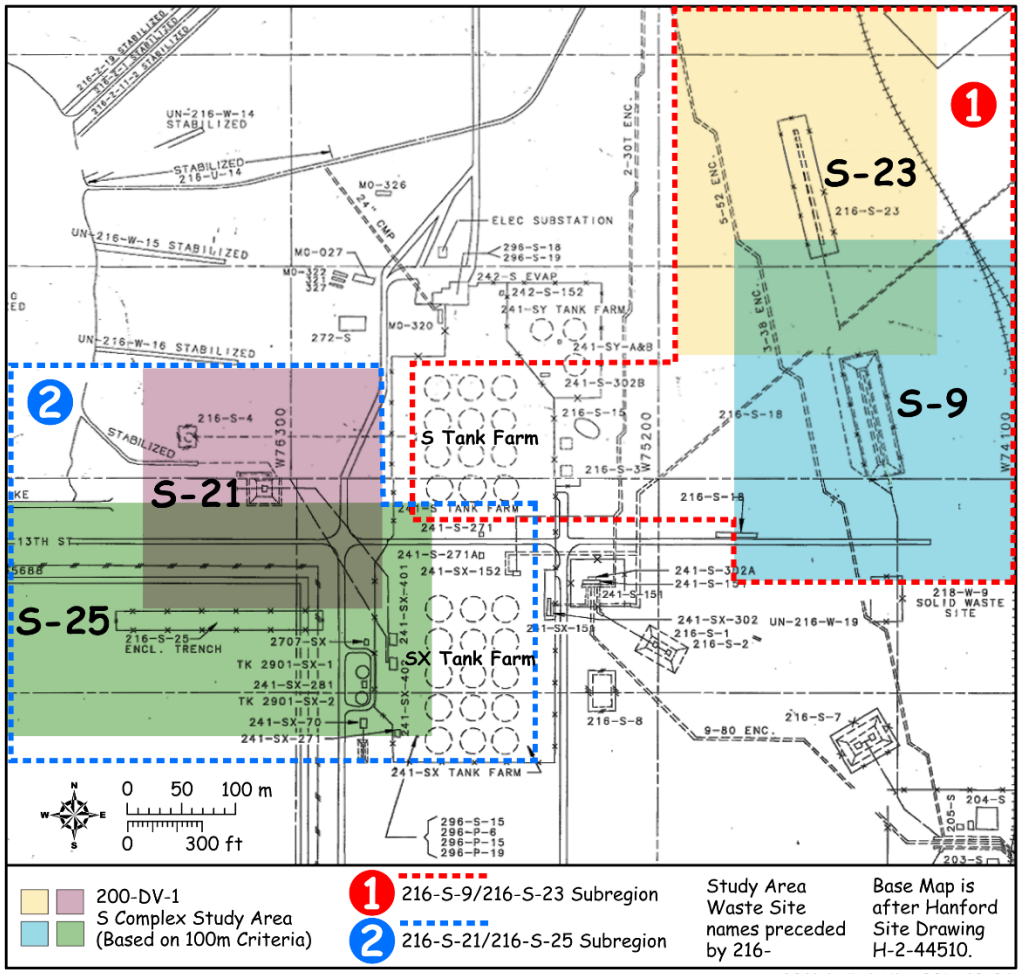

Figure ES-1. Location of 200-DV-1 OU Waste Sites near the S-SX Tank Farm Waste Management Area and Extent of Associated Subregions

These zones typically include the Hanford formation unit contacts boundaries (and in some cases may include thin localized lenses within the Hanford formation), and the regional contact between the Hanford formation and the underlying Cold Creek unit (CCu).

In most cases, the borehole gamma logging data for the deep vadose zone—within the CCu and the underlying Ringold Formation under the 200-DV-1 OU waste sites—are too limited to definitively prove or disprove that waste liquids reached the groundwater in significant quantities. There are no useful direct vadose zone sediment measurements of

contaminant or associated chemical concentrations proximal to any of the S Complex Area waste sites. Further, soil resistivity surveys are limited in delineating the vertical extent of the low-resistivity (high-salt) anomalous zones associated with the vadose zone plumes. Soil resistivity field surveys have proven to be useful for delineating the lateral extent of the high-salt vadose zone plumes when the metallic infrastructure does not cause electrical interferences or when interferences can be accounted for during the electrical-resistivity inverse modeling.

Based on groundwater monitoring, waste fluids and contaminants are known to have reached the groundwater below some of the 200-DV-1 OU waste sites in the S Complex Area soon after they were activated. However, no effort was ever performed to quantify the mass of contaminants and volumes of waste fluids that reached the water table in the early years of disposal. To date, no estimate of the mass of contaminants that have reached the groundwater below the S Complex Area has been made. The CSMs for the S Complex Area used the available groundwater monitoring data and a three-dimensional aquifer conceptual model integrated with the groundwater monitoring data to make mass/activity estimates for three of the five mobile contaminants of interest for the recent period ~2005 to 2010. For two of the mobile contaminants, uranium and I-129, no groundwater mass/activity estimates were performed because there is no significant uranium groundwater plume below the study area and the bulk of the I-129 plume that encroaches on a portion of the study area is not currently believed to be sourced from facilities considered in this report[1].

The results of these mass calculations for three of the five mobile contaminants in the groundwater plumes below the S Complex Area over the past 5 to 10 years show relatively small groundwater contaminant mass percentages compared to the total masses released to the waste sites and from the S Complex Area tanks. This partially supports the conservative conceptual model that almost all of the waste and contaminants could still reside in the vadose zone. The major exception is nitrate. The estimate of the mass in the current and recent nitrate groundwater plume below the S Complex Area ranges from 49 to 52 percent of the mass of nitrate released to the waste sites and from two single-shell tanks (included in this report). This large percentage of nitrate is estimated to reside in the current groundwater; it is likely caused by the large percentage of nitrate disposed to the

[1] Some of the groundwater I-129 could be sourced from 216-S-9, but the mass from 216-S-9 is not large compared to estimated mass in groundwater over the entire S Complex Area.

216-S-25 Crib and about 80 percent of that waste volume is estimated to have reached the water table. Another possibility is that a significantly low estimate of the total nitrate released to the vadose zone in the S Complex Area has been used. Because nitrate was a common contaminant in liquid wastes disposed of in 200 West Area, even in the dilute cooling waters sent in very large volumes to ponds, in sanitary sewerage, and in unplanned releases, the mass of nitrate estimated using only the disposal to the S Complex Area and releases from the two tank farms may be unrealistically low.

Because nitrate, I-129, and Tc-99, and to some extent chromium are all considered mobile and exist as anions in the Hanford Site subsurface, they should migrate through the vadose zone sediments without interacting significantly with the sediment. In fact, at most locations where there is adequate vadose zone sediment characterization, nitrate and Tc-99 have been shown to travel at the same rate in both vadose zone pore waters and groundwater at the Hanford Site. Thus, the true mass of nitrate released to the subsurface below the S Complex Area may be much larger than the mass estimated for the individual 200-DV-1 OU waste sites considered in this report. It is possible that the percentage of the nitrate released to the S Complex Area that is in the groundwater today could be closer to the low percentages estimated for Tc-99 (~10 percent) and chromium (~9 percent).

The groundwater contamination sources were derived by reviewing the groundwater plume histories (time of occurrence and location), and comparing the masses or activities estimated to have been in the waste streams disposed of to each waste site in the S Complex Area. A few high-precision isotope signature ratios (groundwater's nitrate, oxygen, nitrogen, and stable strontium) augmented the source attribution exercise. The integration of the vadose zone conceptual site models of residual mass with the groundwater source attributions were applied to provide the following preliminary rankings of the S Complex Area facilities (including the S-SX SST farms) that are likely to impact groundwater today:

- **216-S-9 Crib**—The vadose zone below the 216-S-9 Crib may still contain a significant inventory of nitrate, uranium, and I-129 in comparison to the other three S Complex Area waste sites discussed in this report.

- **216-S-23 Crib**—The vadose zone below and surrounding the 216-S-23 Crib does not contain significant amounts of any of the five mobile contaminants and thus should not be a priority for further characterization.

- **S SSTs**—The area near and/or surrounding the S-104 tank appears to be the source of increasing chromium, Tc-99, and nitrate in the groundwater downgradient (east) of the S Tank Farm. The groundwater concentrations in this location have been increasing since the mid-2000s. It is estimated that a moderate amount of all five mobile contaminants is still present in the vadose zone and will likely continue to supply inventory to the groundwater.

- **216-S-21 Crib**—Because the waste type disposed to the 216-S-21 Crib was not particularly concentrated in any of the five mobile contaminants and the lateral spread was not particularly large, the mass of residual contaminants in the vadose zone is not significant. The 216-S-21 sediments may contain about 1 percent of the total chromium released to the S Complex Area but less than 0.2 percent of any of the other mobile contaminants. Therefore, it is not a priority to perform more characterization below and surrounding the 216-S-21 Crib.

- **216-S-25 Crib**—It is probable that the 216-S-25 Crib is contributing nitrate to the groundwater. There are very little data available at this waste site.

- **SX SSTs**—Of the 15 tanks in the SX Tank Farm, eight are believed to have released liquids to the subsurface. Since the mid-2000s, there has been a large and increasing (in both size and concentration) groundwater plume with an apparent origin[2] near the SX-115 tank's southern perimeter. The estimates of the mass/activity of the five mobile contaminants released from these eight SX tanks are substantial for all but uranium. Characterization of sediments from three boreholes and seven of eleven direct push holes within the SX Tank Farm confirm the presence of significant masses/activities of residual vadose zone contamination above and within the CCu. This preliminary assessment of the S Complex Area yielded similar conclusions as found in PNNL-19277, *Conceptual Models for Migration of Key Groundwater Contaminants Through the Vadose Zone and Into the Upper Unconfined Aquifer Below the B-Complex*, and SGW-49924, *Preliminary Conceptual Models for the 200-DV-1 Operable Unit Waste Sites in the T Complex Area*. For example, there is a fairly direct correlation between the estimates of total mass discharged to the various facilities, and the estimates of how much of the waste remains in the vadose zone, and what current groundwater impacts can be attributed to each facility. This simple

[2] Note that there are no groundwater monitoring wells to the north or west (potentially upgradient of vadose zone contaminant plumes) of 299-W23-19 to aid in locating the source of the waste.

correlation, based on tracking mass in various compartments (or media) in each subregion, supports the utility of the mass-balance construct performed at all 200-DV-1 OU waste sites studied to date. The volume of liquids disposed to the cribs and the volumes of fluids released in the tank farms does not directly correlate with impacts to groundwater as one might expect because of the vadose zone lateral spreading phenomena.

A second finding at all the 200-DV-1 OU waste sites is that lateral spreading along fine-grained layers and lithologic contacts has occurred during and after active waste disposal, and that later dilute waters (natural recharge, pipeline leaks, and episodic off-normal events [rapid snowmelt, large rainstorms, and concentrated recharge through depressions in topography accepting large area runoff, etc.]) could have pushed the more concentrated wastes further distances laterally along the contact boundaries and deeper within the vadose zone.

The one remaining issue regarding tank farm releases is how the contaminants that are present in the relatively low volume releases (relative to the several million-liter disposals to most of cribs and trenches) migrate through the thick vadose zone so far that they affect groundwater. It was not within the scope of this report to assess the details of vadose zone flow or to systematically identify and quantify the sources of water within the tank farms that may also be influencing contaminant migration through the vadose zone. There have been several descriptions (but few explicitly documented reports) suggesting that substantial volumes of water have been released to the vadose zone within the tank farms, including (1) prolonged potable water line leaks; (2) large snowmelt events that flooded tank farms (historical photographs exist for T Farm); (3) enhanced recharge within the tank farm boundaries caused by the gravel covers to prevent spread of surface contamination, and the shedding and focusing of recharge water off the concrete domes to the sides of the tanks; and (4) surface run-on from the surrounding higher elevations. Some of these conditions have been mitigated and some tanks are being covered with interim surface covers to minimize further enhanced recharge. However, since the mid-2000s, both of the tank farms in the S Complex Area currently appear to be releasing Tc-99, chromium, nitrate, and potentially I-129 to the groundwater at rates more significant than the four S Complex Area waste sites. Additionally, the vadose zone below the 216-S-25 Crib is currently providing nitrate to the water table, and the 216-S-9 Crib may be providing low amounts of I-129 to the water

table. There are no indications that the deep vadose zone proximal to the 216-S-21 and 216-S-23 Cribs is providing measureable amounts of mobile contaminants to the current water table.

This page intentionally left blank.

Contents

1 Introduction 1-1

1.1 Project Goal 1-1

1.2 Scope 1-1

1.3 Sources and Rationale of Facility Information 1-3

1.3.1 Waste Release Depth and Area 1-3

1.3.2 Waste Volumes and Contaminant Inventories 1-3

1.4 Data Availability in Vadose Zone 1-6

1.5 Data Availability for the Groundwater 1-7

1.6 Conceptual Site Model Development 1-9

2 S Complex Hydrogeology 2-1

2.1 Summary 2-1

2.2 Regional Hydrogeologic Overview 2-3

2.3 Geomorphology 2-3

2.4 General Stratigraphy 2-4

2.4.1 Holocene Deposits 2-9

2.4.2 Hanford Formation 2-9

2.4.3 Cold Creek Unit 2-14

2.4.4 Ringold Formation 2-20

2.4.5 Columbia River Basalt Group 2-23

2.5 Structure 2-23

2.5.1 Clastic Dikes 2-24

2.6 Site-Specific Hydrogeologic Data for the S Complex Area 2-24

2.7 Water Levels and Flow Directions Beneath the S Complex Area 2-26

2.7.1 Current Water Levels and Flow Direction Beneath the S Complex Area and Vicinity 2-26

2.7.2 Historical Changes in Groundwater Flow Direction and Gradient Beneath S Complex Area and Vicinity 2-32

3 Conceptual Site Models for Vadose Zone Contamination in S Complex Area Subregions ... 3-1

3.1 Subregion 1 – 216-S-9 and 216-S-23 Cribs 3-1

3.1.1 Facility Description, Source Details, and Inventory Released 3-1

3.1.2 Hydrogeology of the 216-S-9 and 216-S-23 Subregion 3-3

3.1.3 Subregion 1 – Vadose Zone Contamination Estimates for 216 S-9 and 216-S-23 Cribs 3-9

3.1.4 Subregion 1 – Vadose Zone Conceptual Model for 216-S-9 and 216-S-23 Cribs 3-11

3.1.5 S Tank Farm 3-15

3.2 Subregion 2 – 216-S-21 and 216-S-25 Cribs 3-20

3.2.1 Facility Description, Source Details, and Inventory Released 3-20
3.2.2 Subregion 2 – Hydrogeology for the 216-S-21 and 216-S-25 Cribs 3-24
3.2.3 Subregion 2 – Vadose Zone Contamination Estimates for 216-S-21 and 216-S-25 Cribs 3-28
3.2.4 Subregion 2 – Vadose Zone Conceptual Model for 216-S-21 and 216-S-25 Cribs 3-29
3.2.5 SX Tank Farm 3-32
3.3 S Complex Area Total Mass of Key Chemicals and Activity of Radionuclides Remaining in the Vadose Zone 3-59
4 Hydraulic Properties of the Vadose Zone and Unconfined Aquifer 4-1
5 Status of Selected Mobile Contaminants in Groundwater Beneath the S Complex Area 5-1
5.1 Groundwater Contamination Beneath the Subregion 1 5-1
5.2 Groundwater Contamination Beneath Subregion 2 5-16
5.3 Vertical Groundwater Contaminant Distribution at Waste Management Area S-SX 5-26
6 Integrated Conceptual Models for Key Contaminants 6-1
6.1 Methodology and Assumptions 6-1
6.2 Estimates of Mass in Current Groundwater Plumes 6-3
6.2.1 Technetium-99 6-6
6.2.2 Nitrate 6-10
6.2.3 Iodine-129 6-11
6.2.4 Chromium 6-12
6.2.5 Uranium 6-16
6.3 Contaminant Mobility Once in the Aquifer 6-16
6.4 Summary of Key Integrated Conceptual Models 6-17
7 Isotopic Systematics for the Identification and Tracking of Hanford Contamination and Related Materials, with a Focus on the S Complex Area 7-1
7.1 S Complex Area Isotopic Data Summary 7-1
7.2 Summary of Isotopic Data Significance to Developing Conceptual Models for Fate of Released Waste in the S Complex Area 7-3
8 Summary 8-1
8.1 Facilities Summary 8-4
8.2 S Complex Area Hydrogeology Conceptual Model 8-5
8.3 Hydraulic and Recharge Parameters 8-6
8.4 Isotopic Signature Studies in S Complex Area 8-6
8.5 Conceptual Model for Subregion 1 8-7
8.6 Conceptual Model for Subregion 2 8-7
8.7 Groundwater Flow Direction and Plume Inventories 8-9
9 References 9-1

Appendices

A S Complex Area Waste Facility Dimensions, Major Chemical Inventories Disposed of by Year for Each Facility, Total Waste Volume Disposed by Year, Waste Stream Definitions ..... A-i

B S Complex Area CSM Support Data ..... B-i

Figures

Figure ES-1. Location of 200-DV-1 OU Waste Sites near the S-SX Tank Farm Waste Management Area and Extent of Associated Subregions iv

Figure 1-1. Location of 200-DV-1 OU Waste Sites near the S Complex Area Tank Farm Complex and Extent of Associated Subregions 1-2

Figure 1-2. Conceptual Model Development Process Flowchart 1-10

Figure 2-1. Major Landforms and General Lateral Distribution of the Three Principal Hanford Formation Facies Within the Central Pasco Basin 2-5

Figure 2-2. Correlation of 200-DV-1 OU Stratigraphy to Generalized Hanford Site Suprabasalt Stratigraphy 2-6

Figure 2-3. A North-South Hydrogeologic Cross Section Shows Stratigraphic Relationships Within the Vadose Zone along the Western Hanford Site 2-7

Figure 2-4. Stratigraphic Units Representative in the Vadose Zone Beneath S Complex Area 2-8

Figure 2-5. Exposure Showing Hanford Formation Sand- and Gravel-Dominated Facies in the Northeastern 200 East Area 2-11

Figure 2-6. Drill Cuttings of Gravel-Dominated Facies of the Hanford Formation (Hf1) 2-11

Figure 2-7. Core Samples of the Sand-Dominated Facies of the Hanford Formation (Hf2) from Borehole 299-W10-27 2-12

Figure 2-8. Sharp Contact between the Hanford Formation Hf2 and the Underlying Cold Creek Unit Silt in Borehole 299-W11-39 2-13

Figure 2-9. Distinct Contact between the Brown Silt-Dominated (CCuz) and White Calcrete (CCuc) of the CCu 2-15

Figure 2-10. Thickness (Isopach) Map of the CCuz Subunit near the S Complex Area 2-17

Figure 2-11. Structure-Contour Map Showing Relief Atop the CCuz Subunit near the S Complex Area 2-18

Figure 2-12. Laminated Silt and Fine Sand of the CCuz Subunit 2-19

Figure 2-13. Cemented Calcic Paleosol (CCuc) Facies of the CCu 2-20

Figure 2-14. Example Geophysical Log, Well 299-W23-08 2-21

Figure 2-15. Laminated, Fine-Grained Sand and Silt of the Ringold Member of Taylor Flat (from borehole C4105, 116 ft bgs Within T Tank Farm, ~25 m northeast of the 216-T-32 Crib) 2-22

Figure 2-16. General Map of Liquid Disposal Facilities and Infrastructure in the S Complex Area 2-27

Figure 2-17. Subregion 1 - Location Map for Facilities and Wells near the 216-S-9 and 216-S-23 Cribs, S Complex Area 2-28

Figure 2-18. Subregion 2 - Location Map for Facilities and Wells near the 216-S-21 and 216-S-25 Cribs, S Complex Area 2-29
Figure 2-19. March 2009 Water Table Map for the South Part of 200 West Area and the S Complex Area 2-31
Figure 2-20. Discharge History for T Pond and U Pond 2-33
Figure 2-21. Hydrographs of Selected Wells near the S Complex Area 2-34
Figure 2-22. Water Table Elevations for the Region of the 200 West Area 2-36
Figure 2-23. Maps Showing the Historical Water Table in 200 West Area 2-39
Figure 2-24. Groundwater Flow Directions near WMA S-SX 2-41
Figure 3-1. Subregion 1 – 216-S-9 and 216-S-23 Cribs, 200-DV-1 Operable Unit 3-2
Figure 3-2. Stratigraphic Type Log for 299-W19-7 3-5
Figure 3-3. Stratigraphic Type Log for 299-W22-69 3-6
Figure 3-4. Hydrogeologic Cross Section L14-L14′ 3-7
Figure 3-5. Hydrogeologic Cross Section L15-L15′ 3-8
Figure 3-6. Soil Resistivity Profiling near the 216-S-9 and 216-S-23 Cribs 3-10
Figure 3-7. Two-Dimensional Modeling 3-11
Figure 3-8. Depiction of Vadose Zone Lateral Spread of Contamination Proximal to the 216-S-9 and 216-S-23 Cribs 3-13
Figure 3-9. Depiction of Vadose Zone Contamination Proximal and Below the 216-S-9 and 216-S-23 Cribs using Spectral Gamma Logs and SGE 3-14
Figure 3-10. Location of Direct Push Probe Holes South of S Tank Farm 3-16
Figure 3-11. Estimated Lateral Extent of Contamination below S Tank Farm Based on Soil Resistivity Data Looking Northeast 3-18
Figure 3-12. Estimated Vertical Extent of Contamination Below S Tank Farm based on Soil Resistivity Data 3-19
Figure 3-13. Subregion 2 – Location of the 216-S-21 and 216-S-25 Cribs, S Complex Area 3-21
Figure 3-14. Subregion 2 – 216-S-21 and 216-S-25 Base Map, S Complex Area 3-25
Figure 3-15. Subregion 2 – Hydrogeologic Cross Section L16-L16′ 3-26
Figure 3-16. Subregion 2 – Hydrogeologic Cross Section L17-L17′ 3-27
Figure 3-17. Subregion 2 – Location of 216-S-21 and 216-S-25 Cribs and Boreholes 3-30
Figure 3-18. Subregion 2 – Conceptual Model for Lateral Spread of Residual Contamination in the 216-S-21 and 216-S-25 Cribs 3-31
Figure 3-19. Conceptual Model for Location of Residual Contamination below the 216-S-21 Crib ... 3-34
Figure 3-20. Subregion 2 – Conceptual Site Model for the 216-S-25 Crib 3-35
Figure 3-21. Location of Three Characterization Boreholes in SX Tank Farm 299-W23-234, Slant Borehole, and 299-W23-19 3-38
Figure 3-22. Location of Direct Push Characterization and Logging Probe Holes 3-38
Figure 3-23. Comparison of Pore Water Electrical Conductivity for Three SX Tank Farm Borehole Sediments 3-43
Figure 3-24. Comparison of Water and Acid Extractable Technetium-99 in Sediments from the Slant Borehole 3-44

Figure 3-25. Comparison of Acid Extractable Technetium-99 in Sediments from the 299-W23-234 and the SX-108 Slant Borehole 3-46
Figure 3-26. Comparison of Water Extractable Chromium in Sediments from 299-W23-234 and the SX-108 Slant Borehole 3-47
Figure 3-27. Comparison of Water and Acid Extractable Technetium-99 in Sediments from 299-W23-19 3-48
Figure 3-28. Estimated Lateral Extent of SX Tank Farm Contamination based on Soil Resistivity Data 3-54
Figure 3-29. Location of Soil Resistivity Surface Electrode Lines 3-54
Figure 3-30. Estimated S-SX Tank Farm Lateral Extent of Contamination based on Soil Resistivity Modelling at 40 m (131 ft) bgs 3-55
Figure 3-31. Estimated S-SX Tank Farm Lateral Extent of Contamination based on Soil Resistivity Modelling at Several Depths (m bgs) 3-57
Figure 3-32. Location of Laterals Below and Dry Well Monitoring Boreholes around the SX Tanks 3-58
Figure 5-1. Well Location Map for the S Complex Area 5-2
Figure 5-2. Gross Beta Concentrations at Selected Wells in Subregion 1 (216-S-9/216-S-23 Cribs) 5-4
Figure 5-3. Cobalt-60 Concentrations in Wells at the 216-S-9 Crib 5-5
Figure 5-4. Cobalt-60 in Wells from the 216-S-23 Crib 5-6
Figure 5-5. Ruthenium-106 Concentrations in Wells at the 216-S-9/216-S-23 Subregion 5-7
Figure 5-6. Nitrate Concentration in Wells at the 216-S-9/219-S-23 Subregion 5-7
Figure 5-7. Average 2009 Nitrate Concentrations Within the S Complex Area, Upper Portion of the Unconfined Aquifer 5-9
Figure 5-8. Tritium Concentrations in Wells at Subregion 1 (216-S-9/216-S-23 Cribs) 5-10
Figure 5-9. Technetium-99 Concentrations at the 216-S-9/216-S-23 Subregion 5-11
Figure 5-10. Average Technetium-99 Concentrations Within the S Complex Area, Upper Portion of the Unconfined Aquifer 5-12
Figure 5-11. Average Iodine-129 Concentration in the Southern Part of the 200 West Area, Upper Part of the Unconfined Aquifer 5-13
Figure 5-12. Chromium Concentrations (μg/L) in Wells at the 216-S-9 Crib 5-14
Figure 5-13. Average Chromium Concentrations Within the S Complex Area (216-S-9/216-S-23 Cribs) 5-15
Figure 5-14. Uranium Concentrations (μg/L) in Wells in Subregion 1 5-16
Figure 5-15. Gross Beta Concentration in Well 299-W23-4 at the 216-S-21 Crib 5-18
Figure 5-16. Nitrate Concentration in Well 299-W23-4 at the 216-S-21 Crib 5-19
Figure 5-17. Tritium Concentration in Well 299-W23-4 at the 216-S-21 Crib 5-19
Figure 5-18. Cobalt-60 Concentration in Well 299-W23-4 at the 216-S-21 Crib 5-20
Figure 5-19. Uranium Concentration (μg/L) in Well 299-W23-4 at the 216-S-21 Crib 5-21
Figure 5-20. Chromium Concentrations (μg/L) in Wells at the 216-S-21 Crib 5-21
Figure 5-21. Nitrate Concentration in Wells at the 216-S-25 Crib 5-22
Figure 5-22. Tritium Concentrations in Wells at the 216-S-25 Crib 5-23

Figure 5-23. Technetium-99 Concentrations in Wells at the 216-S-25 Crib 5-24
Figure 5-24. Chromium Concentrations (μg/L) in Wells at the 216-S-25 Crib 5-25
Figure 5-25. Uranium Concentration (μg/L) in Wells at Subregion 2 (216-S-21/216-S-25 Cribs) 5-26
Figure 5-26. Carbon Tetrachloride, Nitrate, Technetium-99, and Chromium Concentrations (pCi/L or μg/L) versus Depth in the Aquifer in Well 299-W22-47 at Waste Management Area S-SX 5-27
Figure 5-27. Wellbore-Fluid Specific Conductance Measurements Collected in Well 299-W23-19 at Waste Management Area S-SX 5-29
Figure 6-1. Yearly Volumes of Waste Liquids Disposed or Released to Subsurface at S Complex Area 6-3
Figure 6-2. Technetium-99 Contamination Beneath the S Complex Area 6-7
Figure 6-3. Location of Groundwater Monitoring Wells Surrounding the S and SX Tank Farms 6-9
Figure 6-4. Nitrate Contamination Beneath the S Complex Area 6-11
Figure 6-5. Iodine-129 Contamination Beneath the Southern Portion of the 200 West Area 6-13
Figure 6-6. Chromium Contamination Beneath the S Complex Area 6-14
Figure 7-1. Map Showing the Locations of Groundwater Samples Collected in 2004 Near the WMA S-SX for the Stable Isotopic Analysis of Nitrate ($\delta^{15}N$ and $\delta^{18}O$) 7-2
Figure 7-2. Plot of δ15N vs. δ18O for Nitrate in Groundwater Samples near WMA-S-SX 7-3

Tables

Table 1-1. Boreholes in the S Complex Area with Laboratory Analyses of Vadose Zone Sediment Samples 1-7
Table 2-1. Hanford Site Hydrogeologic Studies 2-1
Table 2-2. Thickness of the Unconfined Aquifer Beneath the S Complex Area 2-30
Table 2-3. Water-Level Changes Beneath the S Complex Area 2-35
Table 3-1. Masses Released over 216-S-9 and 216-S-23 Cribs Lifetime and Percent of Total Released to S Complex Area 3-3
Table 3-2. Tank 241-S-104 Comparison with 216-S-9 and 216-S-23 Cribs 3-16
Table 3-3. Masses Released over S-21 and S-25 Cribs Lifetime and Percent of Total Released to S Complex Area 3-22
Table 3-4. Volumes and Masses Released from the SX Tank and Disposed to 216-S-21 and 216-S-25 Cribs 3-36
Table 3-5. Depth Discrete Water Extractable Concentrations of Mobile Contaminants in SX Tank Farm Sediments 3-39
Table 3-6. Concentrations of Key Mobile Contaminants in the Sediments from the SX Tank Farm Direct Push Probe Holes 3-50
Table 3-7. Estimates of Residual Vadose Zone Contamination and Site Rankings 3-61
Table 5-1. Wells Used to Characterize Groundwater Beneath Subregion 1 (216-S-9/216-S-23 Cribs) 5-3
Table 5-2. Wells Used to Characterize Groundwater Beneath the 216-S-21/216-S-25 Subregion 5-17
Table 5-3. Depth Distribution of Selected Contaminants during Drilling of Well 299-W22-50 5-28

Table 5-4. Vertical Variation of Groundwater Composition Measured in Well 299-W23-19 and Estimated for the Adjacent Aquifer on September 23, 2003 (from PNNL-14548) 5-30

Table 6-1. Estimated Mass of Mobile Contaminants in Current Groundwater Plumes, Below the S Complex Area for 2005-2010 Period 6-4

Table 6-2. Technetium Concentrations Time History for Three Wells Downgradient from S Tank Farm 6-10

Table 6-3. Calendar Year Average Chromium Concentrations in Groundwater Monitoring Wells near and Downgradient of the SX and S Tank Farms 6-15

Table 6-4. Qualitative Description of Strength and Weakness of Integrated Vadose Zone/Groundwater Models Used to Identify Sources of Groundwater Contamination.....6-19

Table 8-1. 200-DV-1 OU Summary by Facility of the Percentage Volume and Mass of Contaminants Released to the S Complex Area.....8-5

Table 8-2. S Complex Area Local Groundwater Flow Direction over Time 8-9

This page intentionally left blank.

Terms

2D	two-dimensional
3D	three-dimensional
amsl	above mean sea level
ATL	Advanced Technologies and Laboratories International
bgs	below ground surface
CCu	Cold Creek unit
CCuc	Cold Creek calcic geosol
CCuz	Cold Creek silt
CERCLA	*Comprehensive Environmental Response, Compensation, and Liability Act of 1980*
Cr(VI)	hexavalent chromium
CRBG	Columbia River Basalt Group
CSM	conceptual site model
DOE	U.S. Department of Energy
DWS	drinking water standard
EC	electrical conductivity
Ecology	Washington State Department of Ecology
EDA	Environmental Dashboard Application
EPA	U.S. Environmental Protection Agency
ERDF	Environmental Restoration Disposal Facility
FIR	Field Investigation Report
FY	fiscal year
GW	groundwater
HDW	Hanford Defined Waste
HEIS	Hanford Environmental Information System
Hf1	Hanford formation subunit 1
Hf2	Hanford formation subunit 2
Hf3	Hanford formation subunit 3
K_d	distribution coefficient

KUT	potassium-40-natural uranium-natural thorium
LAW	low activity waste
Ma	million years ago
Mgal	million gallons
ML	million liters
OU	operable unit
ORIGEN2	Oak Ridge Isotope Generation and Depletion Code
PNNL	Pacific Northwest National Laboratory
PUREX	Plutonium Uranium Extraction
RCRA	*Resource Conservation and Recovery Act of 1976*
REDOX	Reduction Oxidation
RFI/CMS	RCRA Facility Investigation/Corrective Measures Study
RFlm	Ringold Formation-lower mud unit
RFtf	Ringold Formation member of Taylor Flat
RFwia	Ringold Formation member of Wooded Island-unit a
RFwie	Ringold Formation member of Wooded Island-unit e
SGE	surface geophysical exploration
SGLS	Spectral Gamma Logging System
SIM	Soil Inventory Model
SST	single-shell tank
Tc-99	technetium-99
UPR	unplanned release
WIDS	Waste Information Data System
WMA	Waste Management Area
WRPS	Washington River Protection Solutions
VZ	vadose zone

1 Introduction

The objective of this report is to document the current understanding (i.e., conceptual site models) of the distribution and behavior of mobile contaminants associated with waste sites assigned to the 200-DV-1 Operable Unit (OU) near the Waste Management Area (WMA) S-SX in the 200 West Area of the Hanford Site. This area, which includes waste sites and tank farms, is referred to in this report as the S Complex Area.

1.1 Project Goal

Of particular interest in developing these conceptual site models (CSM) is to define the vadose zone geochemical and hydrogeologic mechanisms influencing the migration and fate of mobile contaminants as they travel from the near-ground surface disposal facilities toward the upper unconfined aquifer. An outcome of describing the conceptual models is the identification of data gaps that need to be addressed to sufficiently evaluate risk to groundwater and select appropriate remedies. This work supports the *Resource Conservation and Recovery Act of 1976* (RCRA) facility investigation/corrective measures study (RFI/CMS) and the *Comprehensive Environmental Response, Compensation, and Liability Act of 1980* (CERCLA) remedial investigation/feasibility study work plan for the 200-DV-1 OU. Draft A of the work plan is due March 31, 2015, in accordance with the Tri-Party Agreement (Ecology et al., 1989, *Hanford Federal Facility Agreement and Consent Order*) Milestone M-015-110A.

The U.S. Department of Energy (DOE), U.S. Environmental Protection Agency (EPA), and Washington State Department of Ecology (Ecology) established the 200-DV-1 OU to bring a centralized focus and systematic approach to the challenges presented by contamination below the practical depth of surface excavation or surface engineered barrier influence (DOE/RL-2010-89, *Long-Range Deep Vadose Zone Program Plan*).

1.2 Scope

This report focuses on the 200-DV-1 OU waste sites located within the S Complex Area. For ease of discussion, the 200-DV-1 OU waste sites are grouped into two geographic subregions (Figure 1-1):

- Subregion 1 – 216-S-9 and 216-S-23 Cribs
- Subregion 2 – 216-S-21 and 216-S-25 Cribs

(Note: The 216-S-23 and 216-S-25 Cribs are not 200-DV-1 OU waste sites but were included in the development of the conceptual site models in this report.) For each group of waste sites, the area of investigation is defined as the area within 100 m (328 ft) of the waste sites. The S-SX single-shell tanks (SST) within the subregions that maybe sources of vadose zone contamination are also included in the sections addressing conceptual models. Other nearby waste sites, such as the 216-S-1/S-2 and 216-S-7 Cribs and the 216-S-8 Trench, are not included in this report. The conceptual models address five key mobile contaminants: nitrate, technetium-99 (Tc-99), iodine-129 (I-129), uranium, and hexavalent chromium (Cr(VI)).

Detailed evaluations of available data were conducted for each subregion to acquire and assimilate pertinent data on the following:

- The design and operational use of the disposal facilities
- The volume of waste disposed of
- The masses and activities of key chemicals and radionuclides disposed of

- The vadose zone site-specific geology beneath the facilities
- The current distribution of key constituents in the vadose zone
- Historical and current groundwater concentrations below and proximal to the facilities
- The conceptual models for how key constituents migrate from the disposal facility toward the water table, including subsequent migration into the unconfined aquifer and within the groundwater

In addition, information on the regional and site-specific geology and physical, hydrologic, and geochemical properties of the lithostratigraphic units below the S-SX Complex Area are summarized.

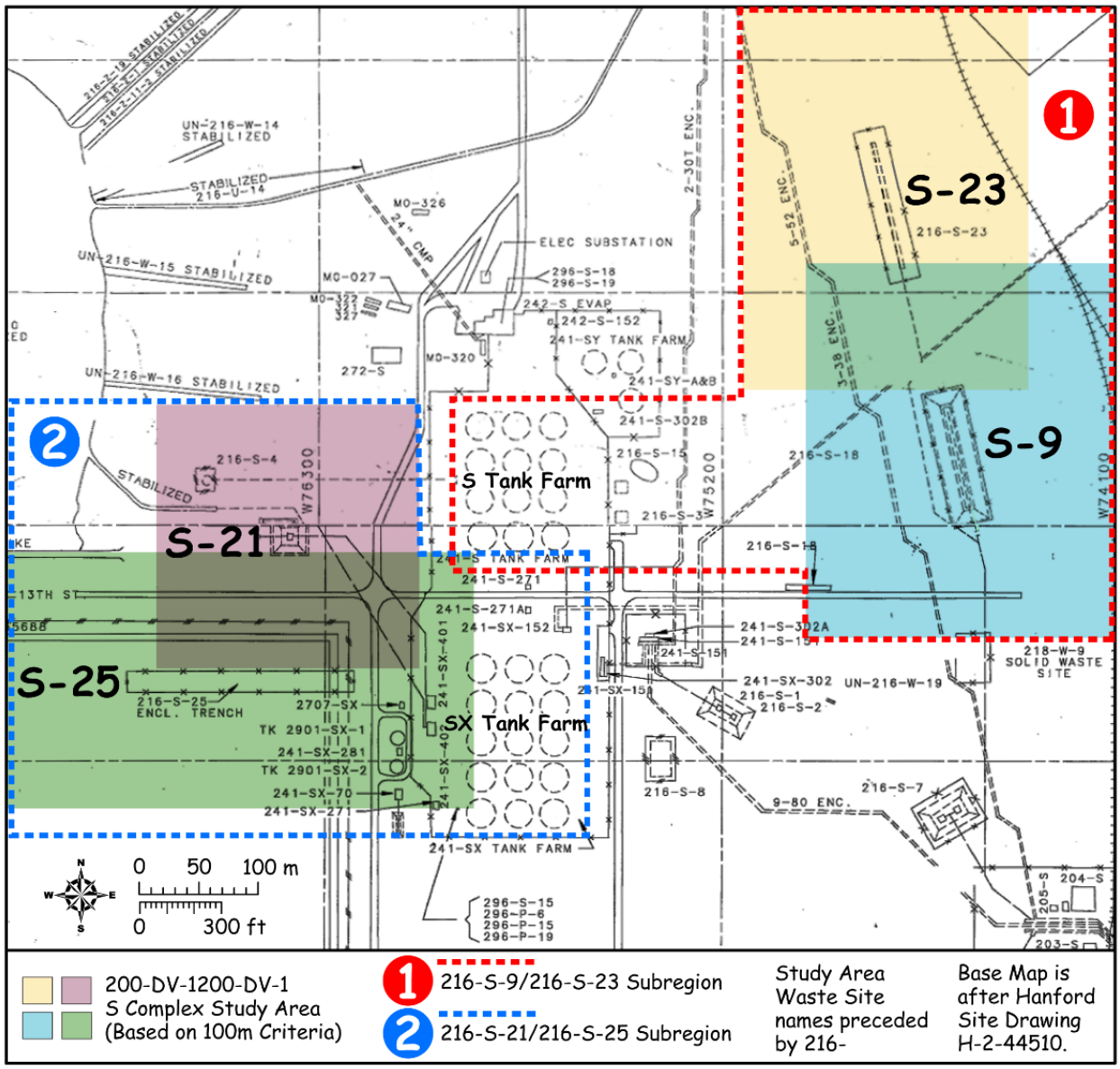

Figure 1-1. Location of 200-DV-1 OU Waste Sites near the S Complex Area Tank Farm Complex and Extent of Associated Subregions

1.3 Sources and Rationale of Facility Information

The primary sources used to describe the physical dimensions and facility construction details of the waste sites included in this report are the detailed drawings that were published in CP-49279, *Central Plateau Waste Site Dimensions*. The drawings relied on historical Hanford Site drawings and reports and the Waste Information Data System (WIDS) database.

The primary source for the liquid volumes and contaminant inventories discharged to the waste sites is the estimate provided in RPP-26744, *Hanford Soil Inventory Model, Rev. 1*, hereinafter called SIM. The volumes and inventories associated with releases from SSTs were obtained from SIM (RPP-26744) and other published reports.

1.3.1 Waste Release Depth and Area

Appendix A provides numerous tables with all pertinent facility dimensions and excavation depths at the times the waste sites were in use. In most cases, excavation depths are assumed to be the depths at which the liquid wastes were released to the vadose zone during active disposal. Most of the engineered facilities had a gravel bed that extended upward from the depth of excavation to and around the disposal pipelines to promote even percolation of the waste liquids throughout the bottom areal footprint. The excavation depth and bottom area, the depth to the water table, average sediment porosity for each sediment type, and the volume of liquid released were used to estimate the number of pore volumes of waste discharged at each facility. These pore volume calculations provide a qualitative indicator of hypothetical effluent volumes that passed through the vadose zone by waste site for assessing and comparing the potential to affect groundwater.

For the adjacent SST farms tank leak evaluations, the liquid was assumed to have been released directly to the subsurface at the bottom outer edge of the tank, and the footprint through which the waste hypothetically percolated was 25 percent of the area of the tank bottom. These are arbitrary assumptions because little objective data are available to describe the extent of structural breaches and the nature of releases from the SSTs. Waste release estimates are based largely on in-tank measurements and gamma and spectral gamma measurements in drywells located 5 to 15 ft from a tank around the tank perimeter. These conservative pore volume estimates do not incorporate lateral spreading.

1.3.2 Waste Volumes and Contaminant Inventories

The volumes of waste that were discharged to the waste sites and the mass of individual waste constituents or radionuclide activities in the waste were extracted from the SIM (RPP-26744) database for cribs and trenches. The activities in SIM were decayed to January 1, 2001. Those activities were decayed to September 30, 2010, in this report. The volumes of waste placed in each crib and trench are also available in the WIDS database, and in general, match the SIM tabulation. In most cases, the two databases used the same primary data, so no independent analysis was done. SIM (RPP-26744) provides more details on mass or activity estimates for the individual constituents that are not available in WIDS. SIM (RPP-26744) relies on the Hanford Defined Waste (HDW) Model, which is a spreadsheet-based engineering estimate of the chemical and radionuclide contents of Hanford Site waste streams. HDW calculations are based on process knowledge, which includes, but is not limited to, reactor fuel irradiation records, irradiated fuel plant dissolver charging records, plutonium (Pu)/uranium (U) separation plant and tank farm process flow sheets, and tank farm waste receipt and transfer records.

Constituent inventories are calculated in the HDW model with Microsoft® Excel[3] software and conventionally available personal computers. The formation of primary waste stream compositions, such

[3] Microsoft and Excel are trademarks of Microsoft Corporation, Redmond, Washington.

as sludge and salt cake (e.g., evaporator concentrates), is estimated by applying waste stream-specific analyte solubility limits to each plant waste stream. A macro-driven subroutine in the HDW Model calculates the fraction of each waste stream that precipitates as sludge or salt cake. It enters the fractions into the waste stream composition calculation such that two distinct compositions (solids and solution) are generated for each waste stream. In addition to estimating the composition of the primary separation process wastes discharged from the Bismuth Phosphate, Reduction Oxidation (REDOX), and Plutonium Uranium Extraction (PUREX) process facilities, HDW calculations also simulate the various reprocessing efforts that occurred and their corresponding waste streams. Reprocessing campaigns includes the tributyl phosphate plant (uranium recovery), Hot Semiworks Plant (strontium recovery), B Plant (cesium and strontium recovery), and various tank farm evaporations (including tank waste self-concentration). The waste streams from these second tier processes are calculated using the principal waste streams discharged from the Bismuth Phosphate, REDOX, and PUREX process facilities as the starting composition. A selected subset of radionuclide concentrations for each waste stream is also calculated from the Oak Ridge Isotope Generation and Depletion Code (ORIGEN2) radionuclide inventory for irradiated fuel processed through each separations plant and assigned using a set of radionuclide distribution factors and solubilities specific to the particular separation process.

It is beyond the scope of this report to perform a critical review of the waste stream compositions and total inventories placed in the facilities found in the S Complex Area. The most current documentation on the HDW waste model is HDW Model, Version 5 (RPP-19822, *Hanford Defined Waste Model-Revision 5.0*). SIM is simply a bookkeeping algorithm that multiplies the volumes of each type of waste stream released to each facility by year with the HDW Model estimates of the chemical compositions of each waste stream. SIM then stores the masses of each chemical and radionuclide by year and facility and sums the overall values of disposal volumes that occurred in each facility. A principal assumption of the HDW Model is that a limited set of waste streams can be used to represent all wastes that emanated from the plutonium separation processes used at the Hanford Site, even though the processes evolved and changed over time. Appendix A lists the set of waste streams that HDW (and thus SIM) uses, and the electronic Appendix D of RPP-26744 contains the chemical composition of the solution and solid phases for each of these "basis" waste streams.

A second key assumption of particular importance to the SIM model calculations is that very few waste streams discharged to the past-practice waste sites (e.g., cribs and trenches) possessed solids. Thus, only the solution portion of the HDW calculations and not the solids portion of each basis waste stream are generally used in the SIM mass and activity estimates that were used in this report. Solids are ignored, in general, because of the waste management and surveillance practices employed during production operations and the general physical constraints of the system with regard to particulate entrainment (e.g., radiation monitors, settling tanks, no agitation, and passive filtration). These active engineering practices in most situations minimized solids piped to the cribs and trenches. Therefore, the default condition for SIM is to exclude the entrained solids. However, for certain waste streams and waste sites, including entrained solids is reasonable from a physical and waste management operations perspective. For example, SIM documentation infers that laboratory wastes, decontamination wastes, cold start wastes, and fuel cladding were all likely to have solids and, in certain instances, the surveillance data suggest that solids were present. In addition, selected process excursions (piping failures, overflow conditions, or poor settling) occurred where the conventional waste management practices were inadequate to maintain particulate containment. Thus, the presence of solids was included in the disposal site description of operations when such information was noted. Solids inclusion in the waste stream was tracked for each site on a yearly basis; that is, if solids were noted at any time during any given year, the entire year's volume discharged was calculated with a certain percentage of solids. The SIM documentation in

RPP-26744 infers that approximately 21 percent of the disposal sites received solids at some point in their operating history.

Although not a principal focus of the 200-DV-1 OU Waste Site evaluation, liquid releases from the nearby SSTs and ancillary equipment are considered in this conceptual model development. Because of the less documented nature of fluid releases from the SSTs and numerous transfers of waste into and out of the tanks, obtaining good estimates of volumes released and the times and masses released is more difficult. Based on the complicated operations history of inputs and exports of fluids to most of the SSTs, determining when fluids were released to the subsurface, the volumes of fluids released, and the chemical composition of the released fluids is challenging. In many cases, a release was assumed when the operating contractor noticed an unexplained drop in the liquid level measured inside a tank. However, chemical reactions and sludge consolidation confound using drops in liquid levels as a definitive sign of lost fluids. The liquid-level gauges have a short operating life in the highly corrosive and high-radiation environment inside the SSTs.

A second monitoring method is to measure the gamma activity in the subsurface around the SSTs through dry wells drilled around the tanks. The areal coverage of these monitoring dry wells around individual tanks varies such that small-volume leaks might not be detected. The highly heterogeneous subsurface lithology can also cause released fluids to channel along discrete flow paths rather than spreading uniformly through the vadose zone porosity, perhaps allowing fluids to travel undetected past the discrete monitoring dry well locations. Further, most gamma-emitting radionuclides interact moderately to strongly with the sediments (adsorption) such that they do not migrate as far as the released fluids. Surface spills and leaks from the shallow pipelines between the SSTs also confound the interpretation of the gamma log results, namely because many of the dry wells were drilled after fluids were released to the sediments, and drag-down of contaminated sediments to deeper depths was common. Thus, only the largest volume releases have a high probability of being discovered by gamma logging through dry wells.

The current reference that tabulates the status of SST integrity, the timing of past fluid releases, and the estimated release volumes is a series of status reports generally called the Hanlon reports (e.g., HNF-EP-0182, *Waste Tank Summary Report for Month Ending December 31, 2012*). These reports are updated when significant new evaluations have been made.

Using estimates on the timing of tank releases and volumes released, SST waste compositions can be calculated as a function of time using additional subroutines within the HDW Model by calculating the cross-product of the waste stream compositions and their respective contributing volumes (both solid and liquid phases) at various points during a tanks operating life. For SST releases, inventories are especially difficult to estimate accurately because the liquids in the tanks were blended to a much greater extent than wastes released to cribs and trenches. Therefore, certain assumptions and technical judgment are needed to define the composition of a tank leak. A key assumption for each tank leak is that the release event was confined to the year specified and does not occur over multiple years. This assumption attempts to make identifying the waste type involved in a release to the sediment easier because the waste type is more important than knowing the release volume to develop the estimate for the mass or activity inventory. For some wastes, the concentration of key contaminants can vary by over four orders of magnitude whereas the release volume generally varies by much lower amounts.

A second resource is RPP-23405, *Tank Farm Vadose Zone Contamination Volume Estimates*, which revisited the timing of past releases and the estimated release volumes. RPP-23405 provided volume estimates that are identical to those used in the current version of SIM. A formal process for updating the SST leak assessments (see RPP-32681, *Process to Assess Tank Farm Leaks in Support of Retrieval and Closure Planning*, for details) was established several years ago. Using this process, the tank farm

contractor (currently Washington River Protection Solutions [WRPS]) and Ecology review historical and new information, including gamma logging and sediment sampling performed in recent direct-push boreholes. This formal process of updating the status of SSTs has been completed for the SX and S Tank Farms (RPP-ENV-39658, *Hanford SX-Farm Leak Assessments Report*; RPP-RPT-48589, *Hanford 241-S Farm Leak Assessment Report*, respectively). The extensive revisions in which tanks released waste, the revised volumes, and the masses presented in these two reports have been incorporated in this conceptual model document and are listed in Appendix A and Chapter 3 tables within this main report where the vadose zone conceptual models for each subsection are explained.

1.4 Data Availability in Vadose Zone

Laboratory measurements of sediment samples and downhole geophysical logging measurements are the primary data types used to estimate the distribution and concentrations of key contaminants in the 200-DV-1 vadose zone. Soil electrical resistivity surveys have also been used at various Hanford Site locations to identify resistivity anomalies in the subsurface. Areas of low resistivity may correlate to zones or strata with a relatively high saline and moisture content. However, when the electrical resistivity surveys are performed with surface electrodes only, the results do not give an accurate indication of the vertical extent of the low-resistivity plume (PNNL-17821, *Electrical Resistivity Correlation to Vadose Zone Sediment and Pore-Water Composition for the BC Cribs and Trenches Area*). Soil resistivity surveys can give an accurate indication of the lateral extent of low resistivity (high-salt) plumes when metallic infrastructure interferences are not severe or can be removed during data analysis. Available soil resistivity survey data are discussed in Chapter 3 for each S Complex Area subregion when available.

The available borehole geophysical logging data have been compiled in a separate report (SGW-50194, *Geophysical Logging Report for 200-DV-1 Operable Unit Waste Sites in the S Complex Area*), and the most relevant information is liberally used in this report, especially in Chapter 3. Geophysical borehole logs are available from many wells within each subregion; combined, these logs are the largest dataset available for assessing the nature and extent of subsurface contamination. In general, for the S Complex Area conceptual models, the gross gamma logging data from the early days of Hanford Site operations are useful for tracking the mobile gamma emitters ruthenium-106 (Ru-106) and cobalt-60 (Co-60). However, by 2000, when spectral gamma logging became available, most of the Ru-106 had decayed to levels below those readily detected by the logging system. Decay also makes cobalt-60 difficult to detect now in all but a few vadose locations where high concentrations were released in the past. The spectral gamma logging data that readily measure more long-lived radionuclides such as cesium-137 (Cs-137), Hanford-derived uranium-239 (U-239), and europium radioisotopes are useful for identifying the lateral and vertical spread of these less-mobile contaminants. The spread of these radioisotopes in the vadose zone can be used to estimate the likely minimum distances traveled by the more mobile contaminants such as Tc-99, I-129, hexavalent chromium (Cr(VI)), and nitrate that were also present in the liquids released to the subsurface. While not always quantitative, the geophysical borehole log data provide a reasonable estimate of the historical and recent distributions of mobile and immobile gamma emitting contaminants and, by association, any chemical contaminants that existing or currently exist in the vadose zone beneath the waste sites. Laboratory measurements of sediment samples collected within and proximal to disposal facilities in the S Complex Area are nonexistent. However, three characterization boreholes and some shallow direct push characterization boreholes are inside the S and SX Tank Farms fence lines with sufficient depth-discrete sediment samples to estimate the vertical extent of species in the vadose zone (Table 1-1).

Table 1-1. Boreholes in the S Complex Area with Laboratory Analyses of Vadose Zone Sediment Samples

Well/Borehole	S Complex Area Location	No. of Sediment Samples	No. of Discrete Depths	Shallowest Depth (ft bgs)	Deepest Depth (ft bgs)
299-W23-234 (41-09-49)	SX Tank Farm	162	122	25	214
299-W23-19	SX Tank Farm	257	232	6.5	205.2
299-W23-64 (Slant Borehole)	SX Tank Farm	24	24	55*	149*
WRPS SX direct push boreholes(13 boreholes)	SX Tank Farm	~50	36	46	154
WRPS S direct push boreholes (south of S and north of SX (5 boreholes)	south of S Tank Farm and north of SX Tank Farm	~20	16	37	161

bgs = below ground surface

WRPS = Washington River Protection Solutions

* vertical ft bgs

The number of boreholes with adequate data is severely limited in comparison to the area encompassed by the S Complex Area (73.7 hectares [182 acres]) and the volume of the vadose zone. Table 1-1 lists 3 boreholes and 18 direct push borings in the S and SX Tank Farms, with 373 discrete sediment samples that had some laboratory analysis. The sediment samples were from ~314 discrete depth intervals. Even with this number of sediment samples, there is very little useful information for the characterization of the S Complex vadose interval below the bottom of the tank farm and waste sites.

These data are integrated (i.e., sediment analytical results, borehole geophysical log data, and surface geophysical exploration [SGE] information) to interrogate the volume of sediment beneath the S Complex Area and determine what is known about the lateral and vertical extent of contamination in the vadose zone.

In addition to these data sets, process knowledge of waste types and volumes disposed of can aid in determining the relative distances contaminants might travel. Geological knowledge on the location of potential lateral spreading zones can aid in predicting where contaminants might exist in the vadose zone.

1.5 Data Availability for the Groundwater

Environmental monitoring data for the Hanford Site have been reported regularly since January 1945. Reports issued before and during the early 1950s are mainly concerned with drinking water and media other than groundwater, although a few analytical results for groundwater samples from monitoring wells at waste management facilities were published. Many more groundwater monitoring data became available during the 1950s as more monitoring wells were installed and an increased emphasis developed on waste management monitoring. Many of these older data from the 1950s and 1960s have been entered into the Hanford Environmental Information System (HEIS) and are easily available for use. Recently, the HEIS database was made available to the public and is now called the Environmental Dashboard Application (EDA). The EDA is available at http://environet.hanford.gov/eda/. The groundwater dataset accessed through EDA is the primary dataset used to analyze groundwater contamination in this document.

The amount of EDA data available for characterization of groundwater beneath the S Complex Area is not large. Only two of the wells used to characterize the groundwater were drilled in the 1950s, limiting the amount of early data. A few gross beta and nitrate results are available in EDA from the 1950s. Other analytes, including gross alpha, cobalt-60, and uranium, which were commonly analyzed in other parts of the Hanford Site in the late 1950s, are not available for the S Complex Area during that time. The first available gross alpha concentrations for wells in the S Complex Area are from 1980. Cobalt-60 was first analyzed from wells used to characterize the S Complex Area groundwater in March 1969. The number of wells and sample frequency for cobalt-60 decreased significantly in the 1990s and 2000s because it was no longer detected in groundwater at most wells due to decay of the isotope (5.7-year half-life).

Although uranium was a common analyte in groundwater in parts of the Hanford Site in the mid to late 1950s, no groundwater uranium data are available for the S Complex Area until early 1983.

Nitrate became a commonly reported groundwater analyte in wells from the S Complex Area and elsewhere around the Hanford Site in the mid to late 1950s. A large data gap for nitrate occurs between 1963 and 1969 in the two wells within the S Complex Area that span that period. Groundwater samples were again analyzed for nitrate after 1969; nitrate continues to be a common groundwater analyte today.

Tritium became a commonly measured groundwater constituent after it was discovered in groundwater in 1962. Interest in tritium mostly resulted from the plume moving from the 200 East Area to the Columbia River, but tritium was measured in two wells in the early to mid-1960s at the S Complex Area. A gap in tritium groundwater analyses occurs between 1966 and 1972 for the S Complex Area wells.

Ruthenium-106 became a commonly reported groundwater analyte in 1971 and was measured in several wells in the S Complex Area throughout the 1970s and into the 1980s. The number of available ruthenium-106 (1.02 years half-life) results decreases rapidly in the late 1980s and 1990s because it had undergone sufficient radiological decay that it was no longer detected.

Very few groundwater I-129 data are available from the wells used to characterize the S Complex Area in the EDA. Of the 37 results in the EDA, 27 are nondetects and only four exceed the drinking water standard (DWS) of 1 pCi/L. The first I-129 analysis was in 1988, but the first detectable I-129 was found in 1992.

The first groundwater analyses for chromium were in 1987 for wells in the S Complex Area, but the first detectable chromium results are from 1991. The first detected Tc-99 groundwater concentration in the S Complex Area occurred in 1986. These analytes were added after that time, with the onset of environmental monitoring for RCRA and CERCLA purposes. Chromium groundwater data are available in EDA for both filtered and unfiltered samples. Samples for analyses of both filtered and unfiltered metals were collected in the late 1980s and early 1990s. However, the practice of analyzing metals from unfiltered samples was stopped in about 1992 because it was realized that several spurious results were obtained from groundwater samples containing particulate material from the sediment formation or from deteriorating well casings and screens. Since the analyte of interest was soluble Cr(VI), there was no loss of information in analyzing samples only after the particulates had been filtered from the groundwater.

The practice of analyzing both filtered and nonfiltered groundwater for metals began again in 2007, at the direction of Ecology, and that practice continues today. There is a continuum of filtered chromium data from 1991 to the present. There is a long gap in the data for unfiltered chromium from about 1991 to 2008. There are 272 analyses for chromium in EDA from wells used to characterize the S Complex Area. Of those, 82 filtered samples show detectable results, and 40 unfiltered samples show detectable results. Both filtered and unfiltered results are reported in this document, and the reader is cautioned against interpreting unfiltered results as representative of groundwater conditions.

Not all of the previously mentioned analytes are mobile constituents of interest for the deep vadose zone beneath the S Complex Area. Their results, however, can be useful because they act as surrogates for one or more of the constituents of interest. The historical groundwater concentration results and trends for gross alpha, gross beta, cobalt-60, and nitrate indicate the period when released liquid wastes first entered groundwater from the vadose zone. The older results may also be used to track and trend historical groundwater flow rates and directions.

Sampling methods also have changed. Samples were collected using bailers before the late 1970s and before March 1956, the only effort to limit cross-contamination among wells was to sample wells with lower contaminant concentrations before sampling wells with higher concentrations (Earth Sciences Personnel 1956, *Earth Sciences' Waste Disposal Monitoring Activities Summary, March 1956*). After March of 1956, individual bailers were provided for each disposal area to limit concentration ranges to which each bailer was exposed. This and other potentially undocumented practices require careful interpretation of data collected before strict environmental protocols were adopted.

Water-level data accessed through EDA extend back to the late 1940s and early 1950s for a few wells. These data are useful for tracking changes in water table elevation and changes in groundwater flow direction, both of which influence contaminant distribution. As with the analytical data, care needs to be taken when using the historical water level data. Potential problems may result from different vertical data having been used, changes in the ground surface elevation at a well, or changes in the length of well casing stick-up. Historical water-level data also were entered into HEIS from handwritten data sheets and notebooks, which, may have resulted in transcription errors.

1.6 Conceptual Site Model Development

Figure 1-2 describes the process used to develop the conceptual models for the vadose zone distribution of contaminants for each facility and the groundwater plumes for each subregion. The SIM database (RPP-26744) is used to obtain estimates for the volumes of waste and masses of chemicals and radionuclides released into each facility. All of the geophysical and geological data collected for boreholes in each subregion and soil resistivity model interpretations were compiled and evaluated to create the best geologic model of each subregion's lithology and stratigraphic architecture. When available, vadose zone sediment laboratory analytical data were merged with geophysical logs and soil resistivity models to define the lateral spread and vertical extent of current (residual) contamination in the vadose zone. This became the first iteration of the vadose zone conceptual model for the location and extent of vadose zone contamination. Using assumed or measured moisture contents for the contaminated sediments and the percentage of discharged liquid that remains in the vadose zone, the mass of residual mobile contaminants was approximated. This calculation assumed that no interaction (sorption or precipitation) occurred between the mobile contaminants and the sediments, and the pore water in the contaminated sediment volume is waste liquid that contains the original waste stream concentrations of mobile contaminants. Based on these assumptions, the percentage of waste fluid volume still residing in the vadose zone plume is the same value as the percentage of the contaminant inventory present.

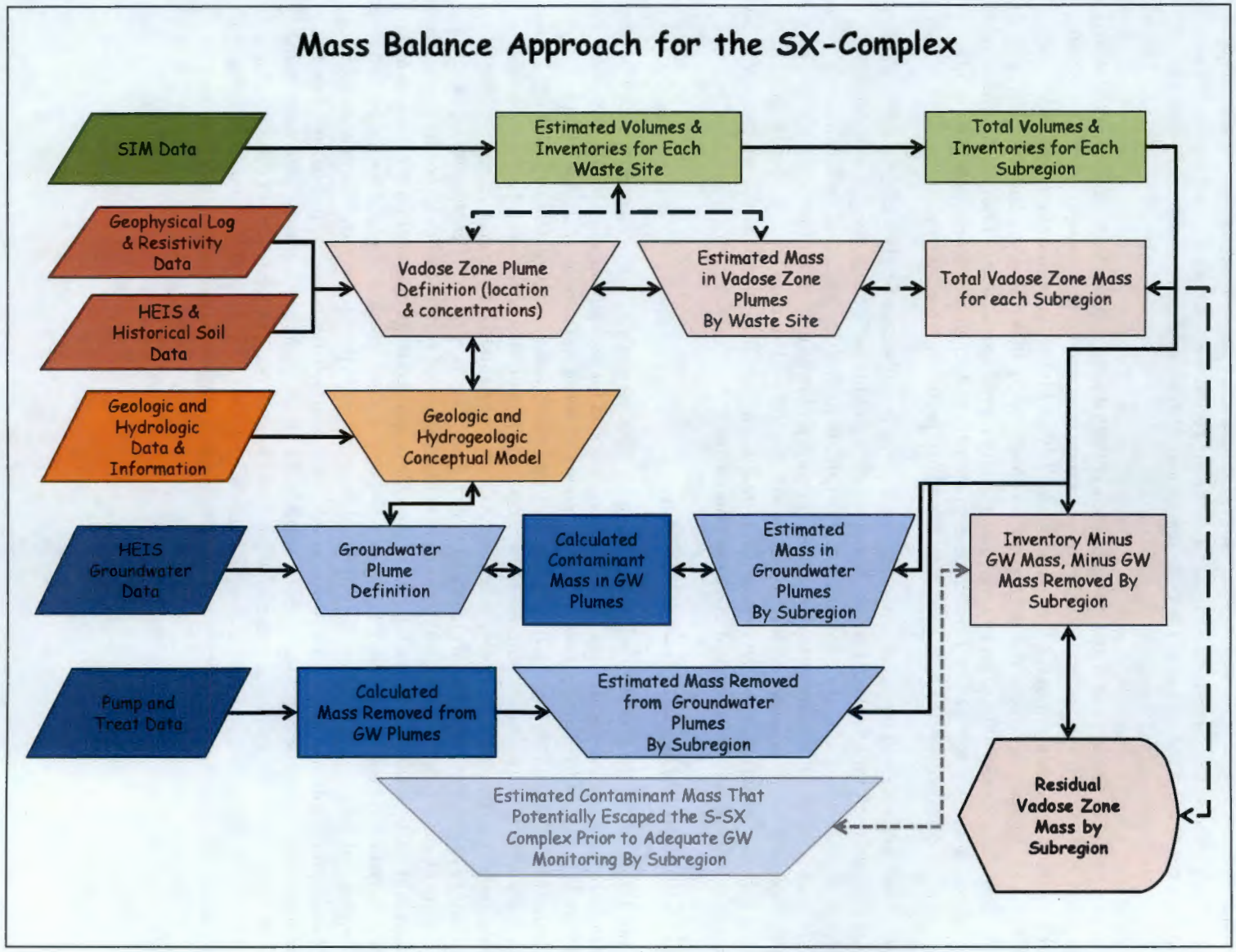

Figure 1-2. Conceptual Model Development Process Flowchart

The mass of contaminants residing in the groundwater was calculated using the annually averaged groundwater concentrations and water table elevations at each monitoring well from year to year to delineate the shape (area of the plume) and volume of contaminated water in the plume. Using a three-dimensional (3D) model of the groundwater plume and the point (well) concentrations (including any depth discrete groundwater concentrations), a geostatistical smoothing routine was used to assign concentrations to each representative grid cell volume that constitutes the groundwater plume. The smoothing routine creates a fixed concentration for each contaminant in each volumetric grid cell, and sums all the masses (concentration times grid cell volume) for the entire 3D plume. The final step was to assign porosity for aquifer sediments because the entire volume of each grid cell is not composed only of water. After making the porosity correction, the result is the mass of each contaminant in its volumetric plume for each year modeled. For the S Complex Area, the groundwater mass calculation was performed for only one period, covering the time interval 2005 to 2010 because the groundwater database is not robust. Thus, no quantitative estimate on whether mass is increasing or decreasing was performed to assess whether the mass in the aquifer is growing with time (being augmented by influx from the vadose zone or from groundwater entering the S Complex Area from outside the defined boundaries) or decreasing (by groundwater leaving the defined boundaries of the S-SX Complex). The sum of the residual mass in the vadose zone plus the current mass in the groundwater plume, plus mass removed by pump-and-treat activities should equal the estimated mass disposed of to the S Complex Area (obtained from the SIM [RPP-26744]) as long as no mass has left the S Complex Area aquifer region before groundwater data became available.

Because the dataset available to estimate the residual mass of contaminants in the vadose zone is relatively limited, the mass balance calculations are better used to provide a conservative estimate of the mass that may still be in the vadose zone. The preliminary estimate of residual mass in the vadose zone becomes the difference between the mass estimate from SIM (RPP-26744) for the disposed of mass and the sum of the current mass in the groundwater plume (the mass removed by pump-and-treat activities in the S Complex Area is too small to impact the calculation). This approach is based on the assumption that no mass escaped from the S Complex Area in the early years when groundwater monitoring was not adequate or not being performed for mobile contaminants.

This page intentionally left blank.

2 S Complex Hydrogeology

This chapter summarizes the geologic setting, including the geomorphology, stratigraphy, lithology, and structure of the vadose zone sediments and presents the most recent conceptual geohydrologic model of the area near the S Complex Area. This analysis is based on a limited network of boreholes and geophysical surveys located in the area. The information in this chapter provides the framework for interpreting stratigraphic and structural controls on moisture and contaminant movement through the vadose zone to groundwater. Stratigraphic type logs, stratigraphic cross sections, isopach maps, and structure contour maps of the suprabasalt units pertinent to this discussion are included in SGW-50900, *Geologic Cross Section Development in the Vicinity of S-Complex and T-Complex to Support the 200-DV-1 Operable Unit Conceptual Models*.

2.1 Summary

Understanding the geologic framework is fundamental to the vadose zone CSM developed to define contaminant distribution below the S Complex Area. Chapter 3 provides the detailed subregion geology for each 200-DV-1 OU waste site.

The vadose sediment is composed of unconsolidated to strongly consolidated sedimentary deposits. Of particular significance to liquid disposal and percolation through and/or to sequestration within these sediments are the interrelationships between the coarser and finer grained sediment strata and the degree of contrast in their physical and geochemical properties. The geology of the western Hanford Site where the S Complex Area is located is based on a long history of hydrogeologic studies published in numerous reports (Table 2-1).

Table 2-1. Hanford Site Hydrogeologic Studies

Document Number	Document Title
BHI-00184	*Miocene- to Pliocene-Aged Suprabasalt Sediments of the Hanford Site, South-Central Washington*
BHI-01203	*Nature and Variability of the Plio-Pleistocene Unit in the 200 West Area of the Hanford Site*
DOE/RL-91-61	*T-Plant Source Aggregate Area Management Study Report*
DOE/RW-0164	*Site Characterization Plan: Reference Repository Location, Hanford Site, Washington* (Consultation Draft)
HNF-4936	*Subsurface Conditions Description for the S-SX Waste Management Area*
HW-61780	*Subsurface Geology of the Hanford Separation Areas*
PNL-6820	*Hydrogeology of the 200 Areas Low-Level Burial Grounds—An Interim Report*
PNL-7336	*Geohydrology of the 218-W-5 Burial Ground, 200 West Area, Hanford Site*
PNNL-13757-1	*Characterization of Vadose Zone Sediment: Uncontaminated RCRA Borehole Core Samples and Composite Samples*
PNNL-13757-2	*Characterization of Vadose Zone Sediment: Borehole 299-W23-19 [SX-115] in the S-SX Waste Management Area*
PNNL-13757-3	*Characterization of Vadose Zone Sediment: Borehole 41-09-39 in the S-SX Waste Management Area*

Table 2-1. Hanford Site Hydrogeologic Studies

Document Number	Document Title
PNNL-13757-4	*Characterization of Vadose Zone Sediment: Slant Borehole SX-108 in the S-SX Waste Management Area*
PNNL-13858	*Revised Hydrogeology for the Suprabasalt Aquifer System, 200-West Area and Vicinity, Hanford Site, Washington*
PNNL-15955	*Geology Data Package for the Single-Shell Tank Waste Management Areas at the Hanford Site*
PNNL-17913	*Hydrogeology of the Hanford Site Central Plateau – A Status Report for the 200 West Area*
USGS Professional Paper 717	*Geology and Ground-Water Characteristics of the Hanford Reservation of the U.S. Atomic Energy Commission, Washington* (Newcomb and Strand, 1972)
RHO-ST-23	*Geology of the Separations Areas, Hanford Site, South-Central Washington*
RPP-7884	*Field Investigation Report for Waste Management Area S-SX*
RPP-43548	*Completion Report for 241-SX Tank Farm Direct Push Barrier Characterization*
RPP-47274	*2010 Completion Report for the 241-S/SX Tank Farm Direct Push Barrier Characterization*
SD-BWI-DP-039	*Suprabasalt Stratigraphy Within and Adjacent to the Reference Repository Location*
USGS-W-P-8	*Parker and Piper (1949), Geologic and Hydrologic Features of the Richland Area, Washington, Relevant to Disposal of Waste at the Hanford-Directed Operations of the Atomic Energy Commission*
WHC-SD-EN-TI-008	*Geologic Setting of the 200 West Area: An Update*
WHC-SD-EN-TI-014	*Hydrogeologic Model for the 200 West Groundwater Aggregate Area*
WHC-SD-EN-TI-290	*Geologic Setting of the Low-Level Burial Grounds*

Note: Complete reference citations are provided in Chapter 9.

The stratigraphy of the S Complex Area consists of unconsolidated sedimentary deposits that overlie the volcanic Columbia River basalt and associated sedimentary interbeds. This report focuses on stratigraphic units associated with the unsaturated zone beneath the S Complex Area. The principal units occurring wholly or partially within the unsaturated zone beneath the S Complex Area are (from youngest to oldest):

- Holocene surficial deposits (primarily of anthropogenic and eolian origin)
- Hanford formation
- Cold Creek unit
- Ringold Formation

Eolian materials blanketed the area with up to 2 m (5 ft) of windblown sand and silt before the S Complex Area facilities were installed. Backfill materials, composed of the mostly gravel-dominated Hanford

formation subunit 1, were introduced during the construction of the cribs, trenches, and tile fields in the S Complex Area.

Hanford formation sediments are approximately 30 m (98 ft) thick beneath the S Complex Area. The uppermost Hanford formation consists of a gravel-dominated facies referred to informally as the Hanford formation subunit 1 (Hf1). To the south of the area, the Hf1 transitions laterally into a sand-dominated facies, referred to as the Hanford formation subunit 2 (Hf2); Hf2 also underlies Hf1 beneath the S Complex Area. To the west of the S Complex Area, another sequence of gravel-dominated facies, referred to as the Hanford formation subunit 3 (Hf3), exists locally beneath Hf2. The southerly dips of strata within the Hanford formation are probably associated with the depositional surface that existed along the south flank of the Cold Creek flood bar as it prograded south and east during subsequent Ice Age floods.

Underlying the Hanford formation below the S Complex Area is the Cold Creek unit (CCu). This sedimentary sequence is approximately 8 m (27 ft) thick in this area. The CCu forms a continuous layer beneath the S Complex Area that occurs approximately midway between the ground surface and the water table. The uppermost Cold Creek silt-dominated subunit z (CCuz) consists of cohesive, compacted, and massive-to-laminated, fine-grained sand and silt. The underlying Cold Creek calcic geosol subunit (CCuc) consists of gravels, sands, silt, and clay that are cemented with one or more layers of secondary, pedogenic calcium carbonate (calcrete). Like the Hanford formation, the Cold Creek unit gradually dips to the south toward the Cold Creek syncline beneath the S Complex Area.

The upper contact of the Ringold Formation member of Taylor Flat (RFtf) is gradational with the overlying CCuc paleosol sequence and consists of interstratified, well-bedded, fine to coarse sand and silt. Post-Ringold Formation erosion has made the RFtf laterally discontinuous across the Pasco Basin. The RFtf is present locally in a few places, such as near the T Complex Area, as thin (2 to 6 m [6 to 20 ft]) erosional remnants. The Ringold Formation member of Wooded Island-unit e (RFwie) sequence is 82 to 85 m (270 to 280 ft) thick, and consists predominantly of fluvial conglomerate with occasional thin beds and lenses of mud and sand. The RFwie generally consists of a bimodal, clast-supported, pebble-cobble gravel within a moderately to well-sorted sandy matrix. Most gravel clasts are very well rounded and frequently polished—typical of fluvial deposits. The top of the unit dips very gently to the southwest toward the Cold Creek syncline. Beneath the S Complex Area, the water table (i.e., saturated zone) lies strictly within the RFwie. Underlying the RFwie are the Ringold Formation member of Wooded Island-lower mud unit (RFlm) and Ringold Formation member of Wooded Island-unit a (RFwia). These units occur entirely within the saturated zone and are not discussed further in this report.

2.2 Regional Hydrogeologic Overview

The next several sections provide a discussion of the regional geomorphology and stratigraphy. The Hanford Site and Pasco Basin lie within the Columbia Plateau of south-central Washington State. This broad, uneven plain is situated between the Cascade Mountains to the west and the Rocky Mountains to the east. It is underlain by a thick sequence of volcanic Columbia River basalt, which forms the bedrock for the Central Plateau. Since the Miocene, the basalt bedrock in this area has been folded into a series of east-west trending anticlines and synclines called the Yakima Fold Belt. Locally, over 1,000 ft of sediment has accumulated in the down-warped synclines in the Pasco Basin.

2.3 Geomorphology

The S Complex Area lies within the west-central portion of the Hanford Site at an elevation of about 200 m (660 ft) above mean sea level (amsl). The Site lies in a low-relief area atop Cold Creek bar, a large

compound flood bar formed during Pleistocene Ice Age floods (Figure 2-1). The S Complex Area lies along a north-south trending secondary cataclysmic flood channel that bisects Cold Creek bar. Present topography indicates the last Ice Age flood that overtopped Cold Creek bar incised a wide, shallow channel immediately west of the tank farms at an elevation of 200 m (656 ft). A thin (1 m or less) sheet of windblown sand occurs at the surface in undisturbed areas within the S Complex Area. The semi-arid climate, in combination with the relatively young age and high permeability of the near-surface sediments, has resulted in the lack of any natural surface-drainage channel development in the immediate vicinity of the S Complex Area.

2.4 General Stratigraphy

The generalized stratigraphy beneath the Hanford Site consists of, in descending order, Holocene alluvium, colluvium, and/or eolian sediments and backfill materials (all discontinuous), the Hanford formation, the CCu, the Ringold Formation, the Columbia River Basalt Group, and intercalated sediments of the Ellensburg Formation (Figure 2-2)[4]. The CCu and Hanford formation are informal stratigraphic designations adapted for the Hanford Site. The regional suprabasalt stratigraphy is described in more detail in (RHO-BWI-ST-4, *Geologic Studies of the Columbia Plateau—A Status Report*; RHO-BWI-ST-14, *Subsurface Geology of the Cold Creek Syncline*; BHI-00184; and Lindsey, 1996, *The Miocene to Pliocene Ringold Formation and Associated Deposits of the Ancestral Columbia River System, South Central Washington and North Central Oregon.*). Figure 2-3 shows a north-south cross section L4-L4' depicting the detailed vadose zone geologic framework for the western Hanford Site beneath the S Complex Area.

Considerable heterogeneity exists in the sedimentary deposits for the Pasco Basin and Hanford Site because of the uniquely dynamic geologic setting that exists here. Examples of the many different stratigraphic units represented within the vadose zone beneath the S Complex Area are shown in Figure 2-4.

Geologic cross sections (SGW-50900) show the general distribution and thicknesses of the lithostratigraphic units within the vadose zone.

[4] Complete reference citations are provided in Chapter 9.

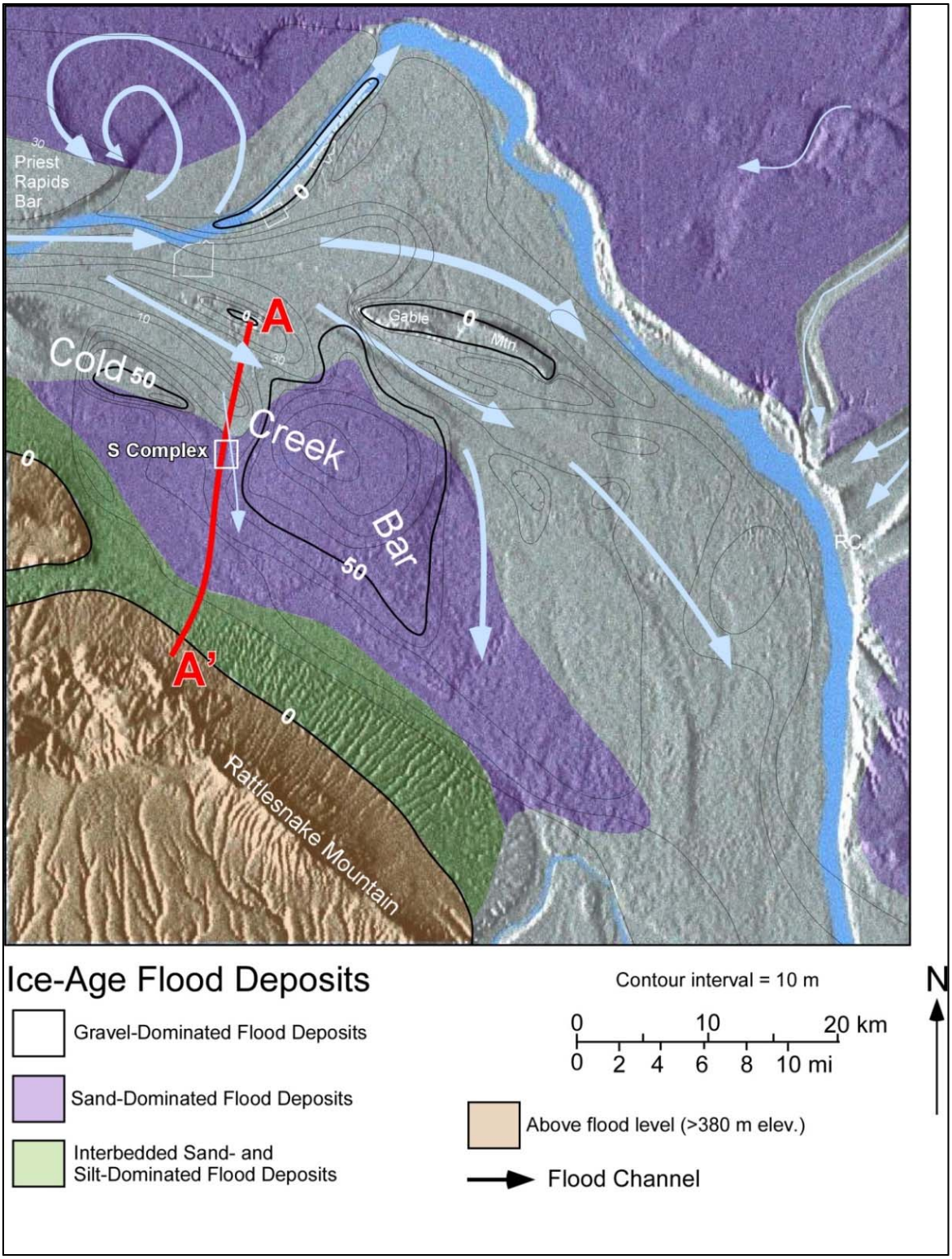

Note: Flood deposits of the Hanford formation are thickest (~100 m [328 ft]) beneath Cold Creek flood bar east of the S Complex Area. A smaller portion of Cross section A-A' (L4-L4') is presented in Figure 2-2 (DOE/RL-2002-39, Standardized Stratigraphic Nomenclature for Post-Ringold-Formation Sediments within the Central Pasco Basin).

Figure 2-1. Major Landforms and General Lateral Distribution of the Three Principal Hanford Formation Facies Within the Central Pasco Basin

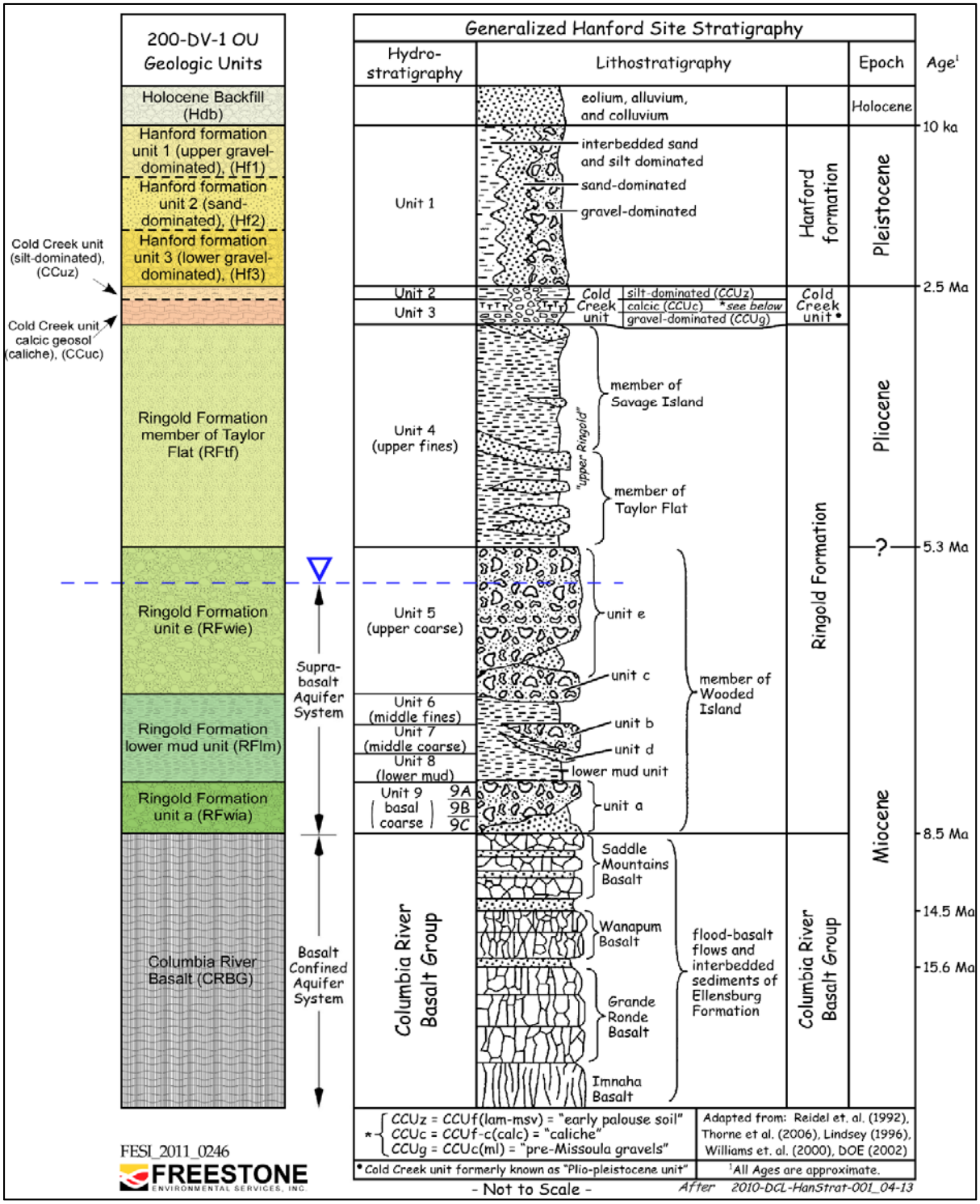

Note: Chapter 9 provides complete reference citations.
Sources: WHC-MR-0391, *Field Trip Guide to the Hanford Site* (Reidel et al., 1992); PNNL-14753, *Groundwater Data Package for Hanford Assessments* (Thorne et al., 2006); Lindsey, 1996, *The Miocene to Pliocene Ringold Formation and Associated Deposits of the Ancestral Columbia River System, South-central Washington and North-central Oregon*; PNNL-12261, *Revised Hydrogeology for the Suprabasalt Aquifer System, 200-East Area and Vicinity, Hanford Site, Washington* (Williams et al., 2000); DOE/RL-2002-39, *Standardized Stratigraphic Nomenclature for Post-Ringold-Formation Sediments Within the Pasco Basin* (DOE, 2002).

Figure 2-2. Correlation of 200-DV-1 OU Stratigraphy to Generalized Hanford Site Suprabasalt Stratigraphy

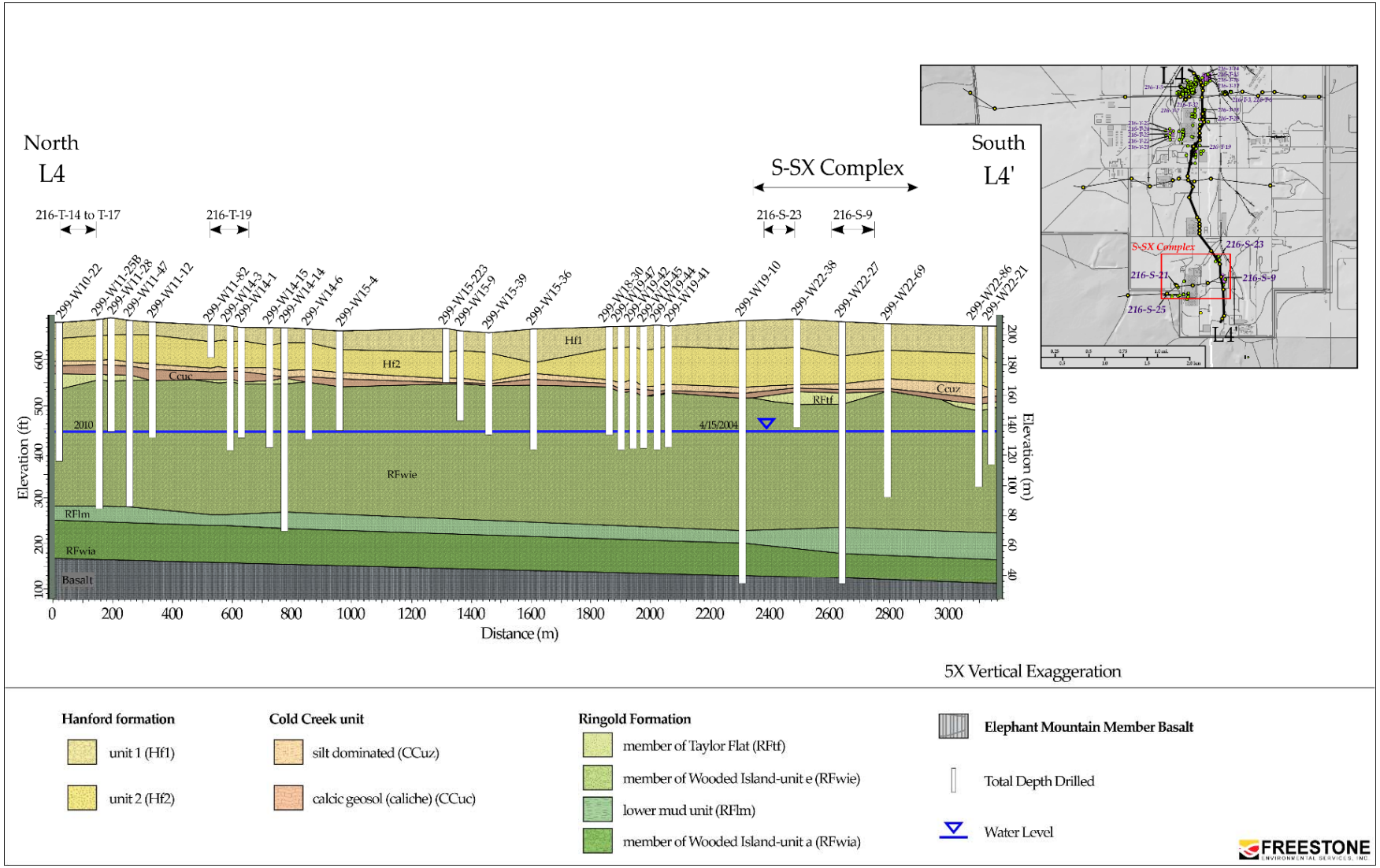

Figure 2-3. A North-South Hydrogeologic Cross Section Shows Stratigraphic Relationships Within the Vadose Zone along the Western Hanford Site

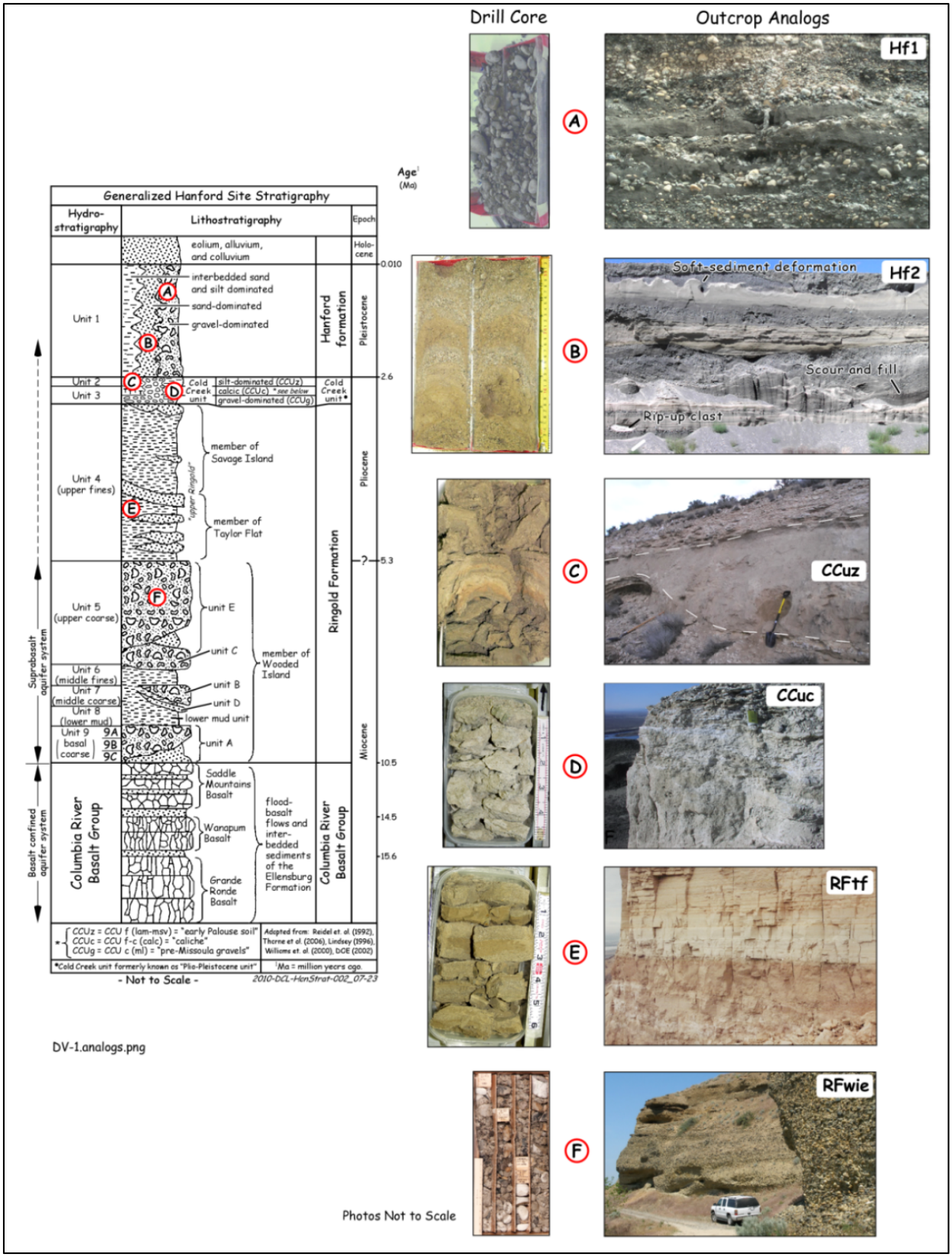

Figure 2-4. Stratigraphic Units Representative in the Vadose Zone Beneath S Complex Area

2.4.1 Holocene Deposits

Holocene deposits include eolian deposits as well as manmade backfill material. Eolian deposits are generally composed of windblown sand and silt. Backfill materials composed of the mostly gravel-dominated Hf1 stockpiled nearby during disposal-facility construction, perhaps mixed with eolian materials that blanketed the area with up to 2 m (5 ft) of windblown sand and silt before the S Complex Area facilities were installed (DOE/RL-2000-61, *Draft Industrial Mineral Resources Management Plan*). The natural layering and stratification of the Hanford formation were destroyed as disposal facilities were excavated; however, some anthropogenic stratification and differential compaction were likely introduced by heavy-equipment movement during the backfill process. Sediments foreign to the waste sites were occasionally introduced during backfill operations to improve traction for construction vehicles.

2.4.2 Hanford Formation

The Hanford formation is the informal name given to all glacio-fluvial deposits from cataclysmic Ice Age (Missoula) floods that occurred as recently as 15,000 years ago (RHO-ST-23, *Geology of the Separation Areas, Hanford Site, South-Central Washington*; DOE/RW-0164; DOE/RL-2002-39, *Standardized Stratigraphic Nomenclature for Post-Ringold-Formation Sediments Within the Pasco Basin*; Baker et al., 1991, "Quaternary Geology of the Columbia Plateau;" Bjornstad, 2006, *On the Trail of the Ice Age Floods: A Geological Field Guide to the Mid-Columbia Basin*). The earliest floods may extend back to the beginning of the Ice Age or 2.6 million years ago (Bjornstad et al., 2001, "Long History of Pre-Wisconsin, Ice Age, Cataclysmic Floods: Evidence from Southeastern Washington State"). The Hanford formation consists of mostly unconsolidated sediments that cover a wide range in grain size from pebble- to boulder-gravel, fine- to coarse-grained sand, silty sand, and silt. Significant amounts of clay are conspicuously absent from the Hanford formation within the Hanford Site's Central Plateau.

The Hanford formation is subdivided into gravel-, sand-, and interbedded sand and silt-dominated facies, which transition into one another vertically as well as laterally with distance from the main, high-energy, flood currents. Figure 2-3 shows how facies of the Hanford formation transition laterally away from higher energy flood channels. Bouldery coarse-grained deposits along flood channels give way to pebble-cobble gravel, sand, and finally silt-dominated lithofacies in slackwater areas around the margins of the valley where flood currents moved more slowly. Within the S Complex Area, subunits Hf1 and Hf2 of the Hanford formation have been defined by delineating contiguous sediments that are predominately composed of one of the following lithofacies types:

1. **Gravel-Dominated Lithofacies (Hf1 and Hf3).** This facies generally consists of poorly sorted, coarse-grained, basaltic sand and granule-to-boulder gravel. The area between gravel clasts is sometimes empty (i.e., openwork fabric), but more often is filled with a poorly sorted mixture of sand to silt grains. Deposits display massive to plane to low-angle bedding and large-scale planar (foreset) cross bedding in outcrop. Gravel-dominated beds may fine upward into sand and, more rarely, thin silt caps. Bedding is highly chaotic and discontinuous (see "A" in Figure 2-4). Gravel clasts are dominantly subangular to subrounded basalt with lesser amounts of well-rounded Ringold Formation clasts, including granite, quartzite, and gneiss (WHC-SD-EN-TI-008, *Geologic Setting of the 200 West Area–An Update*). The gravel-dominated facies was deposited by high-energy floodwaters in or immediately adjacent to principal flood channel ways associated with Ice Age flooding.

2. **Sand-Dominated Lithofacies (Hf2).** This facies consists of moderately to well-sorted, fine- to coarse-grained sand and granule gravel. The sands typically have high basalt content and are commonly referred to as black, gray, or "salt-and-pepper" sands. They may contain small pebbles and rip-up clasts and pebbly interbeds, and they often grade upward into thin (<1 m [3.3 ft]) zones of silt-dominated facies. This facies commonly displays plane-to-ripple lamination and bedding and, less

commonly, channel scour-and-fill sequences (see "B" in Figure 2-4). The sand-dominated facies was deposited on flood bars adjacent to the main flood channelways during the waning stages of flooding. The facies is transitional between the gravel-dominated facies and the interbedded sand-and silt-dominated facies.

3. **Interbedded Sand-and-Silt-Dominated Lithofacies (ISSD).** This facies typically consists of regular graded beds starting with plane- to ripple-laminated sand at the base, grading up into horizontally laminated sandy silt to silt at the tops of the so-called rhythmites (Smith, 1993, "Missoula Flood Dynamics and Magnitudes Inferred from Sedimentology of Slack-Water Deposits on the Columbia Plateau;" DOE/RW-0164; DOE/RL-2002-39; Bjornstad, 2006). Beds are typically a few inches to several tens of inches thick. Sediments of this facies were deposited under slack water conditions in mostly back-flooded areas. Each graded-bed rhythmite may represent deposition from a separate Ice Age flood event (Waitt, 1980, "About Forty Last-Glacial Lake Missoula Jökulhlaups Through Southern Washington"). This lithofacies occurs around the margins of the Pasco Basin (e.g., at south end of cross section A-A′ in Figure 2-3).

It is important to emphasize that each of these three facies transition from one to the other, both laterally and vertically, across the Hanford Site. Furthermore, considerable heterogeneity exists within each of the Hanford formation facies, and it is common to observe the different facies interfinger with each other. Therefore, delineation of which lithofacies dominates at each location is important for understanding vadose zone moisture movement and controlling conditions, and in choosing appropriate hydrogeologic values for computer modeling. Across the Central Plateau, a sequence of gravel-dominated facies usually makes up the uppermost Hanford formation. This lithostratigraphic unit is referred to informally in this report as Hf1. To the south, away from the high-energy flood currents, Hf1 transitions laterally into a sand-dominated facies, referred to as Hf2. Locally within the Central Plateau, another sequence of gravel-dominated facies exists beneath Hf2, known as Hf3.

The sand and gravel fractions of the Hanford formation generally consist of about 50 percent basalt and 50 percent felsic material (RHO-ST-23; RHO-BWI-ST-14). This mineral assemblage gives the Hanford formation its characteristic "salt and pepper" appearance, often noted in driller and geologist logs. The felsic component is composed of quartz, feldspar, and mica with some samples containing greater than 10 percent pyroxene, amphibole, mica, chlorite, ilmenite, and magnetite. The silt- and clay-sized fractions consist of quartz, feldspar, mica, and smectite.

Figure 2-5 shows composite photograph and facies analysis of a portion of the 218-E-12B Burial Ground (submarine trenches). The walls of this 15 m (49.2 ft) deep open pit, photographed and surveyed soon after excavation, expose a sequence of flood gravels, sands, and silts deposited during the last late-Pleistocene cataclysmic floods (PNNL-13757-1, *Characterization of Vadose Zone Sediment: Uncontaminated RCRA Borehole Core Samples and Composite Samples*). Within the excavation, an upper gravel-dominated sequence overlies a sand-dominated sequence, interpreted to represent deposition during at least two separate flood events. The pebbly sand (i.e., sand-dominated facies) lies directly beneath and grades upward into the upper silty sand layer (sand-dominated facies). The silty sand is overlain in sharp contact by sandy gravel (i.e., gravel-dominated facies) along an erosional unconformity. An unknown amount of the silty sand may have been eroded before the overlying sandy gravel was deposited during a subsequent cataclysmic flood. The higher moisture content of the silty sand layer, evidenced by its darker color, is typical of these fine-grained layers as they represent preferential absorption of meteoric water.

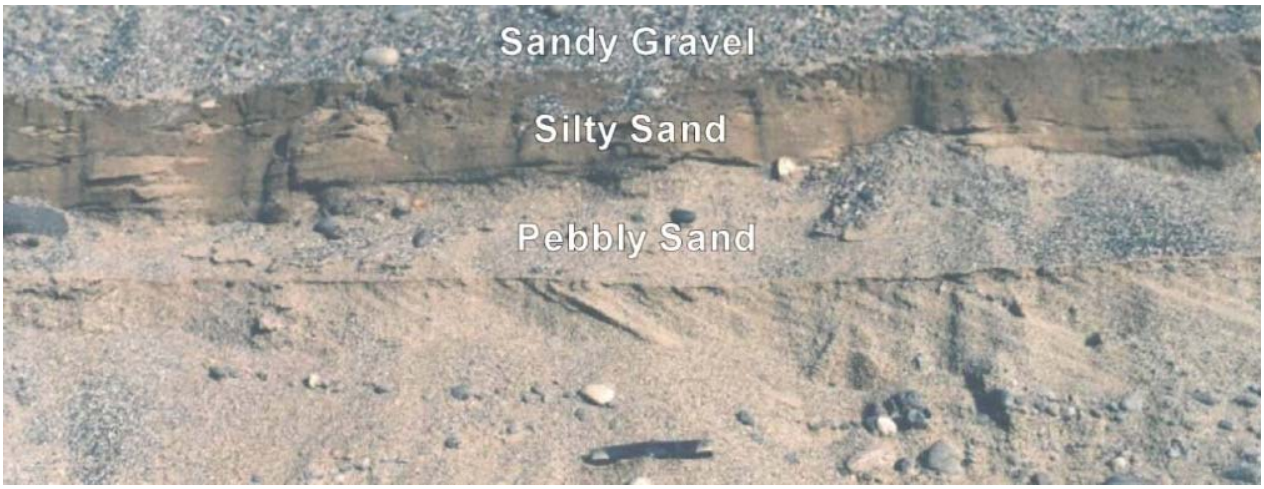

Source: PNNL-13757-1, *Characterization of Vadose Zone Sediment: Uncontaminated RCRA Borehole Core Samples and Composite Samples*.

Figure 2-5. Exposure Showing Hanford Formation Sand- and Gravel-Dominated Facies in the Northeastern 200 East Area

2.4.2.1 Hanford Formation Gravel-Dominated Sequence (Hf1)

The Hanford formation gravel-dominated sequence overlies the Hanford formation sand-dominated sequence over most of the central Hanford Site, including the S-SX Complex Area. Based on observations of outcrop and intact core samples, the Hanford formation gravel sequence is interpreted to consist of the high-energy, gravel-dominated facies interbedded with lenticular and discontinuous layers of the sand-dominated facies. Occasional silt-dominated lenses may also be present, although they constitute a relatively small percentage of the total. Figure 2-6 shows sediment typical of Hf1 (see also "A" in Figure 2-4). Most of the material used for backfill around S-SX Complex waste facilities is from the gravels and sands of Hf1 removed during tank installation. Within the S-SX Complex Area, the Hf1 consists of sandy granule-to-pebble-cobble-size gravel (Figure 2-6). Variable amounts of silt may also be present in the matrix. Overall, the Hf1 grain size decreases to the south away from the main paleo-flood channel paths.

Note: Distinguishing characteristics are its subangular to subrounded clasts of mostly basalt in a brownish gray, poorly sorted, silt and sand matrix; from borehole 299-W11-39, 23 to 24 ft depth.

Figure 2-6. Drill Cuttings of Gravel-Dominated Facies of the Hanford Formation (Hf1)

2.4.2.2 Hanford Formation Sand-Dominated Sequence (Hf2)

The contact between Hf1 and Hf2 is typically distinct and indicated by an abrupt change from gravel-dominated to sand-dominated lithofacies. When the contrasting unit grain sizes are significant enough, the contact and units can be distinguishable on borehole geophysical total- and spectral-gamma logs. Often total gamma counts increase below the Hf1-Hf2 contact downward into the finer-grained Hf2 (this is associated with increases in naturally occurring potassium-40 [K-40] and, to a lesser degree, naturally occurring uranium-238 [U-238] and thorium-232 [Th-232]).

The Hf2 consists of predominantly sand-dominated facies (Figure 2-7). Internally, this Hanford formation sequence contains multiple beds of moderately to well-sorted, loose, plane-bedded sand to pebbly sand 1 m (3.3 ft) or greater thick. Sand-dominated beds occasionally grade upward and are capped by thin (<10 cm [0.4 in.]) beds of sandy silt or silt (Figure 2-7, right). The total calcium carbonate ($CaCO_3$) content is generally a few weight percent or less. Typically, this unit consists of loose, moderately sorted, fine-to coarse-grained sand. It is often described as "salt and pepper" owing to its combination of light-colored felsic and dark-colored mafic sand grains.

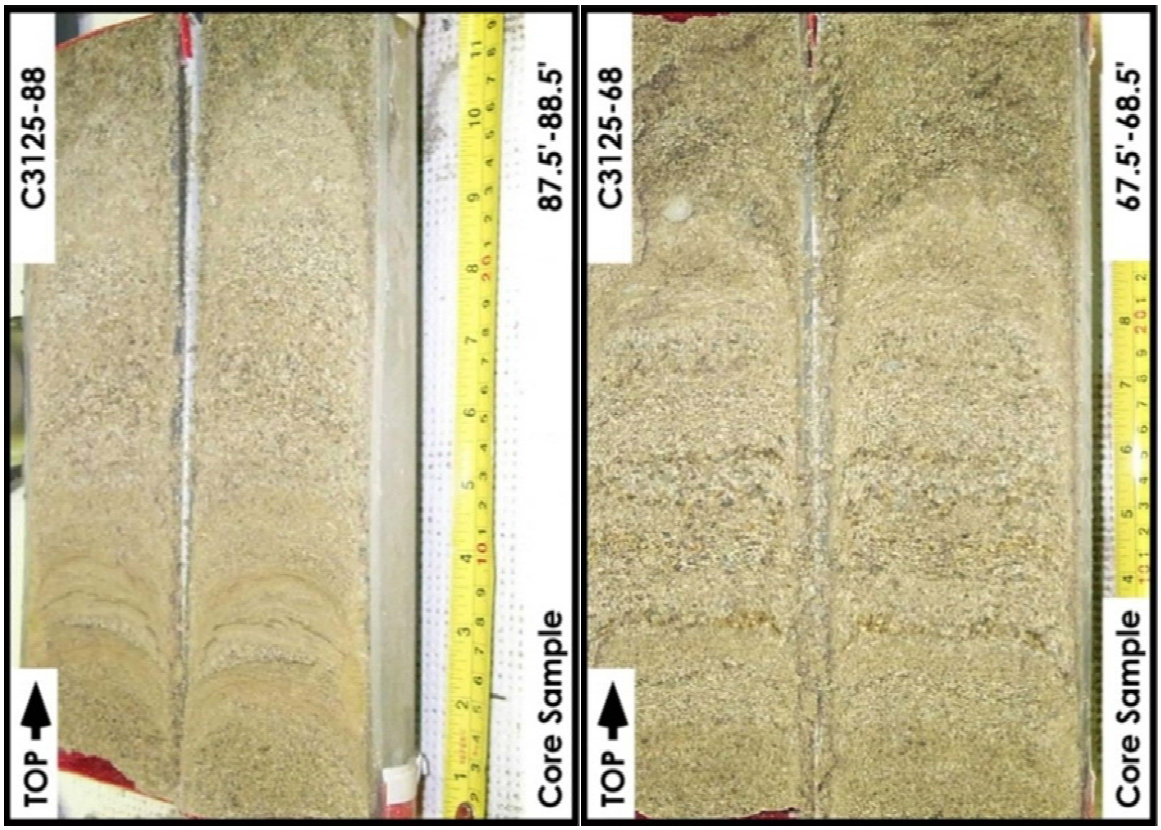

Note: Left: Fine silty sand separates two layers of medium to coarse sand. This sequence appears to represent deposition during two flood pulses, separated by an interval of slack water sedimentation.
Right: Horizontal to low-angle cross-laminated sand with multiple internal micro-gradations is typical of Hf2. Curving laminations are drag-folding created during drilling.

Figure 2-7. Core Samples of the Sand-Dominated Facies of the Hanford Formation (Hf2) from Borehole 299-W10-27

The Hf2 is continuous beneath the S Complex Area; the base is well defined by a change from well-stratified, fine- to coarse-grained, salt and pepper-like sands to silt-dominated deposits of the upper

CCu (Figure 2-8). A diagnostic increase in total natural gamma and/or K-40 activity, as well as moisture, typically distinguish this unit contact boundary at the base of Hf2.

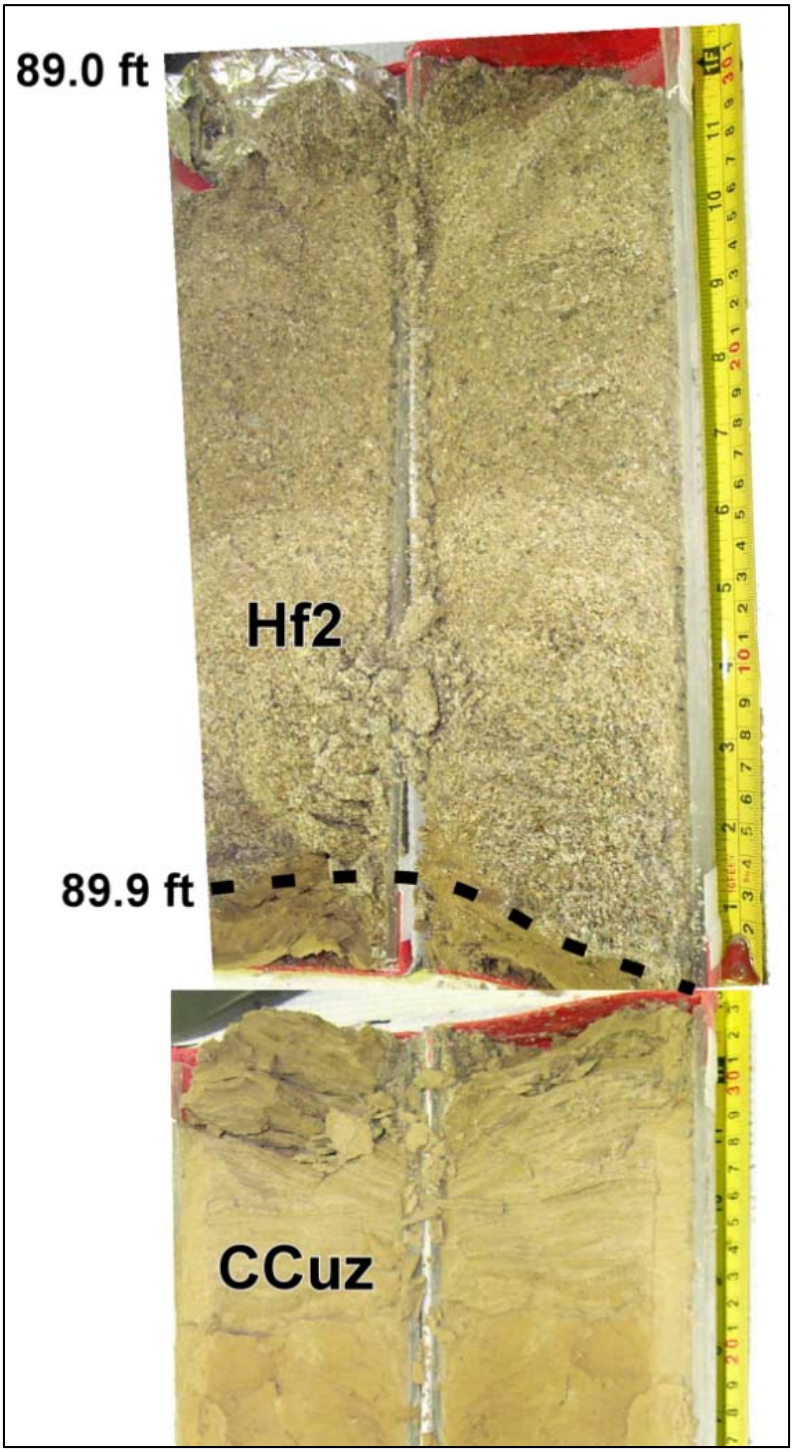

Note: Loose, gray, fine- to medium grained, “salt and pepper” sands of the Hf2 immediately overlie compacted, yellowish-brown, laminated to massive, micaceous and calcareous, silty fine sand to fine sandy silt of the CCuz subunit.

Figure 2-8. Sharp Contact between the Hanford Formation Hf2 and the Underlying Cold Creek Unit Silt in Borehole 299-W11-39

2.4.3 Cold Creek Unit

The CCu includes the sedimentary sequence that overlies the Ringold Formation and underlies cataclysmic flood deposits of the Hanford formation. After a period of post-Ringold incision, the eroded surface of the Ringold Formation was locally weathered and covered with a sequence of CCu deposits. The CCu forms a continuous layer beneath the S Complex Area that lies midway between the ground surface and the water table.

CCu deposits beneath the S Complex Area consist of fine-grained eolian and overbank alluvial deposits overlying a calcic paleosol sequence. The CCu includes those deposits formerly referred to as the "Plio-Pleistocene unit" and "pre-Missoula Gravels," as well as the "early Palouse soil" and "caliche layer" within the 200 West Area. The CCu appears to be correlative to other sidestream alluvial, eolian, and pedogenic deposits found near the base of the ridges bounding the Pasco Basin on the north, west, and south. These sedimentary deposits are inferred to have a late Pliocene to early Pleistocene Epoch (DOE/RW-0164; DOE/RL-2002-39). The upper surfaces of the Ringold Formation and the CCu in the 200 West Area generally dip to the south (PNNL-17913, *Hydrogeology of the Hanford Site Central Plateau–A Status for the 200 West Area*).

The CCu is divided into five subunits within the central Pasco Basin, two of which occur in the 200 West Area (DOE/RL-2002-39). The CCu facies represented in this report are the silt-dominated (CCuz subunit) and the calcic geosol (otherwise known as "caliche" or "calcrete paleosol"), referred to here as the CCuc subunit. The CCuz is hypothesized to have been deposited in an overbank-eolian type of environment (HW-67549, *An Eolian Deposit Beneath 200-West Area*, RHO-ST-23; SD-BWI-DP-039, *Suprabasalt Stratigraphy Within and Adjacent to the Reference Repository Location*; DOE/RW-0164; DOE/RL-2002-39). The underlying CCuc subunit represents a long period of subaerial weathering and soil development in semi-arid moisture conditions (Retallack, 1988, "Field recognition of paleosols;" Retallack, 2001, *Soils of the Past; An Introduction of Peleopedology*) similar to those of today. Extremely well-cemented, Stage IV to V calcic soil horizons (Gile et al., 1996, "Morphological and Genetic Sequences of Carbonate Accumulation in Desert Soils;" Machette, 1985, *Calcic soils of the southwestern United States*; RPP-7123) indicate that the land surface remained relatively stable and unchanging with little or no sedimentation for as much as 1 to 2 million years during the development of the CCuc subunit. Toward the end of the Cold Creek period, however, a sudden influx of fine-grained, mostly windblown, loess-like sediment (CCuz) that quickly buried the calcic soil horizons of the CCuc subunit. This is indicated by the sharp boundary (Figure 2-9) and the lack of any well-developed soil horizons within the CCuz. This may be associated with climate change accompanying the onset of the early Ice Age (~2.6 million years ago) and/or perhaps a changing wind regime associated with the growing Cascade Mountains to the west. In conclusion, it appears that a change in the strength and/or direction of surface winds may have accompanied the change in climate (Sweeney et al., 2004, "Glacial anticyclone recorded in Palouse loess of northwestern United States") that marked the beginning of CCuz subunit, perhaps during the earliest Pleistocene Epoch.

Note: From 97.5-98.5 ft depth in Well 299-W10-.27 (~50 m northwest of the 216-T-26 Crib).

Figure 2-9. Distinct Contact between the Brown Silt-Dominated (CCuz) and White Calcrete (CCuc) of the CCu

The CCu in the 200 West Area is important, hydrologically, because of its very fine-grained texture and carbonate cementation can have a significant impact on contaminant movement in the vadose zone. Perched water zones above the CCu have been encountered in many wells in the 200 West Area; however, no perching is known to have occurred beneath the S Complex Area.

2.4.3.1 Cold Creek Silt-Dominated Subunit

The lithologic contact between the CCuz and the overlying Hanford formation Hf2 is very distinct beneath the S Complex Area (Figure 2-8). It is also easily distinguishable based on borehole geophysical total-gamma and/or the more recent spectral-gamma logs. Particularly useful in the delineation of stratigraphic boundaries and correlations are logs of naturally occurring K-40, U-238, and Th-232 (also known as the potassium-40-natural uranium-natural thorium (KUT) set of geophysical logs [see Figure 2-14]). The lithologic boundary between the Hf2 and CCuz is especially apparent because of a consistently sharp increase in total gamma activity that is based on elevated activity associated with

natural radioisotopes, particularly K-40 and, to lesser degree, Th-232 and U-238. The changes in the amount of KUT activity are assumed to be caused by differences in grain size, mineralogy, and/or degree of pedogenesis within these and other deposits. More study is needed to decipher the exact causes of these geophysical signatures. An increase in moisture also typically occurs in the CCuz, apparent in neutron-moisture logs where available, caused by the higher moisture-retention capacity of the silt-dominated interval.

The CCuz ranges from about 6 to 14 m (20 to 46 ft) thick (Figure 2-10) and dips slightly to the southwest beneath the S-SX Complex (Figure 2-11). The unconsolidated, silt-rich sediments of the silt-dominated CCuz consist of cohesive, compacted, massive-to-laminated and stratified, fine-grained sand and silt (Figure 2-12). This brown- to yellow-colored unit is also characterized as micaceous, very well sorted, and moderately to strongly calcareous, with relatively high natural background-gamma (e.g., KUT) activity (DOE/RL-2002-39). It is equivalent to the "early Palouse soil" (HW-67549; RHO-ST-23; RHO-BWI-ST-14; SD-BWI-DP-039; PNL-7336, *Geohydrology of the 218-W-5 Burial Ground*; DOE/RW-0164; PNL-6820; WHC-SD-EN-TI-008), and the "Hanford Formation/Plio-Pleistocene deposits" described in RPP-7123, and most recently identified as the CCUf (laminated-massive) facies of the CCu in DOE/RL-2002-39.

2.4.3.2 Cold Creek Calcic Geosol Subunit

The lithologic contact between the CCuc and the overlying CCuz subunits is also very distinct beneath the S Complex Area (Figure 2-9). The contact is distinguishable on borehole geophysical logs based on sharp decreases in total-gamma (i.e., KUT) activity. This is likely related to a long period of leaching, translocation, and pedogenic eluviation associated with soil development atop the Cold Creek geosol (Retallack, 2001). Diagnostic features of the CCuc include advanced induration with pedogenic calcium carbonate, local increases in grain-size (up to gravel) with variable sorting, white color, and the presence of pedogenic structures (e.g., root traces, animal burrows, and soil horizonation).

A corresponding decrease in the borehole geophysical log total gamma (KUT) response at the upper boundary, and reduced moisture in the neutron-moisture logs also characterize this interval (DOE/RW-0164; PNL-7336; PNNL-13858, *Revised Hydrogeology for the Suprabasalt Aquifer System, 200 West Area and Vicinity, Hanford Site, Washington*; DOE/RL-2002-39). The upper boundary of the CCuc subunit is normally sharp and distinct in contrast to the lower boundary, which is commonly gradational as to be expected for a buried paleosol sequence. The overlying CCuz is easily distinguished from the CCuc based on the sharp contrast in color, grain size, and degree of cementation (Figure 2-9), as well as a sudden change in geophysical logs (concomitant decrease in total gamma, K-40, and Th-232 activity). Furthermore, while the upper CCuz is generally compacted and cohesive, it is uncemented, unlike the underlying pedogenically altered CCuc. Even though the upper CCuz may contain moderate to high concentrations of calcium carbonate, the carbonate appears to be evenly disseminated as detrital grains. The bulk of the detrital calcium carbonate in the CCuz is likely derived from the disintegration and mechanical reworking/redeposition of the underlying CCuc. The top of the CCuc is well defined as the top of the first pedogenically altered, carbonate-rich, cemented zone, accompanied by a sudden drop in total-gamma activity.

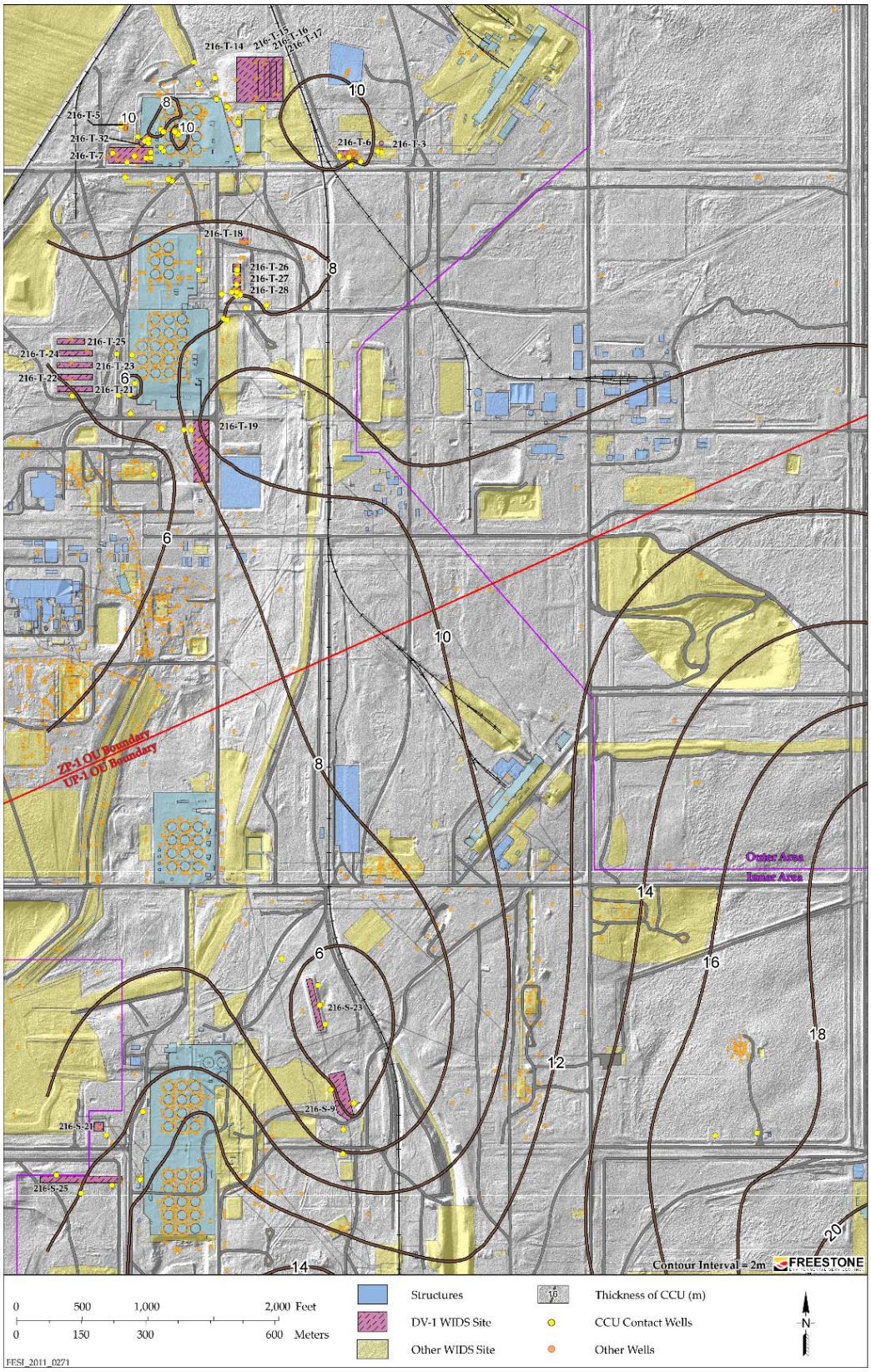

Figure 2-10. Thickness (Isopach) Map of the CCuz Subunit near the S Complex Area

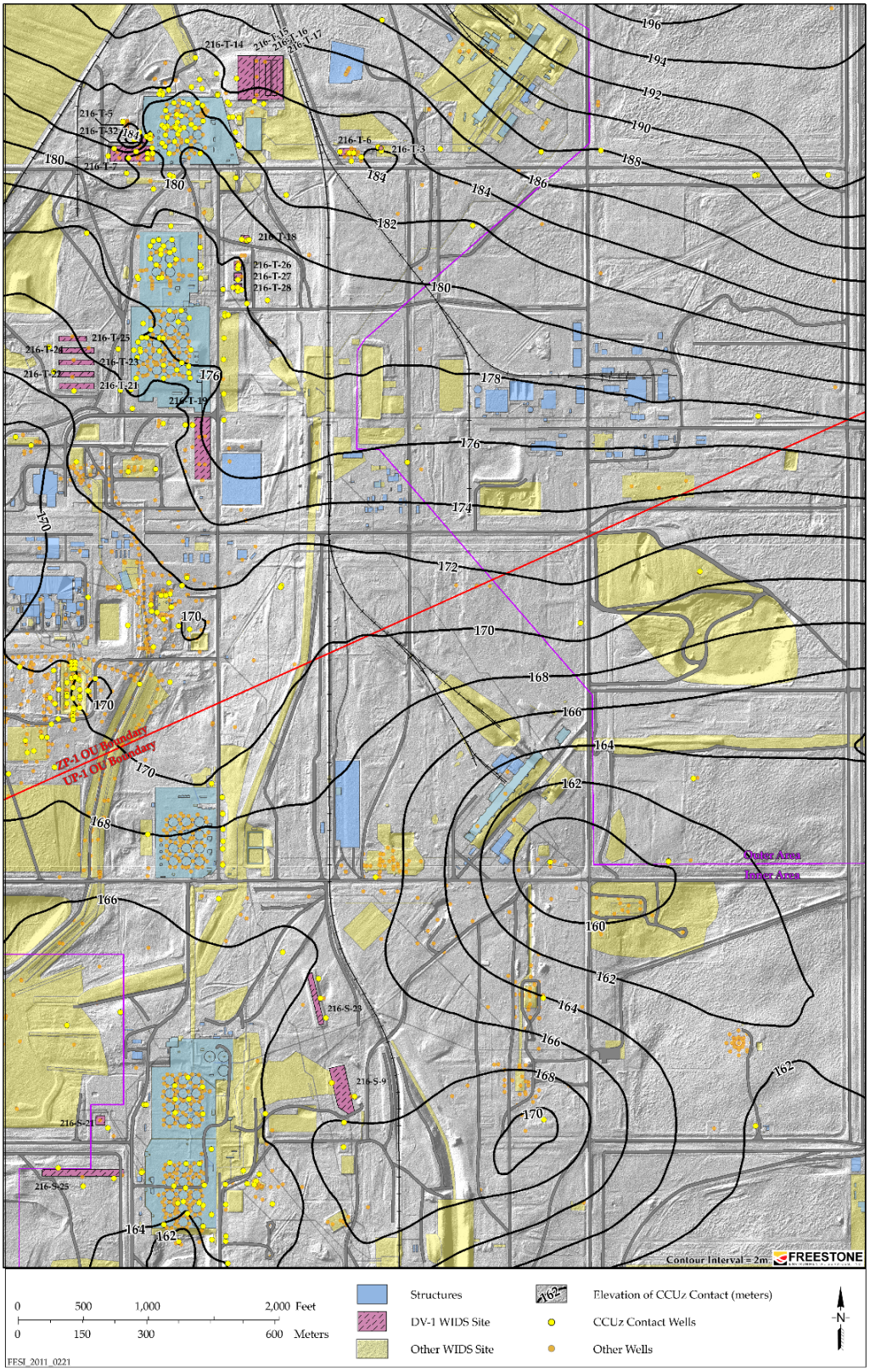

Figure 2-11. Structure-Contour Map Showing Relief Atop the CCuz Subunit Near the S Complex Area

Note: Borehole C4104, 87 ft bgs. Described as moist, well-laminated, compacted, well-sorted olive-brown silt to fine sandy silt, and strongly calcareous. Since the original sedimentary structure is preserved, the high concentration of $CaCO_3$ appears to be the result of erosion and fluvial reworking of the underlying CCuc calcic paleosol and not from in situ soil development, which would have destroyed the structure. Top of the core is to the left.

Figure 2-12. Laminated Silt and Fine Sand of the CCuz Subunit

The CCuc represents a highly weathered paleosurface that is partially developed on top of the Ringold Formation (HW-61780; HW-67549) within the central Pasco Basin following incision of the Ringold Formation. Other names used to describe the CCuc have included "caliche" (HW-61780) and "calcrete" (DOE/RW-0164). The CCuc consists of basaltic to quartzitic gravels, sands, silt, and clay that are cemented with one or more layers of secondary, pedogenic calcium carbonate (Figure 2-13). Soil development associated with the CCuc is frequently overprinted onto the underlying Ringold Formation. The concentration of calcium carbonate within the CCuc is generally 20 to 30 wt%, but ranges anywhere from 5 to 70 wt%. The overall thickness of the CCuc beneath the S Complex Area is generally 1 to 5 m (3 to 14 ft) and dips to the southeast.

Considerable variability may exist within the CCuc because of the natural heterogeneity inherent in soils and soil-forming processes that vary under different physical, chemical, and biological conditions (e.g., moisture, grain size, structural aspect, mineralogy, bioturbation, and microbial activity). An additional complicating factor is that the land surface during late Pliocene time was locally undergoing changes via fluvial and eolian activity, which resulted in variable rates of aggradation, degradation, and soil development (SD-BWI-DP-039; PNL-7336; DOE/RW-0164; Slate, 1996, "Buried Carbonate Paleosols Developed in Pliocene-Pleistocene Deposits of the Pasco Basin, South-Central Washington;" BHI-01203; RPP-7123). The calcium carbonate overprint is superimposed onto a variety of rock types, including silt, quartz-feldspar-rich sand and gravel, and locally derived basaltic sand and gravel (Slate, 1996; BHI-01203; RPP-8531).

Note: Secondary, $CaCO_3$ cement binds a poorly sorted mixture of clay and silt particles along with grains of dark basaltic sand. From Borehole C4105, 103 ft depth, located ~25 m northeast of the 216-T-32 Crib.

Figure 2-13. Cemented Calcic Paleosol (CCuc) Facies of the CCu

2.4.4 Ringold Formation

The Ringold Formation records fluvial-lacustrine deposition associated with the ancestral Columbia River drainage system, following the last emplacement of basalt in the central Hanford Site about 10.5 million years ago (RHO-BWI-ST-14; DOE/RW-0164; WHC-SD-EN-TI-290, *Geologic Setting of the Low-Level Burial Grounds*; BHI-00184). Deformation of the Yakima folds, which began in the middle Miocene Epoch, concurrent with the Columbia River basalt volcanism, continued into Ringold time. As a result, the centers of down-warped basins received more sediments than the margins. The Ringold Formation is up to 185 m (600 ft) thick in the center of the basin and pinches out against the basin-bounding basalt ridges.

The Ringold Formation consists of semi-indurated clay, silt, fine- to coarse-grained sand, and variably cemented granule to cobble gravel. Ringold Formation sediments have been classified into five sediment facies associations: fluvial gravel, fluvial sand, overbank deposits, lacustrine deposits, and alluvial fan deposits. More-detailed descriptions of these facies are presented in BHI-00184; Lindsey, 1996; and RPP-8531.

Sediments associated with the Ringold Formation filled the basin to at least 274 m (900 ft) elevation (Lindsey, 1996) during the late Miocene to Pliocene period (10.5 to 3.4 million years ago). Since then, however, the Ringold Formation has been significantly eroded by fluvial down-cutting of the ancestral Columbia River and cataclysmic Ice Age flooding. The fluvial-lacustrine Ringold Formation, which overlies basalt over most of the central Pasco Basin, is present as several subunits: the Ringold Formation member of Taylor Flat (RFtf), the Ringold Formation member of Wooded Island-unit e (RFwie), the Ringold Formation member of Wooded Island-lower mud unit (RFlm), and the Ringold Formation member of Wooded Island-unit a (RFwia).

The Ringold Formation makes up the lower half of the vadose zone within the S Complex Area (Figure 2-3). Typically, only the RFtf and the uppermost portion of the RFwie are present in the vadose

zone beneath the S Complex Area; the suprabasalt aquifer in the 200 West Area comprises the lower RFwie, RFlm, and RFwia units.

In the 200 West Area, erosional remnants of the RFtf consist of fine-grained fluvial sand and overbank facies with localized stringers of calcium carbonate. The RFtf is discontinuous and only locally present beneath the 200 West Area[5] (Figure 2-2).

RFwie, on the other hand, completely underlies the 200 West Area and the S Complex Area. It is the thickest of the Ringold Formation units present in the Central Plateau and the 200 West Area and contains the unconfined aquifer beneath the region. It consists of well-rounded gravel in a sand and silt matrix deposited by the ancestral Columbia River. Gravel lithologies are varied with sources outside the Columbia Basin, predominantly quartzite, granite, and gneiss as well as indigenous basalt. Consolidation varies from well to poorly indurated. The thickness of the RFwie is largely influenced by structural (i.e., Cold Creek syncline) and differential erosion (i.e., Cold Creek and Missoula floods) processes.

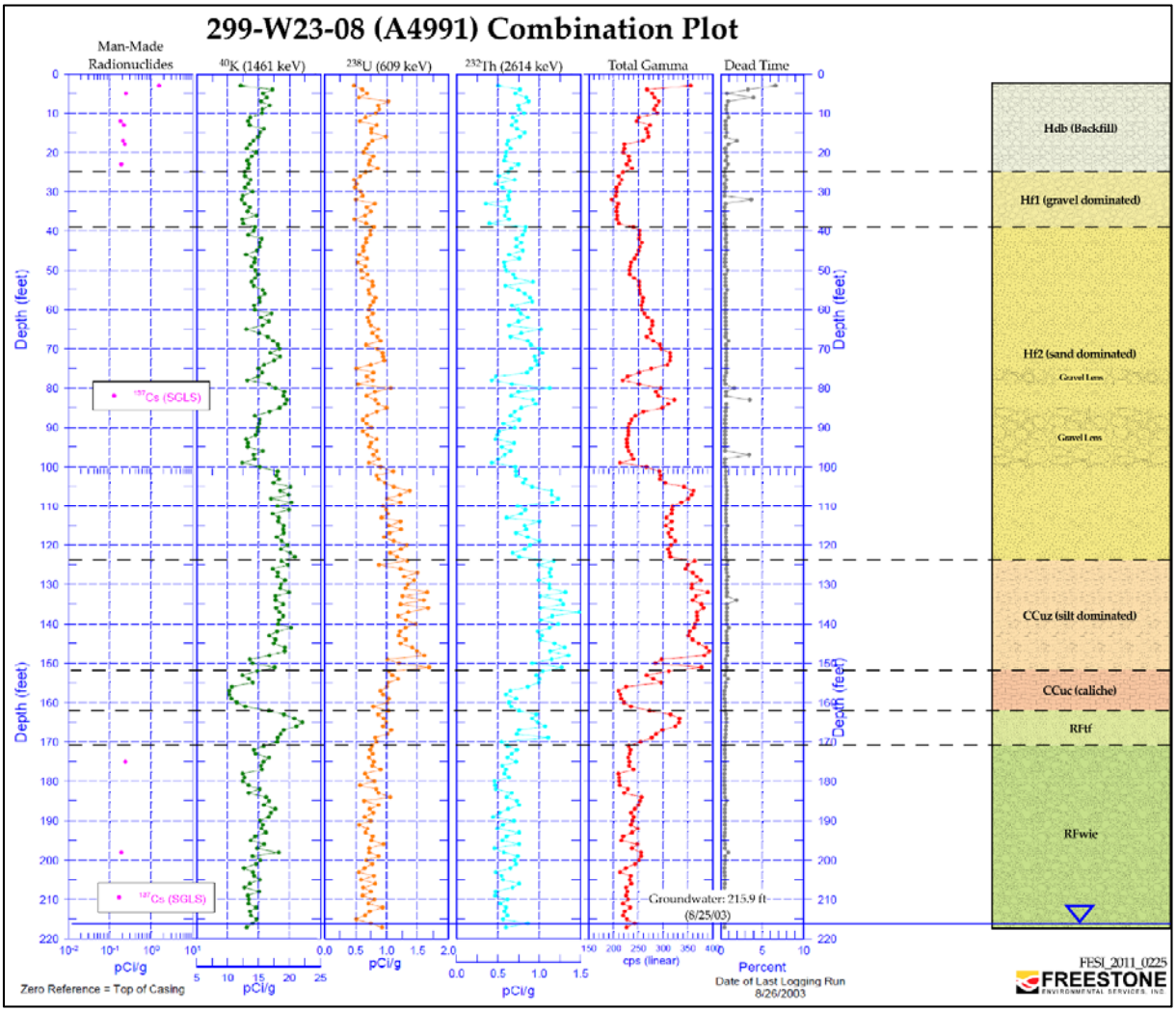

Figure 2-14. Example Geophysical Log, Well 299-W23-08

[5] Complete reference citations provided in Chapter 9.

2.4.4.1 Ringold Formation Member of Taylor Flat (RF_{tf})

Where present, the upper contact of the RFtf is gradational with the overlying CCu calcic geosol (CCuc). This is because Cold Creek paleosols partially developed and were superimposed onto the eroded Ringold surface. The effects of the Cold Creek geosol soil-forming processes gradually diminished with depth below the former ground surface once immediately underlain by the Ringold Formation. Thus, the boundary between these two overlapping units is not always clear cut.

The Rftf consists of interstratified, well-bedded fine-to-coarse sand to silt (Figure 2-15) belonging to a mixture of fluvial-sand and overbank facies associations. Post-Ringold Formation erosion locally stripped away most of this member from the central Pasco Basin, but in a few places, such as the S Complex Area, thin 1 to 9 m [4 to 28 ft]) erosional remnants of this unit remain (RPP-7123).

Figure 2-15. Laminated, Fine-Grained Sand and Silt of the Ringold Member of Taylor Flat (from borehole C4105, 116 ft bgs Within T Tank Farm, ~25 m northeast of the 216-T-32 Crib)

Weathering and soil development associated with the overlying CCu are often overprinted onto the RFtf. Because the degree of post-Ringold Formation pedogenesis decreases with depth, the contact with the overlying CCu is gradational and generally defined by an upward decrease in natural-gamma (KUT) on geophysical logs (see Figure 2-14), an increase in calcium-carbonate ($CaCO_3$) content, and/or a decrease in silt/clay content (higher concentration of $CaCO_3$ cement).

2.4.4.2 Ringold Formation Member of Wooded Island—Unit E

The lithologic boundary between RFwie and the overlying RFtf is generally sharp and distinct and usually accompanied by a sudden decrease in borehole geophysical log total-gamma (KUT) activity below the RFtf-RFwie contact (see Figure 2-14). Where the overlying RFtf is missing, there may actually be a slight increase in total gamma (KUT) activity, where the CCuc subunit directly overlies the RFwie unit. The RFwie typically contains a higher percentage of felsic minerals and clay (i.e., higher concentration of naturally occurring K-40).

The RFwie consists predominantly of a thick sequence of fluvial conglomerate with occasional thin beds and lenses of mud and sand. RFwie generally consists of a bimodal, clast-supported, pebble-cobble gravel

within a moderately to well-sorted sandy matrix (see "F" in Figure 2-4). Most gravel clasts are very well rounded and frequently polished—typical of fluvial deposits. The surfaces of sand and gravel clasts are often stained in oxidized shades of red, orange, and yellow, giving the unit an overall brown appearance. The most common clasts are composed of basalt, quartzite, porphyritic volcanics, and greenstone. Silicic plutonic rocks, gneisses, and volcanic breccias also are found. Sand is quartzo-feldspathic, with the basalt content usually ranging between 5 and 25 percent. More easily weathered clasts, like basalt, often show weathering rinds generally ≤1 cm (0.4 in.) thick. Weathering rinds and clay skins that surround gravel clasts attest to the greater age (at least several million years) and longer period of exposure of the Ringold Formation to interactions with groundwater. The RFwie is weakly to moderately indurated because of long-term compaction and local cementation. Low-angle to planar stratified, massive bedded, and large-scale cross-bedded facies are found in outcrops. The top of the unit dips very gently to the southwest (SGW-50900), consistent with the top of the basalt and underlying Ringold Formation units. The water table lies within the RFwie beneath the 200 West Area (Figure 2-3).

2.4.5 Columbia River Basalt Group

The Columbia River Basalt Group (CRBG) is divided into three formations that underlie this region: the Grande Ronde Basalt, the Wanapum Basalt, and the Saddle Mountains Basalt. About 300 separate CRBG flows have been identified on the Columbia Plateau (DOE/RW-0164).

The Elephant Mountain Member forms the youngest basalt flows near the S-SX Complex. Dated at about 10.5 million years (DOE/RW-0164), it forms the base of the suprabasalt aquifer about 150 m (500 ft) below ground surface (bgs) and is composed of a medium to fine-grained tholeiitic basalt with abundant microphenocrysts of plagioclase (DOE/RW-0164). The Elephant Mountain member is about 30 m (100 ft) thick beneath the S Complex Area.

2.5 Structure

Basalt flows and sediments of the Pasco Basin have been folded and faulted, creating broad structural and topographic basins separated by asymmetric anticlinal ridges. These structures are part of the Yakima Fold Belt structural subprovince, which formed from north-south regional compression of the crust that began in the Miocene Epoch (DOE/RW-0164). The northern limbs of these anticlines generally dip steeply to the north, are vertical, or even overturned; thrust or high-angle reverse faults with fault planes that generally parallel fold axial trends occurring on the north sides of these anticlines. The southern limbs of Yakima folds dip gently to the south. The anticlinal ridges are separated by broad synclines or basins that, in many cases, contain thick accumulations of Neogene- to Quaternary-Period sediments.

The S Complex Area within the 200 West Area lies along the north limb of the Cold Creek syncline, about 5 km (1.5 mi) northeast of the synclinal axis (DOE/RW-0164). The second-order Gable Mountain and Gable Butte segments of the first-order Umtanum Ridge-Gable Mountain anticline lies to the north of the study area (PNNL-19702, *Hydrogeologic Model for the Gable Gap Area, Hanford Site* [Figure 5.1]). The bedrock surface (i.e., top of basalt) beneath the S Complex Area dips gently (about 0.7°) to the southwest toward the axis of the Cold Creek syncline, with up to 150 m (500 ft) of sediments overlying the basalt (RPP-7123).

It appears that most bedding surfaces within the post-basalt sediments generally dip to the south beneath the S Complex Area. The dip on the older Ringold Formation units is likely from tectonic deformation associated with the downwarping Cold Creek syncline (DOE/RW-0164). The southerly dip on the younger CCu may be from topographic relief that developed along the north side of the ancestral Cold Creek valley after incision into the Ringold Formation, but before the Ice Age flooding and accumulation of the Hanford formation. Southerly dips on strata within the Hanford formation, on the other hand, are probably strictly

associated with the depositional surface that existed along the south flank of Cold Creek flood bar as it grew and prograded south and east during subsequent Ice Age floods (see PNNL-19702 [Figure 8.1]).

2.5.1 Clastic Dikes

Clastic dikes are vertical to subvertical sedimentary structures that crosscut normal sedimentary layering (BHI-01103, *Clastic Injection Dikes of the Pasco Basin and Vicinity*). In outcrop, regular clastic dikes are common in the sand-dominated Hanford formation facies, but relatively rare in the gravel-dominated facies.

Where clastic dikes intersect the ground surface and are not covered with younger deposits, a feature known as "patterned ground" can be observed. Well-developed "patterned ground" is found just south of the 200 West Area (Bjornstad, 2006). Within the 200 West Area and the S Complex Area, however, visible patterned ground is rare because of the many manmade surface disturbances and/or because it is buried under a thin cover of recent eolian sand. Clastic dikes are likely a common geologic feature of the Hanford formation in the 200 Areas, especially in the sand- and interbedded sand- and silt-dominated facies (the frequency and distribution of dikes are not known because they are covered over at the surface; vertical boreholes do not intersect many of the vertical dikes). This would include Hf2 near the S-SX Complex Area.

Clastic dikes occur in swarms and form four types of networks: regular-shaped polygonal-patterns, irregular-shaped, polygonal-patterns, pre-existing fissure fillings, and random occurrences (BHI-01103). Regular polygonal networks resemble 4- to 8-sided polygons and typically range from 3 cm (1.2 in.) to 1 m (3.3 ft) in width, from 2 m (6.6 ft) to greater than 20 m (65.6 ft) in depth, and from 1.5 to 100 m (4.9 to 328.1 ft) along the strike. Smaller dikelets, sills, and small-scale faults and shears are commonly associated with master dikes that form the polygons.

In general, clastic dikes consist of multiple, alternating vertical to subvertical layers (dikelets) of sand, silt, and clay that cut through horizontally layered sediments. Individual dikelets display an outer skin of silt clay with coarser, more permeable infilling material. Silt clay linings are commonly 0.03 to 1.0 mm (0.001 to 0.04 in.) thick, but linings up to about 10 mm are known. The width of individual infilling layers ranges from as little as 0.01 mm (0.0004 in.) to more than 30 cm (11.8 in.), and their length can range from about 0.2 m (0.7 ft) to more than 20 m (65.6 ft).

The exact mechanism for the formation of clastic dikes is debatable. Some evidence suggests the dikes developed from upward hydraulic injection associated with the rapid dewatering (and subsequent unweighting of sediment) after one or more Ice Age flood events. Other evidence suggests that at least some dikes infilled from above. In either case, they have the potential to act as vertical conduits that could transfer contaminants more rapidly from waste sites downward into the deep vadose zone.

Clastic dikes are occasionally observed in drill core. One example of a clastic dike was revealed in borehole C4104 within the Ringold Formation (see Section 2.4 in SGW-49924, *Preliminary Conceptual Models for the 200-DV-1 Operable Unit Waste Sites in the T Complex Area*) near the T Complex. Two other clastic dikes near the T Complex Area were intersected in characterization Borehole 299-W10-27, located northwest of T-26 Crib (see Section 2.4 in SGW-49924). The paucity of observed clastic dikes in boreholes, however, is not surprising considering that most Hanford Site boreholes, like the dikes, are oriented vertically.

2.6 Site-Specific Hydrogeologic Data for the S Complex Area

Principal hydrogeologic data sources used to interpret and develop the 200-DV-1 OU CSMs include driller's and geologist's logs and borehole geophysical logs for hundreds of wells drilled near the S Complex Area. In addition, core photographs and penetration resistance (hammer blow counts) also

provide useful information on the hydrogeologic characteristics of the sediments. Within the S Complex Area, the borehole geophysical log database provided the most abundant and useful source for defining and correlating subsurface geology and defining the extent of the gamma contamination. A limited number of detailed geologic borehole and core logs were used to supplement and verify interpretations based on the borehole geophysical logs.

Borehole geophysical logs were used extensively within the S Complex Area to evaluate the subsurface distribution and migration of manmade gamma-emitting radionuclides (i.e., radioactive contaminants) over time (ARH-2874, *241-T-106 Tank Leak Investigation*; RHO-ST-1, *Status of Liquid Waste Leaked from the 241-T-106 Tank*; GJO-99-101-TAR, GJO-HAN-27; GJO-97-30-TAR, GJO-HAN-16; Sobczyk, 2001, *Subsurface Interpretation of the T Tank Farm, Hanford Site, Washington, Based on Gamma-Ray Logging*). More recently, geoscientists have used naturally occurring gamma results (i.e., KUT logs) obtained from improved geophysical logging tools to differentiate stratigraphy and aid lithologic correlation. Within the tank farms, high-level radiological contamination masks and often overwhelms lower natural gamma activity, so spectral-gamma (KUT) logs from nearby and surrounding boreholes are used for interpreting lithology, defining stratigraphic contacts, and aiding in correlation into highly contaminated areas. One limitation of the Hanford Site geophysical logging program is that data collection is typically at half-foot intervals; this reduces the ability to resolve strata less than 0.6 m (2 ft) thick (Sobczyk, 2001). This can make it difficult to define thin beds, particularly low-permeability, fine-grained layers, such as those that commonly cap sand sequences within the Hf2 (e.g., see Figure 2-7). Defining these thin fine-grained lenses is important because they have been shown to result in the significant lateral spreading of moisture and contaminants. At present, the only way to identify the frequency and distribution of these thin, fine-grained layers positively is via continuous coring.

Generally, where no radiological contamination occurs, the total gamma count rate (from higher concentrations of natural gamma emitters associated with silts and clays) increases in finer grained sediments with a corresponding increase in moisture content caused by the moisture-retaining properties of these sediments. The neutron-moisture log is generally used to depict the relative moisture content within a 20 to 30 cm (8 to 12 in.) radius around the borehole. Neutron-moisture logs can also reveal anomalous or highly saturated sediments above and/or within fine-grained intervals (perching horizons) or along sharp sediment interface boundaries (e.g., contact).

In most cases, the lithostratigraphic contacts picked from driller's and geologist's logs generally correlate with contacts interpreted on the borehole geophysical logs. However, the borehole geophysical logs provide more precise contact boundaries compared to drilling logs (which are typically based on a much greater sampling interval). Occasional cases with disagreement are explained by the recording of inaccurate drill depths in the field, variation in drilling methodology (i.e., cable tool versus air-rotary drilling), or the presence of gradational contacts resulting in indistinct boundaries between units. Here, the choosing of the contact is more subjective and open to individual interpretation. It is typically shown as a dashed contact line on cross sections in this report.

To develop the subregion specific conceptual geohydrologic models presented in Chapter 3 of this report, all available data from select boreholes included in the study (i.e., within 100 m [328 ft] of each of the 200-DV-1 OU waste site) were compiled and summarized onto borehole-type log summary sheets (SGW-50900).

The next step in building a hydrogeologic model of the subsurface was to construct scaled cross sections linking boreholes together using correlated contact boundaries to differentiate and identify hydraulically significant hydrogeologic units. These cross sections are included in the site-specific development of the hydrogeologic model for each subregion in Chapter 3 and in SGW-50900.

2.7 Water Levels and Flow Directions Beneath the S Complex Area

This subsection describes the aquifer properties beneath the S Complex Area and adjacent parts of the southern 200 West Area including aquifer thickness, and current flow directions and flow rates. The subsection also describes historical changes in the aquifer properties caused by past fuel processing operations and waste management. Changes in the aquifer properties during the past 60 years have significant implications for direction and rate of contaminant movement in the aquifer and for residual vadose zone contamination where the water table has decreased elevation. Most of the information was taken from RPP-23748, *Geology, Hydrogeology, Geochemistry, and Mineralogy Data Package for the Single-Shell Tank Waste Management Areas at the Hanford Site*, and PNNL-15837, *Data Package for Past and Current Groundwater Flow and Contamination Beneath Single-Shell Tank Waste Management Areas*, and updated using the latest groundwater sampling results.

Figure 2-16 shows the entire S Complex Area. Figures 2-17 and 2-18 show the locations of most of the wells discussed in this subsection. The locations of wells not shown in the figures are described in the text.

2.7.1 Current Water Levels and Flow Direction Beneath the S Complex Area and Vicinity

The base of the unconfined aquifer beneath the southern part of the 200 West Area and the S Complex Area is the top of the Ringold Formation lower mud unit (RFlm), known as hydrogeologic unit 8 in PNL-8971, *Three-Dimensional Conceptual Model for the Hanford Site Unconfined Aquifer System, FY 1993 Status Report*. The RFlm forms a confining layer that separates the suprabasalt aquifer into the uppermost unconfined aquifer and the underlying confined aquifer in the Ringold Formation (PNNL-13858). Thus, the unconfined aquifer in the area of interest extends from the water table down to the RFlm (hydrogeologic unit 8) and consists of variably cemented and compacted coarse sands and gravels of the RFwie, which is hydrogeologic unit 5 in PNL-8971.

Two wells extend to the bottom of the unconfined aquifer in the S Complex Area and can be used to estimate the thickness of the aquifer in this area. Table 2-2 lists the wells that penetrate the entire thickness of the unconfined aquifer, March 2010 water levels from those wells, and the calculated aquifer thickness. The data in the table show that the uppermost aquifer beneath the S Complex Area ranges from about 65 to 70 m (213 to 230 ft) thick. PNNL-13858 used similar data to make an isopach map of the aquifer thickness in the 200 West Area.

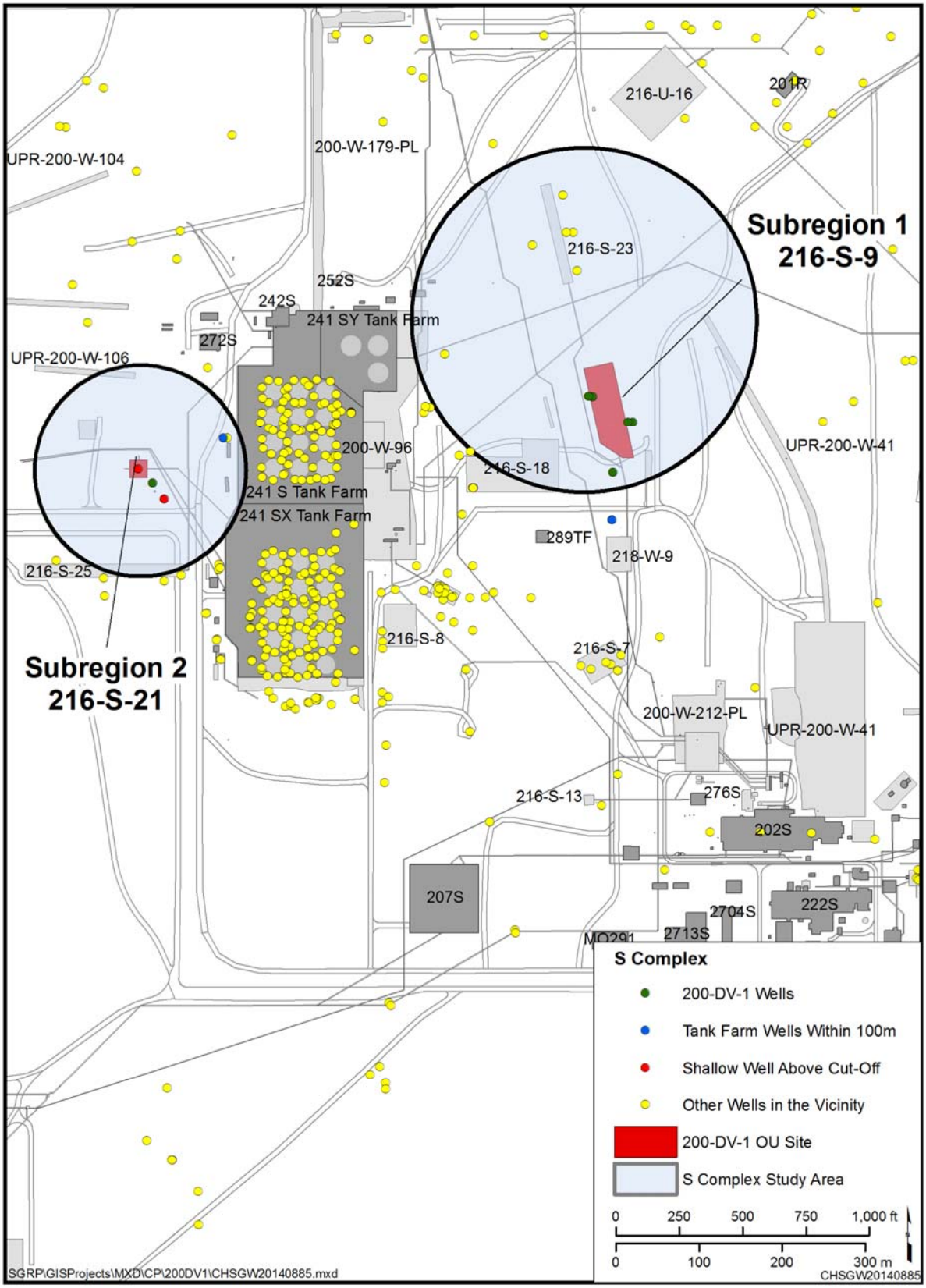

Figure 2-16. General Map of Liquid Disposal Facilities and Infrastructure in the S Complex Area

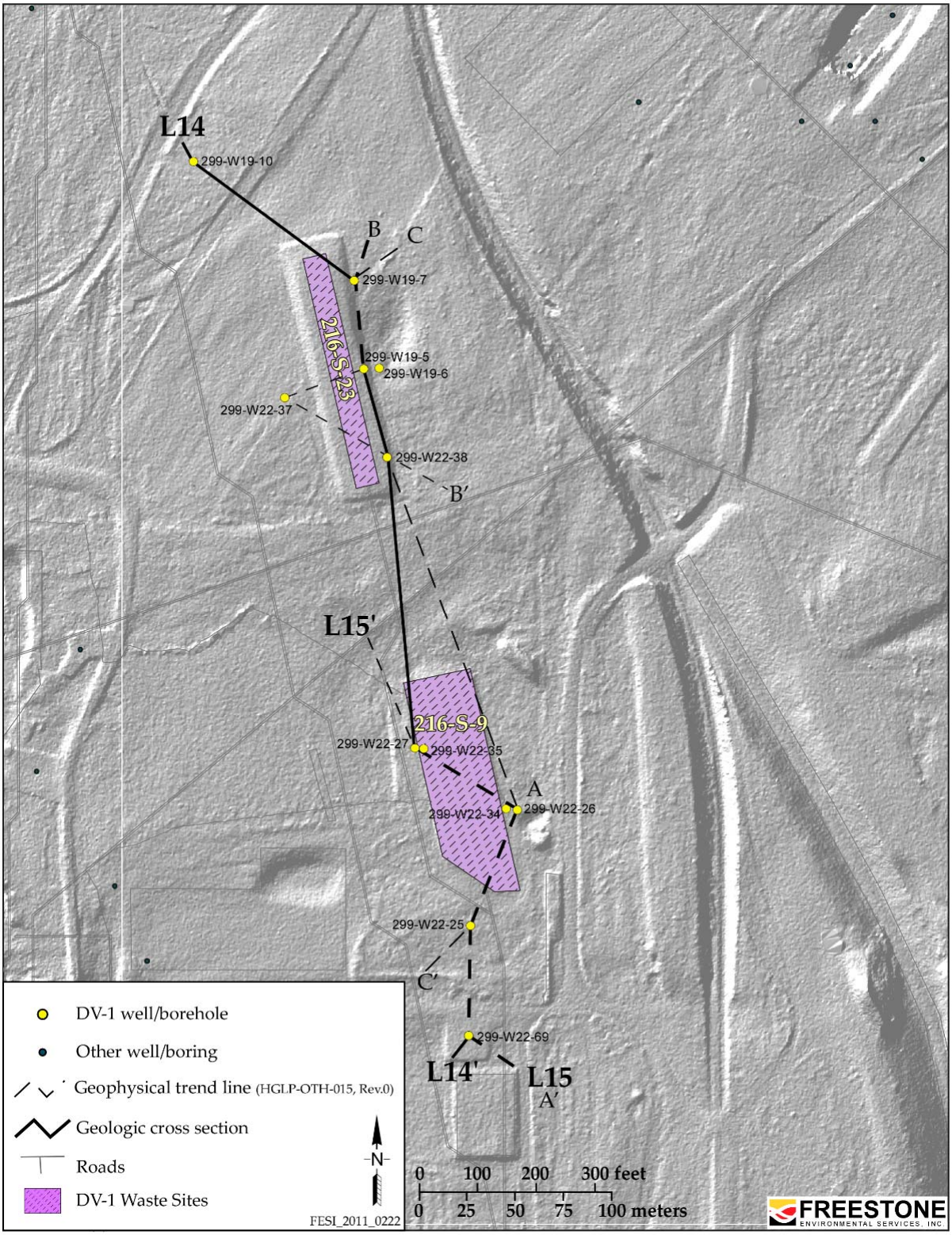

Figure 2-17. Subregion 1 - Location Map for Facilities and Wells near the 216-S-9 and 216-S-23 Cribs, S Complex Area

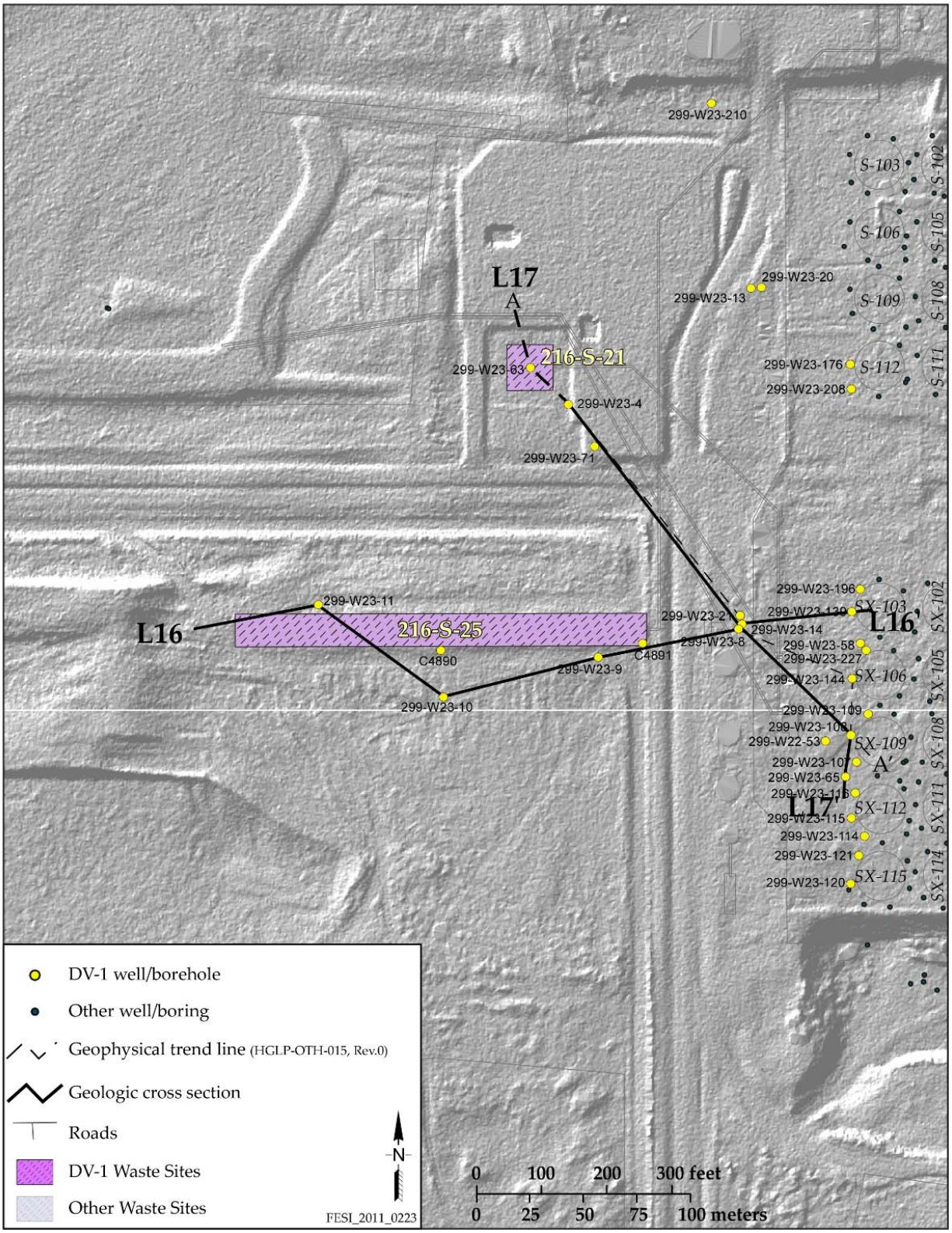

Source: DOE/RL-2010-11, *Hanford Site Groundwater Monitoring and Performance Report for 2009 Volumes 1 & 2*.

Figure 2-18. Subregion 2 - Location Map for Facilities and Wells near the 216-S-21 and 216-S-25 Cribs, S Complex Area

Table 2-2. Thickness of the Unconfined Aquifer Beneath the S Complex Area

Well Name	Well Location	Elevation of Aquifer Bottom[a] (m amsl)	Elevation of Water Table[b] (m amsl)	Aquifer Thickness (m)
299-W22-50	At the southeast corner of WMA S-SX	64.3	134.66	70.4
299-W19-10	~ 300 m north of the 216-S-9 Crib	68.6	134.1[c]	65.5

a. PNNL-13858, *Revised Hydrogeology for the Suprabasalt Aquifer System, 200-West Area and Vicinity, Hanford Site, Washington*.

b. March 2010 data except where noted

c. Well is dry, measured at Well 299-W22-26 also located at the 216-S-9 Crib

amsl = above mean sea level

WMA = Waste Management Area

Figure 2-19 is the general water table map for the southern part of the 200 West Area (DOE/RL-2010-11, *Hanford Site Groundwater Monitoring and Performance Report for 2009 Volumes 1 & 2*) and shows that the general flow direction is toward the east beneath S Complex Area, although the flow direction takes on a slight southern component beneath 216-S-23 and 216-S-9 subregion where the flow direction is east-southeast. Current groundwater flow directions and flow rates specific to WMA S-SX are given in the 2009 annual groundwater report as east to east-southeast at 0.7 to 0.14 m/day based on inferred contaminant travel times, and as 0.012 to 0.3 m/day based on the Darcy equation (DOE/RL-2010-11).

Several trend-surface analyses, tracer dilution tests, tracer pumpback tests, constant rate pumping tests, and slug tests have been done at selected wells located within the S Complex Area during the past ten years to support RCRA assessments at WMA S-SX, (PNNL-13514, *Results of Detailed Hydrologic Characterization Tests – Fiscal Year 2000*; PNNL-14113, *Results of Detailed Hydrologic Characterization Tests – Fiscal Year 2001*; PNNL-14186, *Results of Detailed Hydrologic Characterization Tests – Fiscal Year 2002*; PNNL-17348, *Results of Detailed Hydrologic Characterization Tests—Fiscal and Calendar Year 2005*).

These tests have given values for hydraulic conductivity, transmissivity, specific yield, effective porosity, and groundwater flow rate and flow direction. The results of those analyses are summarized and tabulated in PNNL-15837.

Although some conditions in the aquifer may have changed during the past 10 years, the data obtained from the aquifer tests, along with data obtained from geologist's logs, geophysical logs, and development pumping data, all indicate heterogeneity in the aquifer properties within the screened intervals of individual wells and among wells in the S Complex Area. No widespread trends have been identified.

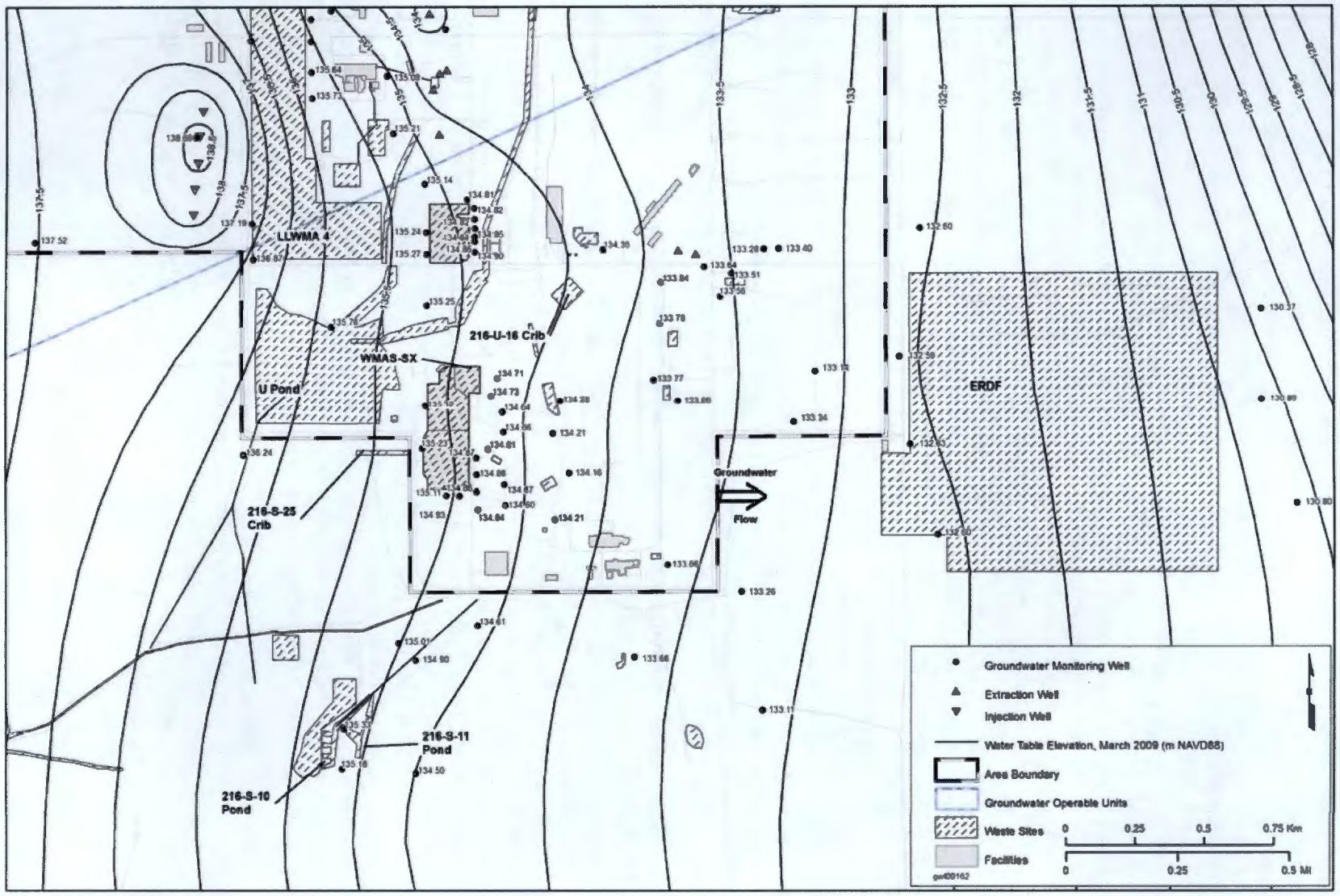

Source: DOE/RL-2010-11, *Hanford Site Groundwater Monitoring and Performance Report for 2009 Volumes 1 & 2.*

Figure 2-19. March 2009 Water Table Map for the South Part of 200 West Area and the S Complex Area

A significant feature of the tracer dilution test results was evidence for upward vertical hydraulic gradients within the upper portion of the aquifer in two of the wells tested in the S Complex Area. Vertical flow in Wells 299-W22-47, 299-W22-49, and 299-W22-80 was first noted by electromagnetic flowmeter surveys (QET-T-132, *Results of Field Tests with the Electromagnetic Borehole Flowmeter at the Pacific Northwest National Laboratory, Richland, WA*). The vertical flow in two of the wells (299-W22-49 and 299-W22-80) was confirmed by tracer tests (Well 299-W22-47 did not receive tracer tests). Vertical flow was identified in four additional wells by tracer-dilution studies and later (at two of the wells) by vertical tracer tests specifically designed to detect vertical flow within a borehole (PNNL-13514). More recently, vertical flow was measured in two wells in the S Complex Area with an electromagnetic borehole flowmeter (Newcomer, 2005, *Preliminary Electromagnetic Borehole Flowmeter Survey Results for Hydrologic Assessment Task Characterization Wells 299-W14-11, 299-W22-47, and 299-W22-80*). Data from all tests are summarized and tabulated in PNNL-15837.

The existence of vertical flow in a well does not necessarily reflect actual groundwater flow conditions within the surrounding aquifer, but its presence implies a vertical flow gradient and also has implications pertaining to the representativeness of groundwater samples collected from the wells and vertical contaminant distribution in the aquifer. For example, PNNL-14548, *Hanford Site Groundwater Monitoring for Fiscal Year 2004*, and PNNL-15670, *Hanford Site Groundwater Monitoring for Fiscal Year 2005*, attributed a small "island" of low contaminant concentrations at Well 299-W22-80 located within the larger contaminant plume south of WMA S-SX, to upward flow of relatively uncontaminated groundwater, from the bottom of the well into and diluting that portion of the plume. The reason for vertical flow is not known. In some areas, such as within the T Area Complex, vertical flow is downward in some wells and upward in others. Only upward vertical flow has been found in the S Complex Area. Whatever the mechanism for vertical flow, such flow may affect observed groundwater contaminant distribution patterns.

2.7.2 Historical Changes in Groundwater Flow Direction and Gradient Beneath S Complex Area and Vicinity

Water levels in the unconfined aquifer have risen as much as 26 m (85 ft) beneath the 200 West Area (PNNL-13282, *Groundwater Quality Assessment for Waste Management Area U: First Determination*) because of artificial recharge from liquid waste disposal operations active from the mid-1940s to 1995. The largest volumes of discharge were to the 216-T Pond (T Pond) system and the 216-U-10 Pond (U Pond). (See Figure 1-1 for T Pond and U Pond locations.) Figure 2-20 shows the liquid discharge history for the two ponds. The T Pond system is estimated to have received approximately 42.5 billion L (11.23 billion gal) of effluent and U Pond to have received about 162 billion L (42.8 billion gal) of effluent (see Figure 2-20 references). These large volumes poured into the ponds (with lesser volumes being discharged to cribs and ditches) artificially recharged the unconfined aquifer, creating large water table mounds. The increase in water table elevation was most rapid from 1949 to 1956 and was somewhat stabilized between the late 1960s and the late 1980s. Water levels began to drop in the late 1980s when wastewater discharges in the 200 West Area were reduced.

Figure 2-21 shows hydrographs for the wells in and around the S Complex Area. The hydrographs illustrate the changes in water table elevations that occurred beneath much of the S Complex Area since the early 1950s. All data used to make the hydrographs were obtained from the HydroDat database. HydroDat is a database of water level measurements maintained by the CH2M HILL Plateau Remediation Company and accessible through the EDA.

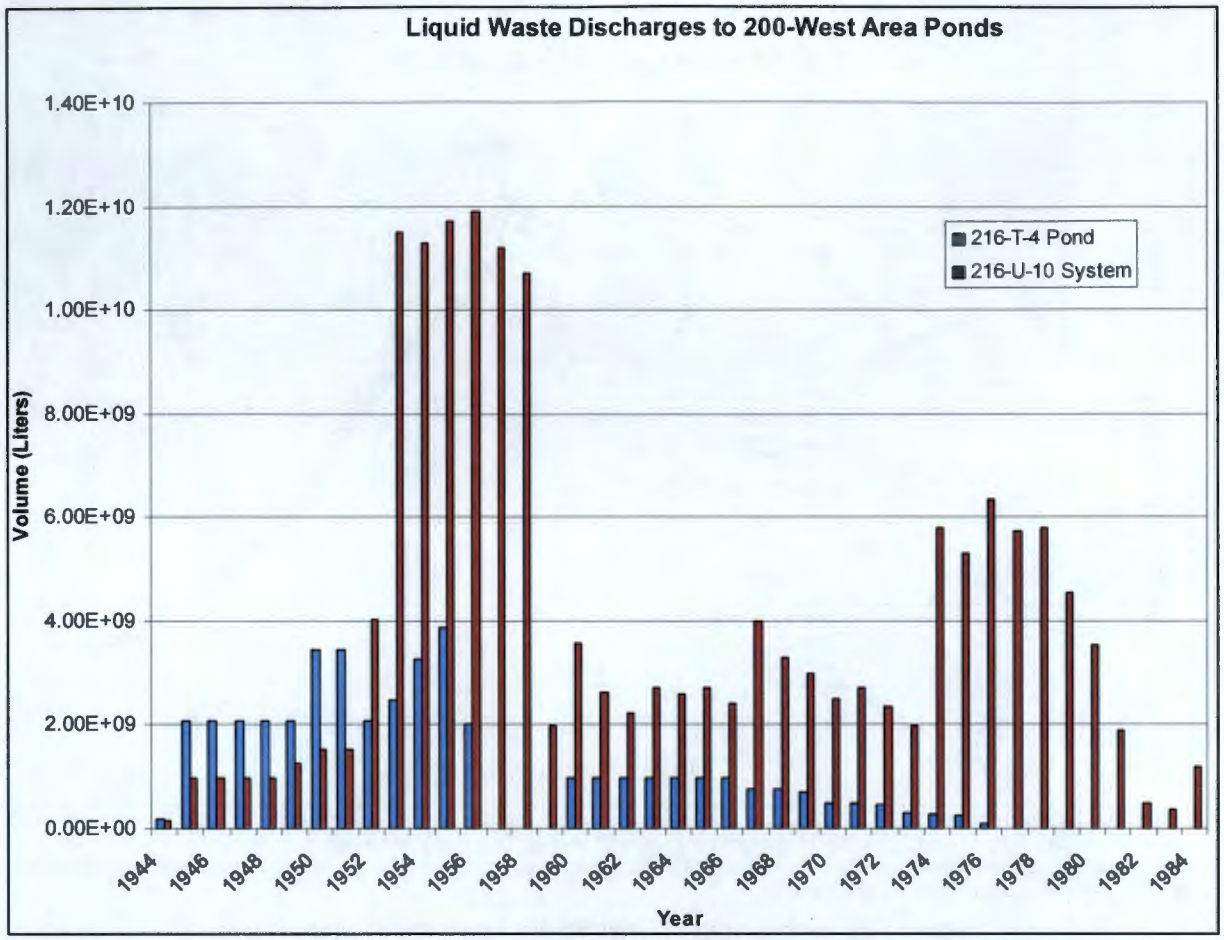

Note: Figure is from PNNL-15837; data are from ARH-CD-369-4Q, *Summary of Radioactive Solid Waste Burials in the 200 Areas During 1975*; Mirabellea, 1977; RHO-CD-27-3Q, *Summary of Radioactive Solid Waste Burials in the 200 Areas During 1977*; RHO-LD-78-24-4Q, 1979, *Summary of Radioactive Solid Waste Burials in the 200 Areas During 1978*; RHO-CD-79-34 4Q, *Radioactive Liquid Wastes Discharged to Ground in the 200 Areas During 1979*; RHO-HS-SR-81-3, *Radiactive Liquid Wastes Discharged to Ground in the 200 Areas During 1981*; RHO-HS-SR-82-3-4Q-LIQ-P, *Radioactive Liquid Wastes Discharged to Ground in the 200 Areas During 1982*; RHO-HS-SR-84-3-4Q-LIQ-P, *Radioactive Liquid Wastes Discharged to Ground in the 200 Areas During 1984*; RHO-HS-SR-85-3-4Q-LIQ-P, *Radioactive Liquid Wastes Discharged to Ground in the 200 Areas During 1985*; RHO-CD-80-34-4Q, *Radioactive Liquid Wastes Discharged to Ground in the 200 Areas During 1980*. Wells 299-W22-11 and 299-W22-17 are very near each other and can be considered a continuum in water level elevation time series. Wells 299-W22-11 and 299-W22-17 are located about 150 m (500 ft) east of WMA S-SX, near the 216-S-1,2 Cribs; Well 299-W23-1 is located inside the S Tank Farm; Well 299-W23-4 is located southeast of the 216-S-21 Crib; and Well 299-W23-15 is located just south of the SX Tank Farm.

Figure 2-20. Discharge History for T Pond and U Pond

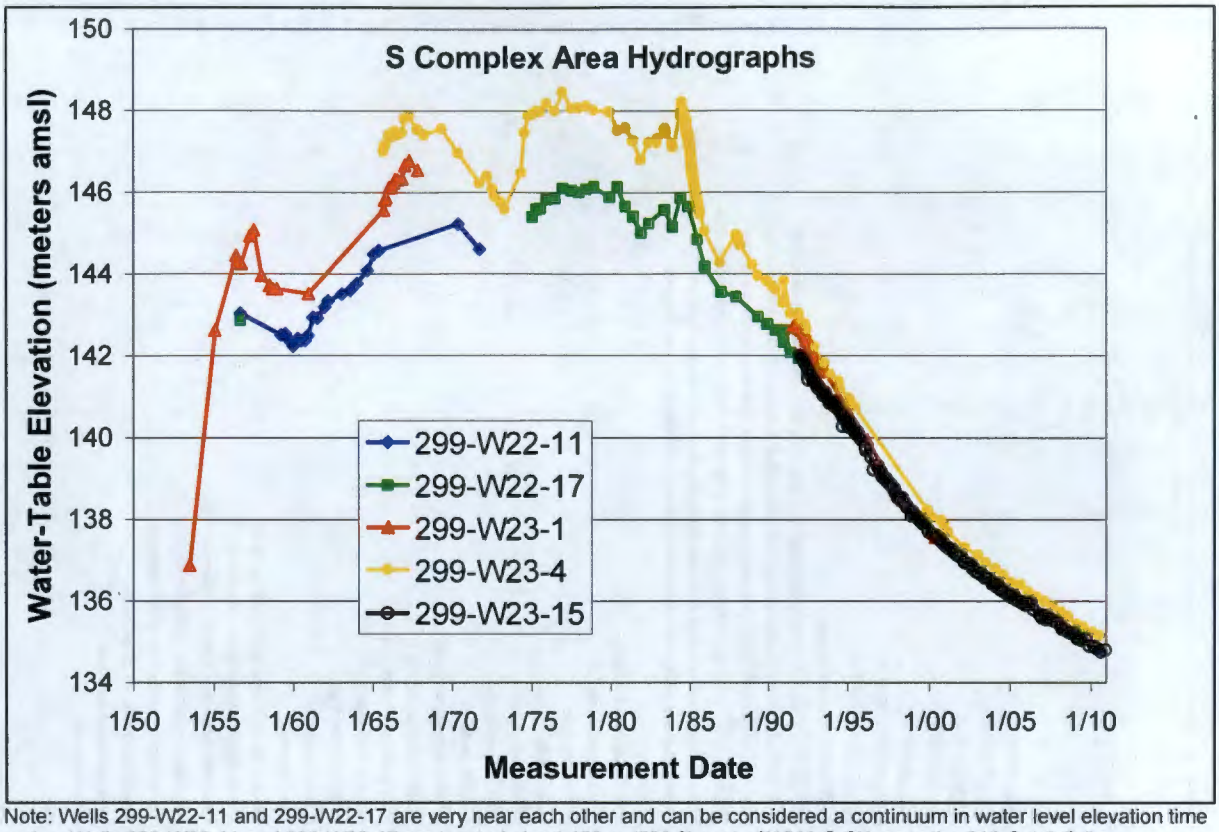

Note: Wells 299-W22-11 and 299-W22-17 are very near each other and can be considered a continuum in water level elevation time series. Wells 299-W22-11 and 299-W22-17 are located about 150 m (500 ft) east of WMA S-SX, near the 216 S-1,2 Cribs; Well 299-W23-1 is located inside the S Tank Farm; Well 299-W23-4 is located southeast of the 216-S-21 Crib; and Well 299 W23 15 is located just south of the SX Tank Farm.

Figure 2-21. Hydrographs of Selected Wells near the S Complex Area

The hydrographs in Figure 2-21 show an initial and very rapid rise in the water table because of discharges to the T Pond and the U Pond in the late 1940s and early 1950s. The water table was at its highest elevation in December 1976 after having risen about 25 m (82 ft) beneath the S Complex Area. The initial increase in the water table in the 1950s was followed by a 19-year period between 1964 and 1985 during which the water table remained high with only slight variation in elevation. The water table began a steady and sharp decline in 1985, following cessation of discharges to the U Pond in 1984, and that decline continues today, although the rate of decrease has lessened slightly (Figure 2-22).

The pre-Manhattan Project maximum water table was at approximately 123 m (403.5 ft) above sea level (BNWL-B-360, *Selected Water Table Contour Maps and Well Hydrographs for the Hanford Reservation, 1944-1973*). In 2000, the elevation of the water table beneath the Hanford Site was modeled for PNNL-13400, *Groundwater Flow and Transport Calculations Supporting the Immobilized Low-Activity Waste Disposal Facility Performance Assessment*. Their model, however, resulted in a water table elevation of about 128 to 132 m (420 to 433 ft) above sea level in the 200 West Area after all influences from the Hanford Site were dissipated. PNNL-13400 analysis considered recharge from agricultural activities, just west of the Hanford Site, which did not exist at the time of the BNWL-B-360 analysis. The PNNL-13400 analysis assumed the agricultural irrigation would continue after Hanford Site influences on the water table stopped. The assumed continuing agricultural input to the unconfined aquifer probably accounts for the differences in the pre-Hanford Site water table elevation and the predicted future (post Hanford) water table elevation.

Table 2-3 gives the average rate of water table decline in the two subregions of the S Complex Area during the past 5 years. The data show that the water table beneath the area is declining at a rate of about 0.25 m/year (<1 ft/yr). At the current rate of decline, the water table should reach the estimated post-Hanford water table elevation (PNNL-13400) in approximately 7 to 14 years for the 216-S-9/216-S-23 subregion and about 12 to 19 years for the 216-S-21/216-S-25 subregion.

Table 2-3. Water-Level Changes Beneath the S Complex Area

Subregion	Approximate Pre-Hanford Water Table Elevation[a] (m amsl)	Estimated Post-Hanford Water Table Elevation[b] (m amsl)	Approximate Maximum Water Table Elevation and Date of Measurement (m amsl)	Approximate Current Water Table Elevation (m amsl)	Approximate Rate of Decline in the Past 5 Years (m/yr)
216-S-9/ 216-S-23	123 to 125	130 to 132	145.09 – April 1967 (299-W22-25)	133.82 – Mar 2011 (299-W22-25)	0.26
216-S-21/ 216-S-25	123 to 125	130 to 132	148.17 – Dec 1976 (299-W23-4)	135.13 – Aug 2010 (299-W23-4)	0.25

a. BNWL-B-360, *Selected Water Table Contour Maps and Well Hydrographs for the Hanford Reservation, 1944-1973.*

b. PNNL-13400, *Groundwater Flow and Transport Calculations Supporting the Immobilized Low-Activity Waste Disposal Facility Performance Assessment.*

amsl = above mean sea level

Accompanying the changes in water level were changes in groundwater flow direction. Pre-Hanford Site groundwater flow direction was generally toward the east (BNWL-B-360). Beginning in the late 1940s, groundwater flow direction changed due to intentional discharges of large volumes of liquid to the ground. Groundwater flow direction changed several times during Hanford Site operations due to changes in waste management practices as liquids were discharged to different facilities during different times.

HNF-4936, *Subsurface Conditions Description for the S-SX Waste Management Area*, published a series of water table maps showing changes in groundwater flow directions from 1944 to 1998. Groundwater flow direction beneath WMA S-SX changed from the easterly pre-Hanford Site flow direction to a south-southeast flow direction by 1951. In 1955, groundwater flow direction was toward the southeast and it remained toward the southeast or the east southeast until after 1987.

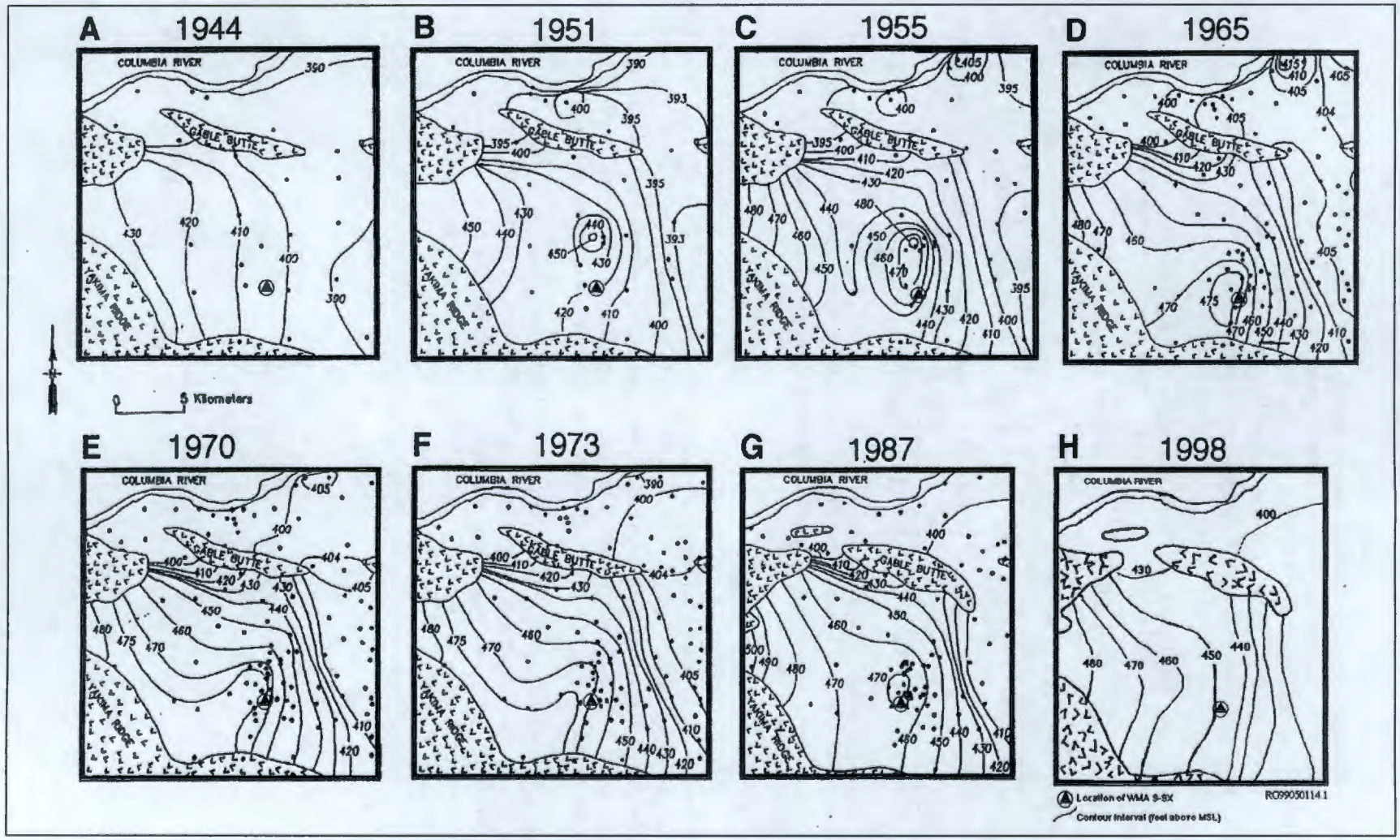

Note: The circled triangle is the location of WMA S-SX (from HNF-4936, *Subsurface Conditions Description for the S-SX Waste Management Area*).

Figure 2-22. Water Table Elevations for the Region of the 200 West Area

PNNL-16069, *Development of Historical Water Table Maps of the 200 West Area of the Hanford Site (1950–1970)*, included a similar study to that of HNF-4936, but at a smaller scale, and a series of water table maps for the 200 West Area were published using available historical data from HydroDat. Figure 2-23 shows four of the maps.

Figure 2-23A shows the water table mound that developed beneath T Pond by 1951. This mound resulted in southeasterly groundwater flow beneath the 216-S-9/216-S-23 subregion and southerly groundwater flow beneath the 216-S-21/216-S-25 subregion. By 1954, the U Pond mound dominated groundwater flow beneath the S Complex Area and the groundwater flow direction changed toward the southeast beneath the 216-S-21/216-S-25 subregion and toward the east-southeast direction beneath the 216-S-9/216-S-23 subregion (Figure 2-23B). Both T Pond and U Pond continued to influence groundwater flow in the southern half of 200 West Area until sometime between 1958 and 1960 when the effects of T Pond are no longer seen (Figure 2-23C and Figure 2-23D). Groundwater flow direction remained toward the southeast at least through 1970 (the date of the last map in PNNL-16069) and probably through most of the 1980s, as shown by the 1987 map in HNF-4936.

PNNL-15837 used water level measurements from the HydroDat database to solve a series of three-point problems to calculate groundwater flow directions and presented the results as rose diagrams. The rose diagrams showed the general changes in groundwater flow directions beneath WMA S-SX from 1992 to 2002. The results are shown as Figure 2-24. The rational for choosing the wells and the data points for the analyses and potential sources of error are discussed in PNNL-15837.

PNNL-13441, *RCRA Groundwater Quality Assessment Report for Waste Management Area S-SX (November 1997 through April 2000)*, noted differences in hydraulic conductivity in wells beneath the S Tank Farm in the northern part of WMA S-SX and wells in the SX Tank Farm to the south. Therefore, the results shown on Figure 2-24 are separated into two parts: northern and southern. The diagrams in Figure 2-24 show that between 1996 and 2002, the groundwater flow direction has been slightly south of east similar to the current flow directions beneath the 216-S-9/216-S-23 subregion (Figure 2-19). The current flow direction beneath the 216-S-21/216-S-25 subregion is more directly east (Figure 2-24). The most recent published flow direction at WMA S-SX, from March 2009 water level data, is almost due east at 88 degrees azimuth and the hydraulic gradient is 0.0019 m/m (DOE/RL-2010-11).

This page intentionally left blank.

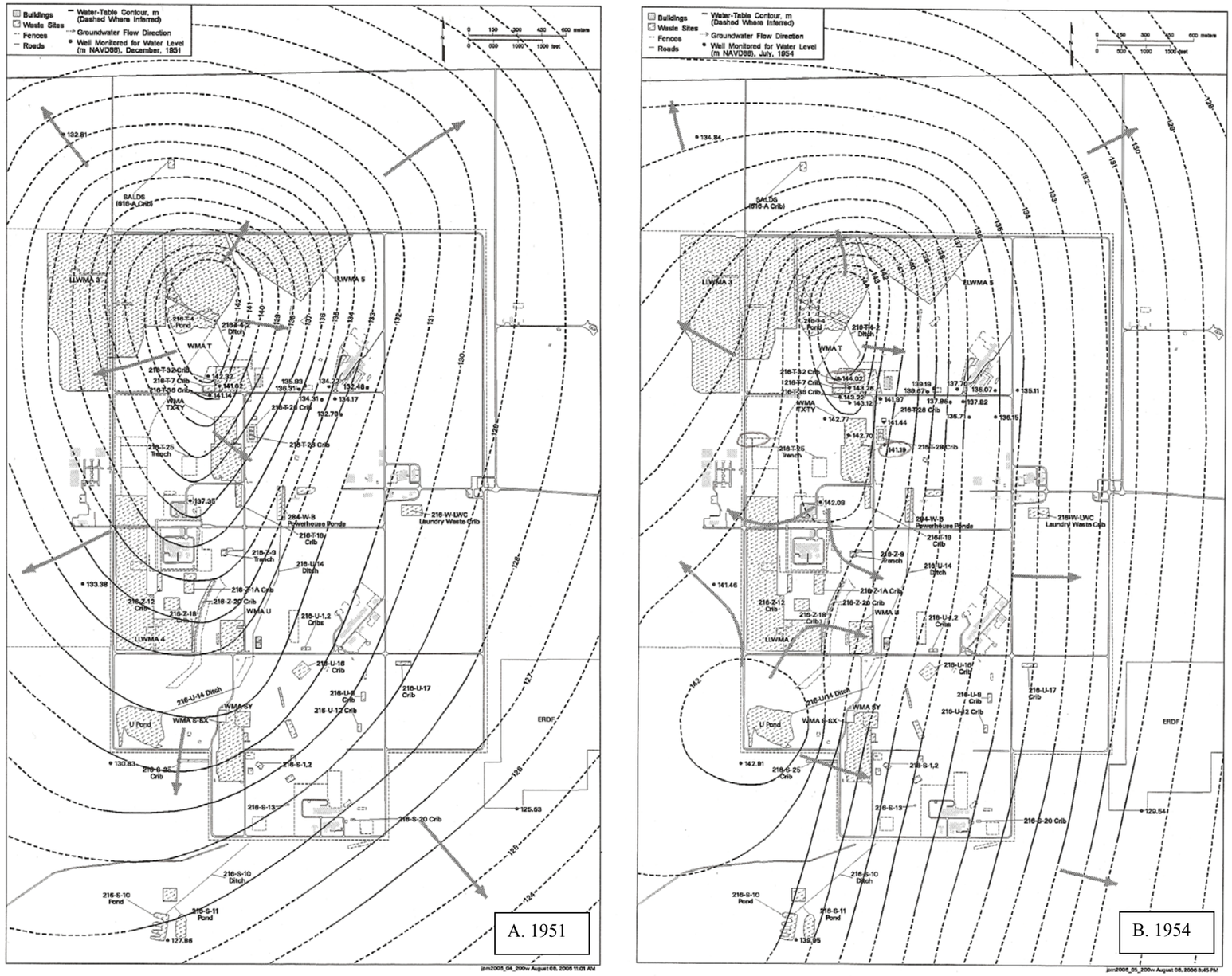

Source: PNNL-16069, *Development of Historical Water Table Maps of the 200 West Area of the Hanford Site (1950-1970)*.

Figure 2-23. Maps Showing the Historical Water Table in 200 West Area

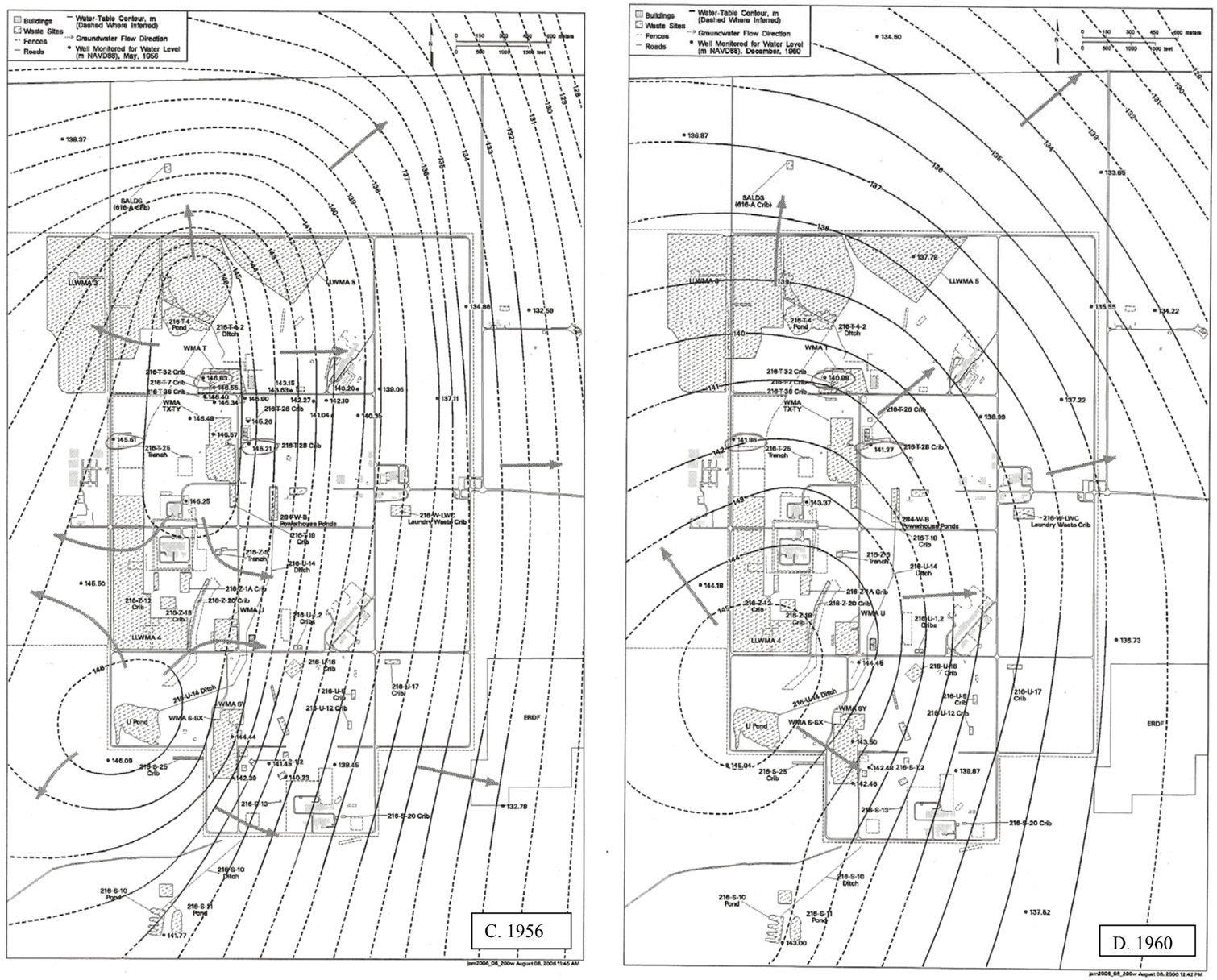

Figure 2-23. Maps Showing the Historical Water Table in 200 West Area (continued)

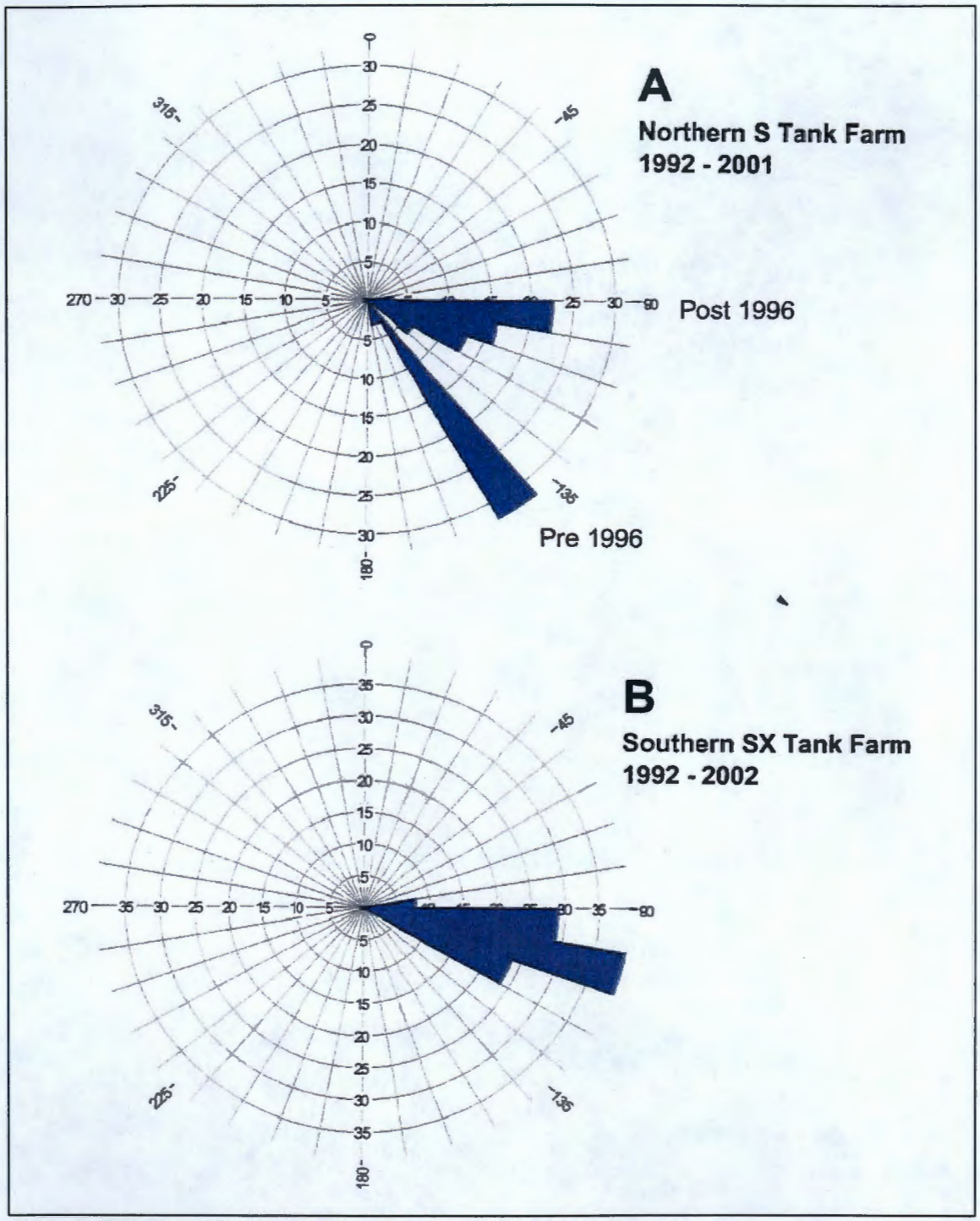

Notes: A. The northern S Tank Farm (1992 to 2001), one well triplet, 31 measurements.
B. The southern SX Tank Farm (1992 to 2002), one well triplet, 38 measurements.
Source: PNNL-15837, *Data Package for Past and Current Groundwater Flow and Contamination Beneath Single-Shell Tank Waste Management Areas.*

Figure 2-24. Groundwater Flow Directions near WMA S-SX

This page intentionally left blank.

3 Conceptual Site Models for Vadose Zone Contamination in S Complex Area Subregions

The S Complex Area has been divided into two subregions that will be discussed in Chapters 3 and 5 of this conceptual model report. This chapter focuses on the vadose zone below and proximal to each subregion and Chapter 5 focuses on groundwater plumes below each subregion as well as some discussion on how individual groundwater plumes have merged into more regional plumes. Additional supporting data used in the development of the CSMs is contained in Appendix B.

3.1 Subregion 1 – 216-S-9 and 216-S-23 Cribs

This subregion is located in the northern portion of the S Complex Area, as shown in Figure 1-1. Figure 3-1 is a more detailed, localized subregion map. This subregion contains two inactive waste disposal facilities that are part of the 200-DV-1 OU: the 216-S-9 and 216-S-23 Cribs. The two cribs are east and northeast of the S Tank Farm, respectively. The S Tank Farm is also considered part of this subregion for conceptual model discussions.

3.1.1 Facility Description, Source Details, and Inventory Released

Table 3-1 shows the SIM, Rev. 1 database (RPP-26744) with details for the two 200-DV-1 OU facilities over their lifetimes. Appendix A provides other details, such as yearly values for chemicals and radionuclides released and facility dimensions and depths to the water table.

The 216-S-9 Crib has bottom dimensions of 90.8 m (298 ft) long by 9.1 m (30 ft) wide with sloping sides that manifest at the ground surface with dimensions 97 m (319 ft) by 15.5 m (51 ft). The bottom of the crib is 9.1 m (30 ft) bgs and the crib was filled with 2.1 m (7 ft) of gravel according to CP-49279 drawings and 7 m (23 ft) of overburden once the crib was deactivated. The crib received liquid wastes (REDOX decontamination) from 1965 through 1969, but the bulk of the waste was disposed in the first four years (1965-1968) with a total disposal of 49.58 million liters (ML) (13.1 million gal [Mgal]). Based on the bottom dimensions, a depth to groundwater from the bottom of the crib at the time of active disposal of 52.46 m (172 ft) and an assumed volumetric water content of 25 percent, the volume of liquid waste disposed would represent 4.55 pore volumes of fluid. Assuming that the entire crib footprint percolated the disposed waste equally straight down to the water table, the wastes would have affected groundwater.

The 216-S-23 Crib has bottom dimensions of 110 m (360 ft) long by 3 m (10 ft) wide with sloping sides that manifest at the ground surface with dimensions 111 m (364 ft) by 43 m (141 ft). The bottom of the crib is 9.1 m (30 ft) bgs and the crib was filled with 0.6 m (2 ft) of gravel according to CP-49279 drawings and 8.5 m (28 ft) of overburden once the crib was deactivated. The crib received liquid wastes (REDOX cooling water) from 1969 through 1972, with a total disposal of 34.07 ML (9 Mgal). Based on the bottom dimensions, a depth to groundwater from the bottom of the crib at the time of active disposal of 54.24 m (177.9 ft) and an assumed volumetric water content of 25 percent, the volume of liquid waste disposed would represent 7.5 pore volumes of fluid. Assuming that the entire crib footprint percolated the disposed waste equally straight down to the water table, the wastes would have affected groundwater.

Table 3-1 shows the volume of waste, the masses (or radioactivity) of chemicals, and radionuclides disposed in the two cribs as a percentage of the total liquid waste disposed of or released via SST and associated piping leaks to the entire S Complex Area. The total volume of waste disposed in these two cribs represents 18 percent of the total volume of waste released to the S Complex Area. The mass of uranium disposed (almost all going to 216-S-9) represents 90 percent of the total uranium released to the S Complex Area from facilities designated as being in the 200-DV-1 OU. The nitrate disposed to the two

cribs represents 12 percent of the total nitrate released to the S Complex Area. The wastes disposed to the two cribs did not contain any chromium. I-129 disposed to 216-S-9 constitutes 36 percent of the total I-129 released to the S Complex Area, but only 0.3 percent of the total Tc-99 disposed to the S Complex Area came from the two cribs and essentially all of it was disposed in 216-S-9.

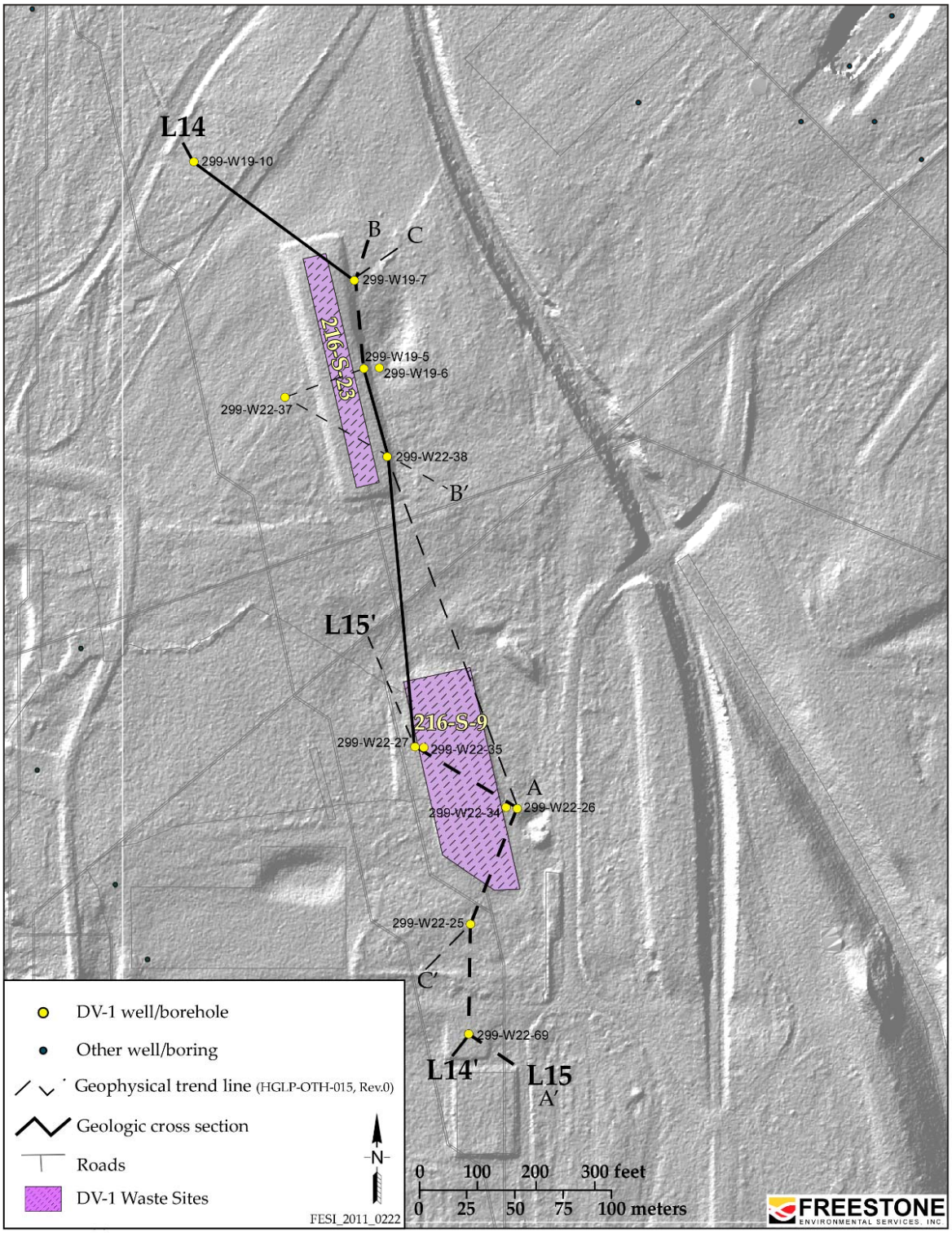

Figure 3-1. Subregion 1 – 216-S-9 and 216-S-23 Cribs, 200-DV-1 Operable Unit

Table 3-1. Masses Released over 216-S-9 and 216-S-23 Cribs Lifetime and Percent of Total Released to S Complex Area

	216-S-9	216-S-23	Subregion Totals	216-S-9 % Subregion	216-S-23 % Subregion	216-S-9 & 216-S-23 % of Total S Complex Area
Total Volume Released (ML)	49.58	34.07	83.74	59.3	40.7	18.21
Mass Released (kg)						
Sodium (Na)	742	443.9	1185.9	62.6	37.4	1.14
Nitrate (NO_3)	**41784.8**	**1913.2**	**43698.0**	**95.6**	**4.4**	**12.00**
Nitrite (NO_2)	0	1696.5	1696.5	0.0	100.0	5.05
Phosphate (PO_4)	0	0	0			0.00
Sulfate (SO_4)	0	1.01E-03	0.001	0.0	100.7	0.00
Fluorine (F)	0	0	0			0.00
Uranium (U)	**275.6**	**1.57E-05**	**275.6**	**100.0**	**0.0**	**90.33**
Chromium (Cr)	**0**	**1.28E-03**	**1.28E-03**	**0.0**	**100.0**	**0.00**
Activity Released (Ci)						
Cobalt-60	3.12E-03	9.43E-07	3.12E-03	100.0	0.0	0.01
Iodine-129	**2.95E-02**	**2.93E-08**	**2.95E-02**	**100.0**	**0.0**	**36.03**
Technetium-99	**1.04E-01**	**1.86E-05**	**1.04E-01**	**100.0**	**0.0**	**0.30**
Tritium	6.75E+02	2.45E-05	6.75E+02	100.0	0.0	21.05
Plutonium-238	1.98E-01	8.21E-08	1.98E-01	100.0	0.0	17.63
Plutonium-239	2.90E+00	2.57E-06	2.90E+00	100.0	0.0	7.65
Cesium-137	4.83E+01	4.70E-02	4.83E+01	99.9	0.1	0.07

Note: Volume and inventory estimates for the facilities were taken from RPP-26744, *Hanford Soil Inventory Model, Rev. 1.*
Cobalt-60, tritium, and cesium-137 activities decay corrected to 9/30/2010.
The five potentially mobile contaminants of concern are in **bold type**.
ML = mega liters (million liters).

3.1.2 Hydrogeology of the 216-S-9 and 216-S-23 Subregion

This hydrogeologic summary supports the conceptual model development for the 216-S-9 and 216-S-23 (Subregion 1) (Figure 3-1). The 200-DV-1 OU remedial investigation focuses on the nature and extent of contamination in the vadose zone sediments. As such, this hydrogeologic summary also focuses primarily on the stratigraphic units occurring in the vadose zone interval.

The vadose zone underlying the 216-S-9 and 216-S-23 Cribs is approximately 76 m (249.4 ft) thick. The suprabasalt aquifer system in this area is estimated to be approximately 99 m (324.8 ft) thick. Aquifer

thickness is inferred from a regional top of basalt map (PNNL-17913) since only one well (299-W22-27) in this area was drilled to basalt. Groundwater generally flows to the east (based on Figure 2-2 in DOE/RL-2010-11) beneath this subregion and is known to contain dissolved contaminants from past disposal facilities within the 200 West Area. Perched groundwater was not identified during review of borehole logs near the 216-S-9 and 216-S-23 Cribs.

The 216-S-9 and 216-S-23 Cribs are constructed in the near-surface Hanford formation sediments of the vadose zone. The bottom of the cribs lie within the gravel dominated Hf1 at 9.1 m (30 ft) bgs (see facility details in Appendix A).

Type logs based on borehole spectral-gamma geophysical logs were created using Wells 299-W19-7 (Figure 3-2) and 299-W22-69 (Figure 3-3) to define and constrain stratigraphic contacts within this subregion. Geologic information for this subregion is limited to the driller's logs, most of which are extremely old and qualitative. More quantitative data, from which to interpret lithology, is available in the ROCSAN[6] database in addition to the downhole geophysical logs (gross gamma and spectral gamma). Cross sections depicting the geology of the subregion are shown in Figures 3-4 and 3-5. A detailed description of the individual geologic units beneath 216-S-9 and 216-S-23 follows.

3.1.2.1 Holocene Deposits

Most of the recent (Holocene age) fine-grained (eolian) sediment has been removed or highly disturbed in this subregion. Several meters of backfill are present across the subregion above the Hanford formation and are located within the construction areas of 216-S-9 and 216-S-23 Cribs. The backfill is native Hanford formation (sand and gravel) material that was stockpiled nearby during crib construction. During crib construction, all natural layering/stratification was disrupted such that the backfill is rather homogeneous and featureless compared to the undisturbed Hf1 unit.

3.1.2.2 Hanford formation

The Hanford formation makes up the majority of the vadose zone sediment beneath the subregion (Figures 2-3 and 3-5), ranging in thickness from 37 to 44 m (121.4 to 144.4 ft). Both the Hf1 subunit (coarse-grained sandy gravel or gravel) and the Hf2 subunit (predominately sand) are present.
The gravel-dominated Hf1 unit consists of sandy gravel to silty sandy gravel. Overall, the Hf1in this subregion contains a greater amount of sand (i.e., borehole log for 299-W22-69 described the top 14 m [46 ft] of sediments as a poorly sorted sand with less than 10 percent gravel) and displayed an interfingering of coarse gravel lenses. Driller's logs and geophysical log plots indicate there may be discontinuous finer-grained lenses within the Hf1 in Wells 299-W19-7 (Figure 3-2) and 299-W19-5. The sand-dominated Hf2 unit consists of predominantly fine to coarse sand. Driller's logs and geophysical log plots indicate there may be discontinuous coarse-grained lenses within the Hf2 in the central portion of the subregion.

The top of the Hf2 generally dips to the southeast (PNNL-17913) in this area. Differentiating the Hanford subunits using geophysical logging data was sometimes complicated by the occurrence of radiological contamination, drilling methods, and the sometimes-gradational nature of the unit contacts.

[6] Database that includes particle size and calcium carbonate content of sediments from the Hanford Site.

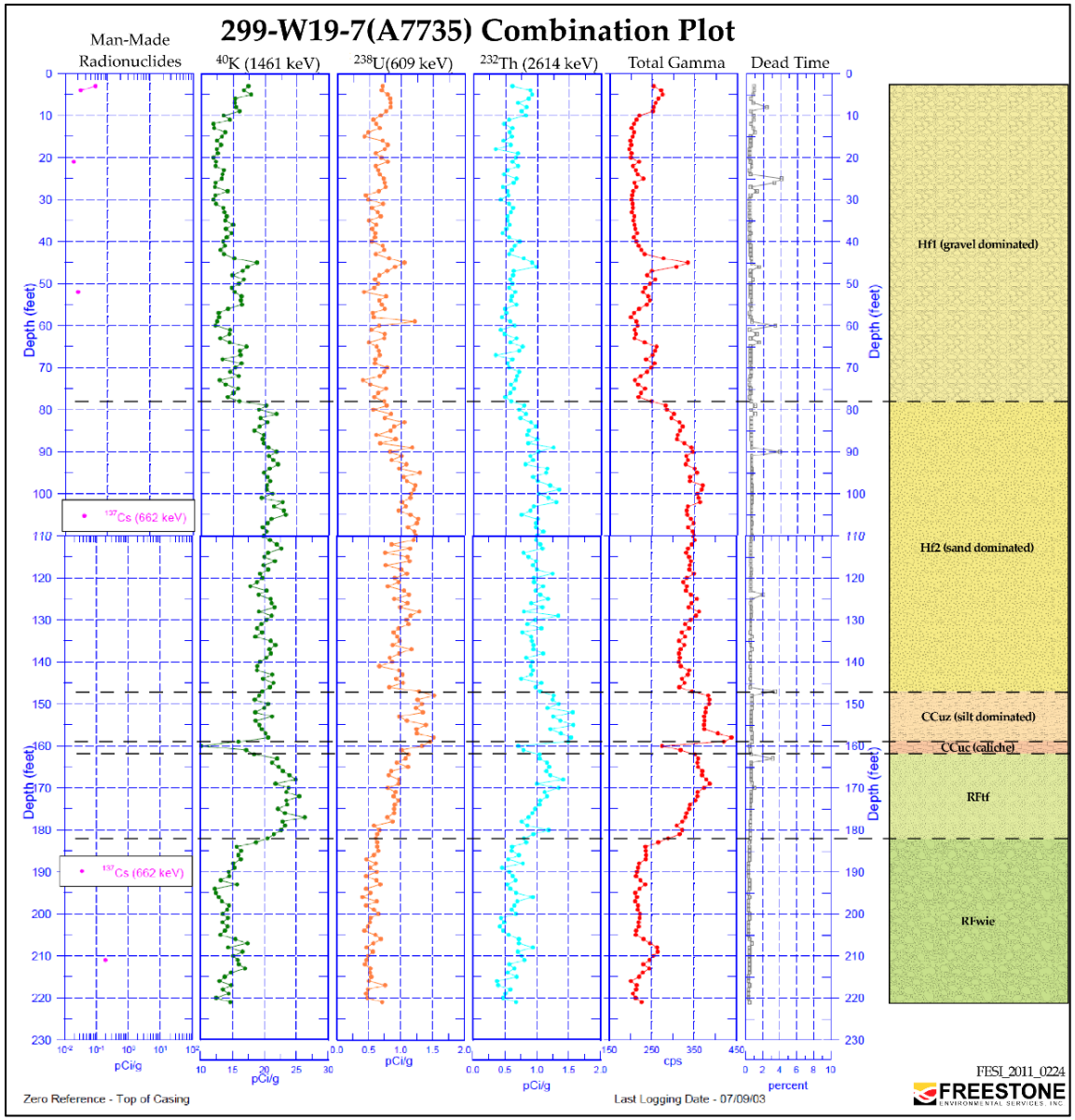

Figure 3-2. Stratigraphic Type Log for 299-W19-7

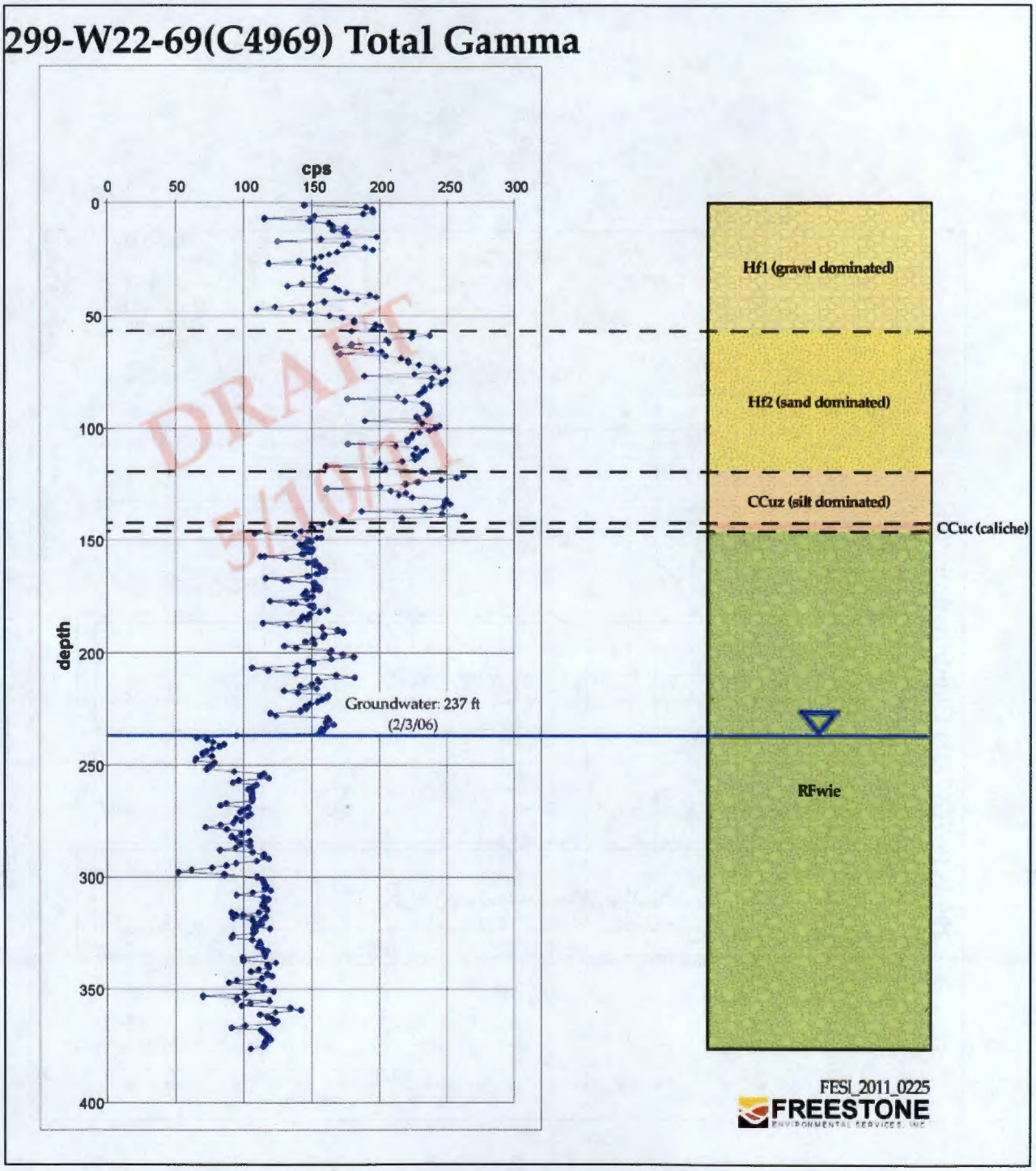

Figure 3-3. Stratigraphic Type Log for 299-W22-69

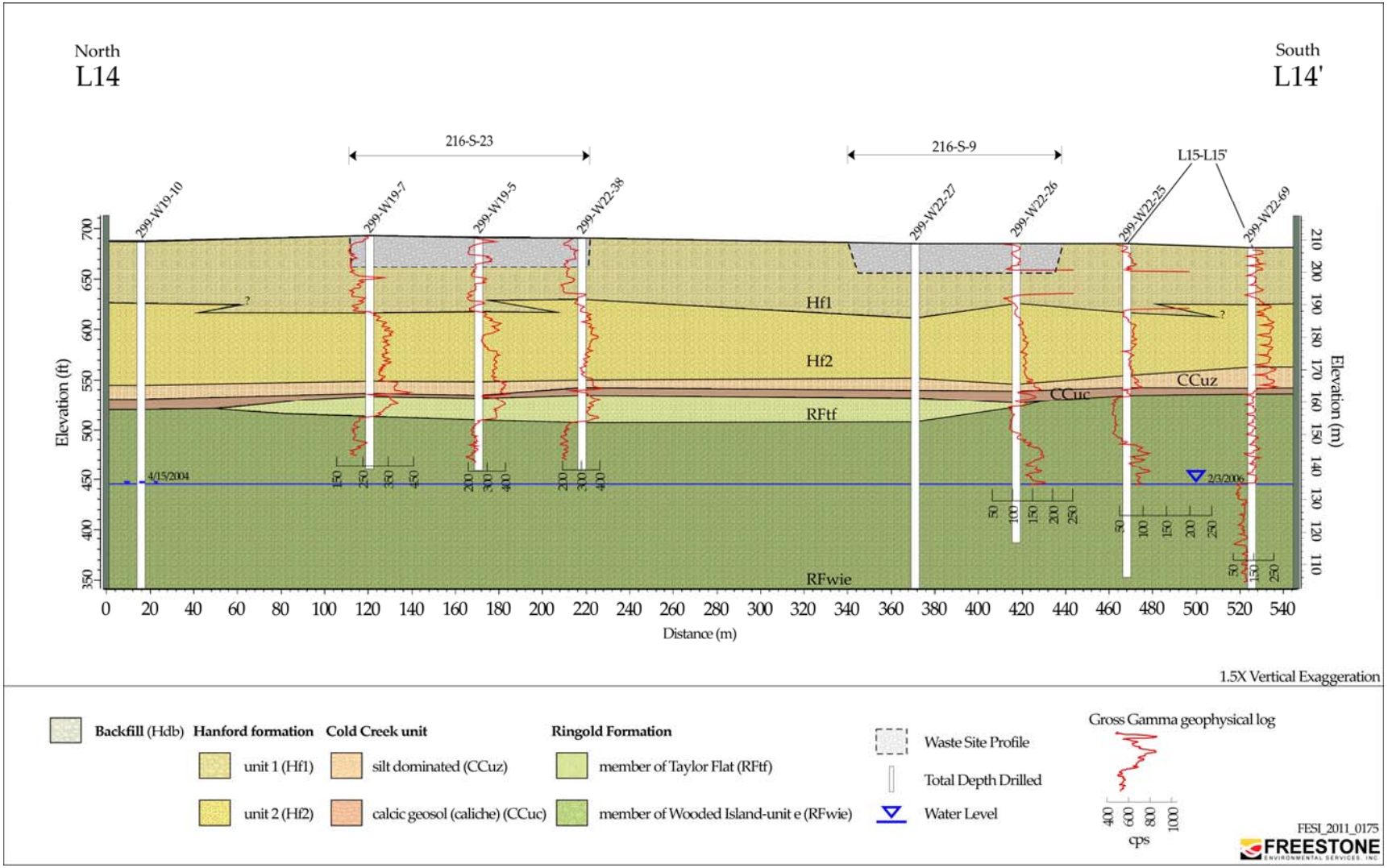

Figure 3-4. Hydrogeologic Cross Section L14-L14'

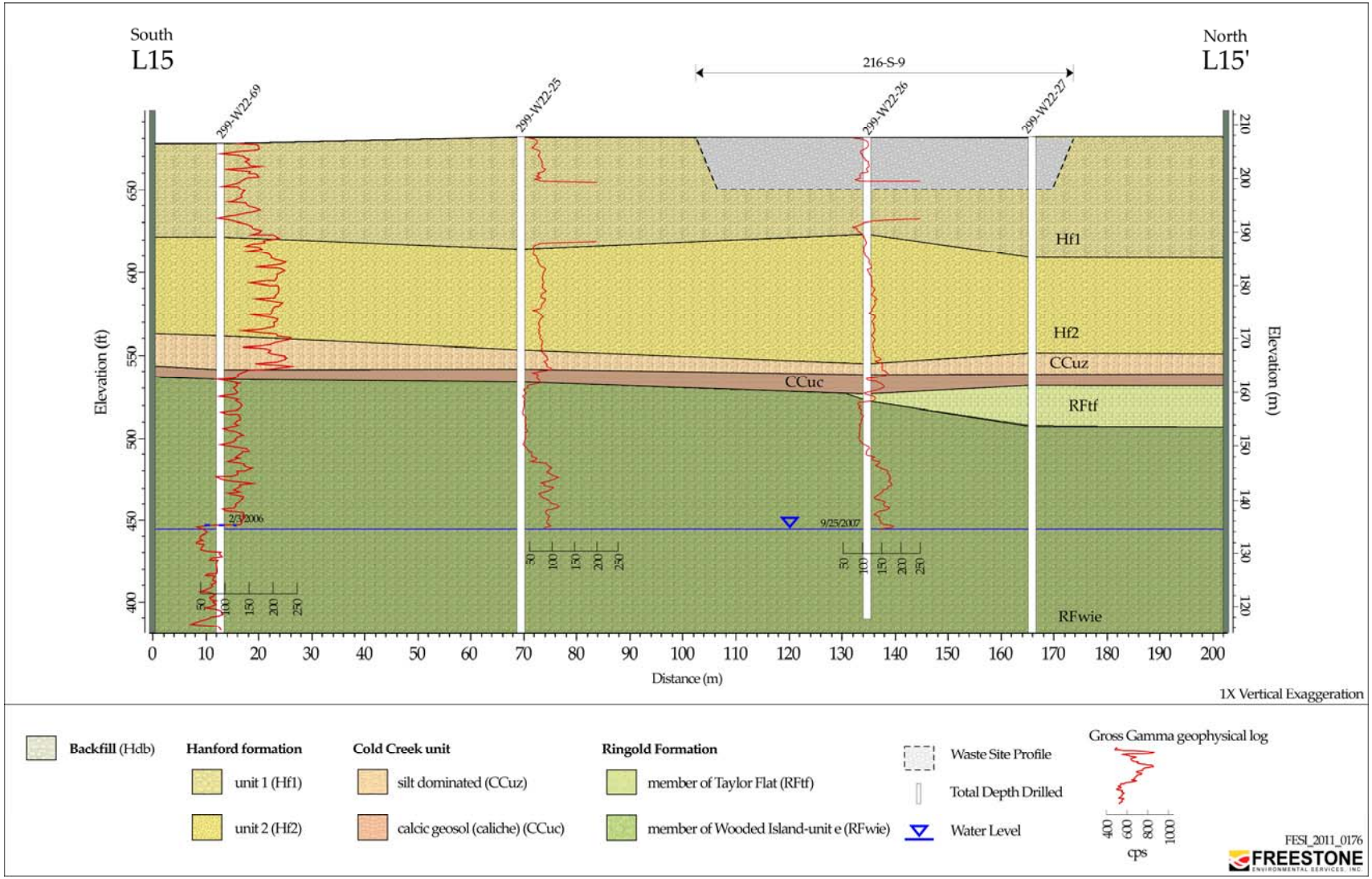

Figure 3-5. Hydrogeologic Cross Section L15-L15'

3.1.2.3 Cold Creek Unit

The CCu underlies the Hanford formation and is locally subdivided into two subunits: CCuz and CCuc. Both the CCuz and CCuc are laterally continuous throughout the subregion. The upper and lower contacts of these subunits were largely defined using the spectral and gross gamma borehole geophysical log plots as shown in stratigraphic type logs (Figures 3-2 and 3-3). CCuz is generally indicated by the occurrence of "fine sand and clay" noted on the driller's logs and was described in the geologist's borehole log (Well 299-W22-69) as a reddish brown sandy-silt with "clay nodules in matrix up to 3 cm."

The CCuc is described in the geologist's borehole logs as a calcium carbonate-rich silty sand overlying an interval containing caliche "nodules up to 4 in." The base of the CCuc beneath the caliche layer consists of dark reddish-brown silty sandy-gravel with gravel clasts up to 4 in. The overall thickness of the CCuc in this subregion is thin relative to the more northern waste sites. The characteristic apposing K-40 and Th-232 peak that correlates with highly cemented calcrete layers in most of the other subregions in the 200-DV-1 OU is not visible in this subregion, suggesting that the cemented nature of the CCuc interval changes from nearby areas. Spectral Gamma Logging System (SGLS) geophysical logs from 299-W19-7 show only a single low signature of K-40 and Th-232 (Figure 3-2). The existence of only a single cemented calcrete in this subregion suggests one of the calcrete layers was eroded away at this location prior to the deposition of the CCuz subunit, or aggradation and accretion of soil deposits was much slower so that only a single pedogenic calcrete horizon developed.

The CCuz ranges in thickness from 2.1 to 6.4 m (7 to 21 ft) and CCuc ranges in thickness from 0.9 to 4.9 m (3 to 16 ft). Both subunits appear to dip gently to the north-northwest beneath the subregion (Figure 2-11).

3.1.2.4 Ringold Formation

The total thickness of the Ringold Formation was penetrated by two of the eight wells (299-W19-10 and 299-W22-27) evaluated for the subregion. Based on geologic descriptions in the subregion vicinity (PNNL-15955), the Ringold Formation is composed of units RFtf, RFwie, RFlm, and RFwia.

The uppermost Ringold Formation unit, where present, is the RFtf, which is composed predominately of well-sorted sand with minor silt described by driller's logs as a "fine sand" or "sand and silt." Where present in this subregion, the RFtf ranges in thickness from 6.1 to 8.5 m (20 to 28 ft) and is relatively flat. The RFtf thickens substantially toward the south of 216-S-23 and north of 216-S-9, then thins and disappears in the areas south, west, and north of the subregion (Figures 3-4 and 3-5).

The RFtf overlies the RFwie, which represents the lowermost Ringold Formation unit in the vadose zone. The contact between the RFtf and RFwie is distinct both in the geologist's borehole logs and in the geophysical logging plots. RFwie is described as well-rounded pebble-to-cobble gravel with a fine-to coarse-grained sand matrix. Gravel content is usually greater than 60 to 70 percent and poorly sorted; iron oxide staining is common (PNNL-15955). The sediments in the RFwie are variably consolidated. In Wells 299-W19-10 and 299-W22-27, the RFwie is 87.9 and 81.7 m (288.5 and 268 ft) thick, respectively, and dips slightly to the southeast (PNNL-15955). The RFwie, RFlm, and RFwia comprise the suprabasalt aquifer system in this subregion. The RFlm (confining unit) and RFwia (a confined aquifer interval) are not described in this report due to their occurrence in the deeper portion of the saturated zone.

3.1.3 Subregion 1 – Vadose Zone Contamination Estimates for 216 S-9 and 216-S-23 Cribs

There are no quantitative data for direct measurements of contaminant concentrations in sediments from within or near the Subregion 1waste sites. The only information that can be used to estimate the vertical and horizontal spread of mobile contaminants from the two cribs are borehole geophysical logs (gross and

spectral gamma) taken through well casings of nearby boreholes and available soil resistivity field surveys that were performed at the S Tank Farm.

SGW-50194 provides an analysis of all historical and recent borehole gamma logs. The following material is summarized from the report. The borehole geophysical log data evaluation for wells near the 216-S-9 Crib, suggest that gamma-emitting contaminants affected the deep vadose zone all the way to groundwater by February 1968. The gamma activity significantly decayed by 1976, suggesting short-lived fission products such as ruthenium-106 was the dominant radionuclide.

The current contaminant profile shows cesium-137 existing from approximately 9.1 to 18.3 m (30 to 60 ft) bgs with concentrations up to 50,000 pCi/g near the crib. This contamination remains mostly within the Hf1, above the Hf1/Hf2 geologic contact and near the crib. Most of the gamma emitting radionuclides that were evident in the deep vadose zone in 1968 have decayed away. Data also indicate that the upper unconfined aquifer became polluted with gamma emitting contamination around the same time as the vadose zone. The data suggest that mobile non-gamma emitting contaminants present in the waste stream could be present throughout the vadose zone down to the water table. The location (lateral and vertical extent) of the non-gamma contaminants is a data gap for this crib.

The 216-S-23 Crib was activated in 1969 after the 216-S-9 Crib was closed. There is some evidence in two boreholes east of the crib that short-lived radionuclides contaminated the deep vadose zone to groundwater (SGW-50194). Activity exhibited in these two boreholes was much less than that found near the 216-S-9 Crib. The activity in the two boreholes near 216-S-23 decayed away by 1976, similar to the activity measured near the 216-S-9 Crib. No significant cesium-137 was found in the boreholes around the 216-S-23 Crib. At the time of logging in the two wells, groundwater contamination was noticeable at the artificially elevated water table.

Another source of vadose zone information was the surface soil electrical resistivity field survey of the S Tank Farm just west of the 216-S-9 Crib. Figure 3-6 shows the array of surface electrodes that were used to interrogate the subsurface sediments of this subregion.

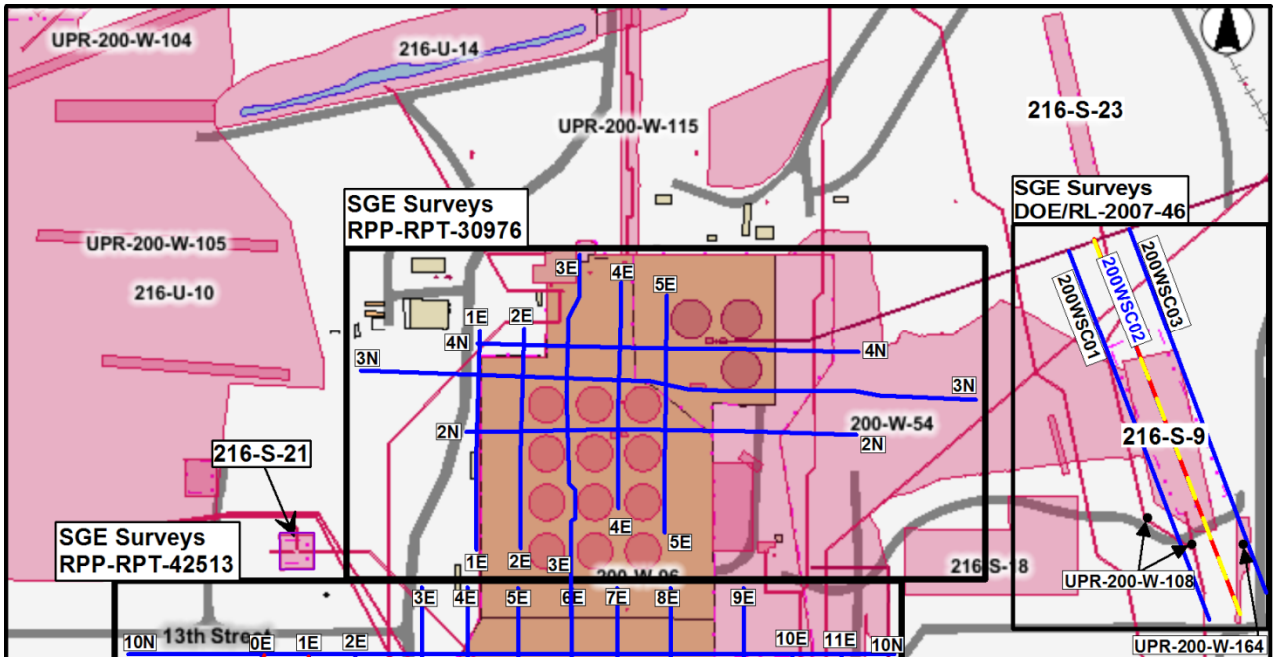

Figure 3-6. Soil Resistivity Profiling near the 216-S-9 and 216-S-23 Cribs

Three SGE resistivity profiles were acquired along a SE-NW orientation over 216-S-9 (Figure 3-6). SGE investigations at 216-S-9 were also scoped to image subsurface conditions beneath UPR-200-W-108 and UPR-200-W-164, both of which are located immediately to the south and southwest of 216-S-9. A two-dimensional (2D) computer modeling exercise of the raw soil resistivity data yielded the soil resistivity conceptual model shown in Figure 3-7. The lowest resistivity regions, which indicate either metallic infrastructure or soils with high salt and/or moisture content, are depicted with blue and green colors. Regions with high resistivity, such as dry native sediments, are depicted in brown, red, and purple colors. The conceptual model shown in Figure 3-7 has been interpreted to show high-resistivities (>350 ohm-m, brown-to-red colors) within the upper 40 m (131 ft), which is consistent with the presence of unsaturated sands and gravels of the Hanford formation. Relative lower resistivities (180-280 ohm-m) are modeled to 6 to 10 m (20 to 33 ft) in depth under most of 216-S-9, and form a broader region trending vertically downward from the southeast end of the waste site (cyan and magenta outline). Lower resistivities at depth are most likely due to salt laden sediments. Contractor interpreted the anomaly near profile coordinate 220 m (721.8 ft) (magenta oval) as caused by buried pipes. The SGE electrode lines did not extend far enough to interrogate the 216-S-23 Crib.

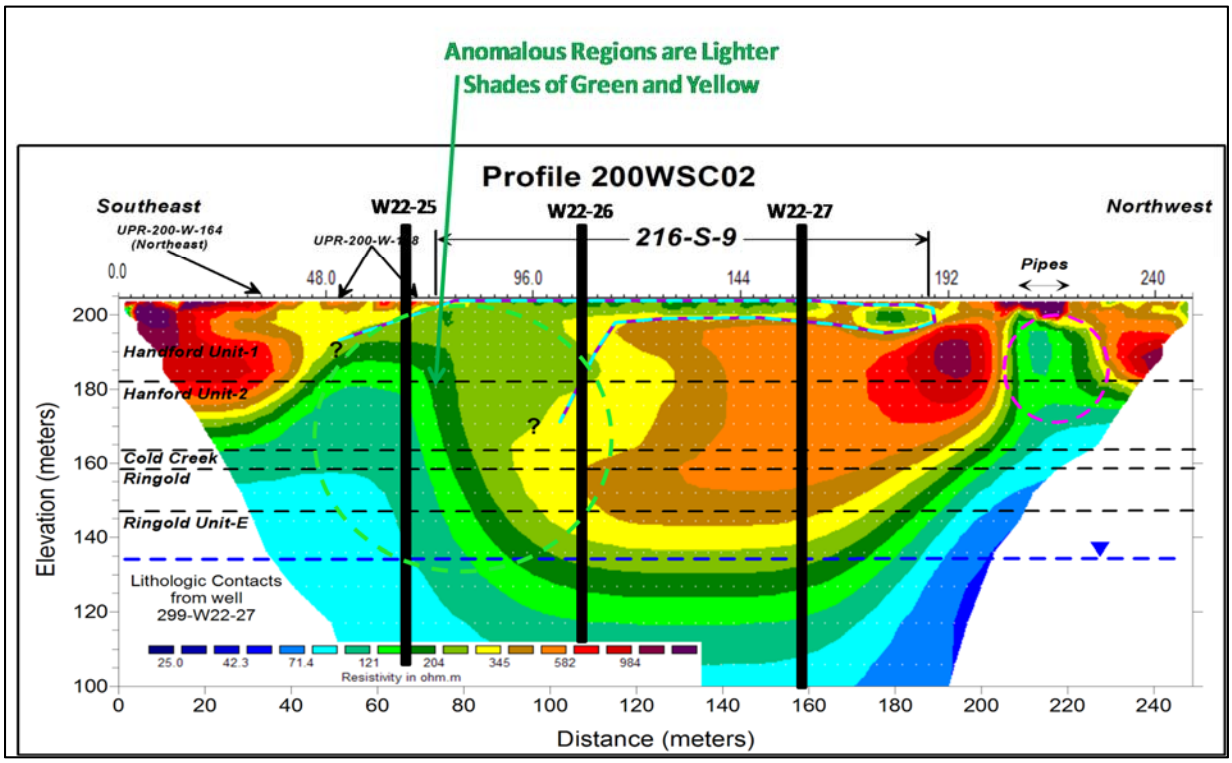

Note: See Figure 3-6 for profile location.

Figure 3-7. Two-Dimensional Modeling

3.1.4 Subregion 1 – Vadose Zone Conceptual Model for 216-S-9 and 216-S-23 Cribs

The conceptual model for the distribution of contaminants below the 216-S-9 and 216-S-23 Cribs subregion relies almost exclusively on historical gross gamma field logs, recent spectral gamma logs coupled with the detailed geological model of stratigraphy and lithology, and knowledge of the volumes of liquid released to each facility. The soil electrical resistivity survey information adds some information on the location of moderate salt within the subsurface around the 216-S-9 Crib, but is not as definitive on the vertical extent of the past liquid waste migration.

Using the conservative assumption that all the liquid released to the two cribs percolated into the sediment directly beneath the footprint of the facilities (i.e., no lateral spreading) from the bottom of the facilities to the water table and wetted the sediments within the footprint to 25 vol%, then both would have affected groundwater. A second pore-volume calculation that considers the observed and inferred lateral spread based on the gamma logging and soil resistivity information will be discussed later in this subsection.

Based on the available gamma logs and soil electrical resisitivity field survey of the 216-S-9 Crib, the following conceptual model of the lateral spread and vertical extent of vadose zone contamination was generated.

Beneath 216-S-9, gamma contamination was detected in boreholes 299-W22-25 and 299-W22-26 throughout most of the vadose zone. The most recent geophysical log data indicate that gamma contamination remains from 9.4 to 20.7 m (31 to 68 ft) bgs and from 9.1 to 17.7 m (30 to 58 ft) bgs, respectively. Total gamma logs record this contamination by a sharp increase at approximately 200 m (656 ft) elevation on cross sections L14-L14′ and L15-L15′. Figures 3-4 and 3-5 delineate the extent of gamma contamination (recent logs generally detect cesium-137 and, in a few cases, cobalt-60). Cesium-137 is sorbed well by the Hanford sediments and this indicates a minimum extent of migration, but cobalt-60 is relatively mobile in Hanford sediments and thus gives a more realistic depiction of the extent of migration of the disposed liquid wastes. Historical gross gamma logs detected the very mobile ruthenium-106 gamma-emitting isotope and thus when available can be used to estimate the leading edges of the liquid waste vadose zone plumes. Keep in mind that the gamma logs do not give a quantitative estimate of the concentrations of the five key (nitrate, Tc-99, I-129, chromium, and uranium) contaminants of interest. The gamma logging and field soil resistivity survey information can only yield indications of the volume of vadose sediment impacted by the disposed liquid wastes. The conceptual model for the lateral spread of contaminants disposed to the two cribs is shown in Figure 3-8. Figure 3-8 suggests that the contamination at 216-S-9 exists in an area below almost the entire crib footprint and extends to the south a considerable distance to commingle with UPR-200-W-108. At the 216-S-23 Crib, it appears that liquid waste only spread below the southern two-thirds of the footprint nearer to the inlet. There is currently no cesium-137 gamma detected around the 216-S-23 Crib, which is logical based on the very low inventory of cesium-137 disposed to the crib.

Figure 3-9 gives the conceptualization for the vertical extent of contamination below both cribs. Mobile contaminants are depicted to exist from both crib bottoms all the way to the water table (both the historical high water and current) at 216-S-9 with more concentrated residually elevated Cs-137 located mostly within the Hf1 above the Hf1/Hf2 contact. For the 216-S-23 Crib, the vertical extent is less well defined by the available field gamma logs but more than likely mobile contaminants did reach the high water table during the active disposal period. Even today, there appears to be remnant gamma contamination sorbed to the casings of the boreholes between the historical high water table and the current water table. With the exception of the Hf1/Hf2 contact, there are no definitive or significant lateral spreading zones depicted in Figure 3-9 at the major contacts between the strata. Whether this is caused by the sparsity of boreholes surrounding the cribs is not determinable.

The volume of residual contamination below the two facilities can be estimated by combining the plan view in Figure 3-8 and vertical extent shown in the Figure 3-9 cross section. The dimensions of the perceived residual contamination for 216-S-9 Crib are represented by a solid oval with north-south dimensions of 170 m (557.8 ft) and east-west dimensions of 100 m (328 ft), yielding a cross-sectional area of 13,350 m^2, a depth to the water table of 52.5 m (172.2 ft), and a residual moisture content of 10%vol. The calculated pore volume for the volume is 0.7, suggesting all the disposed waste could still reside within the vadose zone. Based on historical groundwater data and the gross gamma logs at the historical monitoring wells, wastes disposed to 216-S-9 Crib did reach the water table. Thus, the estimate

for the lateral spread or the volumetric water content in the vadose zone through which the wastes percolated appears to be overestimated. However, for conservatism, it will be assumed that all the inventory of mobile contaminants disposed of to the 216-S-9 Crib remain in the vadose zone sediments.

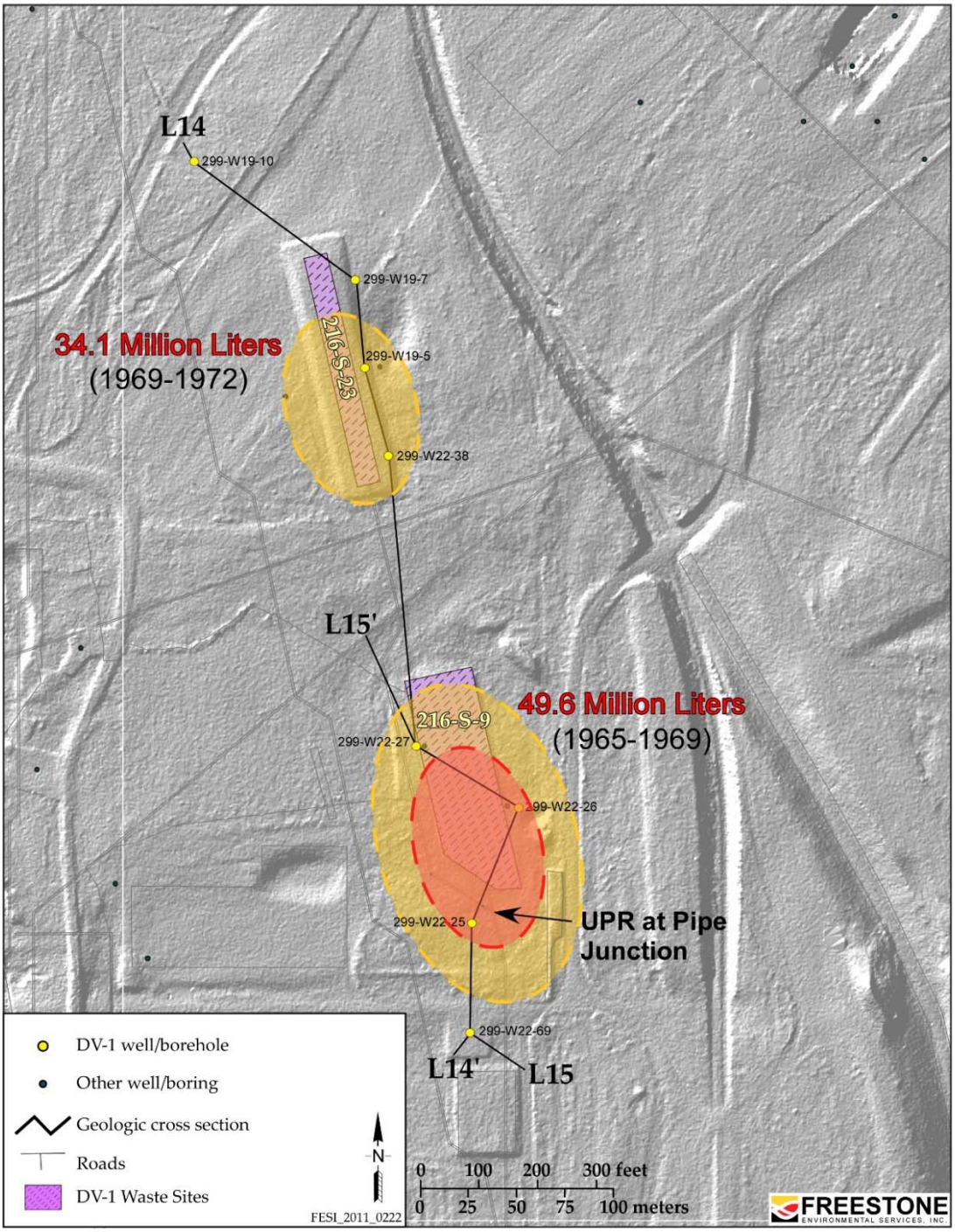

Note: The dark red-orange area represents the region with currently detectable cesium-137 ≥10 pCi/g contamination (less mobile) and the faint yellow-orange area represents the region of past historical gamma contamination (mobile short half-life [e.g., ruthenium-106]).

Figure 3-8. Depiction of Vadose Zone Lateral Spread of Contamination Proximal to the 216-S-9 and 216-S-23 Cribs

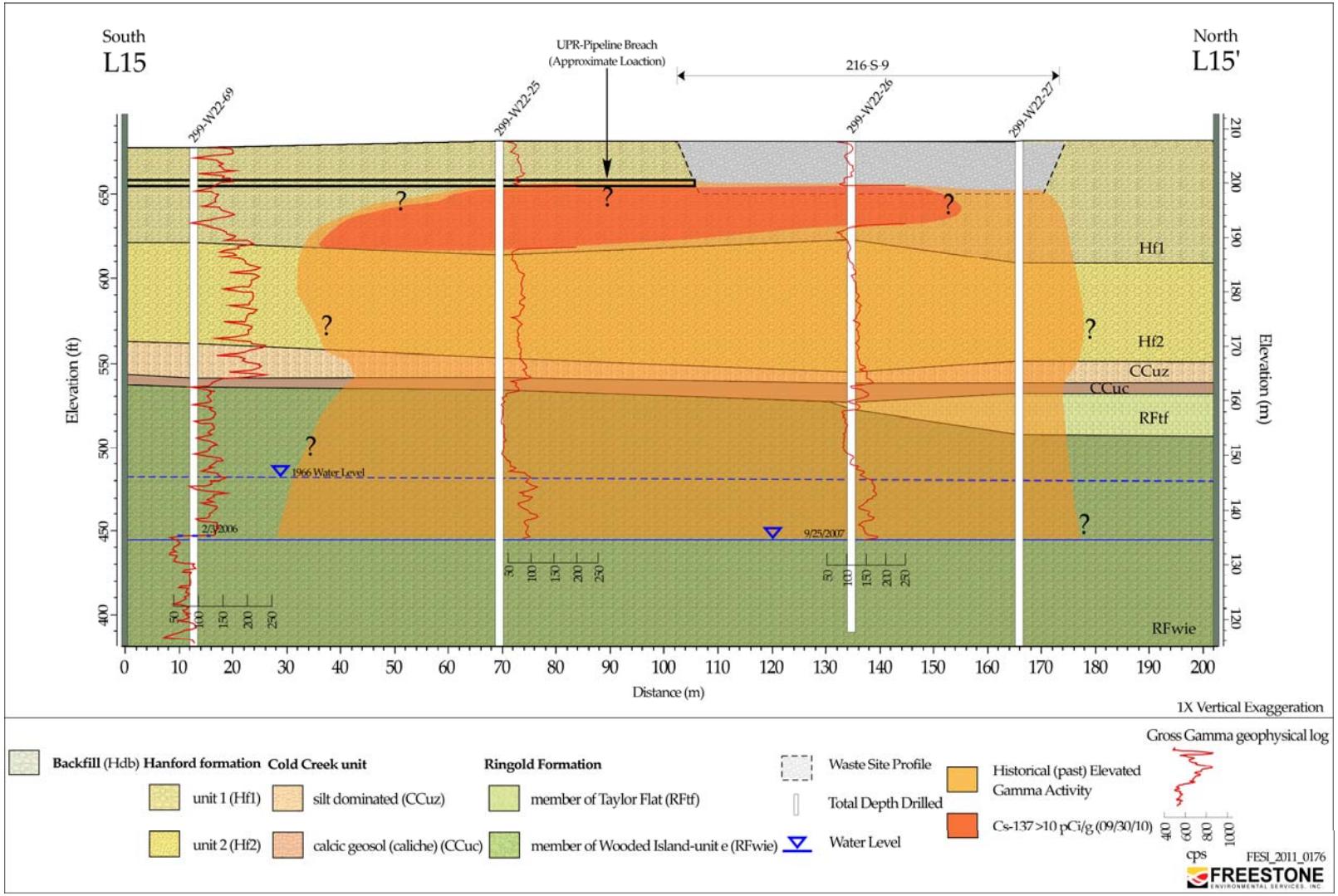

Figure 3-9. Depiction of Vadose Zone Contamination Proximal and Below the 216-S-9 and 216-S-23 Cribs using Spectral Gamma Logs and SGE

A similar calculation to estimate residual waste fluids below the 216-S-23 Cribs, based on a solid oval with dimensions 72 m (236.2 ft) E-W, 85 m (279 ft) N-S, and a thickness of 54.3 m (178 ft) yields a lateral spread pore volume of 1.3, suggesting that about 77 percent of the waste disposed to the 216-S-23 Crib could still reside within the vadose zone. Based on historical groundwater data and the gross gamma logs at the historical monitoring wells, wastes disposed to 216-S-23 Crib did reach the water table so the estimate that 23 percent might have reached the water table could be realistic.

Because there are no direct measurements of residual nitrate, Tc-99, I-129, chromium, or uranium in the vadose zone sediments below the 216-S-9 and 216-S-23 Subregion, there is no objective way to measure the inventories of these key mobile contaminants in the vadose zone. The key point of the lateral spread calculations is to suggest that a large percentage of the masses of chemicals and radionuclides disposed of to the two cribs could remain in the vadose zone sediments.

3.1.5 S Tank Farm

The S Tank Farm is directly west and upgradient of the 216-S-9 Crib. Any waste liquids released from the S Tank Farm that reach the water table would flow under the contaminated vadose zone below the 216-S-9 Crib and would appear at downgradient groundwater monitoring wells destined to monitor the crib. Thus, impacts of the S Tank Farm on the S Complex Area Subregion #1 conceptual model need to be considered.

Based on the most current tank leak assessment activities, only the 241-S-104 tank appears to have released waste that has reached the deep vadose zone (RPP-RPT-48589). RPP-RPT-48589 also presents substantial evidence to suggest that the release from 241-S-104 was likely a spare inlet overflow not a leak from the tank. Table 3-2 shows the volume of liquids released and the masses thought to be present in the liquids along with the same information for the 216-S-9 and 216-S-23 Cribs (excerpted from Table 3-1). Tank S-104 released almost 30 times as much Tc-99 and 50,000 times as much chromium and about half as much nitrate, about one-tenth as much I-129 and one-twentieth as much uranium as the two cribs combined. As discussed in Section 5, it appears that waste liquids from 241-S-104 did reach groundwater and that the Tc-99 and chromium groundwater plumes downgradient of both the S Tank Farm and 216-S-9 Crib are likely sourced from 241-S-104.

There are no sediment characterization boreholes inside the S Tank Farm fence and the few direct push probe holes south of the S Tank Farm (locations shown on Figure 3-10) are too far away from 241-S-104 tank to find lateral spread of the vadose zone plume. The sediment characterization data from the probe holes shown as green dots on Figure 3-10 were obtained at depths between 13.7 and 49 m (45 and 161 ft) bgs (generally three depths per probe hole). The two probe holes C7738 (north of tank SX-101) and C7742 (farther to the northeast of tank SX-101) did show some water extractable nitrate varying between 7 and 16 μg/g sediment and acid-extractable Tc-99 (varying between 0.7 and 3 pCi/g). Details can be found in RPP-47274 and Advanced Technologies and Laboratories International (ATL) Document No. 20100311, *Final Analytical Report for Soil Samples in Support of an Interim Barrier Southeast of S Farm, Bordering SX Farm.*

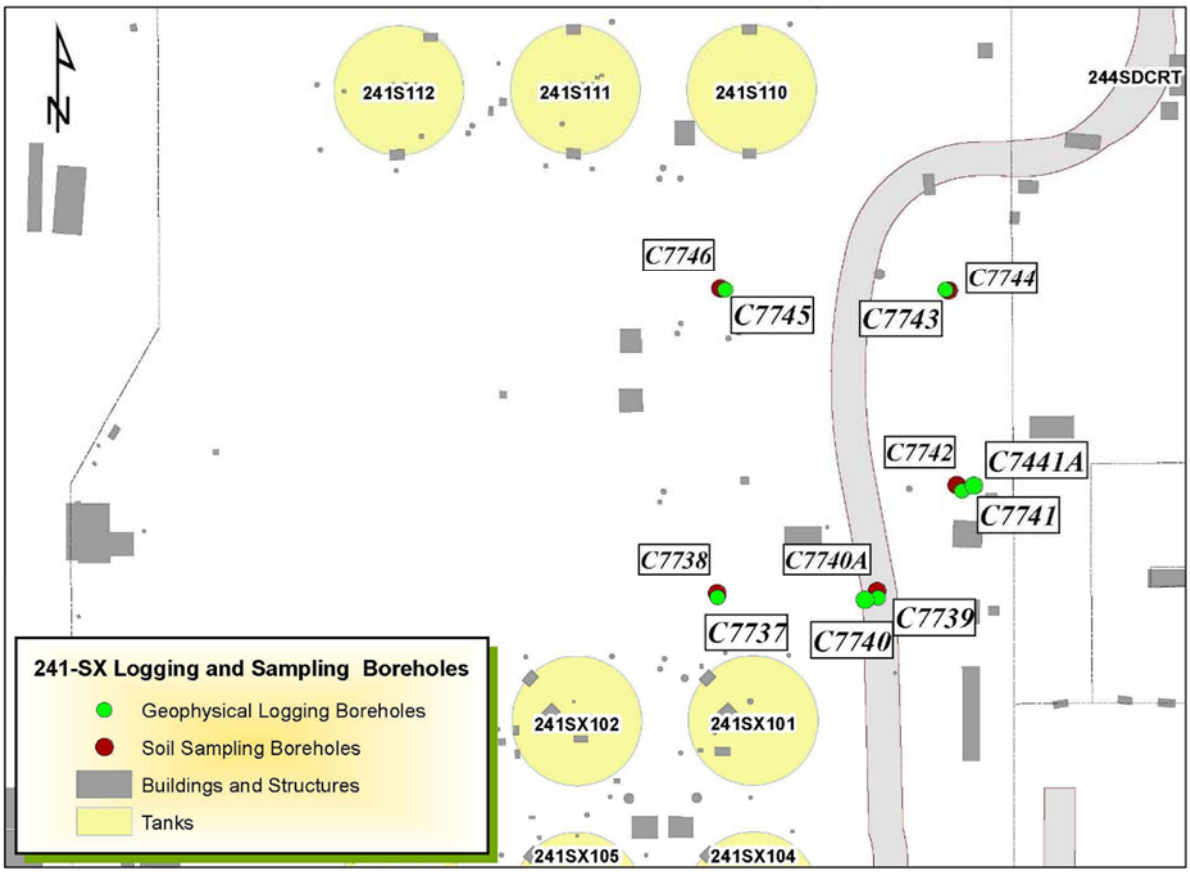

Figure 3-10. Location of Direct Push Probe Holes South of S Tank Farm

Table 3-2. Tank 241-S-104 Comparison with 216-S-9 and 216-S-23 Cribs

	216-S-9 & 216-S-23	241-S-104	241-S-104/ 216-S-9 & 216-S-23 Total	216-S-9 & 216-S-23% of Total S Complex Area	241-S-104 % of Total S Complex Area
Total Volume Released (ML)	**83.65**	0.0908	1.09E-03	18.2	0.02
Mass Released (kg)					
Sodium (Na)	1185.9	443.9	1185.9	62.6	37.4
Nitrate (NO_3)	**43698.0**	**1913.2**	**43698.0**	**95.6**	**4.4**
Nitrite (NO_2)	1696.5	1696.5	1696.5	0.0	100.0
Phosphate (PO_4)	0.000	0	0		
Sulfate (SO_4)	0.001	1.01E-03	0.001	0.0	100.7
Fluorine (F)	0.000	0	0		
Uranium (U)	**275.6**	**1.57E-05**	**275.6**	**100.0**	**0.0**
Chromium (Cr)	**0.001**	**1.28E-03**	**1.28E-03**	**0.0**	**100.0**

Table 3-2. Tank 241-S-104 Comparison with 216-S-9 and 216-S-23 Cribs

	216-S-9 & 216-S-23	241-S-104	241-S-104/ 216-S-9 & 216-S-23 Total	216-S-9 & 216-S-23% of Total S Complex Area	241-S-104 % of Total S Complex Area
Activity Released (Ci)					
Cobalt-60	0.003	42.395	1.36E+04	0.01%	95.15%
Iodine-129	**0.029**	**0.004**	**1.32E-01**	**36.0**	**4.8**
Technetium-99	**0.104**	**2.880**	**2.78E+01**	**0.3**	**8.4**
Tritium	675.4	1029.1	1.52E+00	21.0	32.1
Plutonium-238	0.198	0.824	4.16E+00	17.6	73.4
Plutonium-238	2.9	32.2	1.11E+01	7.7	85.1
Cesium-137	48.3	6550.9	1.36E+02	0.1	9.4

Note: The volume and inventories are estimates for S-9 and S-23 from RPP-26744, *Hanford Soil Inventory Model, Rev. 1*, and for S-104 from RPP-RPT-48589, *Hanford 241-S Farm Leak Assessment Report.*

Cobalt-60, tritium, and cesium-137 activities decay corrected to 9/30/2010.

The five potentially mobile contaminants of concern are in **bold type.**

ML = Mega (million) liters

The available soil resistivity data (RPP-RPT-48589) concluded there is a vadose zone plume of low resistivity surrounding the 241-S-104 tank (Figure 3-11). Inverse modeling of the raw data suggest the vertical extent of the low resisitivity (high salt waste) could have reached groundwater[7].

The low resistivity/high conductivity region appears to originate near tank 241-S-104 at about 6 m (20 ft) bgs in the 4 or 5 o'clock position from the north (i.e., to the southeast) near the tank edge Figure 3-11 for lateral extent) and continues downward in a west southwesterly direction in the vadose zone, most likely following the dip direction of the vadose sediments, toward the water table (Figure 3-12). More details are found in RPP-RPT-30976, *Surface Geophysical Exploration of S Tank Farm at the Hanford.*

[7] Although RPP-RPT-48589 suggests that the low resistivity (2-5 ohm-m region) may have reached the water table, RPP-RPT-30976 only discusses the fact that the lowest resistivity (1-2 ohm-m) region did not reach the water table. It is unclear whether the main authors of RPP-RPT-30976 wanted to make any conclusions on the meaning of the 2-5 ohm-m region in their modeled data.

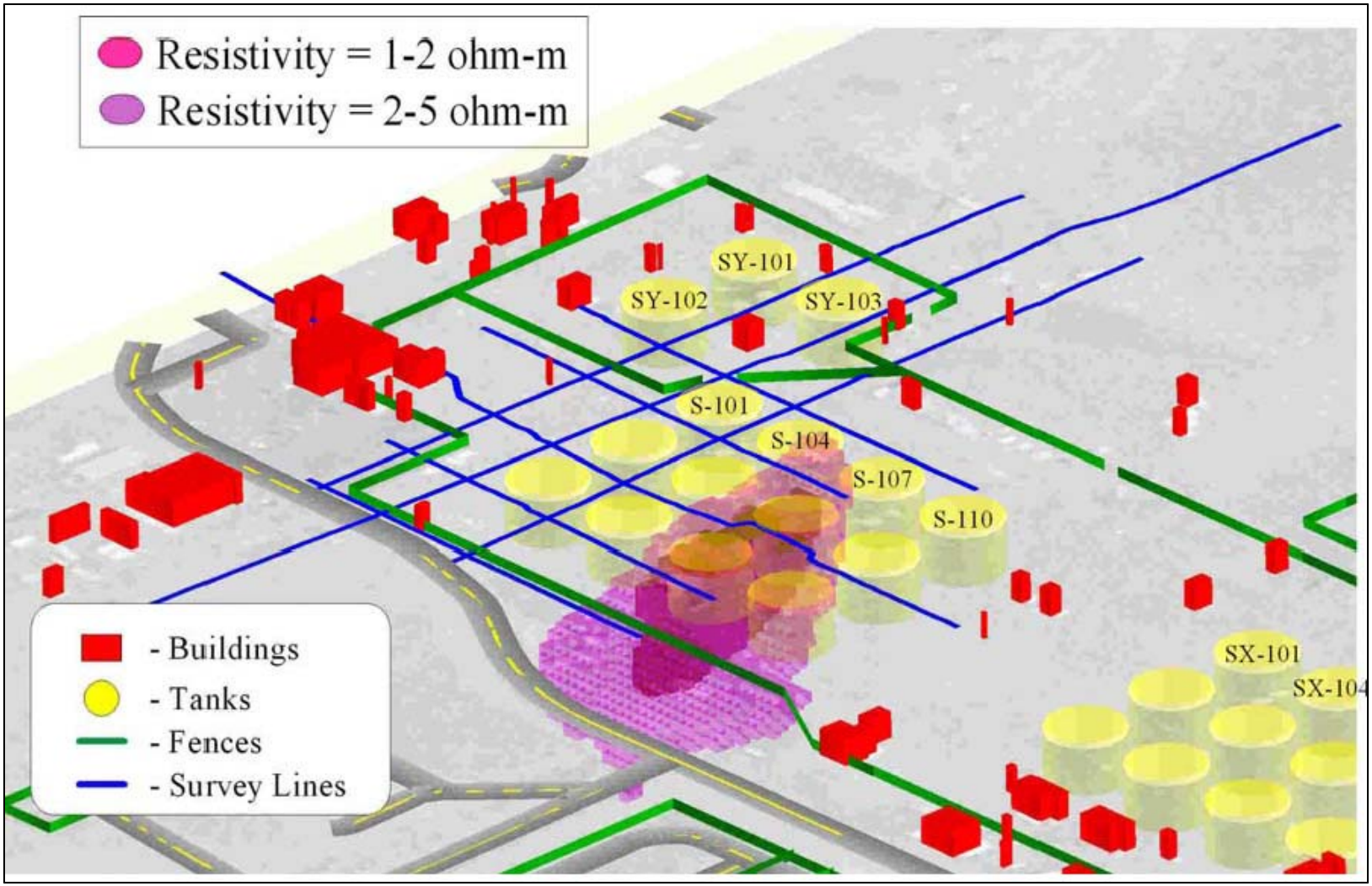

Source: RPP-RPT-48589, *Hanford 241-S Farm Leak Assessment Report*.

Figure 3-11. Estimated Lateral Extent of Contamination below S Tank Farm Based on Soil Resistivity Data Looking Northeast

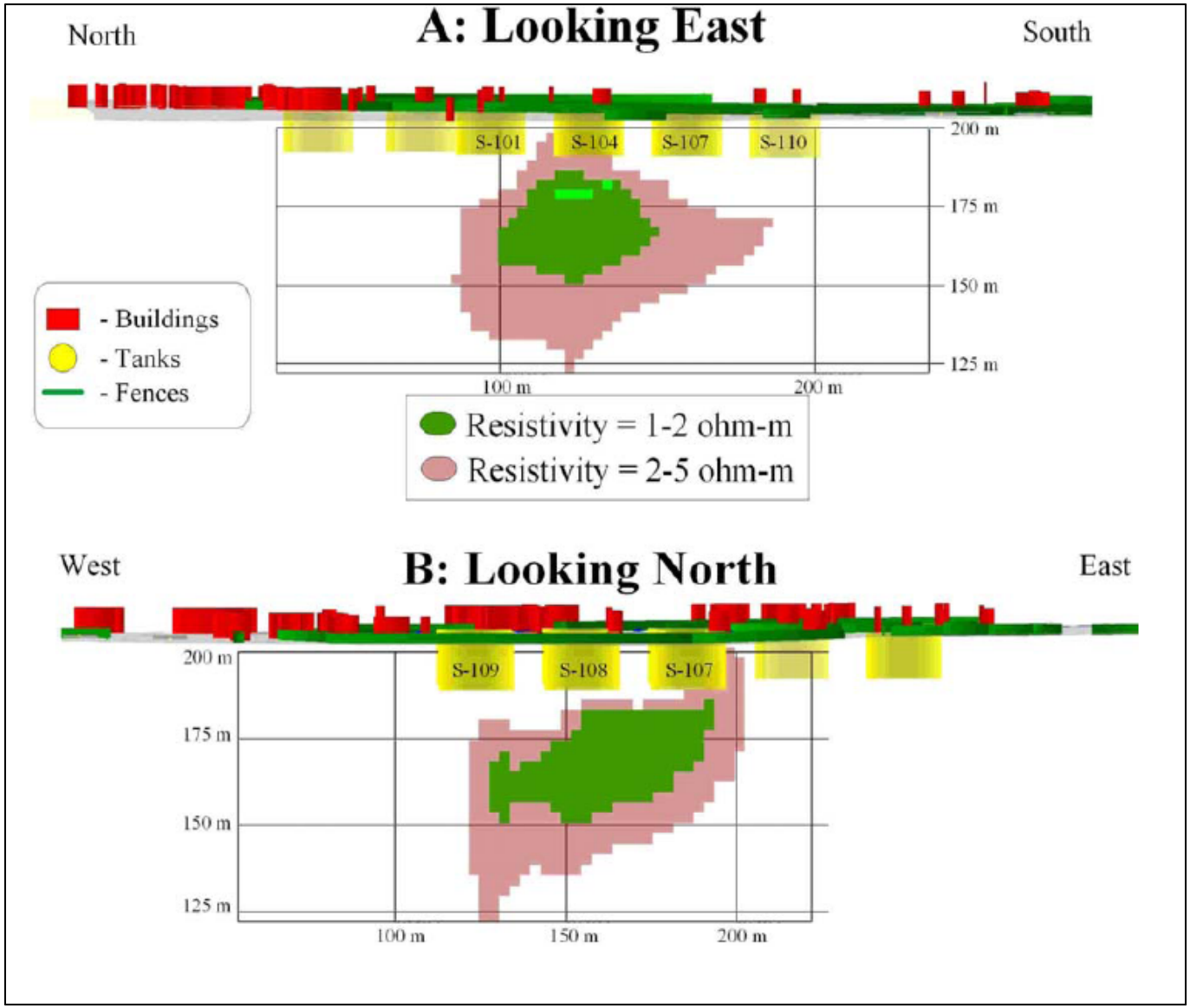

Figure 3-12. Estimated Vertical Extent of Contamination Below S Tank Farm based on Soil Resistivity Data

The only other available data to estimate the location of vadose zone contamination within the S Tank Farm is gamma logging data from dry wells surrounding the tanks and a dry well-to dry well soil electrical resistivity survey. The S Tank Farm gamma logging data are available in RPP-RPT-48589. Review of this report suggested that the only significant signs of gamma contamination below the base of tanks in the S Farm occurred at dry Well 40-04-05 (southeast) of 241-S-104. This dry well was drilled in May 1970 (after the leak) to 30 m (100 ft), then deepened in May 1973 to 41 m (135 ft) bgs. A 1991 spectral gamma log shows measurable cesium-137 from 0 to 6.7, 8.2 to 29.6, and 30 to 41 m (0 to 22, 27 to 97 and 100 to 135 ft) bgs. From 18.0 to 40.8 m (62 to 134 ft) bgs, the analysts could not determine if cesium-137 was truly present in the sediments or was drag down of some of the very high activity at 13 to 13.4 m (43 to 44 ft) bgs below tank foundation. All the available gamma logging data for the S Tank Farm has been previously tabulated and reviewed in RPP-7884, *Field Investigation Report for Waste Management Area S-SX* (Vol. 1, Main Text, and Appendices A-C); GJO-97-31-TAR, GJO-HAN-17, *Hanford Tank Farms Vadose Zone S Tank Farm Report*; and GJO-97-31-TARA, GJO-HAN-17, *Hanford Tank Farms Vadose Zone, Addendum to the S Tank Farm Report.*

The key points from the available S Tank Farm gamma logging and soil electrical resistivity information is that there is a vadose zone plume of tank related waste in the subsurface surrounding and below the 241-S-104 tank. Some of the waste may have reached the groundwater. The more immobile cesium-137 may be in the formation as deep as 41 m (135 ft) bgs, the total depth of the available dry wells surrounding 241-S-104. The available data do not allow any estimate of the sediment concentrations of the mobile contaminants of interest. If one-tenth of the tank footprint is the active area through which the waste is released, and assuming that the S Tanks bottoms are 12.8 m (42 ft) bgs and that the fluids fill 25 percent of the vadose zone below the tank, about 0.5 ML (0.13 Mgal) of leaked tank liquor could be retained in the vadose zone during the active waste release period. Further, after years of gravity draining to a final volumetric moisture content of 10 percent, 0.2 ML (0.05 Mgal) could be retained. For a larger footprint or porosity, proportionally more fluids could be retained during the leak period. The volume of fluids released by the 241-S-104 tank is estimated at 0.09 ML (0.02 Mgal); thus, it is reasonable to assume that the entire inventory of key contaminants shown in Table 3-2 still resides in the vadose zone below 241-S-104 tank. For conservative purposes, the current best estimate of residual contamination within the vadose zone below the S Tank Farm will be set equal to the masses tabulated in Table 3-2, which essentially suggests that all the released mass is still present despite the fact that groundwater plumes sourced to the S Tank Farm have been present for at least the past decade. Chapter 6 will provide an estimate for the mass of these mobile contaminants currently in the groundwater so a comparison with the mass released can be made.

3.2 Subregion 2 – 216-S-21 and 216-S-25 Cribs

This subregion is located south and west of Subregion 1 and west of the SX Tank Farm (Figure 1-1. This subregion contains two inactive waste disposal facilities, 216-S-21 and 216-S-25 Cribs (Figure 3-13. Subregion 2 – Location of the 216-S-21 and 216-S-25 Cribs, S Complex Area) that are part of the conceptual model effort. The SX Tank Farm is included in the conceptual model for this subregion as it is downgradient from the two inactive cribs.

3.2.1 Facility Description, Source Details, and Inventory Released

Table 3-3 shows the SIM, Rev. 1 database (RPP-26744) details for the two cribs over their lifetimes. Other details, such as yearly values for chemicals and radionuclides released and facility dimensions and depths to water table, are found in Appendix A.

The 216-S-21 Crib is located northwest of the 241-SX Tank Farm, due west from the southernmost row of tanks in 241-S Tank Farm and north of the 216-S-25 Crib. It was used in November 1954 through either February 1969 (SIM, Rev. 1 [RPP-26744]) or perhaps December 1970 (WIDS) to accept mainly condensates recovered during cooling of the stored SX tank wastes using air circulators.

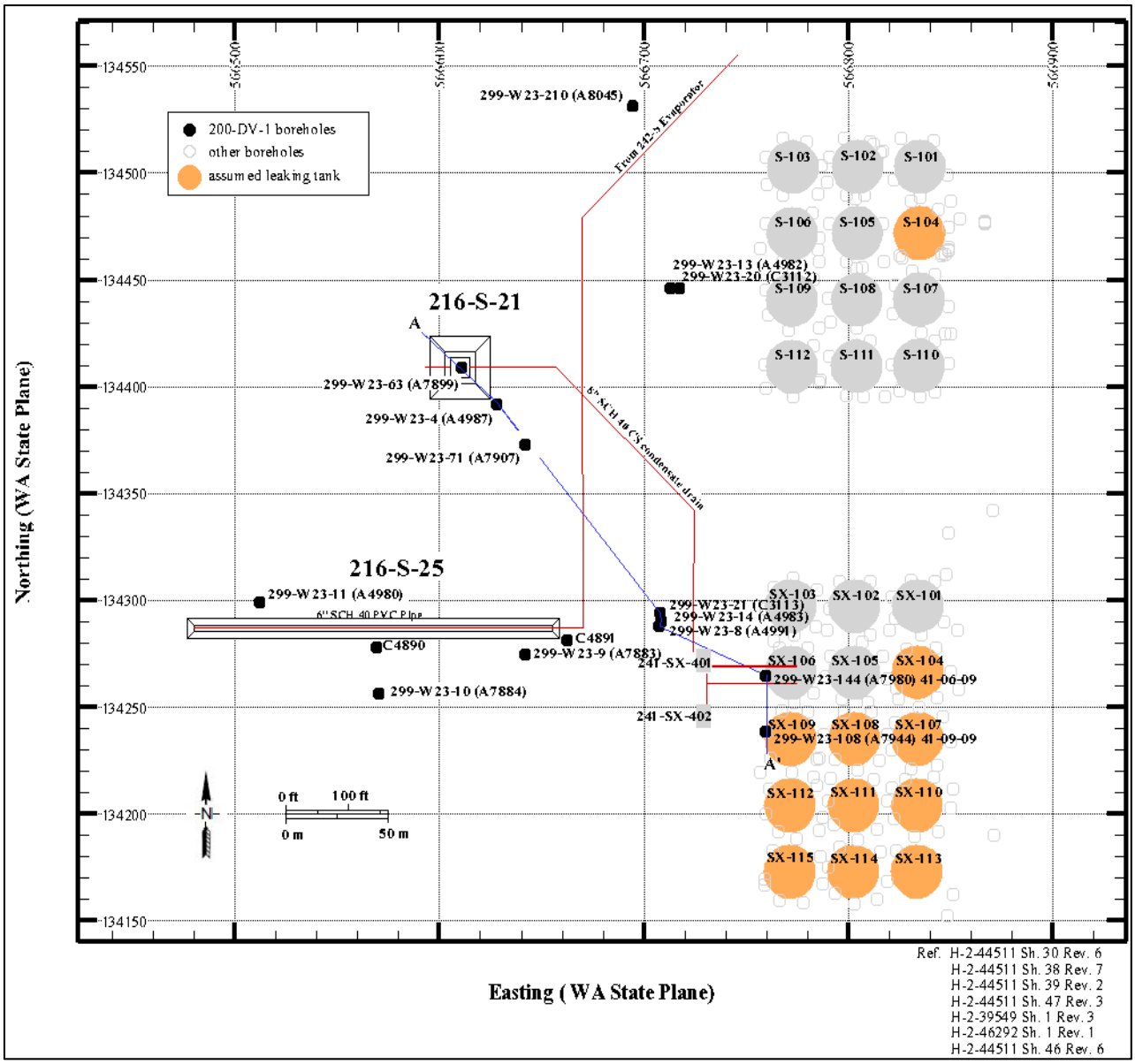

Figure 3-13. Subregion 2 – Location of the 216-S-21 and 216-S-25 Cribs, S Complex Area

Table 3-3. Masses Released over S-21 and S-25 Cribs Lifetime and Percent of Total Released to S Complex Area

	216-S-21	216-S-25	Subregion Totals	216-S-21 % Subregion	216-S-25 % Subregion	216-S-21 & 216-S-25% of Total S-SX Complex
Total Volume Released (ML)	87.1	288.0	375.1	23.2	76.8	81.7
Mass Released (kg)						
Na	712.6	925.0	1637.7	43.5	56.5	1.6
NO_3	**491.4**	**222643.7**	**223135.1**	**0.2**	**99.8**	**61.3**
NO_2	207.2	0.0	207.2	100.0	0.0	0.6
PO_4	0.10	3905.5	3905.6	0.0	100.0	99.7
SO_4	1248.9	3877.2	5126.1	24.4	75.6	3.58
F	21.9	427.3	449.2	4.9	95.1	99.8
U	**0.11**	**0.69**	**0.8**	**13.4**	**86.6**	**0.3**
Cr	**50.8**	**139.7**	**190.5**	**26.7**	**73.3**	**14.1**
Activity Released (Ci)						
Cobalt-60	9.339E-03	6.457E-05	9.403E-03	99.3	0.7	0.02
Iodine-129	**3.233E-04**	**0.000E+00**	**3.233E-04**	**100.0**	**0.0**	**0.4**
Technetium-99	**2.108E-01**	**0.000E+00**	**2.108E-01**	**100.0**	**0.0**	**0.6**
Tritium	1.469E+03	2.094E+03	3.563E+03	41.2	58.8	67.2
Plutonium-238	3.305E-03	9.470E-03	1.278E-02	25.9	74.1	1.1
Plutonium-239	5.990E-02	1.385E-01	1.984E-01	30.2	69.8	0.5
Cesium-137	5.016E+02	1.838E-05	5.016E+02	100.0	0.0	0.7

Notes: The volume and inventories are estimates for S-21 and S-25 are from RPP-26744, *Hanford Soil Inventory Model, Rev. 1.*

Cobalt-60, tritium, and cesium-137 activities decay corrected to 9/30/2010.

The five potentially mobile contaminants of concern are in **bold type**.

ML = mega (million) liters

The 216-S-21Crib received waste through an 8 in. schedule 40 carbon steel pipeline originating from the 241-SX-401 condenser facility that lies west of the 241-SX-106 tank. The waste is low in salt, is neutral to basic, and mainly consisted of sodium and ammonium nitrate.

This waste site consists of a 4.9 m (16 ft) by 4.9 m 16 ft) square wooden crib box. This crib box sits in a gravel layer in the bottom of a square pit. The rest of the pit is backfilled. The bottom dimensions of the excavation for the crib are 15.2 m (50 ft) by 15.2 m (50 ft) by 6.7 m (22.1 ft) deep. The top of the excavation had dimensions of 21.3 m (70 ft) by 21.3 m (70 ft). There is either 2.5 m (8.25 ft) of gravel

backfill within the crib and excavation according to WIDS or 3 m (10 ft) according to CP-49279 waste site drawings. According to WIDS, the site was interim stabilized in 1991 with 0.3 to 0.6 m (1 to 2 ft) of contaminated material and clean backfill may have been placed over the crib. It is not known if the reported 2.5 m (8.25 ft) of backfill reported in WIDS includes the possible additional backfill material. A borehole (299-W23-63 [A7899]) was drilled through the center of the crib but there is no record of sediment characterization data in the EDA database.

The 216-S-25 Crib is located west of the northern row of tanks in the 241-SX Tank Farm and south of the 216-S-21 Crib. The bottom dimensions of the waste site excavation are 175.3 m (575 ft) long by 3.1 m (10 ft) wide and 3.1 m (10 ft) deep. The slope of the excavation is 1:1 (WIDS) such that the top dimensions at the ground surface were 177.6 by 5.5 m (583 ft by 18 ft) wide. A 15.2 cm (6 in.) perforated polyvinyl chloride pipe serves as the distributor pipe throughout the length of the excavation. The bottom of the crib is filled with 1.2 m (4 ft) of gravel with the distributor pipe being 2.1 m (~7 ft) bgs. Above the gravel fill is backfill sediments from the excavation. An underground 10.1 cm (4 in.) pipeline from the 242-S evaporator building enters the crib at the east end. In 1984, the pipeline from the 241-SX-402 condenser was tied into the 216-S-25 pipeline (WIDS).

The 216-S-25 Crib operated from 1973 to 1980 and received the condensate wastes. In 1985, the crib also received effluent (31.54 ML) from a pump and treat effort to extract U-238 from groundwater underneath the 216-U-1 & -2 cribs. The 216-S-25 Crib might also have received waste from the 242-S Evaporator building and the 241-SX-402 Condenser facility in 1985. SIM, Rev. 1 (RPP-26744) does note contributions of two types of waste in 1985. Table 3-3 shows the estimated volume of waste, the masses of chemicals and radionuclides disposed in the two cribs as a percentage of the total liquid waste disposed of or released via SST and associated piping leaks to the entire S Complex Area. The total volume of waste disposed in these two cribs represents ~82 percent of the total volume of waste released to the entire S Complex Area and the volume of waste released to 216-S-25 Crib represents 63 percent of all waste released (0.817 × 0.768) released to the S Complex Area.

Based on the bottom dimensions for 216-S-21 Crib, a depth to groundwater from the bottom of the crib at the time of active disposal of 51.86 m (170.2 ft) and an assumed volumetric water content of 25 percent, the volume of liquid waste disposed would represent 29 pore volumes of fluid. Using a conservative estimate that assumes that effluent percolated directly beneath the crib footprint to the water table with no lateral spreading, the wastes would have affected groundwater.

The 216-S-25 Crib received almost all the phosphate and fluoride and about 60 percent of the nitrate and 10 percent of the chromium released in the S Complex Area. However, the radionuclide content of waste disposed to the 216-S-25 Crib was quite low for all nuclides but tritium. About 40 percent of all tritium released to the subsurface from the facilities constituting the S Complex Area was disposed into the 216-S-25 Crib. The percentages for the key mobile radionuclides, plutonium, and cesium-137 were between 0 and 0.8 percent, essentially inconsequential. The 216-S-21 Crib received about 18, 5, and 28 percent of the total sulfate, fluoride, and tritium, respectively, released in the S Complex Area but less than 1 percent of any other chemical and radionuclides.

Based on the bottom dimensions for 216-S-25, a depth to groundwater from the bottom of the crib at the time of active disposal of 50 m (164 ft) and an assumed volumetric water content of 25 percent, the conservative estimate of the volume of liquid waste disposed would represent 43 pore volumes of fluid. Using this same conservative, no lateral spreading methodology used for previous comparisons, the wastes would have affected groundwater.

3.2.2 Subregion 2 – Hydrogeology for the 216-S-21 and 216-S-25 Cribs

This section provides the detailed hydrogeology used for the conceptual model development for the 216-S-21 and 216-S-25 subregion (Figure 3-14). This hydrogeologic summary focuses primarily on the stratigraphic units occurring in the vadose zone interval. The vadose zone underlying the 216-S-21 and 216-S-25 Cribs is approximately 70.1 m (230 ft) thick. The suprabasalt aquifer system in this area is estimated to be approximately 105 m (344.5 ft) thick. Aquifer thickness is inferred from a regional top of basalt map (PNNL-17913) since none of the wells in this area were drilled to basalt. Groundwater generally flows to the east-northeast (based on Figure 2-2 in DOE/RL-2010-11) beneath this subregion and is known to contain dissolved contaminants from past disposal facilities within the 200 West Area. Perched groundwater was not identified during review of borehole logs near the 216-S-21 and 216-S-25 Cribs. The Subregion 2 location map (Figure 3-14) illustrates the orientation of the two hydrogeologic cross sections (Figures 3-15 and 3-16).

The 216-S-21 and 216-S-25 Cribs are constructed in the near-surface Hanford formation. The bottoms of the 216-S-21 and 216-S-25 Cribs lie within the gravel dominated Hanford formation unit 1(Hf1) at 6.7 m (22.1 ft) and 3 m (10 ft) bgs, respectively (see Appendix A for facility dimensions and details).

A type log based on the geophysical logging data from Well 299-W23-8 and borehole log from Well 299-W23-14 provides the stratigraphic contact correlation within this subregion (Figure 2-14). Well 299-W23-14 is the only well in this subregion with a geologist's borehole log, and provides the best lithologic descriptions of the subsurface sediments. This well is included on the geologic cross section (Figure 3-16).

Except for the geologic log for Well 299-W23-14, geologic information for this subregion is limited to the driller's logs, most of which are extremely old and qualitative. More quantitative data, which is used to interpret stratigraphy, is available in the ROCSAN database in addition to the downhole geophysical logs (gross gamma and spectral gamma). A detailed description of the individual geologic units beneath the 216-S-21 and 216-S-25 Cribs follows.

3.2.2.1 Holocene Deposits

Most of the recent (Holocene age), fine-grained (eolian) sediment has been removed or highly disturbed in this subregion. Several meters of backfill are present across the subregion above the Hanford formation and located within the construction areas of 216-S-21 and 216-S-25 Cribs. The backfill is native Hanford formation (gravelly sand) material that has been recovered from several "borrow pits" on site (DOE/RL-2000-61). During crib construction, all natural layering/stratification was disrupted such that the backfill is rather homogeneous and featureless compared to the undisturbed Hf1 unit.

3.2.2.2 Hanford formation

The Hanford formation makes up the majority of the vadose zone sediment beneath the subregion, with a thickness of 37.8 m (124 ft). Both the Hf1 subunit (coarse-grained sandy gravel or gravel) and the Hf2 subunit (predominately sand) are present. The gravel-dominated Hf1 unit consists of poorly sorted sandy gravel to silty sandy gravel. Overall, the Hf1in this subregion is finer-grained: borehole log for 299-W23-14 indicates gravel content was at or below 40 percent, predominately fine-grained (less than 8 mm) and did not contain cobbles. The sand-dominated Hf2 unit consists of predominantly fine to very fine sand and silt though driller's logs and geophysical logging data (example noted on Figure 2-14) indicate the presence of discontinuous gravel lenses, with occasional cobbles noted. The top of the Hf2 unit generally dips to the south-southeast (PNNL-17913).

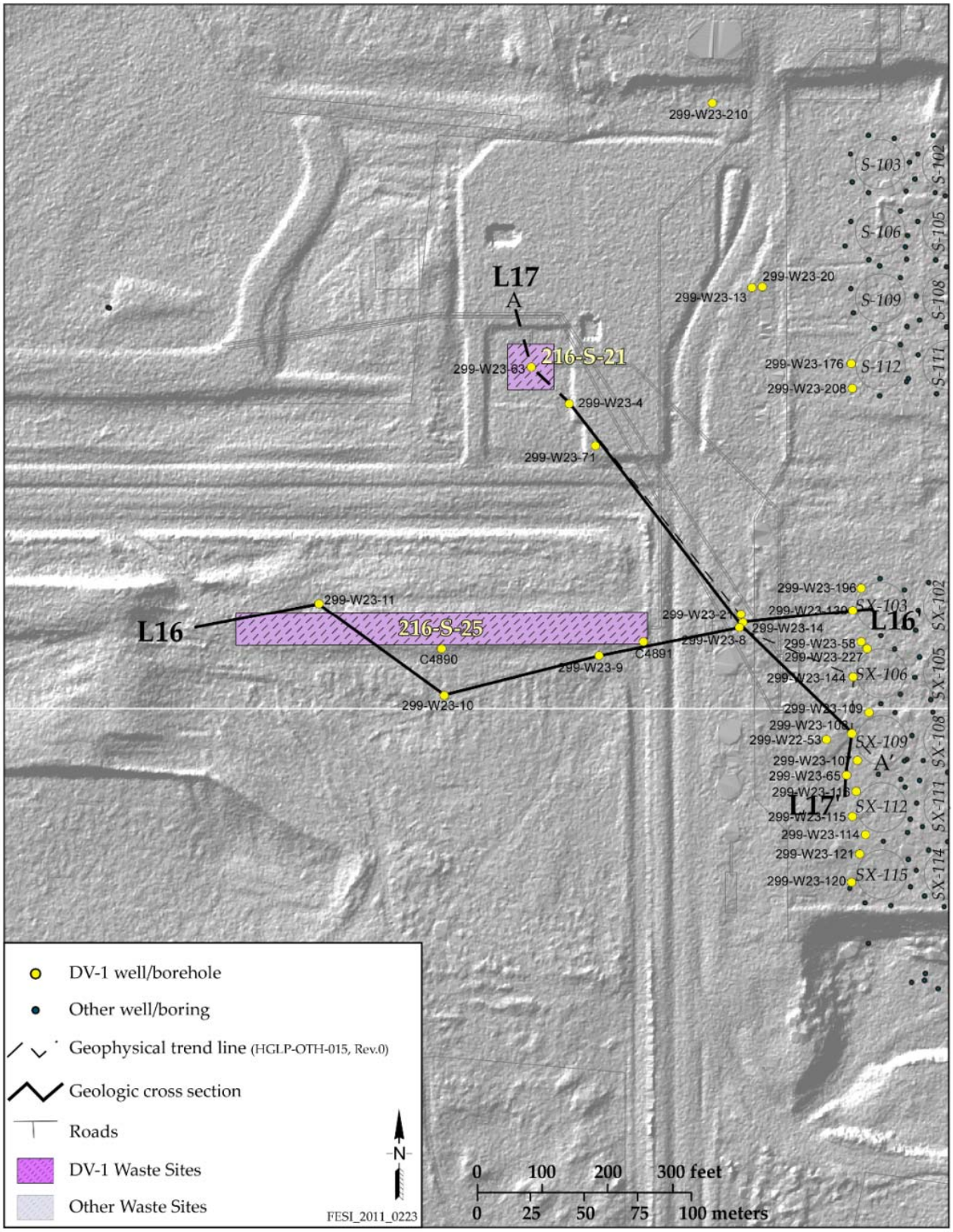

Figure 3-14. Subregion 2 – 216-S-21 and 216-S-25 Base Map, S Complex Area

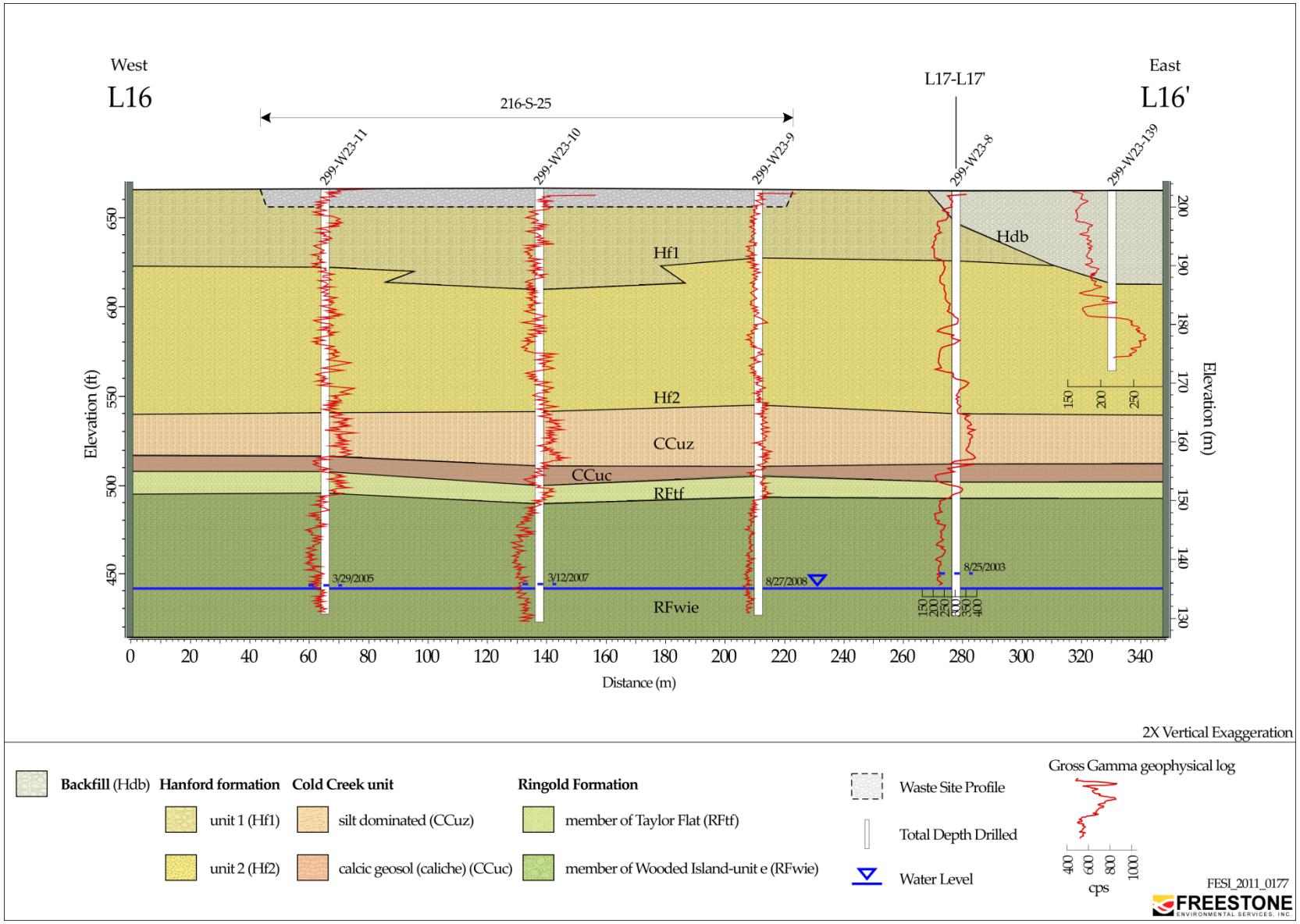

Figure 3-15. Subregion 2 – Hydrogeologic Cross Section L16-L16'

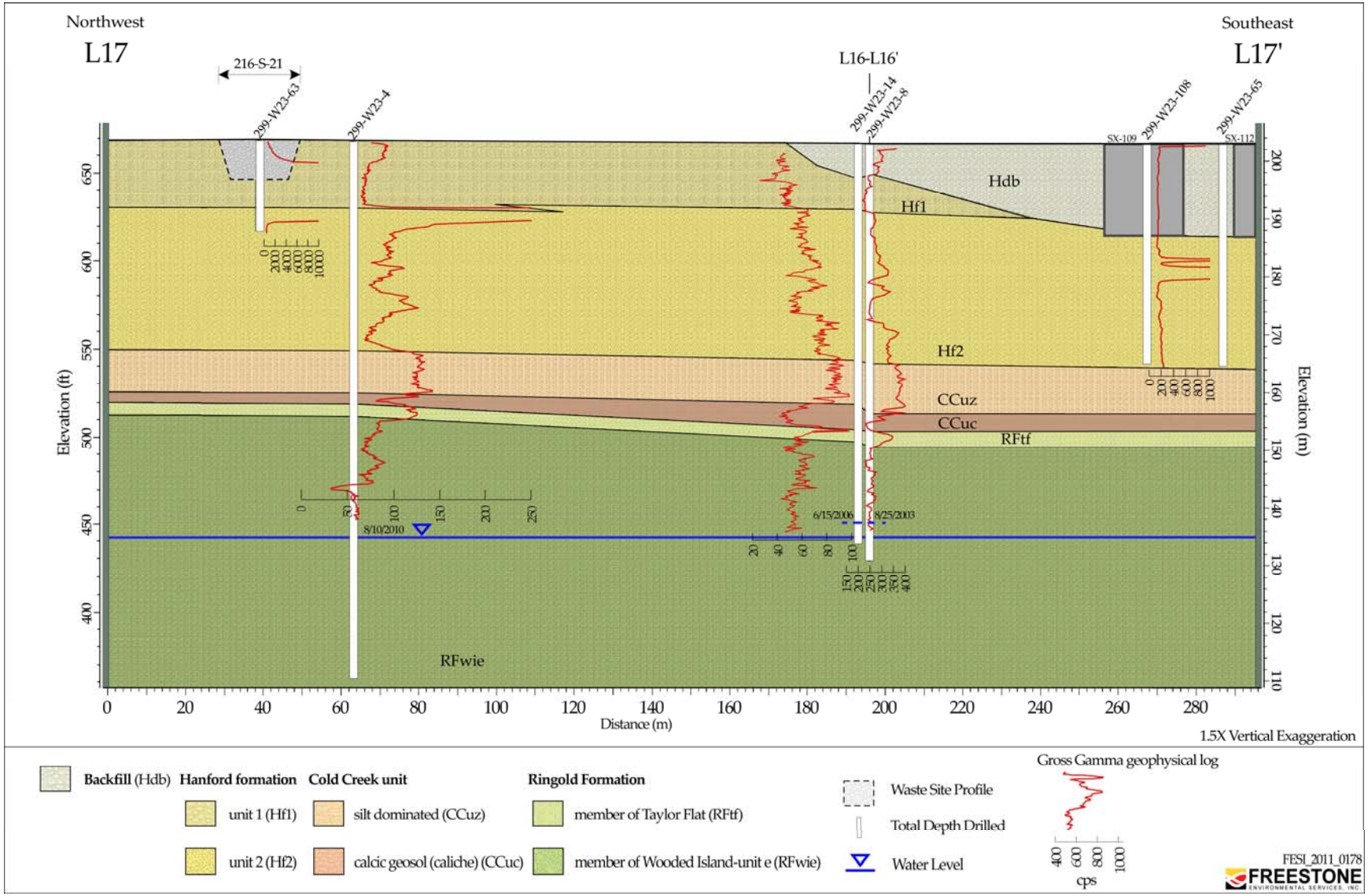

Figure 3-16. Subregion 2 – Hydrogeologic Cross Section L17-L17'

3.2.2.3 Cold Creek Unit

The CCu underlies the Hanford formation and consists of two subunits, the CCuz and the CCuc. Both the CCuz and CCuc are laterally continuous throughout the subregion. The upper and lower contacts of these subunits were largely defined using the spectral and gross gamma borehole geophysical log plots as shown in the stratigraphic type log (Figure 2-14). CCuz is generally indicated by the occurrence of "heavy silt" or "brown sand and silt" noted on the driller's logs and was described by a geologist (borehole log for 299-W23-14) as a dark yellowish-brown silt with "iron staining in places."

The CCuc is described as an unconsolidated, light olive-brown, silty sandy gravel in which "gravels were coated with calcium carbonate." The base of the CCuc beneath the calcium carbonate-rich layer consists of dark grayish-brown sand with a trace of gravel. SGLS geophysical logs from 299-W23-8 show only a single, relatively thin CCuc interval (Figure 2-14). The CCuz ranges in thickness from 7.3 to 10.4 m (24 to 34 ft) and CCuc ranges in thickness from 1.5 to 3.7 m (5 to 12 ft). The surface of both subunits are relatively flat (horizontal) beneath the subregion (Figure 2-11).

3.2.2.4 Ringold Formation

The total thickness of the Ringold Formation was not penetrated during drilling of the ten wells evaluated for the subregion. Based on geologic descriptions in the vicinity (PNNL-15955), the Ringold Formation is composed of units RFtf, RFwie, RFlm, and RFwia.

RFtf is present beneath the 216-S-25, even though it is missing over much of the area to the north, south, and west (PNNL-17913). The RFtf maintains a uniform thickness of ~3 m (10 ft) and is relatively flat (horizontal) beneath 216-S-25. The RFtf overlies the RFwie, which represents the lowermost Ringold Formation unit in the vadose zone. The contact between the RFtf and RFwie was sometimes difficult to distinguish from borehole or driller's logs due to the hard-tool, Becker Hammer, or Air Rotary drilling methods used in this area. Driller's logs described the RFwie formation as "very tightly packed" and containing "silt and brown sand with 4-in gravel." RFwie is described as well-rounded pebble-to-cobble gravel with a fine- to coarse-grained sand matrix. The sediments in the RFwie are variably consolidated. The RFwie is estimated to be approximately 82 m (249.9 ft) thick; the upper boundary of RFwie dips slightly toward the south or southeast beneath SX Tank Farm (PNNL-17913). The RFwie, RFlm, and RFwia comprise the suprabasalt aquifer system in this subregion. The RFlm and RFwia are not described in this report due to their occurrence deep in the saturated zone.

3.2.3 Subregion 2 – Vadose Zone Contamination Estimates for 216-S-21 and 216-S-25 Cribs

There are no quantitative data for direct measurements of contaminant concentrations in sediments from within or near the two cribs. The only information that can be used to estimate the vertical and horizontal spread of mobile contaminants from the two cribs are borehole geophysical logs of gross and spectral gamma taken through well casings of nearby boreholes and a soil resistivity field survey that was performed at the SX Tank Farm.

SGW-50194 provides an analysis of all historical and recent borehole geophysical logs for the S Complex Area. The following material is summarized from the report. The 216-S-21 Crib is characterized by Borehole 299-W23-63 that was drilled through the center of the crib to 15.5 m (51 ft) bgs. Gamma contamination was detected to the bottom of the borehole, which reached total depth in the Hf2 sand. The shallow portion of the 216-S-21 Crib is reasonably well characterized by this borehole. However, there is evidence from historical logs that the deep vadose zone may have been contaminated-a nearby borehole (299-W23-4) southeast of the crib indicated potential contamination by short-lived radionuclides to at least 50.9 m (167 ft) bgs. Current log data indicate remnants of cobalt-60 near this depth.

Further characterization beneath the 216-S-21 Crib may be necessary to determine the extent of deep vadose contamination.

At the 216-S-25 Crib borehole, geophysical gamma logs obtained in 1976 from nearby boreholes show no evidence of contamination. Since 1976, there have been no further measurements acquired in the boreholes close to 216-S-25; however, the crib remained in service until 1985. Additional characterization may be necessary to confirm that no significant contamination was introduced into the crib since 1976.

Soil resistivity measurements performed at the SX Tank Farm did allow for some interrogation of the subsurface under the 216-S-25 Crib but did not extend far enough to the northwest to interrogate the 216-S-13 crib adequately. Three reports describe the soil resistivity survey results for the SX Tank Farm: RPP-RPT-38322, *Surface Geophysical Exploration of the S and SX Tank Farms at the Hanford Site*; RPP-RPT-42513, *Surface Geophysical Exploration of the SX Tank Farm at the Hanford Site*; and RPP-RPT-47851, *Three-Dimensional Surface Geophysical Exploration of S/SX Tank Farm*. Interpretation of the soil resistivity results below the 216-S-25 crib is not provided in any of these reports and further review of these three reports concluded that soil resistivity modeling results for 216-S-25 do not indicate a strong electrical signature that can be correlated with past waste streams. The region below some of the surface electrode lines that were close to 216-S-25 Crib showed a subtle zone of low-to-intermediate resistivity beneath the 216-S-25. However, this feature is not imaged in several other surface lines, one of which parallels the southern edge of 216-S-25. Two other strong low-resistivity zones observed below two other north-south lines are tentatively interpreted as either buried infrastructure or some other non-216-S-25 related source.

3.2.4 Subregion 2 – Vadose Zone Conceptual Model for 216-S-21 and 216-S-25 Cribs

The conceptual model for the distribution of contaminants below Subregion 2 (216-S-21 and 216-S-25 Cribs) relies exclusively on historical borehole geophysical gross- and spectral gamma logs integrated with the hydrogeological conceptual model, and knowledge of the volumes of liquid released to each facility. The soil electrical resistivity survey information does not add any useful information on the location of anomalous moisture or moderate salt within the subsurface around the 216-S-21 or 216-S-25 Cribs.

Figure 3-17 shows the available boreholes/wells around the two cribs. Two boreholes at the 216-S-21 Crib provide the only characterization data available for this waste site. The borehole 299-W23-63 directly in the 216-S-21Crib only reaches 15.5 m (51 ft) bgs and the adjacent deeper well, 299-W23-4, provided useful gamma logs with short-lived gamma contamination observed historically down to 51 m (167 ft) bgs.

Using this gamma information and the geologic conceptual model for the subregion, Figure 3-18 portrays the estimated lateral extent of vadose zone contaminant for the 216-S-21 Crib, and Figure 3-19 shows the vertical extent of contamination detected based on the gamma logging results.

The conceptual model for contamination below and surrounding the 216-S-21 Crib suggests that contamination has spread laterally with a bias toward the south from the crib footprint, forming two concentric circles. The smaller represents the location of higher concentrations of more immobile (sorbing) contaminants, such as cesium-137, and the larger represents the extent and location of mobile contaminants. The estimated diameters of the lateral spread for these two concentric circles are ~36.5 and ~82.3 m (~120 and ~270 ft) compared to the surface dimensions of the 216-S-21 Crib of 21 m by 21 m (70 ft by 70 ft). Thus, the lateral spread for mobile contaminants is estimated to create an area ~12 times larger than the top of the crib excavation and ~25 times larger than the bottom of the crib excavation.

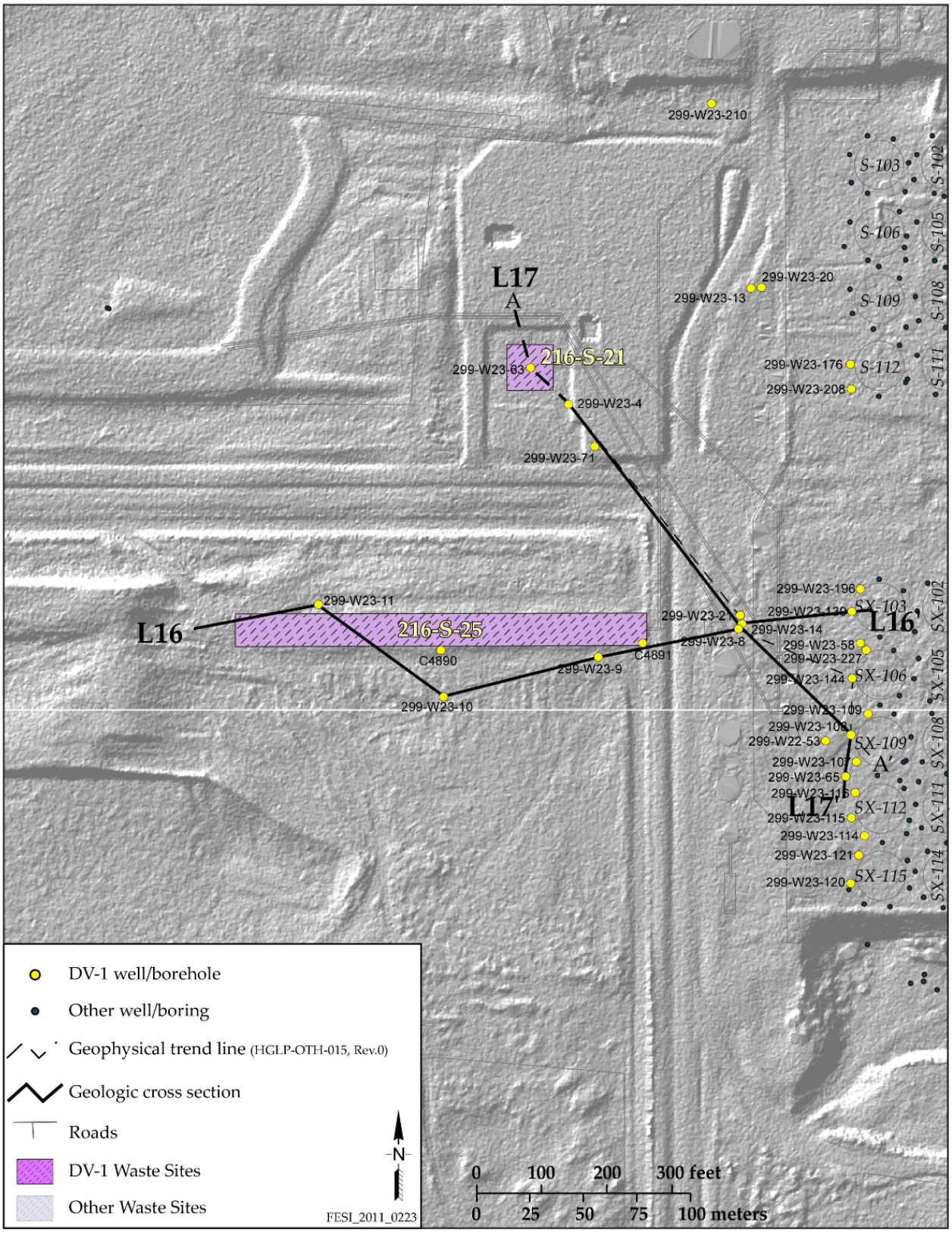

Figure 3-17. Subregion 2 – Location of 216-S-21 and 216-S-25 Cribs and Boreholes

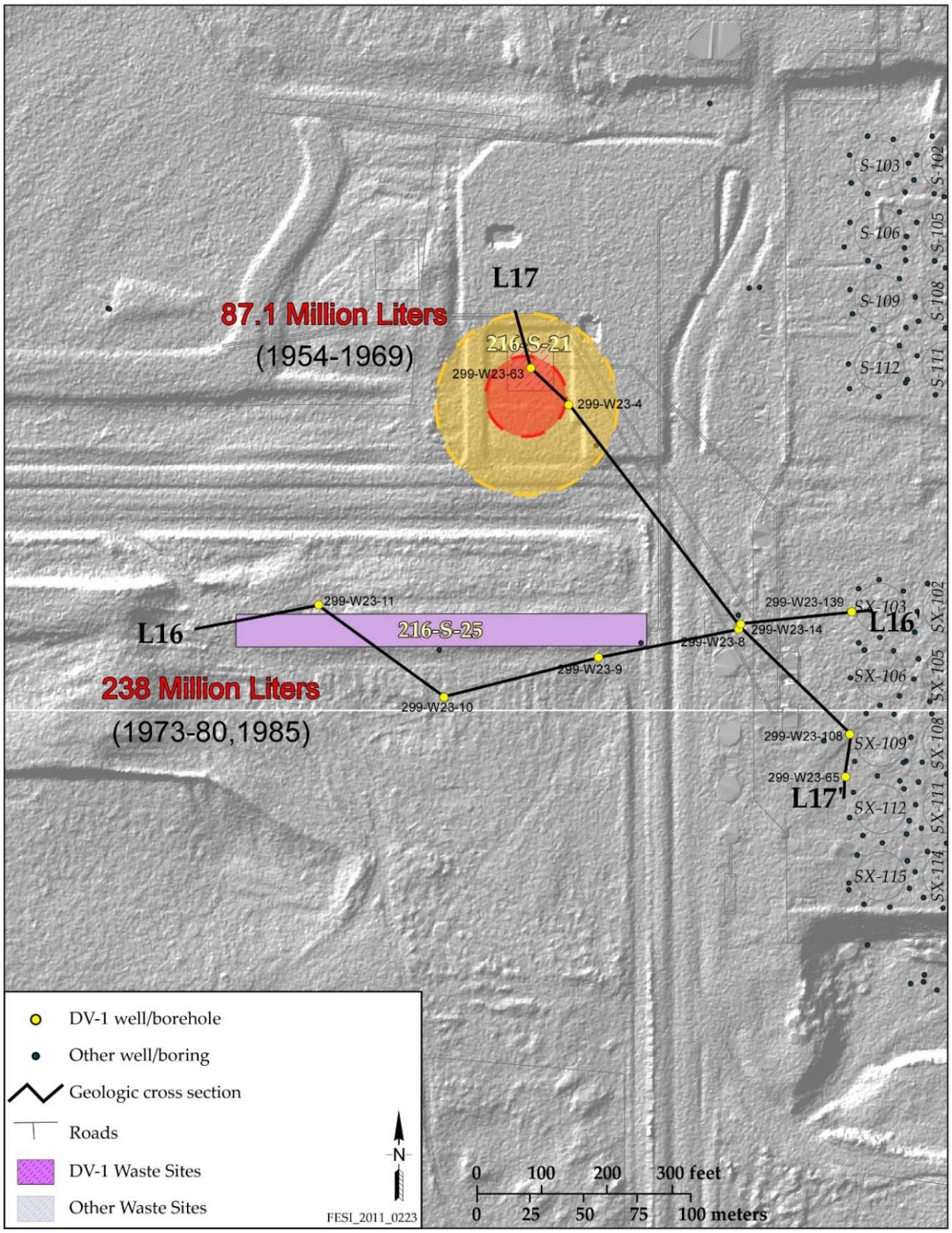

Note: The dark red-orange area represents the region with currently detectable cesium-137 ≥10 pCi/g contamination (less mobile) and the faint yellow-orange area represents the region of past historical gamma contamination (mobile short half-life [e.g., ruthenium-106]).

Figure 3-18. Subregion 2 – Conceptual Model for Lateral Spread of Residual Contamination in the 216-S-21 and 216-S-25 Cribs

The maximum vertical extent of mobile contamination is not defined (Figure 3-19) but is assumed to have reached the top of the CCuc where it may have been held up and, thus, did not reach the water table at the time of active disposal. Sorbing contaminants, such as cesium-137, are retained shallow (near 15 m [50 ft] bgs), not extending very far into the Hf2 just below the Hf1 (coarser) and Hf2 (typical Hanford sand) contact. Figure 3-19 also suggests that the lateral spread of contamination was not sustained at about 82.3 m (270 ft) at depth. The largest lateral spread likely occurred at the contact of the Hf1 and Hf2 subunits and the vertical spread was estimated to 58 m (~190 ft). Using a solid right cylinder configuration for the two estimates of lateral spread for the mobile constitutes of 82.3 and 58 m (270 and 190 ft) diameters and assuming that the vadose zone has drained to 10%vol moisture content, the total volume of liquid disposed to 216-S-21 Crib would represent between 3.2 and 6.4 pore volumes. This suggests that about two-thirds to 85 percent of the waste liquid disposed to 216-S-21 should have reached the groundwater and dispersed into a contaminant plume. For conservative purposes, it will be assumed that 33 percent of the inventories disposed to the 216-S-21 Crib are retained today in the vadose zone sediments.

At the 216-S-25 Crib, there was no elevated gamma observed in historical geophysical logs; however, the most recent was obtained in 1976, which is before the crib became inactive in 1985. The historical gross gamma logs for nearby boreholes are shown in Figure 3-20. The soil resistivity field surveys also are not useful in delineating the lateral and vertical extent of contamination. However, as shown in Table 3-3, the mass of mobile contaminants of interest disposed in the 216-S-25 Crib in comparison to the entire S Complex Area is not significant for any but nitrate (61 percent of total released nitrate was to 216-S-25 Crib) and chromium (10 percent of total released was to 216-S-25 Crib). Interestingly, 216-S-25 Crib also received almost all the fluoride released in the S Complex Area. Therefore, if elevated fluoride was observed in groundwater below the S Complex Area, it should be traceable back to wells proximal to the 216-S-25 Crib or east of this crib in the direction of groundwater flow. Assuming a lateral spreading that increases the impacted area beneath the crib by a factor of 10 or even 20 and assuming that the vadose zone drains to 10%vol, the volume of waste disposed to 216-S-25 Crib would represent between 5.4 and 10.8 pore volumes. Thus, between 80 and 90 percent of the disposed liquid should have reached the groundwater and dispersed into a groundwater contaminant plume.

Given the tenuous nature of all the vadose zone data available for the 216-S-21 and 216-S-25 Cribs, a conservative assumption is made that only one-third of the wastes disposed to the 216-S-21 Crib and one-fifth of the wastes disposed to the 216-S-25 Crib still reside in the vadose zone sediments above the current water table. However, the exact location both in vertical and lateral extent is not well defined.

3.2.5 SX Tank Farm

The SX Tank Farm is directly east and downgradient of the 216-S-25 Crib. Any waste liquids released from the 216-S-25 Crib that reach the water table would flow under the SX Tank Farm and might be difficult to differentiate from tank waste without some isotopic fingerprint technique. Such techniques are discussed in Chapter 7. In this subsection the impacts of the SX Tank Farm on the S Complex Area subregion 2 conceptual model is discussed.

The most current tank leak assessment activities, documented in RPP-ENV-39658, provide significant revisions to SIM, Rev. 1 (RPP-26744) as to which tanks in the SX Tank Farm released wastes, and the volumes and the masses of constituents released to the subsurface. Table 3-4 shows the volume of liquids released and the masses of key constituents thought to be present in the SX tanks liquids along with a comparison to the totals for 216-S-21 and 216-S-25 Cribs (excerpted from Table 3-3). Table 3-4 shows that 8 of the 15 SX tanks released fluids to the subsurface with SX-115, SX-108, and SX-112 releases being the largest (each greater than 10+05 L). From largest to least, the tanks that released (leaked) chemicals are SX-108, SX-115, and SX-112, respectively. For the two key radionuclides (Tc-99 and I-129), the order of release is SX-108, SX-112, and then SX-115. The SX Tank Farm releases of the

following constituents represent very high percentages for the entire S Complex Area: Tc-99 (91 percent), Cs-137 (90 percent), chromium (81 percent), sodium (80 percent), iodine (59 percent), and nitrate (20 percent).

Compared to the SX Tank Farm, the 216-S-21 and 216-S-25 Cribs contributed much lower masses of all these constituents, with the exception of nitrate. Therefore, if SX tank wastes, especially from the three releases (SX-108, SX-112, and SX-115), reached groundwater below the subregion, their contribution of the mobile constituents Tc-99, Cr(VI), sodium, and I-129 would dominate over any masses disposed to the two cribs that potentially affect groundwater.

Sediment characterization data are available for the vadose zone from below and around several of the SX tanks obtained by conventional and slant cable tool drilling and several direct push probe holes (Table 3-5). The locations of the boreholes and direct push probe holes are shown Figure 3-21 and Figure 3-22, respectively. As shown in Table 3-5, over 100 depth-discrete samples from 299-W23-234 were obtained near tank SX-109 from 7.6 m (25 ft) bgs to the water table and most were characterized for the key mobile contaminants as well as other macro cations and anions. For borehole 299-W23-19 (near tank SX-115), more than 200 depth discrete samples were obtained and most were characterized for the key mobile contaminants as well as other macro cations and anions from near the ground surface to almost the groundwater table. At 299-W23-64 (the slant borehole below SX-108), 24 depth-discrete sediment samples were obtained and characterized in detail from vertical depths representing 16.7 to 45.4 m (55 to 149 ft) bgs. The most useful direct push samples around the SX tanks consisted of 13 probe holes that each were sampled at two to four discrete depths between 14 to 47 m (46 and 154 ft) bgs. The direct push samples were characterized for the five key mobile contaminants and other macro cations and anions. All of the sediment characterization data gives direct information on the location, depth, and concentration of constituents in the vadose zone.

The results of the sediment characterization of the three boreholes are found in PNNL-13757-3, PNNL-13757-2, and PNNL-13757-4, respectively. The following summarizes key vadose zone characterization data.

The concentrations of the key mobile constituents in the vadose sediments as a function of depth are shown in Table 3-5. The available soil electrical resistivity field survey data suggest that the fluid released from SX-107, SX-108, SX-109, SX-111, and SX-112 and perhaps the three most southern tanks (SX-113 through SX-115) likely have commingled below the tanks into one vadose plume. Thus, comparing the vertical distribution and concentrations of mobile contaminants is reasonable. The two boreholes, 299-W23-234 (near tank SX-109) and 299-W23-64 (the slant borehole below SX-108), intercept the commingled plume. The electrical conductivity (EC) of sediment water extracts suggests that tank fluids dominate the pore water at the slant borehole to a depth of 39.3 m (129 ft) bgs, about 1.5 m (5 ft) into the CCuz silt subunit. The EC of the two deepest samples from the slant borehole does not drop to natural background levels, but the EC is significantly lower than all the shallower samples in the profile. Thus, the leading edge of the contaminant plume below SX-108 is below the total depth sampled, but the bulk of the salt is still above 39.3 m (129 ft) bgs. The EC of the water extracts from 299-W23-234 is elevated between depths of 25 and 38.7 m (82 and 127 ft) bgs and appears to return to near background levels at ~41 m (135 ft) bgs (see EC comparisons for all three boreholes in Figure 3-23). Based on the nitrate profile at borehole 41-09-39, which does show the whole extent of the plume, we estimate that the leading edge of the tank waste plume beneath tank SX-108 may have stopped at the contact of the CCuz and CCuc contact near 45.7 m (150 ft) bgs.

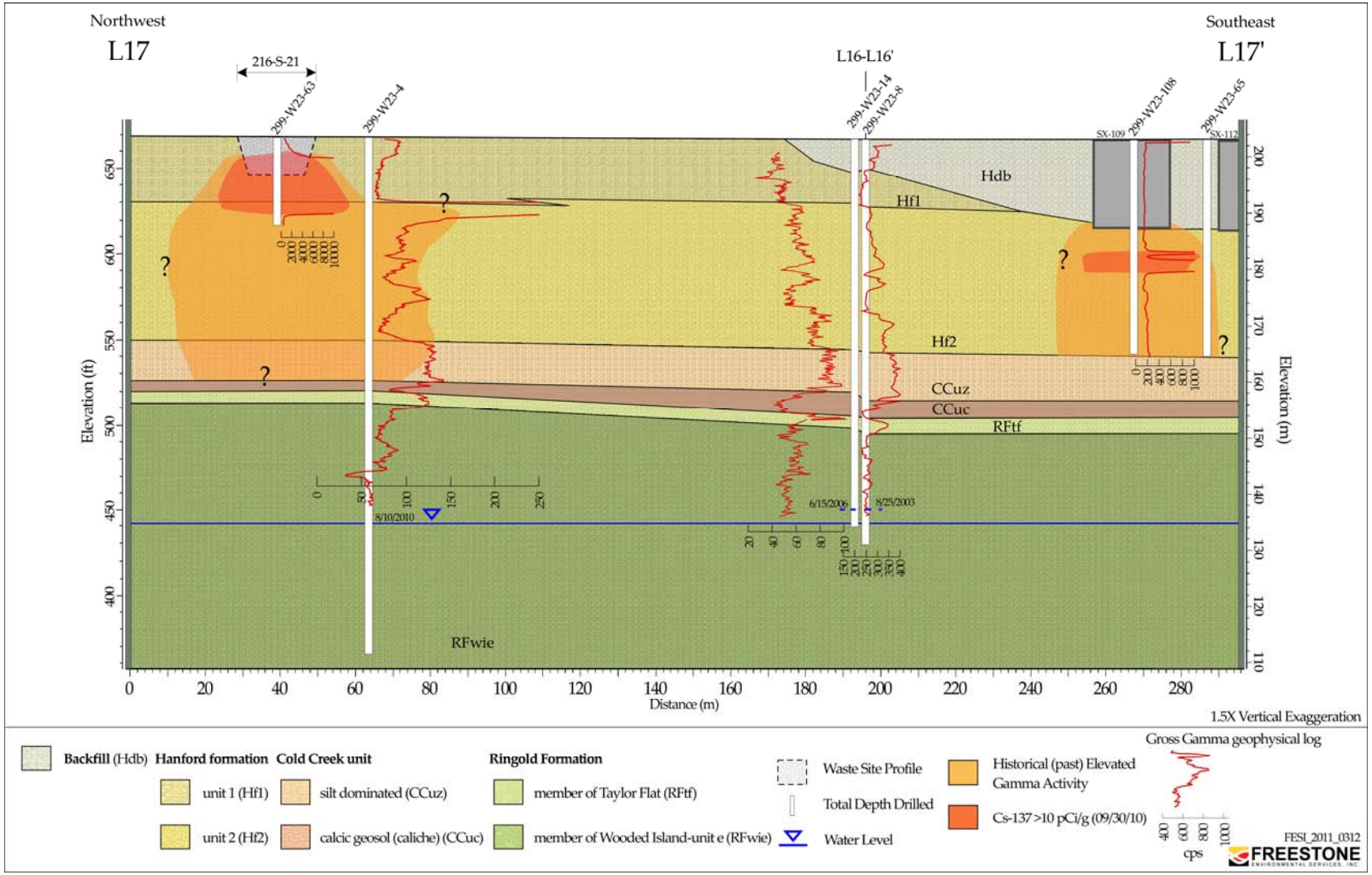

Figure 3-19. Conceptual Model for Location of Residual Contamination below the 216-S-21 Crib

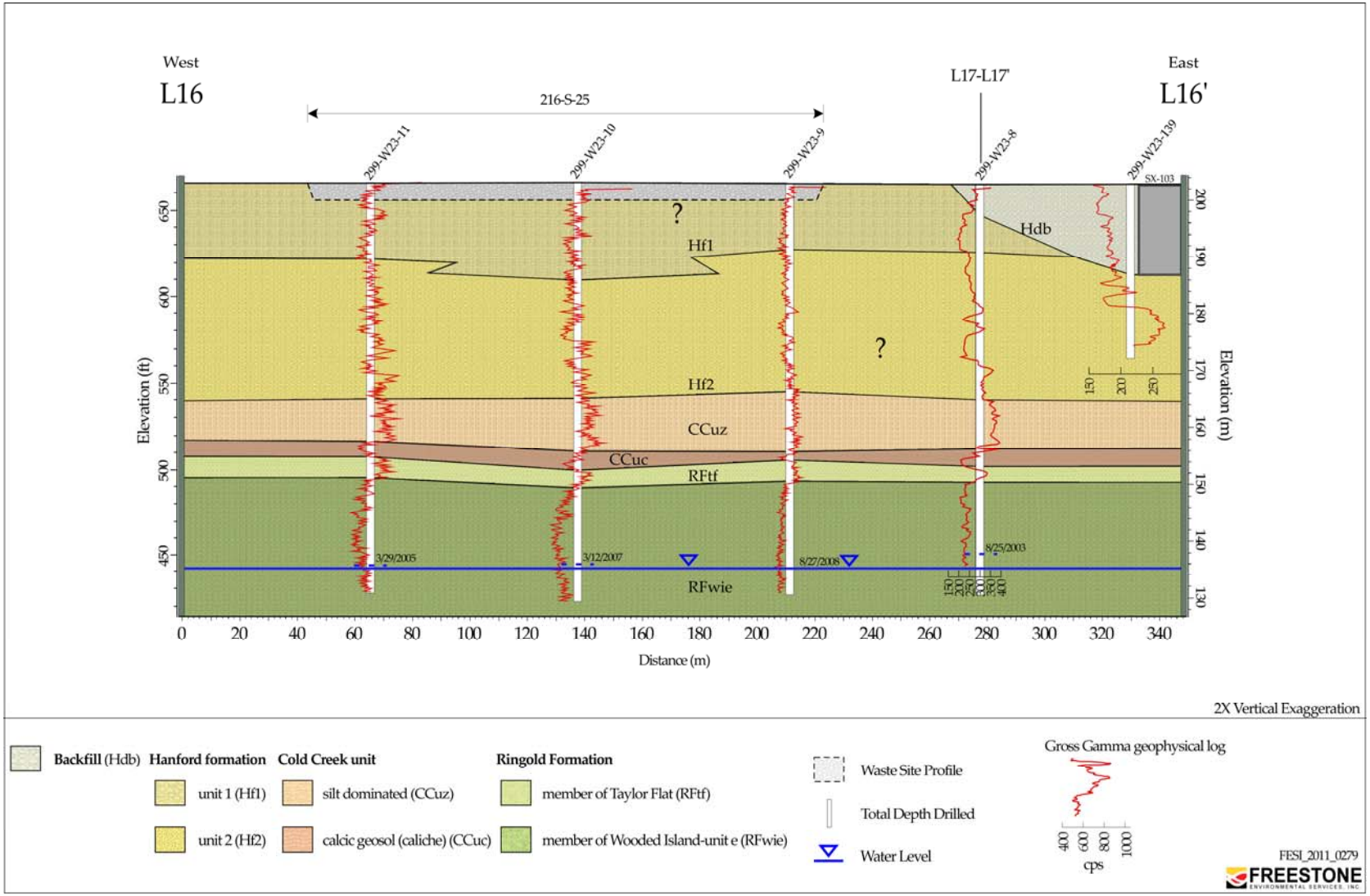

Note: No gamma contamination detected in wells.

Figure 3-20. Subregion 2 – Conceptual Site Model for the 216-S-25 Crib

Table 3-4. Volumes and Masses Released from the SX Tank and Disposed to 216-S-21 and 216-S-25 Cribs

	241-SX-107	241-SX-108	241-SX-109	241-SX-111	241-SX-112	241-SX-113	241-SX-114	241-SX-115	SX Farm Totals	216-S-21 & S-25 Totals	SX Farm/ 216-S-21 & 216-S-25 Cribs	SX Tank Farm % of Total S-SX Complex	216-S-21 and 216-S-25 Cribs % of Total S-SX Complex
Total Volume Release (ML)	0.023	0.132	0.008	0.011	0.105	0.058	0.008	0.198	0.542	375.1	0.001	0.1180	81.7
Mass Released (kg)													
Na	1.19E+04	2.86E+04	1.88E+03	1.54E+03	1.57E+04	6.97E+03	1.25E+02	1.68E+04	8.36E+04	1.6E+03	51.06	80.1	1.6
NO_3	**9.98E+03**	**2.40E+04**	**1.57E+03**	**1.29E+03**	**1.32E+04**	**7.60E+03**	**1.03E+02**	**1.61E+04**	**7.39E+04**	**2.2E+05**	**0.33**	**20.3**	**61.3**
NO_2	4.80E+03	1.15E+04	7.57E+02	6.23E+02	6.35E+03	1.93E+03	5.04E+01	0.00E+00	2.61E+04	2.1E+02	125.70	77.5	0.6
PO_4	2.38E+00	5.74E+00	3.76E-01	3.09E-01	3.16E+00	0.00E+00	7.26E-01	7.92E-02	1.28E+01	3.9E+03	0.003	0.33	99.7
SO_4	2.45E+02	5.90E+02	3.87E+01	3.18E+01	3.25E+02	1.01E+02	1.03E+01	2.96E+02	1.64E+03	5.1E+03	0.32	23.4	3.6
F	1.84E-01	4.42E-01	2.90E-02	2.38E-02	2.43E-01	4.93E-05	5.06E-02	6.23E-03	9.78E-01	4.5E+02	0.002	0.22	99.8
U	**1.43E+00**	**3.43E+00**	**2.25E-01**	**1.85E-01**	**1.89E+00**	**1.69E+00**	**3.94E-02**	**6.60E+00**	**1.55E+01**	**7.9E-01**	**19.47**	**5.1**	**0.3**
Cr	**1.32E+02**	**3.18E+02**	**2.09E+01**	**1.72E+01**	**1.75E+02**	**1.57E+02**	**2.02E+00**	**2.68E+02**	**1.09E+03**	**1.9E+02**	**5.73**	**80.8**	**14.1**
Activity Released (Ci)													
Cobalt-60	2.16E-01	5.20E-01	3.41E-02	2.81E-02	2.86E-01	3.08E-02	7.79E-03	1.02E+00	2.15E+00	9.403E-03	228.28	4.8	0.02
I-129	7.52E-03	1.81E-02	1.19E-03	9.76E-04	9.95E-03	2.31E-03	1.11E-04	7.96E-03	4.81E-02	3.233E-04	148.79	**58.8**	0.4
Tc-99	4.87E+00	1.17E+01	7.68E-01	6.32E-01	6.45E+00	1.44E+00	1.63E-01	5.12E+00	3.12E+01	2.108E-01	147.79	**90.7**	0.6
Tritium	1.97E+00	4.74E+00	3.11E-01	2.55E-01	2.61E+00	8.69E-01	2.01E-02	2.50E+01	3.58E+01	3.563E+03	0.01	0.68	67.2
^{238}Pu	9.11E-03	2.19E-02	1.43E-03	1.18E-03	1.20E-02	5.28E-03	2.89E-04	3.71E-02	8.84E-02	1.278E-02	6.92	7.9	1.1
^{239}Pu	2.33E-01	5.62E-01	3.69E-02	3.03E-02	3.09E-01	2.78E-01	6.44E-03	1.08E+00	2.54E+00	1.984E-01	12.78	6.7	0.5

Table 3-4. Volumes and Masses Released from the SX Tank and Disposed to 216-S-21 and 216-S-25 Cribs

	241-SX-107	241-SX-108	241-SX-109	241-SX-111	241-SX-112	241-SX-113	241-SX-114	241-SX-115	SX Farm Totals	216-S-21 & S-25 Totals	SX Farm/ 216-S-21 & 216-S-25 Cribs	SX Tank Farm % of Total S-SX Complex	216-S-21 and 216-S-25 Cribs % of Total S-SX Complex
Cesium-137	1.16E+04	2.79E+04	1.84E+03	1.46E+00	1.53E+04	3.26E+03	1.05E+03	1.34E+03	6.23E+04	5.016E+02	124.18	89.8	0.7

Notes: The volume and inventory estimates for SX tanks come from RPP-ENV-39658, *Hanford SX-Farm Leak Assessments Report*, and RPP-RPT-48589, *Hanford 241-S Farm Leak* Assessment *Report*; data for 216-S-21 and 216-S-25 Cribs come from RPP-26744, *Hanford Soil Inventory Model, Rev. 1.*

Cobalt-60, tritium, and cesium-137 activities decay corrected to 9/30/2010.

The five potentially mobile contaminants of concern are in **bold type**.

Blue type represents a high (>30%) of total mass of constituents released to the entire S-SX Complex.

ML = mega (million) liters

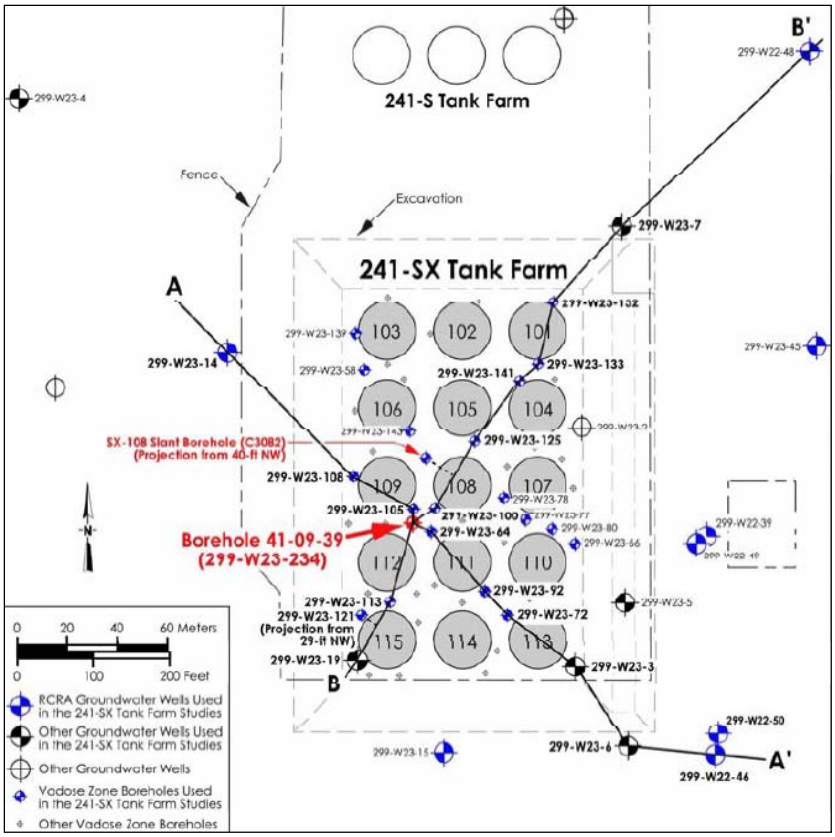

Figure 3-21. Location of Three Characterization Boreholes in SX Tank Farm 299-W23-234, Slant Borehole, and 299-W23-19

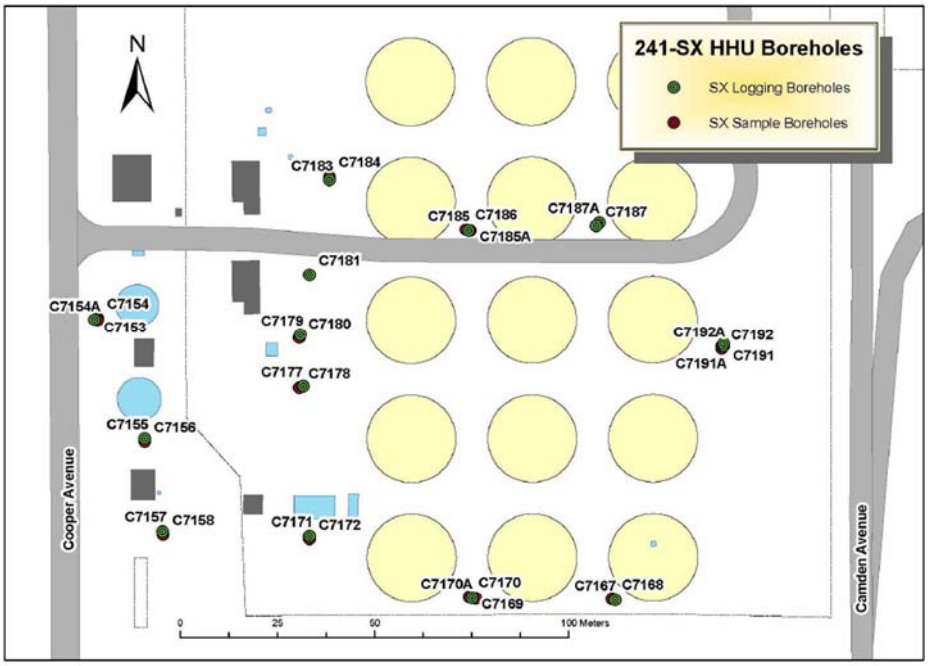

Figure 3-22. Location of Direct Push Characterization and Logging Probe Holes

Table 3-5. Depth Discrete Water Extractable Concentrations of Mobile Contaminants in SX Tank Farm Sediments

ID Slant Borehole	Vertical Depth (ft)	Tc-99 pCi/g	Nitrate µg/g soil	Cr (OES) µg/g soil	Cr (ICP-MS) µg/g soil	I-129 pCi/g soil
S0070-01A-WE	55.37	<1.70E+01	6.95E+00	(1.55E-02)	0.009	NA
S0070-02A-WE	64.03	No Sample Recovery				
S0070-03AB-WE	68.37	3.46E+00	2.96E+01	9.97E-01	8.05E-01	NA
S0070-04A-WE	72.75	1.70E+00	2.35E+01	8.55E-01	7.70E-01	NA
S0070-05A-WE	77.08	1.02E+01	9.29E+01	3.65E+00	3.52E+00	NA
S0070-06A-WE	81.36	4.07E+01	**1.17E+04**	**4.84E+02**	**4.03E+02**	1.397E+02
S0070-07A-WE	85.69	**1.02E+03**	**4.67E+04**	**3.10E+02**	**2.80E+02**	NA
S0070-08A-WE	90.02	**2.86E+03**	**3.97E+04**	**8.30E+02**	**7.58E+02**	1.978E+02
S0070-09A-WE	94.35	**3.96E+03**	**2.28E+04**	**5.12E+02**	**4.47E+02**	NA
S0070-10A-WE	98.68	**4.53E+03**	**1.90E+04**	**3.98E+02**	**3.56E+02**	NA
S0070-11A-WE	103.06	**4.54E+03**	**9.52E+03**	**8.95E-01**	**8.84E-01**	NA
S0070-12A-WE	107.13	**5.95E+02**	**1.53E+03**	**2.88E-01**	**2.09E-01**	NA
S0070-13A-WE	115.61	**7.40E+03**	**2.27E+04**	**4.40E+02**	**3.91E+02**	NA
S0070-14A-WE	124.45	**7.38E+03**	**2.23E+04**	**3.09E+02**	**2.96E+02**	1.845E+02
S0070-15A-WE	133.11	**1.15E+04**	**3.46E+04**	**3.37E+02**	**3.06E+02**	2.904E+02
S0070-16A-WE	141.77	**1.44E+03**	**4.19E+03**	1.06E-01	1.98E-02	NA
S0070-17A-WE	148.87	**5.51E+02**	**2.39E+03**	8.69E-02	3.40E-03	NA
SX-41-09-39	**Depth**	**Tc-99 pCi/g soil**	**Nitrate µg/g soil**	**Cr (OES) µg/g soil**	**Cr (ICP-MS) µg/g soil**	**I-129 pCi/g soil**
15A/B/C	25-26	1.53E-01	13.0	3.78E-03	5.00E-04	NA
14A/B/C	44-45	9.64E-01	13.0	<0.03	2.89E-03	NA
13A/B/C	56-57	5.21E-01	13.2	<0.03	3.53E-03	NA
12A/B/C	61-62	6.97E-01	13.0	4.50E-03	8.16E-03	NA
11A/B	65-66	7.81E+00	17.6	3.67E-01	3.42E-01	NA
11C	65-66	4.07E+00	29.1	4.21E-01	3.44E-01	NA
10A/B/C	69-70	5.53E+00	33.5	5.05E+00	5.07E+00	NA
9A/B/C	74-75	7.72E+00	44.3	4.19E+00	4.09E+00	NA
8A/B/C	79-80	1.82E+01	**371.2**	7.24E-01	7.19E-01	NA
7A/B/C	82-83	**3.93E+02**	**2838.0**	**7.34E+02**	**7.46E+02**	NA
SX-41-09-39	**Depth**	**Tc-99 pCi/g soil**	**Nitrate µg/g soil**	**Cr (OES) µg/g soil**	**Cr (ICP-MS) µg/g soil**	**I-129 pCi/g soil**
6A/B	90	**2.75E+03**	**2.8E+04**	**7.07E+02**	**7.11E+02**	NA
3A/B/C	95-96	**6.14E+03**	**3.2E+04**	**2.51E+02**	**5.28E+02**	NA
5A/B/C	102-103	**1.19E+04**	**4.2E+04**	**4.91E+02**	**4.82E+02**	NA
4A/B/C	108-109	**7.04E+03**	**3.3E+04**	**4.39E+02**	**2.60E+02**	NA
2B/C	112	**8.59E+03**	**3.3E+04**	**1.67E+02**	**1.76E+02**	NA

Table 3-5. Depth Discrete Water Extractable Concentrations of Mobile Contaminants in SX Tank Farm Sediments

1A/B/C	127.4	**3.34E+02**	**1.3E+04**	3.47E-02	1.15E-02	NA
2C/2D	133.2	**333**	**291.00**	NA	0.001	NA
2A/2B	134.2	**134**	**268.00**	NA	<0.001	NA
3A/3B	135.2	**158**	**362.00**	NA	<0.001	NA
	135.9	**55**	**165.00**	NA	<0.001	NA
6D	143.3	0.2	42.00	NA	<0.001	NA
6C	144.1	16	58.00	NA	<0.001	NA
10A/10B	153.9	2.3	49.00	NA	<0.001	NA
12A/12B	156.8	2.9	9.00	NA	<0.001	NA
17A/17B	9.4	<2	9.40	NA	<0.001	NA
38A/38B	188.3	<2	1.90	NA	<0.001	NA
47A/47B	196.9	<2	18.00	NA	<0.001	NA
58A/58B	208.6	<2	6.58	NA	<0.001	NA
	214	<2	0.6	NA	<0.001	NA
299-W23-19	**Near SX-115**					
SAMPLE #	**Depth (ft) Mid**	**Tc-99 pCi/g**	**Nitrate µg/g soil**	**Cr (OES) µg/g soil**	**Cr (ICP-MS) µg/g soil**	**I-129 pCi/g**
B8809-09E	32.95	<0.85	1.0	<0.003	NA	NA
B8809-15A	54.5	<0.85	0.8	<0.001	NA	NA
B8809-16A	57.45	<0.85	3.1	<0.000	NA	NA
B8809-17J	61.75	<0.85	1.35	5.13E-04	NA	NA
B8809-17G	63.25	<0.85	5.25	<0.001	NA	NA
B8809-17F	63.75	<0.85	8.83	1.44E-03	NA	2.71E+00
B8809-17E	64.25	<0.85	NA	4.76E-04	NA	NA
B8809-17C	65.25	<0.85	12.43	<0.001	NA	NA
B8809-18I	67.45	<0.85	19.93	1.67E-02	NA	NA
B8809-18E	69.45	<0.85	10.26	3.02E-02	NA	NA
B8809-18B	70.95	<0.85	27.69	5.01E-01	NA	NA
B8809-19H	73.25	1.29E+01	136.86	1.56E+00	NA	NA
B8809-19G	73.75	3.58E+01	**344.35**	4.30E+00	NA	NA
B8809-19F	74.25	4.71E+01	**431**	**6.85E+00**	NA	<1.57E+00
B8809-19D	75.25	3.91E+01	**379.66**	3.74E+00	NA	NA
B8809-20F	79.25	2.51E+01	**241.81**	3.08E+00	NA	NA
B8809-20E	79.75	2.54E+01	**275.88**	2.72E+00	NA	NA
B8809-20D	80.25	3.21E+01	**359.00**	3.31E+00	NA	NA
B8809-21A	86	4.25E+00	44.96	2.44E-01	NA	NA
B8809-22D	88.1	4.77E+01	**446.00**	**6.47E+00**	NA	<1.57E+00
B8809-24A	95	3.05E+01	**340.00**	3.77E+00	NA	NA

Table 3-5. Depth Discrete Water Extractable Concentrations of Mobile Contaminants in SX Tank Farm Sediments

B8809-25B	99.06	7.15E+00	142.51	1.65E+00	NA	<1.27E+00
B8809-25A	100.06	2.73E+01	**334.61**	5.93E+00	NA	NA
B8809-26E	102.95	1.29E+01	156.90	2.61E+00	NA	<1.57E+00
B8809-26A	104.95	1.27E+01	75.39	1.32E+00	NA	NA
B8809-27G	107.05	3.63E+01	**342.00**	**8.15E+00**	NA	<1.57E+00
B8809-29D	116.35	3.70E+01	**468.00**	6.85E+00	NA	NA
B8809-30G	123.85	**8.26E+01**	**865.00**	**7.30E+00**	NA	NA
B8809-30D	125.35	**1.76E+02**	**1727.23**	4.97E+00	NA	5.96E+00
B8809-30B	126.35	**3.63E+02**	**3304**	3.62E-01	NA	NA
B8809-31G	129.15	**4.97E+02**	**3932.00**	2.67E-03	NA	8.77E+00
B8809-31A	132.15	**3.94E+02**	**3202.71**	<0.002	NA	NA
B8809-32D	134.25	**8.34E+01**	**683.02**	<0.002	NA	NA
B8809-32A	135.8	**3.65E+02**	**2776.00**	<0.002	NA	NA
B8809-33G	137.65	**3.46E+02**	**2734.00**	<0.003	NA	8.93E+00
B8809-33B	140.15	**3.27E+02**	**2738.00**	<0.002	NA	NA
B8809-35K	141	**2.53E+02**	**2594.00**	<0.002	NA	NA
B8809-35H	142.35	**2.82E+02**	NA	<0.002	NA	NA
299-W23-19	**Near SX-115**					
SAMPLE #	**Depth (ft) Mid**	**Tc-99 pCi/g**	**Nitrate µg/g soil**	**Cr (OES) µg/g soil**	**Cr (ICP-MS) µg/g soil**	**I-129 pCi/g**
B8809-35F	143.35	**2.17E+02**	NA	8.57E-04	NA	NA
B8809-35C	144.85	**1.85E+02**	**1552.00**	2.50E-03	NA	NA
B8809-35A	145.85	**2.87E+02**	**2454.00**	9.63E-04	NA	NA
B8809-36D	147.45	**1.15E+02**	**762.00**	<0.002	NA	NA
B8809-36B	148.45	**1.92E+02**	**1385.00**	<0.002	NA	NA
B8809-37D	149.65	**1.87E+02**	**2140.00**	2.50E-03	NA	NA
B8809-38G	152.1	**5.49E+01**	**408.83**	<0.002	NA	NA
B8809-38E	153.1	2.08E+01	**242.00**	<0.002	NA	NA
B8809-38A	155.1	3.41E+00	NA	<0.002	NA	NA
B8809-39D	155.35	2.55E+01	**241.26**	<0.002	NA	NA
B8809-39C	155.85	1.06E+01	90.00	2.50E-03	NA	NA
B8809-40B	157.75	1.14E+00	34.47	<0.002	NA	NA
B8809-40	158.65	3.70E+00	34.40	<0.002	NA	NA
B8809-17SK	158.5-161.0	2.58E+00	32.25	5.42E-03	NA	NA
B8809-18SKA	161	1.63E+00	23.29	2.96E-03	NA	NA
B8809-18SKB	Near 161.0'	2.74E+00	29.33	4.37E-03	NA	NA
B8809-18SKC	Near 166.5'	1.59E+00	17.30	<0.002	NA	NA
B8809-19SKA	Near 166.5'	9.17E-01	11.37	<0.002	NA	NA

Table 3-5. Depth Discrete Water Extractable Concentrations of Mobile Contaminants in SX Tank Farm Sediments

B8809-19SKB	166.5-185	5.60E-01	5.65	<0.00	NA	NA
B8809-41A	184.55	<0.85	6.53	<0.002	NA	NA
B8809-19SKC	Near 185'	<0.85	3.89	<0.00	NA	NA
B8809-20SKA	Near 185.0'	<0.85	0.78	<0.00	NA	NA
B8809-20SKB	Near 189.5'	<0.85	2.95	<0.00	NA	NA
B8809-42	194.55	<0.85	1.14	<0.002	NA	NA
B8809-43B	204.5	3.14E+00	76.80	<0.002	NA	NA
B8809-43A	205.15	4.26E+00	25.31	<0.002	NA	NA

Note: **Bold type** represents peak concentrations in the vadose zone plume.
ICP-MS = Inductively coupled plasma- mass spectrometry.
NA = Not analyzed
OES = Inductively coupled plasma -optical emission spectroscopy.

The Tc-99 data (both sediment 1:1 water extracts and strong acid extracts) from boreholes 299-W23-234 and 299-W23-64 (the slant borehole below SX-108) show that there are significant concentrations of Tc-99 between the depths of 24 to 43.3 m (80 to 142 ft) bgs. The leading edge of the Tc-99 plume appears to reach 41.4 m (136 ft) bgs at 299-W23-234 near tank SX-109 and appears to be deeper below SX-108, because the deepest sample from the slant borehole at 45.4 m (148.9 ft) bgs also contains elevated Tc-99. Figure 3-24 shows the concentrations of Tc-99 in both the acid and water extracts of the slant borehole sediments. Tc-99 is quite mobile in that a water leach removes as much Tc-99 as the acid extracts.

Figure 3-25 compares the acid extractable Tc-99 for both boreholes, which are similar to the water extractable Tc-99 concentrations shown in Table 3-5.

Tc-99 concentrations in these two boreholes are the highest observed in vadose zone sediments collected in the Central Plateau. The Tc-99 in situ distribution coefficient (K_d) (determined from a comparison of the water to acid extractable Tc-99) varies from 0.01 to about 5 mL/g over the whole zone of contamination in both boreholes.

The most significant chemical contaminant in the sediment is chromium. The water leachable chromium profiles are shown in Figure 3-26. The leading edge of the chromium plume appears to stop at 34.1 m (112 ft) bgs in the sediments from 299-W23-234 and at 40.5 m (133 ft) bgs in the SX-108 slant borehole, which suggests that it does not migrate as far as technetium. The bulk of the water-leachable chromium has been confirmed as chromate by its distinct yellow color and by ion chromatography. This is true also at the other boreholes within the SX Tank Farm.

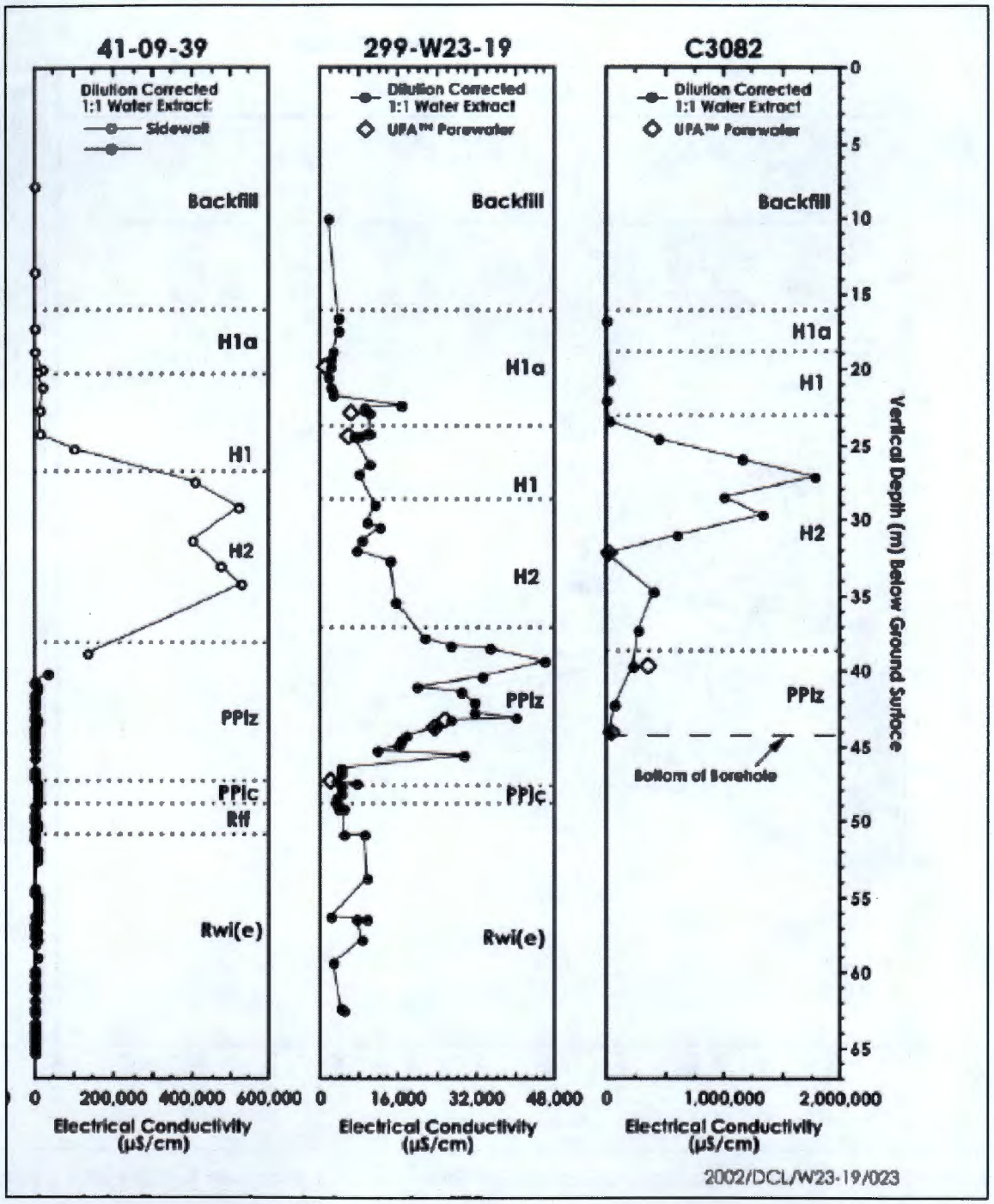

Figure 3-23. Comparison of Pore Water Electrical Conductivity for Three SX Tank Farm Borehole Sediments

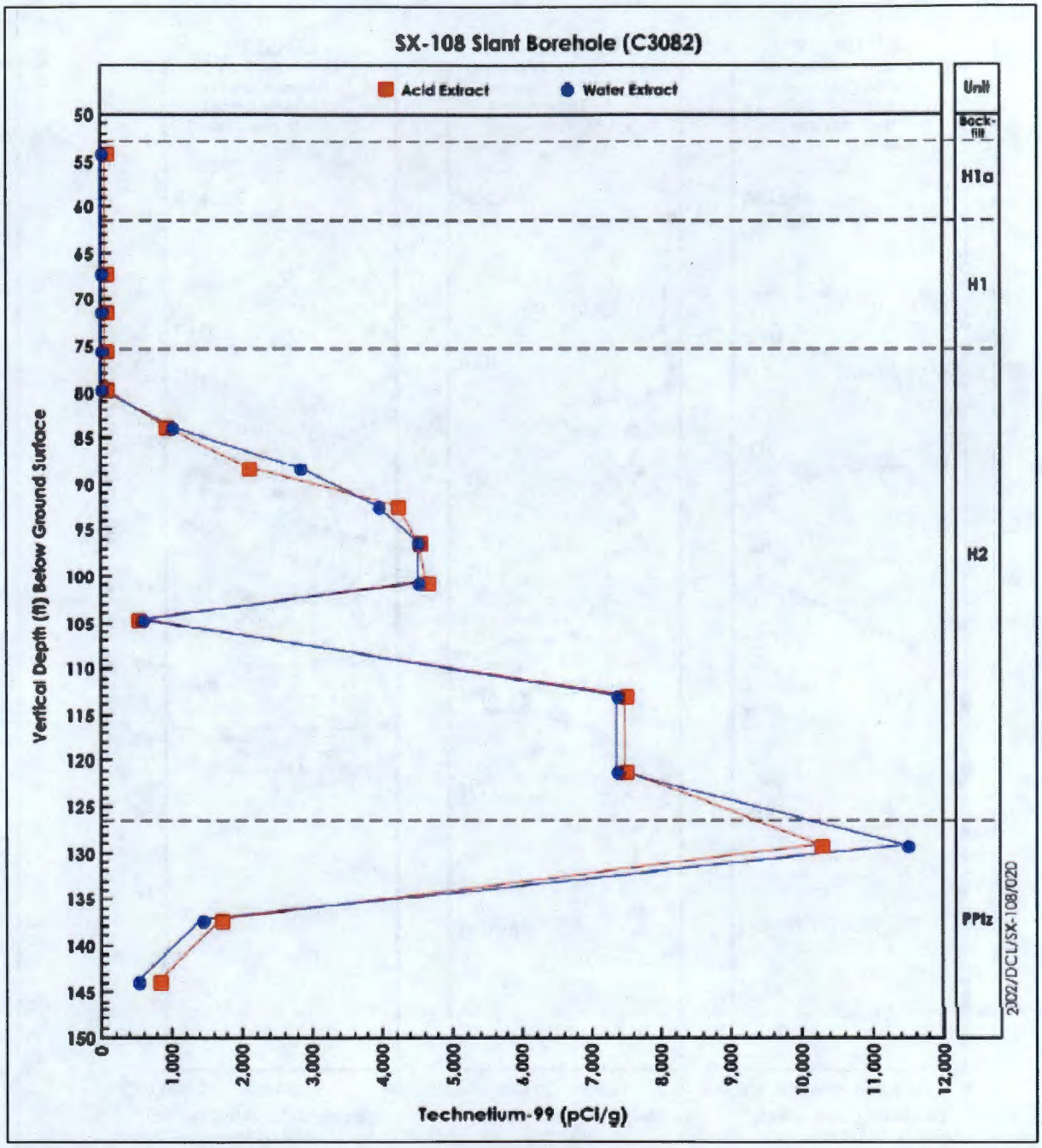

Figure 3-24. Comparison of Water and Acid Extractable Technetium-99 in Sediments from the Slant Borehole

Water extract sodium, nitrate, and Tc-99 all indicate the leading edge of the vadose plume is near 41.4 m (136 ft) bgs at Borehole 299-W23-234 but the leading edge of the plume below SX-108 tank was not found because the slant borehole did not go deep enough. The mobile constituent profiles all suggest that the leading edge of the plume at Borehole 299-W23-234 resides about 3.4 m (11 ft) into the fine grained CCuz unit at 41.4 m (136 ft) bgs.

Three groundwater samples were collected at borehole 299-W23-234 between April 1998 and May 1999. Nitrate concentrations ranged from 17.9 to 19.1 mg/L and only tritium appeared to be elevated (ranged between 130,000 to 172,000 pCi/L. A sample from August 1998 had an EC of about 250 µS/cm and, aside from the tritium, showed no signs of elevated concentrations of other constituents. This suggests that the groundwater beneath the SX Tank Farm at this location still shows the influence of the large volumes of dilute-salt waste liquids disposed to facilities upgradient (north and west). Based on the SIM, Rev. 1 model (RPP-26744), the 216-S-25 Crib wastes disposed between 1973 and 1980 had nitrate concentrations of 0.52 mg/L and tritium concentrations of 7.66×10^6 pCi/L. In 1985, contaminated groundwater from a pump and treat at the 216-U1&2 Cribs was disposed in 216-S-25 Crib. According to SIM, Rev. 1 (RPP-26744), this contaminated groundwater had a nitrate concentration of 7,050 mg/L and a tritium concentration of 4.10×10^6 pCi/L. It would appear that the contaminated groundwater from the 216-U1&2 Cribs had not reached the location of Borehole 299-W23-234 by the 1998-1999 period.

EC and water extractable chromium, nitrate, sodium, and technetium concentrations were found to be good indicators of the plume distribution. Data for the other measured contaminants indicate that leaked tank fluids have affected the vadose zone. Beneath tank SX-115, the water extract EC from vadose zone sediments at 299-W23-19 suggests that tank fluids descended from about 22.2 m (73 ft) depth to the base of the upper CCuz at about a 47.5 m (156 ft) depth (see Figure 3-23). However, Tc-99 concentrations in sediments between 48 and 56 m (158 and 185 ft) bgs are not consistently at background levels (non-detectable) and the two deepest samples near 62.5 m (205 ft) show between 3 and 4 pCi/g of Tc-99 (Table 3-5 and Figure 3-27). It is unclear whether fluids leaked from the SX-115 tank have reached the groundwater table at this location but a nearby well, 299-W23-19, was converted into a monitoring well and has shown high concentrations of Tc-99 ever since it was developed. There remains considerable mass of Tc-99 near SX-115 in the upper CCuz subunit between 38.1 m (125 ft) and 47.5 m (156 ft) depth. Concentrations of Tc-99 in the sediments (based on water extracts is most likely dissolved in the pore water) vary from a few pCi/g above 30 m (100 ft) bgs to about 50 pCi/g below and exceed 100 pCi/g between the depths of 38 and 45.7 m (125 and150 ft) bgs with a peak water extractable concentration of ~450 pCi/g near 41.4 m (136 ft) bgs. As mentioned, the leading edge of the main Tc-99 plume in the CCuz sediments at 47.5 m (156 ft) bgs, which is slightly deeper than the contamination investigated at tank SX-108 and tank SX-109, both of which have the bulk of contamination in the Hanford formation. It is noted that the volume of tank liquor released from SX-115 is larger (0.198 ML) than any other SX tank (see Table 3-3). However, concentrations of Tc-99 in the Hanford formation sediments below SX-108 and SX-109 reach concentrations greater than 11,000 pCi/g.

Pore water from all of the SX Tank Farm sediment cores in three tank farm defined Hanford formation units (H1a, H1, and H2) were dominated by sodium and nitrate. The most concentrated pore water found in sediments from 41-09-39 borehole was 5 to 6 molar mass (M) sodium nitrate with several tenths molar concentrations of calcium and chromate. At the slant borehole, the most concentrated pore water was in the H2 unit and was 16 to 17 M sodium nitrate with 1 M concentration of calcium, 0.5 M chromate, and several tenths molar sulfate, chloride, potassium, and magnesium. This extremely hypersaline composition is about three times higher in all constituents as found in the H2 pore water at borehole 41-09-39, but the increase is caused more by sediment desiccation than different leak chemical compositions. The species present in the contaminated pore water at both boreholes are remarkably similar. The pore fluids in the sediments from 299-W23-19 are more dilute but contain the same major constituents.

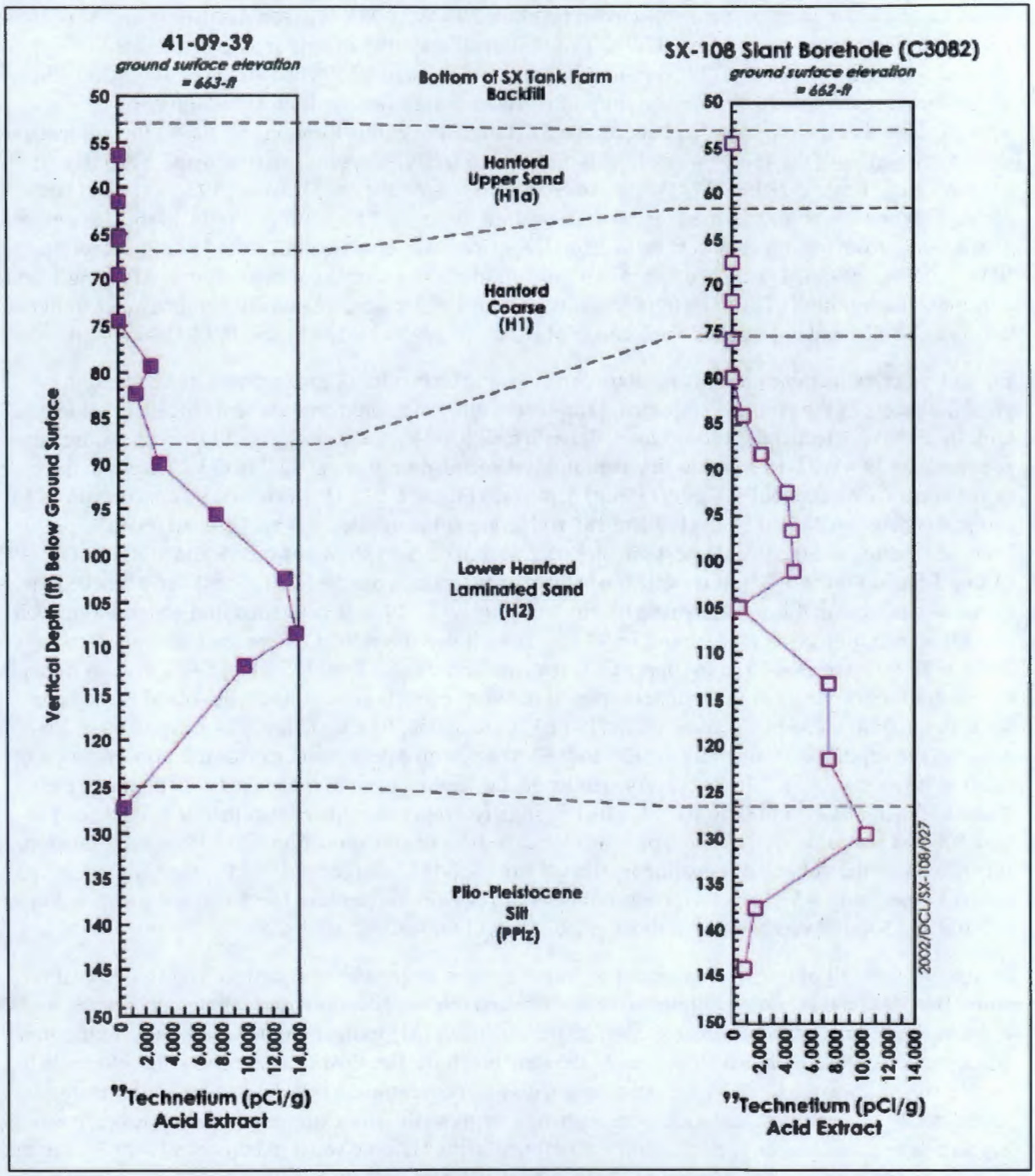

Figure 3-25. Comparison of Acid Extractable Technetium-99 in Sediments from the 299-W23-234 and the SX-108 Slant Borehole

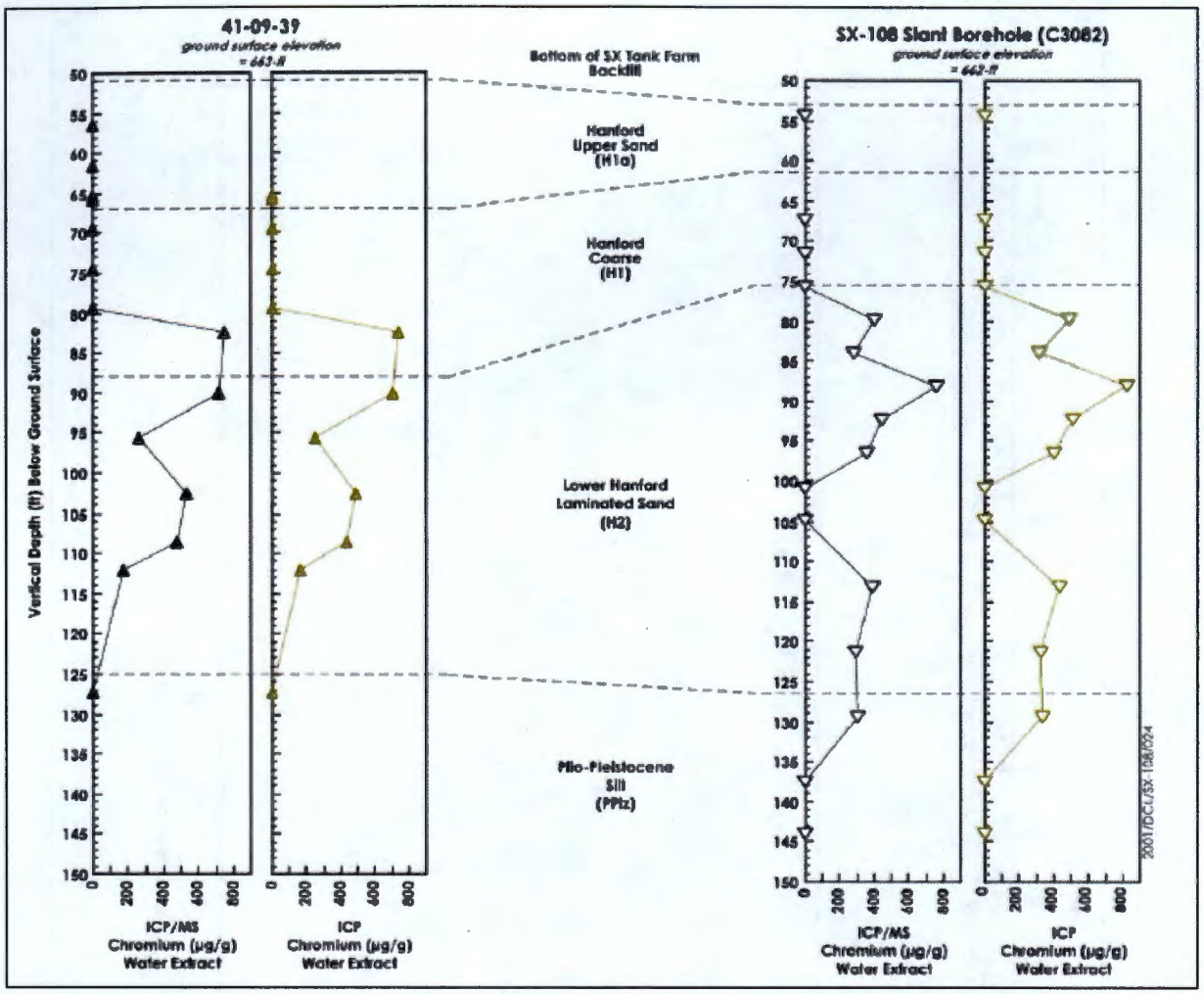

Figure 3-26. Comparison of Water Extractable Chromium in Sediments from 299-W23-234 and the SX-108 Slant Borehole

Overall, the interaction of the SX tank liquors with native vadose zone sediments are controlled by common ion exchange and heterogeneous (solid phase-liquid solute) redox reactions. Significant indications of caustic alteration of the sediment mineralogy or porosity were not observed in the sediments, suggesting that the zone of most impact is small perhaps within 4.6 m (15 ft) in all directions from the point of the entry of the tank liquors. However, we did observe slightly elevated pH values and faint indications of caustic reactions out to a maximum distance of 9.1 m (30 ft) from the SX-108 tank bottom. The pH values in water extracts at SX-41-09-39 also are not nearly as high as would be expected for tank liquor completely saturating sediment.

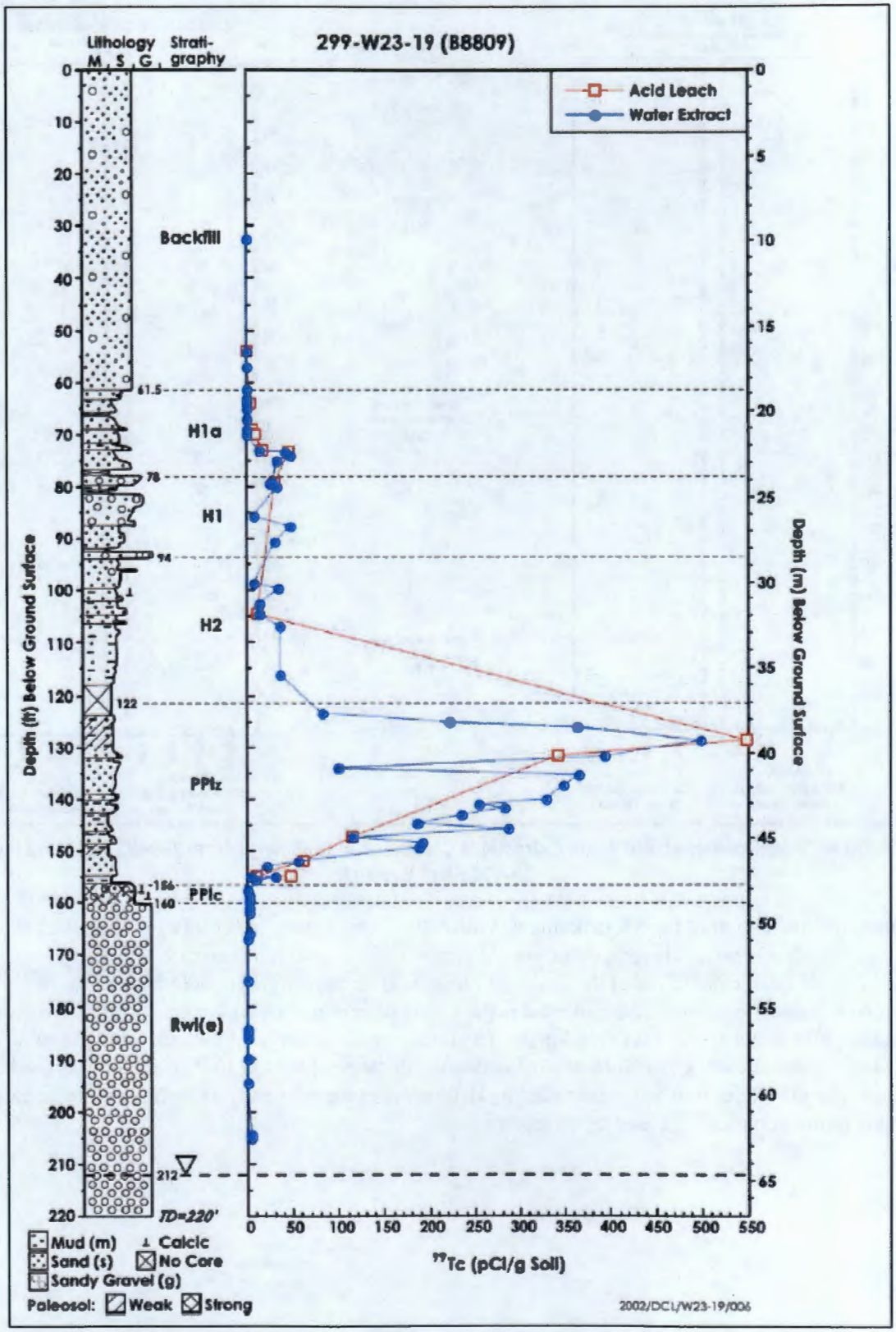

Figure 3-27. Comparison of Water and Acid Extractable Technetium-99 in Sediments from 299-W23-19

Therefore, it would appear that significant pH reactions occur only from the SX tank bottoms at ~16.8 m (~55 ft) to a maximum of 27.4 m (90 ft) bgs for sediment surrounding the SX tanks.

Based on comparing the depth of penetration of various contaminants and comparing the percentages that are water leachable, it can be stated that chromium and molybdenum migrate faster than cesium-137 but slower than Tc-99, selenium, and nitrate. Tc-99 desorption data are consistently near zero, meaning that Tc-99 is not interacting with the sediment. Despite the findings that approximately one-third of the chromium appears to be reduced via caustic dissolution of ferrous containing minerals, the chromium desorption K_d values are still <1 mL/g in the entire zone where the bulk of the tank fluid currently resides.

The near horizontally bedded, slightly southwesterly dipping sediment likely caused anisotropic flow of the migrating contaminants. The vertical distribution of cesium-137 at both the slant borehole under tank SX-108 and at the adjacent 41-09-39 borehole suggest that much of the tank fluid that leaked from surrounding tanks traveled to the southwest within the coarse-grained Hanford formation H1 unit. At the slant borehole under tank SX-108, there is also a large mass of cesium-137 in the fine sand of the Hanford formation H2 unit that lies below the H1 unit. At the slant borehole, there is a fine-grained lens within the H2 unit at 32.2 m (105.6 ft) bgs that was not affected much by the hypersaline tank liquors. The migrating plume of cesium-137 seems to have bypassed the sediment in this area under the tank, making it difficult to fully interpret the vertical distribution of contaminants under SX-108. Compared to the cesium-137 distributions, there is very little strontium-90 in the sediment, suggesting that strontium is not mobile in the redox fluid that leaked from the SX tanks.

Based on the data collected to date, it appears unlikely that the source of the contamination in the groundwater just south and east of the SX Tank Farm (see more discussion in Section 5) is the pore fluids in the vadose zone directly beneath tank SX-108. A more plausible source of the contamination reaching the groundwater appears to be the fluid originally lost from tank SX-115. Vadose zone pore fluids proximal to the SX-115 tank show a Tc-99 to nitrate ratio closer to that present in the groundwater than the leaked fluid from tank SX-108. However, the ratios for the pore waters in the SX-108 slant borehole (299-W23-64) are not constant, possibly caused by irregular mixing between the plumes of two separate leak events and/or dynamic convection currents driven by the time varying heat and fluid head load under the tank. Temperature measurements at the wall of the slant borehole casing, previous in-tank temperature measurements, and thermal modeling (see Field Investigation Report [FIR]) suggest that complicated convection cells of water vapor and liquid water were active under tank SX-108.

As shown on Figure 3-22, several direct push probe holes were placed to the west and south of the SX tanks. Additionally, a few were pushed inside the perimeter (mainly along the edges of the SX-104 through SX-106 row of tanks) to investigate the lateral extent of the vadose zone plume from all the tanks (SX-107 through SX-115) directly to the south, which all released tank fluids (exception being SX-110). In general, two probe holes were placed close together with one being used for gamma logging and the other one used to collect sediment samples at two to four depths (dependent on gamma logging results from the companion probe hole) for characterization. Table 3-6 lists the concentrations of key mobile contaminants found in 1:1 sediment water extracts as well as acid-extractable (total) Tc-99 concentrations at the discrete depths sampled. The table lists the probe hole number (see Figure 3-22 for location) and depth as well as a range of gravimetric moisture contents measured on several aliquots of each sample, electrical conductivity of the water extract; Tc-99 concentrations per gram of sediment (both water and acid extractable); water extractable nitrate, chromium, and sodium concentrations; and total I-129 concentrations in the sediment. When duplicate measurements of an analyte were performed, both values are shown. The sediments with high moisture content are in general fine-grained material compared to typical Hanford formation sands and when shallower than the contact with the CCuz subunit represent thin silt lenses in the Hanford Hf2 unit.

Table 3-6. Concentrations of Key Mobile Contaminants in the Sediments from the SX Tank Farm Direct Push Probe Holes

SX Direct Push	ft bgs	%wt	µmho/cm	pCi/g	pCi/g	µg/g soil	µg/g soil	pCi/g	µg/g soil
Probe Hole	Depth	Moisture Content	Elec. Cond.	Technetium-99-WE	Technetium-99-AE	NO_3-WE	Cr(ICP-MS)-WE	Iodine-129	Na-WE
C7154	74-76	16.86-18.59	200 204	9.51E-02	<1.7808	9.72	<0.013	<1.34E-01	32.4
	106-108	11.58-12.79	189	6.07E-02	<1.7808	6.1	<0.018	<1.69E-01	24.9
C7156	92-94	12.23-13.74	190	7.77E-02	1.26E+00	8.5	<0.015	<1.52E-01	36.5
	126-128	10.65-17.92	252	8.36E+00	8.69E+00	46.4	<0.016	<1.53E-01	30.2
	140-142	21.13-21.73	879	1.15E+02	9.16E+01	521	<0.017	<1.47E-01	72.3
C7158	87-89	2.16-3.38	138	6.58E-02	1.45E+00	0.3	<0.018	<1.73E-01	24.5
	124-126	14.08-18.10	224	8.21E-01	1.98E+00	24.9	<0.019	<1.36E-01	40
	141-143	13.89-18.04	322	4.88E+00	6.00E+00	62.3	<0.020	<1.55E-01	41.9
C7168	81-83	9.9-10.86	1880	5.07E+01	5.51E+01	757	7.76	<1.65E-01	441
	129-131	13.94-16.39	3.07	1.55E+02	1.11E+02	2140	0.027	<1.51E-01	171
	145-147	17.03-18.37	310	2.83E+00	3.95E+00	<0.2	0.013	<1.39E-01	32.6
C7170	81.5-83.5	5.50-9.01	684	25.95 3.22E+01	4.68E+01	290 366	0.07	<1.51E-01	49.4 55.3
	113-115	12.39	3.39	1.34E+02	163.8 186.56	2110	0.36	<1.50E-01	178
	133-135	9.87-15.69	228	8.72E-01	<6.5	15	<0.01	<1.42E-01	22.6
	150-152	18.67-19.75	268	<0.070	<3.5	37.7	<0.014	<1.54E-01	36.4
C7172	46-48	7.56-13.84	166	<0.054	<6.5	3.53	<0.011	<1.54E-01	26.8
	75.5-77.5	10.88-14.28	205	1.83E-01	3.83E+00	17.7	<0.011	<1.54E-01	41.8
	97.5-99.5	16.61-18.96	738	4.31E+01	3.70E+01	303	6.2	<1.54E-01	172
	126-128	19.68-20.33	1120	1.20E+02	7.63E+01	619	12.8	<1.54E-01	273

Table 3-6. Concentrations of Key Mobile Contaminants in the Sediments from the SX Tank Farm Direct Push Probe Holes

SX Direct Push	ft bgs	%wt	µmho/cm	pCi/g	pCi/g	µg/g soil	µg/g soil	pCi/g	µg/g soil
Probe Hole	Depth	Moisture Content	Elec. Cond.	Technetium-99-WE	Technetium-99-AE	NO_3-WE	Cr(ICP-MS)-WE	Iodine-129	Na-WE
C7178	89-91	2.75-6.22	6.2	9.85E+02	7.90E+02	3150	114	1.46E+00	1180
	127-129	17.53-19.26	12.5	2.14E+03	1.85E+03	10,700	0.59	<1.54E-01	878
	151-153	11.0-17.4	379	3.07E+00	<6.5	57.5	0.015	<1.54E-01	30
C7180	93-95	3.80-5.54	5.48 5.78	839.52 880.2	844.6 853.1	3840 4150	22.7 24.3	5.28E-01	771 784
	104-106	4.42-7.70	1870	153.1 157.9	2.41E+02	955	<0.01	<1.54E-01	54.7
	127-129	11.83-12.75	708	4.36E+01	6.53E+01	367	<0.01	<1.54E-01	37.4
	152-154	15.31-15.68	224	7.24E-01	<6.5	39.3	<0.01	<1.54E-01	24.8
C7184	83-85	2.49-4.56	127	6.60E-02	1.76E+00	1.85	<0.01	<1.54E-01	13.4
	104-106	12.37-14.69	376	8.92E+00	<15.7	118	<0.01	<1.54E-01	36.4
C7184	128-130	11.66-14.52	219	2.87E-01	<6.5	23.7	<0.01	<1.54E-01	22
	141-143	17.06-19.36	223	<0.066	<6.5	42.2	<0.01	<1.54E-01	23.6
C7186	105-107	9.75-15.02	313	4.51E+00	6.94 8.53	112	<0.01	<1.54E-01	31.5
	128-130	16.10-18.52	323 298	2.39E+00	4.26E+00	91	<0.01	<1.54E-01	31.2
	145-147	12.38-13.67	251 239	6.1 6.2	1.05E+01	67.7 67.6	<0.01	<1.54E-01	24.3 23.0
C7192	100-102	15.81-17.03	580	4.05E+01	3.99E+01	216	5.95	<1.54E-01	146
	128-130	18.34-18.52	3970	2.14E+02	6.90E+02	3040 3030	0.047	<1.54E-01	187
	140-142	17.35-17.99	700	1.06E+02	1.61E+02	<0.03	<0.01	<1.54E-01	46.7

bgs = below ground surface

ICP-MS = Inductively coupled plasma-mass spectroscopy

The top of the CCuz subunit is found at ~38 ± 0.9 m (~125 ± 3 ft) bgs below the SX Tank Farm and is quite fine grained and thus retains moisture. The top of the CCuc subunit (caliche) is found at ~47.5 ± 0.9 m (~156 ± 3 ft) bgs below the SX Tank Farm and exhibits highly variable moisture content as well as sediment particle sizes and degree of cementation. The details on the direct push field activities and analytical measurements are available in RPP-43548 and RPP-RPT-47008, *Final Analytical Report for Soil Samples in Support of an Interim Barrier at SX Farm*, respectively.

Of particular note are the high concentrations of Tc-99, nitrate, chromium, and detectable I-129 in Hf2 and at the contact of Hf2 with the CCuz subunit at probe holes C7178 and C7180 just southwest and west of tank SX-109. These probe holes definitely are intercepting the same high concentration vadose plume that the two boreholes (299-W23-234 and 299-W23-64) intercepted around SX-109 and below SX-108. There is no significant contamination in the sediments from probe hole C7184 about 24 m (80 ft) north of C7180, so the lateral extent of the commingled vadose zone plume below SX-109 and SX-108 in a northwesterly direction might be delineated. Farther to the west at C7154, there also does not seem to be any signs of significant contamination in the Hanford formation; this probe hole did not interrogate the CCu units. To the northeast is probe hole C7186, near the 4 o'clock position of tank SX-106. At the three depths probed at this location, there is some signs of Tc-99 and nitrate but no chromium at 32, 39, and 44.5 m (106, 129, and 146 ft) bgs. This location may be delineating the lateral extent of the commingled SX-108 and SX-109 vadose zone plume in the northeast direction. To the west of the SX tanks and south of C7154 are two more probe holes. C7156 does not show any contamination in the Hf2 sediments but does show Tc-99 and nitrate in the CCuz subunit with higher concentrations at 43 m (141 ft) bgs. Farther to the south at C7158, there is a trace of Tc-99 and nitrate contamination at 43.3 m (142 ft) bgs in the CCu sediments. This distribution may delineate the extent of vadose zone contamination in the CCu unit from the SX tanks in the second and third N-S tank rows down the southwesterly dip of the Hanford and CCus. Probe hole C7172, which is west of tank SX-115 at about the 10 o'clock position, shows moderate concentrations of Tc-99, nitrate, and chromium at 30 m (98 ft) bgs in the Hf2 unit and larger concentrations of the same three mobile contaminants at 48.7 m (127 ft) bgs, near the contact of the Hf2 and CCuz subunits. The Tc-99 and nitrate concentrations in the sediments from this probe hole are similar to those found in the 299-W23-19 borehole sediments, which suggest this probe hole is intercepting the same vadose zone plume assigned to the leak at SX-115. Probe hole C7170, near SX-115 at about the 5 o'clock position and probe hole C7168 near SX-113 at the 7 o'clock position both show some Tc-99 and nitrate contamination near 25 m (82 ft) bgs in the Hf2 and greater concentrations at 34.7 m (114 ft) bgs deep in the Hf2 subunit. However, neither probe hole shows significant contamination deeper at 40.8 and 46.3 m (134 and 152 ft) bgs in the CCu formation. This may suggest that the relatively small volume releases from tanks SX-114 and SX-113 remain in the Hanford formation sediments and the larger leak at SX-115 occurred on the tanks western edge and migrated deeper toward the southwest with the dip in vadose zone sediments. Probe hole C7192 near tank SX-107 at the 4 o'clock position shows medium concentrations of Tc-99, nitrate, and chromium at 30.7 m (101 ft) bgs and about an order of magnitude higher Tc-99 and nitrate but no chromium at 39.3 m (129 ft) bgs. The contamination may have come from the moderate volume release from SX-107 or perhaps is a continuation of the vadose zone plume formed by the commingled release from SX-108 and SX-109.

The probe holes within the SX Tank Farm region corroborate the findings from the three boreholes that suggest chromium is slightly less mobile than the Tc-99 and nitrate released from SX tanks.
The chromium, in general, has not penetrated below the Hf2 subunit in appreciable concentrations, except directly below the SX-108 tank. The only probe holes with detectable I-129 are C7178 and C7180 that intercepted the highly concentrated commingled vadose zone plume from SX-108 and SX-109.
This suggests that the detection limit for determining I-129 is not sensitive enough to detect I-129 when not near its highest concentrations. The probe hole data corroborate that the contact between the Hf2 and

CCuz subunits are acting as a lateral spreading and possibly a perching plane and that, in places, contamination has penetrated deeper into the CCuz subunit. The vadose zone plume(s) also migrate in a southwesterly direction along the dip of the sedimentary units. It is unlikely that any of the probe holes and only two of the boreholes have penetrated deeper into the CCuc subunit and the Ringold Formation below so that it is difficult to determine if and where contamination from the SX tank releases has reached the water table.

Three soil resistivity survey reports (RPP-RPT-38322, RPP-RPT-42513, and RPP-RPT-47851) have been published that evaluate low resistivity "anomalies" in the vadose zone. The first report (RPP-RPT-38322) used the dry well casings and surrounding groundwater monitoring well casings as electrodes in the well-to-well electrical resistivity survey. The results yield only a two-dimensional portrayal of the lateral spread of low resistivity with no depth information. Figure 3-28 shows the results on a conceptual model of the raw data using mainly the dry wells surrounding the SX tanks. The results are grouped into two values: the smallest and lowest resistivity anomaly in semitransparent red represents values less than 1.5 ohm-m; the larger anomaly in transparent green represents values between 1.5 and 3 ohm-m. There is clear spatial correlation between the low-resistivity features and the tanks designated as historically leaking. Tank SX-108 appears to be at the epicenter of the anomaly. Other inverted models that used raw electrical resistivity data from the surrounding groundwater wells as electrodes (thus, including a larger region that covered both the S and SX Tank Farms) shows an apparent minor low resistivity anomaly in the area between S and SX Tank Farms. The authors warn that the low resistivity feature between the farms should be interpreted with caution as there are no wells (or electrodes in the region) and some noisy raw data are still present in the modeling domain. This region between the two tank farms was the focus of the third report. The soil electrical resistivity conceptualization suggests that all the fluids released from the SX tanks may have commingled and formed one larger vadose zone plume with localized higher concentration hot spots centralized around tank SX-108. The borehole and probe hole sediment characterization activities suggest there may be several discrete vadose zone plumes with different concentrations of mobile contaminants dependent on the waste types released from each tank and separated by zones of uncontaminated sediments.

The second report, RPP-RPT-42513, describes surface-to surface electrode surveys that were performed to augment and refine more localized well-to-well electrode surveys previously documented in RPP-RPT-38322. The surface-to-surface survey involved the installation of permanent surface electrodes and subsequent data acquisition along 23 orthogonal survey lines. In total, the linear coverage of the resistivity profiles was approximately 10 km (3 mi), as shown in Figure 3-29. The raw data from all 23 lines were combined and inverse modeled using a single, large 3D domain for the entire SX project site. To account for the metallic infrastructure, a series of a priori modeling tests was conducted to incorporate estimated resistivity values and known dimensions of the tank structures into the inverse model. Interestingly, the a priori information did not significantly change overall estimates of soil resistivity when compared to results for models with no a priori information. A sequence of depth slices, corresponding to depths between 5 and 70 m (16 and 230 ft) bgs, was extracted from the 3D inversion results. Data for each depth level were interpolated and visualized using 2D algorithms, which produced better differentiation of features (i.e., better feature resolution) and less smoothing than 3D. An example of a plan view depth slice at a depth of 40 m (131 ft) bgs can be viewed in Figure 3-30. Low resistivity values are shown in cool shades (violet and purple) while high resistivity values are indicated by warm colors (yellow and red).

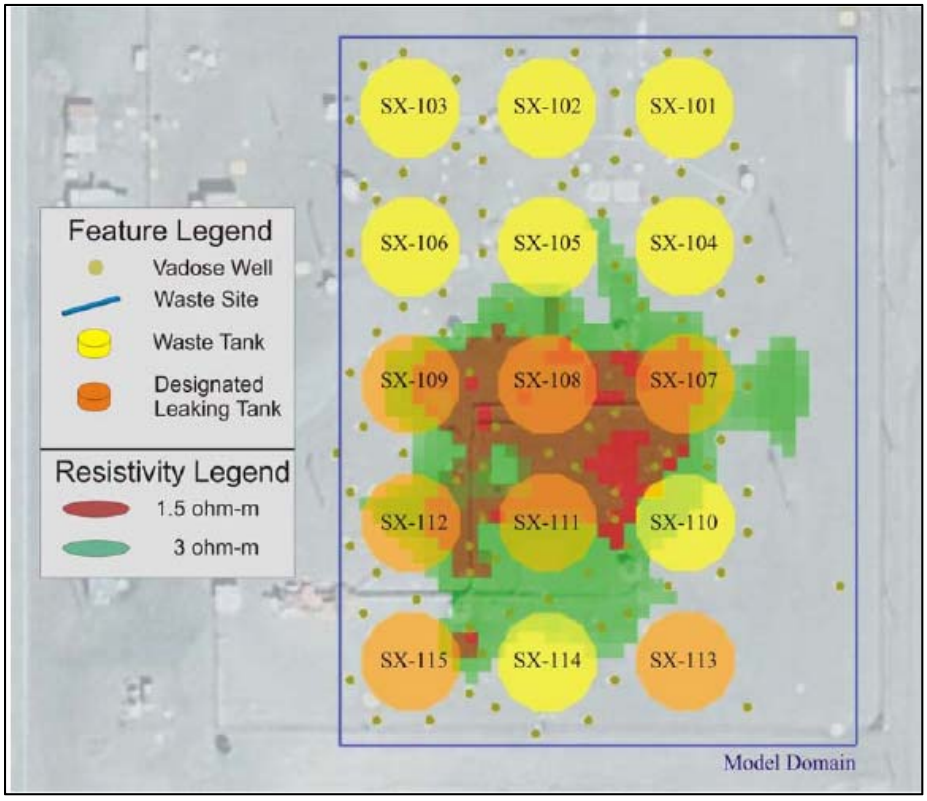

Figure 3-28. Estimated Lateral Extent of SX Tank Farm Contamination based on Soil Resistivity Data

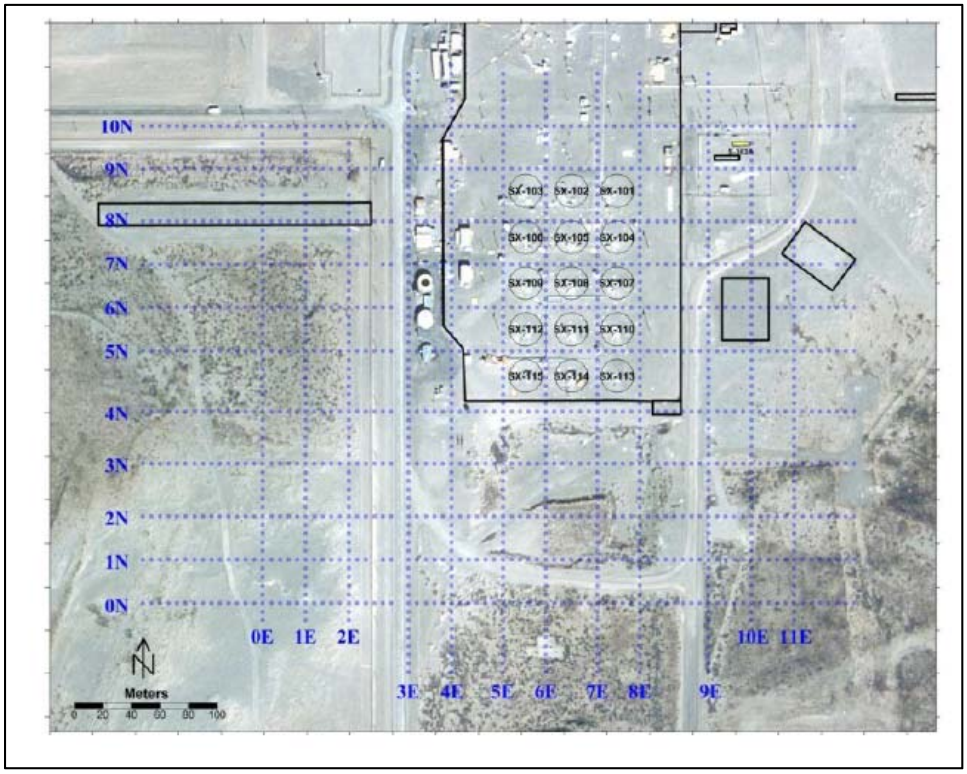

Figure 3-29. Location of Soil Resistivity Surface Electrode Lines

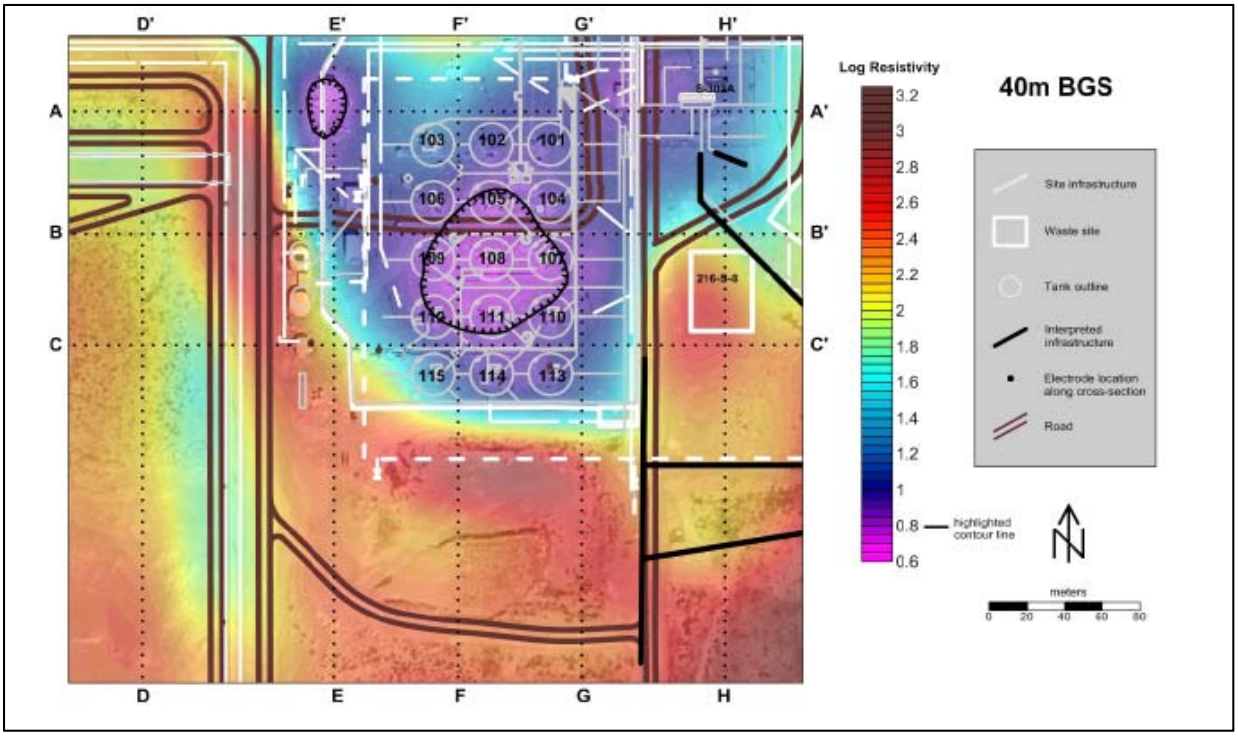

Figure 3-30. Estimated S-SX Tank Farm Lateral Extent of Contamination based on Soil Resistivity Modelling at 40 m (131 ft) bgs

The most conductive regions vary with depth, but were grouped into three areas within the SX Tank Farm. A large, highly conductive feature is indicated near the center of the SX Tank Farm. Two small conductive features are indicated to the northwest of tank 241-SX-103 along the fence line and to the northeast of 241-SX-102 near the 241-S-302A tank. It is expected that the low resistivity responses likely represent the combined effects of increased soil moisture and waste salts and the influence of conductive infrastructure. The authors of RPP-RPT-42513 suggest there was sufficient variation in the correlation of infrastructure to resistivity responses to suggest that areas containing the lowest resistivity values provide the highest confidence in locating subsurface contamination. Figure 3-31 shows a stack of the 0.8 log ohm-meter isopleths for depths bgs. Contrary to the direct sediment measurements from 299-W23-19 and several of the SX probe holes, the surface-to-surface resistivity response shows little indication of increased soil moisture or salts near SX-115, which reportedly leaked 193,056 L (51,000 gal), but there is good correlation between the conductive response and the SX-107/108 combined 211,983 to 401,253 L (56,000 to 106,000 gal) release. Conductive responses for depths 60 and 70 m (197 and 230 ft) bgs are proximal to the 56,781 L (15,000 gal) released at SX-113. There are no reported surface or tank waste releases near the two low resistivity responses to the northeast of SX-102 and northwest of the SX-103. Therefore, these smaller, isolated low resistivity responses were most likely caused by infrastructure or unreported surface and-or pipeline leaks in the vicinity. The fact that the soil resistivity conceptual models do not show indications of tank waste around and west of tank SX-115 is particularly puzzling because the Borehole 299-W23-19 and probe holes C7172, C7158, and C7170 all suggest that tank fluids reside in the vadose zone that likely originated from SX-115. It is true that the waste leaked from SX-115 is more dilute than most of the other SX tank waste fluids; however, the ionic strength of the SX-115 fluids is large enough such that it should be causing low resistivity anomalies.

RPP-RPT-47851 describes soil resistivity survey results for the region between the S and SX Tank Farms where the direct push sediments described in RPP-47274 and shown in Figure 3-10 were obtained.

Electrodes were placed in several of the direct push probe holes after sediment sampling and backfilling. The main conclusion of the report was that low soil resistivity and inverse modeling of the subsurface below 20 m (65.6 ft) seemed to correlate with high moisture zones that sediment measurements showed were fine-grained sediments. The soil characterization data described in ATL Document No. 20100311 showed there was detectable nitrate at concentrations between 6 and 16 μg/g and barely detectable (0.8 to 3 pCi/g) Tc-99 at depths between 14 and 40 m (46 and 131 ft) bgs. It is doubtful that these sediments contained high percentages of the tank fluids that were released from many of the tanks SX-107 through SX-115 to the south of these probe holes.

The third type of data that can be used to delineate the vadose zone contamination below and surrounding the SX Tank Farm is gamma logging activities. It was beyond the scope of this effort to provide critical review of all the available historical gross gamma logs and more recent spectral gamma logs. Besides the typical gamma logging activities through the borehole and dry well casings, the SX Tank Farm has laterals placed about 3.1 m (10 ft) below the tank bottoms that have been logged using gamma detectors. Figure 3-32 shows the location of the laterals, and RPP-RPT-27605, *Gamma Surveys of the Single-Shell Tank Laterals for A and SX Tank Farms*, includes data that have been collected in the recent past (1995). Earlier measurements of gamma activity in the laterals are found in many operations memos and reports that are cited in the most recent effort to evaluate tank releases and, to a lesser extent, the vadose zone contamination (RPP-ENV-39658).

A complete listing of documents that contain the gamma logging data for the SX Tank Farm is found in HGLP-OTH-015, *Hanford Geophysical Logging Project S-SX Focus Area.* Included in the listing are DOE/ID/12584-268, GJO-HAN-4, *Vadose Zone Characterization Project at the Hanford Tank Farms SX Tank Farm Report*; DOE/ID/12584-268A, GJO-HAN-4, *Hanford Tank Farms Vadose Zone, Addendum to the SX Tank Farm Report*; Sobczyk, 2000, *Subsurface Interpretation of the SX Tank Farm Hanford Site, Washington Based on Gamma-Ray Logging*; RPP-7884; and DOE/ORP-2008-001, *RCRA Facility Investigation Report for Hanford Single-Shell Tank Waste Management Areas.* A brief summary of the gamma logging findings is that the Hanford formation sediment around the SX tanks indicates several significant releases of tank fluids, especially around SX-115, SX-112, SX-108, SX-113, and SX-107.

Small releases are indicted around SX-109 and SX-114. Very few of the gamma logs extend below the CCuz subunit because the dry wells were not drilled to depth to avoid becoming conduits for tank fluids to short circuit to the water table. Thus, there is little direct evidence from the gamma logs to delineate a connection through the vadose zone to the water table for tank fluids. The gamma logs are most useful for indicating which SX tanks released fluids that have penetrated to depths below the tank bottoms and, by finding several dry wells close to each other that show similar gamma distributions, one can infer a relative volume of waste that likely was released from each tank or where plumes likely coalesced into one larger vadose zone plume.

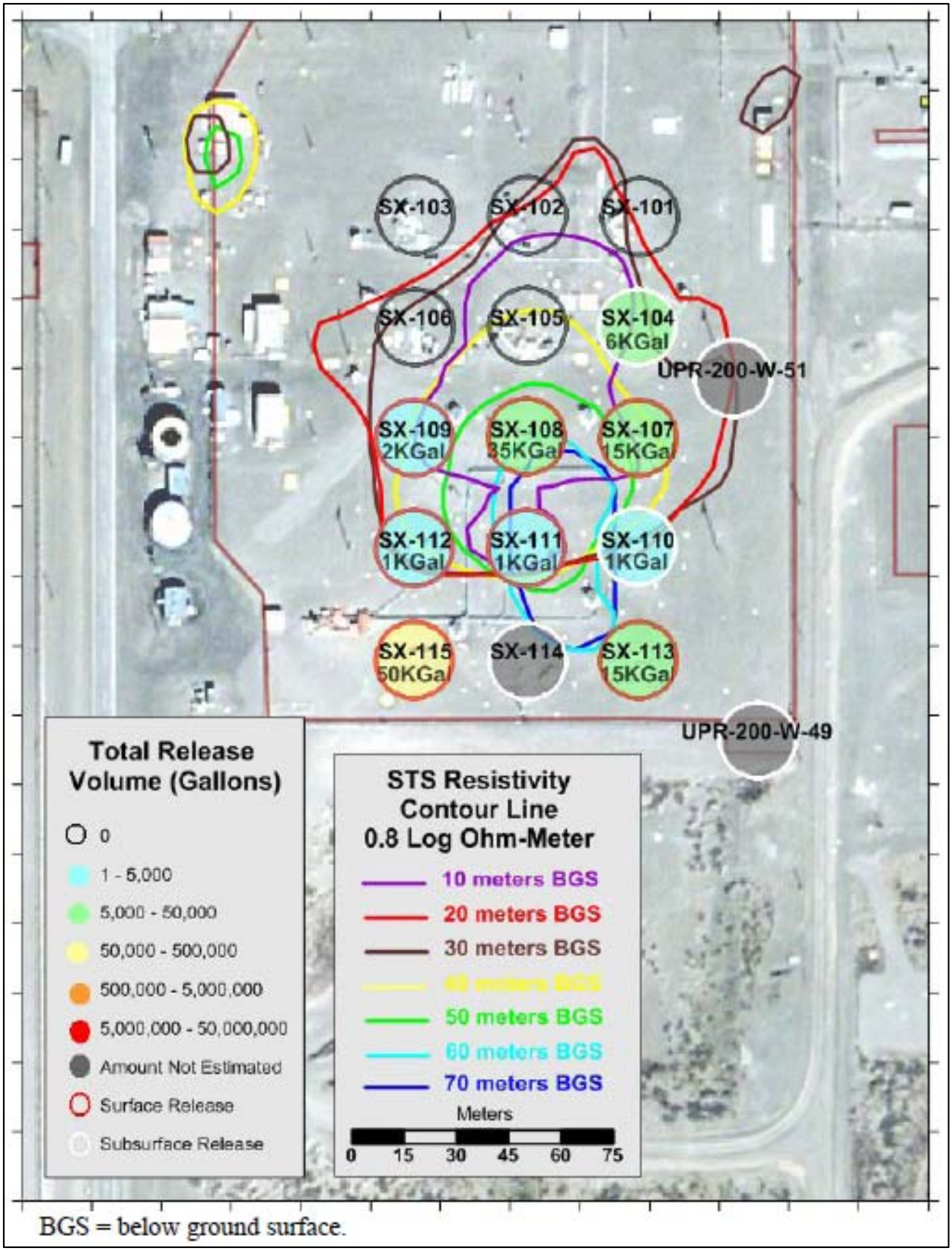

Figure 3-31. Estimated S-SX Tank Farm Lateral Extent of Contamination based on Soil Resistivity Modelling at Several Depths (m bgs)

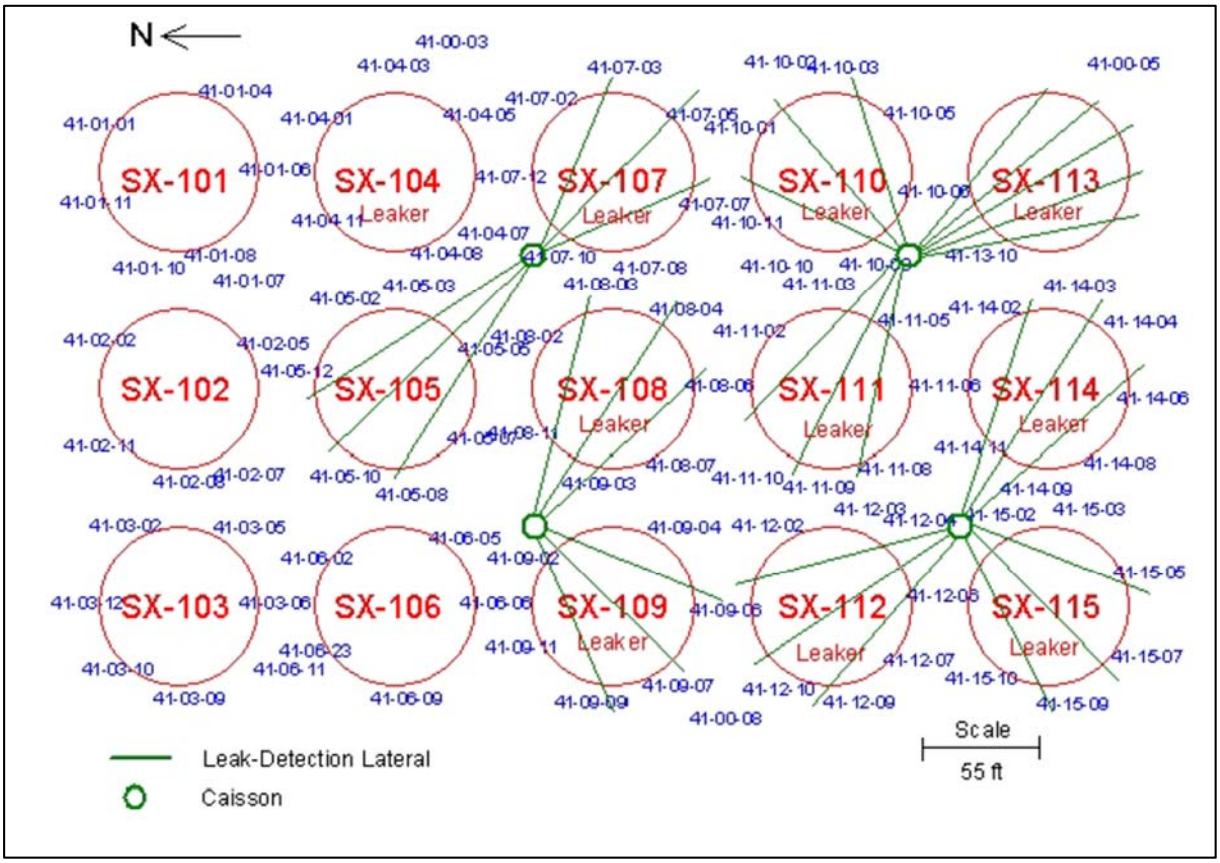

Figure 3-32. Location of Laterals Below and Dry Well Monitoring Boreholes around the SX Tanks

A detailed vadose zone conceptual model that estimates in a quantitative fashion the residual contamination below the SX Tank Farm is not possible at this time. However, the information reviewed in this subsection makes it quite clear that the vadose zone below the SX tanks does contain significant mass of mobile nitrate, Tc-99, chromium, and likely I-129. Based on the concentrations measured in vadose zone sediments around and below the SX-108 and SX-109 tanks and the inventories tabulated in Table 3-3, the vadose zone below the SX Tank Farm contains more radionuclide and chromium contamination than the two neighboring cribs (216-S-21 and 216-S-25) and considerable nitrate, as well. As will be discussed in Chapter 5, the S and SX Tank Farms appear to be the source of current groundwater chromium and Tc-99 in the S Complex Area.

If the tank wastes are released over one-tenth the footprint of each tank, the bottom of the SX tanks are 16.5 m (54 ft) bgs, and the fluids fill 25 percent of the volume, about 0.5 ML of tank fluid could be retained in the vadose during the active leak period and, after years of gravity draining to a final volumetric moisture content of 10 percent, 0.2 ML could be retained. For a larger footprint or porosity, proportionally more fluids could be retained during the leak period. As shown in Table 3-3, the largest estimated volume released from the SX tanks was 0.2 ML from SX-115. For conservative purposes, the current best estimate of residual contamination within the vadose zone below the SX Tank Farm will be set equal to the masses tabulated in Table 3-4, which essentially suggests that all the released mass is still present despite the fact that groundwater plumes sourced to the two tank farms have been present for at least the past decade. Section 6 will provide an estimate for the mass of these mobile contaminants currently in the groundwater so a comparison with the mass released can be made.

3.3 S Complex Area Total Mass of Key Chemicals and Activity of Radionuclides Remaining in the Vadose Zone

The process of estimating the residual masses/activities of the five key mobile contaminants that may currently remain in the S Complex Area vadose zone relied on a combination of data consisting primarily of the borehole geophysical logging data, soil-resistivity survey data, vadose zone hydrogeologic interpretations, SIM inventory data, and process knowledge. There is no sediment analytical data available within or near the four 200-DV-1 OU waste sites to support the estimation. There are a limited number of sediment analytical results available from boreholes near the S Tank Farm and several boreholes and probe holes within the SX Tank Farm. Tank farm studies suggest that eight SX tanks may have released waste fluids to the subsurface. In this area, 3 boreholes and 13 direct push probe holes have been sampled and their sediments characterized. Further, most of these SX Tank Farm sediment samples were obtained from depths above the CCuc subunit; only two boreholes (299-W23-234 and 299-W23-19) provide samples deeper into the underlying Ringold Formation where the water table resides.

Based on the available data, expert judgment supported by gamma logging and soil resistivity survey data were combined with the vadose zone hydrogeology to generate estimates of the volume of vadose zone sediments that may contain contamination and the residual waste fluids. During this evaluation, it was assumed that mobile contaminants do not interact significantly with the sediments and, therefore, are present mainly in the residual pore water.

Based on the estimates of vadose zone sediments that are contaminated and the assumed moisture contents of that sediment volume, the estimated volume of pore water contained in the contaminated sediment exceeds the volume of liquid waste released to the S Complex Area Cribs and leaked from the S-SX SSTs. These data indicate that, with the exception of the 216-S-25 Crib, almost all the liquid waste released to the vadose zone beneath the S Complex Area waste sites could still be present in the vadose zone, regardless of what the groundwater plumes' time history data show (discussed in Chapter 5).

The primary assumption for the residual contaminant mass/activity estimates is that if the disposed waste fluids are still present in the vadose zone, then the mobile and, certainly, the less mobile contaminants also remain in the vadose zone. This assumption assumes that artificial and natural recharge has not significantly pushed (or displaced) residual waste fluids deeper and into the unconfined aquifer where they would disperse and migrate within the underlying unconfined aquifer. Transport modeling of the fate of the waste fluids and contaminants therein was not part of the scope of this preliminary S Complex Area CSM report. Table 3-7 shows the summary and ranking of the estimates of residual vadose zone masses/activities below each S Complex Area Waste facility. The following paragraphs summarize the waste estimates for the five contaminants:

- **Nitrate**—Based on the assumptions defined previously, approximately 25 percent of the nitrate released to the S Complex Area may still be present below the 216-S-9 and 216-S-25 Cribs with each containing about 12 percent. Sediments below and around the 216-S-23 Crib are estimated to contain only 0.4 percent of the nitrate released to the entire S Complex Area. The 216-S-21 Crib sediments account for an insignificant 0.04 percent of the nitrate. These estimates suggest that approximately 50 percent of the nitrate disposed to the S Complex Area reached the groundwater in the past, most of it originally disposed to the 216-S-25 Crib. The S Complex Area CSM estimates that all nitrate released from the 241-S-104 tank and any associated piping remains in the vadose zone and represents approximately 6.4 percent of the total nitrate released. The eight SX tanks that released fluids to the subsurface account for another 20.4 percent of the total nitrate released to the S Complex Area, with tanks 241-SX-108 and 241-SX-115 releasing about half of this value.

- **Chromium**—Chromium waste estimates for the S Complex Area vadose zone CSMs, indicate that two of the cribs (216-S-25 and 216-S-21) account for 3.3 percent of the total chromium released and the sediments below the SX Tank Farm fence line contains approximately 81 percent of the chromium released. The sediments below and around S Tank Farm (tank 241-S-104) contain about 5 percent of the total chromium released. Because the four S Complex Area Cribs contribute such a small percentage of the total chromium (even though we believe significant amounts of the fluids disposed reached the water table), the total mass of chromium remaining in the vadose zone (primarily beneath the SSTs) represents about 90 percent of the total released. The deep vadose zone below the SX Tank Farm would be priority for future characterization if chromium were considered a high priority groundwater threat.

- **Uranium**—As will be discussed in Chapter 5, there does not currently appear to be any significant uranium plume in the groundwater below the S Complex Area. However, one well (299-W23-11) near the 216-S-9 Crib does show persistent values of approximately 10 μg/L, which is above the estimated background level of 3 μg/L The vadose zone sediments below the 216-S-9 Crib are estimated to contain 90 percent of the total uranium released to the S Complex Area and, therefore, is the likely source of the low uranium groundwater concentrations observed at 299-W23-11. The uranium releases from the 241-S-104 tank and the SX tanks are estimated to be approximately 4.3 percent and 5.1 percent, respectively, of the total uranium released to the S Complex Area. Thus, the vadose zone below the 216-S-9 Cribs would be the first priority for future characterization for uranium contamination if there were concern that uranium might be a future groundwater threat. Note that the ~10 μg/L uranium found in 299-W23-11 are below the drinking water maximum permissible concentration of 30 μg/L.

- **Technetium-99**—For Tc-99, vadose zone sediments below the four cribs are estimated to contain an insignificant amount of the total mass of Tc-99 released to the entire S Complex Area (only 0.5 percent of the total or 0.17 Ci). The bulk (91 percent) of the Tc-99 released to the S Complex Area is estimated to currently reside below the SX Tank Farm and an additional 8.4 percent of the Tc-99 currently resides around and below 241-S-104 tank. As will be discussed in Chapter 5, we feel that these two tank farms are the source of the increased Tc-99 in the groundwater observed below the S Complex Area in the last decade or more.

- **Iodine-129**—The 216-S-9 Crib probably has the most I-129 still remaining in the vadose zone (estimated at 36 percent). The sediments below the SX Tank Farm are estimated to contain 59 percent of all the I-129 with tanks SX-108, SX-112, and SX-115 accounting for 44 percent of the 59 percent. I-129 was detected in the borehole sediments and a few of the direct push sediments around and below these tanks. The sediments from around and below 241-S-104 are estimated to currently contain 4.8 percent of the total I-129 released to the S Complex Area.

Table 3-7. Estimates of Residual Vadose Zone Contamination and Site Rankings

Ranking	NO_3	%	Chromium	%	Uranium	%	Technetium	%	Iodine-129	%
1	**S-25**	**12.2%**	SX-108	23.6%	**S-9**	**90.3%**	SX-108	34.1%	**S-9**	**36.0%**
2	**S-9**	**11.5%**	SX-115	19.9%	S-104	4.3%	SX-112	18.8%	SX-108	22.1%
3	SX-108	6.6%	SX-112	13.0%	SX-115	2.2%	SX-115	14.9%	SX-112	12.2%
4	S-104	6.4%	SX-113	11.6%	SX-108	1.1%	SX-107	14.2%	SX-115	9.7%
5	SX-115	4.4%	SX-107	9.8%	SX-112	0.6%	S-104	8.4%	SX-107	9.2%
6	SX-112	3.6%	S-104	5.0%	SX-113	0.6%	SX-113	4.2%	S-104	4.8%
7	SX-107	2.7%	**S-25**	**2.1%**	SX-107	0.5%	SX-109	2.2%	SX-113	2.8%
8	SX-113	2.1%	SX-109	1.5%	SX-109	0.1%	SX-111	1.8%	SX-109	1.5%
9	SX-109	0.4%	SX-111	1.3%	SX-111	0.1%	SX-114	0.5%	SX-111	1.2%
10	**S-23**	**0.4%**	**S-21**	**1.2%**	**S-25**	**0.0%**	**S-9**	**0.3%**	SX-114	0.1%
11	SX-111	0.4%	SX-114	0.1%	SX-114	0.0%	**S-21**	**0.2%**	**S-21**	**0.1%**
12	**S-21**	**0.04%**	**216-S-23**	**0.00%**	**S-21**	**0.0%**	**S-23**	**0.000%**	**S-23**	**0.0%**
13	SX-114	0.03%	**216-S-9**	**0.00%**	**S-23**	**0.0%**	**S-25**	**0.0%**	**S-25**	**0.0%**
	Total	50.9%	Total	89.2%	Total	99.8%	Total	99.6%	Total	99.7%

Note: Residual contaminant inventories do not total 100% because some mass/activity is estimated to have reached water table.

Bold Type Identifies S Complex Area 200-DV-1 OU waste sites and corresponding values.

Waste site number prefix "216-" and tank number prefix "241-" omitted.

This page intentionally left blank.

4 Hydraulic Properties of the Vadose Zone and Unconfined Aquifer

This chapter of the 200-DV-1 OU CSM specifies available published hydraulic and transport parameter values for both the vadose zone and the unconfined aquifer near the S Complex Area. These references also provide best estimates of recharge rates for near-surface soil types and vegetated conditions existing within the study region to serve as a model for upper boundary conditions for future flow and contaminant transport modeling. For the S Complex Area, the available data have been aptly reviewed and tabulated in published reports that should be consulted. No additional hydraulic parameter values estimated from laboratory tests of sediment samples from the S Complex Area since the following available tabulations were published.

The values recommended in the following documents should be used after carefully assessing their applicability to any site-specific aspects at the S Complex Area that warrant "case-by-case" considerations.

These documents are good compilations of hydraulic parameters:

- PNNL-14702, *Vadose Zone Hydrogeology Data Package for Hanford Assessments*
- PNNL-17913, *Hydrogeology of the Hanford Site Central Plateau – A Status Report for the 200 West Area*
- RPP-9223, *Modeling Data Package for B-BX-BY Field Investigation Report (FIR)*
- RPP-13310, *Modeling Data Package for an Initial Assessment of Closure for C Tank Farm*
- RPP-RPT-35222, *Far-Field Hydrology Data Package for the RCRA Facility Investigation (RFI) Report*
- WHC-EP-0883, *Variability and Scaling of Hydraulic Properties for 200 Area Soils, Hanford Site*

The following documents discuss field techniques and provide field-scale measured hydraulic parameters:

- PNNL-14753, *Groundwater Data Package for Hanford Assessments*
- PNL-7330, *Hydrologic Testing at the Single-Shell Tanks*
- PNNL-16945, *Slug Test Characterization Results for Multi-Test/Depth Intervals Conducted During the Drilling of CERCLA Operable Unit OU ZP-1 Wells 299-W10-33 and 299-W11-48*
- PNNL-17675, *BP-5 Remedial Investigation Slug-Test Characterization Results for Well 699-52-55A*
- PNL-7333, *Hydrologic Testing at the Low-Level Burial Grounds*
- PNNL-13378, *Results of Detailed Hydrologic Characterization Tests – Fiscal Year 1999*
- PNNL-13514, *Results of Detailed Hydrologic Characterization Tests – Fiscal Year 2000*
- PNNL-14186, *Results of Detailed Hydrologic Characterization Tests – Fiscal Year 2002*
- PNNL-17348, *Results of Detailed Hydrologic Characterization Tests—Fiscal and Calendar Year 2005*
- PNNL-18732, *Field Test Report: Preliminary Aquifer Test Characterization Results for Well 299-W15-225: Supporting Phase I of the 200-ZP-1 Groundwater Operable Unit Remedial Design*

- PNNL-18279, *Aquifer Testing Recommendations for Well 299-W15-225: Supporting Phase I of the 200-ZP-1 Groundwater Operable Unit Remedial Design*
- PNNL-19491, *Slug Test Characterization Results for Multi-Test/Depth Intervals Conducted During the Drilling of CERCLA Operable Unit OU ZP-1 Wells 299-W11-43, 299-W15-50, and 299-W18-16*
- PNNL-19482, *Slug Test Characterization Results for Multi-Test/Depth Intervals Conducted During the Drilling of CERCLA Operable Unit OU UP-1 Wells 299-W19-48, 699-30-66, and 699-36-70B*
- PNNL-16688, *Recharge Data Package for Hanford Single-Shell Tank Waste Management Areas has a good discussion and tabulation of recharge rates for the Hanford Site.*

5 Status of Selected Mobile Contaminants in Groundwater Beneath the S Complex Area

This chapter summarizes the status of groundwater contamination beneath the S Complex Area. The S Complex Area has been divided into two subregions: the 216-S-9/216-S-23 Subregion 1, located east and downgradient of the S Tank Farm; and the 216-S-21/216-S-25 Subregion 2, located just west and upgradient of the SX Tank Farm. Local subregion-specific groundwater plumes include Tc-99, chromium, nitrate, uranium, and tritium, although only the uranium and tritium may have a source from the cribs. In addition to current contamination, cobalt-60 and gross beta plumes existed at one time beneath the S Complex Area. The gross beta plumes probably reflected the presence of ruthenium-106, which has since decayed to such small concentrations that it can no longer be detected. These historical groundwater plumes are discussed in this chapter.

5.1 Groundwater Contamination Beneath the Subregion 1

The wells used to characterize Subregion 1 (the 216-S-9/216-S-23 Cribs) are shown in Figure 5-1 and listed in Table 5-1, with their completion date, the latest water level elevations, and elevations of the wells open interval. One of the four wells at the 216-S-9 Crib and all four wells at the 216-S-23 Crib used for groundwater characterization are decommissioned. Well 299-W22-26 was on the eastern (downgradient) edge of the 216-S-9 Crib, and Well 299-W22-27 was on the western (upgradient) edge. Wells 299-W22-25 and 299-W22-69 are about 15 and 75 m (49 and 246 ft) south of the 216-S-9 Crib, respectively. At the 216-S-23 Crib, Wells 200-W19-5, 299-W19-7, and 299-W22-38 were on the eastern (downgradient) side of the crib, and Well 299-W22-37 was on the western (upgradient) side of the crib.

The earliest groundwater monitoring data from wells in the 216-S-9/216-S-23 subregion are from 1966 and 1967 and the groundwater already had been contaminated with gross beta, cobalt-60, and tritium by that time. Recall that these two cribs received wastes from 1965 to 1969 and from 1969 to 1972, respectively.

At the 216-S-9 Crib, gross beta concentrations were extremely high in late 1966 and early 1967 in Wells 299-W22-26 and 299-W22-25 reaching 80 million pCi/L and 38 million pCi/L, respectively (Figure 5-2). Additionally, gross beta concentrations were over 7,000 pCi/L in Well 299-W22-27. Concentrations decreased rapidly and were less than 30,000 pCi/L by May 1973, under 1,000 pCi/L by August 1976, and under 100 pCi/L by August 1978. Concentrations have remained low since that time. The 216-S-9 Crib received 53 ML (14 Mgal) of effluent between July 1965 and January 1969, and the high gross beta concentrations in the groundwater in the late 1960s and early 1970s are probably from the crib and probably represent mostly ruthenium-106.

At the 216-S-23 Crib, gross beta concentrations were much lower in the surrounding groundwater wells than in wells at 216-S-9 in the late 1960s and early 1970s. Active disposal to the 216-S-23 Crib occurred between 1969 and 1972. Gross beta concentrations began to increase in Well 299-W19-5 (monitored 216-S-23 Crib) in September 1969 when it was 4,000 pCi/L. Gross beta was not measured again until January 1971 when the concentration had reached 120,000 pCi/L. The concentration peaked at 140,000 pCi/L the following month and then began a steady decline until October 1974 when the concentration was less than 100 pCi/L. The gross beta concentration remained at <100 pCi/L until August 1988 after which the well was no longer sampled for gross beta analysis.

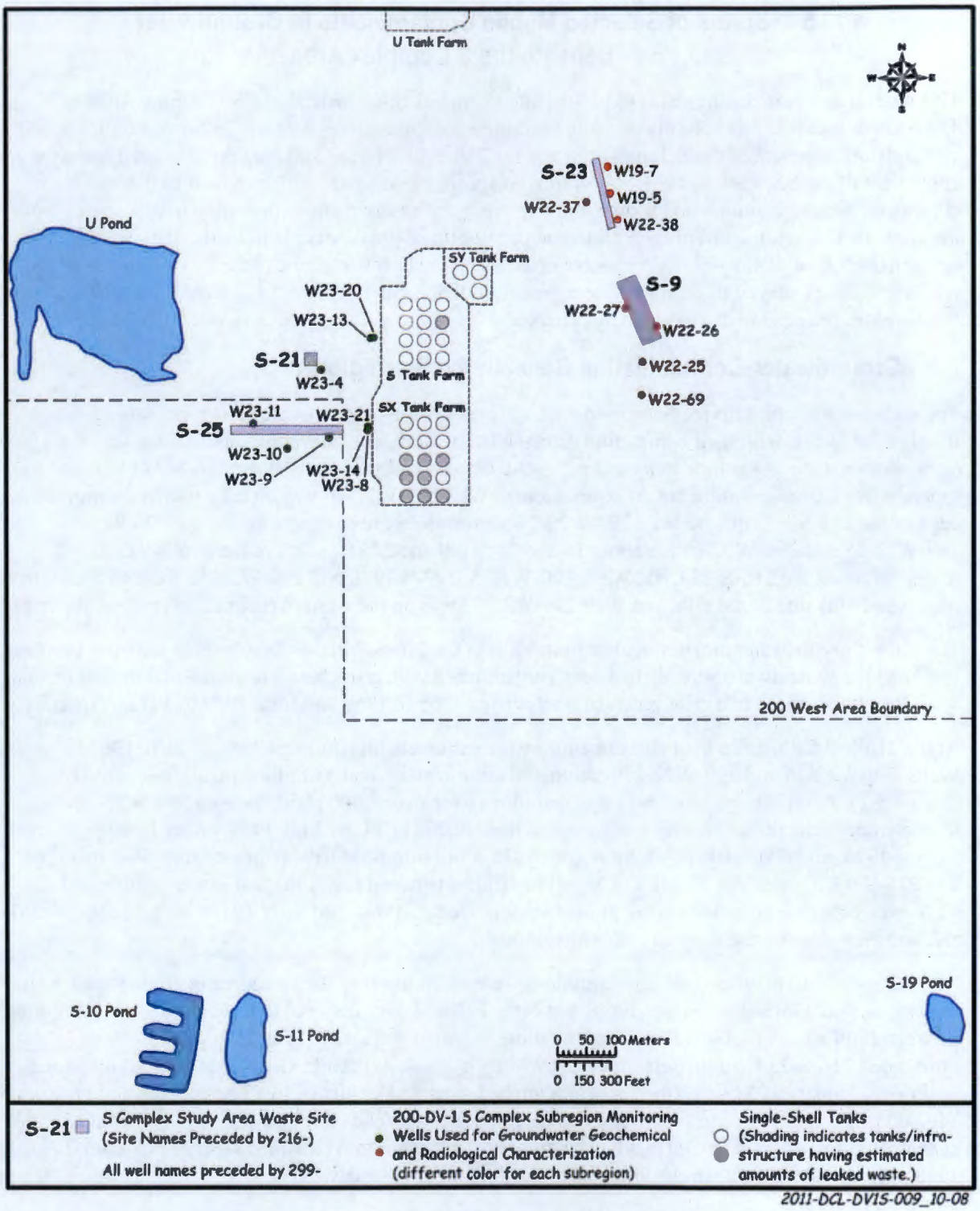

Figure 5-1. Well Location Map for the S Complex Area

Table 5-1. Wells Used to Characterize Groundwater Beneath Subregion 1 (216-S-9/216-S-23 Cribs)

Well Name	Completion Date	Elevation of the Water Table (Date) (m amsl)	Elevation of Open Interval (m amsl)	Water Above Bottom of Open Interval (m)
216-S-9 Crib				
299-W22-25	January 1964	143.93 (April 1973)	134.4 – 146.8 (perforated)	9.5
299-W22-26	December 1963	133.82 (March 2011)	133.0 – 141.4 (perforated)	0.8
299-W22-27	April 1964	143.76 (April 1973)	40 – 149.7 (perforated)	Decommissioned
299-W22-69	March 2006	134.02 (December 2010)	124.1 – 134.8 (screened)	9.9
216-S-23 Crib				
299-W19-5	November 1968	142.20 (August 1988)	Not available	Decommissioned
299-W19-7	November 1968	None available	127.9 – 150.1 (perforated)	Decommissioned
299-W22-37	November 1968	133.47 (July 2010)	127.3 – 149.5 (perforated)	Decommissioned
299-W22-38	November 1968	135.72 (March 2002)	127.1 – 149.3 (perforated)	Decommissioned

amsl = above mean sea level

The decrease in gross beta concentration between February 1971 and October 1974 in Well 299-W19-5 is more rapid than can be explained on the basis of ruthenium-106 radioactive decay alone (ruthenium-106 half-life is 367 days). Thus, the concentration decrease must have resulted from a combination of plume migration and radioactive decay without significant additional contamination entering groundwater after disposal stopped 1969 (assuming most of the gross beta was due to ruthenium-106). The plume would have moved toward the east since that was the direction of groundwater flow at that time.

Gross beta concentrations in the other three wells (299-W19-7, 299-W22-37, and 299-W22-38) were less than about 200 pCi/L throughout the 1970s and into the 1980s until they were no longer sampled for gross beta analysis. The relatively high gross beta concentrations in Well 299-W19-5 and low concentrations in the other wells at the 216-S-23 Crib is likely caused by Well 299-W19-5 being the closest downgradient well and near the middle of the crib. Well 299-W22-37 is west of the crib and upgradient and 299-W19-7 is at the far end of the crib opposite from the inlet and likely did not experience as much liquid disposal. Well 299-W22-38 near the inlet end of 216-S-23 Crib and downgradient shows moderate gross beta concentrations in the early 1970s.

In Subregion 1, cobalt-60 was first detected in Well 299-W22-25 at the southern end of the 216-S-9 Crib, where the pipeline that fed both cribs had a junction in March 1967 at a concentration of 38,000 pCi/L (Figure 5-3). Cobalt-60 was not measured again in the well until two years later, by which time the

concentration had decreased to 3,300 pCi/L. The large decrease in concentration cannot be explained by radioactive decay alone, so that the highly contaminated part of the plume encountering the well in 1967 had moved east 2 years later.

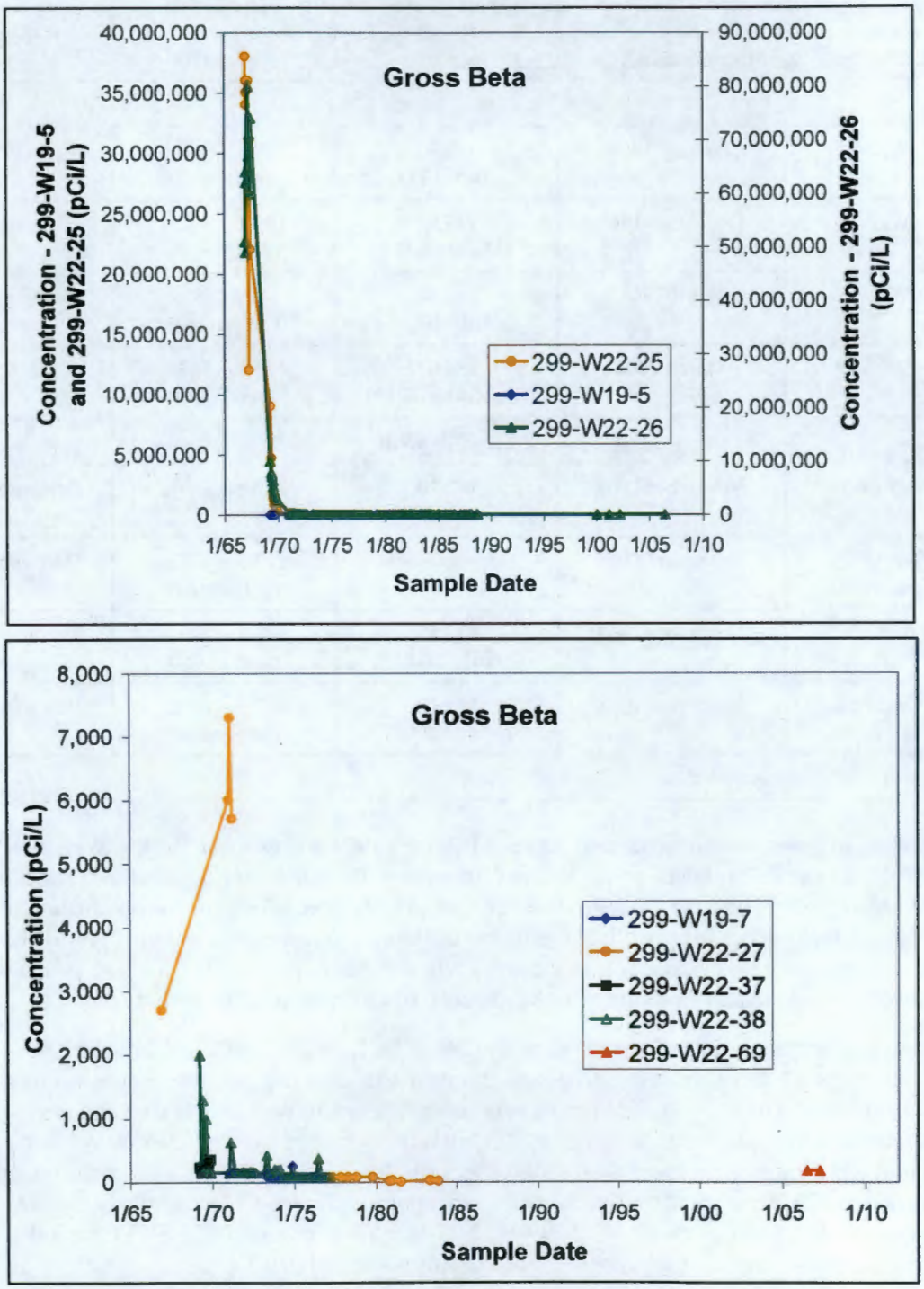

Figure 5-2. Gross Beta Concentrations at Selected Wells in Subregion 1 (216-S-9/216-S-23 Cribs)

Borehole 299-W22-25 is located near UPR-200-W-108 where contaminated water leaked into the vadose zone in January 1969. The amount of waste released from the pipeline leak is unknown. However, this pipeline leak appears to have occurred after the high cobalt-60 was observed in the well.

Cobalt-60 was found next in Well 299-W22-26 in March 1969 at a concentration of 3,300 pCi/L. The concentration had decreased to 350 pCi/L in January 1971 and was less than about 6 pCi/L after 1980. Again, the decrease in cobalt-60 concentration cannot be explained by radioactive decay alone (cobalt-60 half-life is 5.27 years). The source for the cobalt-60 may have been the 216-S-9 Crib since concentrations as great as 27,900 pCi/L were discharged to the crib in 1965 (concentration from RPP-26744 decay corrected to November 1965).

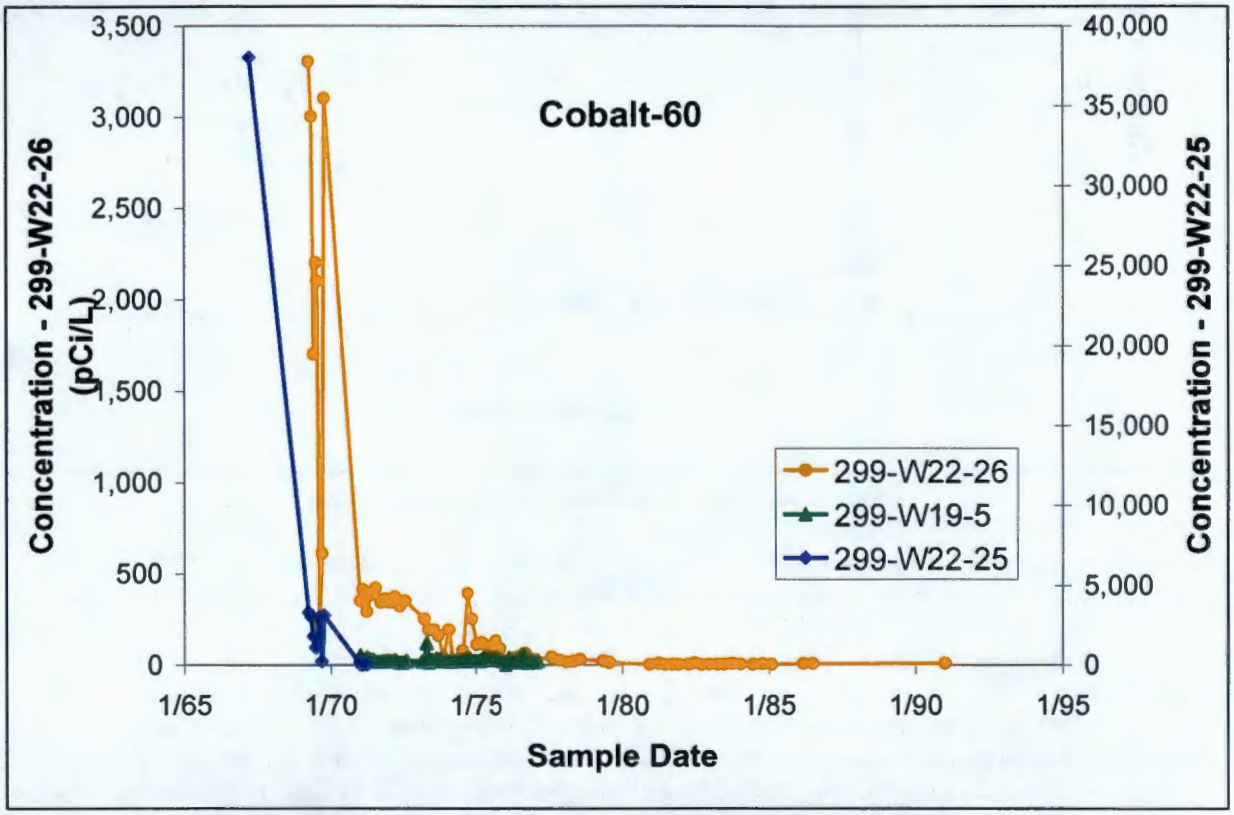

Figure 5-3. Cobalt-60 Concentrations in Wells at the 216-S-9 Crib

There also are data in the database for cobalt-60 from wells at the 216-S-23 Crib. However, the results from the late 1960s are almost certainly not valid although they are not flagged as such in HEIS. Figure 5-4 shows that the results are exactly the same for each of the four wells monitoring the 216-S-23 Crib for the six sampling events between March 1969 and October 1969. This is probably a result of transcription errors. The first "good" results are from January 1971 when the cobalt-60 concentration was between 17 and 63 pCi/L in wells at the 216-S-23 Crib (Figure 5-4). The cobalt-60 concentration ranged between about 15 and 45 pCi/L between 1972 and 1977. The only subsequent analysis was in August 1987 when the cobalt-60 concentration was 5.7 pCi/L. All wells at the 216-S-23 Crib are now decommissioned.

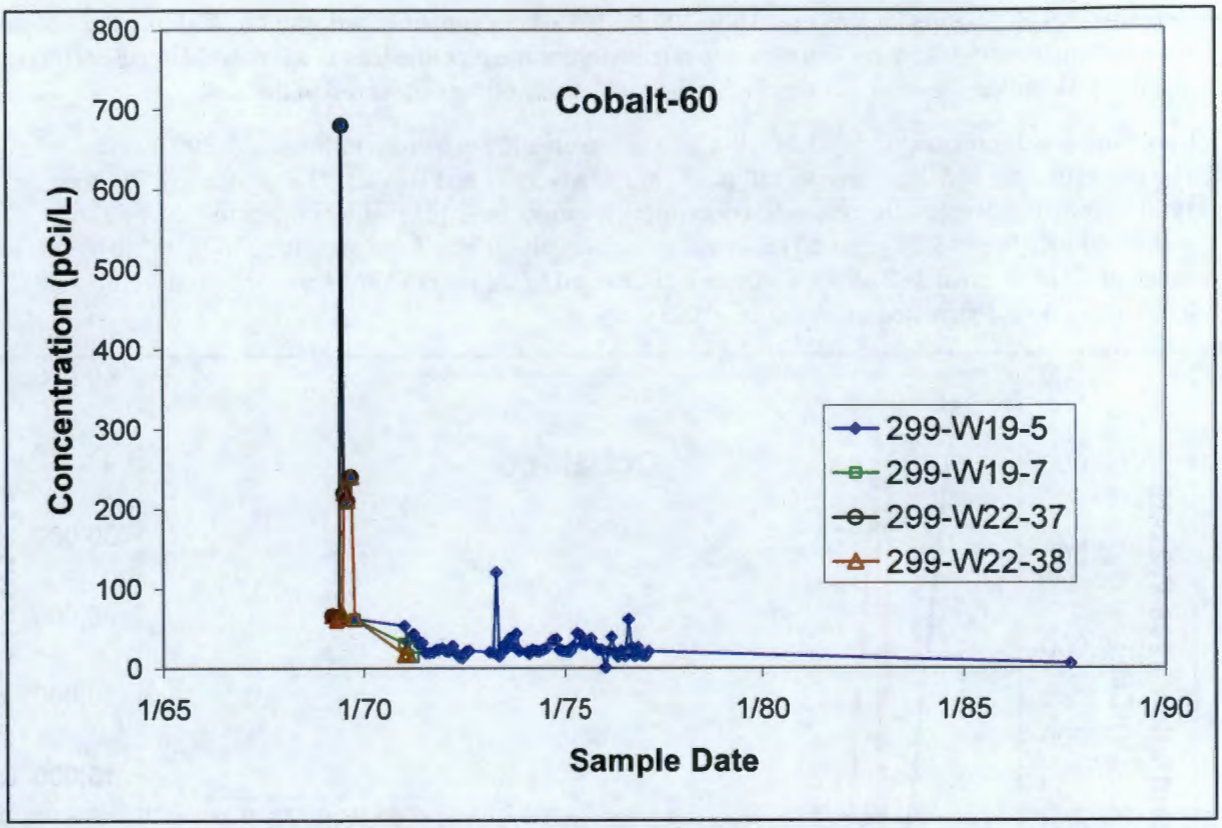

Figure 5-4. Cobalt-60 in Wells from the 216-S-23 Crib

Ruthenium-106 was found in one well at the 216-S-9 Crib and one well at the 216-S-23 Crib in early 1971 (Figure 5-5). The initial concentration in Well 299-W19-5, at the 216-S-23 Crib, was 130,000 pCi/L and the initial concentration in Well 299-W22-26, at the 216-S-9 Crib was 55,000 pCi/L. There was a rapid decrease in ruthenium-106 concentration throughout the 1970s and concentrations were less than 100 pCi/L in 1980. The decrease in concentration was the result of radioactive decay (ruthenium-106 half-life is 368 days) and movement and dispersion of the plume in the aquifer. The source for the ruthenium-106 in groundwater at the 216-S-9/216-S-23 subregion is not known but probably was not the 216-S-9 or 216-S-23 Cribs because RPP-26744 cites concentrations of less than 1 pCi/L discharged to the cribs (decay corrected to November 1965).

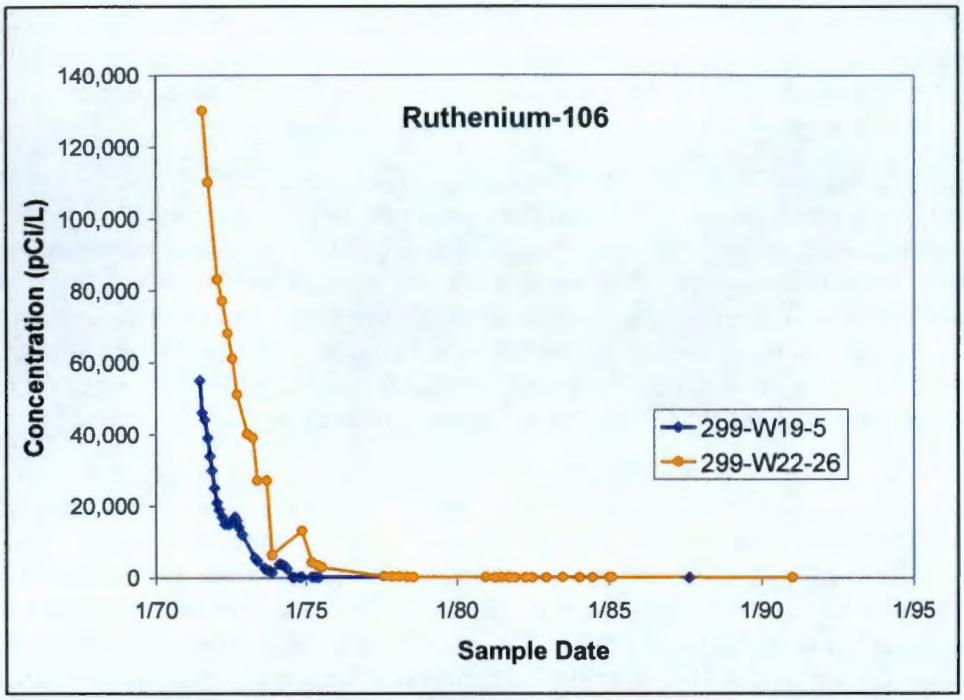

Figure 5-5. Ruthenium-106 Concentrations in Wells at the 216-S-9/216-S-23 Subregion

Nitrate concentrations have been measured in three wells within Subregion 1 (216-S-9/216-S-23 Cribs) (Figure 5-6). Nitrate concentrations have been less than 30 mg/L in all samples from Well 299-W22-69, since it was first sampled in 2006 until the present, and are not shown on Figure 5-6.

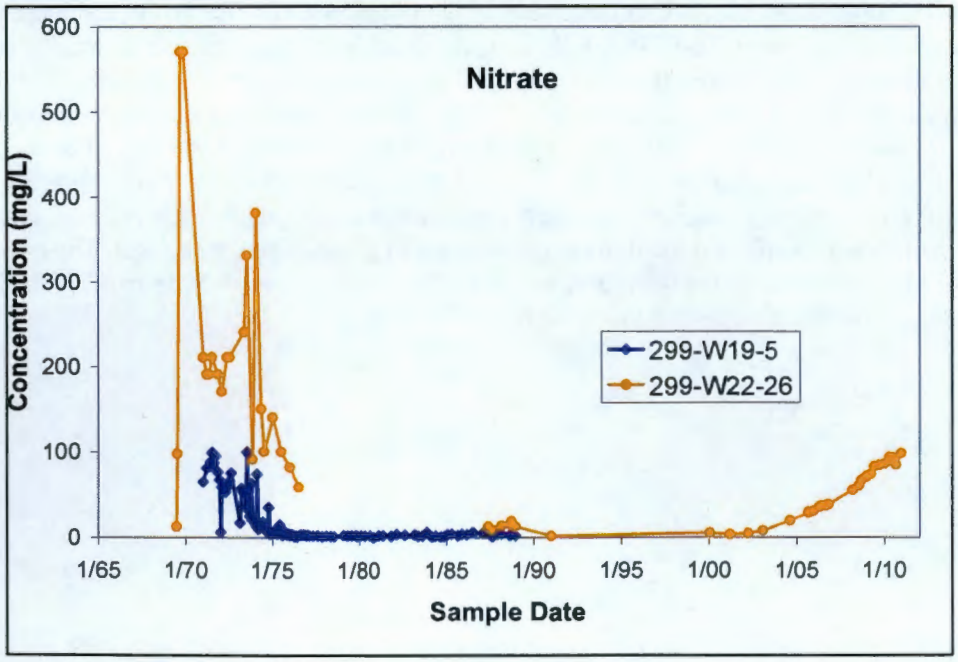

Figure 5-6. Nitrate Concentration in Wells at the 216-S-9/219-S-23 Subregion

The nitrate concentrations in groundwater from Well 299-W22-26 during the late 1960s and 1970s are difficult to interpret because of the large concentration range in the database. The data show that in July 1969, the nitrate concentration was slightly less than 100 mg/L; two months later, and eight months after termination of disposal to the crib, the nitrate concentration was 570 mg/L.

A second sample collected November 1969 also had 570 mg/L nitrate. The well was not sampled again until July 1971 when the nitrate concentration had dropped to 210 mg/L and then remained between about 200 and 250 mg/L until July 1973. Between July 1973 and May 1974, the nitrate concentration varied greatly, and seemingly unreasonably, between 91 mg/L and 380 mg/L. None of these data is flagged as suspect in the database but the high variability in concentrations seems unreasonable for such a short period. Possibly, the two higher concentrations between August 1973 and ay 1974 are in error and the nitrate concentration continued to decrease from the early 1970s until August 1976 when the last sample was taken from the well (until 1987) when the concentration was 59 mg/L.

The large nitrate increase of about 475 mg/L in the two-month period between July 1969 and September 1969 also is suspect, although the September concentration was verified in November 1969. It is certainly possible that the 216-S-9 Crib contributed to nitrate groundwater contamination. The crib received 50 ML (13.2 Mgal) of effluent and the effluent contained over 1,000 mg/L nitrate in 1965 and 1966. It is possible that waste solutions reached Well 299-W22-26 and very rapidly descended the outside of the well casing to the aquifer. Well 299-W22-26 was drilled in 1963 and was retrofitted with a grout seal from the surface to 59.4 m (195 ft) in 1971. Regardless of the specific concentration trends in this well, it does appear that the nitrate concentration exceeded the DWS (45 mg/L) throughout the 1970s and the source of the nitrate was most likely the 216-S-9 Crib.

The nitrate concentration was not measured again in Well 299-W22-26 until June 1986. Between that time and August 2004, the nitrate concentration remained well below 20 mg/L. The nitrate concentration began to increase in August 2004 and continued to increase at a steady rate until the present. The latest nitrate concentration was 97.8 mg/L in December 2010. The nitrate increase in mid and late 2000 is coincident with an increase in Tc-99 (see following discussion) and is due to encroachment of a nitrate plume from the 241-S Tank Farm, likely from the 241-S-104 SST (Figure 5-7). Nitrate also has been found in Well 299-W19-5, located at the 216-S-23 Crib. Nitrate concentrations were first measured in 1971, and the initial concentration throughout 1971 ranged between 65 and 99 mg/L. The concentration decreased after 1971 and was at or below the 5.7 mg/L background (DOE/RL-96-61, *Hanford Site Background: Part 3, Groundwater Background*) during the last 13 years that the well was sampled. The 216-S-23 could have contributed to nitrate contamination of groundwater in the area. The crib received 34.1 ML (9 Mgal) of effluent, but the nitrate concentration in the effluent was 56 mg/L (RPP-26744)—too dilute to account for the concentrations measured in 1971.

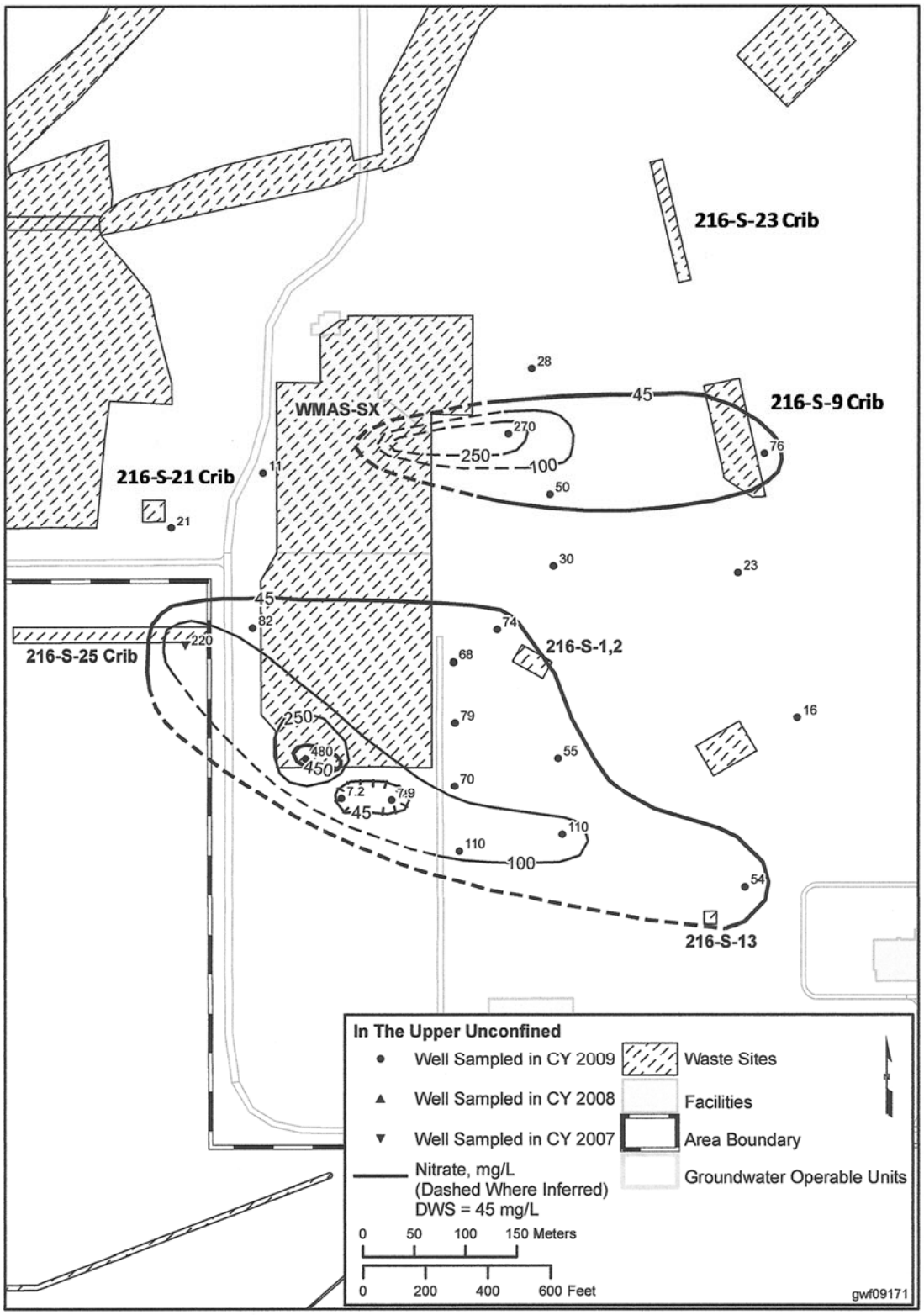

Source: DOE/RL-2010-11, *Hanford Site Groundwater Monitoring and Performance Report for 2009 Volumes 1 & 2*.

Figure 5-7. Average 2009 Nitrate Concentrations Within the S Complex Area, Upper Portion of the Unconfined Aquifer

Tritium has been found in two wells at the 216-S-9 Crib and one well at the 216-S-23 Crib (Figure 5-8). The 216-S-9 Crib was used from July 1965 to January 1969. The initial tritium concentration measured in Well 299-W22-25, located just south of the crib, in December 1965 was 2,000 pCi/L. Two months later, in February 1966, the concentration had increased to 55,000 pCi/L and, eight months after that; the concentration had reached 150 million pCi/L. That was the last tritium sample collected from the well.

Well 299-W22-26, located just east (downgradient) of the 216-S-9 Crib showed a similar, very large increase in the tritium concentration in 1966 when the concentration went from 4,000 pCi/L in December 1965 to 200 million pCi/L in August 1966 to 160 million pCi/L in October 1966 (Figure 5-8). The next tritium measurement was from a sample collected in 1972 and the concentration had drastically decreased to 20 million pCi/L. Since that time, the tritium concentration has steadily decreased to 1 million pCi/L in July 1978 to 150,000 pCi/L in 1985, to 132,000 pCi/L in 1988. The next tritium sample was collected in January 1991 and had only 1,240 pCi/L tritium. The tritium concentration has remained at less than the DWS (20,000 pCi/L) since that time.

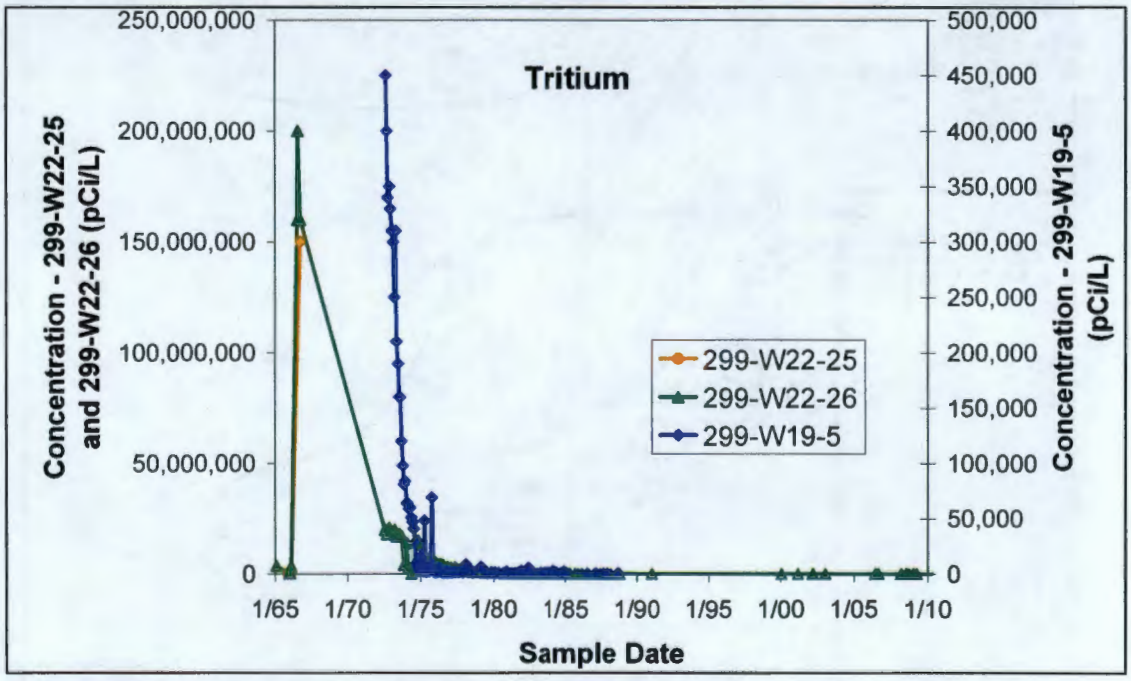

Figure 5-8. Tritium Concentrations in Wells at Subregion 1 (216-S-9/216-S-23 Cribs)

The 216-S-9 Crib is almost certainly the source of the tritium in groundwater in the 1960s and 1970s. The crib received 50 ML (13.2 Mgal) of effluent containing at least 166 million pCi/L (data from RPP-26744 decay corrected to November 1965). A second potential contributor to the tritium contamination is the 216-S-3 French drain, located approximately 250 m (820 ft) upgradient of the 216-S-9 Crib. The 216-S-3 French drain received 4.2 ML (1.1 Mgal) of effluent containing at least 200 million pCi/L tritium between 1953 and 1956. The rapid decrease in concentration between October 1966 and August 1972, a decrease of 140 million pCi/L, is difficult to explain. The plume could have moved downgradient and away from the well but this would require that the source of tritium entering the aquifer from the vadose zone either stopped or decreased in concentration between 1966 and 1972. It is unlikely that the vadose zone source of tritium was depleted by 1966 and there is no mechanism for the vadose zone to affect a decreasing tritium concentration entering the aquifer.

The tritium concentration in Well 299-W19-5 at the 216-S-23 Crib was 450,000 pCi/L when the well was first sampled in August 1972. The concentration quickly decreased to below the DWS by September 1974 as the plume moved away from the well. The tritium concentration remained below the DWS since that time, but no wells in the vicinity have been sampled since August 1988. The tritium concentration decreased to below the DWS at the 216-S-9 Crib (Well 299-W22-26) in 1987 but increased briefly to 132,000 pCi/L in 1988 before again decreasing below the DWS in 1991. The latest tritium concentration was 5,000 pCi/L in August 2010.

The earliest Tc-99 analyses from Subregion 1 (216-S-9/216-S-23 Cribs) were from the late 1980s and early 1990s and all concentrations were less than about 120 pCi/L (Figure 5-9). No subsequent Tc-99 analyses were made until the early 2000s when Tc-99 concentrations were undetectable in Well 299-W22-26. Sometime between 2002 and 2005, the Tc-99 concentration began to increase in Well 299-W22-26 at the 216-S-9 Crib (Figure 5-9). The increase probably began in 2003 and 2004 when the nitrate concentration began to increase. The Tc-99 concentration increased from 1,450 pCi/L in October 2006 to 5,600 pCi/L in September 2009. Since that time, the Tc-99 concentration has remained constant or has increased only slightly. The most recent concentration was 6,000 pCi/L in December 2010.

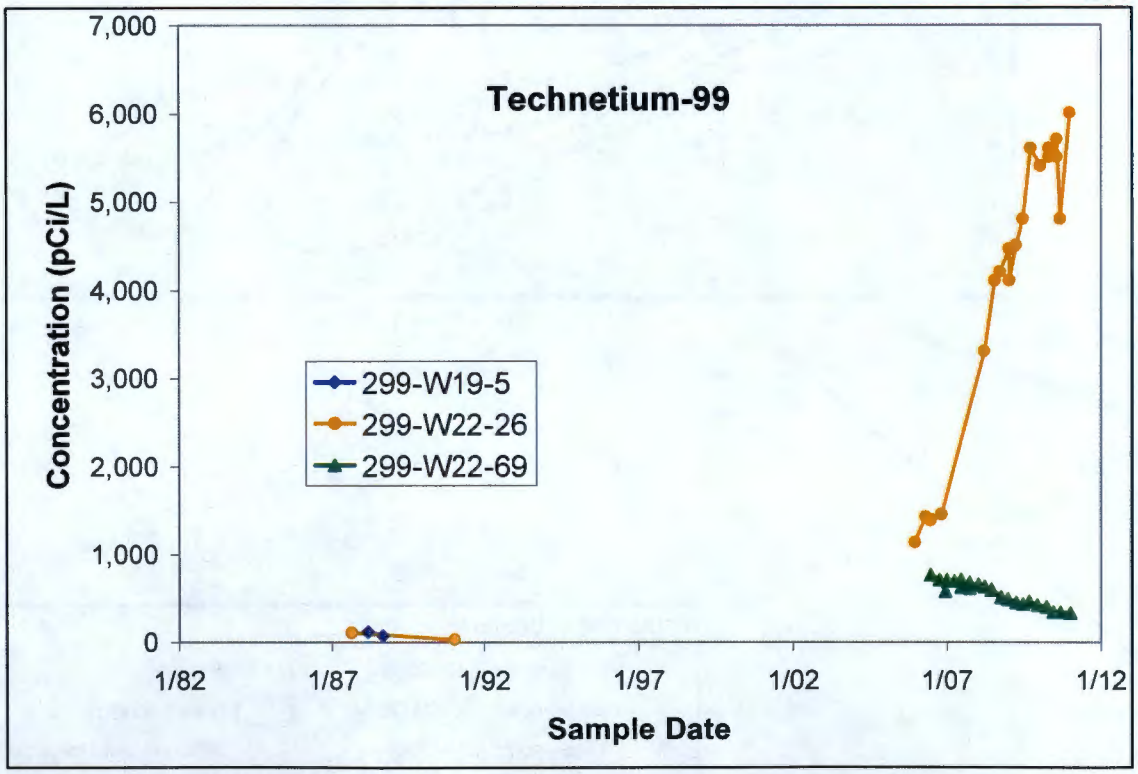

Figure 5-9. Technetium-99 Concentrations at the 216-S-9/216-S-23 Subregion

A Tc-99 plume emanating from the 241-S Tank Farm has been mapped since at least 1999 (PNNL-13116). At that time, the plume was oriented in a northwest-southeast direction and the 900 pCi/L isopleths was entirely within the 241-S Tank Farm. Since then, the Tc-99 plume has reoriented to an east-west direction and the 900 pCi/L isopleths extends beyond the 216-S-9 Crib (Figure 5-10). The Tc-99, nitrate, and chromium currently found beneath the 216-T-9/216-T-23 Cribs is part of plumes coming out of the WMA S-SX with two apparent localized sources, 241-S-104 and tanks in the southern portion of the SX Tank Farm.

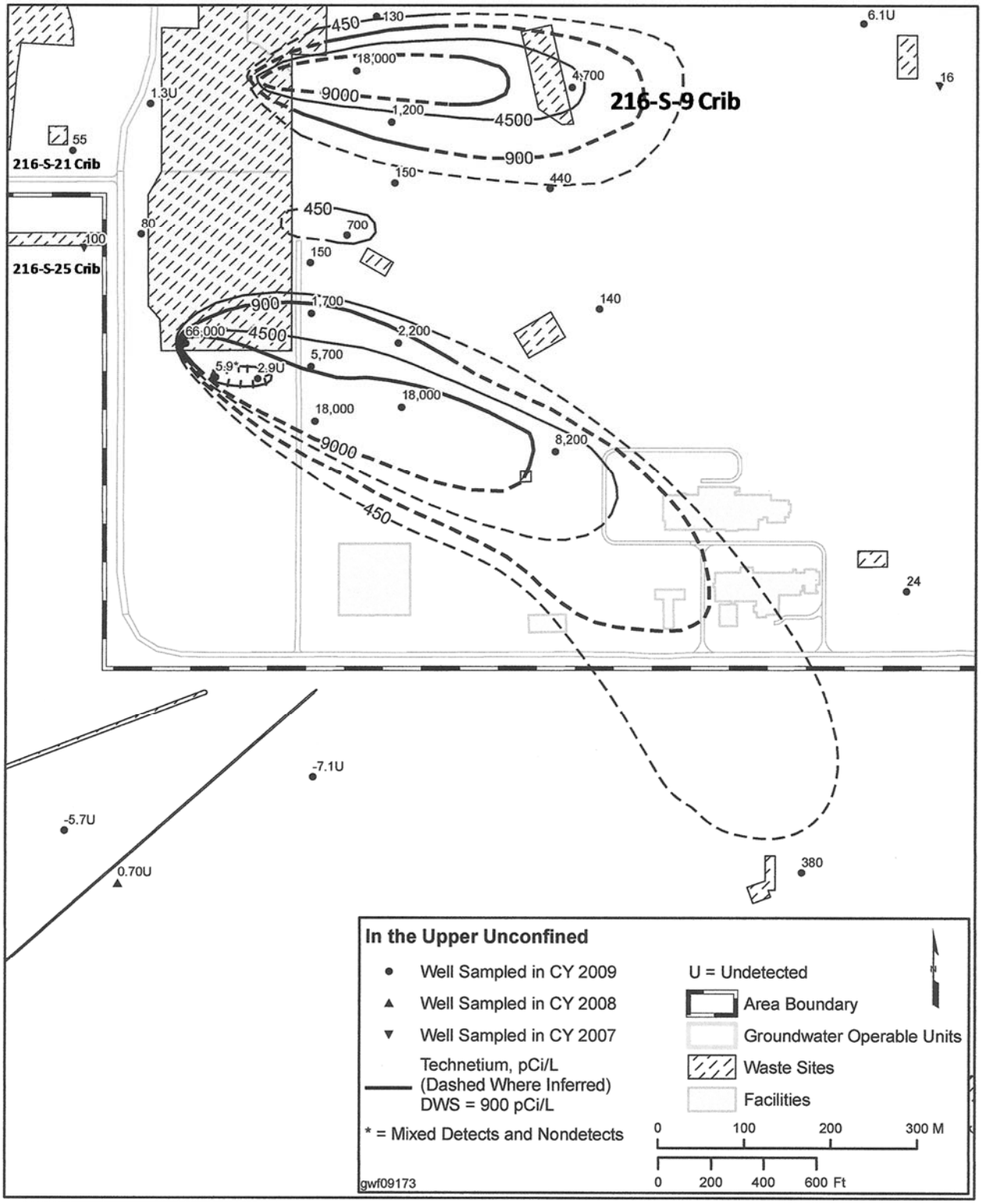

Source: DOE/RL-2010-11, *Hanford Site Groundwater Monitoring and Performance Report for 2009 Volumes 1 & 2*.

Figure 5-10. Average Technetium-99 Concentrations Within the S Complex Area, Upper Portion of the Unconfined Aquifer

Very little data exist concerning the depth distribution of Tc-99 in the 216-S-9/216-S-23 Cribs. Five depth discrete groundwater samples were collected and analyzed for Tc-99 when Well 299-W22-69 was drilled in early 2006. One sample, from 7 m (23 ft) below the water table, had detectable Tc-99 at 1,080 pCi/L. The four other samples, from deeper in the aquifer, did not contain detectable Tc-99. The sample from 7 m (23 ft) below the water table had a similar, but slightly higher, Tc-99 concentration than the first sample collected after the monitoring well was completed from the screened interval, which is from 0.5 to 11.2 m (1.6 to 36.7 ft) below the water table. Because the screened interval included the depth discrete sample, little can be said about the depth distribution of Tc-99 in the area.

Detectable I-129 has been found in 4 of 26 samples collected from Well 299-W22-26, located at the 216-S-9 Crib, since the beginning of 2000. The I-129 concentration was between about 1.5 and 1.7 pCi/L in 2009 and 2010. The 216-S-9 Crib lies at the upgradient end of a large, regional I-129 plume that extends from the crib (and the 216-U1/2 Cribs that also contributes I-129 to the plume) to the east, past the Environmental Restoration Disposal Facility (ERDF), and into the 600 Area (Figure 5-11). Part of the I-129 forming the regional plume in the southern part of the 200 West Area could have come from the 216-S-9 Crib, which received effluent containing up to 903 pCi/L of I-129 (RPP-26744).

Chromium has been found above the DWS of 100 µg/L in one well at the 216-S-9 Crib (Figure 5-12). The chromium concentration was low in Well 299-W22-26 before the late 2000s. The groundwater chromium concentration began to increase in the well in 2006 concomitant with increases in the nitrate and Tc-99 concentrations. The increasing chromium (and nitrate and Tc-99) concentrations are believed to result from a plume emanating from the 241-S Tank Farm encroaching on wells at the 216-S-9 Crib (Figure 5-13).

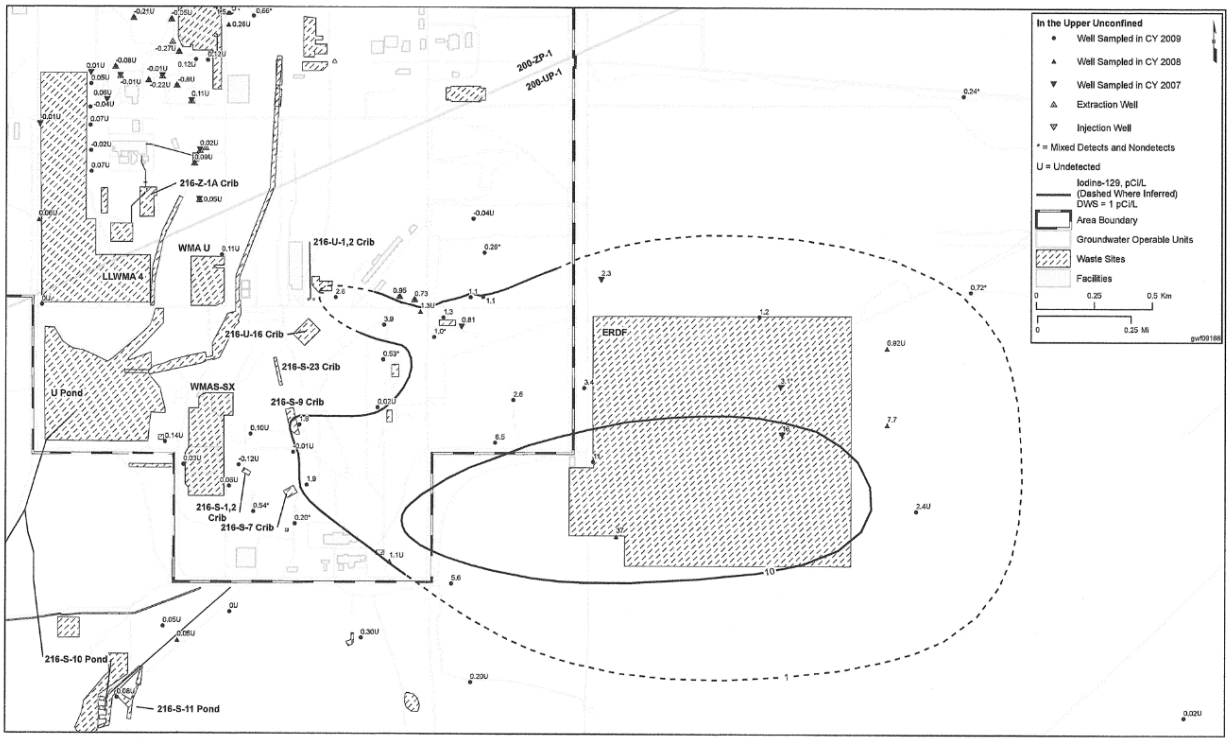

Source: DOE/RL-2010-11, *Hanford Site Groundwater Monitoring and Performance Report for 2009 Volumes 1 & 2*.

Figure 5-11. Average Iodine-129 Concentration in the Southern Part of the 200 West Area, Upper Part of the Unconfined Aquifer

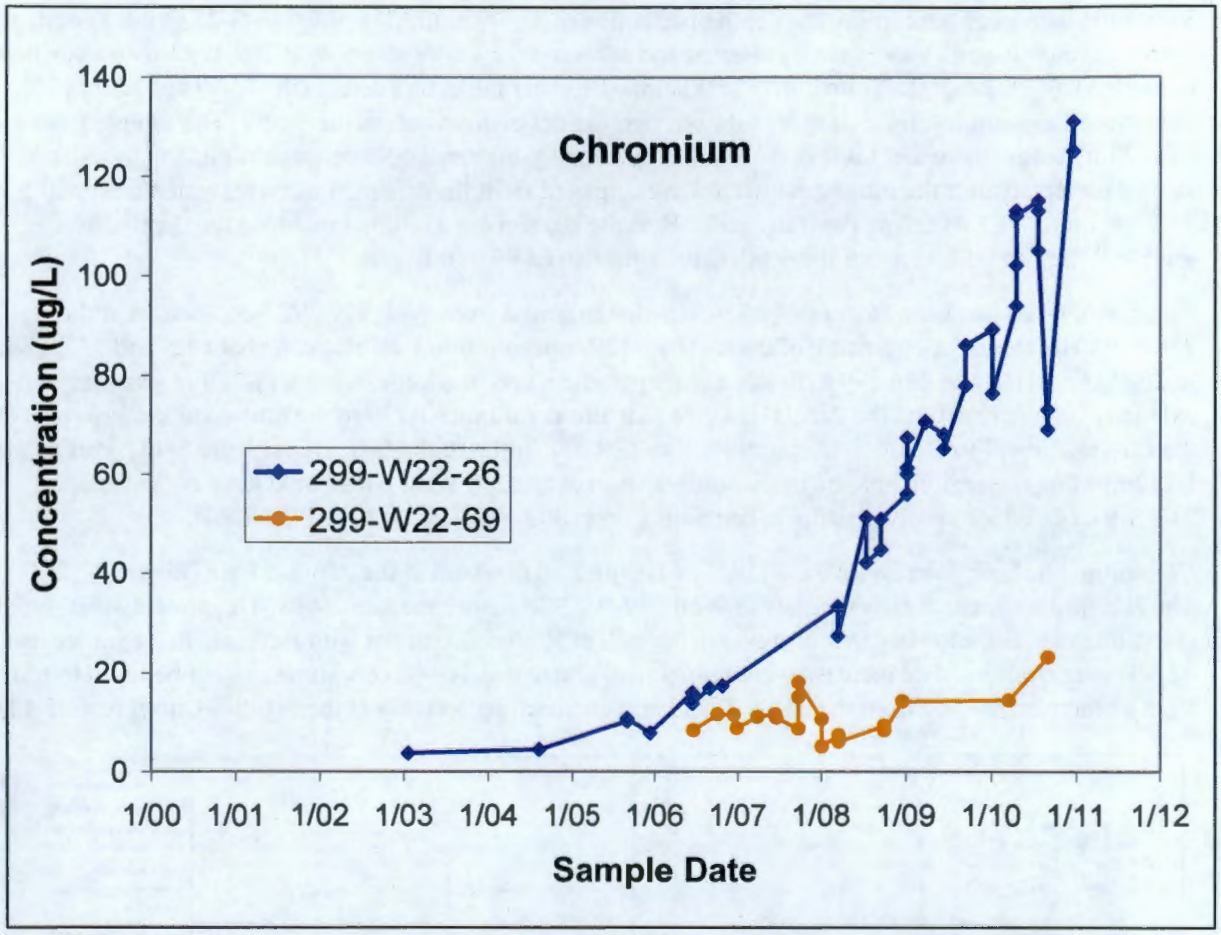

Figure 5-12. Chromium Concentrations (µg/L) in Wells at the 216-S-9 Crib

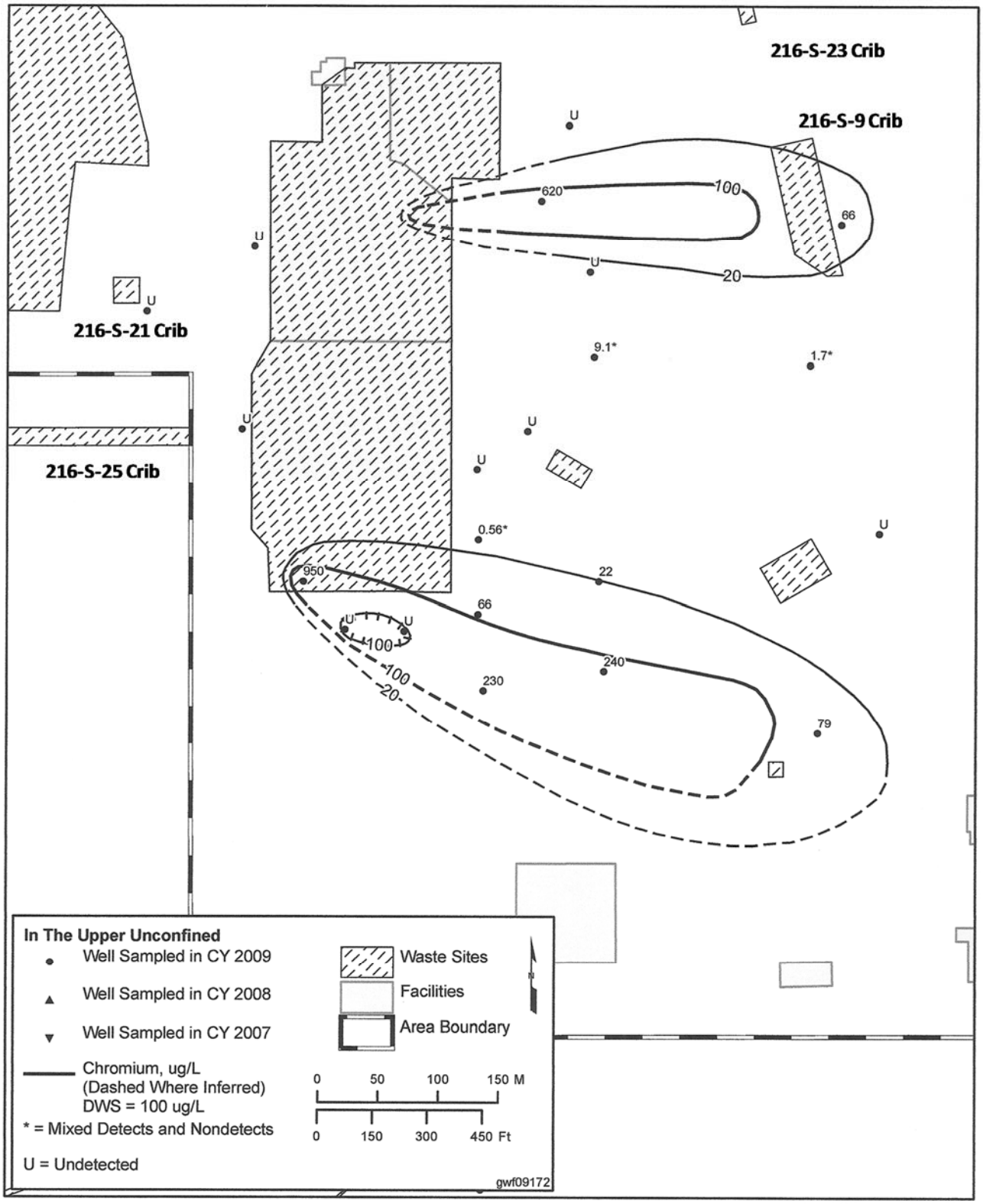

Figure 5-13. Average Chromium Concentrations Within the S Complex Area (216-S-9/216-S-23 Cribs)

Slightly elevated uranium concentrations were found in some wells in Subregion 1(216-S-9/216-S-23 Cribs) in the mid to late 1980s (Figure 5-14). The uranium contamination in Well 299-W22-26 may have been from the 216-S-9 Crib, which received liquid waste containing between 3,336 and 6,711 µg/L uranium between 1965 and 1969 (RPP-26744). However, uranium disposed to the 216-S-9 Crib cannot account for the uranium in samples from Wells 299-W19-5, located at the 216-S-23 Crib. The 216-S-23 Crib has never been downgradient of the 216-S-9 Crib and waste disposed to the 216-S-23 Crib contained negligible uranium concentrations if the waste stream designation in RPP-26744 is correct. Uranium concentrations in wells from Subregion 1 have been below 3 µg/L since January 1991.

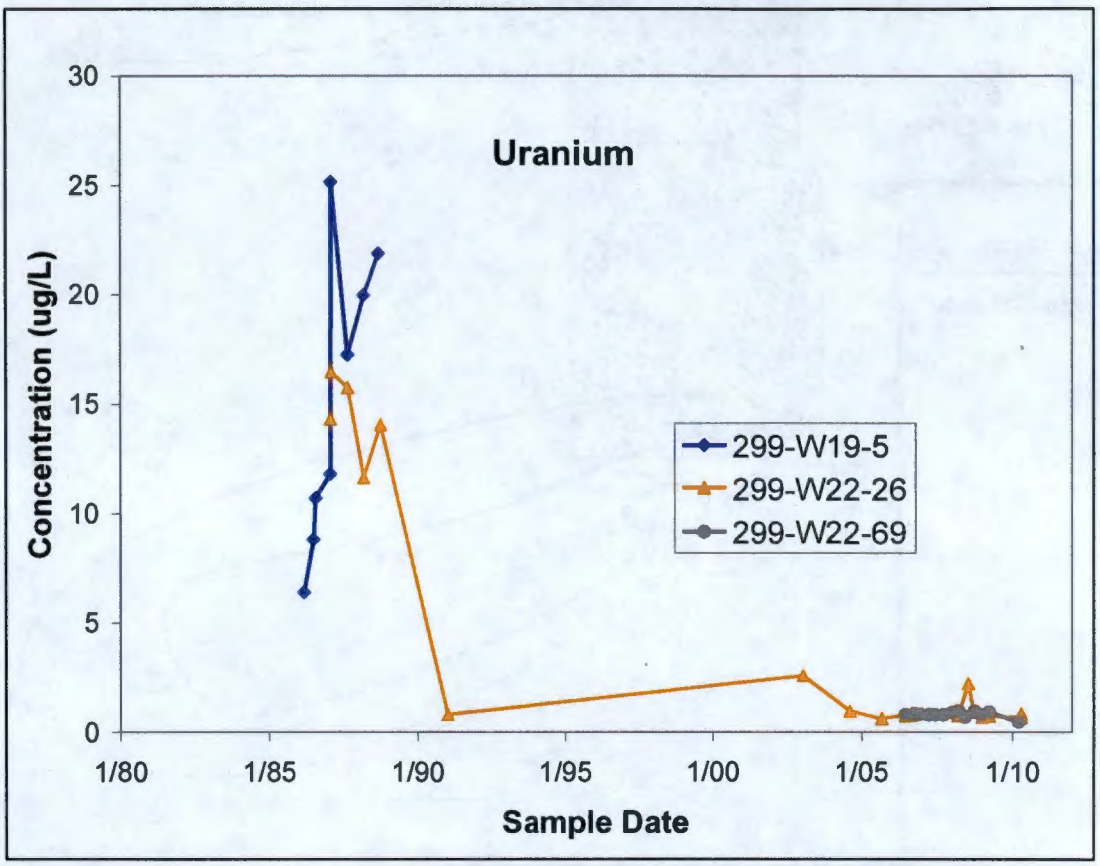

Figure 5-14. Uranium Concentrations (µg/L) in Wells in Subregion 1

5.2 Groundwater Contamination Beneath Subregion 2

This subsection discusses current and historical groundwater contamination beneath Subregion 2 of the S Complex Area (216-S-21/216-S-25 Cribs). The wells used to characterize the Subregion 2 are shown on Figure 5-15 and listed in Table 5-2 along with their completion date, the latest water level, and elevations of the open interval.

Well 299-W23-4 is near the southeast corner of the 216-S-21 Crib; Wells 299-W23-13 and 299-W23-20 are located about 85 m (279 ft) northeast of the crib and do not monitor the crib but were used to characterize groundwater in the area. Wells 299-W23-8, 299-W23-14, and 299-W23-21 are located at the head end and downgradient of the 216-S-25 Crib. Wells 299-W23-9, 299-W23-10, and 299-W23-11 are located adjacent to and along the length of the crib.

The earliest contamination found within Subregion 2 (216-S-21/216-S-25 Cribs) is from the late 1950s and is associated with Well 299-W23-4, which monitors the 216-S-21 Crib. The 216-S-21 Crib received 87.1 ML (23 Mgal) of effluent between 1954 and either 1969 or 1970, dependent on which records are chosen. Groundwater from Well 299-W23-4 was contaminated with gross beta and nitrate by the end of the 1950s.

Table 5-2. Wells Used to Characterize Groundwater Beneath the 216-S-21/216-S-25 Subregion

Well Name	Completion Date	Elevation of the Water Table (Date) (m amsl)	Elevation of Open Interval (m amsl)	Water Above Bottom of Open Interval (m)
		216-S-21 Crib		
299-W23-4	June 1957	135.1 (August 2010)	126.9 – 147.68 Perforated	8.2
299-W23-13	December 1990	137 (March 2002)	137.03 – 143.64 Screened	Decommissioned
299-W23-20	August 2000	134.7 (March 2011)	127.60 – 138.27 Screened	7.1
		216-S-25 Crib		
299-W23-10	October 1972	136 (May 2007)	135.9 – 153.5 Perforated	Dry
299-W23-11	November 1972	136.5 (March 2005)	136.0 – 153.26 Perforated	Dry
299-W23-14	April 1991	137 (September 2002)	137.83 – 144.32 Screened	Decommissioned
299-W23-21	July 2000	134.8 (March 2011)	127.24 – 138.58 Screened	7.6
299-W23-8	September 1972	139.8 (June 1996)	133.34 – 153.15 Perforated	Decommissioned
299-W23-9	August 1972	135.2 (August 2008)	134.9 – 153.72 Perforated	Dry

amsl = above mean sea level

The gross beta concentration was slightly over 1,000 pCi/L by the end of the 1950 in Well 299-W23-4 (Figure 5-16). No subsequent samples were collected until March 1967, by which time the gross beta concentration had decreased to about 160 pCi/L. The measured concentrations of gross beta were sporadic between 1967 and 1973, but generally remained between 150 and 200 pCi/L. The concentration decreased to less than 100 pCi/L after 1973, where it remained until 2002 when the well was last sampled.

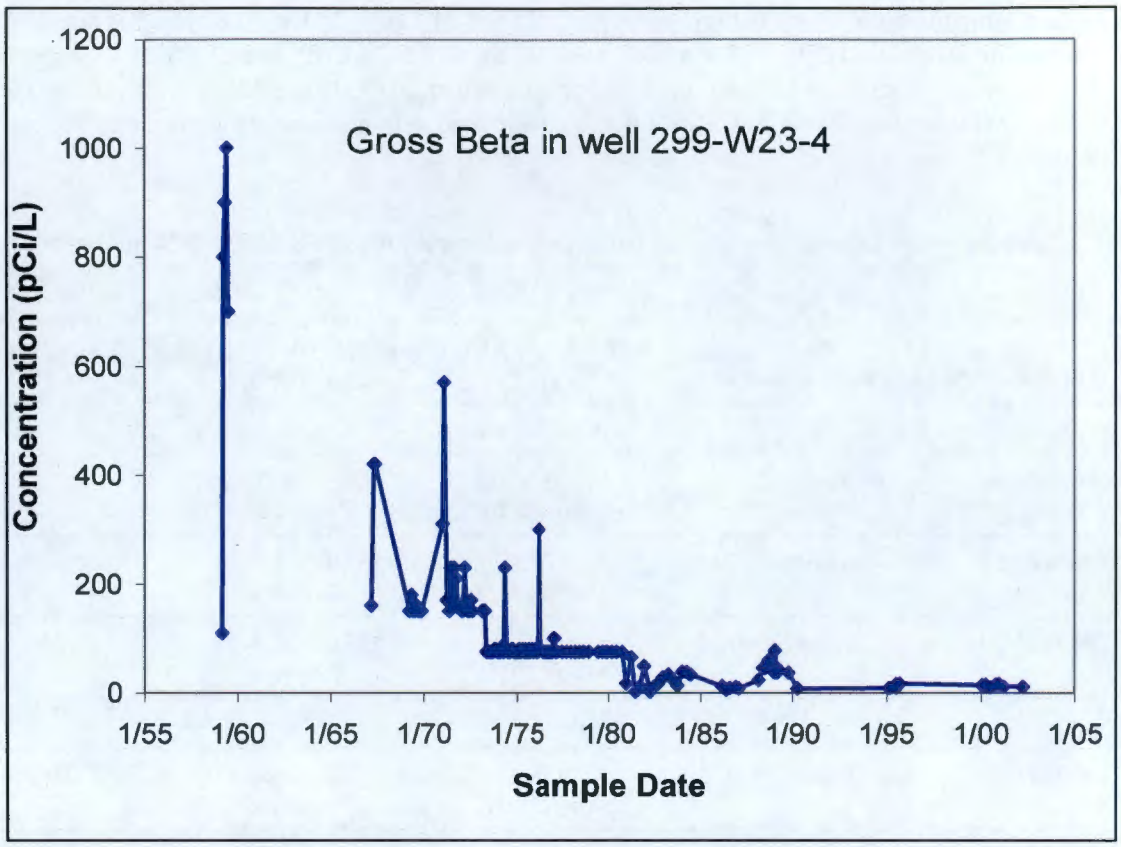

Figure 5-15. Gross Beta Concentration in Well 299-W23-4 at the 216-S-21 Crib

The nitrate concentration reached 150 mg/L in the early 1960s in Well 299-W23-4 (Figure 5-17). The concentration dropped to 120 mg/L in 1963. The well was not sampled for nitrate again until January 1971, when the concentration had decreased to 20 mg/L. The concentration remained between 20 and 30 mg/L throughout the early 1970s and further decreased to less than 10 mg/L in the mid-1970s, where it remained until 2004. In 2004, the nitrate concentration began to increase to the 22 mg/L concentration measured in 2010. The high nitrate concentrations found in groundwater at the 216-S-21 Crib in the 1950s and 1960s cannot have originated from the crib because effluent disposed to the crib during that time is estimated to have contained only 0.5 mg/L nitrate (RPP-26744). However, the effluent disposed to the crib in 1968 had 19,495 mg/L nitrate, which can account for the nitrate concentrations found in the 1970s. Perhaps the waste type chosen to represent the early years of disposal to the crib was not correct.

The tritium concentration was already 29 million pCi/L in Well 299-W23-4 when it was first analyzed in February 1962 (Figure 5-17). The tritium concentration soon rose to 110 million pCi/L in 1963 and 1964, but dropped to 930,000 pCi/L in February 1966. The well was not sampled again for tritium until July 1972 when the concentration was 27 million pCi/L. The concentration decreased quickly to less than the 20,000 pCi/L DWS by June 1977 and remained below the DWS until the late 2000s except for a short increased interval in 1988 when the concentration reached 5.45 million pCi/L (Figure 5-18). The brief increase in concentration to 73 million pCi/L in May 1974 (shown on Figure 5-17) is probably not real but the data are not flagged in EDA. Recently, the tritium concentration has increased to 50,000 pCi/L in August 2010. The 216-S-21 Crib may have been the source for the tritium found in the 1960s since the effluent disposed to the crib contained at least 388 million pCi/L tritium (data from RPP-26744 decay corrected to November 1954).

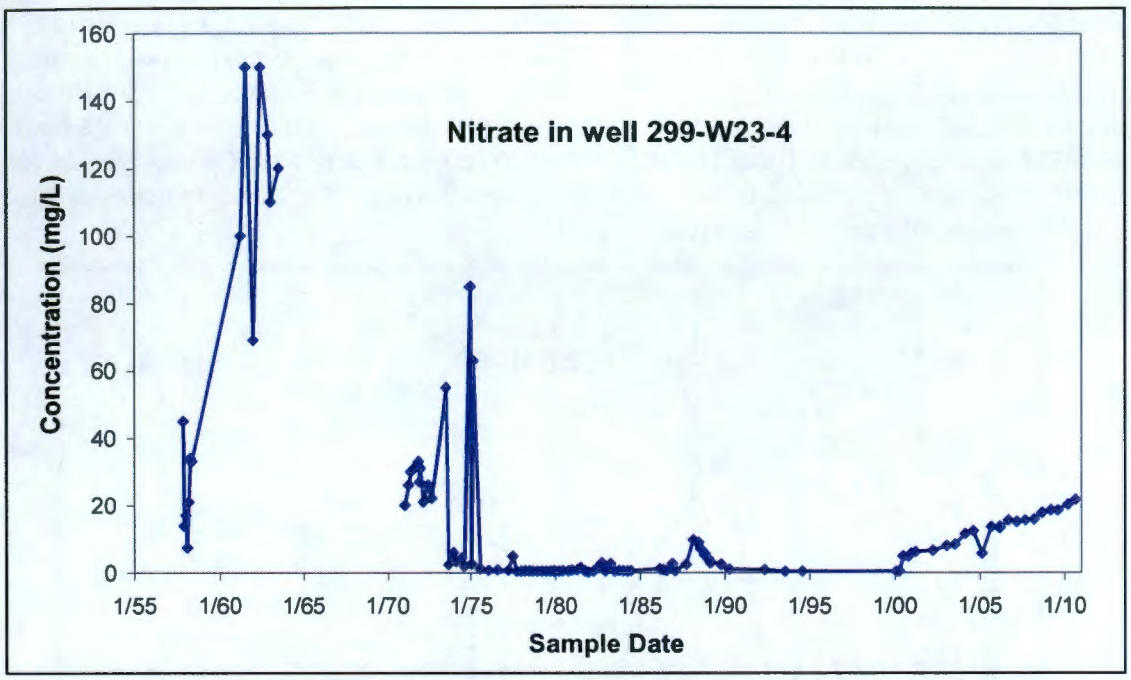

Figure 5-16. Nitrate Concentration in Well 299-W23-4 at the 216-S-21 Crib

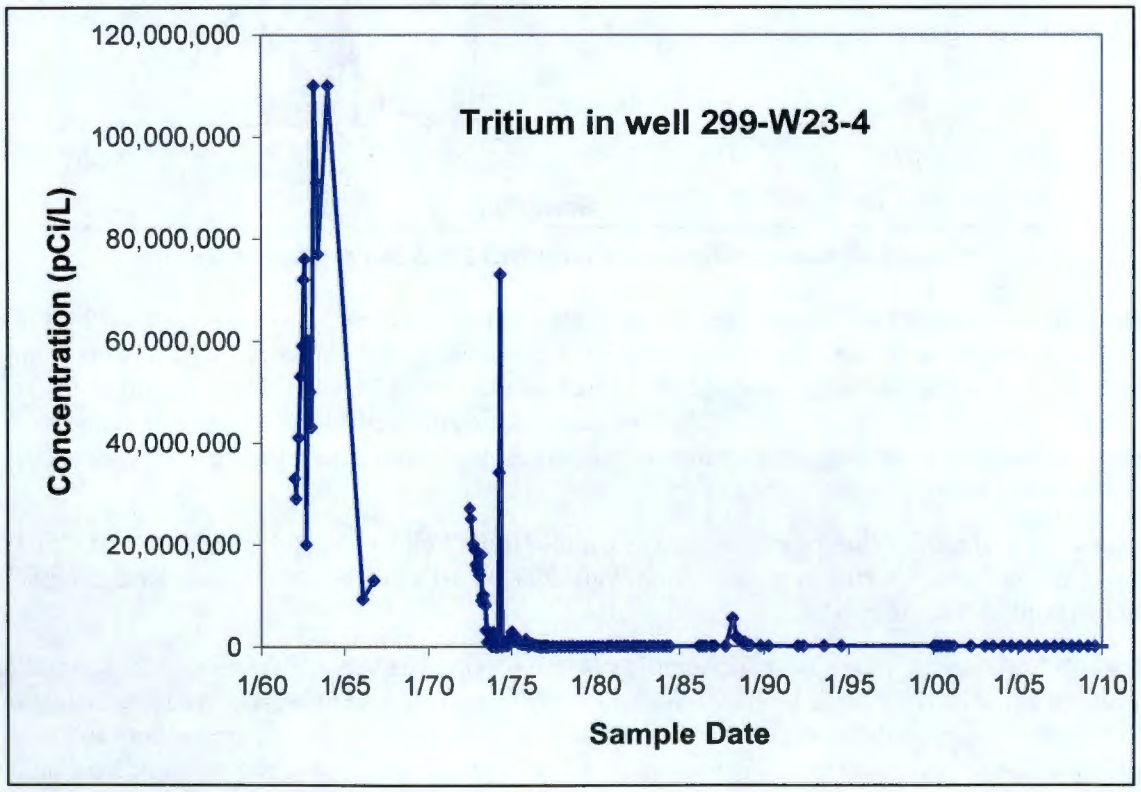

Figure 5-17. Tritium Concentration in Well 299-W23-4 at the 216-S-21 Crib

The cobalt-60 concentration was about 10 pCi/L in 1971 and increased to 34 pCi/L by August 1975 (Figure 5-19). No additional analyses for cobalt-60 were made in groundwater from the well so the subsequent cobalt-60 contaminant history at the 216-S-21 Crib is not known. The 216-S-21 Crib received negligible cobalt-60 between 1954 and 1967, but received 962 million pCi/L cobalt-60 in 1968 (data from RPP-26744 decay corrected to 1968). However, cobalt-60 sent to the crib in 1968 cannot account for the concentrations found in groundwater before that time, unless the waste type chosen to represent the disposals between 1954 and 1967 is wrong.

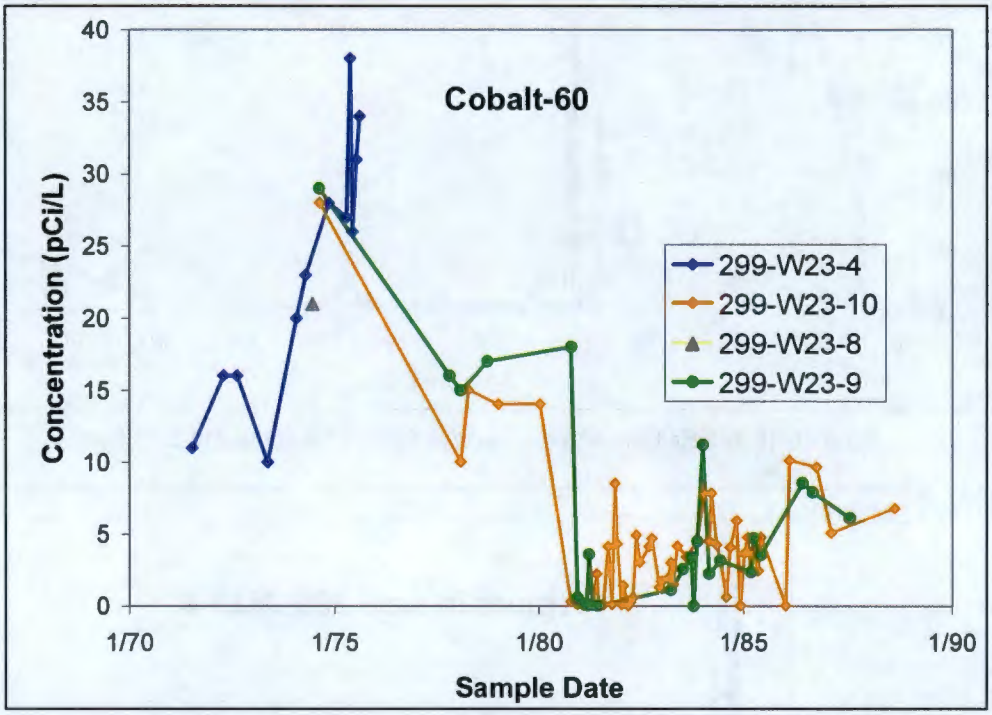

Figure 5-18. Cobalt-60 Concentration in Well 299-W23-4 at the 216-S-21 Crib

The uranium concentration was elevated in the 1970s and 1980s (Figure 5-20) in Well 299-W23-4 at the 216-S-21 Crib. The uranium concentration was 363 µg/L in March 1970 when the well was first sampled for uranium. The concentration increased to 417 µg/L in October 1970 before decreasing to 60 to 120 µg/L in the late 1970s and early 1980s. The concentration increased from about 16 to 32 µg/L between March 1986 and May 1990 and remained near 35 µg/L until 2000 when the well was last sampled for uranium.

No detectable chromium has been measured in samples from Well 299-W23-4 at the 216-S-21 Crib. Chromium has been detected in samples from Wells 299-W23-13 and 299-W23-20, located about 85 m (279 ft) northeast of the crib[8].

Figure 5-21 shows the chromium concentrations in those wells. The very high chromium concentrations measured in the early 1990s in Well 299-W23-13 are from unfiltered samples. The well was drilled in 1990 and completed with carbon steel casing and screen. The high chromium concentrations in the unfiltered samples probably represent particulate material (likely iron oxide rust with sorbed chromium)

[8] Note that the groundwater flow direction is toward the east, which places the wells downgradient, but not directly downgradient of the 216-S-21 Crib. Solid symbols are filtered samples; open symbols are unfiltered samples.

in the sample and do not represent ambient groundwater conditions. Filtered samples show appreciably lower chromium concentrations that are representative of groundwater.

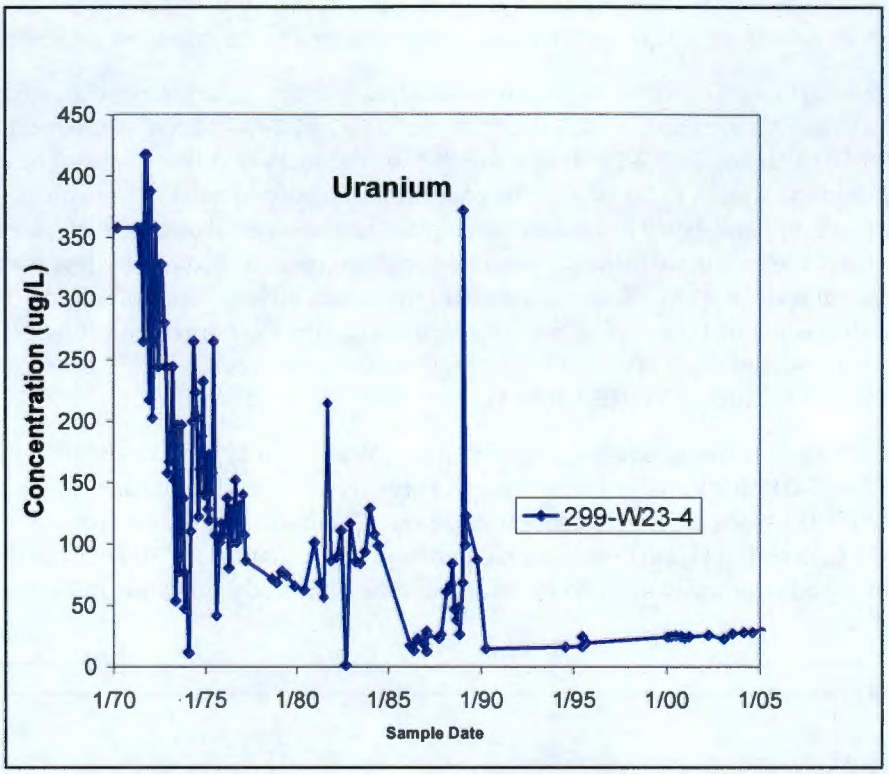

Figure 5-19. Uranium Concentration (µg/L) in Well 299-W23-4 at the 216-S-21 Crib

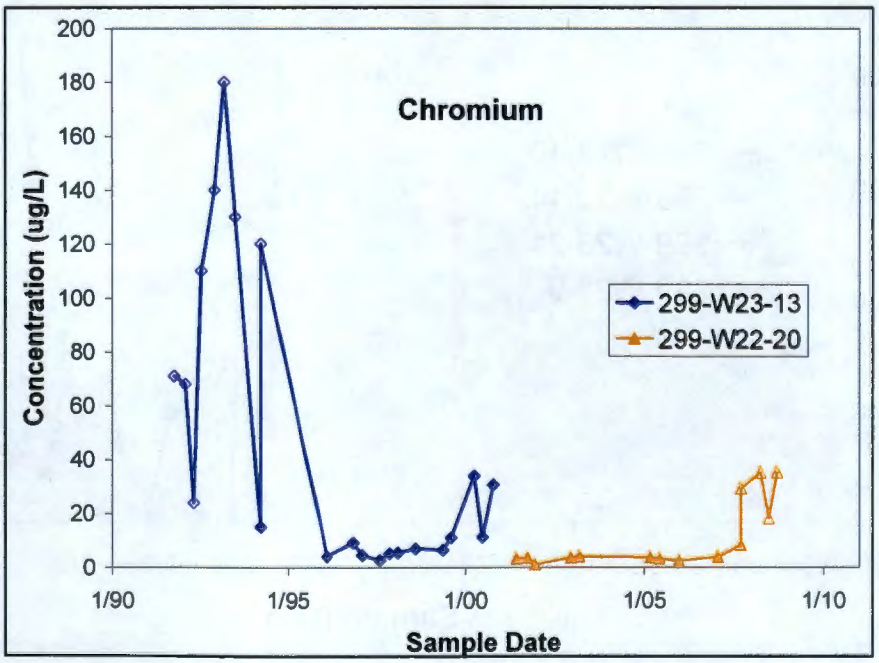

Note: Solid symbols are filtered samples; open symbols are unfiltered samples.

Figure 5-20. Chromium Concentrations (µg/L) in Wells at the 216-S-21 Crib

The 216-S-25 Crib operated continuously from November 1973 to November 1980 and received 300 ML (79 Mgal) of effluent from the 242-S Evaporator. In February 1985, the crib received a one-time discharge from a pump-and-treat operation to remediate uranium in groundwater at the 216-U-1/2 Cribs. Approximately 31.54 ML (8.3 Mgal) of effluent were discharged to the crib from the remediation effort.

Cobalt-60, nitrate, tritium, and uranium contamination was found in groundwater beneath the 216-S-25 Crib during and shortly after the facility's operating period. Cobalt-60 concentrations were elevated in two wells (299-W23-10 and 299-W23-9) near the crib in August 1974 (Figure 5-18). The concentration in those wells at the time was 28 to 29 pCi/L. The concentration dropped quickly from about 15 to 20 pCi/L to less than 1 pCi/L in late 1980. The concentration remained between about 1 and 10 pCi/L from that time until the early 1990s, after which all measured cobalt-60 concentrations were less than detectable. The 216-S-25 Crib could not have been the source of the cobalt-60 in groundwater in the 1970s since the effluent to the crib contained only 0.8 pCi/L cobalt-60 throughout the normal operating period of the crib. The U pond is a possible source of cobalt-60; U pond received between 29 and 32 p/Ci/L of cobalt-60 each year between 1952 and 1973 (RPP-26744).

The nitrate concentration increased abruptly in Well 299-W23-10 in 1976 from about 23 mg/L to over 300 mg/L (Figure 5-21) and remained high through February 1972. No subsequent nitrate analyses were made until early 1983 when the nitrate concentration was 233 mg/L. The nitrate concentrations disposed to the 216-S-25 Crib and to U pond were not high enough to account for the 300 mg/L and greater concentrations found in groundwater and the source for the nitrate contamination in 1976 and 1977 is not known.

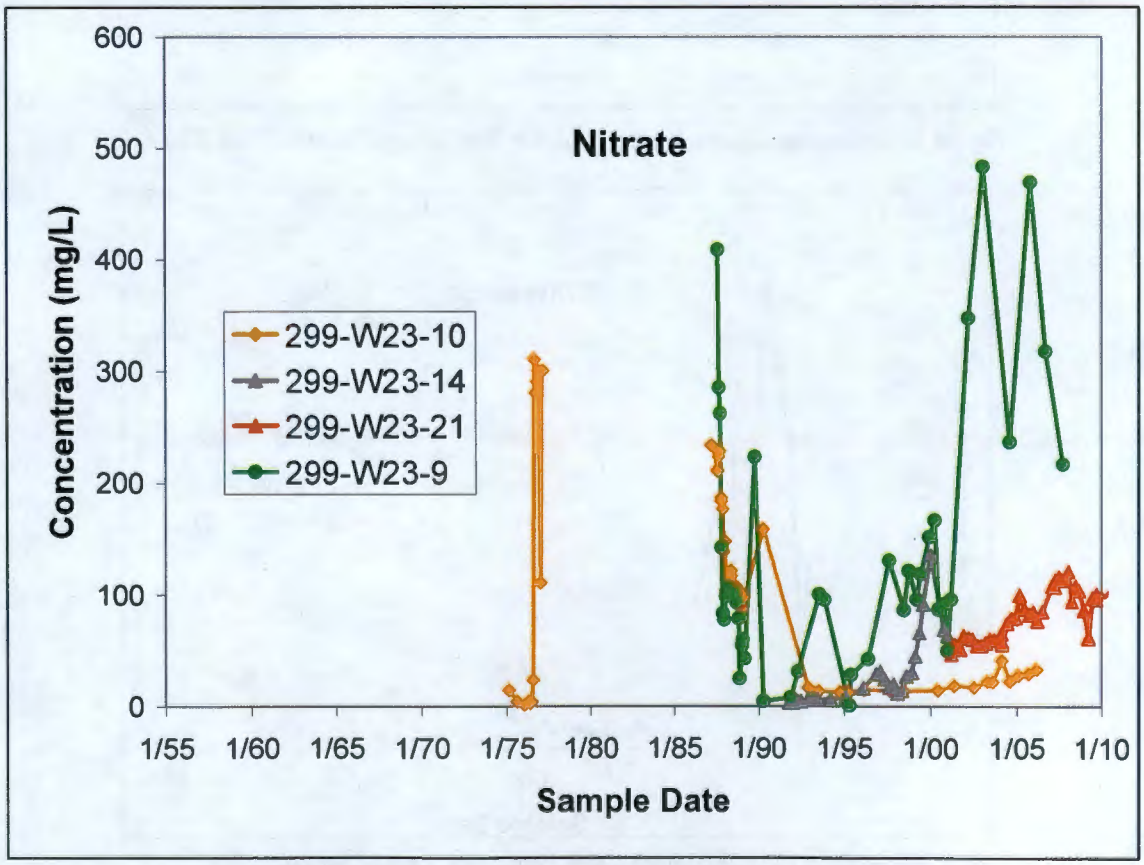

Figure 5-21. Nitrate Concentration in Wells at the 216-S-25 Crib

The nitrate concentration was high in two wells monitoring the 216-S-25 Crib in 1987 with a maximum of 407 mg/L in Well 299-W23-9 (Figure 5-21). The source for the high nitrate in the late 1980s is the 30 ML (7.9 Mgal) of effluent from the 216-U-1/2 pump-and-treat operation disposed to the 216-S-25 Crib in 1985. That effluent had 7,055 mg/L nitrate (RPP-26744). Later spikes of high nitrate concentrations in the 2000s are additional releases from the vadose zone beneath the crib (PNNL-15070, *Hanford Site Groundwater Monitoring for Fiscal Year 2004*).

The tritium concentrations were very high in wells monitoring the 216-S-25 Crib in the late 1970s with concentrations reaching 9.2 million pCi/L in Well 299-W23-10 in April 1976 (Figure 5-22). The concentrations decreased fairly rapidly by the early 1980s but remained above the DWS of 20,000 pCi/L in most wells surrounding the crib. An increase in tritium concentrations in the mid-1980s to about 1.5 million pCi/L resulted from disposal of the 216-U-1/2 pump-and-treat effluent to the crib. The tritium in groundwater at that time may have been from the pump-and-treat effluent, which contained over 7 million pCi/L, or from earlier disposal of evaporator condensate from the S and SX Tank Farms, which was highly enriched in tritium (13 million pCi/L decayed to January 1, 2001 [Corbin et al. 2010]) compared to other waste constituents. The most recent tritium concentrations in wells near the 216-S-25 Crib are more than twice the DWS and are near 50,000 pCi/L (Figure 5-22).

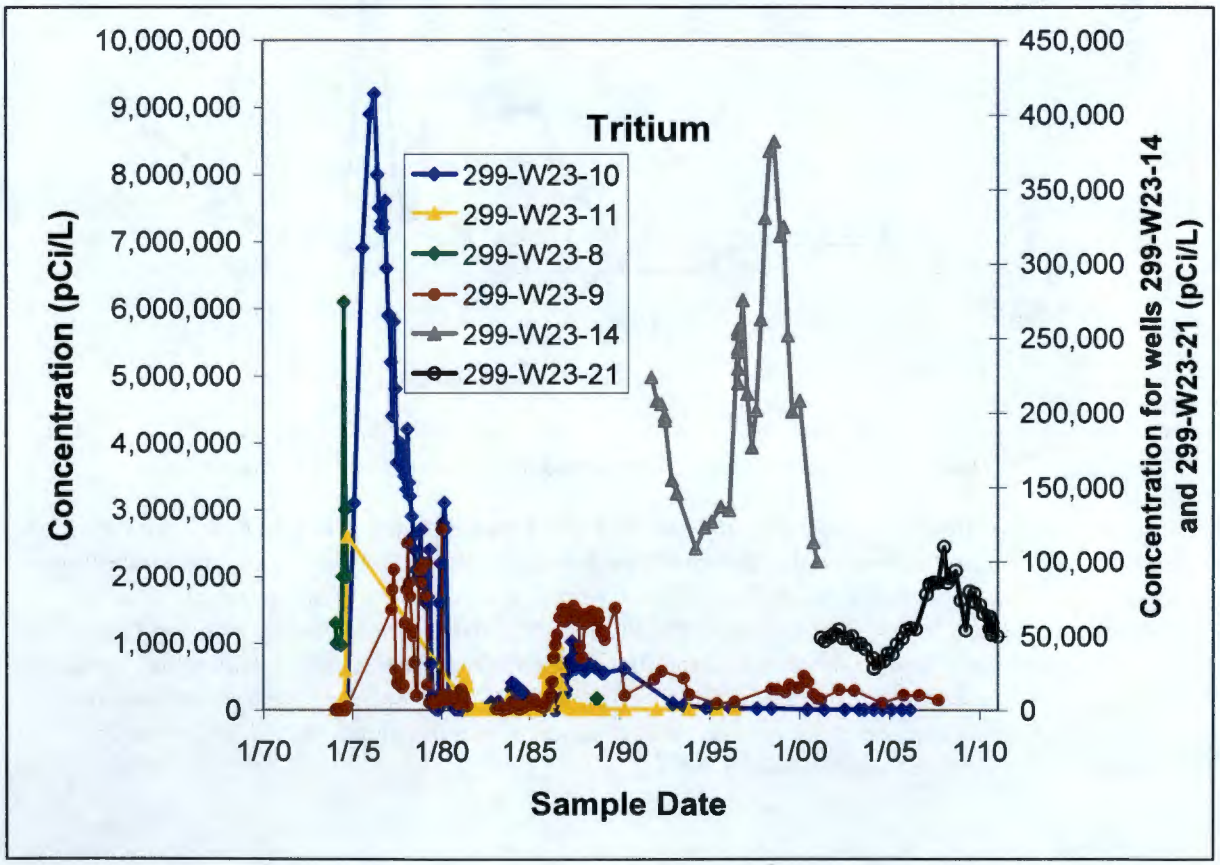

Figure 5-22. Tritium Concentrations in Wells at the 216-S-25 Crib

The highest Tc-99 concentrations near Subregion 2 (216-S-21/216-S-25 Cribs) are downgradient of the WMA S-SX, which is the source of the Tc-99 in the groundwater (Figure 5-10). Tc-99 concentrations in wells surrounding the 216-S-25 Crib are low and have never exceeded the 900 pCi/L DWS (Figure 5-23). The small amount of Tc-99 in groundwater beneath the 216-S-25 Crib may be from the 216-U-1/2

pump-and-treat effluent disposed to the crib, since RPP-26744 reports that no Tc-99 was in the evaporator condensate sent to the crib between 1973 and 1980.

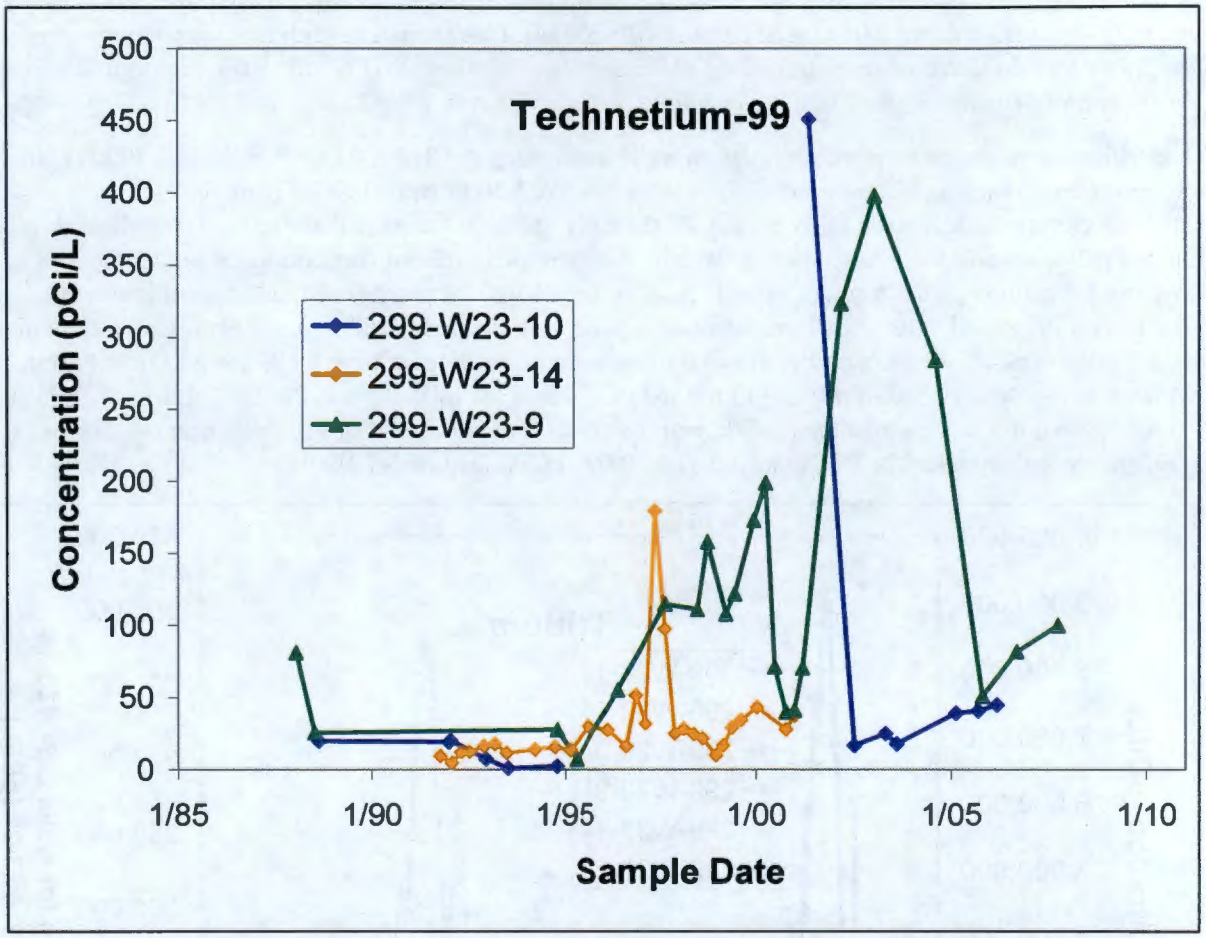

Figure 5-23. Technetium-99 Concentrations in Wells at the 216-S-25 Crib

Figure 5-24 shows the chromium concentrations in wells surrounding the 216-S-25 Crib. The very high chromium concentrations measured in the early 1990s in Well 299-W23-14 are from unfiltered samples. The high chromium concentrations in the unfiltered samples probably represent particulate material (likely iron oxide rust with sorbed chromium) in the sample and do not represent groundwater conditions. Filtered samples show appreciably lower chromium concentrations that are representative of groundwater. The chromium concentration has not exceeded the DWS of 100 µg/L in filtered samples at the 216-S-25 Crib. Elevated chromium concentrations occur downgradient of Subregion 2 (216-S-21/216-S-25 Cribs) but are caused by releases from the WMA S-SX.

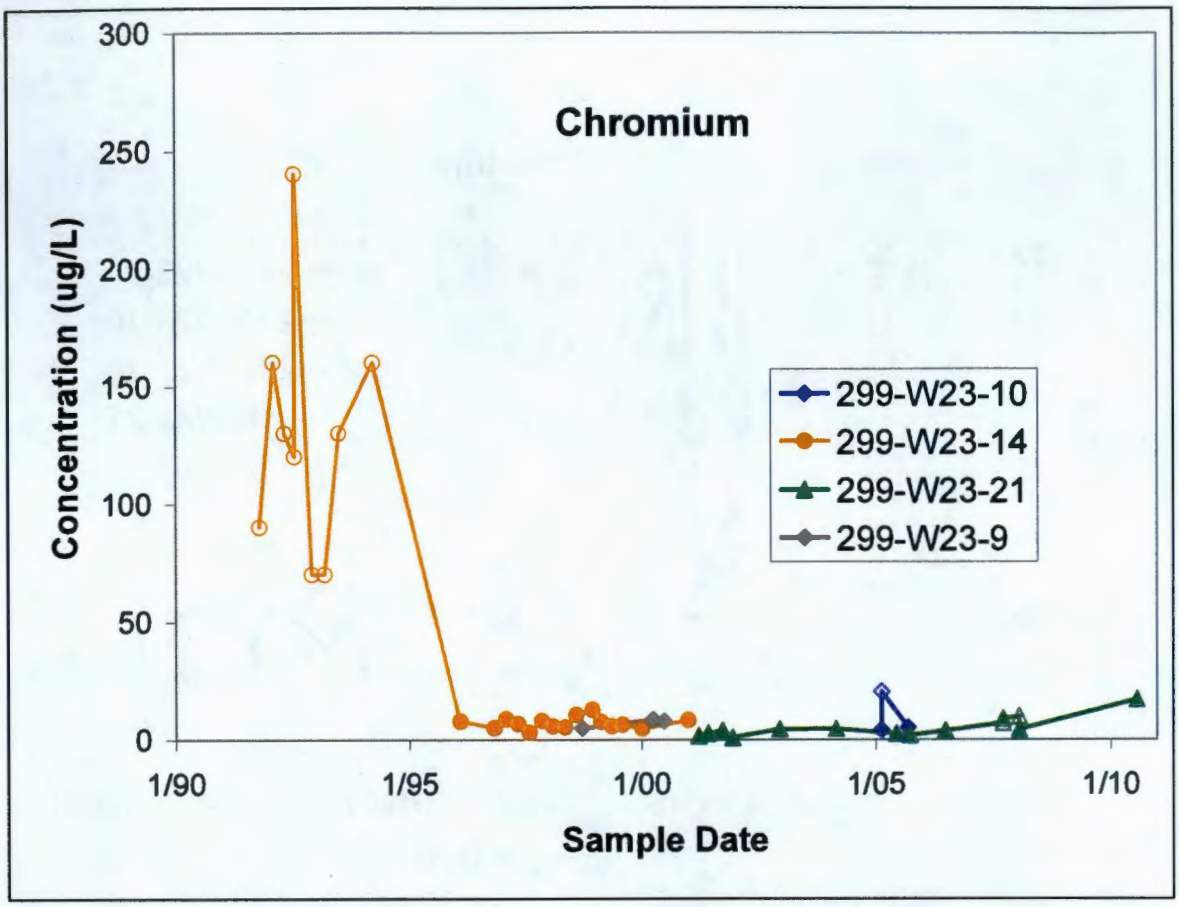

Note: Open symbols are unfiltered samples; solid symbols are filtered samples.

Figure 5-24. Chromium Concentrations (µg/L) in Wells at the 216-S-25 Crib

The groundwater uranium concentration was high in Well 299-W23-11 when it was first measured in July 1982 and it remained fairly high (between about 10 and 30 pCi/L [30 and 90 µg/L]) throughout the early- and mid-1980s (Figure 5-25). The source for the uranium in groundwater in the early 1980s is not known since the uranium concentration disposed to the 216-S-25 Crib is reported to be 0.3 µg/L between 1973 and 1980. A second period of high uranium concentrations occurred between 1987 and 1989 when the uranium concentration exceeded 60 µg/L in Wells 299-W23-9 and 299-W23-10 (Figure 5-25).
The source for the elevated uranium during the late 1980s may have been the effluent from the 216-U-1/2 Cribs uranium remediation. However, RPP-26744 reports that the pump-and-treat effluent disposed to the 216-S-25 Crib contained 19.4 µg/L uranium, which is insufficient to account for the greater than 60 µg/L found in groundwater during the late 1980s. The estimated uranium concentration given by RPP-26744 may be too small. An alternative potential uranium source is the 216-U-10 pond, which received more than 2,000 kg of uranium. However, the uranium concentrations disposed to the pond were too dilute to account for the concentrations found in groundwater near Well 299-W23-11 (at 216-S-25 Crib) in the late 1980s. The most recent uranium groundwater concentrations in wells near the 216-S-25 Crib are slightly greater than 10 µg/L and exceed the background concentration of 2.57 µg/L (DOE/RL-96-61).

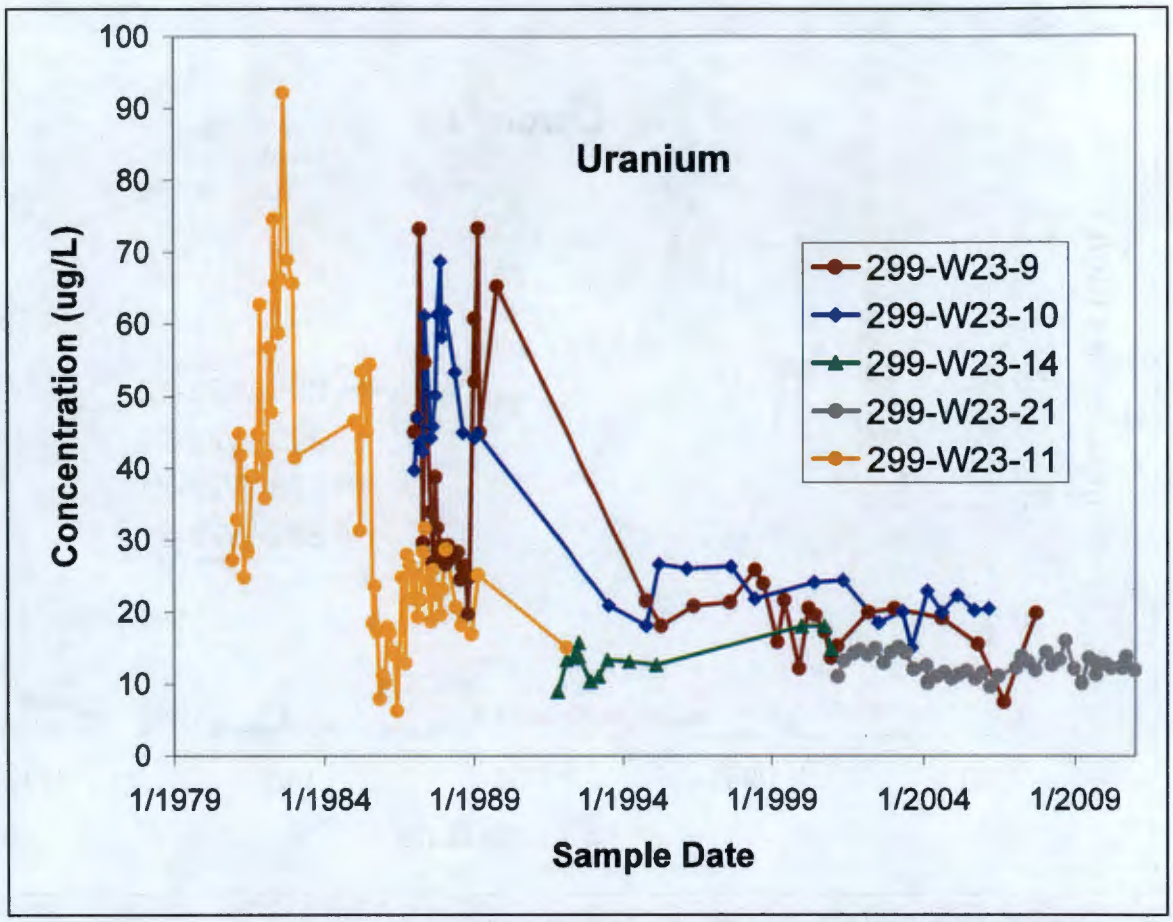

Figure 5-25. Uranium Concentration (µg/L) in Wells at Subregion 2 (216-S-21/216-S-25 Cribs)

5.3 Vertical Groundwater Contaminant Distribution at Waste Management Area S-SX

Knowledge of the variation in contaminant concentrations as a function of depth in the aquifer is necessary to estimate the mass of a contaminant in the various plumes and can be used to identify potential sources of the contamination. Because concentrations of contaminants in the groundwater are known to vary with depth from the top of the water table, to estimate the mass requires some estimate of vertical variability. Past mass estimates based on the simple assumption that the concentrations are uniform from the top of the water table to the bottom of the aquifer are not technically defensible, especially in thick aquifers. In most cases, the screened portions of the wells are near the water table surface and, thus, obtaining an accurate estimate of the variation in concentrations versus depth within the identified groundwater plumes is challenging. The following data provide our current understanding and database for contaminant concentrations as a function of depth.

Two sources of information provide indications of the depth distribution of contaminants within the aquifer below the S Complex Area: depth-discrete sampling in the aquifer downgradient of the S-SX SST during drilling of Well 299-W22-47 during 2004 and specific conductance measurements in Well 299-W23-19. Depth-discrete sampling also was done earlier in 1999 during drilling of Well 299-W22-50 downgradient of the WMA S-SX SST.

Sampling During Drilling. Well 299-W22-47 is located southeast of the southeast corner of the SX Tank Farm fence line in the center of the Tc-99, nitrate, and chromium plume emanating from the SX Tank Farm. The well was drilled to a depth of 36.6 m (120 ft) below the water table. Groundwater samples were collected during drilling of the well at 1.5 m (4.9 ft) depth intervals and were analyzed for anions, Tc-99, chromium (filtered), and carbon tetrachloride. Analytical results are shown on Figure 5-26 as a function of depth.

Only the pumped groundwater samples are included for chromium in Figure 5-26. The groundwater associated with the air lifted samples was in contact with the drill cuttings for up to several days before a filtered sample was collected. During this time, the chromium in solution is believed to have been reduced by freshly exposed sediment surfaces (ground up basalt particles) and precipitated from solution, resulting in artificially low chromium concentrations. A similar situation was seen in samples collected from WMAs T and TX-TY.

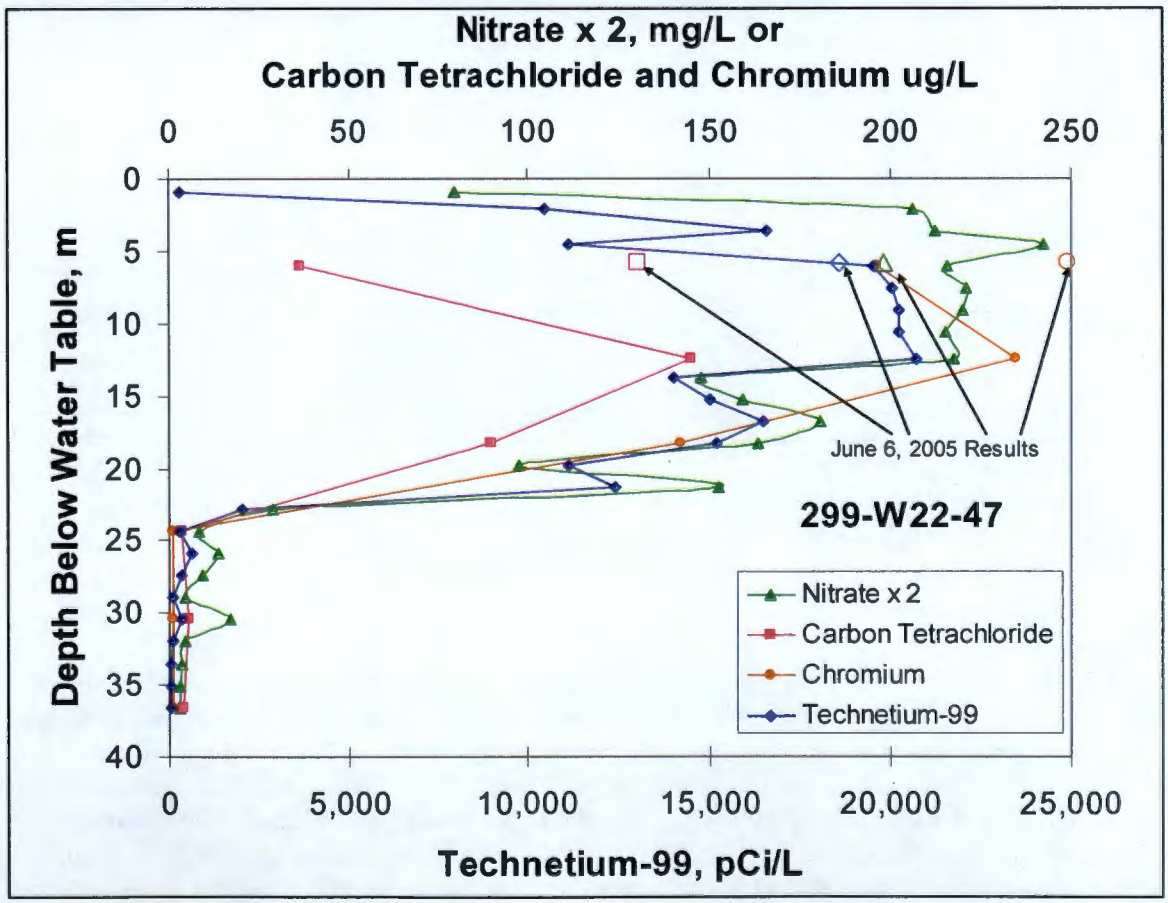

Source: Modified from PNNL-14548, *Hanford Site Groundwater Monitoring for Fiscal Year 2003.*

Figure 5-26. Carbon Tetrachloride, Nitrate, Technetium-99, and Chromium Concentrations (pCi/L or µg/L) versus Depth in the Aquifer in Well 299-W22-47 at Waste Management Area S-SX

Based on the data (Figure 5-26, the chromium, nitrate, and Tc-99 plume is present throughout almost the entire upper 23 m (75 ft) of the aquifer at Well 299-W22-47. Subsequent routine, quarterly samples (screened in upper 10 m [32 ft]) collected from the well in 2005 yielded concentrations at the same levels as reported in Figure 5-26.

PNNL-13441 presents results from depth-discrete sampling during drilling of Well 299-W22-50, located approximately 60 m (197 ft) north of Well 299-W22-47. Their results are tabulated in Table 5-3. The samples were collected at predetermined depths. One sample was collected just above and one sample from just below the Ringold Formation lower mud unit. (The lower mud unit is between 72.5 and 84.4 m (238 and 277 ft) below the water table in Well 299-W22-50.) The drilling and sampling details are found in PNNL-13441 and PNNL-13200, *Borehole Data Package for Wells 299-W22-48, 299-W22-49, and 299-W22-50 at Single-Shell Waste Management Area S-SX.*

Table 5-3. Depth Distribution of Selected Contaminants during Drilling of Well 299-W22-50

Sample Depth (m)	Sample Mode	Technetium-99 (pCi/L)	Nitrate (mg/L)	Chromium (µg/L)	Tritium (pCi/L)	Uranium (µg/L)	Carbon Tetrachloride (µg/L)
0.2	B	4,240	57	3 U	31,400	0.78	13
2.3	S	3,230	30	10.4	24,200	4.29	11
6.7	P	812	12	3 U	19,900	3.34	5.6
11.9	P	7.03 U	2	3 U	969	1.09	0.94
28.7	P	0 U	1	3 U	304	0.58	1.5
53.0	P	0 U	3	3 U	185 U	0.79	5.6
67.7	P	0.577 U	12	3 U	0 U	0.43	0.89
99.4	P	0 U	4	3 U	0 U	30.90	0.23

Source: PNNL-13441, RCRA Groundwater Quality Assessment Report for Waste Management Area S-SX: (November 1997 through April 2000.

Note: U denotes analytical result is non-detect.

S = sample collected by pumping from 4.5 m (146 ft) screened interval

P = sampled during drilling using temporary pump/screen and packer assembly

B = bailed during drilling

The data from Well 299-W22-50 (Table 5-3), located near the northern edge of the Tc-99 and nitrate plume, show that the concentrations of Tc-99 and nitrate decrease fairly rapidly from the water table to about 7 m (23 ft) depth in the aquifer. This is in contrast to the broader and deeper plume found in Well 299-W22-47 located near the axis of the plume (Figure 5-27). Additionally, the magnitudes of the concentrations are smaller in Well 299-W22-50 than they are in Well 299-W22-47. The distribution of nitrate concentrations with depth in Well 299-W22-50 shows a second smaller magnitude maximum between about 60 and 80 m (197 and 262 ft) below the water table. The second, deeper maximum is corroborated by several field measurements of nitrate collected from air lifted samples during drilling and is associated with a second, deeper concentration maximum for carbon tetrachloride (PNNL-13441). PNNL-13441 attributes the concentration profiles found in Well 299-W22-50 to two different plumes intercepted by the well. These include a shallow-depth plume consisting of tank waste constituents of Tc-99, tritium, and nitrate, and a deeper plume containing carbon tetrachloride and nitrate that were probably from past-practice wastewater discharges from the Plutonium Finishing Plant routed to U Pond.

Specific Conductance Measurements in Well 299-W23-19. Well 299-W23-19 was drilled in 1999 adjacent to tank SX-115. The well was originally drilled as a characterization borehole next to a tank that is suspected to have leaked about 0.198 ML (0.05 Mgal) in 1965 (RPP-ENV-39658). Groundwater sampled from the

well in October 1999 showed the highest Tc-99 concentrations yet observed in Hanford Site groundwater (PNNL-13441). For that reason, the borehole was completed as a monitoring well. A permanent sampling pump and four specific conductance probes were installed in the well in early 2003.

Specific conductance measurements were recorded at intervals no longer than 30 minutes from March through September 2003. Those data reveal sharp discontinuities (Figure 5-27) that represent pumping and sampling events. According to PNNL-14548, during pumping for sampling purposes, the water passing Probes 1, 2, and 3 is a blend of water entering the well above their respective depths because the pump intake is lower than Probe 3. Using a simple mixing model, they calculated the average concentration of water entering the well within the specific interval of each probe. (Probe 4 was not considered because it malfunctioned.) For example, Probe 1 reflects the composition of water entering the uppermost 1.2 m (3.9 ft) of the aquifer with specific conductance of about 2,100 µS/cm (Table 5-4). Probe 2 represents a blend of water from the upper 3.1 m (10.1 ft) of the aquifer, but the concentration of the water entering the aquifer between the two probes is greater than that entering above Probe 1. Thus, to achieve the composition of water measured by Probe 2 (2,600 µS/cm), water with specific conductance of 2,915 µS/cm must be mixing with water passing Probe 1. Table 5-4 shows the results of applying this same logic to all probes and depth intervals. The results suggest that the plume at Well 299-W23-19, as indicated by elevated specific conductance, is located in mainly the upper 3 to 4 m (9.8 to 13.1 ft) of the aquifer. The lower plume boundary is reasonably sharp with the groundwater composition falling significantly over, at most, a 2 m (6.6 ft) interval (PNNL-14548).

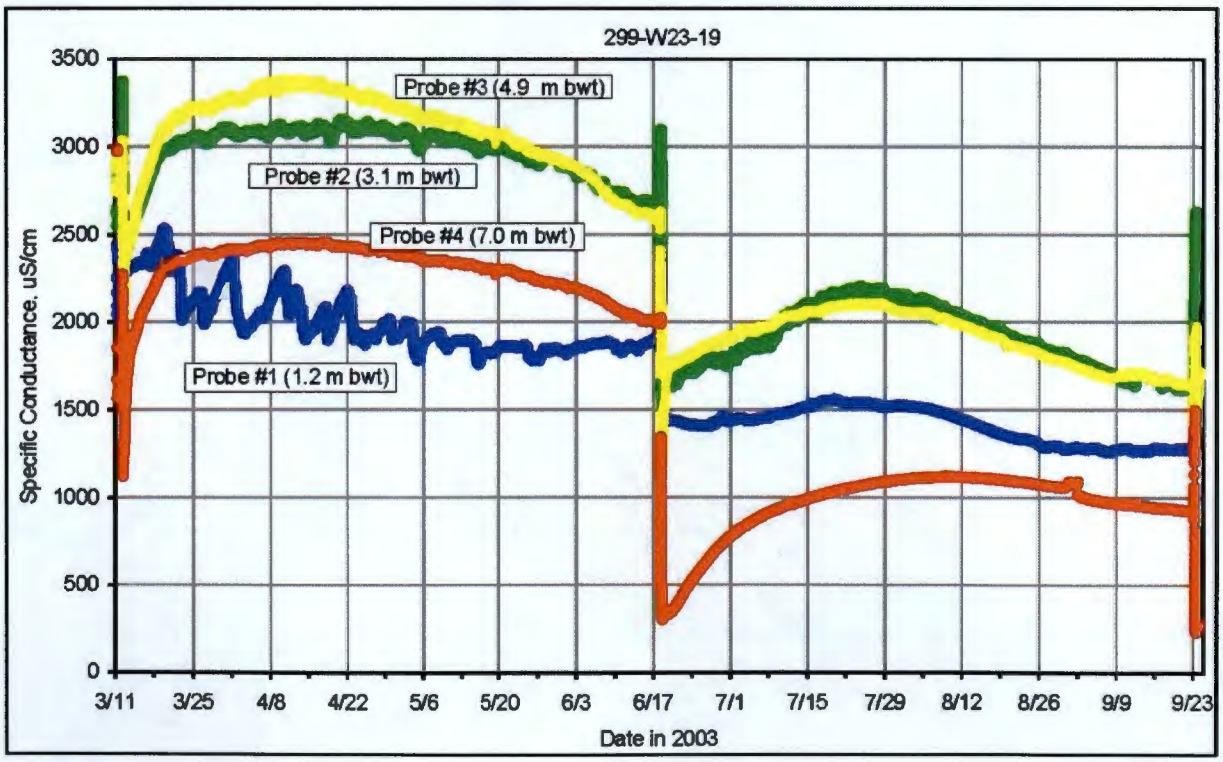

Source: PNNL-14548, *Hanford Site Groundwater Monitoring for Fiscal Year 2003.*
bwt = below water table

Figure 5-27. Wellbore-Fluid Specific Conductance Measurements Collected in Well 299-W23-19 at Waste Management Area S-SX

Table 5-4. Vertical Variation of Groundwater Composition Measured in Well 299-W23-19 and Estimated for the Adjacent Aquifer on September 23, 2003 (from PNNL-14548)

Measurement Point[a]	Depth Below Water Table (m)	Interval Length[a] (m)	Measured In-Well Specific Conductance (µS/cm)	Estimated Aquifer Specific Conductance Over the Interval[b] (µS/cm)
Probe 1	1.2	1.2	2,100	2,100
Probe 2	3.1	1.9	2,600	2,915
Probe 3	4.9	1.8	1,900	694
Pump Intake	5.8	0.9	1,450	663
Well Bottom	7.7	1.9	Not measured	

a. The interval length is the distance between Probe 1 and the water table, between Probe 2 and Probe 1, between Probe 3 and Probe 2, between Probe 3 and the pump intake, and between the pump intake and the well bottom.

b. It is assumed that the aquifer is homogeneous and isotropic, i.e. water enters the well uniformly across the entire saturated portion of the screen during pumping. Therefore, the specific conductance in the aquifer for an interval was computed assuming that the quantity of water entering the well across that interval is only a function of the interval length.

6 Integrated Conceptual Models for Key Contaminants

In this chapter, the information used to develop vadose zone conceptual models for the distribution of key mobile contaminants (Chapter 3) has been combined with the observed groundwater plumes (Chapter 5) for the two S Complex Area subregions. This chapter provides preliminary comparisons and estimates of the mass/activity of key risk drivers remaining in the vadose zone below each subregion in relation to present groundwater plumes.

6.1 Methodology and Assumptions

Combined vadose zone-aquifer conceptual models for the distribution of Tc-99, nitrate, chromium, I-129, and uranium below the S Complex Area subregions were developed (Chapters 3 and 5). These were based on the review and synthesis of all available historical gamma logging, soil resistivity surveys, vadose zone sediment characterization data, detailed vadose zone hydrogeology, and groundwater monitoring and depth discrete characterization data.

A goal of the combined conceptual models is to estimate the masses of each mobile contaminant in each medium and to perform a mass balance check. To perform a mass balance evaluation, five compartments were chosen to represent locations and the subsurface media where contaminants reside. Figure 1-2 shows the five compartments that were used in the mass balance estimation process: inventory released to each facility, residual mass in vadose zone, current mass in groundwater plumes, mass removed by pump-and-treat activities, and mass that escaped the S Complex Area and missed detection because monitoring was unavailable.

The mass of contaminants in each compartment is based on the following assumptions:

Compartment 1 is inventory released to each facility. The SIM database was used as an accurate estimate of inventory disposed of or released to each facility.

Compartment 2 is residual mass in the vadose zone sediment (actually, in pore water for mobile contaminants, because sorption or precipitation of mobile contaminants is assumed to be negligible)[9] was developed in Chapter 3. As mentioned, because there is such a dearth of measurements of concentrations of the key contaminants in actual sediments, in most cases, the conservative estimate is that almost the entire disposed inventory remains in the vadose zone for the releases from the two tank farms and the 216-S-9 Crib. Based on the estimates of lateral spread of the contaminants in the vadose zone below the 216-S-21, 216-S-23, and 216-S-25 Cribs compared to the volumes of waste liquids disposed, we estimate that 33 percent, 77 percent, and 20 percent, respectively, of the inventories remain in the vadose zone.

Compartment 3 is the mass in the groundwater plumes. The mass currently in groundwater plumes is based on the data discussed in Chapter 5.

Compartment 4 is the mass removed by pump-and-treat activities. The mass removed by pump-and-treat actives for the S Complex Area is currently ignored, although some Tc-99 has been removed from pumping 299-W23-19.

Compartment 5 is the mass that escaped in groundwater that has left the S Complex Area (and likely dispersed below detectable concentrations) before adequate monitoring was available, is assumed to be negligible in this first iteration.

---

[9] It is acknowledged that uranium is not a non-sorbing contaminant in most subsurface environments at the Hanford Site. Making the non-sorbing assumption for uranium is very conservative and most applicable for only one particular Hanford waste stream (neutralized metals waste from the bismuth phosphate fuel reprocessing method).

The fact that the size and shape of the groundwater plume may not change appreciably with time suggests that mass has likely been removed by migration beyond the boundaries of the S Complex Area and dispersed and diluted to concentrations not detectable. Therefore, there is no objective way or defensible idea on how to estimate the value for this escaped mass, which is the fifth compartment in the mass balance calculation. Additionally, as discussed in Chapter 3, in general, there is not sufficient data to estimate the residual mass in the vadose zone for each subregion and for each mobile contaminant (thus, compartment 2 and compartment 4 cannot be quantified with much certainly). The only compartment with the potential for having a sufficient data set is compartment 3 (mass in the current groundwater plume). However, after inspection of the available groundwater monitoring data for the S Complex Area, the estimate of mass for many of the five mobile contaminants has only been practical during the last five years because of well coverage and sampling frequency. Therefore, the mass balance calculation for the S Complex Area using the five compartments is of limited value.

Next, the available groundwater data that was used to quantify compartment 3 (mass in the current S Complex Area groundwater plume) is discussed. As mentioned in Chapter 5, the time when monitoring for the five mobile constituents commenced varied with contaminant and often time; the earliest measurements were for limited wells and not very frequent. Figure 6-1 shows the volumes of waste disposed to the four cribs and when releases were estimated to have occurred in the S and SX Tank Farms for comparison to the timing of commencement of groundwater monitoring.

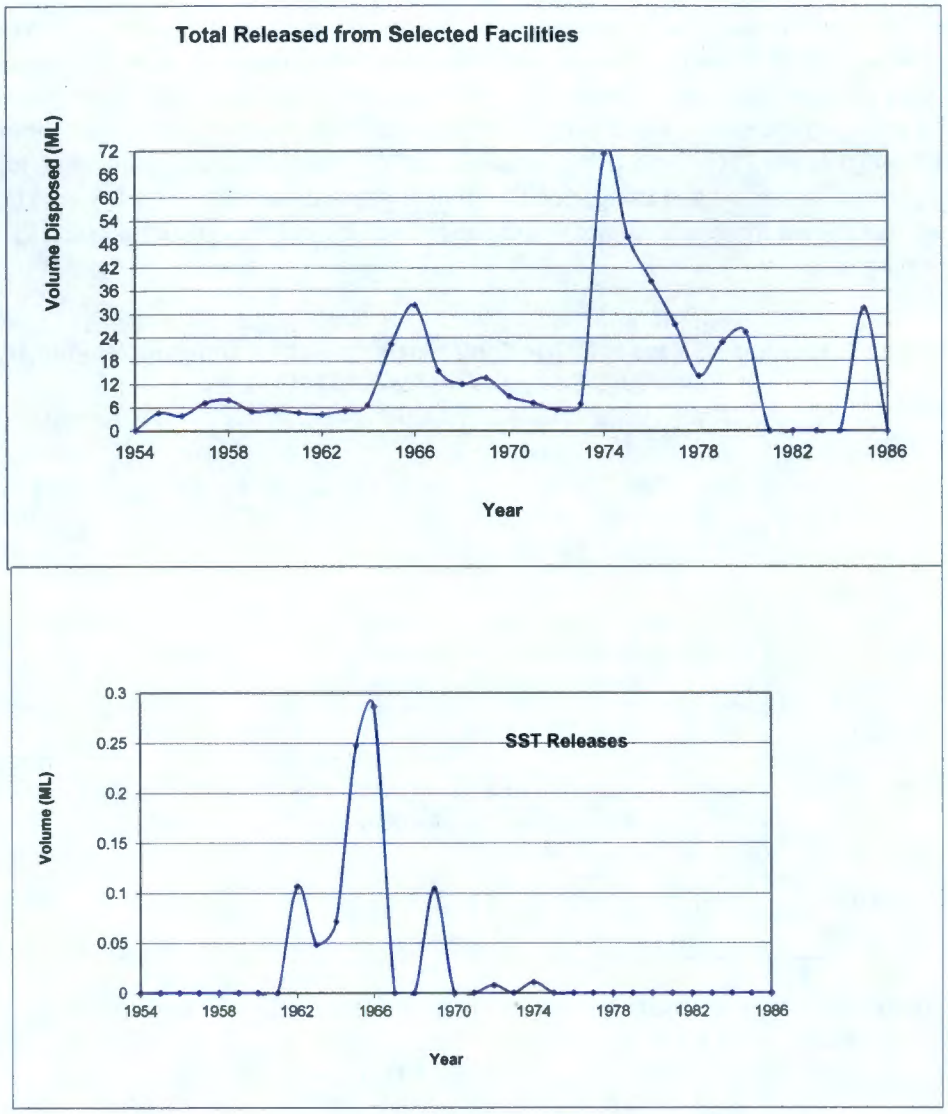

Figure 6-1. Yearly Volumes of Waste Liquids Disposed or Released to Subsurface at S Complex Area

6.2 Estimates of Mass in Current Groundwater Plumes

This section provides estimates of the masses of contaminants in groundwater beneath the S Complex Area that are believed to have been sourced by the four cribs and S and SX Tank Farms. Some other facilities, such as the 216-U-10 Pond and the 216-S-1 and 216-S-2 Cribs, have also contributed to groundwater contamination within the S Complex Area. Additionally, some groundwater contamination may have occurred from broken or leaking pipelines throughout the years of operation, but these unplanned releases are not considered in this report.

Separate contaminant plumes for the two subregions of the S Complex Area were not mapped because, in most cases, groundwater plumes from individual disposal facilities or subregions have mixed with plumes from other facilities or subregions and cover large areas. To distinguish plumes from individual subregions, large cut off concentrations are necessary, such that areas of lower concentrations would

separate the high concentrations within each plume. This would exclude the contaminant masses in the low concentration areas from being included in the overall mass estimates. In addition, to include the entire mass of a given contaminant, groundwater plumes were traced beyond the boundaries of the S Complex Area when necessary. Table 6-1 summarizes the mass/activity estimates for chromium, nitrate, and Tc-99 that were generated using EarthVision[10] (a 3D geosciences computer code) from the historical groundwater data without using specific cutoff concentrations (i.e., no background natural concentration was chosen for the chromium or nitrate values that would be ignored as being a contributor to the contaminant plume).

Table 6-1. Estimated Mass of Mobile Contaminants in Current Groundwater Plumes, Below the S Complex Area for 2005-2010 Period

Contaminant	Mass in Groundwater (assumes porosity = 20% vol)	Total Mass Released to S Complex Area	% of Mass/Activity in Groundwater Versus Total Released
Technetium-99 (Ci)	3.2 Ci	34.4 Ci	9.3
Iodine-129 (Ci)	Groundwater database is too sparse to effectively estimate mass	0.08 Ci	
Nitrate (kg)	1.83E+05 kg	3.64E+05 kg	50.3
Chromium (kg)	107.4 kg 111.2 kg if include mass attributed to U Pond	1350 kg	8.0 8.2
Uranium (kg)	There is no significant U in groundwater in S Complex Area	305 kg	

No mass/activity estimates were made for uranium or I-129 because there is no uranium groundwater plume above the DWS and the I-129 groundwater database is very sparse (number of analyses at a well versus time and well coverage is also sparse) below the S Complex Area in the last ~20 years.

Some details on the groundwater mass calculations used and the assumptions made to estimate the masses follow, and there is additional discussion in Sections 1.5, 1.6, and 6.1. Approximate 3D groundwater plume distributions for the recent period 2005 to 2009 were modeled in EarthVision, based on concentrations observed in wells during the period of interest, and for some wells that have not been sampled recently, data collected in the period 2000 to 2005 were added to increase the area of well coverage. In a few instances, groundwater data from the late 1990s were added for wells that are no longer sampled. EarthVision uses an interpolation algorithm to fill in concentrations for all grid cells representing the volume of the plume and control points selected by a Hanford Site team of groundwater experts. Control points are synthetic data points and were used to control extrapolation of the contaminant concentrations to areas within and outside the plume where no data were available. The EarthVision representation of the S Complex Area consisted of 1,072,162 cells with dimensions of 20 × 20 × 1 m (65.6 × 65.6 × 3.28 ft) thick. The volume of each cell was 400 m^3 (14,125 ft^3).

[10] EarthVision and the EarthVision logo are trademarks of Dynamic Graphics, Inc. Alameda, California.

The initial set of groundwater concentration measurements and control points used for the period of interest (~2005 to 2010) for Tc-99, nitrate, and chromium were taken from an earlier groundwater plume interpretation developed by Intera, Inc. in support of the 200-UP-1 and 200-BP-5 Remedial Investigation Reports (ECF-200UP1-10-0373, *200-UP-1, Remedial Investigation Report; Groundwater Contaminant Fate and Transport Model*; ECF-200BP5-10-0351, *200-BP-5 Remedial Investigation Report-Groundwater Fate and Transport Modeling*). The Intera, Inc. data sets included the most recent available concentrations measured for wells from 2005 to 2010, but included older measurements where no recent measurements were available for wells that are within the S Complex Area of interest. The control points included contour concentration values assigned along contour maps produced for the fiscal year (FY) 2009 annual groundwater report (DOE/RL-2010-11). Additional control points were added in some areas to control extrapolation of the concentration data into areas outside the plume where no measurements were available.

The hydrogeologic solid model for the modeled area was also imported from the earlier Intera, Inc. model. Groundwater contamination is primarily within the Ringold Formation sand and gravel deposits (RFwie subunit). The porosity of RFwie sediment was assumed to be 20 percent for the base calculations. However, the porosity of this unit is quite variable, and there is uncertainty in the value that should be applied to the groundwater plume mass calculations. The total mass of each contaminant was calculated by summing the cell concentration over the entire 3D grid and multiplying by the cell volume and the assumed porosity of 0.20. To estimate the mass/activity for any of the contaminants using a different porosity value (that differs from 20 vol.%), requires a simple multiplication of the ratio of the desired porosity expressed as a fraction divided by 0.20. Because the groundwater database for the five mobile contaminants in the S Complex Area as a function of time is not robust, no assessments of the changes of mass of contaminants in groundwater over time were calculated. Future mass estimates should use the most current/updated S Complex Area hydrogeologic interpretation.

Another complication for the thick aquifer below the S Complex Area is the fact that there are vertical variations in contaminant concentrations, and the data set for concentrations as a function of depth below the water table is very limited in time. Measurements of the vertical distribution of contaminants were and continue to be primarily obtained from samples taken at the time of drilling, and in the past, focused primarily on the few relatively deep groundwater wells. To honor the information on vertical distribution of contaminants from these deeper groundwater wells in addition to other wells that were recently installed, the past contaminant vertical distributions were estimated, based on the ratios of past to current concentrations in the upper part of the aquifer where more data are available. The measured ratios at each time-plane were used to create a 2D grid of the ratio representing changes in concentration in the upper portion of the aquifer, which was multiplied by the current 3D contaminant distribution to estimate the earlier contaminant vertical distributions. If earlier groundwater concentration measurements were not available, and a concentration-change ratio was, therefore, missing at that location, then the ratio grid value was interpolated from other more recent measured vertical concentration ratios. In essence, this assumes there is a linear time-dependence to changes in the vertical distribution of contaminants at any given well.

The last column of Table 3-7 shows the percentages of the total inventory disposed to the S Complex Area that the groundwater plume mass/activity represents. The following subsections discuss the groundwater mass estimates in current S Complex Area plumes for the three mobile contaminants that mass/activity estimates were possible (Tc-99, nitrate, and chromium). By using no-concentration-cutoff for groundwater concentrations, the calculated masses shown in Table 6-1 for nitrate and chromium should be conservative.

Because Section 3.3 estimates for residual mass in the vadose zone assumed that essentially all of the Tc-99 and chromium released from the S Complex Area came from the two tank farms and that, because

the volumes of fluid released below the tank farms were small, all fluid and associated contaminants remain in the vadose zone below the tank farms. However, based on the groundwater plume findings, about 8 percent of Tc-99 and chromium are found in the current groundwater plumes, which require that the Table 3-5 values for residual mass in the vadose zone be reduced from 100 percent of the total released to ~90 percent to honor the mass balance process. Regardless, the mass balance exercise still projects that the bulk of the Tc-99 and chromium released below the S Complex Area likely remains in the vadose zone sediments, although at depths not readily determined because of the sparse sediment concentration database.

6.2.1 Technetium-99

Figure 6-2 shows the plume map for Tc-99 for the past 5 years. Two sources for Tc-99 contamination exist in the groundwater beneath the S Complex Area. The first source is at the southwest corner of the S-SX Tank Farm, and this large plume continues to migrate downgradient to the east and southeast.

An ad hoc pump and treat removal operation using Well 299-W23-19 (located adjacent to the SX Tank Farm near the source) is one explanation for the apparent separation of the higher concentration isopeth into two hot spots. After samples are collected from this well each quarter, well purging is continued at a higher flow rate until a minimum of 3,785 L (1,000 gal) of water is removed from the aquifer. This water is transferred to the Effluent Treatment Facility for treatment and disposal. This practice has the objective of reducing the Tc-99 concentration in the aquifer, and is to continue until four consecutive quarterly sample results are below 9,000 pCi/L. Through 2009, about 8.4×10^{-3} curies of Tc-99 have been removed since this ad hoc pump and treat process was started in 2003 (DOE/RL-2010-11; see Section 6.3.3). Alternatively, the separation of the Tc-99 plume into two contiguous plumes with distinct hot spots could be an artifact of the gridding process and data interpolation used to construct the conceptual model. Figure 5.10, taken from DOE/RL-2010-11, presents an alternative Tc-99 groundwater plume estimate. The two alternative conceptual groundwater plume representations should be vetted in the future as more data become available.

The following discussion is based on the interpretation presented in Figure 6-2. At extraction Well 299-W23-19, Tc-99 was present when the well was first sampled in October 1999 at 39,000 pCi/L and peaked at 188,000 pCi/L in January 2003. During the ad hoc pump and treat, Tc-99 activity has varied between 35,000 and 137,000 pCi/L but has stabilized at an activity range between 46,000 to 75,000 pCi/L since 2008.

The southwestern boundary of this Tc-99 plume appears to be near Well 299-W23-15, located just south and a bit east of 299-W23-19. From 1992 through early 1994, Tc-99 activity in 299-W23-15 varied from 2000 to 7,500 pCi/L. Then, the activity consistently dropped to 300 and then to ~20 pCi/L between 1995 and 2002; since 2002, it has varied narrowly from 20 to <5 pCi/L.

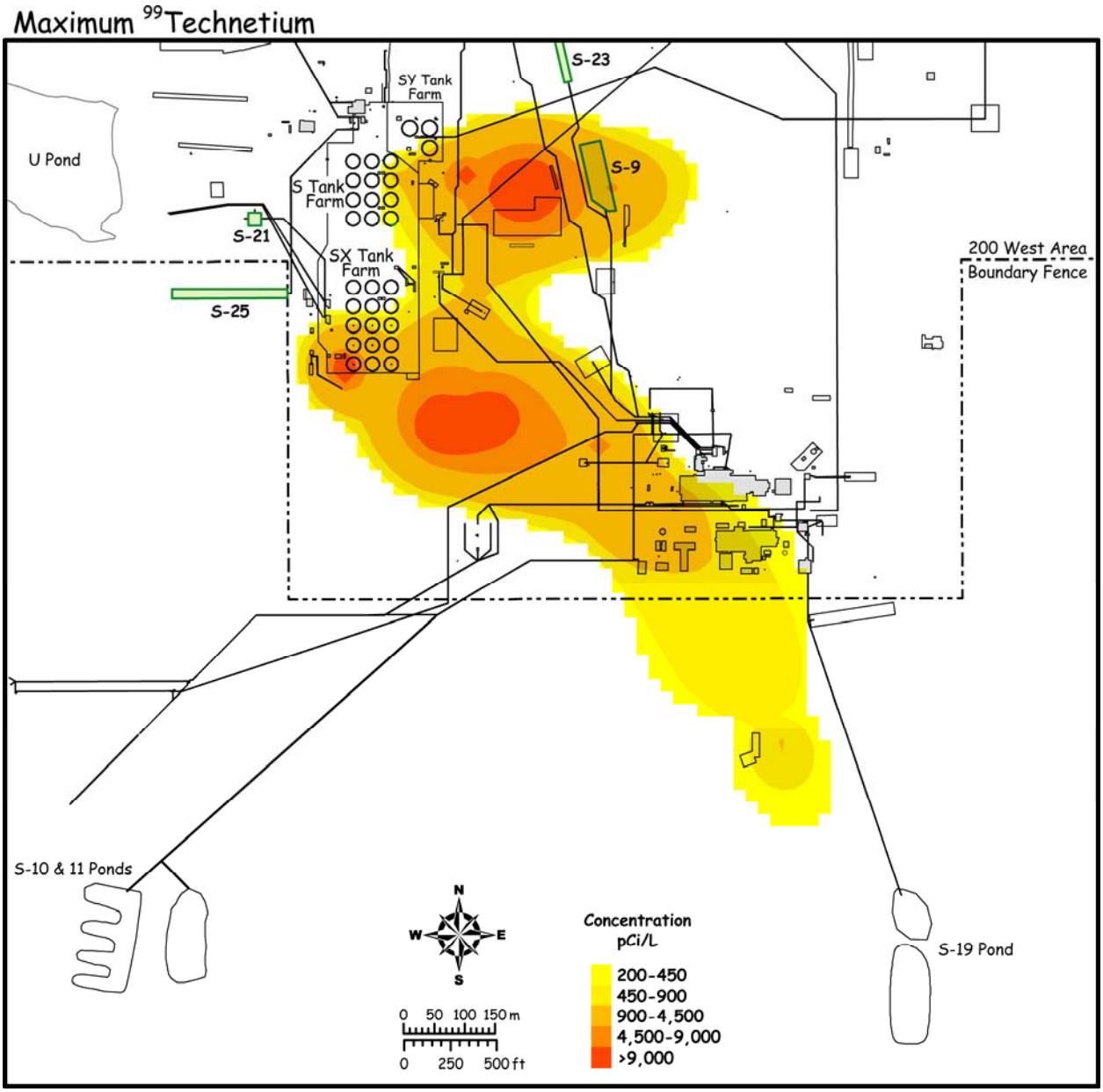

Figure 6-2. Technetium-99 Contamination Beneath the S Complex Area

Two downgradient wells (299-W22-50 and W22-47) intercept the plume farther east of 299-W23-19, 299-W23-15, and 299-W22-80. Tc-99 concentrations in 299-W22-50 and 299-W22-47 range from 3,000 to 13,800 pCi/L over the period 2005 to 2011, and 10,700 to 20,000 pCi/L over the period 2005 to 2011, respectively. Well 299-W22-80 lies between the high Tc-99 groundwater concentrations at 299-W23-19 and the moderate Tc-99 concentrations measured in 299-W22-50 and 299-W-22-47. One would logically assume that the Tc-99 concentration in the groundwater at 299-W22-80 would be intermediate to the values near the "source" Well 299-W23-19 and the more distance Wells 299-W22-47 and 299-W-22-50. However, Tc-99 measured at 299-W22-80 has varied between <5 to 20 pCi/L from 2001 to mid-2004 and from 2006 to the present. From mid-2004 through the end of 2005, the Tc-99 concentration in 299-W22-80 ranged from 30 to 150 pCi/L. Overall, these values are much lower than would be expected for this location within the plume. As mentioned in Section 2.6.1 the water inside the casing of

299-W22-80 exhibits upward vertical flow. The upward vertical flow likely is bringing uncontaminated water into the casing during the sampling episodes and thus diluting the observed actual Tc-99 concentrations used to represent the plume in the upper portion of the aquifer at this well location. Another yet untested possibility is that sediment (or the well completion) surrounding 299-W22-80 has a lower intrinsic permeability that restricts the flow of contaminated water through this area. Essentially, a localized low permeability zone around 299-W22-80 could force the contaminated water to divert around 299-W22-80. This all could be related to the mechanism causing the upward flow within the casing. Even though this upward flow phenomenon is not understood, it is most likely the reason for the observed low Tc-99 groundwater concentrations.

The second Tc-99 plume is located east of the S Tank Farm and appears to be sourced by tank fluids released in or near the 241-S-104 tank. The three closest monitoring wells downgradient (to the east) from the S Tank Farm are 299-W22-44, farther east 299-W22-26, and 299-W22-48 located south and east Note: Well 299-W-22-26 (near 216-S-9 Crib) is off the map east of the midpoint between W-22-44 and W22-48.

Figure 6-3 shows the closest groundwater monitoring wells surrounding the S and SX Tank Farms). The time history of Tc-99 concentrations for these three wells is shown in Table 6-2. In general, Tc-99 started to appear in the groundwater just east of the S Tank Farm in early 2000 and farther to the east at 299-W22-26 sometime between 2000 and the end of 2005 (no samples were measured between 2001 and early 2005 at this well). Directly east of 241-S-104 tank, the groundwater Tc-99 has been steadily increasing over the last ten years and may be stabilizing to the south at 299-W22-48.

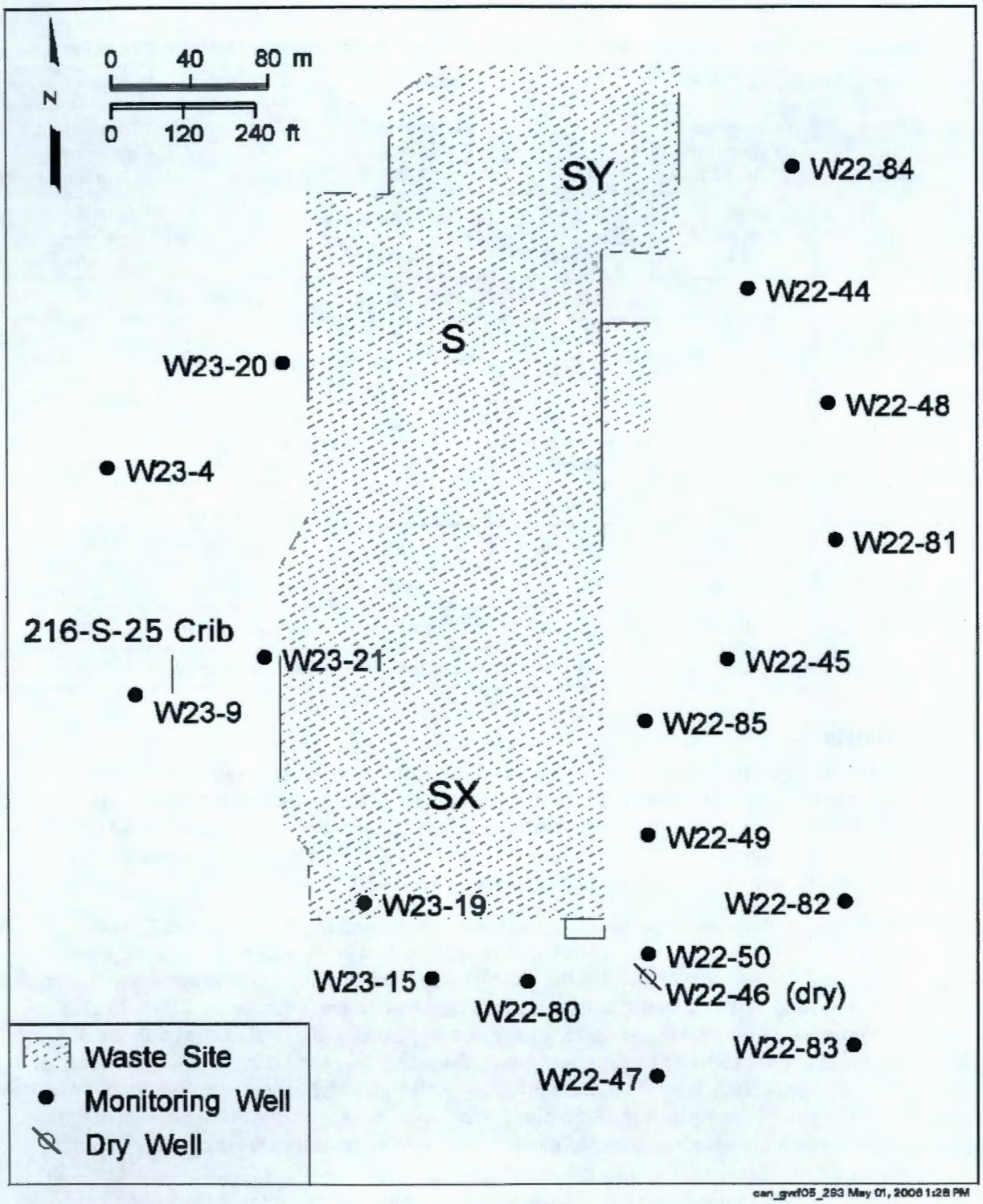

can_gwf05_293 May 01, 2006 1:28 PM

Note: Well 299-W-22-26 (near 216-S-9 Crib) is off the map east of the midpoint between W-22-44 and W22-48.

Figure 6-3. Location of Groundwater Monitoring Wells Surrounding the S and SX Tank Farms

Table 6-2. Technetium Concentrations Time History for Three Wells Downgradient from S Tank Farm

Well 299-W22-44		Well 299-W22-48		Well 299-W22-26	
Date	Technetium-99 Concentration (pCi/L)	Date	Technetium-99 Concentration (pCi/L)	Date	Technetium-99 Concentration (pCi/L)
Jan-00	40	Mar-00	720		
Jan-01	140	Mar-01	2,950	1st qtr 2001	<5
		Mar-02	4,140	2nd qtr 2002	<5
Jan-03	385	Mar-03	3,360		
Jan-04	927	Mar-04	3,010		
Jan-05	1,200	Mar-05	1,980	4th qtr 2005	1,130
		Mar-06	1,120	4th qtr 2006	1,450
Jan-07	7,300	Mar-07	1,270		
Jan-08	14,000	Mar-08	1,100	4th qtr 2008	4,200
Jan-09	16,000	Mar-09	1,300	3rd qtr 2009	5,600
Jan-10	18,000	Mar-10	1,400	4th qtr 2010	6,000

Note: Years with no technetium-99 value represents years with no sample results reported (well not sampled).

6.2.2 Nitrate

Figure 6-4 shows the nitrate plume map for the past 5 years; the lowest concentration isopleth is 20 mg/L. This figure can be compared to the nitrate groundwater plume depiction shown in DOE/RL-2010-11 (Figure 5-7), which considered only data down to the 45 mg/L DWS. Both conceptualizations of the nitrate groundwater plume in the S Complex Area suggest three sources for the nitrate found in the groundwater: the 216-S-25 Crib and the two tank farms (S and SX).

The estimated mass of nitrate in the groundwater (assuming no concentration cutoff and 20 vol% porosity) is $1.83 \times 10^{+05}$ kg. This mass represents about 50 percent of the total released to the entire S Complex Area. The percentage found in the groundwater is significantly larger than the 8 to 9 percent of the chromium and Tc-99 estimated to have reached the groundwater. Because the 216-S-25 Crib received 63 percent of the total liquid waste volume and 61 percent of the total nitrate of all the S Complex Area facilities included in this report but contained no Tc-99 and only 10 percent of the total chromium (see Appendix A Worksheet Mass Inventory Roll Up), a higher percentage of nitrate would be expected in the groundwater below the S Complex Area. Table 3-5 shows that about 50 percent of the nitrate mass remains in the vadose zone sediments, which is in agreement with the estimate of nitrate mass in the aquifer. Therefore, the mass balance calculation is quite satisfactory. Of course, given the uncertainty in the data available to make the calculation of residual nitrate mass in the vadose zone, the even split of the total nitrate between the vadose zone and groundwater plume may be completely fortuitous. However, because most of the nitrate found in the groundwater in the S Complex Area would have come from disposal to the 216-S-25 Crib, which did affect groundwater over its active disposal period (1975 to 1980 and 1985), this preliminary nitrate mass balance has merit. Unlike the large

discrepancy in the nitrate estimate in the groundwater and nitrate remaining in the vadose zone below the T Complex Area (SGW-49924), because of the possibility of additional nitrate sources such as sewerage, the nitrate mass balance for the S Complex Area is very good.

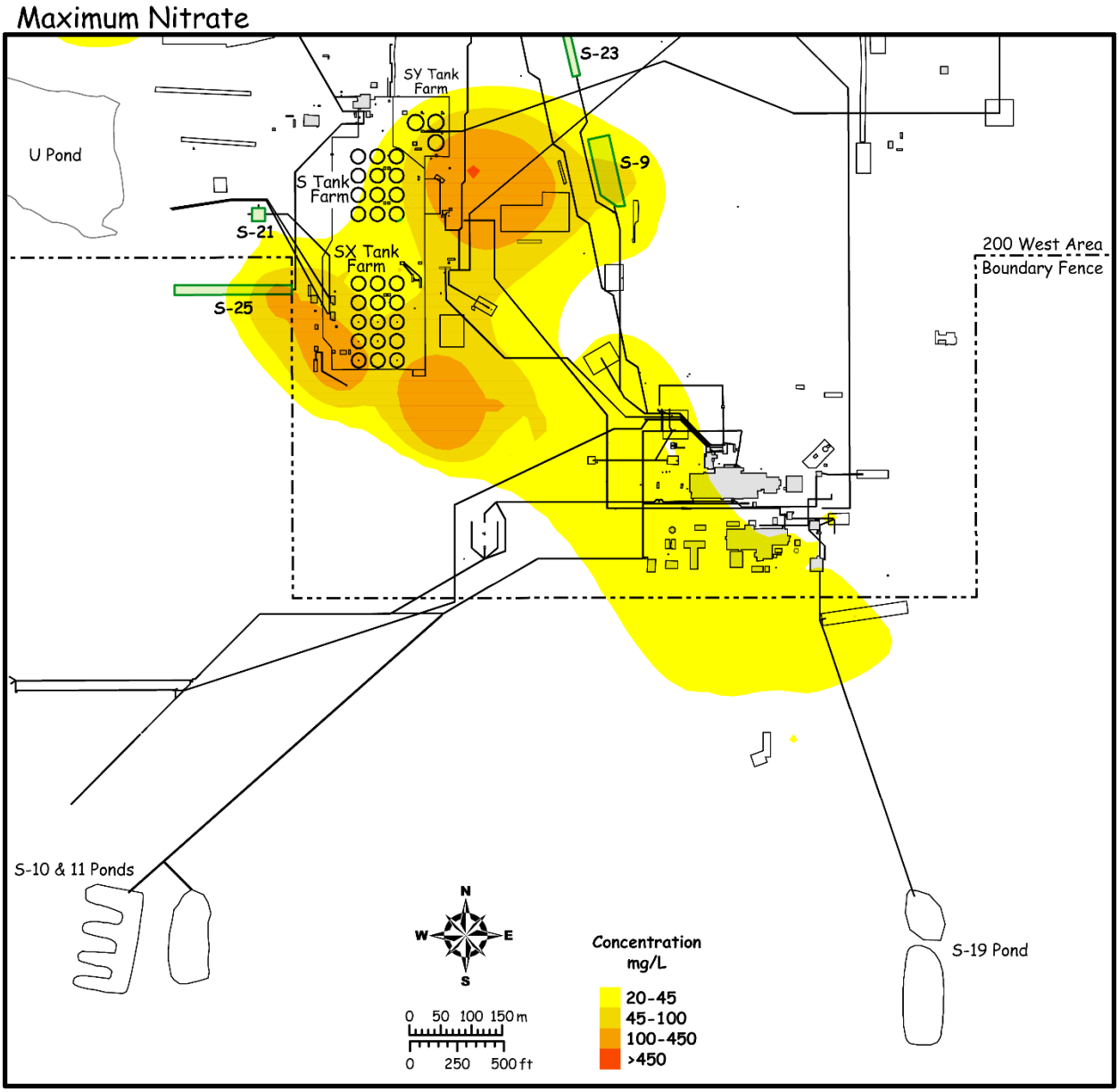

Figure 6-4. Nitrate Contamination Beneath the S Complex Area

6.2.3 Iodine-129

There is insufficient I-129 groundwater data in the S Complex Area to make a meaningful groundwater plume map and, as shown in Figure 6-5 (from DOE/RL-2010-11); the I-129 in this southern portion of the 200-W Area is sourced primarily from both U Plant and REDOX Plant disposal facilities. One plume originates from the 216-U-1 & 2 Cribs, and a second plume originates from the southern portion of the 200 West Area. At the current level of monitoring detail, these plumes merge downgradient and become indistinguishable. The 216-S-9 Crib may have sourced some of the I-129 feeding this relatively large comingled plume. As shown in Table 3-5, the 216-S-9 Crib did receive the most I-129 released to the

S Complex Area. Thus, it is likely that some of the groundwater I-129 plume found to the east did originate from 216-S-9 Crib. The total activity of I-129 released in the S Complex Area is 0.082 Ci, which is slightly larger than the 0.074 Ci released to the T Complex Area just north of this region (Figure 6-4).

6.2.4 Chromium

Figure 6-6 shows the chromium plume map generated for the period 2005 to 2010. Chromium contamination appears as four localized smaller plumes that appear to be sourced from the southwest edge of the SX Tank Farm, the east edge of the S Tank Farm, the southeast edge of the S Complex Area near the 216-S-20 and 216-S-22 Cribs (which are not facilities discussed in this report), and near the southwest edge of the S Complex Area below the 216-S-10 Pond. Figure 6-5 differs somewhat from a FY 2008 chromium plume map presented in DOE/RL-2009-122, *Remedial Investigation/Feasibility Study for the 200-UP-1 Groundwater Operable Unit* (see Figure 4-20 therein) and, once additional characterization is performed in the S Complex Area, the chromium plume interpretation will be updated. Both groundwater plume estimates suggest that the most chromium mass is associated with the plumes that appear to originate from the two tank farms, and (Figure 6-6) that the localized chromium groundwater plumes from the SX Tank Farm and southeast corner of the S complex Area (near 216-S-20) have started to coalesce into one larger commingled plume with the three elevated hot spots. The groundwater chromium plume conceptualization in DOE/RL-2009-122 does not show the same degree of coalescence and does not show the relatively small low concentration plume midway along the S-10 Pond and Ditch.

Table 6-3 lists the calendar year average total dissolved chromium concentrations in three wells south of the SX Tank Farm (299-W23-19, 299-W22-50, and 299-W22-47) and three wells east of the S Tank Farm (299-W22-44, 299-W22-48, and 299-W22-46).

Chromium concentrations as high as 1,750 µg/L have been found in the groundwater to the south of the SX Tank Farm at Well 299-W23-19 (December 2005) and the yearly average concentrations have ranged from approximately 700 to 1,175 µg/L since 2005. The current groundwater chromium values measured at this well are approximately 1,000 µg/L. East of the S Tank Farm, chromium in Well 299-W22-44 (closest to S-104 tank) started to increase significantly sometime between 2006 and 2007. Since 2007, the average Chromium concentration for each year has ranged from 310 to 608 µg/L. To the south and east (downgradient) at 299-W22-48, there is no evidence of a significant increase since 2006. Farther east, at 299-W22-26, the chromium plume originating from/near the 241-S-104 tank release started to appear sometime between 2006 and 2008 and has been increasing in concentration since 2008. Concentrations of chromium near the southern border of the SX tank farm are larger than the concentrations found east of S-104 tank. The mass of chromium entering the aquifer from these two sources appear to be slowly increasing over the last three years, although the ad hoc pump-and-treat of Well 299-W23-19 may be influencing the flux rate.

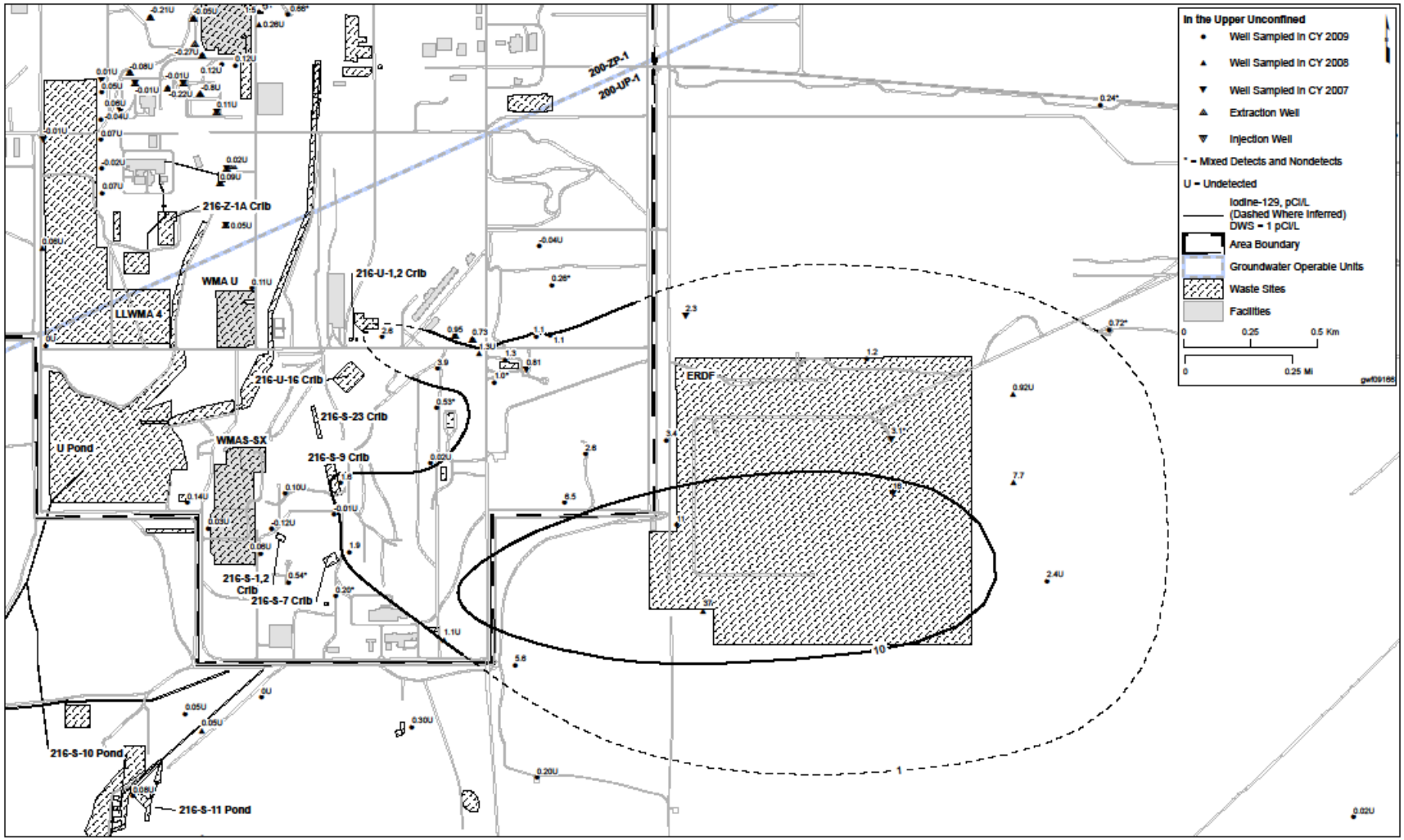

Figure 6-5. Iodine-129 Contamination Beneath the Southern Portion of the 200 West Area

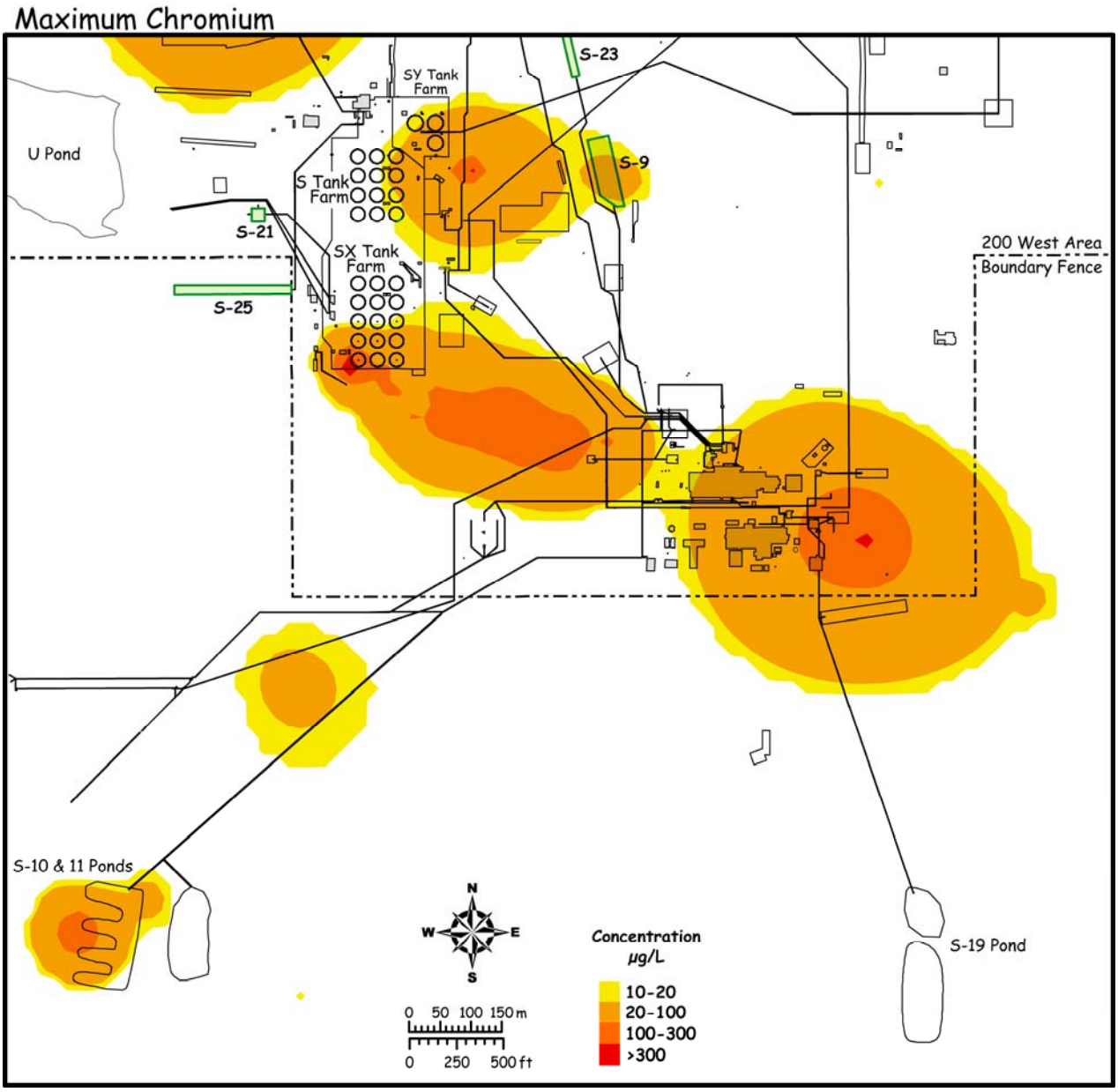

Figure 6-6. Chromium Contamination Beneath the S Complex Area

Table 6-3. Calendar Year Average Chromium Concentrations in Groundwater Monitoring Wells near and Downgradient of the SX and S Tank Farms

Wells Near SX Tank Farm					
Well 299-W23-19		Well 299-W22-50		Well 299-W22-47	
Date	Cr (µg/L)	Date	Cr (µg/L)	Date	Cr (µg/L)
1999	77	1999	<3	1999	
2000	103	2000	11	2000	
2001	74	2001	17	2001	
2002	16	2002	69	2002	
2003	60	2003	115	2003	
2004	284	2004	105	2004	
2005	1175	2005	110	2005	138
2006	1038	2006	87	2006	281
2007	692	2007	85	2007	283
2008	768	2008	80	2008	258
2009	950	2009	70	2009	229
2010	980	2010	70	2010	219
Wells Near S Tank Farm					
Well 299-W22-44		Well 299-W22-48		Well 299-W22-26	
Date	Cr (µg/L)	Date	Cr (µg/L)	Date	Cr (µg/L)
2000	<10	2000	18	2000	
2001	<10	2001	33	2001	<10
2002		2002	40	2002	<10
2003	<10	2003	35	2003	<10
2004	16.4	2004	26	2004	<10
2005	17	2005	17	2005	10.5
2006		2006	11	2006	16
Date	Cr (µg/L)	Date	Cr (µg/L)	Date	Cr (µg/L)
2007	310	2007	17	2007	
2008	546	2008	15	2008	42
2009	629	2009	<13	2009	68
2010	608	2010	<14	2010	102

Note: Years with no chromium value represent years with no sample results reported (well not sampled).

6.2.5 Uranium

There has been no significant uranium groundwater contamination detected beneath the S Complex Area in the last 20 years. Uranium concentrations are elevated in wells west and northwest of WMA S-SX near U Pond. Uranium concentrations exceed the DWS in only one well in the S Complex Area, 299-W23-4 (near the 216-S-21 Crib), which had a peak concentration of ~350 µg/L in the early 1970s that dropped to about 150 µg/L in the mid-1970s, to 50 to 100 µg/L in the early- to mid-1980s, to 30 to 80 µg/L in the late-1980s, and has stabilized in the range of 20 to 35 µg/L from the mid-1990s through 2010. Thus, no mass estimates were performed for uranium existing in the groundwater today below the S Complex Area. As mentioned in Chapter 5, there was some elevated uranium in the groundwater below some of the cribs in the period of active disposal or shortly thereafter, but the concentrations in the groundwater have dissipated by dilution and/or the uranium has adsorbed onto aquifer sediments.

Apparently, the uranium that traveled through the vadose zone to the water table in the past has either stopped or the uranium flux rate has dropped to an un-measureable concentration that is within the range of natural uranium background concentrations. The driving force that promoted the influx to groundwater decades ago has abated, and the groundwater plume has interacted with the aquifer sediments such that some of the uranium has adsorbed and is no longer in the aqueous phase. Dissolved uranium in waste streams and pore waters in the Hanford subsurface is a moderately sorbing species and not as mobile as the anions pertechnetate, iodide, chromate, and nitrate. The most mobile form of aqueous uranium is associated with pH neutralized metals waste from the bismuth phosphate process waste because it is strongly complexed to bicarbonate, carbonate, and sulfate present in the waste stream (for more discussion, see PNNL-14120, *Laboratory-Scale Bismuth Phosphate Extraction Process Simulation to Track Fate of Fission Products*; PNNL-19277, *Conceptual Models for Migration of Key Groundwater Contaminants Through the Vadose Zone and Into the Upper Unconfined Aquifer Below the B-Complex*; RPP-10098, *Field Investigation Report for Waste Management Area B-BX-BY*). This type of waste was present at the 241-BX-102 overfill event that has sourced the large uranium groundwater plume below the B Complex Area in the 200 East Area but was not present in the wastes disposed or released from the S Complex Area Cribs and tank farms.

6.3 Contaminant Mobility Once in the Aquifer

Conservative conceptual models for Tc-99, I-129, chromium as chromate, and nitrate once they reach the water table are that they will migrate at the same velocity as the groundwater (i.e., retardation factor equals 1, and K_d equals 0 mL/g). All of these contaminants are anions in the geochemical conditions of the Hanford groundwater. Anions rarely exhibit retardation caused by chemical bonding with the sediments at the Hanford Site as long as the typical oxidizing and near-neutral pH conditions are present. In addition, the aquifer sediments below the S Complex Area are coarse-grained and thus are not generally considered good adsorbents for most contaminants. Other Hanford K_d databases (e.g., PNNL-13037, *Geochemical Data Package for the 2005 Hanford Integrated Disposal Facility Performance Assessment*) used for groundwater risk assessments assign a non-zero K_d value (0.25 mL/g) for I-129 for the unconfined aquifer sediments. For conservative groundwater risk assessment predictions, it is recommended that both I-129 K_d values (0 and 0.25 mL/g) be used in sensitivity analyses.

There are also several Hanford documents that discuss K_d values for vadose sediments impacted by various waste fluids (PNNL-13037; PNNL-18564, *Selection and Traceability of Parameters to Support Hanford-Specific RESRAD Analyses: Fiscal Year 2008 Status Report*; PNNL-17154, *Geochemical Characterization Data Package for the Vadose Zone in the Single-Shell Tank Waste Management Areas at the Hanford Site*) that can be used for vadose zone fate and transport sensitivity modeling.

The conceptual model for uranium, once it reaches the water table, is that it will interact slightly with the aquifer sediments and travel somewhat more slowly than the groundwater itself. PNNL-13037 recommended a most probable uranium K_d value of 1 mL/g for the Hanford unconfined aquifer and PNNL-13895, *Hanford Contaminant Distribution Coefficient Database and Users Guide*, recommended a uranium K_d range from 0.2 to 4 mL/g be used in sensitivity studies. However, no elevated concentrations of uranium in the groundwater currently exist below the S Complex Area and there are no indications of elevated concentrations of uranium in any of the vadose zone sediments below the CCu unit within the S Complex Area, albeit the vadose zone sediment database for this area is very sparse, especially for sediments in the Ringold Formation (deep vadose zone).

6.4 Summary of Key Integrated Conceptual Models

Table 3-5 presented one conservative estimate of the residual contamination in the vadose zone that assumed all of the contaminants released to the vadose zone below the S and SX tanks remain in the vadose zone because the estimate of lateral spread below each tank is large enough to have retained all the waste fluids released. After estimating that ~8 to 9 percent of the chromium and Tc-99 released to the S Complex Area (and most likely from the S and SX Tank Farms) appears to be in the current groundwater plumes, the masses/activities for the releases from the S and SX Tank Farms for the four mobile contaminants (Tc-99, chromium, nitrate, and I-129) shown in Table 3-5 should be reduced by 10 percent.

Using the lateral spread estimates, based solely on gamma logging and soil electrical resistivity surveys described in Chapter 3, below the four cribs of interest, the percentage of disposed waste and contaminants that remain in the vadose is estimated at 20 percent (216-S-25 Crib), 33 percent (216-S-21 Crib), 77 percent (216-S-23 Crib), to 100 percent (216-S-9 Crib). These corrections were already captured in the values listed in Table 3-5.

There are no direct measurements of the contaminant concentrations and the major salts concentrations in the vadose zone below the four cribs of interest for this report. The lack of actual measured concentration data from the vadose zone beneath the S Complex Area Cribs reduces the certainty with which the mass estimates can be made.

Based on groundwater monitoring data, wastes and contaminants did in fact reach the groundwater at many of the S Complex Area facilities soon after they were activated. However, there has not been any effort to quantify the mass of contaminants and volumes of waste fluids that reached the water table in the early years of disposal. Further, there has not been any effort to estimate the mass of contaminants that have reached the groundwater below the S Complex Area in the recent past. Therefore, as discussed in Chapter 5, the available groundwater data was reviewed and then integrated with the 3D aquifer conceptual model to make mass estimates for the five mobile contaminants of interest for the period 2005 through 2010.

The results of the mass/activity calculations are provided in Table 6-1. As discussed, these estimates of the mass currently within the groundwater in general show relatively small percentages compared to the total masses released to the S Complex Area. The major exception is nitrate for which the estimate of the mass in the current groundwater plume below the S Complex area is 50 percent of the mass of nitrate released to the S Complex Area waste sites.

Because nitrate, I-129, Tc-99, and chromium are all considered mobile and are anions in the Hanford subsurface, they should migrate through the vadose zone sediments without interacting significantly with the sediment. In fact, nitrate and Tc-99 have been shown many times to travel together in both vadose zone pore waters and groundwater at the Hanford Site (see also the B Complex conceptual model report (PNNL-19277) and groundwater annual reports (DOE/RL-2008-66, *Hanford Site Groundwater*

Monitoring for Fiscal Year 2008; DOE/RL-2008-77, *200-UP-1 and 200-ZP-1 Operable Units Pump-and-Treat System Annual Report for Fiscal Year 2008*; DOE/RL-2010-11).

Table 6-4 provides a summary of the qualitative evaluation of the integrated CSMs for the 200-DV-1 OU waste sites within the S Complex Area. The evaluation considers the robustness of the various data sets that were used to create the CSMs for the residual masses of the contaminants in the vadose zone and to estimate which inactive facilities or tank farms are the likely sources of the contaminants in the groundwater plumes below the S Complex Area. Table 6-3 includes comments on additional activities that would improve the understanding of the contamination in the vadose zone below the waste sites suspected of supplying the bulk of the contamination currently reaching the water table. The details of these findings are presented in Chapters 3 and 5.

Lessons learned from developing the B Complex Conceptual Model (PNNL-19277) are as follows:

- There was a fairly direct correlation between the percentages of total B Complex mass estimates disposed to the various facilities and the estimates of how much of the waste remains in the vadose zone and what percentage of the current groundwater mass estimates can be attributed to various facilities. This simple correlation, based on tracking mass in various compartments (or media), was encouraging, and supports the mass-balance exercise performed in this report.

- Lateral spreading along fine-grained layers has occurred during and after active waste disposal, and later dilute waters (natural recharge, pipeline leaks, episodic off-normal events [e.g., rapid snowmelt, large and heavy rain storms, and concentrated recharge through depressions in topography accepting large area runoff]) could have pushed the earlier, more concentrated wastes further distances and deeper within the vadose zone. The groundwater time series mass (inventory) plume maps for the last 15 years at the T Complex Area are not consistently showing mass increases with time. However, the time series groundwater plume maps from the last 15 years for the B Complex more consistently showed increasing masses in the groundwater over time, suggesting that the deep vadose zone was adding contaminants at an increasing rate; however, at the B Complex, there have not been any pump-and-treat activities to remove mass as is ongoing in and to the south of the T Complex Area. Thus, the less consistent increasing groundwater mass (inventory) found below the T Complex Area may be related to pump-and-treat activities. In addition, the rate of groundwater flow beneath the B Complex has slowed, based on the extremely flat gradient that exists today, compared to decades earlier when water table heads in the area were artificially elevated. This reduced flow rate may potentially reflect a perceived localized increase in some groundwater contaminant concentrations at known B Complex sites of impact because groundwater is not moving away from the area as quickly, thus allowing vadose concentrations (even at steady flux rates) to impact the B Complex aquifer longer, creating a higher concentration for a given volume of aquifer.

- The one remaining issue regarding tank farm releases is how do the contaminants that are present in a relatively low volume release from the tanks, relative to the several million liter disposals to many cribs and trenches, migrate so far from the source. It was not within the scope of this report to assess the details on vadose zone flow and to systematically identify and quantify the sources of water to the vadose zone. There have been numerous reports of substantial water sources to the vadose zone within the tank farms, including prolonged potable water line leaks; large snow melt events that flooded tank farms; enhanced recharge within the tank farm boundaries caused by the gravel covers to prevent spread of surface contamination; and perhaps surface runoff into low lying topography.

Table 6-4. Qualitative Description of Strength and Weakness of Integrated Vadose Zone/Groundwater Models Used to Identify Sources of Groundwater Contamination

Source	Vadose Zone Sediment Analytical Details	Vadose Zone Sediment Analytical Quality	Borehole Gamma Logging	Soil Resistivity Survey	Vadose Zone Data Consistency	Groundwater Plume Review	Groundwater/ VZ Consistency	Overall Rating	Comments
S-9	No sediments were characterized.	No VZ sediment analytical measurements for 5 COCs of interest. Quality poor.	4 deep boreholes on S-9 Crib perimeter. Results for before and during active disposal. Good temporal coverage. Only two boreholes got recent spectral gamma logs. Consistent results but none through crib footprint. Early logging indicates contamination made it to water table.	Low resistivity shallow below crib footprint and much deeper penetration at southern end where waste was disposed (and UPR- pipeline leak).	Gamma logs and soil resistivity consistent - indicate most waste is below southern end of crib and significant lateral spread occurred.	Soon after active disposal ended or during disposal, GW showed signs of gross beta, gross gamma and nitrate. Current I-129 plume shows some association with area below S-9 so cannot rule it out as a contributor.	Inadequate VZ data to assess current fact that groundwater below S-9 is not a contributor of any of the mobile contaminants.	Inadequate data set; however, masses of Tc-99 and chromium disposed of are low. Uranium, I-129, and nitrate disposed of are significant for S-Complex Area. Early GW impacts do not seem to be sustained currently.	The S-9 Crib could be a contributor of I-129 to groundwater. S-9 also received almost all the uranium disposed to S Complex Area so its vertical profile in a VZ would be very useful.

Table 6-4. Qualitative Description of Strength and Weakness of Integrated Vadose Zone/Groundwater Models Used to Identify Sources of Groundwater Contamination

Source	Vadose Zone Sediment Analytical Details	Vadose Zone Sediment Analytical Quality	Borehole Gamma Logging	Soil Resistivity Survey	Vadose Zone Data Consistency	Groundwater Plume Review	Groundwater/ VZ Consistency	Overall Rating	Comments
S-23	No sediment characterization	No VZ sediment analytical measurements for 5 COCs of interest. Quality poor.	Five deep boreholes were available before active disposal and logs were done before during and after disposal. No logging since 2003. Early logging indicates contamination made it to water table. No gamma detected when last logged in 2003.	No electrode lines in vicinity to interrogate.	Only gamma logging data available so there is no chance to assess consistency.	Over last 5 years, groundwater plume data indicate this crib is not contributing any contaminants. However, during and right after active disposal, crib did affect GW.	Lack of VZ sediment analytical data to compare with gamma logging and current GW limits any consistency check. In last 5 years, GW under this facility has not shown impacts. S-23 residual inventory for all 5 contaminants is very low; so likely not a GW threat.	Inadequate data set; however, masses of COCs disposed are low. Early GW impacts do not seem to be sustained currently.	Based on low estimates for inventories of residual mass in S-23, VZ sediments and no current GW impacts, further characterization is low priority.

Table 6-4. Qualitative Description of Strength and Weakness of Integrated Vadose Zone/Groundwater Models Used to Identify Sources of Groundwater Contamination

Source	Vadose Zone Sediment Analytical Details	Vadose Zone Sediment Analytical Quality	Borehole Gamma Logging	Soil Resistivity Survey	Vadose Zone Data Consistency	Groundwater Plume Review	Groundwater/ VZ Consistency	Overall Rating	Comments
S-21	No sediment characterization.	No detailed sediment characterization. Quality poor.	One shallow borehole in footprint to 51 ft bgs and one borehole to SE with data. Other boreholes had no gamma logs done. Only borehole to SE had good time history coverage. Shallow borehole in footprint logged only in 2006.	No electrode lines in vicinity to interrogate.	No sediment characterization and deep contamination in gamma logs need to be confirmed with more reliable SGLS in W23-4.	Last 5 years, GW plume data do not show this facility as contributing to aquifer, and inventory of disposed mobile contaminants is low.	VZ data is too sparse to make any consistency check.	Inadequate.	Based on low estimates for inventories of residual mass in S-21 VZ sediments, and no current GW impacts, further characterization is low priority.

Table 6-4. Qualitative Description of Strength and Weakness of Integrated Vadose Zone/Groundwater Models Used to Identify Sources of Groundwater Contamination

Source	Vadose Zone Sediment Analytical Details	Vadose Zone Sediment Analytical Quality	Borehole Gamma Logging	Soil Resistivity Survey	Vadose Zone Data Consistency	Groundwater Plume Review	Groundwater/ VZ Consistency	Overall Rating	Comments
S-25	No sediment analytical characterization.	No sediment characterization. Quality poor.	Four deep boreholes close around perimeter; 1 borehole far to south and 2 far to east. Some gamma logging in mid-1970s (when crib was active). No logging since 1976, yet crib was active through 1985. No contamination detected in any logs; wastes very dilute.	The salt plume is so dilute that soil resistivity interpretation is not possible.	No sediment data to quantify lateral or vertical extent. No gamma log data since 1976 and none observed in earlier logs. No VZ data to assess anything.	Last 5 years and earlier historical. GW plume data suggest S-25 may be contributing nitrate to GW. Inventory of nitrate disposed ranks #1 in all of S Complex Area. Sustained nitrate plume is present in groundwater.	VZ data do not exist so cannot make any consistency check.	Inadequate quantitative understanding. Important to characterize vadose zone sediments below crib inlet.	High priority Future VZ characterization should be coordinated with similar activity within SX Tank Farm and west of tank farm fence line. Key need is determining nitrate isotopic fingerprint signature for S-25 versus SX-115 and SX-108,-109, SX-112 type wastes.

Table 6-4. Qualitative Description of Strength and Weakness of Integrated Vadose Zone/Groundwater Models Used to Identify Sources of Groundwater Contamination

Source	Vadose Zone Sediment Analytical Details	Vadose Zone Sediment Analytical Quality	Borehole Gamma Logging	Soil Resistivity Survey	Vadose Zone Data Consistency	Groundwater Plume Review	Groundwater/ VZ Consistency	Overall Rating	Comments
S Tank Farm	A few direct push samples characterized but no significant contamination observed. Pushes not very close to S-104, which is only confirmed leaker.	Direct push locations not useful for aiding in determining extent of S-104 release. Quality poor.	Borehole gamma logging was not assessed but past analyses for tank farm needs show S-104 as only significant source.	Does show region below S-104 is low resistivity. Volume of low resistivity is larger than logging suggest.	Sparse sediment data but soil electrical resistivity and gamma logs consistent.	Last 5 to 10 years indicate a plume of Tc-99, chromium, and nitrate is presently originating from region below S-104 tank and heading east with regional GW flow.	Qualitatively okay but need quantitative data on deep VZ to project future impacts of chemicals. Already ongoing source of GW Tc-99, chromium, and nitrate.	Inadequate quantitative understanding.	High priority for additional vadose characterization to define location where fluids descend through the CCUc into Ringold and water table. Vertical extent of VZ contamination for all 5 mobile contaminants is needed. Could be future source of I-129 and uranium. Already an active source for GW Tc-99, chromium, and nitrate.

Table 6-4. Qualitative Description of Strength and Weakness of Integrated Vadose Zone/Groundwater Models Used to Identify Sources of Groundwater Contamination

Source	Vadose Zone Sediment Analytical Details	Vadose Zone Sediment Analytical Quality	Borehole Gamma Logging	Soil Resistivity Survey	Vadose Zone Data Consistency	Groundwater Plume Review	Groundwater/ VZ Consistency	Overall Rating	Comments
SX Tank Farm	Thirteen direct push locations; many identified significant contamination. Three boreholes identified highest concentration Tc-99, chromium, and nitrate VZ plumes observed at Hanford Site.	Geochemical data good quality but only reached depth >155 ft bgs in two boreholes. Quality good for shallow sediments above CCuc. Little sediment characterization in CCuc or Ringold.	No analyses of borehole logging data inside the SX Tank Farm were performed for this report. Past analyses for SX Tank Farm show 8 of the tanks in the three southern rows may have released fluids to the VZ. Dry well depths do not reach deep enough to delineate vertical extent of contaminant penetration.	A large areal plume of low resistivity centered below the SX-108-109 tanks is observed. Lateral spread by soil resistivity is larger than gamma logging suggests.	All three VZ data sets indicate numerous VZ contaminant plumes but vertical extent is not delineated below CCuz subunit. It is difficult to determine how commingled the VZ plumes are. One significant discrepancy is no low resistivity around SX-115 yet sediment and logging data show lots of contamination	In the last 5 to 10 years, a significant GW plume containing high concentrations of Tc-99, chromium, and nitrate is observed below the southern fence line of SX Tank Farm. SX-115 is closest.	Adequate.	Marginal. Need more deep vadose zone sediment characterization to delineate vertical extent of mobile contaminants and where wastes are reaching water table.	Priority for additional vadose zone characterization. Suggest nitrate isotope data relating SX-115, and SX-108 and SX-112 fluids. Should be coordinated with characterization activities at S-25 Crib. Could be future source of I-129 and uranium. Already the greatest active source of GW Tc-99 and chromium in S Complex Area.

bgs = below ground surface
CCuc = Cold Creek calcic geosol
CCuz = Cold Creek silt
COC = contaminants of concern
gw = groundwater
SE = southeast direction
SGLS = Spectral Gamma Logging System
UPR = unplanned release
VZ = vadose zone
Waste site number prefix "216-" and tank number prefix "241-" omitted

7 Isotopic Systematics for the Identification and Tracking of Hanford Contamination and Related Materials, with a Focus on the S Complex Area

This section discusses the use of high-precision isotopic signature measurements that have been performed on a few water extracts of vadose zone sediments and groundwater from the S Complex Area. Besides presenting the data and its interpretation, some general background information is presented on how the isotope signature protocol can be applied to gain more understanding on pathways contaminants take through the subsurface, their rates of transport, and facilities that are the likely sources for the contamination.

7.1 S Complex Area Isotopic Data Summary

As part of a survey of Hanford groundwater samples for nitrate isotopic composition (δ15N and δ 18O) Lawrence Berkeley National Laboratory staff analyzed a series of samples collected in 2004 near the S-SX WMA (Singleton et al., 2005, "Tracking Sources of Unsaturated Zone and Groundwater Nitrate Contamination Using Nitrogen and Oxygen Stable Isotopes at the Hanford Site, Washington"). The locations of these groundwater samples are plotted on Figure 7-1. The nitrate isotopic compositions of these samples are presented in Figure 7-2, a plot of δ 15N vs. δ 18O, along with groundwater and vadose zone samples related to the T WMA for comparison. In such a plot different sources of nitrate, and their relative proportions, can be distinguished; in particular natural sources of nitrate from the vadose zone, industrial synthetic nitrate (nitric acid) from low-activity waste, and nitrate related to tank waste (higher temperature conditions [boiling and subboiling with air ventilation] and radiolysis) can alter nitrate isotopic composition. The ten 2004 samples can be divided into three groups as to source based on their isotopic composition. Two samples fall at the edge of the range of natural background nitrate sourced in the vadose zone, and come from monitoring Wells 299-W22-44 and 299-W22-49 from near the east side of the S and SX Tank Farms, respectively (see Figure 6-3 for locations). These groundwater samples are relatively moderate in nitrate concentration (45 mg/L) and the isotopic signature indicates the nitrate came from natural sources in the vadose zone washed through to groundwater by percolation. Two other groundwater samples, from monitoring Wells 299-W23-15 (south of the SX Tank Farm fence line) and 299-W23-20 just west of the S Tank Farm fence line), have nitrate isotopic compositions consistent with a component (about 25 percent of the total nitrate) of synthetic industrial nitrate (from nitric acid) likely from low-activity waste such as the 216-S-25 and 216-S-21 Cribs, respectively. These samples are also quite low (6 and 8 mg/L) in nitrate concentration and represent relatively dilute nitrate waste. The waste present at the time that SX-115 released waste to the subsurface was not a typical REDOX tank waste; rather, its composition was dilute and might have the low-activity nitrate waste signature.

Six groundwater samples (nitrate concentrations range from 22 mg/L to 333 mg/L) fall in or very close to the range of tank related waste and come from two sets of wells, one (299-W23-9, 299-W23-21, and 299-W23-10) near the western edge (upgradient to groundwater flow) of WMA S-SX and the adjacent 216-S-25 Crib, and a second (299-W23-19, 299-W22-50, and 299-W22-26) along the southern end of SX Tank Farm within a Tc-99 and chromium contaminant plume. The highest nitrate concentration samples from each group (299-W23-9 [nitrate]=236 mg/L; 299-W23-19 [nitrate]=336 mg/L) also have the highest δ 15N (15.1 ‰ and 16.8 ‰, respectively) and are distinct in their isotopic compositions, suggesting distinct tank-related waste sources.

Groundwater samples from these same nine wells were taken in 1999 and 2001 were also analyzed for strontium isotopic composition. The range of strontium-86/-87 was 0.70838 to 0.70950, relatively low compared to areas such as the WMA T-TX that received large volumes of water locally flushed through

the vadose zone, carrying strontium with high strontium-86/-87 locally to groundwater. Since the samples for strontium-86/-87 and nitrate isotopic composition were collected 3 to 5 years apart, the relationship between the strontium-86/-87 (earlier) and nitrate isotopic data (later) is not clear. Future sampling and analysis for strontium-86/-87 and nitrate isotopic composition on the same sample could clarify the relationship, and whether any of the nitrate isotopic signatures are associated with large throughputs of water through the vadose zone.

No groundwater samples collected from monitoring wells near Cribs 216-S-9 and 216-S-23 were obtained/received for nitrate or strontium isotopic analysis. Therefore, the groundwater sample coverage is quite sparse and, more importantly, there are no isotopic analyses on vadose zone sediment water extracts for the S Complex Area. Vadose zone sediment water extracts of uncontaminated and contaminated sediments that can be unequivocally attributed to specific disposal facilities are key to establishing which source is affecting the groundwater.

The results for the WMA S-SX suggest that analyzing additional vadose zone pore water and groundwater samples for isotopic composition would be useful for characterizing contamination sources in the S Complex Area.

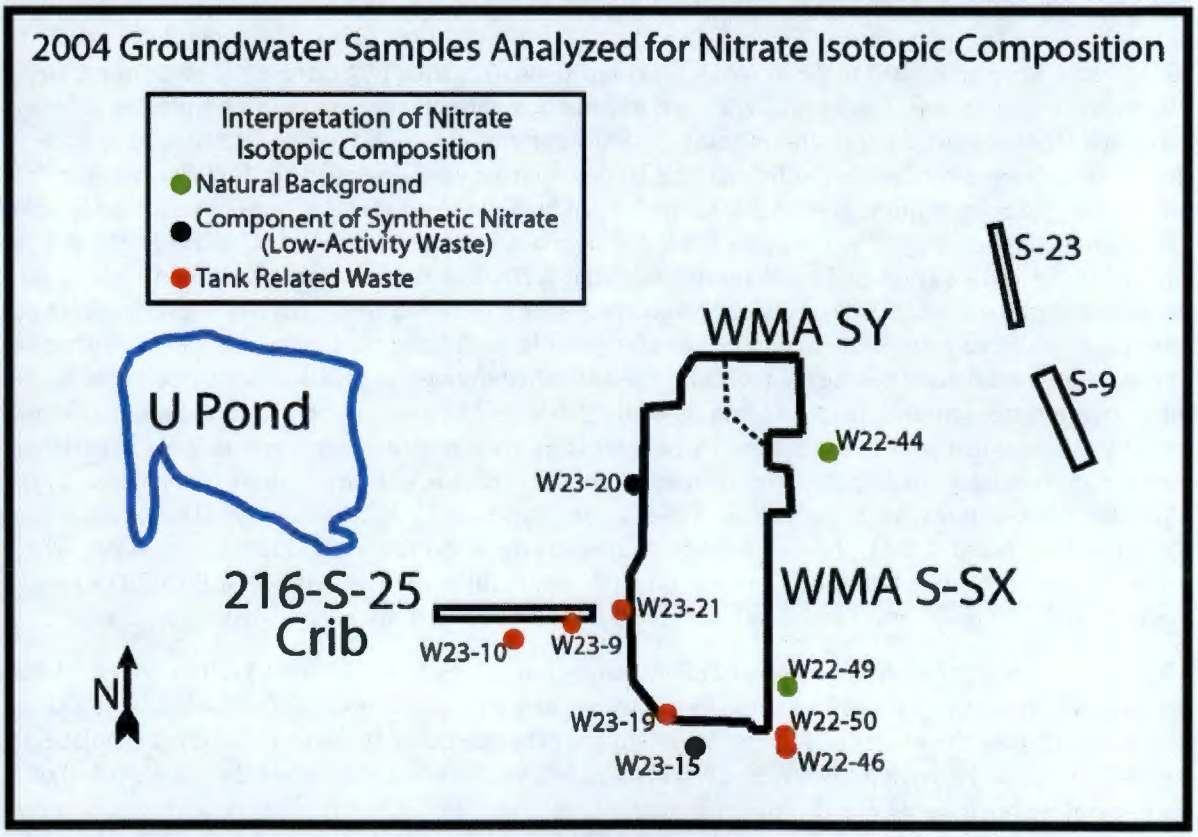

Note: The locations of the wells are color coded to indicate the interpreted significant source of the nitrate at those locations based on nitrate isotopic composition (see text and Figure 7-2).

Figure 7-1. Map Showing the Locations of Groundwater Samples Collected in 2004 Near the WMA S-SX for the Stable Isotopic Analysis of Nitrate ($\delta^{15}N$ and $\delta^{18}O$)

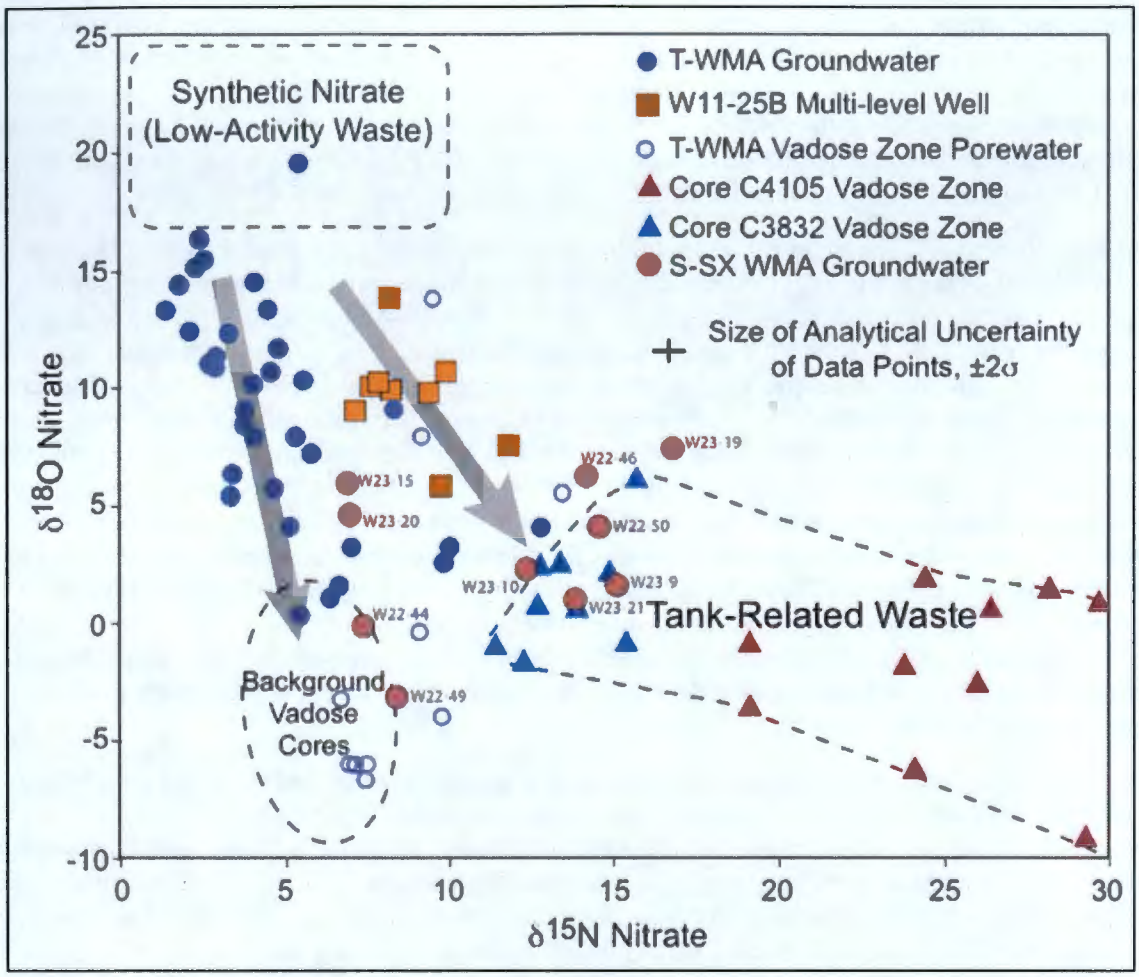

Note: For comparison groundwater and vadose pore water samples from the WMA-T and for the sub-water table depth discrete samples from W11-25B are shown. Additional data on the plot includes the field for uncontaminated (background) sediments, and data for contaminated vadose sediments from Singleton et al., 2005, "Tracking Sources of Unsaturated Zone and Groundwater Nitrate Contamination Using Nitrogen and Oxygen Stable Isotopes at the Hanford Site, Washington" (blue triangles = C3832, purple triangles = C4105). The field for synthetic nitrate (representing low-activity waste) is from Kendall and McDonnell, 1998, *Isotope Tracers in Catchment Hydrology*, and Amberger and Schmidt, 1987, "Natürliche Isotopengehalte von Nitrat als Indikatoren für dessen Herkunft".

Figure 7-2. Plot of δ15N vs. δ18O for Nitrate in Groundwater Samples near WMA-S-SX

7.2 Summary of Isotopic Data Significance to Developing Conceptual Models for Fate of Released Waste in the S Complex Area

The value of high-precision isotopic ratio measurements (fingerprinting) is unparalleled in their capability to identify the sources of wastes in the subsurface as shown in the previous two 200-DV-1 OU CSM reports (PNNL-19277; SGW-49924). Even when the total concentrations of constituents such as uranium, strontium, or nitrate are low and not distinguishable from uncontaminated background concentrations, the isotope ratio measurements can often differentiate sources. Because Tc-99 is often associated with the ubiquitous nitrate released at Hanford, isotopic composition measurements of its common co-contaminant nitrate offers the ability to distinguish between low activity wastes (LAW) (generally released to cribs, trenches, and ponds) from natural vadose zone pore waters and tank-related waste. In the T Complex Area, the nitrate isotopic composition of groundwater that have been studied to date indicates the involvement of all three sources, with certain sets of samples indicating binary mixes of industrial nitrate (related to LAW

disposal) and natural background vadose zone nitrate. This pattern involves groundwater from wells spread over much of the region surrounding the T Tank Farm. A similar pattern of nitrate isotopic signatures is hinted at with the sparse WMA S-SX data shown in Figure 7-2. At the T Complex, the highest groundwater concentrations of nitrate and the strongest nitrate isotopic signature for industrial nitrate are associated with wells near former low-activity disposal cribs/trenches (e.g., 299-W10-4 and 299-W10-33) south of the 216-T-32 and 216-T-7 large commingled vadose zone plume and near the 216-T-36 Crib).

The strontium isotopic signature values for groundwater samples in the T Complex especially from 299-W11-25B where multi-level (several discrete depths below the water table) were quite useful in sourcing both the nitrate and Tc-99. The peak for the strontium-86/-87 was at the same depths as the highest concentration of Tc-99. This same correlation between the highest strontium isotopic ratio and the highest Tc-99 concentration is also seen at 299-W11-45, suggesting that Tc-99 at 299-W11-45 is related to the same source as 299-W11-25. This is consistent with groundwater migration roughly due east from 299-W11-25B. The high strontium isotope signature comes from the tank waste liquids interacting with the vadose zone sediments more aggressively than crib waste and releasing vadose zone related natural strontium with a higher strontium-86/-87 ratio. That is, the more caustic and aggressive tank wastes interact with the vadose zone sediments and cause the release of more natural strontium, which has an inherent high strontium-86/-87 ratio, to the descending pore waters that eventually reached the water table and mixed with the migrating groundwater. Unfortunately, strontium isotopic data are severely lacking at the S Complex, but we suggest that the same useful observations on the type of waste that percolated through the vadose zone to the water table as have been made from data in the T Complex would be found at the S Complex.

The uranium isotopic analyses of vadose pore water and groundwater can also be quite valuable for source identification. At the T Complex, uranium isotope signatures from borehole C4104 (near Tank T-106) provided a unique isotopic signature that will be useful in source identification of groundwater contamination nearby once, as is quite possible, uranium from the vadose zone below the T Tank Farm reaches the water table. Analysis of groundwater samples with low U concentration (< 3 parts per billion) may well detect the early arrival of contaminant uranium from the T Tank Farm that is retarded relative to tank-related nitrate and Tc-99 that is already being observed to the northeast of the T Tank Farm. The same early arrival of minute amounts of waste uranium from the S and SX Tank Farms waste fluids as well as from S facility cribs might occur and thus provide valuable source attribution. In addition, high-precision uranium isotopic signature measurements on even low total uranium concentration groundwater could be used to define the timing and location of wastes entering the water table in the S Complex. On the other hand, the CCus are known strong adsorbents for any uranium that has been released from S Complex facilities such that the groundwater samples might show no signs of Hanford derived uranium. If this turns out to be the case, then a valuable observation would be that uranium disposed to the various S Complex facilities has not reached the aquifer.

8 Summary

This report offers detailed vadose zone and aquifer plume conceptual models for the distribution of key groundwater contaminants, Tc-99, nitrate, chromium, I-129, and uranium in the S Complex Area, located within the Deep Vadose Zone (200-DV-1 OU) of the 200 West Area. It also presents information on where the groundwater plumes are migrating.

The methodology used to create the conceptual models started with review and assembly of pertinent background information on the facilities that received the wastes. Key background information includes facility location; period of operation; volumes and types of waste streams disposed of; and total masses of constituents released to the vadose zone sediments. All the pertinent data are found in Appendix A.

The second step was to assemble the available data on the vertical and lateral distribution of the mobile contaminants and species that control the mobility of the contaminants in the vadose zone sediments. Emphasis was placed on evaluating the distribution of Tc-99, I-129, uranium, chromium, and nitrate. Plots of the available vadose zone contaminant data for the two subregions below the S Complex Area were superimposed on detailed vadose zone stratigraphic cross sections, and include available geophysical surveys (borehole gamma logs and soil resistivity) to aid in constructing models of the lateral and vertical extent of the key contaminants within the vadose zone. Results are presented in Chapter 3. The S Complex Area database for lateral and vertical extent of the key mobile contaminants is based almost exclusively on information generated from the borehole gamma logs and surface based soil resistivity surveys. More direct characterization of vadose zone sediments are necessary (especially for non-gamma emitting contaminants), to determine total contaminant concentrations, including an accurate measurement of the lateral and vertical extent.

A similar effort was performed using the available groundwater monitoring data (discussed in detail in Chapter 5), with emphasis on the last 5 to 10 years (2005-2010), to develop current contaminant plume maps. The shapes of the groundwater plumes also revealed the net direction of flow of groundwater flow. Using a 3D aquifer conceptual model and the aquifer thicknesses from the geologic conceptual model, the mass of selected contaminants was calculated for the past 5 to 10 years, dependent on contaminant and groundwater data availability. The masses within the groundwater plumes could then be calculated and the source region where the mass appears to be entering the aquifer was delineated. The results of these 3D groundwater plume estimates are found in Chapter 6. The vadose zone contaminant distribution data and groundwater data were then combined to create integrated models that define where the bulk of the contaminants remain, where they enter the water table, and how the plumes have migrated over the last 5 to 10 years. These results are also found in Chapter 6.

Most importantly, the report provides preliminary bounding estimates for the mass of each contaminant that remains in the vadose zone and within the current S Complex Area groundwater plumes. There is one ongoing ad-hoc pump-and-treat at Well 299-W23-19 at the southern edge of the SX Tank Farm that each quarter removes some contaminated groundwater. Thus, contaminant mass from the region. Therefore, to perform a mass balance on any given contaminant from its disposal to current conditions, our conceptual model requires mass estimates for five compartments. The first compartment is the starting mass that was assumed to be adequately estimated based on the SIM, Rev. 1 (RPP-26744) database inventory values for each facility and the tank farm contractor's revised estimates for each suspected SST waste fluid release. The starting mass for mobile contaminants, which are assumed not to interact significantly with the sediments by sorption or precipitation reactions, then must be distributed in one of the remaining four compartments: residual mass in vadose zone, current mass in groundwater plumes, mass removed by pump-and-treat activities, and mass that escaped the S Complex Area before monitoring was adequate.

At this time, we have not attempted to construct a rationale to estimate masses of contaminants that belong in compartment 5.

Because the vadose zone sediment database for contaminant location and extent in the S Complex Area only exists within the S and SX Tank Farms, the first iteration for estimated masses remaining in the vadose zone (compartment 2) is estimated by the percentage of the disposed of liquid volume that could be held in the vadose zone sediment volume. This estimate is based solely on field gamma logs and soil resistivity surveys and assumes that the impacted sediments retain 10%vol fluids. A second iteration or mass balance check considers subtracting the masses in the current groundwater plumes (compartment 3) and, when available, minus the masses removed from the groundwater by pump and treat operations (compartment 4). The estimate for residual mass in the vadose zone assumes that the gamma logs and soil resistivity interpretations accurately describe the degree of lateral and vertical spreading in the vadose zone (i.e., Hanford formation and CCus). For three of the cribs considered (216-S-21, 216-S-23, and 216-S-25), the degree of lateral spreading was not found to be sufficient to cause the retention of all of the fluids released above the high water table. Thus, for these three cribs, a portion of the waste was assumed to have reached the groundwater sometime during active disposal and the time that the vadose zone re-equilibrated to a field capacity drainage condition. The lateral spreading areas for these three cribs were combined with the vadose zone thickness to the high water table to create the impacted volume of sediment. The final drained volumetric moisture content was assumed to average 10%vol. For the 216-S-21 Crib, the impacted vadose zone accommodates 33 percent of the total liquid waste volume disposed. For 216-S-23 Crib, the impacted vadose zone retains 77 percent of the total liquid volume disposed, and for the 216-S-25 Crib, the vadose zone retains 20 percent of the total volume disposed. For the 216-S-9 Crib, the calculated impacted volume of vadose zone sediment can hold 100 percent of the volume disposed to the crib.

All releases from the various S and SX tanks were assumed to be retained in the vadose zone for the first iteration. For the second iteration, after the groundwater plume compartment was estimated, the tank releases remaining in the vadose zone was reduced to 90 percent of the estimated releases. These conceptual models differ significantly from past vadose zone conceptual models that assume waste fluids descend directly to the water table below and within the footprint of each facility under the hydraulic forces present during active disposal and then followed by gravity drainage after active disposal ceases.

Of course, it is well established that contaminants reached the groundwater below many of the 200-DV-1 OU facilities soon after active disposal started. However, groundwater monitoring in the early years of Hanford Site operations was limited to a few constituents, the well coverage was limited, and sampling frequency was variable with gaps of several years to even decades when no sampling was performed in certain regions. This makes performing a mass balance for the mobile contaminants of interest in the S Complex Area from the active disposal periods to the present day very difficult.

The estimates for masses currently in the groundwater plumes below the S Complex Area in the last 5 to 10 years in general are based on a better data set than is available for previous years. However, compared to the groundwater monitoring network in the T Complex, the current database for the S Complex Area groundwater plumes is not as robust to allow yearly plume depictions and yearly masses/activities to be estimated. For the S Complex Area analysis present in this report, an I-129 groundwater activity was not estimated at all because the well coverage is so sparse and the source of most of the I-129 is not likely from facilities assigned to the S Complex Area. Also for uranium, no groundwater plume map was constructed and no mass estimates were attempted because there is no significant mass of uranium in the current groundwater below the S Complex Area.

Currently, there are no records on the masses of chromium, nitrate, and I-129 removed by the ad hoc pump-and-treat activities at the WMA SX Tank Farm (i.e., Well 299-W23-19) so compartment 4 can only be estimated for Tc-99. Based on this, the activity removed (~0.0084 curies) is insignificant compared to the mass disposed to the entire S Complex Area (34.4 curies) and the activity estimated to be in the current groundwater plume (3.2 curies). Thus, for the S Complex Area, compartment 4 mass/activity was set to zero. As mentioned previously, we have not explored defensible methods to estimate compartment 5–mass that escaped the S Complex Area before an adequate groundwater monitoring network and database was available, so compartment 5 is also set to zero.

The mass estimates for two of the mobile contaminants (Tc-99 and chromium) in groundwater that appear to be sourced from the S and SX Tank Farms have been increasing since the early to mid-2000s to the present. It is probable that nitrate was sourced from the 216-S-25 Crib sometime in the past, but no similar time series statements can be made since there is very little monitoring data available. There are no current groundwater uranium or I-129 plumes sourced by the S Complex Area facilities that can be used to assess whether more mass is present in the aquifer today than in the past, which would imply that the vadose zone is currently supplying additional contamination to the aquifer.

A comparison of the Tc-99 and chromium masses in the groundwater plumes to the total masses released to the S Complex Area suggest about 9 to 10 percent of the Tc-99 and 8 to 9 percent of the chromium is currently present in the groundwater. Assuming that compartment 5 (mass that escaped the S Complex Area before monitoring was adequate) is not large, this suggests there is a significant mass of these two mobile contaminants still residing in the vadose zone.

For nitrate, approximately 50 percent of the total nitrate disposed to the S Complex Area currently is in the groundwater. Because nitrate and the other mobile constituents generally migrate in concert, this much larger percentage reflects the fact that most of the nitrate disposed to the S Complex Area was from the 216-S-25 Crib, which had very low concentrations of the other mobile contaminants. It is estimated that 80 percent of the 216-S-25 Crib waste volume (and thus mobile contaminants) reach the water table. Therefore, more of the total nitrate disposed or released to the S Complex Area reached the groundwater. Another possibility that was a key conclusion for the T Complex conceptual model report (SGW-49924) is the possibility that other sources of nitrate such as sanitary septic systems and the various high volume pond disposals have added significant quantities of nitrate to the water table below the S Complex Area that need to be accounted for. In the next mass balance iteration, more diligence needs to be taken to improve the estimate of nitrate released to the S Complex Area, and some efforts need to be expended to decide if there are ways to bound the mass belonging to compartment 5.

Of course, the most direct way to improve the estimate for the residual mass of mobile contaminants in the vadose zone is to initiate direct sediment sampling and characterization with emphasis on the deep vadose zone below the Hanford formation to evaluate how much mass is present in the vadose zone within and below the less permeable CCus. After further vadose zone sediment characterization and the aforementioned refinements on estimating compartment 1 nitrate and compartment 4 masses, a more realistic mass balance can be undertaken.

The objective of these mass-balance comparisons is to provide baseline information on two key issues:

- How well has the mass (and thus distribution in the vadose zone and aquifer) of the contaminant been identified?
- Can the contaminant mass distribution in the deep vadose zone and aquifer be used to project future risks and guide the selection of remediation alternatives?

Some of the strengths, weaknesses, and inconsistencies in the mass-balance estimates for the key contaminants for the CSMs for each subregion are presented in Table 6-4. In addition to performing mass estimates for the various compartments and then the mass balance exercise, this report includes a detailed hydrogeologic conceptual model and points the reader to resources to gather hydrologic and geochemical input parameters needed for fate and transport predictive modeling.

The remaining summary material discusses the adequacy of the historical records on the 200-DV-1 OU facilities within the S Complex Area that were critically analyzed, briefly describes the hydrogeologic conceptual model and where to find resources for hydraulic and recharge values, and then reviews the key findings and conceptual models for nature and extent of residual contamination in the vadose zone sediments and for the historical and current groundwater status for each subregion.

8.1 Facilities Summary

The key points from the review of facility history follow. A total of approximately 459 ML (121.2 million gal) of waste were released, either intentionally or unintentionally, into the subsurface below the S Complex Area (in comparison, 725 ML (191.5 Mgal) was released to the subsurface below the T Complex Area). Further, the groundwater underlying the S Complex Area has been influenced by dilute wastewaters from the billions of liters disposed of to the S, U, and T Ponds. Little information is available on the volumes and timing for water lost from water-line leaks and the volume of enhanced recharge from denuding the ground surface or from the use of gravel covers over the tank farms. All these water sources likely promoted contaminant migration within the vadose zone. The estimates for the masses of key mobile contaminants released to the subsurface below the S Complex Area Waste Sites (an area covering about 73.7 hectares or 182 acres) include 3.64E+05 kg of nitrate (1.24E+07 kg disposed at T Complex Area), 305 kg of uranium (2,190 kg disposed of at T Complex Area), 1,350 kg of chromium (57,675 kg disposed at T Complex Area), 34.4 Ci of Tc-99 (49.5 Ci disposed at T Complex Area) and 0.08 Ci of I-129 (0.073 Ci disposed at T Complex Area). By comparison, the masses of mobile chemicals released to the T Complex Area far exceed the masses released to the S Complex Area, but the activity of the two key radionuclides (Tc-99 and I-129) are very similar. As mentioned, the total volume of wastes released at the S Complex Area was 63 percent of the volume released to the T Complex Area.

The largest volumes of waste fluids disposed to the S Complex Area occurred at the 216-S-25 Crib (288 ML) but this waste contained only significant quantities of nitrate and moderate amounts of chromium in comparison to inventories of the other mobile contaminants released to the S Complex Area. The next largest volume of waste fluids disposed was at the 216-S-21 Crib, which received 87 ML (23 Mgal) of waste with only small amounts of chromium being noteworthy.

In terms of radionuclides, releases from the SX and S Tank Farm account for 91 percent and 8.4 percent of the total Tc-99 activity and 58.8 percent and 4.8 percent of the total I-129 activity, respectively. The two tank farms' releases also account for 80.8 percent and 5 percent of the chromium released to the subsurface, respectively. The 216-S-9 Crib received 36 percent of the I-129 and 90.3 percent of all the uranium released to the subsurface at the S Complex Area. These facilities are the most likely waste sites contributing contaminants that have reached the water table; for the tank farms, this assumes that additional water was available to transport the limited leaked volumes of tank fluids accidently released through the vadose zone.

Table 8-1 summarizes the percentages of the waste volumes and masses of each key mobile contaminant released compared to the entire S Complex Area, and tabulates the best estimate of the inventory remaining in the vadose zone below each S Complex Area Waste Site. As discovered during the B Complex Area CSM (see PNNL-19277), the masses of mobile contaminants released to each facility or subregion are likely of greater concern than the volume disposed.

Table 8-1. 200-DV-1 OU Summary by Facility of the Percentage Volume and Mass of Contaminants Released to the S Complex Area

	Volume and Inventory % of Total Released to S Complex Area						Residual Waste in Vadose Zone Sediments % of Total Released to S Complex Area				
Facility	Vol Disposed	NO_3	U	Cr	I-129	Tc-99	NO_3	U	Cr	I-129	Tc-99
	(%)	(%)	(%)	(%)	(%)	(%)	(%)	(%)	(%)	(%)	(%)
216-S-9	**10.79**	**11.47**	**90.33**	0.00	**36.03**	0.30	**11.5**	**90.3**	0.00	**36.0**	0.3
216-S-23	7.42	0.53	0.00	0.00	0.00	0.00	0.4	0.0	0.00	0.0	0.00
S Tank Farm (241-S-104)	0.02	6.44	**4.34**	**5.04**	**4.76**	**8.38**	5.8	**3.9**	**4.5**	**4.3**	**7.5**
216-S-21	**18.97**	0.13	0.03	3.77	0.40	0.61	0.04	0.0	1.2	0.1	0.2
216-S-25	**62.69**	**61.14**	0.23	**10.35**	0.00	0.00	**12.2**	0.0	**2.1**	0.0	0.0
SX Tank Farm	0.12	**20.29**	**5.07**	**80.85**	**58.82**	**90.70**	**18.3**	**4.6**	**72.8**	**52.9**	**81.6**
Total	100	100	100	100	100	100	48.2	98.9	80.6	93.4	89.7

Notes: Total for residual in vadose zone sediments does not sum to 100% because some inventory reached groundwater.

Bold % values represent the largest releases or residual inventories for each parameter.

8.2 S Complex Area Hydrogeology Conceptual Model

The hydrogeology of the S Complex Area consists of unconsolidated sedimentary deposits that overlie the older Columbia River Basalt Group and associated sedimentary interbeds. The hydrogeologic conceptual model focused on stratigraphic units associated with the unsaturated zone beneath the S Complex Area. The principal units occurring wholly or partially within the unsaturated zone beneath the S Complex Area are (from youngest to oldest):

- Holocene surficial deposits (primarily anthropogenic and eolian origin)
- Hanford formation
- Cold Creek unit
- Ringold Formation

Eolian materials blanketed the area with up to 3.7 m (12 ft) of windblown sand and silt before installing S Complex Area facilities. Backfill materials now replace the surficial deposits, and are composed of mostly gravel-dominated Hanford formation unit 1, which were introduced during the construction of the cribs and single-shell tanks.

Hanford formation sediments are approximately 40.8 m (134 ft) thick beneath the S Complex Area. The uppermost Hanford formation consists of a gravel-dominated facies referred to informally as the Hf1 and the sand-dominated facies referred to as the Hf2. The contact boundary between these two units has consistently created a lateral spreading layer beneath most of the waste sites. Most of the detected less mobile gamma contamination is contained within the Hf1 above this contact. Underlying the Hanford

formation is the CCu. This sedimentary sequence ranges in thickness from 4.6 m (15 ft) in the northern portion of the S Complex Area, to 12.8 m (42 ft) in the southern portion. The CCu forms a continuous layer beneath the S Complex Area that occurs approximately midway between the ground surface and the water table. The CCu consists of two subunits, the silt-dominated subunit z (CCuz) and the CCuc (also known as caliche). The CCu gently dips to the south to southeast toward the Cold Creek syncline in the S Complex Area (Figure 2-11). This unit exhibits perching and extensive lateral spreading throughout the 200 West Area. However, there is not enough data beneath the S Complex Area waste sites to determine the significance of this phenomenon.

The upper contact of the RFtf is gradational with the overlying CCuc and consists of interstratified, well-bedded, fine to coarse sand and silt. Because of post-Ringold Formation erosion, the RFtf is not laterally continuous across the Pasco Basin. The RFtf is present locally in a few places, as thin (1.2 to 8.5 m [4 to 28 ft]), discontinuous erosional remnants. The RFwie sequence is between 81.7 to 88.1 m (268 to 289 ft) thick, and consists predominantly of fluvial conglomerate with occasional thin beds and lenses of mud and sand. The top of the unit dips very gently to the south to southeast toward the Cold Creek syncline. Beneath the S Complex Area, the water table (i.e., saturated zone) occurs within the RFwie.

Based on numerous borehole geophysical logs, significant lateral spreading of fluids along bedding interfaces, and thus the spreading of mobile contaminants disposed to the S Complex Area facilities, can be documented. Lateral spreading is particularly apparent along the contact between the Hf1 and Hf2 units of the Hanford formation. Details on these localized lateral spreading locations are found in Chapter 2 and within the various geological descriptions of the two subregions found in Chapter 3. Illustrations of the known lateral spreading locations are provided in many of the vadose zone hydrogeologic cross sections presented in Chapter 3 and SGW-50900.

8.3 Hydraulic and Recharge Parameters

Chapter 4 lists useful resources that describe hydraulic and transport parameter values and estimates of recharge rates for near-surface soil types for nonvegetated and vegetated conditions that can be used for predictive modeling of the vadose zone portion of subsurface flow and contaminant transport below the S Complex Area.

8.4 Isotopic Signature Studies in S Complex Area

In the S Complex Area, very few high-precision isotopic signature measurements have been performed. The few measurements that are available are on groundwater samples from the S Complex Area. The value of high-precision isotopic ratio measurements (fingerprinting) is unparalleled in their capability to identify and differentiate the sources of wastes in the subsurface. Even when the total concentrations of constituents such as uranium, strontium, or nitrate are low and not distinguishable from uncontaminated background concentrations, the isotope ratio measurements can often still differentiate sources. Because Tc-99 is often associated with the ubiquitous nitrate released at Hanford, isotopic composition measurements of its common co-contaminant nitrate offers the ability to distinguish between low activity wastes (generally released to cribs, trenches, and ponds) from natural vadose zone pore waters and from tank-related waste.

In the S Complex Area, the nitrate isotopic composition of groundwater that has been studied to date indicates the involvement of all three sources, with certain samples indicating binary mixes of industrial nitrate (related to LAW disposal) and natural background nitrate and tank sourced nitrate and natural background nitrate.

Chapter 7 provides more detail on isotopic signature studies.

The rest of the summary focuses on the combined vadose zone and aquifer conceptual models for the two subregions in the S Complex Area.

8.5 Conceptual Model for Subregion 1

Subregion 1 contains the two inactive cribs (216-S-9 and 216-S-23) and the S Tank Farm. The 216-S-9 Crib received more waste (49.6 ML [13.1 Mgal]) than the 216-S-23 Crib (34 ML [9 Mgal]), but because the 216-S-23 Crib has smaller bottom dimensions, the estimated hypothetical number of pore volumes of liquid that could drain beneath the crib footprint (7.5) is larger than for the 216-S-9 Crib (4.6). However, it was concluded that each facility likely affected groundwater during or at the end of the active disposal periods (1965 through 1969 for 216-S-9 Crib and 1969 through 1972 for the 216-S-23 Crib). There are no direct chemical or radiological measurements of the sediments from either crib. Therefore, using a combination of borehole geophysical gamma logs and soil resistivity information to determine the extent of contamination, it was concluded that the lateral spread of wastes disposed to 216-S-9 was large enough that most all the fluids could still be retained in the vadose zone. Based on this interpretation, the vadose zone conceptual model for the 216-S-9 Crib assumes that the entire waste inventory disposed is still present within the vadose zone.

For the 216-S-23 Crib, only borehole geophysical gamma logs are available to estimate the extent (lateral spread) of contamination within the vadose zone. The CSM formulated from the logs suggests that lateral spreading was not sufficient to retain all the disposed waste in the vadose zone sediments. The vadose zone CSM for 216-S-23 Crib assumes that only 77 percent of the disposed waste inventory remains in the vadose zone.

Within the S Tank Farm, there appears to be only one significant tank release to the subsurface, 241-S-104.

The vadose zone CSMs for subregion 1 waste sites, and associated volumes and inventories of waste disposed, lead to the values shown in Table 8-1 and the following observations.

The vadose zone below the 216-S-9 Crib may still contain a significant inventory of nitrate, uranium, and I-129 in comparison to the other S Complex Area facilities. Iodine-129 may be affecting groundwater at detectable concentrations below this crib. Additional characterization would provide data to determine the mass of contaminants remaining in the vadose zone and validate the CSM.

The vadose zone below and surrounding the 216-S-23 Crib does not contain any significant mass/activity of the five mobile contaminants and, thus, should not be a priority for further characterization. The 241-S-104 tank and/or surrounding piping within the S Tank Farm appears to be the source of increasing chromium, Tc-99, and nitrate in the groundwater downgradient (east) of the tank farm. The groundwater concentrations in this location have been increasing since the mid-2000s. As shown in Table 8-1, it is estimated that a moderate amount of all five mobile contaminants is still present in the vadose zone and is likely going to continue to affect the groundwater.

8.6 Conceptual Model for Subregion 2

This subregion contains two inactive cribs (216-S-21 and 216-S-25) and the SX Tank Farm. In terms of volumes of waste released to the subsurface, the 216-S-25 Crib received the largest (288 ML [76 Mgal]) of the S Complex Area waste sites, equaling 63 percent of the total volume released to the entire S Complex Area. The 216-S-21 Crib received 87 ML (23 Mgal) (19 percent of the total volume released to the S Complex Area). Using the bottom dimensions of the two cribs, the estimated pore volumes of effluent that hypothetically could drain beneath each crib were 43 and 29 for the 216-S-25 and 216-S-21

Cribs, respectively. Therefore, it is highly likely that both cribs affected groundwater during and after the active disposal periods until the vadose zone drained back to field capacity. The S and SX Tank Farms are reported to have eight tanks that released liquid wastes to the subsurface, and the tank farm leaks are known to be affecting groundwater within the S Complex Area.

Borehole geophysical gamma logs and soil electrical resistivity surveys were the primary data used to evaluate vadose zone contaminant extent for the two cribs because there is no sediment characterization data around either crib.

At the 216-S-21 Crib, the available characterization data includes borehole geophysical logs for one shallow borehole down to 15.5 m (51 ft) bgs through the center of the crib footprint and one borehole geophysical log in an adjacent well located to the southeast. These limited data did allow a lateral spread estimate to be made based on gamma contamination detected in the logs. It suggests that the vadose zone below the 216-S-21 Crib could contain about 33 percent of the liquid wastes disposed and that 67 percent might have descended to the water table.

At the 216-S-25 Crib, none of the boreholes surrounding the long crib showed any detectable gamma activity probably because the waste effluent disposed had very low concentrations of radionuclides. The soil resistivity survey results also were not definitive on delineating where high salt (low resistivity regions) exist below the crib. Without adequate data, some very tentative interpretations were made. The comparison of the wastes disposed to the other three cribs in the S Complex Area provided qualitative guidance for a lateral spread guesstimate that suggests 20 percent of the waste fluid disposed to the 216-S-25 Crib still resides in the vadose zone above the high water table.

The vadose zone CSMs for subregion 2 waste sites and associated volumes and inventories of waste disposed lead to the values shown in Table 8-1 and the following observations:

216-S-21 Crib–Because the waste type disposed to the 216-S-21 Crib was not particularly concentrated in any of the five mobile contaminants and the lateral spread was not particularly large, the mass of residual contaminants in the vadose zone are not significant. Comparatively, the 216-S-21 Crib sediments may contain about 1 percent of the total chromium released to the S Complex Area but less than 0.2 percent of any of the other mobile contaminants. Therefore, the 216-S-21 Crib is given a low priority for additional characterization.

216-S-25 Crib–At the 216-S-25 Crib, the inventory estimates of residual contamination in the vadose zone suggest a significant amount of nitrate (12 percent of the total released to the S Complex Area), a small amount of chromium (2 percent of the total released to the S Complex Area), and none of the three radioactive mobile species remain in the vadose zone. Groundwater monitoring and plume mapping over the last 5 to 10 years indicate that the 216-S-25 Crib is a likely source of nitrate in groundwater. There is also data indicating that some of the nitrate in the groundwater plume (immediately downgradient of the 216-S-25 Crib) is sourced from the S-SX Tank Farm region. Obtaining a total nitrate distribution to improve the nitrate isotope signature database would help differentiate these two potential sources. Any sediment characterization at the 216-S-25 Crib should also be coordinated with similar sediment characterization in the SX tank farm.

SX Tank Farm–Of the 15 tanks in the SX Tank Farm, 8 are believed to have released liquids to the subsurface. All eight of the tanks are in the southern portion of the tank farm. Since the mid-2000s, there has been a large and increasing (in both size and concentration) groundwater plume with an apparent origin near the SX-115 tank's southern perimeter. As shown in Table 3-3 and Table 8-1, the estimates of the mass/activity of the five mobile contaminants released from these eight SX tanks is substantial for all but uranium. Compared to the entire S Complex Area contaminant volumes, the SX tank leak estimates

consist of 91 percent of the Tc-99, 81 percent of the chromium, 59 percent of the I-129, and 20.3 percent of the nitrate. Three boreholes and 7 of 11 of the direct push probe holes in the SX Tank Farm yielded sediments with Tc-99 concentrations measured over 100 pCi/g, some approaching or exceeding 3,000 pCi/g. These values represent the highest activity found in vadose sediment samples at Hanford. The sediment characterization data from the boreholes and direct push holes substantiate the presence of high concentrations of water extractable (mobile) Tc-99, chromium, nitrate, and I-129 in vadose zone sediments in the Hanford formation and CCus. However, sample data are limited primarily to sediment above the Ringold Formation (do not include the complete vadose interval), so determination of which tanks and/or related leaking pipe are affecting groundwater still has not been conclusively determined.

8.7 Groundwater Flow Direction and Plume Inventories

Based on the groundwater analyses discussed in Chapter 2 (Section 2.6), the localized groundwater flow direction in the two S Complex Area subregions has differed slightly from each other over the last 15 to 20 years.

Figure 2-22 and Table 8-2 show the flow direction from pre-Hanford times to the present for discrete time intervals for the two subregions. The localized groundwater flow in the Subregion 1 (216-S-9/216-S-23 Cribs and the S Tank Farm) has been directly eastward since 1996 and before 1996 was toward the east-southeast back to 1954. For Subregion 2 (216-S-21/216-S-25 Cribs and the SX Tank Farm) the current flow direction has been east southeast extending back to 1992, and before 1992, the flow direction was southeast, dating back to 1954. The most recent published (2010) flow direction below the WMA S-SX, from March 2009 water level data, is almost due east at 88 degrees azimuth and the hydraulic gradient is 0.0019 m/m and flow rates of 0.14 to 0.7 m (0.46 to 2.3 ft) per day, based on inferred contaminant travel times and as 0.012 to 0.3 m (0.04 to 1 ft) per day based on the Darcy equation (DOE/RL-2010-11).

In the past, the water table mound that developed beneath T Pond by 1951 resulted in southeasterly groundwater flow beneath Subregion 1 (216-S-9/216-S-23 Cribs) and southerly groundwater flow beneath Subregion 2 (216-S-21/216-S-25 Cribs). By 1954, the U Pond mound dominated groundwater flow beneath the SX Tank Farm and the groundwater flow direction changed from a southerly to a southeasterly flow beneath the Subregion 2 (216-S-21/216-S-25 Cribs) and toward the east southeast direction beneath Subregion 1 (216-S-9/216-S-23 Cribs). Both T Pond and U Pond continued to influence groundwater flow in the southern half of 200 West Area until sometime between 1958 and 1960 when the effects of T Pond are no longer seen. Groundwater flow direction remained toward the southeast probably through the early 1990s in Subregion 2 (216-S-21/216-S-25 Cribs) and a more east-southeast direction a bit to the north in Subregion 1 (216-S-9/216-S-23 Cribs). Pre-Hanford Site groundwater flow direction was generally toward the east (BNWL-B-360). Thus, for almost the entire period since active disposal, the groundwater plumes should have trended to the east with some southerly spreading, especially in the southern portion of the S Complex Area.

Table 8-2. S Complex Area Local Groundwater Flow Direction over Time

Subregion	Period	Period	Period	Period	Period
	1940 to 1951	**1951 to 1954**	**1954 to 1960**	**1960 to 1996**	**1996 to present**
1 (216-S-9/216-S-23 Cribs)	East	Southeast	East-Southeast	East-Southeast	East
				1960 to 1992	**1992 to present**
2 (216-S-21/216-S-25 Cribs)	East	South	Southeast	Southeast	East-Southeast

This page intentionally left blank.

9 References

Amberger, Annette, and H.-L. Schmidt, 1987, "Natürliche Isotopengehalte von Nitrat als Indikatoren für dessen Herkunft," *Geochim. Cosmochim. Acta* 51(10):2699-2705.

ARH-2874, 1973, *241-T-106 Tank Leak Investigation*, Atlantic Richfield Hanford Company, Richland, Washington.

ARH-CD-369-4Q, 1976, *Summary of Radioactive Solid Waste Burials in the 200 Areas During 1975*, Atlantic Richfield Hanford Company, Richland, Washington.

ATL Document No. 20100311, 2011, *Final Analytical Report for Soil Samples in Support of an Interim Barrier Southeast of S Farm, Bordering SX Farm*, Advanced Technologies and Laboratories International, Inc., Richland, Washington.

Baker, V.R., B.N. Bjornstad, A.J. Busacca, K.R. Fecht, E.P. Kiver, U.L. Moody, J.G. Rigby, D.F. Stradling, and A.M. Tallman, 1991, "Quaternary Geology of the Columbia Plateau," *Quaternary Nonglacial Geology; Conterminous U.S.*, The Geology of North America Volume K-2, R.B. Morrison (ed.), Geological Society of America, Boulder, Colorado, pp. 215-250. Available at: http://pbadupws.nrc.gov/docs/ML0037/ML003756793.pdf.

BHI-00184, 1995, *Miocene- to Pliocene-Aged Suprabasalt Sediments of the Hanford Site, South-Central Washington*, Rev. 00, Bechtel Hanford, Inc., Richland, Washington.

BHI-01103, 1999, *Clastic Injection Dikes of the Pasco Basin and Vicinity*, Geologic Atlas Series, Rev. 0, Bechtel Hanford, Inc., Richland, Washington. Available at: http://pdw.hanford.gov/arpir/index.cfm/viewDoc?accession=0084337.

BHI-01203, 2000, *Nature and Variability of the Plio-Pleistocene Unit in the 200 West Area of the Hanford Site*, Rev. 0, Bechtel Hanford, Inc., Richland, Washington.

Bjornstad, B.N., 2006, *On the Trail of the Ice Age Floods: A Geological Field Guide to the Mid-Columbia Basin*, Keokee Books, Sandpoint, Idaho.

Bjornstad, Bruce N., Karl R. Fecht, and Christopher J. Pluhar, 2001, "Long History of Pre-Wisconsin, Ice Age Cataclysmic Floods: Evidence from Southeastern Washington State," *The Journal of Geology* 109(6):695-713.

BNWL-B-360, 1974, *Selected Water Table Contour Maps and Well Hydrographs for the Hanford Reservation, 1944-1973*, Pacific Northwest Laboratory, Richland, Washington. Available at: http://pdw.hanford.gov/arpir/index.cfm/viewDoc?accession=D196069236.

Comprehensive Environmental Response, Compensation, and Liability Act of 1980, 42 USC 9601, et seq., Pub. L. 107-377, December 31, 2002. Available at: http://epw.senate.gov/cercla.pdf.

CP-49279, 2011, *Central Plateau Waste Site Dimensions*, Rev. 0, CH2M HILL Plateau Remediation Company, Richland, Washington.

DOE/ID/12584-268, GJO-HAN-4, 1996, *Vadose Zone Characterization Project at the Hanford Tank Farms SX Tank Farm Report*, U.S. Department of Energy, Albuquerque Operations Office and Grand Junction Projects Office, Grand Junction, Colorado. Available at: http://www.osti.gov/scitech/servlets/purl/437723.

DOE/ORP-2008-01, 2009, *RCRA Facility Investigation Report for Hanford Single-Shell Tank Waste Management Areas*, Rev. 1, U.S. Department of Energy, Richland Operations Office, Richland, Washington. Available at:
http://www5.hanford.gov/arpir/?content=findpage&AKey=1001051140.
http://www5.hanford.gov/arpir/?content=findpage&AKey=1001051141.
http://www5.hanford.gov/arpir/?content=findpage&AKey=1001051142.
http://www5.hanford.gov/arpir/?content=findpage&AKey=1001051143.
http://www5.hanford.gov/arpir/?content=findpage&AKey=1001051144.
http://www5.hanford.gov/arpir/?content=findpage&AKey=1001051145.
http://www5.hanford.gov/arpir/?content=findpage&AKey=1001051146.
http://www5.hanford.gov/arpir/?content=findpage&AKey=1001051147.
http://www5.hanford.gov/arpir/?content=findpage&AKey=1001051148.
http://www5.hanford.gov/arpir/?content=findpage&AKey=0911240059.

DOE/RL-91-61, 1992, *T-Plant Source Aggregate Area Management Study Report*, Rev. 0, U.S. Department of Energy, Richland Operations Office, Richland, Washington. Available at: http://pdw.hanford.gov/arpir/index.cfm/viewDoc?accession=D196124788.

DOE/RL-96-61, 1997, *Hanford Site Background: Part 3, Groundwater Background*, Rev. 0, U.S. Department of Energy, Richland Operations Office, Richland, Washington. Available at: http://pdw.hanford.gov/arpir/index.cfm/viewDoc?accession=D197226378.

DOE/RL-2000-61, 2000, *Draft Industrial Mineral Resources Management Plan*, Rev. 0, U.S. Department of Energy, Richland Operations Office, Richland, Washington.

DOE/RL-2002-39, 2002, *Standardized Stratigraphic Nomenclature for Post-Ringold-Formation Sediments Within the Central Pasco Basin*, Rev. 0, U.S. Department of Energy, Richland Operations Office, Richland, Washington (also cited as DOE, 2002). Available at: http://media.wix.com/ugd/12afd0_9dbdbd7be68232c47fabe26b53360660.pdf.

DOE/RL-2008-66, 2009, *Hanford Site Groundwater Monitoring for Fiscal Year 2008*, Rev. 0, U.S. Department of Energy, Richland Operations Office, Richland, Washington. Available at:
http://pdw.hanford.gov/arpir/index.cfm/viewDoc?accession=0905131281.
http://pdw.hanford.gov/arpir/index.cfm/viewDoc?accession=0905131282.

DOE/RL-2008-77, 2009, *200-UP-1 and 200-ZP-1 Operable Units Pump-and-Treat System Annual Report for Fiscal Year 2008*, Rev. 0, U.S. Department of Energy, Richland Operations Office, Richland, Washington. Available at:
http://pdw.hanford.gov/arpir/index.cfm/viewDoc?accession=0906160170.

DOE/RL-2009-122, 2012, *Remedial Investigation/Feasibility Study for the 200-UP-1 Groundwater Operable Unit*, Rev. 0, U.S. Department of Energy, Richland Operations Office, Richland, Washington. Available at:
http://pdw.hanford.gov/arpir/index.cfm/viewDoc?accession=0092342.

DOE/RL-2010-11, 2010, *Hanford Site Groundwater Monitoring and Performance Report for 2009 Volumes 1 & 2*, Rev. 1, U.S. Department of Energy, Richland Operations Office, Richland, Washington. Available at:
http://pdw.hanford.gov/arpir/index.cfm/viewDoc?accession=0084237.

DOE/RL-2010-89, 2010, *Long-Range Deep Vadose Zone Program Plan*, Rev. 0, U.S. Department of Energy, Richland Operations Office, Richland, Washington. Available at: http://pdw.hanford.gov/arpir/index.cfm/viewDoc?accession=0084131.

DOE/RW-0164, 1988, *Site Characterization Plan: Reference Repository Location, Hanford Site, Washington*, 9 vols., Consultation Draft, U.S. Department of Energy, Washington, D.C. Available at: http://pdw.hanford.gov/arpir/index.cfm/viewDoc?accession=D196007701.
http://pdw.hanford.gov/arpir/index.cfm/viewDoc?accession=D196007769.
http://pdw.hanford.gov/arpir/index.cfm/viewDoc?accession=D196007788.
http://pdw.hanford.gov/arpir/index.cfm/viewDoc?accession=D196007871.
http://pdw.hanford.gov/arpir/index.cfm/viewDoc?accession=D196007870.
http://pdw.hanford.gov/arpir/index.cfm/viewDoc?accession=D196007876.
http://pdw.hanford.gov/arpir/index.cfm/viewDoc?accession=D196007901.
http://pdw.hanford.gov/arpir/index.cfm/viewDoc?accession=D196007935.
http://pdw.hanford.gov/arpir/index.cfm/viewDoc?accession=D196027182.

Earth Sciences Personnel, 1956, *Earth Sciences' Waste Disposal Monitoring Activities Summary, March 1956*, General Electric Company, Richland, Washington.

ECF-200BP5-10-0351, 2010, *200-BP-5 Remedial Investigation Report – Groundwater Fate and Transport Modeling*, Rev. 0, CH2M HILL Plateau Remediation Company, Richland, Washington.

ECF-200UP1-10-0373, 2012, *200-UP-1, Remedial Investigation Report; Groundwater Contaminant Fate and Transport Model*, Rev. 1, CH2M HILL Plateau Remediation Company, Richland, Washington.

Ecology, EPA, and DOE, 1989, *Hanford Federal Facility Agreement and Consent Order*, 2 vols., as amended, Washington State Department of Ecology, U.S. Environmental Protection Agency, and U.S. Department of Energy, Olympia, Washington. Available at: http://www.hanford.gov/?page=81.

Environmental Dashboard Application, 2012, U.S. Department of Energy. Available at: http://environet.hanford.gov/EDA.

Gile, L.H., F.F. Peterson, and R.B. Grossman, 1966, "Morphological and Genetic Sequences of Carbonate Accumulation in Desert Soil," *Soil Science* 101(5):347-360. Available at: http://www2.bren.ucsb.edu/~dturney/port/1966_Gile.pdf.

GJO-97-31-TAR, GJO-HAN-17, 1998, *Hanford Tank Farms Vadose Zone S Tank Farm Report*, U.S. Department of Energy, Grand Junction Office, Grand Junction, Colorado. Available at: http://environet.hanford.gov/env/attach//703/data/htfvz/SReport/report.cfm.

GJO-97-31-TARA, GJO-HAN-17, 2000, *Addendum to the S Tank Farm Report*, Vadose Zone Characterization Project at the Hanford Tank Farms, U.S. Department of Energy, Grand Junction Office, Grand Junction, Colorado. Available at: http://environet.hanford.gov/env/attach//703/data/htfvz/SReport/addendum.cfm.

HNF-4936, 1999, *Subsurface Conditions Description for the S-SX Waste Management Area*, Rev. 0, Lockheed Martin Hanford Corporation, Richland, Washington. Available at: http://www.osti.gov/scitech/servlets/purl/798120.

HNF-EP-0182, 2013, *Waste Tank Summary Report for Month Ending December 31, 2012*, Rev. 297, Washington River Protection Solutions, Richland, Washington. Available at: http://pdw.hanford.gov/arpir/index.cfm/viewDoc?accession=1302141456.

HW-61780, 1959, *Subsurface Geology of the Hanford Separation Areas*, General Electric Company, Richland, Washington.

HW-67549, 1960, *An Eolian Deposit Beneath 200-West Area*, General Electric Company, Richland, Washington.

Kendall, C. and J.J. McDonnell (Eds.), 1998, *Isotope Tracers in Catchment Hydrology*, Elsevier Science, pp. 519-576.

Lindsey, Kevin A., 1996, *The Miocene to Pliocene Ringold Formation and Associated Deposits of the Ancestral Columbia River System, South-central Washington and North-central Oregon*, Open File Report 96-8, Washington Division of Geology and Earth Resources, Washington State Department of Natural Resources, Olympia, Washington. Available at: http://www.dnr.wa.gov/Publications/ger_ofr96-8_ringold_formation.pdf.

Machette, Michael N. 1985, *Calcic soils of the southwestern United States*, Geological Society of America Special Paper 203, U.S. Geological Survey, Denver Federal Center, Denver, Colorado. Available at: http://pbadupws.nrc.gov/docs/ML0037/ML003747879.pdf.

Newcomb, R., J. Strand, and F. Frank, 1972, *Geology and Ground-Water Characteristics of the Hanford Reservation of the U.S. Atomic Energy Commission, Washington*, Professional Paper 717, U.S. Geological Survey, Washington, D.C. Available at: http://pubs.usgs.gov/pp/0717/report.pdf.

Newcomer, D.R., 2005, *Preliminary Electromagnetic Borehole Flowmeter Survey Results for Hydrologic Assessment Task Characterization Wells 299-W14-11, 299-W22-47, and 299-W22-80*, letter report to F.A. Spane, Project F8245, Pacific Northwest National Laboratory, Richland, Washington.

PNL-6820, 1989, *Hydrogeology of the 200 Areas Low Level Burial Grounds—An Interim Report: Volume 1: Text*, Vol. 1, Pacific Northwest Laboratory, Richland, Washington. Available at: http://pdw.hanford.gov/arpir/index.cfm/viewDoc?accession=D195066506.

PNL-7336, 1990, *Geohydrology of the 218-W-5 Burial Ground, 200-West Area, Hanford Site*, Pacific Northwest Laboratory, Richland, Washington. Available at: http://www.osti.gov/scitech/servlets/purl/6932537.

PNL-8971, 1993, *Three-Dimensional Conceptual Model for the Hanford Site Unconfined Aquifer System, FY 1993 Status Report*, Pacific Northwest Laboratory, Richland, Washington. Available at: http://www.osti.gov/scitech/servlets/purl/10116050.

PNNL-12261, 2000, *Revised Hydrogeology for the Suprabasalt Aquifer System, 200-East Area and Vicinity, Hanford Site, Washington*, Pacific Northwest National Laboratory, Richland, Washington (cited as Williams et al., 2000). Available at: http://pdw.hanford.gov/arpir/index.cfm/viewDoc?accession=0906180659.

PNNL-13037, 2004, *Geochemical Data Package for the 2005 Hanford Integrated Disposal Facility Performance Assessment*, Rev. 2, Pacific Northwest National Laboratory, Richland, Washington. Available at: http://pdw.hanford.gov/arpir/index.cfm/viewDoc?accession=0911300324.

PNNL-13200, 2000, *Borehole Data Package for Wells 299-W22-48, 299-W22-49, and 299-W22-50 at Single-Shell Waste Management Area S-SX*, Pacific Northwest National Laboratory, Richland, Washington. Available at: http://www.pnl.gov/main/publications/external/technical_reports/PNNL-13200.pdf.

PNNL-13282, 2000, Groundwater Quality Assessment for Waste Management Area U: First Determination, Pacific Northwest National Laboratory, Richland, Washington. Available at: http://www.pnl.gov/main/publications/external/technical_reports/PNNL-13282.pdf.

PNNL-13400, 2000, *Groundwater Flow and Transport Calculations Supporting the Immobilized Low-Activity Waste Disposal Facility Performance Assessment*, Pacific Northwest National Laboratory, Richland, Washington. Available at: http://www.pnl.gov/main/publications/external/technical_reports/PNNL-13400.pdf.

PNNL-13441, 2001, *RCRA Groundwater Quality Assessment Report for Waste Management Area S-SX (November 1997 through April 2000)*, Pacific Northwest National Laboratory, Richland, Washington. Available at: http://www.pnl.gov/main/publications/external/technical_reports/PNNL-13441.pdf.

PNNL-13514, 2001, *Results of Detailed Hydrologic Characterization Tests – Fiscal Year 2000*, Pacific Northwest National Laboratory, Richland, Washington. Available at: http://www.pnl.gov/main/publications/external/technical_reports/PNNL-13514.pdf.

PNNL-13757-1, 2008, *Characterization of Vadose Zone Sediment: Uncontaminated RCRA Borehole Core Samples and Composite Samples*, Rev. 1, Pacific Northwest National Laboratory, Richland, Washington. Available at: http://www.pnl.gov/main/publications/external/technical_reports/PNNL-13757-1rev1.pdf.

PNNL-13757-2, 2008, *Characterization of Vadose Zone Sediment: Borehole 299-W23-19 [SX-115] in the S-SX Waste Management Area*, Rev. 1, Pacific Northwest National Laboratory, Richland, Washington. Available at: http://www.pnl.gov/main/publications/external/technical_reports/PNNL-13757-2rev1.pdf.

PNNL-13757-3, 2002, *Characterization of Vadose Zone Sediment: Borehole 41-09-39 in the S-SX Waste Management Area*, Pacific Northwest National Laboratory, Richland, Washington. Available at: http://www.pnl.gov/main/publications/external/technical_reports/pnnl-13757-3.pdf.

PNNL-13757-4, 2002, *Characterization of Vadose Zone Sediment: Slant Borehole SX-108 in the S-SX Waste Management Area*, Pacific Northwest National Laboratory, Richland, Washington. Available at: http://www.pnl.gov/main/publications/external/technical_reports/pnnl-13757-4.pdf.

PNNL-13858, 2002, *Revised Hydrogeology for the Suprabasalt Aquifer System, 200-West Area and Vicinity, Hanford Site, Washington*, Pacific Northwest National Laboratory, Richland, Washington. Available at: http://www.pnl.gov/main/publications/external/technical_reports/PNNL-13858.pdf.

PNNL-13895, 2003, *Hanford Contaminant Distribution Coefficient Database and Users Guide*, Rev. 1, Pacific Northwest National Laboratory, Richland, Washington. Available at: http://pdw.hanford.gov/arpir/index.cfm/viewDoc?accession=0911300341.

PNNL-14113, 2002, *Results of Detailed Hydrologic Characterization Tests – Fiscal Year 2001*, Pacific Northwest National Laboratory, Richland, Washington. Available at: http://www.pnl.gov/main/publications/external/technical_reports/PNNL-14113.pdf.

PNNL-14120, 2007, *Laboratory-Scale Bismuth Phosphate Extraction Process Simulation to Track Fate of Fission Products*, Pacific Northwest National Laboratory, Richland, Washington. Available at: http://www.pnl.gov/main/publications/external/technical_reports/PNNL-14120.pdf.

PNNL-14186, 2003, *Results of Detailed Hydrologic Characterization Tests – Fiscal Year 2002*, Pacific Northwest National Laboratory, Richland, Washington. Available at: http://www.pnl.gov/main/publications/external/technical_reports/PNNL-14186.pdf.

PNNL-14548, 2004, *Hanford Site Groundwater Monitoring for Fiscal Year 2003*, Pacific Northwest National Laboratory, Richland, Washington. Available at: http://www.pnl.gov/main/publications/external/technical_reports/PNNL-14548.pdf.

PNNL-14702, 2006, *Vadose Zone Hydrogeology Data Package for Hanford Assessments*, Rev. 1, Pacific Northwest National Laboratory, Richland, Washington. Available at: http://pdw.hanford.gov/arpir/index.cfm/viewDoc?accession=0911300343.

PNNL-14753, 2006, *Groundwater Data Package for Hanford Assessments*, Rev. 1, Pacific Northwest National Laboratory, Richland, Washington (also cited as Thorne et al., 2006). Available at: http://www.pnl.gov/main/publications/external/technical_reports/PNNL-14753Rev1.pdf.

PNNL-15070, 2005, *Hanford Site Groundwater Monitoring for Fiscal Year 2004*, Pacific Northwest National Laboratory, Richland, Washington. Available at: http://www.pnl.gov/main/publications/external/technical_reports/PNNL-15070.pdf.

PNNL-15670, 2006, *Hanford Site Groundwater Monitoring for Fiscal Year 2005*, Pacific Northwest National Laboratory, Richland, Washington. Available at: http://www.pnl.gov/main/publications/external/technical_reports/PNNL-15670.pdf.

PNNL-15837, 2007, *Data Package for Past and Current Groundwater Flow and Contamination Beneath Single-Shell Tank Waste Management Areas*, Pacific Northwest National Laboratory, Richland, Washington. Available at: http://pdw.hanford.gov/arpir/index.cfm/viewDoc?accession=0911240061.

PNNL-15955, 2007, *Geology Data Package for the Single-Shell Tank Waste Management Areas at the Hanford Site*, Pacific Northwest National laboratory, Richland, Washington. Available at: http://www.pnl.gov/main/publications/external/technical_reports/PNNL-15955rev1.pdf.

PNNL-16069, 2006, *Development of Historical Water Table Maps of the 200 West Area of the Hanford Site (1950–1970)*, Pacific Northwest National Laboratory, Richland, Washington. Available at: http://www.pnl.gov/main/publications/external/technical_reports/PNNL-16069.pdf.

PNNL-16649, 2007, *Characterization of Direct Push Vadose Zone Sediments from the T and TY Waste Management Areas*, Pacific Northwest National Laboratory, Richland, Washington. Available at: http://www.pnl.gov/main/publications/external/technical_reports/PNNL-16649.pdf.

PNNL-16688, 2007, *Recharge Data Package for Hanford Single-Shell Tank Waste Management Areas*, Pacific Northwest National Laboratory, Richland, Washington. Available at: http://www.pnl.gov/main/publications/external/technical_reports/PNNL-16688.pdf.

PNNL-16945, 2007, *Slug Test Characterization Results for Multi-Test/Depth Intervals Conducted During the Drilling of CERCLA Operable Unit OU ZP-1 Wells 299-W10-33 and 299-W11-48*, Pacific Northwest National Laboratory, Richland, Washington. Available at: http://www.pnl.gov/main/publications/external/technical_reports/PNNL-16945.pdf.

PNNL-17154, 2008, *Geochemical Characterization Data Package for the Vadose Zone in the Single-Shell Tank Waste Management Areas at the Hanford Site*, Pacific Northwest National Laboratory, Richland, Washington. Available at: http://pdw.hanford.gov/arpir/index.cfm/viewDoc?accession=0911240119.

PNNL-17348, 2008, *Results of Detailed Hydrologic Characterization Tests—Fiscal and Calendar Year 2005*, Pacific Northwest National Laboratory, Richland, Washington. Available at: http://www.pnl.gov/main/publications/external/technical_reports/PNNL-17348.pdf.

PNNL-17675, 2008, *BP-5 Remedial Investigation Slug-Test Characterization Results for Well 699-52-55A*, Pacific Northwest National Laboratory, Richland, Washington. Available at: http://www.pnl.gov/main/publications/external/technical_reports/PNNL-17675.pdf.

PNNL-17821, 2008, *Electrical Resistivity Correlation to Vadose Zone Sediment and Pore-Water Composition for the BC Cribs and Trenches Area*, Pacific Northwest National Laboratory, Richland, Washington. Available at: http://www.pnl.gov/main/publications/external/technical_reports/PNNL-17821.pdf.

PNNL-17913, 2009, *Hydrogeology of the Hanford Site Central Plateau – A Status Report for the 200 West Area*, Rev. 1, Pacific Northwest National Laboratory, Richland, Washington. Available at: http://www.pnl.gov/main/publications/external/technical_reports/PNNL-17913rev1.pdf.

PNNL-18279, 2009, *Aquifer Testing Recommendations for Well 299-W15-225: Supporting Phase I of the 200-ZP-1 Groundwater Operable Unit Remedial Design*, Pacific Northwest National Laboratory, Richland, Washington. Available at: http://www.pnl.gov/main/publications/external/technical_reports/PNNL-18279.pdf.

PNNL-18564, 2009, *Selection and Traceability of Parameters to Support Hanford-Specific RESRAD Analyses: Fiscal Year 2008 Status Report*, Pacific Northwest National Laboratory, Richland, Washington. Available at: http://www.pnl.gov/main/publications/external/technical_reports/PNNL-18564.pdf.

PNNL-18732, 2009, *Field Test Report: Preliminary Aquifer Test Characterization Results for Well 299-W15-225: Supporting Phase I of the 200-ZP-1 Groundwater Operable Unit Remedial Design*, Pacific Northwest National Laboratory, Richland, Washington. Available at: http://www.pnl.gov/main/publications/external/technical_reports/PNNL-18732.pdf.

PNNL-19277, 2010, *Conceptual Models for Migration of Key Groundwater Risk Contaminants Through the Vadose Zone and Into the Unconfined Aquifer Below the B-Complex*, Pacific Northwest National Laboratory, Richland, Washington. Available at: http://pdw.hanford.gov/arpir/pdf.cfm?accession=0084238.

PNNL-19482, 2010, *Slug Test Characterization Results for Multi-Test/Depth Intervals Conducted During the Drilling of CERCLA Operable Unit OU UP-1 Wells 299-W19-48, 699-30-66, and 699-36-70B*, Pacific Northwest National Laboratories, Richland, Washington. Available at: http://www.pnl.gov/main/publications/external/technical_reports/PNNL-19482.pdf.

PNNL-19491, 2010, *Slug Test Characterization Results for Multi-Test/Depth Intervals Conducted During the Drilling of CERCLA Operable Unit OU ZP-1 Wells 299-W11-43, 299-W15-50, and 299-W18-16*, Pacific Northwest National Laboratory, Richland, Washington. Available at: http://www.pnl.gov/main/publications/external/technical_reports/pnnl-19491.pdf.

PNNL-19702, 2010, *Hydrogeologic Model for the Gable Gap Area, Hanford Site*, Pacific Northwest National Laboratory, Richland, Washington. Available at: www.pnl.gov/main/publications/external/technical_reports/PNNL-19702.pdf.

QET-T-132, 2000, *Results of Field Tests with the Electromagnetic Borehole Flowmeter at the Pacific Northwest National Laboratory, Richland, WA*, Quantum Engineering Corporation, Loudon, Tennessee.

Resource Conservation and Recovery Act of 1976, 42 USC 6901, et seq. Available at: http://www.epa.gov/epawaste/inforesources/online/index.htm.

Retallack, Greg J., 1988, "Field recognition of paleosols," Geological Society of America, Special Paper 216, 20 pp. Available at: http://blogs.uoregon.edu/gregr/files/2013/07/Retallack-1988-field-recognition-paleosols-166j4g0.pdf.

Retallack, Gregory J., 2001, *Soils of the Past; An Introduction of Paleopedology*, Second Edition, Blackwell Science, London, England.

RHO-BWI-ST-4, 1979, *Geologic Studies of the Columbia Plateau: A Status Report*, Rockwell Hanford Operations, Richland, Washington. Available at:
http://pdw.hanford.gov/arpir/index.cfm/viewDoc?accession=D196002105.
http://pdw.hanford.gov/arpir/index.cfm/viewDoc?accession=D196000171.
http://pdw.hanford.gov/arpir/index.cfm/viewDoc?accession=D196000172.
http://pdw.hanford.gov/arpir/index.cfm/viewDoc?accession=D196000173.
http://pdw.hanford.gov/arpir/index.cfm/viewDoc?accession=D196000174.
http://pdw.hanford.gov/arpir/index.cfm/viewDoc?accession=D196000175.
http://pdw.hanford.gov/arpir/index.cfm/viewDoc?accession=D196000176.
http://pdw.hanford.gov/arpir/index.cfm/viewDoc?accession=D196000177.
http://pdw.hanford.gov/arpir/index.cfm/viewDoc?accession=D196000178.
http://pdw.hanford.gov/arpir/index.cfm/viewDoc?accession=D196000179.
http://pdw.hanford.gov/arpir/index.cfm/viewDoc?accession=D196000180.

RHO-BWI-ST-14, 1981, *Subsurface Geology of the Cold Creek Syncline*, Rockwell Hanford Operations, Richland, Washington. Available at: http://pdw.hanford.gov/arpir/index.cfm/viewDoc?accession=0084338.

RHO-CD-27-3Q, 1978, *Summary of Radioactive Solid Waste Burials in the 200 Areas During 1977*, Rockwell Hanford Operations, Richland, Washington.

RHO-CD-79-34 4Q, 1980, *Radioactive Liquid Wastes Discharged to Ground in the 200 Areas During 1979*, Rockwell Hanford Operations, Richland, Washington.

RHO-HS-SR-81-3, 1982, *Radioactive Liquid Wastes Discharged to Ground in the 200 Areas During 1981*, Rockwell Hanford Operations, Richland, Washington.

RHO-HS-SR-82-3-4Q-LIQ-P, 1983, *Radioactive Liquid Wastes Discharged to Ground in the 200 Areas During 1982*, Rockwell Hanford Operations, Richland, Washington.

RHO-HS-SR-84-3-4Q-LIQ-P, 1985, *Radioactive Liquid Wastes Discharged to Ground in the 200 Areas During 1984*, Rockwell Hanford Operations, Richland, Washington.

RHO-HS-SR-85-3-4Q-LIQ-P, 1986, *Radioactive Liquid Wastes Discharged to Ground in the 200 Areas During 1985*, Rockwell Hanford Operations, Richland, Washington.

RHO-LD-78-24-4Q, 1979, *Summary of Radioactive Solid Waste Burials in the 200 Areas During 1978*, Rev. 1, Rockwell Hanford Operations, Richland, Washington.

RHO-ST-1, 1979, *Status of Liquid Waste Leaked from the 241-T-106 Tank*, Rockwell Hanford Operations, Richland, Washington.

RHO-ST-23, 1979, *Geology of the Separation Areas, Hanford Site, South-Central Washington*, Rockwell Hanford Operations, Richland, Washington. Available at: http://pdw.hanford.gov/arpir/index.cfm/viewDoc?accession=D195065394.

RPP-7123, 2001, *Surface Conditions Description of the T-TX-TY Waste Management Area*, Rev. 0, CH2M HILL Hanford Group, Inc., Richland, Washington. Available at: http://pdw.hanford.gov/arpir/index.cfm/viewDoc?accession=0911240297.

RPP-7884, 2002, *Field Investigation Report for Waste Management Area S-SX*, Rev. 0, CH2M HILL Hanford Group, Inc., Richland, Washington. Available at:
http://pdw.hanford.gov/arpir/index.cfm/viewDoc?accession=D8974033.
http://pdw.hanford.gov/arpir/index.cfm/viewDoc?accession=D8974041.
http://pdw.hanford.gov/arpir/index.cfm/viewDoc?accession=D8974046.
http://pdw.hanford.gov/arpir/index.cfm/viewDoc?accession=D8974049.
http://pdw.hanford.gov/arpir/index.cfm/viewDoc?accession=0911240245.

RPP-8531, 2001, *Vadose Zone Geology of Boreholes 299-W10-27 and 299-W11-39 T-TX-TY Waste Management Area Hanford Site, South-Central Washington*, Rev. 0, CH2M HILL Hanford Group, Inc., Richland, Washington.

RPP-9223, 2001, *Modeling Data Package for B-BX-BY Field Investigation Report (FIR)*, Rev. 0, CH2M HILL Hanford Group, Inc., Richland, Washington.

RPP-10098, 2003, *Field Investigation Report for Waste Management Area B-BX-BY: Volume 1, Main Text and Appendices A-C*, Rev. 0, CH2M HILL Hanford, Group, Inc., Richland, Washington. Available at: http://pdw.hanford.gov/arpir/index.cfm/viewDoc?accession=D9209332.

RPP-13310, 2003, *Modeling Data Package for an Initial Assessment of Closure for C Tank Farm*, Rev. 0, CH2M HILL Hanford Group, Inc., Richland, Washington. Available at: http://www.hanford.gov/docs/gpp/fieldwork/closure/RPP-13310.pdf.

RPP-19822, 2004, *Hanford Defined Waste Model – Revision 5.0*, Rev. 0, CH2M HILL Hanford Group, Inc., Richland, Washington.

RPP-23405, 2006, *Tank Farm Vadose Zone Contamination Volume Estimates*, Rev. 2, CH2M HILL Hanford Group, Inc., Richland, Washington. Available at: http://pdw.hanford.gov/arpir/index.cfm/viewDoc?accession=0911240667.

RPP-23748, 2006, *Geology, Hydrogeology, Geochemistry, and Mineralogy Data Package for the Single-Shell Tank Waste Management Areas at the Hanford Site*, Rev. 0, CH2M HILL Hanford Group, Inc., Richland, Washington.

RPP-26744, 2005, *Hanford Soil Inventory Model, Rev. 1*, Rev. 0, prepared by R.A. Corbin, B.C. Simpson, M.J. Anderson (Nuvotec), W.F. Danielson III (Advanced Imaging Technologies), J.G. Field, T.E. Jones (CH2M HILL Hanford Group, Inc.), and C.T. Kincaid (Pacific Northwest National Laboratory) for the U.S. Department of Energy, Richland, Washington.

RPP-32681, 2007, *Process to Assess Tank Farm Leaks in Support of Retrieval and Closure Planning*, Rev. 0, CH2M HILL Hanford Group, Inc., Richland, Washington.

RPP-43548, 2009, *Completion Report for 241-SX Tank Farm Direct Push Barrier Characterization*, Rev. 0, Washington River Protection Solutions, Richland, Washington.

RPP-47274, 2010, *2010 Completion Report for the 241-S/SX Tank Farm Direct Push Barrier Characterization*, Rev. 0, Washington River Protection Solutions, Richland, Washington.

RPP-ENV-39658, 2010, *Hanford SX-Farm Leak Assessments Report*, Rev. 0, Washington River Protection Solutions, Richland, Washington. Available at: http://www.hanford.gov/files.cfm/RPP-ENV-39658_Rev_0.pdf.

RPP-RPT-27605, 2006, *Gamma Surveys of the Single-Shell Tank Laterals for A and SX Tank Farms*, Rev. 0, CH2M HILL Hanford Group, Inc., Richland, Washington. Available at: http://pdw.hanford.gov/arpir/index.cfm/viewDoc?accession=0911240666.

RPP-RPT-30976, 2006, *Surface Geophysical Exploration of S Tank Farm at the Hanford Site*, Rev. 0, CH2M HILL Hanford Group, Inc., Richland, Washington. Available at: http://pdw.hanford.gov/arpir/index.cfm/viewDoc?accession=0911240536.

RPP-RPT-35222, 2007, *Far-Field Hydrology Data Package for the RCRA Facility Investigation (RFI) Report*, Rev. 1, CH2M HILL Hanford Group, Inc., Richland, Washington. Available at: http://pdw.hanford.gov/arpir/index.cfm/viewDoc?accession=0911240121.

RPP-RPT-38322, 2008, *Surface Geophysical Exploration of the S and SX Tank Farms at the Hanford Site*, Rev. 0, CH2M HILL Hanford Group, Inc., Richland, Washington.

RPP-RPT-42513, 2009, *Surface Geophysical Exploration of the SX Tank Farm at the Hanford Site*, Rev. 0, Washington River Protection Solutions, Richland, Washington.

RPP-RPT-47008, 2010, *Final Analytical Report for Soil Samples in Support of an Interim Barrier at SX Farm*, Rev. 0, Washington River Protection Solutions, Richland, Washington.

RPP-RPT-47851, 2010, *Three-Dimensional Surface Geophysical Exploration of S/SX Tank Farm*, Rev. 0, Washington River Protection Solutions, Richland, Washington.

RPP-RPT-48589, 2011, *Hanford 241-S Farm Leak Assessment Report*, Rev. 0, Washington River Protection Solutions, Richland, Washington.

SD-BWI-DP-039, 1984, *Suprabasalt Stratigraphy Within and Adjacent to the Reference Repository Location*, Rockwell Hanford Operations, Richland, Washington.

SGW-49924, 2011, *Preliminary Conceptual Models for the 200-DV-1 Operable Unit Waste Sites in the T Complex Area*, Rev. 0, CH2M HILL Plateau Remediation Company, Richland, Washington.

SGW-50194, 2011, *Geophysical Logging Report for 200-DV-1 Operable Unit Waste Sites in the S Complex Area*, Rev. 0, CH2M HILL Plateau Remediation Company, Richland, Washington.

SGW-50900, 2014, *Geologic Cross Section Development in the Vicinity of S-Complex and T-Complex to Support the 200-DV-1 Operable Unit Conceptual Models*, Rev. 0, CH2M HILL Plateau Remediation Company, Richland, Washington.

Singleton M.J., K.N. Woods, M.E. Conrad, D.J. DePaolo, and P.E. Dresel, 2005, "Tracking Sources of Unsaturated Zone and Groundwater Nitrate Contamination Using Nitrogen and Oxygen Stable Isotopes at the Hanford Site, Washington," *Environ. Sci. Technol.* 39(10):3563-3570.

Slate, Janet L., 1996, "Buried Carbonate Paleosols Developed in Pliocene-Pleistocene Deposits of the Pasco Basin, South-Central Washington, U.S.A.," *Quaternary International* 34-36:191-196.

Smith, Gary A., 1993, "Missoula Flood Dynamics and Magnitudes Inferred from Sedimentology of Slack-Water Deposits on the Columbia Plateau," *Geological Society of America Bulletin* 105(1):77-100.

Sobczyk, Stanley Michael, 2000, *Subsurface Interpretation of the SX Tank Farm, Hanford Site, Washington, Based on Gamma-Ray Logging*, Environmental Restoration and Waste Management Department, Nez Perce Tribe of Idaho, Lapwai, Idaho.

Sobczyk, Stanley Michael, 2001, *Subsurface Interpretation of the T Tank Farm, Hanford Site, Washington, Based on Gamma-Ray Logging*, Environmental Restoration and Waste Management Department, Nez Perce Tribe of Idaho, Lapwai, Idaho.

Sweeney, Mark R., Alan J. Busacca, Catherine A. Richardson, Mikhail Blinnikov, and Eric V. McDonald, 2004, "Glacial anticyclone recorded in Palouse loess of northwestern United States," *Geology* 32(8):705-708. Available at: http://pnw-winderosion.wsu.edu/Docs/Publications/04%20pubs/Sweeney-Glacial.pdf.

Waitt, Richard B., Jr., 1980, "About Forty Last-Glacial Lake Missoula Jökulhlaups Through Southern Washington," *The Journal of Geology* 88(6):653-679.

WHC-EP-0883, 1995, *Variability and Scaling of Hydraulic Properties for 200 Area Soils, Hanford Site*, Rev. 0, Westinghouse Hanford Company, Richland, Washington. Available at: http://www.osti.gov/scitech/servlets/purl/188564.

WHC-MR-0391, 1992, *Field Trip Guide to the Hanford Site*, Westinghouse Hanford Company, Richland, Washington (cited as Reidel et al., 1992). Available at: http://pdw.hanford.gov/arpir/index.cfm/viewDoc?accession=D196136627.

WHC-SD-EN-TI-008, 1991, *Geologic Setting of the 200 West Area: An Update*, Rev. 0, Westinghouse Hanford Company, Richland, Washington.

WHC-SD-EN-TI-014, 1992, *Hydrogeologic Model for the 200 West Groundwater Aggregate Area*, Rev. 0, Westinghouse Hanford Company, Richland, Washington. Available at: http://pdw.hanford.gov/arpir/index.cfm/viewDoc?accession=D196100569.

WHC-SD-EN-TI-290, 1994, *Geologic Setting of the Low-Level Burial Grounds*, Rev. 0, Westinghouse Hanford Company, Richland, Washington. Available at: http://www.osti.gov/scitech/servlets/purl/10192359.

Appendix A

S Complex Area Waste Facility Dimensions, Major Chemical Inventories Disposed by Year for Each Facility, Total Waste Volume Disposed by Year, Waste Stream Definitions

This appendix consists of spreadsheets that list details on the dimensions of facilities within the Deep Vadose Zone Operable Unit (200-DV-1 OU), the facility bottoms with respect to ground surface, the overall excavation dimensions, thickness of overburden, etc. These facility construction details aid in the development of the conceptual models for contaminant migration through the vadose zone. In addition Appendix A tabulates all the volume, mass, and activity estimates for total liquid and key constituents that were released to the facilities. The estimates for the inactive cribs, trenches, reverse well and drain fields come from the SIM Rev. 1 database cited in the report. The estimates for the single-shell tanks that released waste fluids to the subsurface come from the tank farm contractor's tank leak reassessment documents cited in the main text. The Mass Inventory Roll Up spreadsheet sums the volumes released and mass inventories by subregion or tank farm and compares the sums to the totals for the T Complex such that percentages can be calculated. These percentages were used in the report to identify which specific disposal units (cribs, trenches, SSTs) contributed the most volume released and most inventory of contaminants to the subsurface. Based on these volumes, masses and distances of lateral spread, pore volume calculations were made that aid in determining how deep in the vadose zone mobile contaminants may have reached. In many cases calculations suggested that wastes likely reached the water table and these findings were compared with the historical groundwater contaminant plumes to see if there is agreement. The final suite of worksheets list details on the waste types that were placed in each disposal facility.

This page intentionally left blank.

Table A-1. S Complex Area Waste Site Dimensions

Facility Name	Facility Type	Elevation of Ground Surface from Bechtel Drawings (ft MSL)	Elevation of Ground Surface from Bechtel Drawings (m MSL)	Top Length/ Diameter (ft)	Top Width (ft)	Bottom Length/ Diameter (ft)	Bottom Width (ft)	Total Crib Box Volume (ft^3)	Height/ Depth (ft)	Overburden (ft)	Top Footprint Area (ft^2)	Top Footprint Area (m^2)	Bottom Footprint Area (ft^2)	Bottom Footprint Area (m^2)	Top (ft bgs)	Bottom (ft bgs)	Top of Gravel (ft bgs)	Bottom of Gravel (ft bgs)	Thickness of Gravel (ft)	Bottom Elevation (m MSL)	Date of WIDS report	Notes	Facility Aliases	Source
216-S-9	Crib	678	206.7	319.1	51	298.1	30		7	23	16274.1	1511.8639	8943.0000	830.8047	23	30	23	30	7	197.5	8/24/2010		216-S-9 crib	Waste site dimensions from Bechtel Waste Summary Sheets/Misc site info from WIDS
216-S-13	Crib	669.5	204.1	40	40	20	20	1296	10	23.5	1600	148.6400	400.0000	37.1600	23.5	33.5	23.5	33.5	10	193.9	8/24/2010		276-S Crib, 216-S-6	Waste site dimensions from Bechtel Waste Summary Sheets/Misc site info from WIDS
216-S-14	Trench	670	204.2	109	17	100	8	4800	3	3	1853	172.1437	800.0000	74.3200	3	6	3	6	3	202.4	8/24/2010		Buried Contaminated Hexone, Cold Organic Trench or Grave, 216-T-3 Crib	Waste site dimensions from Bechtel Waste Summary Sheets/Misc site info from WIDS
216-S-21	Crib	661	201.5	70	70	50	50	2048	10	12.1	4900	455.2100	2500.0000	232.2500	12.1	22.1	12.1	22.1	10	194.7	8/25/2010		216-SX-1, 216-SX-1 Cavern or Crib	Waste site dimensions from Bechtel Waste Summary Sheets/Misc site info from WIDS
216-S-23	Crib	684	208.5	364	14	360	10		2	28	5096	473.4184	3600.0000	334.4400	28	30	28	30	2	199.3	6/21/2010	This crib was built to replace the 216-S-9 Crib. The 216-S-23 pipeline was tied into the 216-S-9 pipeline. This crib is located NE of 2410SY Tank Farm and North of 216-S-9 crib.	216-S-23 Crib	Waste site dimensions from Bechtel Waste Summary Sheets/Misc site info from WIDS
216-S-25	Crib	660	201.2	583	18	575	10		4	6	10494	974.8926	5750.0000	534.1750	6	10	6	10	4	198.1	9/15/2009	In 1985, this crib received the effluent from the 216-U-1 & 2 groundwater pump and treat effort. The 241-SX Sludge Cooler Steam Heater was shut off in 1992 due to leaking tubes. A new steam heater unit was installed in 1993 and scheduled to start up in 1995. It was to operate for five months (through winter and early spring) producing approximately 15 to 30 liters (4-8 gallons) of condensate per hour that would be discharged to the 216-S-25 crib.	216-S-25 Crib	Waste site dimensions from Bechtel Waste Summary Sheets/Misc site info from WIDS

Table A-2. Volume and Mass of Constituents Disposed of to the S Complex Area

Facility	Year	Vol. Disposed (million L)	Summation Inventory (kg)-Mean Value											Summation Inventory (Ci)-Mean Values							
			Na	Ca	K	NO3	NO2	CO3	PO4	SO4	F	U-Total	Cr	Co-60-Decay 1/1/2001	Co-60-Decay 9/30/2010*	I-129	Tc-99	H-3 Decay 1/1/2001	H-3-Decay 9/30/2010*	Pu-238	Pu-239
216-S-9 Operational 1965-1969, Waste Type REDOX D-1 (R2), REDOX D-2 (R2)																					
216-S-9	1965	10.0010569	179.77206	0	0	10123.318	0	0	0	0	0	66.76900093	0	0.002722407	**0.0007559**	0.008935335	0.025135072	235.5799724	**136.160375**	0.048119078	0.701356122
216-S-9	1966	18.4800218	332.20355	0	0	18706.813	0	0	0	0	0	123.373868	0	0.005032678	**0.00139737**	0.016502363	0.046402387	435.7785673	**251.871042**	0.088630624	1.295962767
216-S-9	1967	9.066037051	121.96193	0	0	6868.1848	0	0	0	0	0	45.3125848	0	0.001846904	**0.00051281**	0.004032408	0.017056306	213.7116882	**123.520957**	0.032581008	0.476261957
216-S-9	1968	11.94927232	107.32997	0	0	6044.3715	0	0	0	0	0	39.85928051	0	0.001624784	**0.00045114**	0	0.014997193	281.5498855	**162.730039**	0.028590607	0.419124922
216-S-9	1969	0.083269805	0.7479145	0	0	42.116805	0	0	0	0	0	0.277916203		1.13323E-05	**3.1465E-06**	0	0.000104562	1.963335667	**1.1347676**	0.00020002	0.002918243
216-S-9 Summation		49.57965788	742.01542	0	0	41784.804	0	0	0	0	0	277.5926505	0	0.011238106	**0.00312037**	0.029470106	0.10369552	1168.583449	**675.41718**	0.198121337	2.895624011
216-S-13 Operational 1951-1966, Waste Type Dil Misc UNH Streams (R1), REDOX Cold Start (R1) Org, REDOX (R1) Org, Dil Misc UNH Streams (R2), REDOX (R2) Org																					
216-S-13	1951	0.634000518	915.11472	1.3819203	788.77826	1965.9471	252.19535	0.180459293	17.037308	1.4851124	1.571737906	0.554694661	2.2136696	0	**0**	0	0	1.005212436	**0.5809921**	3.1857E-08	1.6774E-06
216-S-13	1952	0.704000093	1016.0829	1.5344764	875.8393	2182.7137	280.05629	0.200282131	18.913228	1.6493973	1.745706174	0.616370282	2.4575952	0	**0**	0	0	1.115470508	**0.64471899**	3.54023E-08	1.86161E-06
216-S-13	1953	0.704001154	1016.1133	1.5346379	876.0239	2183.0114	280.04772	0.200381761	18.912374	1.6491942	1.745491641	0.615894419	2.4574675	0	**0**	0	0	1.115979943	**0.64501344**	3.53685E-08	1.8624E-06
216-S-13	1954	0.704001545	1016.3836	1.5345342	875.64055	2182.9468	280.05021	0.200362996	18.914883	1.6491716	1.744901312	0.615809519	2.4576615	0	**0**	0	0	1.11508999	**0.64449906**	3.5397E-08	1.86417E-06
216-S-13	1955	0.529999609	765.05553	1.1552797	659.28802	1643.4874	210.83094	0.150828202	14.239763	1.2414712	1.313161477	0.463835183	1.8505773	0	**0**	0	0	0.839786388	**0.48537925**	2.66448E-08	1.40306E-06
216-S-13	1956	0.03000006	43.309142	0.0653912	37.327026	93.039337	11.931591	0.008535937	0.8059254	0.0702606	0.074327846	0.026217937	0.1047243	7.73197E-05	**2.1469E-05**	0	0.038910235	0.056867029	**0.03286797**	0.003012149	0.158977467
216-S-13	1957	0.046000118	8.2336491	0.8247314	510.20538	638.52558	3.7675891	0.001474132	11.121639	0.01908	1.026833248	0.00622167	0.0225291	8.83724E-05	**2.4537E-05**	0	0.019951966	0.98532538	**0.56949779**	0.001853103	0.027153744
216-S-13	1958	0.020000043	3.5796319	0.35859	221.82111	277.50813	1.6383556	0.000640831	4.8349768	0.0082963	0.446077319	0.002703267	0.0097964	3.83921E-05	**1.066E-05**	0	0.008679248	0.428015895	**0.24738438**	0.00080574	0.011773633
216-S-13	1959	0.020000026	3.5796686	0.3585744	221.77231	277.57656	1.6382545	0.000640825	4.8353843	0.0082955	0.446051761	0.002703804	0.0097956	3.83619E-05	**1.0652E-05**	0	0.00866812	0.428511076	**0.24767058**	0.000806673	0.011795537
216-S-13	1960	0.029000127	3.7830305	0.537654	332.71902	415.23028	1.6378269	0.000640819	7.2540826	0.0082953	0.669300792	0.003077156	0.0107766	3.84427E-05	**1.0674E-05**	0	0.008675481	0.64108405	**0.37053338**	0.000806932	0.011789542
216-S-13	1961	0.019999967	3.5796461	0.3585661	221.82815	277.53341	1.6383063	0.000640881	4.8349834	0.0082944	0.445965695	0.0027082	0.0097945	3.84467E-05	**1.0675E-05**	0	0.008679942	0.428268045	**0.24753011**	0.000803531	0.01179469
216-S-13	1962	0.021900049	3.7793342	0.3944256	244.04711	305.19683	1.7202137	0.000672863	5.3196006	0.0087105	0.491013714	0.002877645	0.0103839	4.02885E-05	**1.1187E-05**	0	0.009126191	0.47070004	**0.27205493**	0.000845706	0.012393911
216-S-13	1963	0.016200045	3.1815033	0.2868827	177.44688	222.25269	1.4746791	0.000576843	3.8670464	0.0074671	0.357121019	0.002361013	0.0086204	3.45852E-05	**9.6029E-06**	0	0.007805978	0.343263459	**0.19839921**	0.000727685	0.010608713
216-S-13	1964	0.969999796	97.786061	18.345498	11355.452	14154.082	39.730878	0.015544693	247.48823	0.2012011	22.85257628	0.085653122	0.2904861	0.00093088	**0.00025847**	0	0.210176589	21.7979725	**12.5987794**	0.019583725	0.28569993
216-S-13	1965	0.440001124	44.351564	8.3211877	5149.5083	6421.0512	18.019882	0.00704969	112.28969	0.0912453	10.35940929	0.038881998	0.1317732	0.000421989	**0.00011717**	0	0.095436027	9.880038661	**5.71045898**	0.008870786	0.129786201
216-S-13	1966	0.110000228	11.088128	2.0804288	1287.4745	1604.1474	4.5047188	0.001762059	28.075211	0.0228119	2.59050569	0.009723068	0.032939	0.000105743	**2.9361E-05**	0	0.023846465	2.471554479	**1.42850762**	0.002218908	0.032401105
216-S-13 Summation		4.999104502	4955.0013	39.072778	23835.172	34844.25	1390.8828	0.970493957	518.74433	8.1283049	47.88018116	3.049732944	12.07859	0.001852822	**0.00051445**	0	0.439956241	43.12313988	**24.9242872**	0.040335102	0.704183144
216-S-14 Operational 1952, Waste Types REDOX Cold Start (R1) Org																					
216-S-14	1952	0.076000051	121.68745	0.0160492	0.9933376	132.57055	33.592218	0.024029271	0	0.1977691	0	0.073577785	0.2938858	0	**0**	0	0	0	**0**	0	0
216-S-14 Summation		0.076000051	121.68745	0.0160492	0.9933376	132.57055	33.592218	0.024029271	0	0.1977691	0	0.073577785	0.2938858	0	**0**	0	0	0	**0**	0	0
216-S-21 Operational 1954-1969, Waste Types REDOX (R1) Tank Farm Cond, REDOX (R2) Tank Farm Cond, REDOX (P2') Tank Farm Cond, RSLT (R2), REDOX (P2') Tank Farm Cond																					
216-S-21	1954	0.14000005	0.3054204	2.7148968	0.1043532	0.0726785	0	0	0	1.9937443	0.035340101	4.22771E-05	0.0706829	1.16262E-07	**3.2281E-08**	0	0	4.074104156	**2.35474834**	1.43218E-06	7.53644E-05
216-S-21	1955	4.570000035	9.9698616	88.622449	3.4064105	2.3724928	0	0	0	65.081537	1.15324247	0.001380529	2.3071651	3.79333E-06	**1.0533E-06**	0	0	133.026319	**76.8864742**	4.67682E-05	0.002460377
216-S-21	1956	3.789999816	8.2682456	73.496581	2.8249979	1.9675107	0	0	0	53.97328	0.956569212	0.001144363	1.9135798	3.14638E-06	**8.7362E-07**	0	0	110.3341756	**63.7708824**	3.87418E-05	0.002040323
216-S-21	1957	7.160005545	15.620426	138.84783	5.3369353	3.717071	0	0	0	101.96511	1.807041631	0.002162137	3.6151979	5.94317E-06	**1.6502E-06**	0	0	208.3701247	**120.433643**	7.31785E-05	0.00385535
216-S-21	1958	7.930004204	17.300098	153.77877	5.910864	4.116759	0	0	0	112.93176	2.001566456	0.002395755	4.0040092	6.58472E-06	**1.8283E-06**	0	0	230.7906047	**133.392219**	0.000292175	0.004268185
216-S-21	1959	5.020004698	10.951733	97.347927	3.7418162	2.6060499	0	0	0	71.490478	1.266670059	0.001515569	2.5348976	4.16687E-06	**1.157E-06**	0	0	146.0464794	**84.411859**	0.000184891	0.002702927
216-S-21	1960	5.369999377	11.715174	104.13466	4.0026858	2.787786	0	0	0	76.474032	1.355109606	0.001621779	2.7109243	4.45681E-06	**1.2375E-06**	0	0	156.2603208	**90.315249**	0.000197652	0.002891035
216-S-21	1961	4.610004644	10.05717	89.397358	3.4362055	2.3932667	0	0	0	65.651611	1.163020572	0.001392459	2.3274692	3.82805E-06	**1.0629E-06**	0	0	134.1754922	**77.5506727**	0.000169872	0.002482553
216-S-21	1962	4.160000707	9.0754532	80.670741	3.1007729	2.1596399	0	0	0	59.242685	1.049862933	0.001255411	2.1007464	3.45264E-06	**9.5866E-07**	0	0	121.1534619	**70.0242072**	0.000153143	0.002240994
216-S-21	1963	5.160006997	11.257032	100.06314	3.8461505	2.6788381	0	0	0	73.483048	1.302165728	0.001557418	2.6052504	4.28315E-06	**1.1893E-06**	0	0	150.2125448	**86.819759**	0.000190047	0.002778434
216-S-21	1964	6.489999864	14.158751	125.85627	4.8374888	3.3691952	0	0	0	92.424731	1.63800271	0.00195928	3.2767697	5.39102E-06	**1.4969E-06**	0	0	188.788525	**109.115882**	0.000239177	0.003492643
216-S-21	1965	12.1000035	26.397355	234.64357	9.019105	6.2820129	0	0	0	172.31386	3.05346928	0.003655478	6.1112873	1.00476E-05	**2.7898E-06**	0	0	352.2751433	**203.607782**	0.000445833	0.00651675
216-S-21	1966	13.59999026	29.669748	263.73283	10.137145	7.0601758	0	0	0	193.67585	3.432413531	0.004107462	6.8657511	1.12945E-05	**3.136E-06**	0	0	395.9699531	**228.862482**	0.000500492	0.007321471
216-S-21	1967	6.320014286	13.787847	122.55802	4.710827	3.2807949	0	0	0	90.003886	1.595010716	0.001908624	3.1902294	5.2468E-06	**1.4568E-06**	0	0	183.9779143	**106.335448**	0.00023312	0.003403154
216-S-21	1968	0.011000019	261.21764	0.3896862	1.9920154	223.07999	103.68682	1.521551593	0.0514892	5.4034298	0.005265258	0.039930677	3.6019012	0.016724379	**0.00464369**	0.000161382	0.105380622	0.436546796	**0.25231506**	0.000258866	0.006602652
216-S-21	1969	0.70600059	262.8892	13.919841	2.5268646	223.45827	103.55942	1.522844028	0.0514724	12.802952	0.095615942	0.040361863	3.6028067	0.01683754	**0.00467512**	0.000161904	0.105462508	25.68652585	**14.8462832**	0.000280032	0.006766903

Table A-2. Volume and Mass of Constituents Disposed of to the S Complex Area

Facility	Year	Vol. Disposed (million L)	Summation Inventory (kg)-Mean Value											Summation Inventory (Ci)-Mean Values							
			Na	Ca	K	NO3	NO2	CO3	PO4	SO4	F	U-Total	Cr	Co-60-Decay 1/1/2001	Co-60-Decay 9/30/2010*	I-129	Tc-99	H-3 Decay 1/1/2001	H-3-Decay 9/30/2010*	Pu-238	Pu-239
216-S-21 Summation		87.13703459	712.64115	1690.1746	68.934638	491.40253	207.24625	3.044395621	0.1029616	1248.912	21.91036621	0.106391079	50.838668	0.033633671	0.00933873	0.000323286	0.21084313	2541.578236	1468.97991	0.003305419	0.059899116
216-S-23 Operational 1969-1972, Waste Type REDOX (R2) Cool Water																					
216-S-23	1969	12.70001989	165.47737	0.6439529	6.5160753	713.1746	632.38861	4.23636E-05	0	0.0003753	0	5.8385E-06	0.0004763	1.26586E-06	3.5148E-07	1.09113E-08	6.94724E-06	1.58163E-05	9.1415E-06	3.06192E-08	9.57812E-07
216-S-23	1970	8.820008153	114.91205	0.4471954	4.5254669	495.29472	439.19947	2.94219E-05	0	0.0002607	0	4.05385E-06	0.0003308	8.78906E-07	2.4404E-07	7.57698E-09	4.82647E-06	1.09843E-05	6.3487E-06	2.12375E-08	6.65017E-07
216-S-23	1971	7.170003457	93.419981	0.3635266	3.6787219	402.63419	357.02358	2.39185E-05	0	0.0002119	0	3.29571E-06	0.0002689	7.14259E-07	1.9832E-07	6.15719E-09	3.92374E-06	8.93032E-06	5.1615E-06	1.72849E-08	5.4064E-07
216-S-23	1972	5.379999743	70.094419	0.2727704	2.7604513	302.11098	267.89442	1.79465E-05	0	0.000159	0	2.47121E-06	0.0002018	5.35891E-07	1.488E-07	4.62052E-09	2.94265E-06	6.70048E-06	3.8727E-06	1.29925E-08	4.05853E-07
216-S-23 Summation		179.7340861	443.90382	1.7274454	17.480715	1913.2145	1696.5061	0.00011365	0	0.0010069	0	1.56593E-05	0.0012778	3.39491E-06	9.4263E-07	2.92659E-08	1.86401E-05	4.24314E-05	2.4524E-05	8.21341E-08	2.56932E-06
216-S-25 Operational 1973-1980 & 1985, Waste Types mostly 242-S Evap Cond (R2) with Last Year Dil Misc UNH Streams (P2) and 222-S Lab Waste Water (P3)																					
216-S-25	1973	6.960005403	15.183966	134.9687	5.1878582	3.6132571	0	0	0	99.117803	1.756509797	0.002100392	3.5143362	5.77727E-06	1.6041E-06	0	0	92.25862336	53.3235853	0.000256856	0.003747833
216-S-25	1974	71.2000416	155.32915	1380.7089	53.071047	36.962526	0	0	0	1013.9654	17.9699212	0.021517301	35.949867	5.91512E-05	1.6424E-05	0	0	943.290852	545.202696	0.002628382	0.038344924
216-S-25	1975	49.80008401	108.64315	965.72414	37.119834	25.853719	0	0	0	709.19679	12.57034804	0.015036904	25.146007	4.13498E-05	1.1481E-05	0	0	660.1932762	381.578125	0.001833098	0.026812757
216-S-25	1976	38.60004285	84.211017	748.53168	28.771726	20.038694	0	0	0	549.70515	9.739858982	0.011658827	19.48932	3.20489E-05	8.8987E-06	0	0	511.2417642	295.487217	0.001421531	0.020787091
216-S-25	1977	27.5000045	59.99425	533.28205	20.497983	14.275797	0	0	0	391.6274	6.940301921	0.008306406	13.881674	2.28345E-05	6.3402E-06	0	0	364.3213488	210.570241	0.001013067	0.014810701
216-S-25	1978	14.20001012	30.97843	275.36825	10.584386	7.3719547	0	0	0	202.22157	3.583555165	0.004287412	7.1707932	1.1791E-05	3.2739E-06	0	0	188.2211263	108.787937	0.000522898	0.00763648
216-S-25	1979	22.8000234	49.740382	442.12994	16.994714	11.836689	0	0	0	324.69322	5.754933781	0.006882451	11.510485	1.89333E-05	5.257E-06	0	0	302.3012086	174.723876	0.000840255	0.012267513
216-S-25	1980	25.39998553	55.41285	492.56343	18.932615	13.185979	0	0	0	361.73294	6.410111768	0.007671569	12.821812	2.108E-05	5.8531E-06	0	0	336.5326764	194.50896	0.000935032	0.013676701
216-S-25	1985	31.54003768	365.54282	579.43441	179188.59	222510.54	0	212.859433	3905.4758	224.97434	362.5655555	0.611053486	10.171158	1.95757E-05	5.4354E-06	0	0	223.9704949	129.450336	1.8886E-05	0.000388532
216-S-25 Summation		288.0002351	925.03602	5552.7115	179379.75	222643.68	0	212.859433	3905.4758	3877.2346	427.2910962	0.688514748	139.65545	0.000232542	6.4568E-05	0	0	3622.331371	2093.63297	0.009470006	0.13847253
241-S-104 Operational 1965, Waste Type CWR2 (CWR2)																					
241-S-104	1965	0.0908496	3816.33	13.6547	12.4994	4991.46	1202	20.4446	0	53.3694	0	2.81662	14.4666	2.18126	0.60564911	5.56E-05	0.0395868	25.4348	14.7007909	0.0117752	0.460288
241-S-104 Summation		0.0908496	3816.33	4.68206	8.72014	2151.59	1456.04	10.8651	0.142956	53.3694	0	2.81662	14.4666	2.18126	0.60564911	5.56E-05	0.0395868	25.4348	14.7007909	0.0117752	0.460288
241-SX-104 Operational 1988, Waste Types MW1 (BT1),MW2 (BT2),1C1 (BT1),1C2 (BT2),2C2 (BT2),TBP-UR (BT2),PFeCN1 (BT1),PFeCN2 (BT2),TFeCN (BT2),R1 (R1),CWR1 (CWR1),CWR2 (CWR2),PUREX P1 (P1),PUREX P2 (P2),PUREX PL1 (P1),CWP1 (CWP1),CWP2 (CWP2),CWZr1 (CWZr1),PUREX (P2) Org Waste aqu_OWW1,PUREX (P2) Org Waste aqu_OWW2,PUREX (P2') Org Waste aqu_OWW3,Sr-Cs Rec Waste (P1)_HS,TH1 (TH2),TH2 (TH2),Sr-Cs Rec Org Waste (P2)_B,Sr-Cs Rec Org Waste aqu (P2)_BL,Sr-Cs Rec Org Waste (P2')_CSR,Decon Waste (P1),1C Evap (BT2),RSLT (R2),T2-SltCk(P2'),BYSLT (BT2),PUREX (P2') Cool Water-Stream Condensate, PUREX (P2) Cool Water-Stream Condensate																					
241-SX-104	1988	0.0227124	6424.1606	3.2609364	67.477455	4645.5292	2459.1149	538.7542613	110.86257	255.33045	36.15676272	0.66752386	61.659251	0.514747315	0.14292485	0.004384081	4.510173265	0.6173352	0.35680704	0.003981712	0.109196145
241-SX-104 Summation		0.0227124	6424.1606	3.2609364	67.477455	4645.5292	2459.1149	538.7542613	110.86257	255.33045	36.15676272	0.66752386	61.659251	0.514747315	0.14292485	0.004384081	4.510173265	0.6173352	0.35680704	0.003981712	0.109196145
241-SX-107 Operational 1963, Waste Type RSLT (R2)																					
241-SX-107	1963	0.056781	14688.13	8.5323634	113.40222	12318.994	5926.0541	83.14587385	2.9441806	302.81342	0.226821145	1.760670151	163.48848	0.961419315	0.26694789	0.009282631	6.017696204	4.20583818	2.4308879	0.01124876	0.288215292
241-SX-107 Summation		0.056781	14688.13	8.5323634	113.40222	12318.994	5926.0541	83.14587385	2.9441806	302.81342	0.226821145	1.760670151	163.48848	0.961419315	0.26694789	0.009282631	6.017696204	4.20583818	2.4308879	0.01124876	0.288215292
241-SX-108 Operational 1966, Waste Type RSLT (R2)																					
241-SX-108	1966	0.132489	34270.751	19.907032	264.57391	28743.504	13826.477	194.0068062	6.8705595	706.52998	0.529240459	4.104756663	381.46735	2.24277767	0.62273012	0.021663666	14.03012924	9.815484056	5.67314775	0.026266165	0.672589354
241-SX-108 Summation		0.132489	34270.751	19.907032	264.57391	28743.504	13826.477	194.0068062	6.8705595	706.52998	0.529240459	4.104756663	381.46735	2.24277767	0.62273012	0.021663666	14.03012924	9.815484056	5.67314775	0.026266165	0.672589354
241-SX-109 Operational 1966, Waste Type RSLT (R2)																					
241-SX-109	1966	0.0075708	1958.3014	1.1377084	15.119001	1642.5477	790.02698	11.08598705	0.3925613	40.369523	0.03024127	0.234671843	21.797759	0.128231547	0.0356048	0.001237471	0.8018636	0.560588298	0.3240085	0.001495778	0.038464533
241-SX-109 Summation		0.0075708	1958.3014	1.1377084	15.119001	1642.5477	790.02698	11.08598705	0.3925613	40.369523	0.03024127	0.234671843	21.797759	0.128231547	0.0356048	0.001237471	0.8018636	0.560588298	0.3240085	0.001495778	0.038464533
241-SX-110 Operational 1976, Waste Types MW1 (BT1),MW2 (BT2),1C1 (BT1),1C2 (BT2),2C2 (BT2),TBP-UR (BT2),PFeCN1 (BT1),PFeCN2 (BT2),TFeCN (BT2),R1 (R1),CWR1 (CWR1),CWR2 (CWR2),PUREX P1 (P1),PUREX P2 (P2),PUREX PL1 (P1),CWP1 (CWP1),CWP2 (CWP2),CWZr1 (CWZr1),PUREX (P2) Org Waste aqu_OWW1,PUREX (P2) Org Waste aqu_OWW2,PUREX (P2') Org Waste aqu_OWW3,Sr-Cs Rec Waste (P1)_HS,TH1 (TH2),TH2 (TH2),Sr-Cs Rec Org Waste (P2)_B,Sr-Cs Rec Org Waste aqu (P2)_BL,Sr-Cs Rec Org Waste (P2')_CSR,Decon Waste (P1),1C Evap (BT2),RSLT (R2),T2-SltCk(P2'),BYSLT (BT2),PUREX (P2') Cool Water-Stream Condensate,PUREX (P2) Cool Water-Stream Condensate																					
241-SX-110	1976	0.0037854	317.0885	0.5477268	3.855289	286.45285	117.00012	33.14583135	5.4976722	24.135359	2.210011037	0.086664162	4.4330456	0.05763437	0.01600277	0.000258485	0.335125331	0.082583056	0.04773131	0.000571962	0.013755796
241-SX-110 Summation		0.0037854	317.0885	0.5477268	3.855289	286.45285	117.00012	33.14583135	5.4976722	24.135359	2.210011037	0.086664162	4.4330456	0.05763437	0.01600277	0.000258485	0.335125331	0.082583056	0.04773131	0.000571962	0.013755796
241-SX-111 Operational 1958, Waste Types MW1 (BT1),1C1 (BT1),1C2 (BT2),2C2 (BT2),TBP-UR (BT2),PFeCN1 (BT1),PFeCN2 (BT2),TFeCN (BT2),R1 (R1),CWR1 (CWR1),CWR2 (CWR2),PUREX P1 (P1),PUREX P2 (P2),PUREX PL1 (P1),CWP1 (CWP1),CWP2 (CWP2),CWZr1 (CWZr1),PUREX (P2) Org Waste aqu_OWW1,PUREX (P2) Org Waste aqu_OWW2,PUREX (P2') Org Waste aqu_OWW3,Sr-Cs Rec Waste (P1)_HS,TH1 (TH2),TH2 (TH2),Sr-Cs Rec Org Waste (P2)_B,Sr-Cs Rec Org Waste aqu (P2)_BL,Sr-Cs Rec Org Waste (P2')_CSR,Decon Waste (P1),1C Evap (BT2),RSLT (R2),T2-SltCk(P2'),BYSLT (BT2),PUREX (P2') Cool Water-Stream Condensate,PUREX (P2) Cool Water-Stream Condensate																					
241-SX-111	1958	0.0018927	175.43649	0.2814396	1.4594232	143.60705	70.453589	18.70616447	1.0150176	14.438298	0.070708436	0.055036995	2.8234893	0.039241628	0.01089584	0.000155632	0.227539483	0.048582345	0.0280796	0.000404261	0.0090024
241-SX-111 Summation		0.0018927	175.43649	0.2814396	1.4594232	143.60705	70.453589	18.70616447	1.0150176	14.438298	0.070708436	0.055036995	2.8234893	0.039241628	0.01089584	0.000155632	0.227539483	0.048582345	0.0280796	0.000404261	0.0090024

Table A-2. Volume and Mass of Constituents Disposed of to the S Complex Area

Facility	Year	Vol. Disposed (million L)	Summation Inventory (kg)-Mean Value											Summation Inventory (Ci)-Mean Values							
			Na	Ca	K	NO3	NO2	CO3	PO4	SO4	F	U-Total	Cr	Co-60-Decay 1/1/2001	Co-60-Decay 9/30/2010*	I-129	Tc-99	H-3 Decay 1/1/2001	H-3-Decay 9/30/2010*	Pu-238	Pu-239
241-SX-112 Operational 1969, Waste Type RSLT (R2)																					
241-SX-112	1969	No Information																			
241-SX-113 Operational 1958, Waste Types PUREX (P2) Cool Water-Stream Condition, R1 (R1)																					
241-SX-113	1958	0.056781001	7228.22	8.4767425	58.996272	7873.1421	1995.0844	12.71549256	0	104.43184	5.10949E-05	1.74760002	162.36916	0.11493825	**0.03191378**	0.002392245	1.494676175	1.558727597	**0.90091247**	0.005467864	0.288038197
241-SX-113 Summation		0.056781001	7228.22	8.4767425	58.996272	7873.1421	1995.0844	12.71549256	0	104.43184	5.10949E-05	1.74760002	162.36916	0.11493825	0.03191378	0.002392245	1.494676175	1.558727597	0.90091247	0.005467864	0.288038197
241-SX-115 Operational 1965, Waste Types R1 (R1), R2 (R2), CWR1 (CWR1), CWR2 (CWR2), RSLT (R2), PUREX (P2) Cool Water-Stm Cond																					
241-SX-115	1965	0.189269986	14902.807	28.334398	84.63704	14267.783		44.1478721	0.0701002	262.31229	0.005509646	5.842252018	237.48327	3.262065234	**0.90574571**	0.007047984	4.532024348	38.33806769	**22.158614**	0.032841794	0.956084863
241-SX-115 Summation		0.189269986	14902.807	28.334398	84.63704	14267.783	6039.0864	44.1478721	0.0701002	262.31229	0.005509646	5.842252018	237.48327	3.262065234	0.90574571	0.007047984	4.532024348	38.33806769	22.158614	0.032841794	0.956084863

Notes:

shaded cells represent the total inventory summation (volume or mass) for each waste site.

Data in this spreadsheet are from SIM (RPP-26744, *Hanford Soil Inventory Model, Rev. 1*).

* Radiological isotope decayed mass to the date of 09/30/2010. Formula to calculate isotope decay is:

9.74 Years between SIM Report (1/1/2001) and DV-1 Cutoff Date (9/30/2010)			
Isotope	**1/2 life (yrs)**	**λ= ln2/t1/2**	**e-λt**
Cobalt-60	5.271	0.13150203	0.2776602
Tritium	12.32	0.05626195	0.5779794

SIM = soil inventory model

Table A-3. S Complex Area Waste Sites Cs-137 Decay Results (SIM Data)

Facility	Year	Vol Disposed (million L)	Vol Disposed (Gallons)	Summation Inventory (Ci) Mean Values	
				Cs-137 SIM decayed to 1/1/2001	Cs-137 (decayed to 9/30/2010)*
216-S-9	1965	10.0010569	2,642,008	14.65195197	11.7053
216-S-9	1966	18.4800218	4,881,920	27.04305692	21.6043
216-S-9	1967	9.066037051	2,395,001	9.93991495	7.9409
216-S-9	1968	11.94927232	3,156,674	8.747624902	6.9884
216-S-9	1969	0.083269805	21,998	0.060916082	0.0487
216-S-9 Summation		49.57965788	13,097,601	60.44346482	48.2875
			0		
216-S-13	1951	0.634000518	167,486	0.0000E+00	0.0000E+00
216-S-13	1952	0.704000093	185,978	0.0000E+00	0.0000E+00
216-S-13	1953	0.704001154	185,978	0.0000E+00	0.0000E+00
216-S-13	1954	0.704001545	185,978	0.0000E+00	0.0000E+00
216-S-13	1955	0.529999609	140,012	0.0000E+00	0.0000E+00
216-S-13	1956	0.03000006	7,925	10.77036229	8.6043
216-S-13	1957	0.046000118	12,152	6.655565471	5.3170
216-S-13	1958	0.020000043	5,283	2.895517874	2.3132
216-S-13	1959	0.020000026	5,283	2.894494518	2.3124
216-S-13	1960	0.029000127	7,661	2.898567726	2.3156
216-S-13	1961	0.019999967	5,283	2.898047754	2.3152
216-S-13	1962	0.021900049	5,785	3.040456384	2.4290
216-S-13	1963	0.016200045	4,280	2.605531026	2.0815
216-S-13	1964	0.969999796	256,248	70.30751229	56.1678
216-S-13	1965	0.440001124	116,236	31.84142484	25.4377
216-S-13	1966	0.110000228	29,059	7.969602176	6.3668
216-S-13 Summation		4.999104502	1,320,628	144.7770823	115.6605
216-S-14	1952	0.076000051	20,077	0.000E+00	0.000E+00
216-S-14 Summation		0.076000051	20,077	0.000E+00	0.000E+00
			0		
216-S-21	1954	0.14000005	36,984	6.21385E-08	4.964E-08
216-S-21	1955	4.570000035	1,207,270	2.02851E-06	1.621E-06
216-S-21	1956	3.789999816	1,001,215	1.68172E-06	1.344E-06
216-S-21	1957	7.160005545	1,891,479	3.17757E-06	2.539E-06
216-S-21	1958	7.930004204	2,094,892	3.51848E-06	2.811E-06
216-S-21	1959	5.020004698	1,326,149	2.22812E-06	1.780E-06
216-S-21	1960	5.369999377	1,418,608	2.3839E-06	1.904E-06
216-S-21	1961	4.610004644	1,217,838	2.04646E-06	1.635E-06
216-S-21	1962	4.160000707	1,098,959	1.84561E-06	1.474E-06
216-S-21	1963	5.160006997	1,363,134	2.29043E-06	1.830E-06
216-S-21	1964	6.489999864	1,714,482	2.8804E-06	2.301E-06
216-S-21	1965	12.1000035	3,196,493	5.36943E-06	4.290E-06
216-S-21	1966	13.59999026	3,592,749	6.03611E-06	4.822E-06
216-S-21	1967	6.320014286	1,669,576	2.8038E-06	2.240E-06
216-S-21	1968	0.011000019	2,906	313.2250722	250.2315
216-S-21	1969	0.70600059	186,506	314.6819445	251.3953
216-S-21 Summation		87.13703459	23,019,241	627.9070551	501.6268
216-S-25	1973	6.960005403	1,838,645	0	0.0000
216-S-25	1974	71.2000416	18,809,120	0	0.0000
216-S-25	1975	49.80008401	13,155,831	0	0.0000
216-S-25	1976	38.60004285	10,197,084	0	0.0000
216-S-25	1977	27.5000045	7,264,755	0	0.0000
216-S-25	1978	14.20001012	3,751,257	0	0.0000

Table A-3. S Complex Area Waste Sites Cs-137 Decay Results (SIM Data)

Facility	Year	Vol Disposed (million L)	Vol Disposed (Gallons)	Summation Inventory (Ci) Mean Values	
				Cs-137 SIM decayed to 1/1/2001	Cs-137 (decayed to 9/30/2010)*
216-S-25	1979	22.8000234	6,023,148	0	**0.0000**
216-S-25	1980	25.39998553	6,709,987	0	**0.0000**
216-S-25	1985	31.54003768	8,332,022	2.30026E-05	**0.0000**
216-S-25 Summation		**288.0002351**	76,081,850	2.30026E-05	**1.8376E-05**
241-S-104	1965	0.0908496	24,000	118.5817474	**94.7334**
241-SX-104	1988	0.0227124	6,000	5934.942001	**4741.3484**
241-SX-107	1963	0.056781	15,000	17912.52857	**14310.0873**
241-SX-108	1966	0.132489	35,000	41801.56649	**33394.7305**
241-SX-109	1966	0.0075708	2,000	2388.416251	**1908.0748**
241-SX-110	1976	0.0037854	1,000	141.7389007	**113.2334**
241-SX-111	1958	0.0018927	500	52.61567738	**42.0340**
241-SX-113	1958	0.056781001	15,000	4228.242926	**3377.8886**
241-SX-115	1965	0.189269986	50,000	14904.34342	**11906.8871**

Notes:

shaded cells represent the total inventory summation (volume or mass) for each waste site.

Data in this spreadsheet are from SIM (RPP-26744, *Hanford Soil Inventory Model, Rev. 1*).

* Radiological isotope decayed mass to the date of 09/30/2010. Formula to calculate isotope decay is:

9.74 Years between SIM Report (1/1/2001) and DV-1 Cutoff Date (9/30/2010)			
Isotope	**1/2 life (yrs)**	**λ= ln2/t1/2**	**e-λt**
Cesium-137	30.08	0.023043	0.798887

SIM = soil inventory model

Table A-4. S Complex Area Waste Sites and S-SX Single Shell Tanks - Mass Inventory Roll Up

Facility	Total Volume Disposed (ML)	Summation Inventory (kg)-Mean Values											Summation Inventory (Ci)-Mean Values									
		Na	Ca	K	NO3	NO2	CO3	PO4	SO4	F	U-Total	Cr	Co-60	Co-60 decay to 9/30/2010	I-129	Tc-99	H-3	H-3 decay to 9/30/2010	Pu-238	Pu-239	Cs-137	Cs-137 decay to 9/30/2010
216-S-9	49.579658	742.0154216	0	0	41784.804	0	0	0	0	0	275.5926505	0	0.0112381	0.003120375	0.02947	0.103696	1168.583	675.41718	0.198121	2.895624011	60.44346	48.28750
216-S-13	4.999105	4955.001323	39.072778	23835.17198	34844.2503	1390.882806	0.970493957	518.7443278	8.12830494	47.880181	3.049732944	12.07859	0.0018528	0.000514455	0	0.439956	43.12314	24.92428722	0.040335	0.704183144	144.77708	115.66054
216-S-14	0.076000	121.6874529	0.01604925	0.993337579	132.570546	33.59221767	0.024029271	0	0.19776913	0	0.073577785	0.293886	0	0	0	0	0	0	0	0	0.00000	0.00000
216-S-21	87.137035	712.641151	1690.17458	68.93463775	491.402531	207.2462452	3.044395621	0.102961585	1248.912	21.910366	0.106391079	50.83867	0.0336337	0.009338732	0.000323	0.210843	2541.578	1468.979906	0.003305	0.059899116	627.90706	501.62682
216-S-25	288.000235	925.0360193	5552.71154	179379.7485	222643.683	0	212.859433	3905.47576	3877.23456	427.2911	0.688514748	139.6555	0.0002325		0	0	3622.331		0.00947	0.13847253	0.00002	0.000018
S-SX Single Shell Tanks																						
241-S-104	0.090850	3816.33	0.00062316	0.980482	0.0743534	0.0564525	0	7.57508	53.3694	0	2.81662	14.4666	4.0167992	2.18126	5.56E-05	0.039587	0.02288	25.4348	0.011775		118.58175	94.73342
241-SX-104	0.022712	6424.160624	3.26093643	67.47745523	4645.5292	2459.114926	538.7542613	110.8625679	255.330448	36.156763	0.66752386	61.65925	17.12032	0.514747315	0.004384	4.510173	2.606787	0.6173352	0.003982		5934.94200	4741.34836
241-SX-107	0.056781	14688.12997	8.53236339	113.4022237	12318.9942	5926.054104	83.14587385	2.944180641	302.813424	0.2268211	1.760670151	163.4885	45.394246	0.961419315	0.009283	6.017696	3.478105	4.20583818	0.011249		17912.52857	14310.08728
241-SX-108	0.132489	34270.75123	19.9070321	264.5739125	28743.5042	13826.4766	194.0068062	6.870559461	706.529982	0.5292405	4.104756663	381.4674	105.9183	2.24277767	0.021664	14.03013	8.109126	9.815484056	0.026266		41801.56649	33394.73054
241-SX-109	0.007571	1958.30143	1.13770843	15.11900095	1642.5477	790.026982	11.08598705	0.392561254	40.3695232	0.0302413	0.234671843	21.79776	6.0523702	0.128231547	0.001237	0.801864	0.463461	0.560588298	0.001496		2388.41625	1908.07484
241-SX-110	0.003785	317.0885012	0.54772682	3.855289019	286.452845	117.0001206	33.14583135	5.497672175	24.1353592	2.210011	0.086664162	4.433046	1.2308804	0.05763437	0.000258	0.335125	0.193696	0.082583056	0.000572		141.73890	113.23337
241-SX-111	0.001893	175.4364873	0.28143961	1.459423189	143.607051	70.45358872	18.70616447	1.015017559	14.4382981	0.0707084	0.055036995	2.823489	0.7839706	0.039241628	0.000156	0.227539	0.131513	0.048582345	0.000404		52.61568	42.03398
241-SX-112	No Information	No Information	No Information	No Information	No Information	No Information	No Information	No Information	No Information	No Information	No Information	No Information	No Information	No Information	No Information	No Information	No Information	No Information	No Information	No Information	No Information	No Information
241-SX-113	0.056781	7228.219954	8.4767425	58.99627156	7873.14213	1995.084403	12.71549256	0	104.431837	5.11E-05	1.74760002	162.3692	45.083456	0.11493825	0.002392	1.494676	0.863892	1.558727597	0.005468		4228.24293	3377.88856
241-SX-115	0.189270	14902.80663	28.3343981	84.63704004	14267.7828	6039.086383	44.1478721	0.070100215	262.312291	0.0055096	5.842252018	237.4833	65.939653	3.262065234	0.007048	4.532024	2.619417	38.33806769	0.032842		14904.34342	11906.88709

This page intentionally left blank.

Table A-5. Waste Stream Identifiers (from SIM)

SIM Waste Stream Label	Supporting Information
1C Evap (BT2)	RPP-19822, *Hanford Defined Waste Model – Revision 5.0*
1C1 (BT1)	RPP-19822, *Hanford Defined Waste Model – Revision 5.0*
1C2 (BT2)	RPP-19822, *Hanford Defined Waste Model – Revision 5.0*
1CFeCN (BT2)	RPP-19822, *Hanford Defined Waste Model – Revision 5.0*
209-E Reflector Water (BT1)	WHC-EP-0342, Add. 31
209-E Reflector Water (BT2)	WHC-EP-0342, Add. 31
209-E Reflector Water (P1)	WHC-EP-0342, Add. 31
209-E Reflector Water (P2)	WHC-EP-0342, Add. 31
209-E Reflector Water (P2')	WHC-EP-0342, Add. 31
209-E Reflector Water (P3)	WHC-EP-0342, Add. 31
222-S Lab Waste (P1)	WHC-EP-0342, Add. 9 and Add. 13 w/scaling factors
222-S Lab Waste (P2)	WHC-EP-0342, Add. 9 and Add. 13 w/scaling factors
222-S Lab Waste (P2')	WHC-EP-0342, Add. 9 and Add. 13 w/scaling factors
222-S Lab Waste (P3)	WHC-EP-0342, Add. 9 and Add. 13 w/scaling factors
222-S Lab Waste Water (P2)	WHC-EP-0342, Add. 13 and Add. 10
222-S Lab Waste Water (P2')	WHC-EP-0342, Add. 13 and Add. 10
222-S Lab Waste Water (P3)	WHC-EP-0342, Add. 13 and Add. 10
222-S Lab Waste Water (R1)	WHC-EP-0342, Add. 13 and Add. 10
222-S Lab Waste Water (R2)	WHC-EP-0342, Add. 13 and Add. 10
224 (BT1)	RPP-19822, *Hanford Defined Waste Model – Revision 5.0*
224 (BT2)	RPP-19822, *Hanford Defined Waste Model – Revision 5.0*
231-Z Metal Lab (Z2)	WHC Internal Memorandum 12362-90-LHR-072; HNF-1989, Rev. 1; DOE/RL-91-58; HNF-1744
232-Z Inc (Z1)	WHC Internal Memorandum 12362-90-LHR-072; HNF-1989, Rev. 1; HNF-1744
232-Z Inc (Z2)	WHC Internal Memorandum 12362-90-LHR-072; HNF-1989, Rev. 1; HNF-1744
234-5Z (BT1) D-6	HNF-1744; WHC-EP-0342, Add. 8
234-5Z (Z1) D-6	HNF-1744; WHC-EP-0342, Add. 8
234-5Z (Z2) D-6	HNF-1744; WHC-EP-0342, Add. 8
242-A Cond (P2')	WHC-EP-0342, Add. 26
242-A Cond (P3)	WHC-EP-0342, Add. 26
242-A Cond_CT (P3)	WHC-EP-0342, Add. 26
242-B (BT2) Evap Cond	WHC-EP-0342, Add. 17
242-S Evap Cond (R2)	WHC-EP-0342, Add. 29
242-T Evap Cond (R2)	WHC-EP-0342, Add. 17
242-T Evap Cond (Z2)	WHC-EP-0342, Add. 29 w/misc derivation
242-Z Am Rec (Z2)	WHC Internal Memorandum 12362-90-LHR-072; HNF-1989, Rev. 1; *Laboratory Notebook – Biblio 709* (Mercer, 1986); HNF-1744
2C1 (BT1)	RPP-19822, *Hanford Defined Waste Model – Revision 5.0*
2C2 (BT2)	RPP-19822, *Hanford Defined Waste Model – Revision 5.0*
300 CW (Z1)	Mercer (1986) w/RPP-19822, *Hanford Defined Waste Model – Revision 5.0*
300 CW (Z2)	Mercer (1986) w/RPP-19822, *Hanford Defined Waste Model – Revision 5.0*
5-6 (BT1)	RPP-19822, *Hanford Defined Waste Model – Revision 5.0* with assumed dilution
5-6 (BT2)	RPP-19822, *Hanford Defined Waste Model – Revision 5.0* with assumed dilution
A1-SltCk(Z2)	RPP-19822, *Hanford Defined Waste Model – Revision 5.0*
A2-SltSlr(Z2)	Unused; RPP-19822, *Hanford Defined Waste Model – Revision 5.0*
BiPO4 (BT1) Chem Sewer	Derived from RPP-19822, *Hanford Defined Waste Model – Revision 5.0* sources

Table A-5. Waste Stream Identifiers (from SIM)

SIM Waste Stream Label	Supporting Information
BiPO4 (BT1) Cool Water-Stream Condensate	Derived from RPP-19822, *Hanford Defined Waste Model – Revision 5.0* sources
BiPO4 (BT1) Stack Drain	Derived from RPP-19822, *Hanford Defined Waste Model – Revision 5.0* sources
BiPO4 (BT2) Chem Sewer	Derived from RPP-19822, *Hanford Defined Waste Model – Revision 5.0* sources
BiPO4 (BT2) Cool Water-Stream Condensate	Derived from RPP-19822, *Hanford Defined Waste Model – Revision 5.0* sources
BiPO4 (BT2) Stack Drain	Derived from RPP-19822, *Hanford Defined Waste Model – Revision 5.0* sources
BYSLT (BT2)	RPP-19822, *Hanford Defined Waste Model – Revision 5.0*
CEM(NA)	Unused; RPP-19822, *Hanford Defined Waste Model – Revision 5.0*
Conc Misc UNH Streams (P1)	WHC-EP-0342, Add. 19 and RPP-19822, *Hanford Defined Waste Model – Revision 5.0* assumption
Conc Misc UNH Streams (P2)	WHC-EP-0342, Add. 19 and RPP-19822, *Hanford Defined Waste Model – Revision 5.0* assumption
Conc Misc UNH Streams (P2')	WHC-EP-0342, Add. 19 and RPP-19822, *Hanford Defined Waste Model – Revision 5.0* assumption
Conc Misc UNH Streams (P3)	WHC-EP-0342, Add. 19 and RPP-19822, *Hanford Defined Waste Model – Revision 5.0* assumption
Conc Misc UNH Streams (R1)	WHC-EP-0342, Add. 19 and RPP-19822, *Hanford Defined Waste Model – Revision 5.0* assumption
Conc Misc UNH Streams (R2)	WHC-EP-0342, Add. 19 and RPP-19822, *Hanford Defined Waste Model – Revision 5.0* assumption
CWP1 (CWP1)	RPP-19822, *Hanford Defined Waste Model – Revision 5.0*
CWP2 (CWP2)	RPP-19822, *Hanford Defined Waste Model – Revision 5.0*
CWR1 (CWR1)	RPP-19822, *Hanford Defined Waste Model – Revision 5.0*
CWR2 (CWR2)	RPP-19822, *Hanford Defined Waste Model – Revision 5.0*
CWZr1 (CWZr1)	RPP-19822, *Hanford Defined Waste Model – Revision 5.0*
CWZr2 (CWZr2)	Unused; RPP-19822, *Hanford Defined Waste Model – Revision 5.0*
DE(NA)	Unused; RPP-19822, *Hanford Defined Waste Model – Revision 5.0*
Decon Stack Drain (BT2)	Derived from RPP-19822, *Hanford Defined Waste Model – Revision 5.0* sources
Decon Stack Drain (R2)	Derived from RPP-19822, *Hanford Defined Waste Model – Revision 5.0* sources
Decon Waste (BT1)	Derived from RPP-19822, *Hanford Defined Waste Model – Revision 5.0* sources
Decon Waste (BT2)	Derived from RPP-19822, *Hanford Defined Waste Model – Revision 5.0* sources
Decon Waste (P1)	Derived from RPP-19822, *Hanford Defined Waste Model – Revision 5.0* sources
Decon Waste (P2)	Derived from RPP-19822, *Hanford Defined Waste Model – Revision 5.0* sources
Decon Waste (P2')	Derived from RPP-19822, *Hanford Defined Waste Model – Revision 5.0* sources
Decon Waste (P3)	Derived from RPP-19822, *Hanford Defined Waste Model – Revision 5.0* sources
Decon Waste (R1)	Defunct
Decon Waste (R2)	Derived from RPP-19822, *Hanford Defined Waste Model – Revision 5.0* sources
Dil Misc UNH Streams (BT2)	WHC-EP-0342, Add. 19
Dil Misc UNH Streams (P1)	WHC-EP-0342, Add. 19
Dil Misc UNH Streams (P2)	WHC-EP-0342, Add. 19
Dil Misc UNH Streams (P2')	WHC-EP-0342, Add. 19
Dil Misc UNH Streams (P3)	WHC-EP-0342, Add. 19
Dil Misc UNH Streams (R1)	WHC-EP-0342, Add. 19
Dil Misc UNH Streams (R2)	WHC-EP-0342, Add. 19
ITS Cool Water-Condensate (BT2)	Derived using average of 242-B and 242-S Condensates
Laundry Waste Water (BT1)	WHC-EP-0141-1; WHC-EP-0141-2; WHC-EP-0527; WHC-EP-0527-6 and -7; RHO-HS-SR-81-3 to RHO-HS-SR-86-3-4Q-LIQ
Laundry Waste Water (BT2)	WHC-EP-0141-1); WHC-EP-0141-2; WHC-EP-0527; WHC-EP-0527-6 and -7;

Table A-5. Waste Stream Identifiers (from SIM)

SIM Waste Stream Label	Supporting Information
	RHO-HS-SR-81-3 to RHO-HS-SR-86-3-4Q-LIQ
Laundry Waste Water (P2')	WHC-EP-0141-1; WHC-EP-0141-2; WHC-EP-0527; WHC-EP-0527-6 and -7; RHO-HS-SR-81-3 to RHO-HS-SR-86-3-4Q-LIQ
Laundry Waste Water (P3)	WHC-EP-0141-1; WHC-EP-0141-2; WHC-EP-0527; WHC-EP-0527-6 and -7; RHO-HS-SR-81-3 to RHO-HS-SR-86-3-4Q-LIQ
Laundry Waste Water (R2)	WHC-EP-0141-1; WHC-EP-0141-2; WHC-EP-0527; WHC-EP-0527-6 and -7; RHO-HS-SR-81-3 to RHO-HS-SR-86-3-4Q-LIQ
MW1 (BT1)	RPP-19822, *Hanford Defined Waste Model – Revision 5.0*
MW2 (BT2)	RPP-19822, *Hanford Defined Waste Model – Revision 5.0*
N Decon Waste (P2)	Derived from RPP-19822, *Hanford Defined Waste Model – Revision 5.0* sources
NIT(NA)	Unused; RPP-19822, *Hanford Defined Waste Model – Revision 5.0*
OrgSltCk(P2')	Defunct
P3AZ1(P3)	Unused; RPP-19822, *Hanford Defined Waste Model – Revision 5.0*
P3AZ2(P3)	Unused; RPP-19822, *Hanford Defined Waste Model – Revision 5.0*
PASF (P2)	RPP-19822, *Hanford Defined Waste Model – Revision 5.0*; HNF-1744
PASF (P2')	RPP-19822, *Hanford Defined Waste Model – Revision 5.0*; ARH-1972; HNF-1744
PASF (P3)	RPP-19822, *Hanford Defined Waste Model – Revision 5.0*; ARH-1972; HNF-1744
PFeCN1 (BT1)	RPP-19822, *Hanford Defined Waste Model – Revision 5.0*
PFeCN2 (BT2)	RPP-19822, *Hanford Defined Waste Model – Revision 5.0*
Powerhouse Waste Water (NA)	WHC-SD-LEF-RPT-001, Rev. 0
PUREX (all) Stack Drain WC	Reference Working Sheet - Waste Stream Workbook; Appendix D
PUREX (P1) Chem Sewer	WHC-EP-0342, Add. 2 scaled to timeframe
PUREX (P1) Cold Start	RPP-19822, *Hanford Defined Waste Model – Revision 5.0*
PUREX (P1) Cool Water-Stream Condensate	WHC-EP-0342, Add. 20 and 216-A-25 data; DOE/RL-92-05; and RHO-HS-SR-84-3-4Q-LIQ
PUREX (P1) Org Waste	RPP-19822, *Hanford Defined Waste Model – Revision 5.0*; HW-31000-DEL
PUREX (P1) Org Waste aqu_OWW1	RPP-19822, *Hanford Defined Waste Model – Revision 5.0*
PUREX (P1) Org Waste aqu_OWW2	RPP-19822, *Hanford Defined Waste Model – Revision 5.0*
PUREX (P1) Stack Drain	Derived from RPP-19822, *Hanford Defined Waste Model – Revision 5.0* sources
PUREX (P1) Tank Farm Cond	WHC-EP-0342, Add. 26
PUREX (P2) Chem Sewer	WHC-EP-0342, Add. 2 scaled to timeframe
PUREX (P2') Chem Sewer	WHC-EP-0342, Add. 2 scaled to timeframe
PUREX (P2) Cool Water-Stream Condensate	WHC-EP-0342, Add. 20 and 216-A-25 data; DOE/RL-92-05; and RHO-HS-SR-84-3-4Q-LIQ
PUREX (P2') Cool Water-Stream Condensate	WHC-EP-0342, Add. 20 and 216-A-25 data; DOE/RL-92-05; and RHO-HS-SR-84-3-4Q-LIQ
PUREX (P2) Org Waste	RPP-19822, *Hanford Defined Waste Model – Revision 5.0*; HW-31000-DEL
PUREX (P2') Org Waste	RPP-19822, *Hanford Defined Waste Model – Revision 5.0*; HW-31000-DEL
PUREX (P2) Org Waste aqu_OWW1	RPP-19822, *Hanford Defined Waste Model – Revision 5.0*
PUREX (P2) Org Waste aqu_OWW2	RPP-19822, *Hanford Defined Waste Model – Revision 5.0*
PUREX (P2') Org Waste aqu_OWW3	RPP-19822, *Hanford Defined Waste Model – Revision 5.0*
PUREX (P2) Stack Drain	Derived from RPP-19822, *Hanford Defined Waste Model – Revision 5.0* sources
PUREX (P2') Stack Drain	Derived from RPP-19822, *Hanford Defined Waste Model – Revision 5.0* sources
PUREX (P2) Tank Farm Cond	WHC-EP-0342, Add. 23
PUREX (P2') Tank Farm Cond	WHC-EP-0342, Add. 23
PUREX (P3) Chem Sewer	WHC-EP-0342, Add. 2
PUREX (P3) Cool Water-Stream Condensate	WHC-EP-0342, Add. 20 and 216-A-25 data; DOE/RL-92-05; and RHO-HS-SR-84-3-4Q-LIQ

Table A-5. Waste Stream Identifiers (from SIM)

SIM Waste Stream Label	Supporting Information
PUREX (P3) Process Cond	WHC-EP-0342, Add. 12
PUREX (P3) Stack Drain	Derived from RPP-19822, *Hanford Defined Waste Model – Revision 5.0* sources
PUREX (P3) Tank Farm Cond	WHC-EP-0342, Add. 23
PUREX P1 (P1)	RPP-19822, *Hanford Defined Waste Model – Revision 5.0*
PUREX P2 (P2)	RPP-19822, *Hanford Defined Waste Model – Revision 5.0*
PUREX P2' (P2')	Unused; RPP-19822, *Hanford Defined Waste Model – Revision 5.0*
PUREX P3 (P3)	Defunct
PUREX PL1 (P1)	RPP-19822, *Hanford Defined Waste Model – Revision 5.0*
PUREX PL2 (P3)	Unused; RPP-19822, *Hanford Defined Waste Model – Revision 5.0*
R1 (R1)	RPP-19822, *Hanford Defined Waste Model – Revision 5.0*
R2 (R2)	RPP-19822, *Hanford Defined Waste Model – Revision 5.0*
Recuplex (BT1) aqu	WHC Internal Memorandum 12362-90-LHR-072; HNF-1989, Rev. 1; Mercer (1986); HNF-1744
Recuplex (BT1) org.	WHC Internal Memorandum 12362-90-LHR-072; HNF-1989, Rev. 1; Mercer (1986); HNF-1744
Recuplex (Z1) aqu	WHC Internal Memorandum 12362-90-LHR-072; HNF-1989, Rev. 1; Mercer (1986); HNF-1744
Recuplex (Z1) org.	WHC Internal Memorandum 12362-90-LHR-072; HNF-1989, Rev. 1; Mercer (1986); HNF-1744
Recuplex (Z2) aqu	WHC Internal Memorandum 12362-90-LHR-072; HNF-1989, Rev. 1; Mercer (1986); HNF-1744
Recuplex (Z2) org.	WHC Internal Memorandum 12362-90-LHR-072; HNF-1989, Rev. 1; Mercer (1986); HNF-1744
REDOX (P2') Cool Water	Derived from RPP-19822, *Hanford Defined Waste Model – Revision 5.0* sources
REDOX (P2') Stack Drain	Derived from RPP-19822, *Hanford Defined Waste Model – Revision 5.0* sources
REDOX (P2') Tank Farm Cond	WHC-EP-0342, Add. 26
REDOX (P3) Stack Drain	Derived from RPP-19822, *Hanford Defined Waste Model – Revision 5.0* sources
REDOX (R1) Chem Sewer	Defunct
REDOX (R1) Cool Water	Derived from RPP-19822, *Hanford Defined Waste Model – Revision 5.0* sources
REDOX (R1) Org	Derived from RPP-19822, *Hanford Defined Waste Model – Revision 5.0* sources; HW-18700
REDOX (R1) Tank Farm Cond	WHC-EP-0342, Add. 29
REDOX (R2) Chem Sewer	Defunct
REDOX (R2) Cool Water	Derived from RPP-19822, *Hanford Defined Waste Model – Revision 5.0* sources
REDOX (R2) Org	Derived from RPP-19822, *Hanford Defined Waste Model – Revision 5.0* sources; HW-18700
REDOX (R2) Tank Farm Cond	WHC-EP-0342, Add. 29
REDOX Cold Start (R1)	Derived from RPP-19822, *Hanford Defined Waste Model – Revision 5.0* sources
REDOX Cold Start (R1) Org	Derived from RPP-19822, *Hanford Defined Waste Model – Revision 5.0* sources; HW-18700
REDOX D-1 (R1)	HW-59359; HW-60115; DOE/RL-91-60; HNF-1744; RHO-CD-673
REDOX D-1 (R2)	HW-59359; HW-60115; DOE/RL-91-60; HNF-1744; RHO-CD-673
REDOX D-2 (R1)	HW-59359; HW-60115; DOE/RL-91-60; HNF-1744; RHO-CD-673
REDOX D-2 (R2)	HW-59359; HW-60115; DOE/RL-91-60; HNF-1744; RHO-CD-673
REDOX Stack Drain (R1)	Derived from RPP-19822, *Hanford Defined Waste Model – Revision 5.0* sources
REDOX Stack Drain (R2)	Derived from RPP-19822, *Hanford Defined Waste Model – Revision 5.0* sources
RG Process (BT1)	WHC Internal Memorandum 12362-90-LHR-072; HNF-1989, Rev. 1; HNF-1744
RG Process (Z1)	Defunct

Table A-5. Waste Stream Identifiers (from SIM)

SIM Waste Stream Label	Supporting Information
RG Process (Z2)	Defunct
RSLT (R2)	RPP-19822, *Hanford Defined Waste Model – Revision 5.0*
S1-SltCk(P2')	RPP-19822, *Hanford Defined Waste Model – Revision 5.0*
S2-SltSlr(P2')	RPP-19822, *Hanford Defined Waste Model – Revision 5.0*
Salt Slurry(P2')	Unused; RPP-19822, *Hanford Defined Waste Model – Revision 5.0*
Spent Nitric Acid (BT2)	HW-31000-DEL w/misc derivation
Spent Nitric Acid (P1)	HW-31000-DEL
Spent Nitric Acid (P2)	HW-31000-DEL
Spent Nitric Acid (P2')	HW-31000-DEL
Spent Nitric Acid (P3)	HW-31000-DEL
Spent Nitric Acid (R1)	HW-31000-DEL w/misc derivation
Spent Nitric Acid (R2)	HW-31000-DEL w/misc derivation
Sr-Cs Rec (P1) Cool Water	WHC-EP-0342, Add. 22
Sr-Cs Rec (P1) Stack Drain	WHC-EP-0342, Add. 17; w/misc derivation
Sr-Cs Rec (P2') Chem Sewer	WHC-EP-0342, Add. 6
Sr-Cs Rec (P2) Cool Water	WHC-EP-0342, Add. 22
Sr-Cs Rec (P2') Cool Water	WHC-EP-0342, Add. 22
Sr-Cs Rec (P2) Stack Drain	WHC-EP-0342, Add. 17; w/misc derivation
Sr-Cs Rec (P2') Stack Drain	WHC-EP-0342, Add. 17; w/misc derivation
Sr-Cs Rec (P3) Chem Sewer	WHC-EP-0342, Add. 6
Sr-Cs Rec (P3) Cool Water	WHC-EP-0342, Add. 22
Sr-Cs Rec (P3) Stack Drain	WHC-EP-0342, Add. 17; w/misc derivation
Sr-Cs Rec (R1) Chem Sewer	WHC-EP-0342, Add. 6
Sr-Cs Rec (R1) Cool Water	WHC-EP-0342, Add. 22
Sr-Cs Rec (R2) Chem Sewer	WHC-EP-0342, Add. 6
Sr-Cs Rec Org Waste (P2)_B	RPP-19822, *Hanford Defined Waste Model – Revision 5.0*
Sr-Cs Rec Org Waste (P2')_CSR	RPP-19822, *Hanford Defined Waste Model – Revision 5.0*
Sr-Cs Rec Org Waste aqu (P2)_BL	RPP-19822, *Hanford Defined Waste Model – Revision 5.0*
Sr-Cs Rec Org Waste aqu(P2')_AR	RPP-19822, *Hanford Defined Waste Model – Revision 5.0*
Sr-Cs Rec Waste (P1)_HS	RPP-19822, *Hanford Defined Waste Model – Revision 5.0*
Sr-Cs Rec Waste (P2)_SRR	RPP-19822, *Hanford Defined Waste Model – Revision 5.0*
T2-SltCk(P2')	RPP-19822, *Hanford Defined Waste Model – Revision 5.0*
TBP-UR (BT2)	RPP-19822, *Hanford Defined Waste Model – Revision 5.0*
TBP-UR Org Waste (BT2)	RPP-19822, *Hanford Defined Waste Model – Revision 5.0* and HW-19140 w/derivation information
TFeCN (BT2)	RPP-19822, *Hanford Defined Waste Model – Revision 5.0*
TH1 (TH2)	RPP-19822, *Hanford Defined Waste Model – Revision 5.0*
TH2 (TH2)	RPP-19822, *Hanford Defined Waste Model – Revision 5.0*
Z Complex Chem Sewer (NA)	RHO Internal Letters 65930-86-T-090 and 65930-85-A-116
Z Complex Chem Sewer NCT (NA)	RHO Internal Letters 65930-86-T-090 and 65930-85-A-116
Z Complex Cool Water-Condensate (BT1)	WHC-EP-0342, Add. 8
Z Complex Cool Water-Condensate (Z1)	WHC-EP-0342, Add. 8
Z Complex Cool Water-Condensate (Z2)	WHC-EP-0342, Add. 8
Z Complex Lab Waste (BT1)	WHC Internal Memorandum 12362-90-LHR-072; HNF-1989, Rev. 1; HNF-1744
Z Complex Lab Waste (Z1)	WHC Internal Memorandum 12362-90-LHR-072; HNF-1989, Rev. 1; HNF-1744
Z Complex Lab Waste (Z2)	WHC Internal Memorandum 12362-90-LHR-072; HNF-1989, Rev. 1; HNF-1744

Table A-5. Waste Stream Identifiers (from SIM)	
SIM Waste Stream Label	**Supporting Information**
Z Complex Stack Drain (BT1)	Assumed 1.1 dilution of Z Complex cooling water
Z Complex Stack Drain (Z1)	Assumed 1.1 dilution of Z Complex cooling water
Z Complex Stack Drain (Z2)	Assumed 1.1 dilution of Z Complex cooling water
Z Complex Stack Drain NCT (Z2)	Assumed 1.1 dilution of Z Complex cooling water
Z(Z2)	RPP-19822, *Hanford Defined Waste Model – Revision 5.0*

Table A-6. Hanford Defined Waste Streams (after Higley and Place 2004)

Waste Stream	Waste Type Description
Bismuth Phosphate Process Waste (1944-1956)	
MW1	$BiPO_4$ Metal Waste (1944-1949)-high fission product content
MW2	$BiPO_4$ Metal Waste (1950-1956)-high fission product content
1C1	$BiPO_4$ First cycle decontamination waste and Al cladding (coating) waste (1944-1949)
1C2	$BiPO_4$ First cycle decontamination waste and Al cladding (coating) waste (1950-1956)
2C1	$BiPO_4$ Second cycle decontamination waste (1944-1949)-low fission product content
2C2	$BiPO_4$ Second cycle decontamination waste (1950-1956) and low activity cell 5-6 drainage waste (June 1951-1956)
	Low activity cell 5-6 drainage waste (June 1951-1956) -all low fission product content
224-1	Lanthanum Fluoride process 224 Building waste (1944-1949)
224-2	Lanthanum Fluoride process 224 Building waste (1950-1956)
Uranium Recovery And Scavenging Waste (1952-1958)	
TBP (or UR)	Tributyl phosphate process waste (1952-1958), same as UR
PFeCN1	Ferrocyanide sludge from TBP in-plant scavenged supernatant and co-disposed TBP sludge (1954-1955).
PFeCN2	Ferrocyanide sludge from TBP in-plant scavenged supernatant and co-disposed TBP sludge (1955-1958).
TFeCN	Ferrocyanide sludge from supernatant scavenging in 244-CR Vault (1955-1958). These supernatants consisted of TBP supernatant and the commingled supernatants from other wastes stored in the same tanks.
1CFeCN	Ferrocyanide sludge from in-plant scavenging of T-Plant 1C waste (without coating waste). Transferred to TY-Farm (1955-1956).
Reduction And Oxidation (REDOX)"Process Waste(1952-1966)	
R1	REDOX high-level waste (1952-1958)
R2	REDOX high-level waste (1959-1966)
CWR1	REDOX cladding waste, aluminum clad fuel (1952-1960)
CWR2	REDOX cladding waste, aluminum clad fuel (1961-1966)
Plutonium-Uranium Extraction (PUREX) Process Waste Types (1956-1990)	
P1	PUREX high-activity waste (1956-1962)
P2	PUREX high-activity waste (1963-1967)
P2'	PUREX acid waste to B-Plant (1964-1972)
P3AZ1	PUREX high-activity waste to AZ-101 (1983-March 13, 1986)
P3AZ2	PUREX high-activity waste to AZ-102 (March 13, 1986 to 1990)
CWP1	PUREX cladding waste, aluminum clad fuel (1956-1960)
CWP2	PUREX cladding waste, aluminum clad fuel (1961-1972)
CWZr1	PUREX (and REDOX) zirconium cladding waste, (1968-1972)
CWZr2	PUREX zirconium cladding waste (1983-1989)
OWW1	PUREX organic wash waste and non-boiling waste (1956-1962)
OWW2	PUREX organic wash waste and non-boiling waste (1963-1967)
OWW3	PUREX organic wash waste (1968-1972)
PL1	PUREX non-boiling waste (1968-1972)
PL2	PUREX organic wash waste and non-boiling waste (1983-1988)
TH1	Thoria process wastes (1966)
TH2	Thoria process wastes (1970)
PASF	PUREX Ammonia Scrubber Feed
Cesium And Strontium Recovery Waste Types (1961-1985)	
HS	Hot Semiworks strontium purification waste (1961-1968)
AR	Water washed PUREX sludge entrained in decants of recovered sludge or the water washes of this sludge and the solids remaining after acidification (1967-1976).
B	B-Plant high-activity waste – Rare earth (RE) fission products, recovered current acid waste (CAW), solvent wash waste, and any solution containing high activity (including cask station receipts, cell drainage containing product spills) (1967-1972).
BL	B-Plant low-activity waste – 1AW solvent extraction waste stream (includes complexants added for solvent extraction), the
	1CP/organic wash waste during PAS processing, and insoluble solids remaining after treatment of solids centrifuged from
	CAW feed (i.e., acid leached and water washed PUREX high-level waste [HLW] sludge). Cell drainage and Waste
	Encapsulation Storage Facility (WESF) transfers with low radionuclide content (1967-1976).
SRR	High-activity waste from B-Plant processing of PUREX acidified sludge (PAS), solids centrifuged from AR vault feed, strontium purification wastes after solvent extraction (SX), RE or ion exchange (IX) rework, and other solutions containing activity (including cask station receipts, cell drainage containing product spills, WESF returns unsuitable for rework and crude product spills, WESF returns unsuitable for rework and crude RE disposal). (1969-1985)
CSR	Supernatants from which the cesium has been removed by ion-exchange. C-801 cask station (1962-1967). B-Plant Waste Fractionization (1967-1976)

Table A-6. Hanford Defined Waste Streams (after Higley and Place 2004)

Waste Stream	Waste Type Description
Other Process Facility Wastes	
Z	Plutonium Finishing Plant waste (1974-1988)
DW	Decontamination wastes, primarily from T Plant operations (1967-1976)
N	N Reactor decontamination waste (1976-1990)
Miscellaneous Wastes	
CEM	Portland cement added to tank BY-105
DE	Diatomaceous earth added to six tanks (BX-102, SX-113, TX-116, TX-117, TY-106, and U-104)
NIT	Partial neutralization feed for evaporator campaigns (1977-1981)
Saltcakes and Salt Slurries	
BT-SltCk	Saltcake from 242-B Evaporator operation (1951-1953) and the 242-T Evaporator operation (1951-1955). Formerly BSltCk and T1SltCk.
BYSltCk	Saltcake from in-tank solidification (ITS) in BY-Farm (1965-1974)
RSltCk	Saltcake from self-concentration in S- and SX-Farms (1952-1966)
T2SltCk	Saltcake from the last 242-T Evaporator campaign (1965-1976)
A1SltCk	Saltcake from the first 242-A Evaporator campaign using A-102 feed tank (1977-1980)
A2SltCk	Saltcake form the second 242-Evaporator campaign using AW-102 feed tank (1981-1988)
S1SltCk	Saltcake from the first 242-S Evaporator campaign using S-102 feed tank (1973-1976)
S2SltCk	Saltcake from the second 242-S Evaporator campaign using SY-102 feed tank (1977-1980)

Tables A-7 Through A-22
Annual Waste Site Specific Liquid and Solid Waste Disposal Volume Estimates Disposed of During Facility Operation (from SIM [RPP-26744, Rev. 1], Appendix D; table explanations and details are provided in Appendix A of SIM)

Table A-7a. 216-S-9

Site	Year	Waste Stream	Dist Type	Total Volume (ML)			Dist Type	Vol % Solids	
				Parm 1	Parm 2	Parm 3		Parm 1	Parm 2
216-S-9	1965	REDOX D-1 (R2)	1	1.12E-01	1.49E-01	1.86E-01	1	0.00E+00	0.00E+00
216-S-9	1965	REDOX D-2 (R2)	1	7.39E+00	9.85E+00	1.23E+01			
216-S-9	1966	REDOX D-1 (R2)	1	2.06E-01	2.75E-01	3.43E-01	1	0.00E+00	0.00E+00
216-S-9	1966	REDOX D-2 (R2)	1	1.37E+01	1.82E+01	2.28E+01			
216-S-9	1967	REDOX D-1 (R2)	1	5.03E-02	6.70E-02	8.38E-02	1	0.00E+00	0.00E+00
216-S-9	1967	REDOX D-2 (R2)	1	6.75E+00	9.00E+00	1.12E+01			
216-S-9	1968	REDOX D-2 (R2)	1	8.96E+00	1.19E+01	1.49E+01			
216-S-9	1969	REDOX D-2 (R2)	1	6.25E-02	8.33E-02	1.04E-01			

Table A-7b. 216-S-9

Waste Streams	Supernatants Dist Type	Density (g/mL)			Solids Dist Type	Density (g/mL)	
		Parm 1	Parm 2	Parm 3		Parm 1	Parm 2
REDOX D-1 (R2)	4	1.01E+00	1.01E-02	0.00E+00	4	1.79E+00	8.94E-02
REDOX D-2 (R2)	4	1.01E+00	1.01E-02	0.00E+00	4	1.79E+00	8.94E-02

Table A-8a. 216-S-13

Site	Year	Waste Stream	Dist Type	Total Volume (ML)		
				Parm 1	Parm 2	Parm 3
216-S-13	1951	Dil Misc UNH Streams (R1)	1	0.04755	0.0634	0.07925
216-S-13	1951	REDOX Cold Start (R1) Org	1	0.42795	0.5706	0.71325
216-S-13	1952	Dil Misc UNH Streams (R1)	1	0.0528	0.0704	0.088
216-S-13	1952	REDOX Cold Start (R1) Org	1	0.4752	0.6336	0.792
216-S-13	1953	Dil Misc UNH Streams (R1)	1	0.0528	0.0704	0.088
216-S-13	1953	REDOX Cold Start (R1) Org	1	0.4752	0.6336	0.792
216-S-13	1954	Dil Misc UNH Streams (R1)	1	0.0528	0.0704	0.088
216-S-13	1954	REDOX Cold Start (R1) Org	1	0.4752	0.6336	0.792
216-S-13	1955	Dil Misc UNH Streams (R1)	1	0.03975	0.053	0.06625
216-S-13	1955	REDOX Cold Start (R1) Org	1	0.35775	0.477	0.59625
216-S-13	1956	Dil Misc UNH Streams (R1)	1	0.00225	0.003	0.00375
216-S-13	1956	REDOX (R1) Org	1	0.02025	0.027	0.03375
216-S-13	1957	Dil Misc UNH Streams (R2)	1	0.03105	0.0414	0.05175
216-S-13	1957	REDOX (R2) Org	1	0.00345	0.0046	0.00575
216-S-13	1958	Dil Misc UNH Streams (R2)	1	0.0135	0.018	0.0225
216-S-13	1958	REDOX (R2) Org	1	0.0015	0.002	0.0025
216-S-13	1959	Dil Misc UNH Streams (R2)	1	0.0135	0.018	0.0225
216-S-13	1959	REDOX (R2) Org	1	0.0015	0.002	0.0025
216-S-13	1960	Dil Misc UNH Streams (R2)	1	0.02025	0.027	0.03375
216-S-13	1960	REDOX (R2) Org	1	0.0015	0.002	0.0025
216-S-13	1961	Dil Misc UNH Streams (R2)	1	0.0135	0.018	0.0225
216-S-13	1961	REDOX (R2) Org	1	0.0015	0.002	0.0025
216-S-13	1962	Dil Misc UNH Streams (R2)	1	0.01485	0.0198	0.02475
216-S-13	1962	REDOX (R2) Org	1	0.001575	0.0021	0.002625
216-S-13	1963	Dil Misc UNH Streams (R2)	1	0.0108	0.0144	0.018
216-S-13	1963	REDOX (R2) Org	1	0.00135	0.0018	0.00225
216-S-13	1964	Dil Misc UNH Streams (R2)	1	0.691125	0.9215	1.151875
216-S-13	1964	REDOX (R2) Org	1	0.036375	0.0485	0.060625
216-S-13	1965	Dil Misc UNH Streams (R2)	1	0.3135	0.418	0.5225
216-S-13	1965	REDOX (R2) Org	1	0.0165	0.022	0.0275
216-S-13	1966	Dil Misc UNH Streams (R2)	1	0.078375	0.1045	0.130625
216-S-13	1966	REDOX (R2) Org	1	0.004125	0.0055	0.006875

Table A-8b. 216-S-13

Waste Streams	Supernatants Dist Type	Density (g/mL)		
		Parm 1	Parm 2	Parm 3
Dil Misc UNH Streams (R1)	4	1.01E+00	1.01E-02	0.00E+00
REDOX Cold Start (R1) Org	4	0.79	0.079	0
REDOX (R1) Org	4	0.79	0.079	0
Dil Misc UNH Streams (R2)	4	1.01	0.0101	0
REDOX (R2) Org	4	0.79	0.079	0

Table A-9a. 216-S-14

Site	Year	Waste Stream	Dist Type	Total Volume (ML)		
				Parm 1	Parm 2	Parm 3
216-S-14	1952	REDOX Cold Start (R1) Org	1	6.84E-02	7.60E-02	8.36E-02

Table A-9b. 216-S-14

Waste Stream	Supernatants Dist Type	Density (g/mL)		
		Parm 1	Parm 2	Parm 3
REDOX Cold Start (R1) Org	4	7.90E-01		

Table A-10a. 216-S-21

Site	Year	Waste Stream	Dist Type	Total Volume (ML)		
				Parm 1	Parm 2	Parm 3
216-S-21	1954	REDOX (R1) Tank Farm Cond	1	0.126	0.14	0.154
216-S-21	1955	REDOX (R1) Tank Farm Cond	1	4.113	4.57	5.027
216-S-21	1956	REDOX (R1) Tank Farm Cond	1	3.411	3.79	4.169
216-S-21	1957	REDOX (R1) Tank Farm Cond	1	6.444	7.16	7.876
216-S-21	1958	REDOX (R2) Tank Farm Cond	1	7.137	7.93	8.723
216-S-21	1959	REDOX (R2) Tank Farm Cond	1	4.518	5.02	5.522
216-S-21	1960	REDOX (R2) Tank Farm Cond	1	4.833	5.37	5.907
216-S-21	1961	REDOX (R2) Tank Farm Cond	1	4.149	4.61	5.071
216-S-21	1962	REDOX (R2) Tank Farm Cond	1	3.744	4.16	4.576
216-S-21	1963	REDOX (R2) Tank Farm Cond	1	4.644	5.16	5.676
216-S-21	1964	REDOX (R2) Tank Farm Cond	1	5.841	6.49	7.139
216-S-21	1965	REDOX (R2) Tank Farm Cond	1	10.89	12.1	13.31
216-S-21	1966	REDOX (R2) Tank Farm Cond	1	12.24	13.6	14.96
216-S-21	1967	REDOX (R2) Tank Farm Cond	1	5.688	6.32	6.952
216-S-21	1968	REDOX (P2') Tank Farm Cond	1	0.009	0.01	0.011
216-S-21	1968	RSLT (R2)	1	0	0	0.003
216-S-21	1969	REDOX (P2') Tank Farm Cond	1	0.6345	0.705	0.7755
216-S-21	1969	RSLT (R2)	1	0	0	0.003

Table A-10b. 216-S-21

Waste Streams	Supernatants Dist Type	Density (g/mL)		
		Parm 1	Parm 2	Parm 3
REDOX (R1) Tank Farm Cond	4	1.01	0.0101	0
REDOX (R2) Tank Farm Cond	4	1.01E+00	1.01E-02	0.00E+00
REDOX (P2') Tank Farm Cond	4	1.01	0.0101	0
RSLT (R2)	4	1.510602	0.07553	0

Table A-11a. 216-S-23

Site	Year	Waste Stream	Dist Type	Total Volume (ML)			Dist Type	Vol % Solids		
				Parm 1	Parm 2	Parm 3		Parm 1	Parm 2	Parm 3
216-S-23	1969	REDOX (R2) Cool Water	1	1.14E+01	1.27E+01	1.40E+01	17	0.00E+00	0.00E+00	0.00E+00
216-S-23	1970	REDOX (R2) Cool Water	1	7.94E+00	8.82E+00	9.70E+00	17	0.00E+00	0.00E+00	0.00E+00
216-S-23	1971	REDOX (R2) Cool Water	1	6.45E+00	7.17E+00	7.89E+00	17	0.00E+00	0.00E+00	0.00E+00
216-S-23	1972	REDOX (R2) Cool Water	1	4.84E+00	5.38E+00	5.92E+00	17	0.00E+00	0.00E+00	0.00E+00

Table A-11b. 216-S-23

Waste Streams	Supernatants Dist Type	Density (g/mL)			Solids Dist Type	Density (g/mL)		
		Parm 1	Parm 2	Parm 3		Parm1	Parm2	Parm3
REDOX (R2) Cool Water	4	1.01E+00	1.01E-02	0.00E+00	17	0.00E+00	0.00E+00	0.00E+00

Table A-12a. 216-S-25

Site	Year	Waste Stream	Dist Type	Total Volume (ML)			Vol % Solids			
				Parm 1	Parm 2	Parm 3	Dist Type	Parm 1	Parm 2	Parm 3
216-S-25	1973	242-S Evap Cond (R2)	1	6.26E+00	6.96E+00	7.66E+00	17	0.00E+00	0.00E+00	0.00E+00
216-S-25	1974	242-S Evap Cond (R2)	1	6.41E+01	7.12E+01	7.83E+01	17	0.00E+00	0.00E+00	0.00E+00
216-S-25	1975	242-S Evap Cond (R2)	1	4.48E+01	4.98E+01	5.48E+01	17	0.00E+00	0.00E+00	0.00E+00
216-S-25	1976	242-S Evap Cond (R2)	1	3.47E+01	3.86E+01	4.25E+01	17	0.00E+00	0.00E+00	0.00E+00
216-S-25	1977	242-S Evap Cond (R2)	1	2.48E+01	2.75E+01	3.03E+01	17	0.00E+00	0.00E+00	0.00E+00
216-S-25	1978	242-S Evap Cond (R2)	1	1.28E+01	1.42E+01	1.56E+01	17	0.00E+00	0.00E+00	0.00E+00
216-S-25	1979	242-S Evap Cond (R2)	1	2.05E+01	2.28E+01	2.51E+01	17	0.00E+00	0.00E+00	0.00E+00
216-S-25	1980	242-S Evap Cond (R2)	1	2.29E+01	2.54E+01	2.79E+01	17	0.00E+00	0.00E+00	0.00E+00
216-S-25	1985	Dil Misc UNH Streams (P2)	1	1.31E+01	1.45E+01	1.60E+01	17	0.00E+00	0.00E+00	0.00E+00
216-S-25	1985	222-S Lab Waste Water (P3)	1	1.53E+01	1.70E+01	1.87E+01	17	0.00E+00	0.00E+00	0.00E+00

Table A-12b. 216-S-25

Waste Streams	Supernatants Dist Type	Density (g/mL)			Solids Dist Type	Density (g/mL)		
		Parm 1	Parm 2	Parm 3		Parm 1	Parm 2	Parm 3
242-S Evap Cond (R2)	4	1.01E+00	1.01E-02	0.00E+00	17	0.00E+00	0.00E+00	0.00E+00
222-S Lab Waste Water (P3)	4	1.01E+00	1.01E-02	0.00E+00	17	0.00E+00	0.00E+00	0.00E+00
Dil Misc UNH Streams (P2)	4	1.01E+00	1.01E-02	0.00E+00	17	0.00E+00	0.00E+00	0.00E+00

Table A-13a. 241-S-104

Site	Year	Waste Stream	Dist Type	Total Volume (ML)	
				Parm 1	Parm 2
241-S-104	1965	CWR2 (CWR2)	0	9.08E-02	1.00E-15

Table A-13b. 241-S-104

Waste Streams	Supernatants Dist Type	Density (g/mL)	
		Parm 1	Parm 2
CWR2 (CWR2)	4	1.08E+00	4.33E-02

Table A-14a. 241-SX-104

Site	Year	Waste Stream	Dist Type	Total Volume (ML)	
				Parm 1	Parm 2
241-SX-104	1988	MW1 (BT1)	0	1.38E-08	1.00E-15
241-SX-104	1988	MW2 (BT2)	0	3.46E-11	1.00E-15
241-SX-104	1988	1C1 (BT1)	0	5.68E-08	1.00E-15
241-SX-104	1988	1C2 (BT2)	0	6.20E-07	1.00E-15
241-SX-104	1988	2C1 (BT1)	0	1.92E-10	1.00E-15
241-SX-104	1988	2C2 (BT2)	0	5.65E-09	1.00E-15
241-SX-104	1988	224 (BT1)	0	8.16E-07	1.00E-15
241-SX-104	1988	TBP-UR (BT2)	0	3.74E-08	1.00E-15
241-SX-104	1988	PFeCN1 (BT1)	0	1.01E-09	1.00E-15
241-SX-104	1988	PFeCN2 (BT2)	0	1.20E-08	1.00E-15
241-SX-104	1988	TFeCN (BT2)	0	2.27E-08	1.00E-15
241-SX-104	1988	1CFeCN (BT2)	0	1.43E-09	1.00E-15
241-SX-104	1988	R1 (R1)	0	1.38E-05	1.00E-15
241-SX-104	1988	R2 (R2)	0	8.09E-07	1.00E-15
241-SX-104	1988	CWR1 (CWR1)	0	3.99E-07	1.00E-15
241-SX-104	1988	CWR2 (CWR2)	0	2.23E-08	1.00E-15
241-SX-104	1988	PUREX P1 (P1)	0	5.82E-07	1.00E-15
241-SX-104	1988	PUREX P2 (P2)	0	4.34E-07	1.00E-15
241-SX-104	1988	PUREX PL1 (P1)	0	2.54E-06	1.00E-15
241-SX-104	1988	CWP1 (CWP1)	0	2.88E-07	1.00E-15
241-SX-104	1988	CWP2 (CWP2)	0	2.90E-06	1.00E-15
241-SX-104	1988	CWZr1 (CWZr1)	0	2.16E-09	1.00E-15
241-SX-104	1988	PUREX (P2) Org Waste aqu_OWW1	0	1.55E-07	1.00E-15
241-SX-104	1988	PUREX (P2) Org Waste aqu_OWW2	0	2.96E-07	1.00E-15
241-SX-104	1988	PUREX (P2') Org Waste aqu_OWW3	0	1.61E-06	1.00E-15
241-SX-104	1988	Z(Z2)	0	2.46E-12	1.00E-15
241-SX-104	1988	Sr-Cs Rec Waste (P1)_HS	0	3.05E-07	1.00E-15
241-SX-104	1988	TH1 (TH2)	0	1.30E-10	1.00E-15
241-SX-104	1988	TH2 (TH2)	0	3.35E-08	1.00E-15
241-SX-104	1988	Sr-Cs Rec Org Waste aqu(P2')_AR	0	4.64E-06	1.00E-15
241-SX-104	1988	Sr-Cs Rec Org Waste (P2)_B	0	7.33E-07	1.00E-15
241-SX-104	1988	Sr-Cs Rec Org Waste aqu (P2)_BL	0	5.89E-05	1.00E-15
241-SX-104	1988	Sr-Cs Rec Waste (P2)_SRR	0	1.33E-05	1.00E-15
241-SX-104	1988	Sr-Cs Rec Org Waste (P2')_CSR	0	6.51E-05	1.00E-15
241-SX-104	1988	Decon Waste (P1)	0	4.46E-06	1.00E-15
241-SX-104	1988	N Decon Waste (P2)	0	2.36E-06	1.00E-15
241-SX-104	1988	1C Evap (BT2)	0	7.14E-07	1.00E-15
241-SX-104	1988	RSLT (R2)	0	1.53E-05	1.00E-15
241-SX-104	1988	T2-SltCk(P2')	0	6.23E-05	1.00E-15
241-SX-104	1988	BYSLT (BT2)	0	1.12E-06	1.00E-15
241-SX-104	1988	S1-SltCk(P2')	0	7.60E-03	1.00E-15
241-SX-104	1988	S2-SltSlr(P2')	0	1.40E-02	1.00E-15
241-SX-104	1988	PUREX (P2') Cool Water-Stream Condensate	0	7.74E-05	1.00E-15
241-SX-104	1988	PUREX (P2) Cool Water-Stream Condensate	0	7.58E-04	1.00E-15

Table A-14b. 241-SX-104

Waste Streams	Supernatants Dist Type	Density (g/mL)	
		Parm 1	Parm 2
MW1 (BT1)	4	1.10E+00	3.31E-02
MW2 (BT2)	4	1.10E+00	3.31E-02
1C1 (BT1)	4	1.13E+00	3.39E-02
1C2 (BT2)	4	1.13E+00	3.38E-02
2C1 (BT1)	4	1.10E+00	2.19E-02
2C2 (BT2)	4	1.06E+00	2.12E-02
224 (BT1)	4	1.09E+00	3.28E-02
TBP-UR (BT2)	4	1.21E+00	6.06E-02
PFeCN1 (BT1)	4	1.21E+00	6.04E-02
PFeCN2 (BT2)	4	1.21E+00	6.04E-02
TFeCN (BT2)	4	1.19E+00	5.95E-02
1CFeCN (BT2)	4	1.06E+00	2.13E-02
R1 (R1)	4	1.26E+00	6.32E-02
R2 (R2)	4	1.25E+00	6.24E-02
CWR1 (CWR1)	4	1.16E+00	5.80E-02
CWR2 (CWR2)	4	1.08E+00	4.33E-02
PUREX P1 (P1)	4	1.03E+00	2.06E-02
PUREX P2 (P2)	4	1.05E+00	2.11E-02
PUREX PL1 (P1)	4	1.18E+00	4.70E-02
CWP1 (CWP1)	4	1.10E+00	5.51E-02
CWP2 (CWP2)	4	1.07E+00	4.29E-02
CWZr1 (CWZr1)	4	1.03E+00	1.03E-02
PUREX (P2) Org Waste aqu_OWW1	4	1.03E+00	1.03E-02
PUREX (P2) Org Waste aqu_OWW2	4	1.06E+00	2.12E-02
PUREX (P2') Org Waste aqu_OWW3	4	1.08E+00	3.24E-02
Z(Z2)	4	1.18E+00	3.54E-02
Sr-Cs Rec Waste (P1)_HS	4	1.08E+00	3.24E-02
TH1 (TH2)	4	1.19E+00	5.93E-02
TH2 (TH2)	4	1.19E+00	5.93E-02
Sr-Cs Rec Org Waste aqu(P2')_AR	4	1.07E+00	4.27E-02
Sr-Cs Rec Org Waste (P2)_B	4	1.02E+00	1.02E-02
Sr-Cs Rec Org Waste aqu (P2)_BL	4	1.09E+00	2.19E-02
Sr-Cs Rec Waste (P2)_SRR	4	1.15E+00	4.58E-02
Sr-Cs Rec Org Waste (P2')_CSR	4	1.19E+00	5.96E-02
Decon Waste (P1)	4	1.01E+00	1.01E-02
N Decon Waste (P2)	4	1.02E+00	1.02E-02
1C Evap (BT2)	4	1.26E+00	6.29E-02
RSLT (R2)	4	1.51E+00	7.55E-02
T2-SltCk(P2')	4	1.48E+00	7.42E-02
BYSLT (BT2)	4	1.51E+00	7.55E-02
S1-SltCk(P2')	4	1.51E+00	7.55E-02
S2-SltSlr(P2')	4	1.57E+00	7.84E-02
PUREX (P2') Cool Water-Stream Condensate	4	1.01E+00	1.01E-02
PUREX (P2) Cool Water-Stream Condensate	4	1.01E+00	1.01E-02

Table A-15a. 241-SX-107

Site	Year	Waste Stream	Dist Type	Total Volume (ML)	
				Parm 1	Parm 2
241-SX-107	1963	RSLT (R2)	0	5.68E-02	1.00E-15

Table A-15b. 241-SX-107

Waste Streams	Supernatants Dist Type	Density (g/mL)	
		Parm 1	Parm 2
RSLT (R2)	4	1.51E+00	7.55E-02

Table A-16a. 241-SX-108

Site	Year	Waste Stream	Dist Type	Total Volume (ML)	
				Parm 1	Parm 2
241-SX-108	1966	RSLT (R2)	0	1.32E-01	1.00E-15

Table A-16b. 241-SX-108

Waste Streams	Supernatants Dist Type	Density (g/mL)	
		Parm1	Parm2
RSLT (R2)	4	1.51E+00	7.55E-02

Table A-17a. 241-SX-109

Site	Year	Waste Stream	Dist ype	Total Volume (ML)	
				Parm 1	Parm 2
241-SX-109	1966	RSLT (R2)	0	7.57E-03	1.00E-15

Table A-17b. 241-SX-109

Waste Streams	Supernatants Dist Type	Density (g/mL)	
		Parm 1	Parm 2
RSLT (R2)	4	1.51E+00	7.55E-02

Table A-18a. 241-SX-110

Site	Year	Waste Stream	Dist Type	Total Volume (ML)	
				Parm 1	Parm 2
241-SX-110	1976	MW1 (BT1)	0	5.78E-08	1.00E-15
241-SX-110	1976	MW2 (BT2)	0	5.27E-09	1.00E-15
241-SX-110	1976	1C1 (BT1)	0	1.22E-07	1.00E-15
241-SX-110	1976	1C2 (BT2)	0	9.82E-05	1.00E-15
241-SX-110	1976	2C1 (BT1)	0	2.79E-08	1.00E-15
241-SX-110	1976	2C2 (BT2)	0	3.69E-07	1.00E-15
241-SX-110	1976	224 (BT1)	0	1.32E-04	1.00E-15
241-SX-110	1976	TBP-UR (BT2)	0	2.04E-06	1.00E-15
241-SX-110	1976	PFeCN1 (BT1)	0	6.79E-09	1.00E-15
241-SX-110	1976	PFeCN2 (BT2)	0	1.22E-06	1.00E-15
241-SX-110	1976	TFeCN (BT2)	0	1.11E-07	1.00E-15
241-SX-110	1976	1CFeCN (BT2)	0	2.19E-07	1.00E-15
241-SX-110	1976	R1 (R1)	0	8.42E-06	1.00E-15
241-SX-110	1976	R2 (R2)	0	2.16E-05	1.00E-15
241-SX-110	1976	CWR1 (CWR1)	0	7.29E-06	1.00E-15
241-SX-110	1976	CWR2 (CWR2)	0	1.27E-06	1.00E-15
241-SX-110	1976	PUREX P1 (P1)	0	1.82E-06	1.00E-15
241-SX-110	1976	PUREX P2 (P2)	0	2.74E-05	1.00E-15
241-SX-110	1976	PUREX PL1 (P1)	0	1.42E-06	1.00E-15
241-SX-110	1976	CWP1 (CWP1)	0	1.33E-05	1.00E-15
241-SX-110	1976	CWP2 (CWP2)	0	9.59E-05	1.00E-15
241-SX-110	1976	CWZr1 (CWZr1)	0	1.05E-07	1.00E-15
241-SX-110	1976	PUREX (P2) Org Waste aqu_OWW1	0	5.15E-07	1.00E-15
241-SX-110	1976	PUREX (P2) Org Waste aqu_OWW2	0	2.93E-08	1.00E-15
241-SX-110	1976	PUREX (P2') Org Waste aqu_OWW3	0	1.32E-05	1.00E-15
241-SX-110	1976	Z(Z2)	0	4.50E-13	1.00E-15
241-SX-110	1976	Sr-Cs Rec Waste (P1)_HS	0	2.69E-07	1.00E-15
241-SX-110	1976	TH1 (TH2)	0	8.51E-09	1.00E-15
241-SX-110	1976	TH2 (TH2)	0	1.22E-06	1.00E-15
241-SX-110	1976	Sr-Cs Rec Org Waste aqu(P2')_AR	0	2.83E-07	1.00E-15
241-SX-110	1976	Sr-Cs Rec Org Waste (P2)_B	0	6.28E-06	1.00E-15
241-SX-110	1976	Sr-Cs Rec Org Waste aqu (P2)_BL	0	1.65E-04	1.00E-15
241-SX-110	1976	Sr-Cs Rec Org Waste (P2')_CSR	0	1.87E-03	1.00E-15
241-SX-110	1976	Decon Waste (P1)	0	7.92E-05	1.00E-15
241-SX-110	1976	N Decon Waste (P2)	0	8.21E-05	1.00E-15
241-SX-110	1976	1C Evap (BT2)	0	9.96E-05	1.00E-15
241-SX-110	1976	RSLT (R2)	0	4.88E-05	1.00E-15
241-SX-110	1976	T2-SltCk(P2')	0	1.79E-04	1.00E-15
241-SX-110	1976	BYSLT (BT2)	0	1.33E-04	1.00E-15
241-SX-110	1976	PUREX (P2') Cool Water-Stream Condensate	0	3.83E-04	1.00E-15
241-SX-110	1976	PUREX (P2) Cool Water-Stream Condensate	0	3.14E-04	1.00E-15

Table A-18b. 241-SX-110

Waste Streams	Supernatants Dist Type	Density (g/mL)	
		Parm 1	Parm 2
MW1 (BT1)	4	1.10E+00	3.31E-02
MW2 (BT2)	4	1.10E+00	3.31E-02
1C1 (BT1)	4	1.13E+00	3.39E-02
1C2 (BT2)	4	1.13E+00	3.38E-02
2C1 (BT1)	4	1.10E+00	2.19E-02
2C2 (BT2)	4	1.06E+00	2.12E-02
224 (BT1)	4	1.09E+00	3.28E-02
TBP-UR (BT2)	4	1.21E+00	6.06E-02
PFeCN1 (BT1)	4	1.21E+00	6.04E-02
PFeCN2 (BT2)	4	1.21E+00	6.04E-02
TFeCN (BT2)	4	1.19E+00	5.95E-02
1CFeCN (BT2)	4	1.06E+00	2.13E-02
R1 (R1)	4	1.26E+00	6.32E-02
R2 (R2)	4	1.25E+00	6.24E-02
CWR1 (CWR1)	4	1.16E+00	5.80E-02
CWR2 (CWR2)	4	1.08E+00	4.33E-02
PUREX P1 (P1)	4	1.03E+00	2.06E-02
PUREX P2 (P2)	4	1.05E+00	2.11E-02
PUREX PL1 (P1)	4	1.18E+00	4.70E-02
CWP1 (CWP1)	4	1.10E+00	5.51E-02
CWP2 (CWP2)	4	1.07E+00	4.29E-02
CWZr1 (CWZr1)	4	1.03E+00	1.03E-02
PUREX (P2) Org Waste aqu_OWW1	4	1.03E+00	1.03E-02
PUREX (P2) Org Waste aqu_OWW2	4	1.06E+00	2.12E-02
PUREX (P2') Org Waste aqu_OWW3	4	1.08E+00	3.24E-02
Z(Z2)	4	1.18E+00	3.54E-02
Sr-Cs Rec Waste (P1)_HS	4	1.08E+00	3.24E-02
TH1 (TH2)	4	1.19E+00	5.93E-02
TH2 (TH2)	4	1.19E+00	5.93E-02
Sr-Cs Rec Org Waste aqu(P2')_AR	4	1.07E+00	4.27E-02
Sr-Cs Rec Org Waste (P2)_B	4	1.02E+00	1.02E-02
Sr-Cs Rec Org Waste aqu (P2)_BL	4	1.09E+00	2.19E-02
Sr-Cs Rec Org Waste (P2')_CSR	4	1.19E+00	5.96E-02
Decon Waste (P1)	4	1.01E+00	1.01E-02
N Decon Waste (P2)	4	1.02E+00	1.02E-02
1C Evap (BT2)	4	1.26E+00	6.29E-02
RSLT (R2)	4	1.51E+00	7.55E-02
T2-SltCk(P2')	4	1.48E+00	7.42E-02
BYSLT (BT2)	4	1.51E+00	7.55E-02
PUREX (P2') Cool Water-Stream Condensate	4	1.01E+00	1.01E-02
PUREX (P2) Cool Water-Stream Condensate	4	1.01E+00	1.01E-02

Table A-19a. 241-SX-111

Site	Year	Waste Stream	Dist Type	Total Volume (ML)	
				Parm 1	Parm 2
241-SX-111	1958	MW1 (BT1)	0	5.37E-12	1.00E-15
241-SX-111	1958	1C1 (BT1)	0	1.30E-10	1.00E-15
241-SX-111	1958	1C2 (BT2)	0	9.47E-11	1.00E-15
241-SX-111	1958	2C1 (BT1)	0	3.02E-11	1.00E-15
241-SX-111	1958	2C2 (BT2)	0	4.32E-10	1.00E-15
241-SX-111	1958	TBP-UR (BT2)	0	9.12E-10	1.00E-15
241-SX-111	1958	PFeCN1 (BT1)	0	2.01E-10	1.00E-15
241-SX-111	1958	PFeCN2 (BT2)	0	1.00E-10	1.00E-15
241-SX-111	1958	TFeCN (BT2)	0	3.40E-10	1.00E-15
241-SX-111	1958	R1 (R1)	0	1.03E-05	1.00E-15
241-SX-111	1958	R2 (R2)	0	3.08E-05	1.00E-15
241-SX-111	1958	CWR1 (CWR1)	0	8.30E-08	1.00E-15
241-SX-111	1958	CWR2 (CWR2)	0	2.17E-11	1.00E-15
241-SX-111	1958	PUREX P1 (P1)	0	4.21E-09	1.00E-15
241-SX-111	1958	PUREX P2 (P2)	0	1.11E-08	1.00E-15
241-SX-111	1958	PUREX PL1 (P1)	0	9.13E-08	1.00E-15
241-SX-111	1958	CWP1 (CWP1)	0	1.98E-08	1.00E-15
241-SX-111	1958	CWP2 (CWP2)	0	5.28E-05	1.00E-15
241-SX-111	1958	PUREX (P2) Org Waste aqu_OWW1	0	3.29E-09	1.00E-15
241-SX-111	1958	PUREX (P2) Org Waste aqu_OWW2	0	5.34E-12	1.00E-15
241-SX-111	1958	PUREX (P2') Org Waste aqu_OWW3	0	5.37E-05	1.00E-15
241-SX-111	1958	Sr-Cs Rec Waste (P1)_HS	0	2.24E-08	1.00E-15
241-SX-111	1958	TH1 (TH2)	0	3.05E-10	1.00E-15
241-SX-111	1958	TH2 (TH2)	0	2.91E-07	1.00E-15
241-SX-111	1958	Sr-Cs Rec Org Waste (P2)_B	0	1.83E-06	1.00E-15
241-SX-111	1958	Sr-Cs Rec Org Waste aqu (P2)_BL	0	5.18E-05	1.00E-15
241-SX-111	1958	Sr-Cs Rec Org Waste (P2')_CSR	0	1.51E-03	1.00E-15
241-SX-111	1958	Decon Waste (P1)	0	2.29E-08	1.00E-15
241-SX-111	1958	1C Evap (BT2)	0	1.64E-08	1.00E-15
241-SX-111	1958	RSLT (R2)	0	6.13E-05	1.00E-15
241-SX-111	1958	T2-SltCk(P2')	0	4.90E-06	1.00E-15
241-SX-111	1958	BYSLT (BT2)	0	1.07E-06	1.00E-15
241-SX-111	1958	PUREX (P2') Cool Water-Stream Condensate	0	6.71E-05	1.00E-15
241-SX-111	1958	PUREX (P2) Cool Water-Stream Condensate	0	4.87E-05	1.00E-15

Table A-19b. 241-SX-111

Waste Streams	Supernatants Dist Type	Density (g/mL)	
		Parm 1	Parm 2
MW1 (BT1)	4	1.10E+00	3.31E-02
1C1 (BT1)	4	1.13E+00	3.39E-02
1C2 (BT2)	4	1.13E+00	3.38E-02
2C1 (BT1)	4	1.10E+00	2.19E-02
2C2 (BT2)	4	1.06E+00	2.12E-02
TBP-UR (BT2)	4	1.21E+00	6.06E-02
PFeCN1 (BT1)	4	1.21E+00	6.04E-02
PFeCN2 (BT2)	4	1.21E+00	6.04E-02
TFeCN (BT2)	4	1.19E+00	5.95E-02
R1 (R1)	4	1.26E+00	6.32E-02
R2 (R2)	4	1.25E+00	6.24E-02
CWR1 (CWR1)	4	1.16E+00	5.80E-02
CWR2 (CWR2)	4	1.08E+00	4.33E-02
PUREX P1 (P1)	4	1.03E+00	2.06E-02
PUREX P2 (P2)	4	1.05E+00	2.11E-02
PUREX PL1 (P1)	4	1.18E+00	4.70E-02
CWP1 (CWP1)	4	1.10E+00	5.51E-02
CWP2 (CWP2)	4	1.07E+00	4.29E-02
PUREX (P2) Org Waste aqu_OWW1	4	1.03E+00	1.03E-02
PUREX (P2) Org Waste aqu_OWW2	4	1.06E+00	2.12E-02
PUREX (P2') Org Waste aqu_OWW3	4	1.08E+00	3.24E-02
Sr-Cs Rec Waste (P1)_HS	4	1.08E+00	3.24E-02
TH1 (TH2)	4	1.19E+00	5.93E-02
TH2 (TH2)	4	1.19E+00	5.93E-02
Sr-Cs Rec Org Waste (P2)_B	4	1.02E+00	1.02E-02
Sr-Cs Rec Org Waste aqu (P2)_BL	4	1.09E+00	2.19E-02
Sr-Cs Rec Org Waste (P2')_CSR	4	1.19E+00	5.96E-02
Decon Waste (P1)	4	1.01E+00	1.01E-02
1C Evap (BT2)	4	1.26E+00	6.29E-02
RSLT (R2)	4	1.51E+00	7.55E-02
T2-SltCk(P2')	4	1.48E+00	7.42E-02
BYSLT (BT2)	4	1.51E+00	7.55E-02
PUREX (P2') Cool Water-Stream Condensate	4	1.01E+00	1.01E-02
PUREX (P2) Cool Water-Stream Condensate	4	1.01E+00	1.01E-02

Table A-20a. 241-SX-112

Site	Year	Waste Stream	Dist Type	Total Volume (ML)	
				Parm 1	Parm 2
241-SX-112	1969	RSLT (R2)	0	3.79E-03	1.00E-15

Table A-20b. 241-SX-112

Waste Streams	Supernatants Dist Type	Density (g/mL)	
		Parm1	Parm2
RSLT (R2)	4	1.51E+00	7.55E-02

Table A-21a. 241-SX-113

Site	Year	Waste stream	Dist Type	Total Volume (ML)	
				Parm 1	Parm 2
241-SX-113	1958	R1 (R1)	0	5.64E-02	1.00E-15
241-SX-113	1958	PUREX (P2) Cool Water-Stream Condensate	0	3.75E-04	1.00E-15

Table A-21b. 241-SX-113

Waste Streams	Supernatants Dist Type	Density (g/mL)	
		Parm 1	Parm 2
R1 (R1)	4	1.26E+00	6.32E-02
PUREX (P2) Cool Water-Stream Condensate	4	1.01E+00	1.01E-02

Table A-22a. 241-SX-115

Site	Year	Waste Stream	Dist Type	Total Volume (ML)	
				Parm 1	Parm 2
241-SX-115	1965	R1 (R1)	0	2.99E-02	1.00E-15
241-SX-115	1965	R2 (R2)	0	4.50E-02	1.00E-15
241-SX-115	1965	CWR1 (CWR1)	0	8.33E-03	1.00E-15
241-SX-115	1965	CWR2 (CWR2)	0	1.04E-01	1.00E-15
241-SX-115	1965	RSLT (R2)	0	1.35E-03	1.00E-15
241-SX-115	1965	PUREX (P2) Cool Water-Stream Condensate	0	8.00E-04	1.00E-15

Table A-22b. 241-SX-115

Waste Streams	Supernatants Dist Type	Density (g/mL)	
		Parm 1	Parm 2
R1 (R1)	4	1.26E+00	6.32E-02
R2 (R2)	4	1.25E+00	6.24E-02
CWR1 (CWR1)	4	1.16E+00	5.80E-02
CWR2 (CWR2)	4	1.08E+00	4.33E-02
RSLT (R2)	4	1.51E+00	7.55E-02
PUREX (P2) Cool Water-Stream Condensate	4	1.01E+00	1.01E-02

Appendix B

S Complex Area CSM Support Data

This page intentionally left blank.

200-DV-1 OU S-SX Complex Subregions

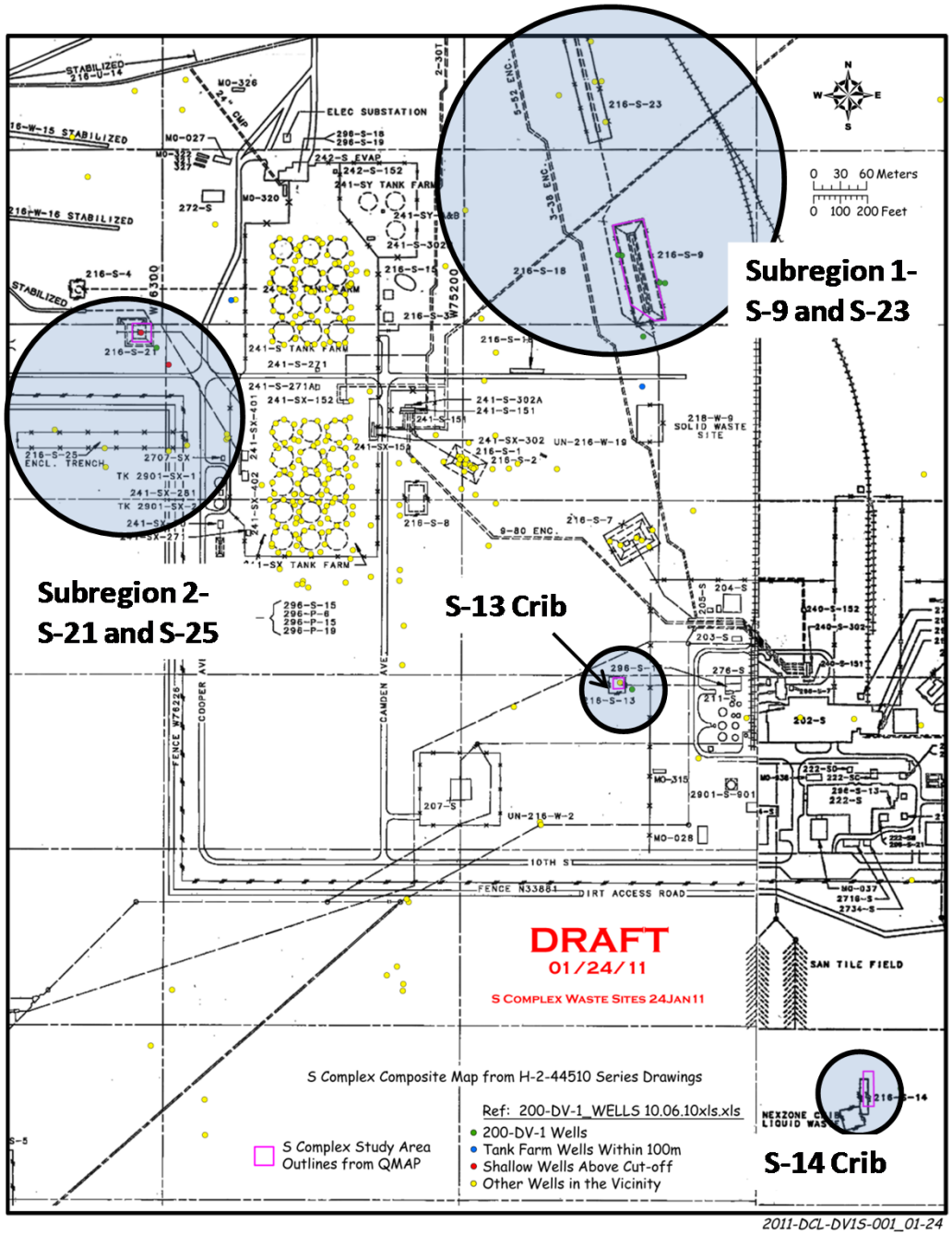

Volume Discharged to the 200-DV-1 OU Waste Sites in the S-SX Area Complex

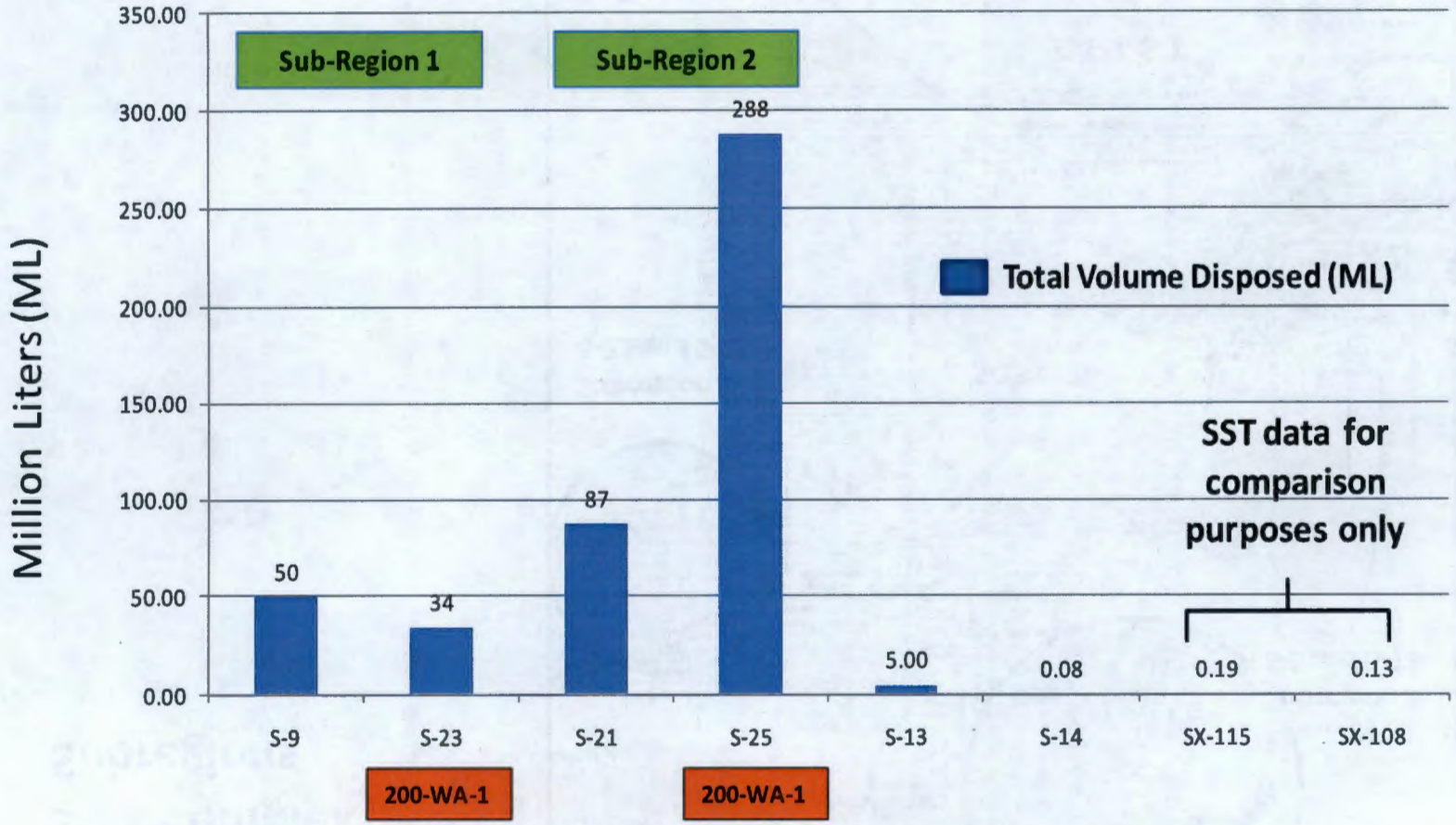

U.S. DEPARTMENT OF ENERGY

Comparison of Liquid Waste Volume Discharged to Available Vadose Zone Pore Volume for Each 200-DV-1 OU Waste Site in S-SX Area Complex

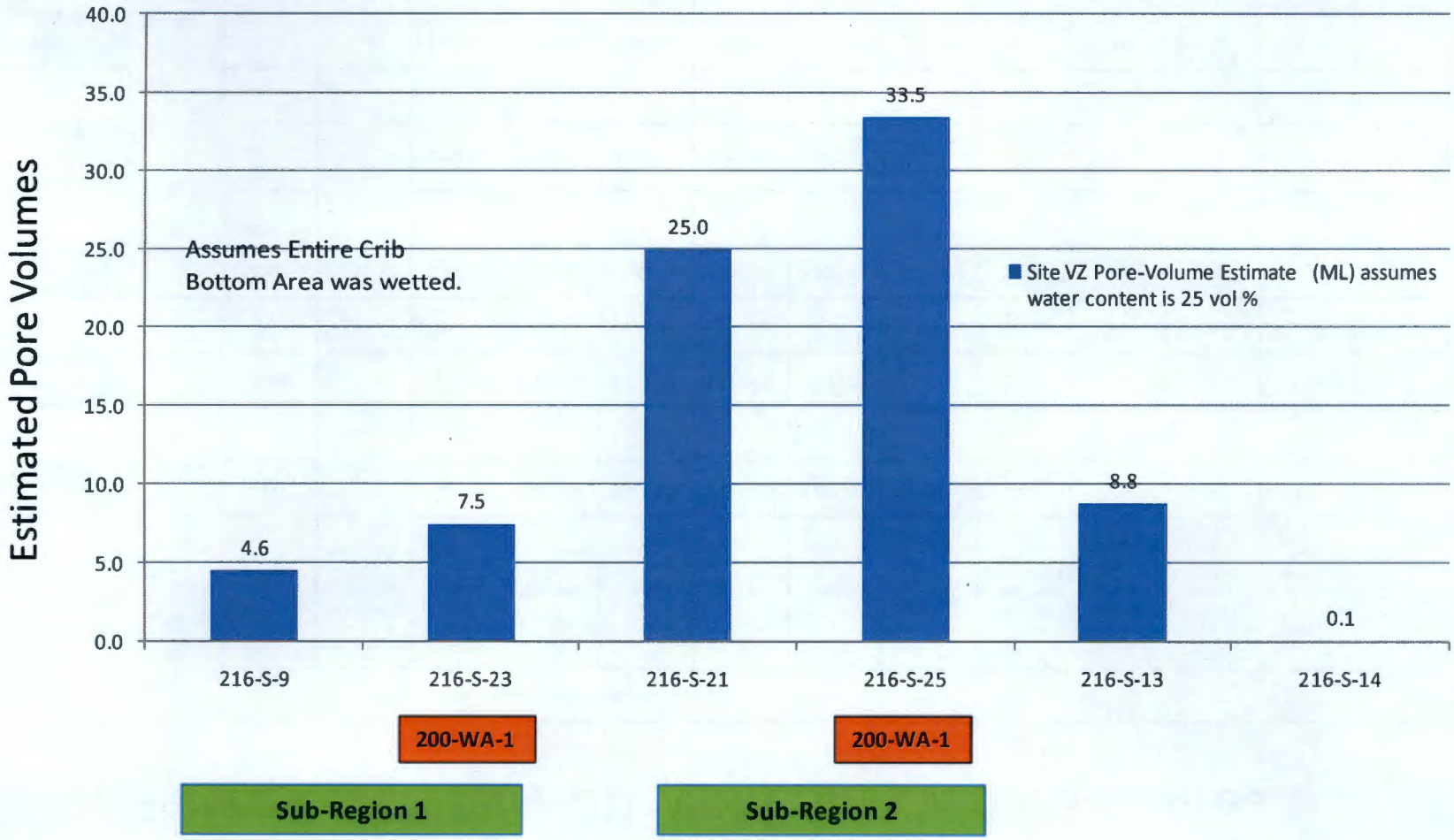

U.S. DEPARTMENT OF ENERGY

Total Mass/Activity of Constituents Discharged and Vadose Zone Extent for200-DV-1 OU Waste Sites in the S-SX Area

Sub region	DV-1 OU Waste Site	Source OU	Disposal Inventory (SIM) (Mean Estimates)												
			Vol disposed (ML)	Vol Disposed by Subregion (ML)	Tc-99 (Ci)	NO3 (kg)	U (kg)	I-129 (Ci)	Cr (kg)	Site Active (Years)	Footprint Area for Bottom (ft2)	Footprint Area for Bottom (m2)	Bottom of Facility (ft bgs)	Depth of Current unconfined Aquifer (ft bgs)	Length of VZ (ft) "bottom of facility" to water table
1	[redacted]	200-DV-1	49.58	83.68	1.04E-01	4.18E+04	2.76E+02	2.95E-02	0.00E+00	65-69(5)	8943	831	30	241	211
	[redacted]	200-WA-1	34.10		1.86E-05	1.91E+03	1.57E-05	2.93E-08	1.28E-03	69-72(4)	3600	334	30	241	211
2	[redacted]	200-DV-1	87.14	375.14	2.11E-01	4.91E+02	1.06E-01	3.23E-04	5.08E+01	54-69 (16)	2500	232	22	219	197
	[redacted]	200-WA-1	288.00		0.00E+00	2.23E+05	6.89E-01	0.00E+00	1.40E+02	73-80 & 85(9)	5750	534	10	221	211
	[redacted]	200-DV-1	5.00	5.00	4.40E-01	3.48E+04	3.05E+00	0.00E+00	1.21E+01	51-66 (16)	400	37	34	234	201
	[redacted]	200-DV-1	0.08	0.08	0.00E+00	1.33E+02	7.36E-02	0.00E+00	2.90E-01	52 (1)	800	74	6	236	230

U.S. DEPARTMENT OF ENERGY

Nitrate Inventory for 200-DV-1 (S-Area Complex)

Mean Nitrate Estimate with Uncertainty

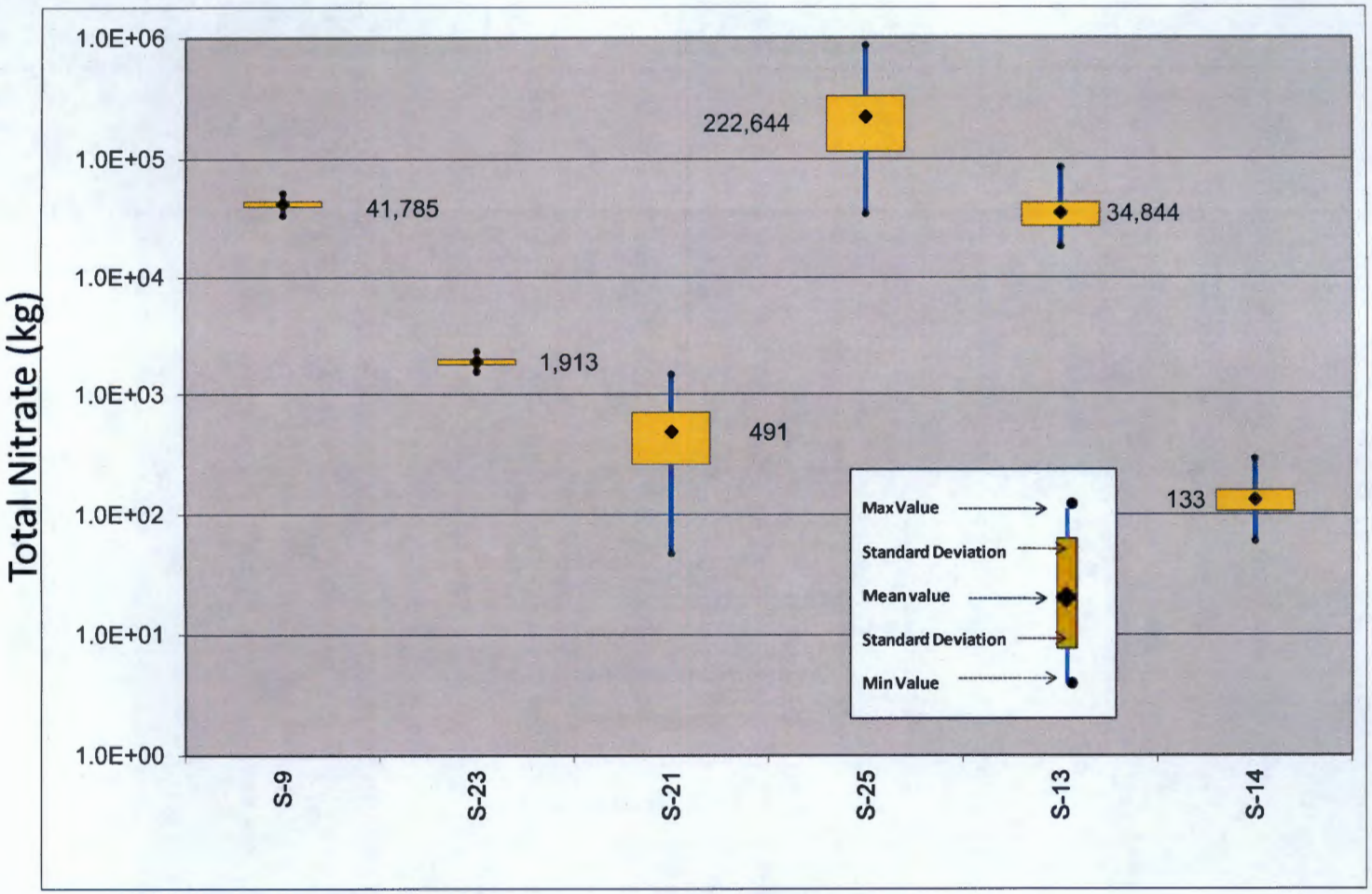

Sub-Region 1

Sub-Region 2

U.S. DEPARTMENT OF ENERGY

Uranium Inventory for 200-DV-1 (S-Area Complex)

Mean Total Uranium Estimate with Uncertainty

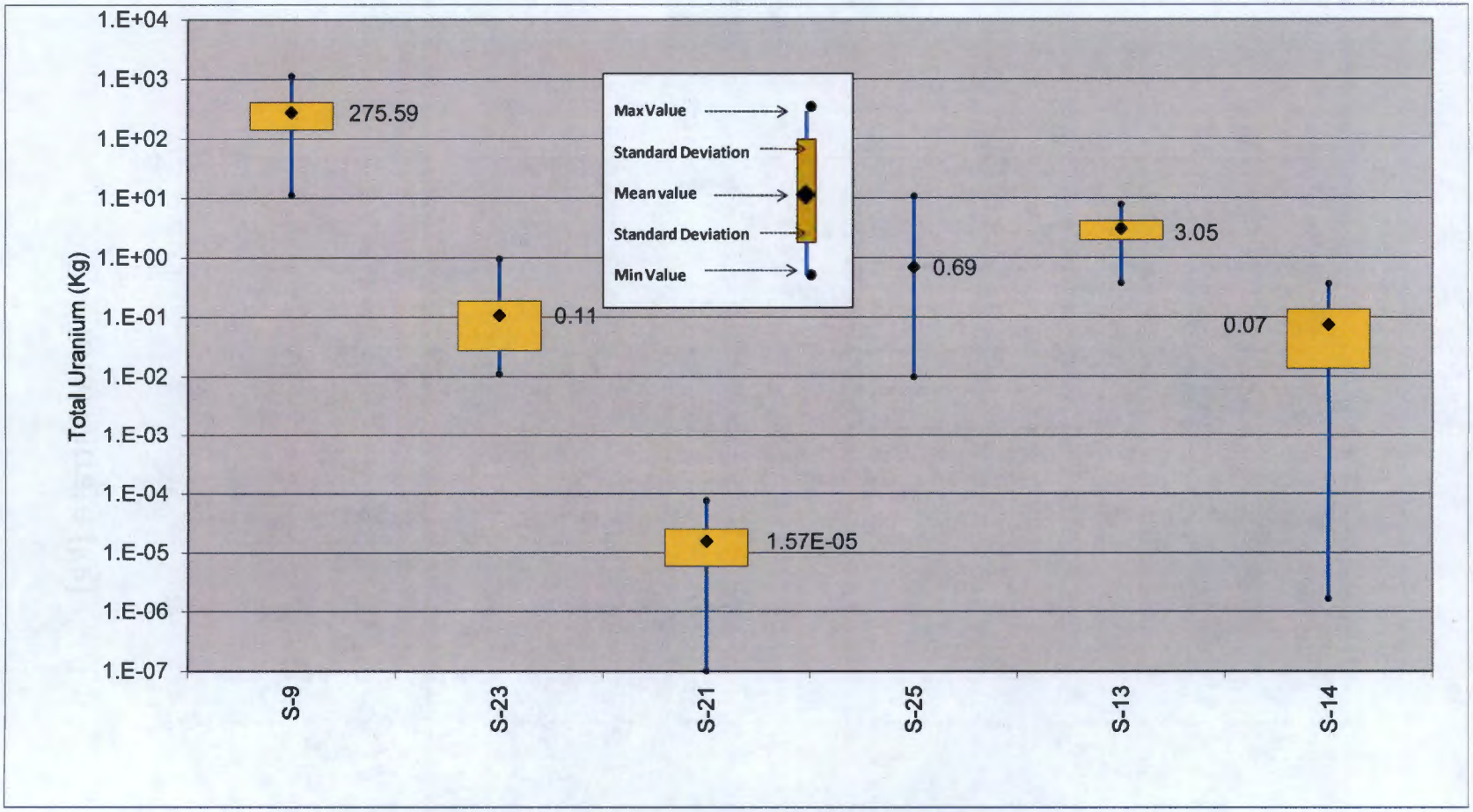

Sub-Region 1

Sub-Region 2

U.S. DEPARTMENT OF ENERGY

Technetium-99 Inventory for 200-DV-1 (S- Area Complex)

Mean Technetium-99 Estimate with Uncertainty

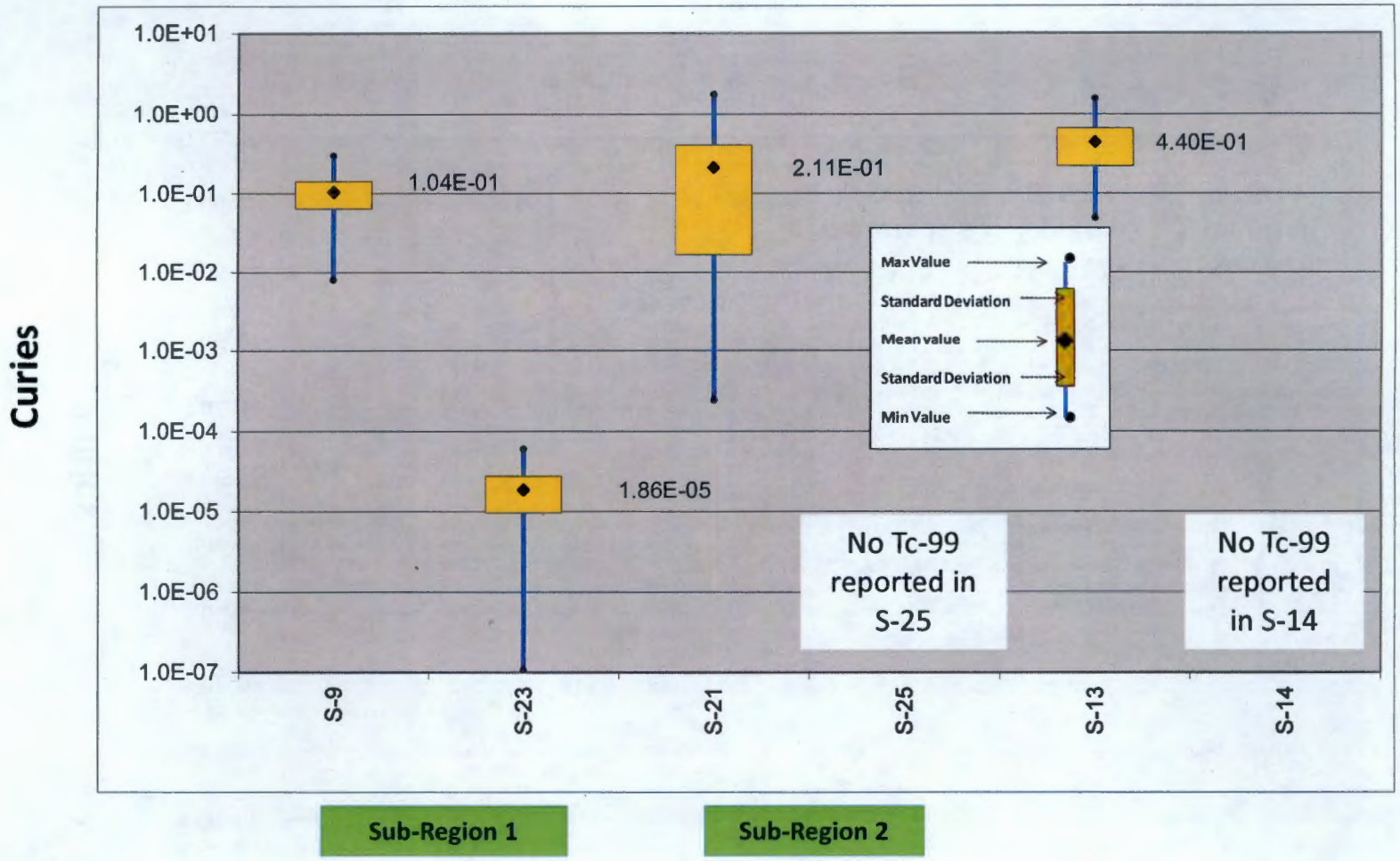

U.S. DEPARTMENT OF ENERGY

Iodine-129 Inventory for 200-DV-1 (S- Area Complex)

Mean Iodine-129 Estimate with Uncertainty

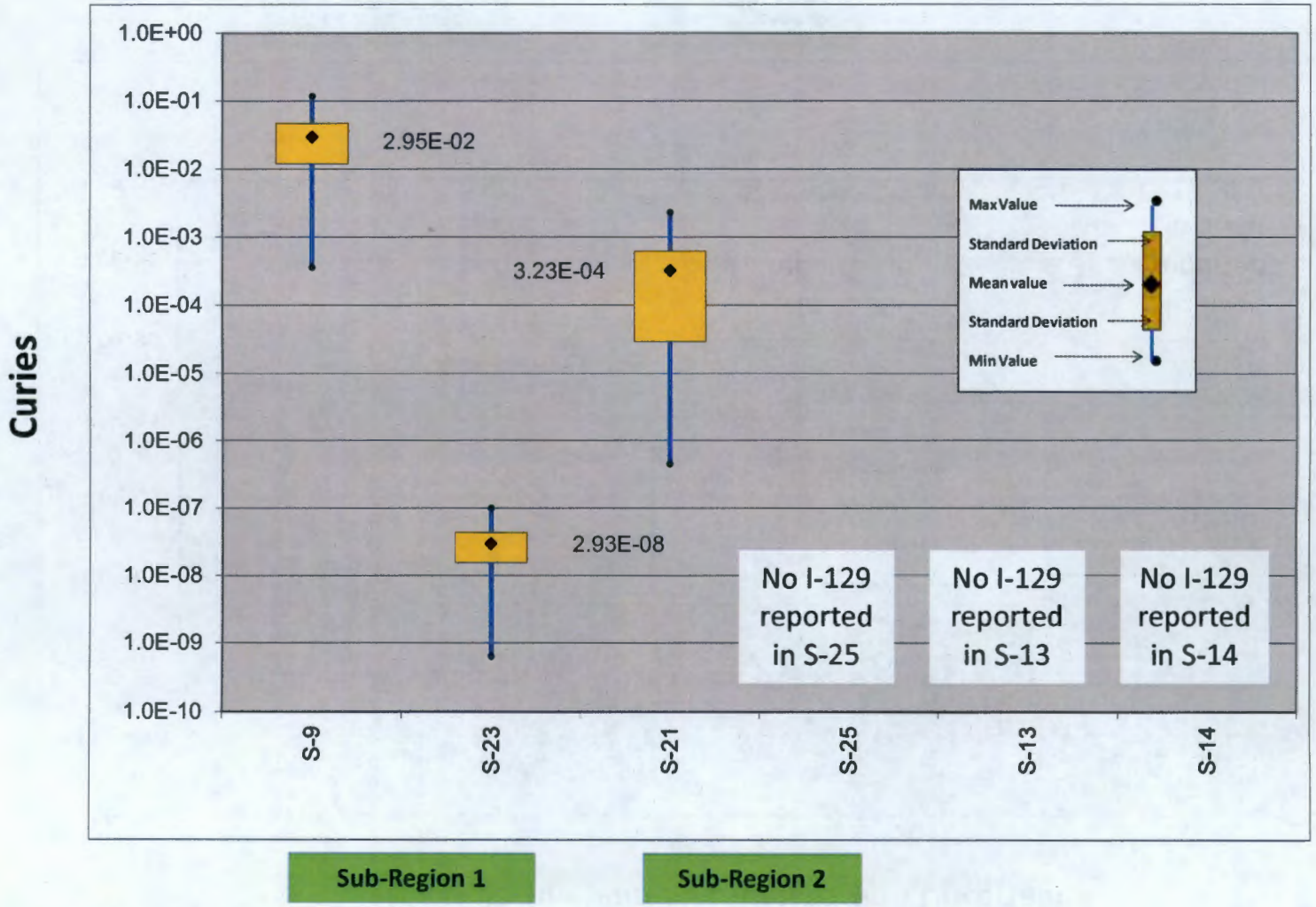

U.S. DEPARTMENT OF ENERGY

200 West Area Water Table Map (2009)

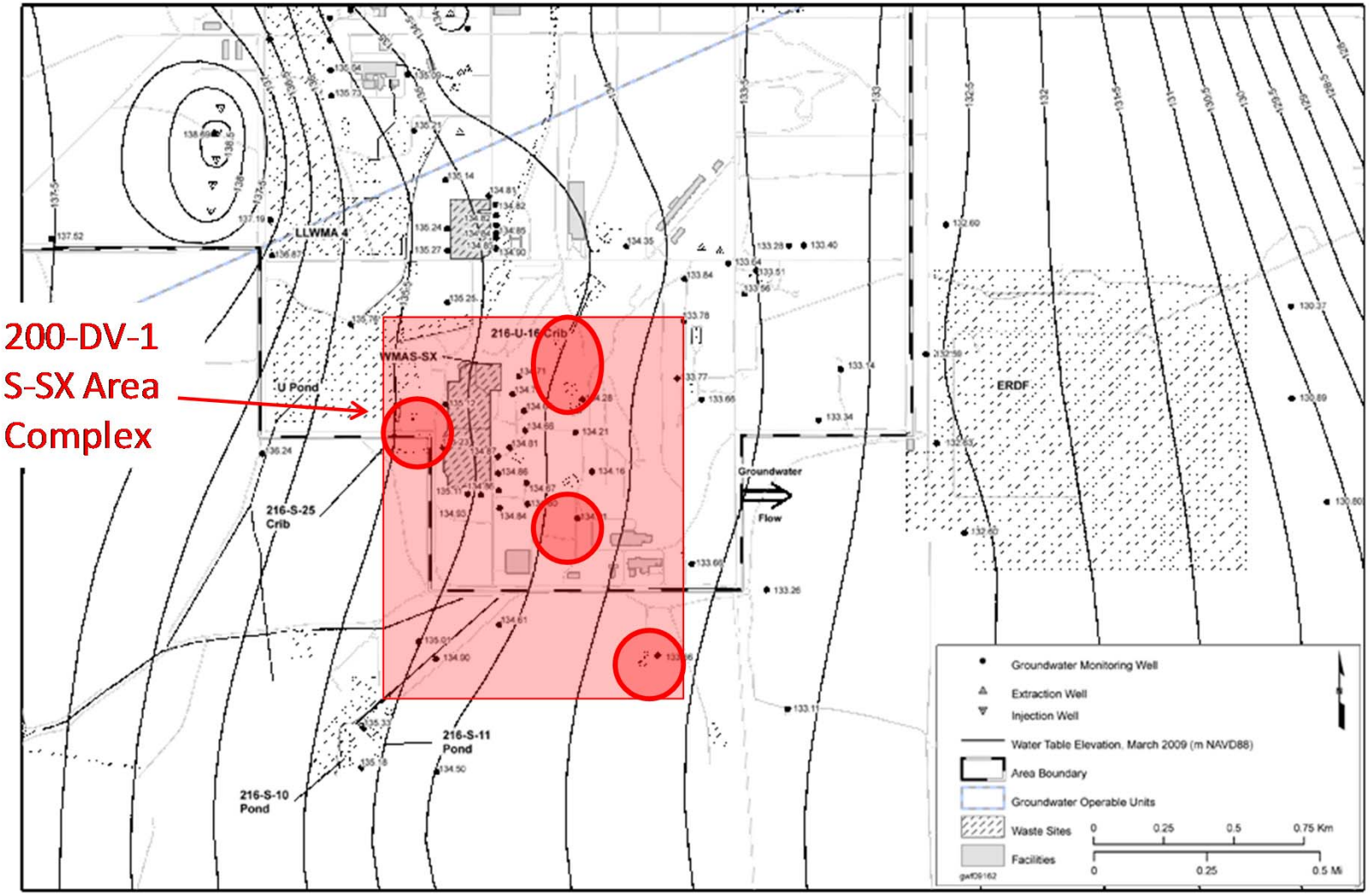

From DOE/RL-2010-11, Rev. 1

U.S. DEPARTMENT OF ENERGY

200 West Area Nitrate Groundwater Plume Map

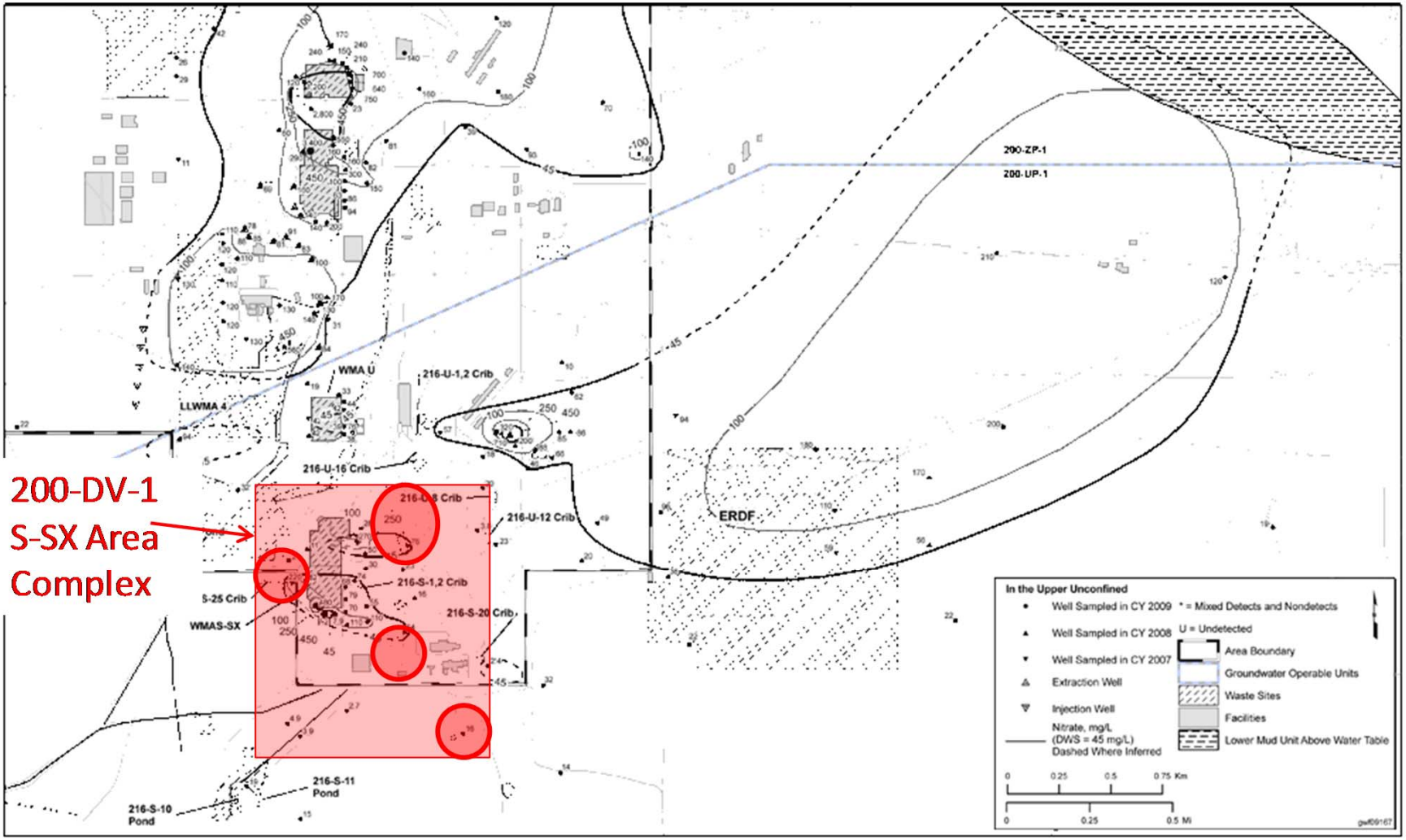

From DOE/RL-2010-11, Rev. 1

U.S. DEPARTMENT OF ENERGY

200 West Area Uranium Groundwater Plume Map

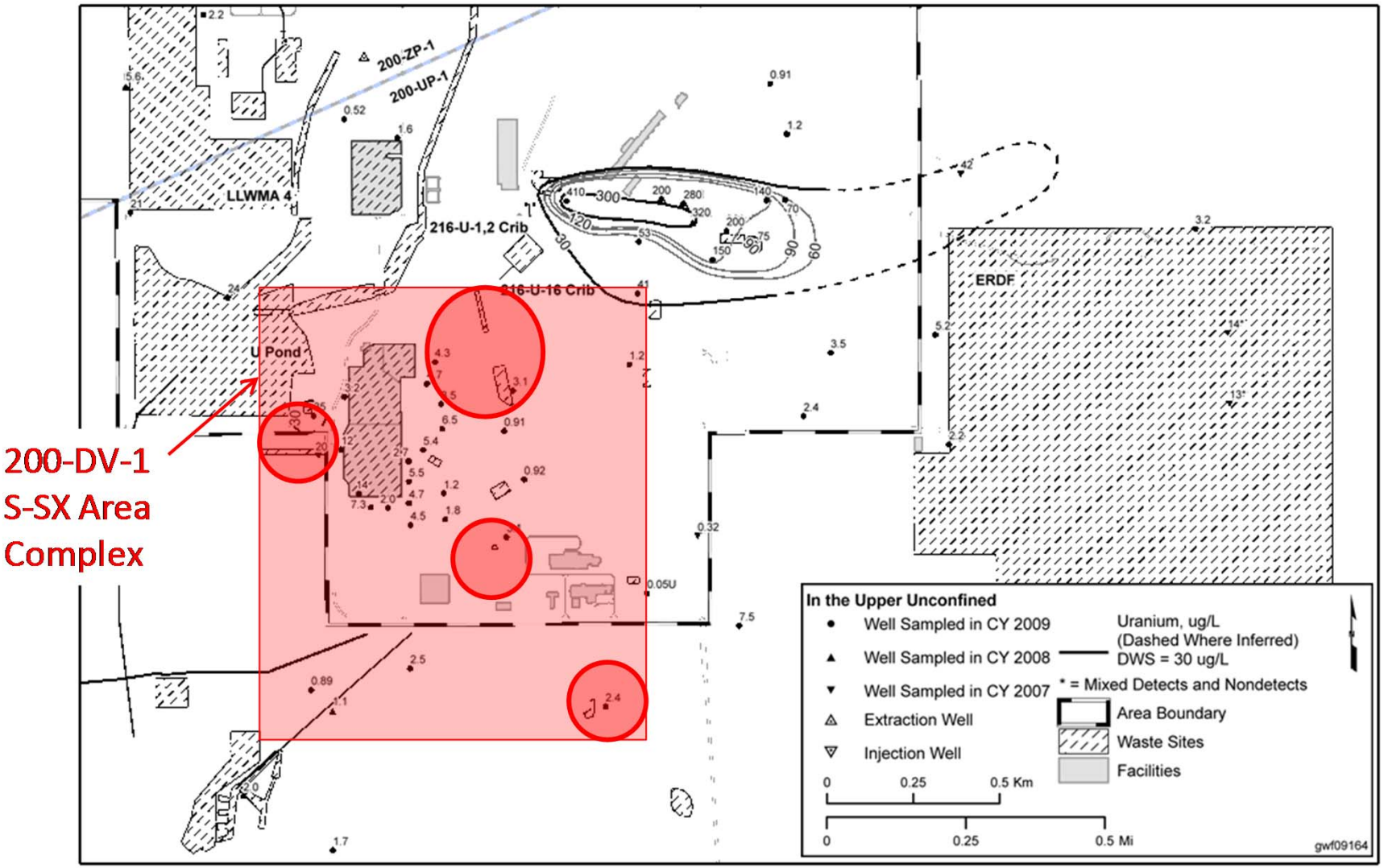

From DOE/RL-2010-11, Rev. 1

U.S. DEPARTMENT OF ENERGY

200 West Area Technetium-99 Groundwater Plume Map

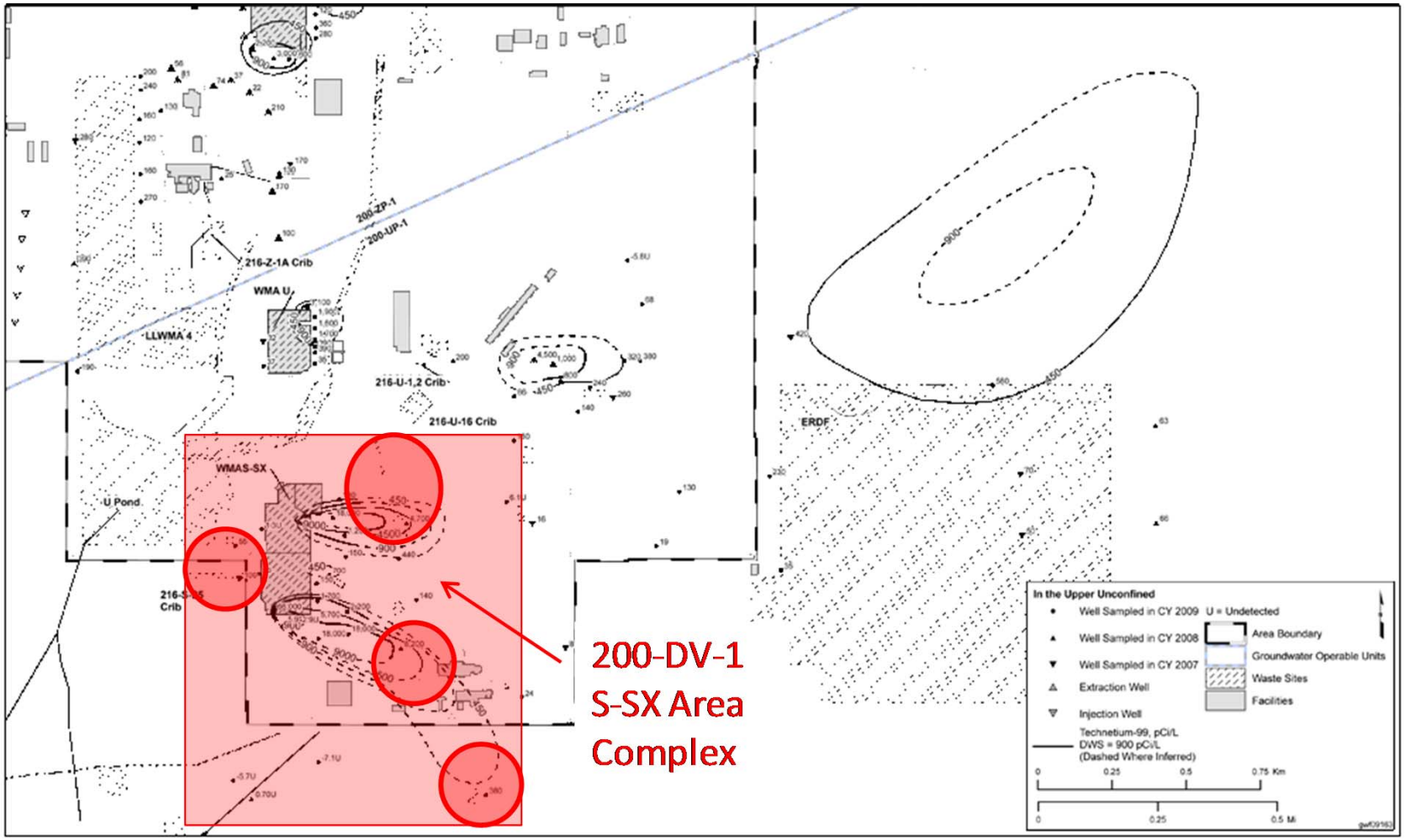

From DOE/RL-2010-11, Rev. 1

U.S. DEPARTMENT OF ENERGY

200 West Area Iodine-129 Groundwater Plume Map

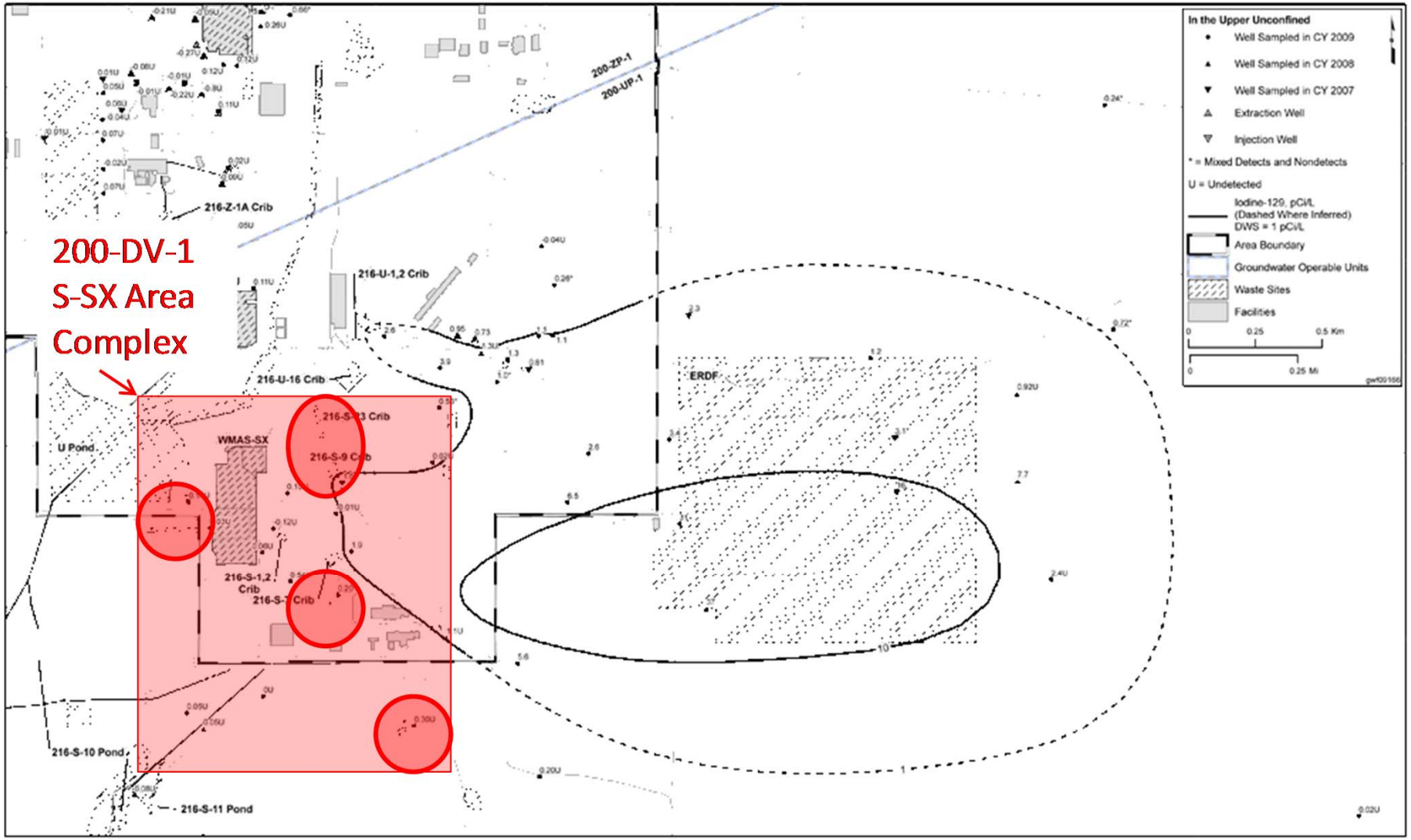

From DOE/RL-2010-11, Rev. 1

U.S. DEPARTMENT OF ENERGY

CCL4 Contaminant Plume Pump and Treat Network and Groundwater Flow

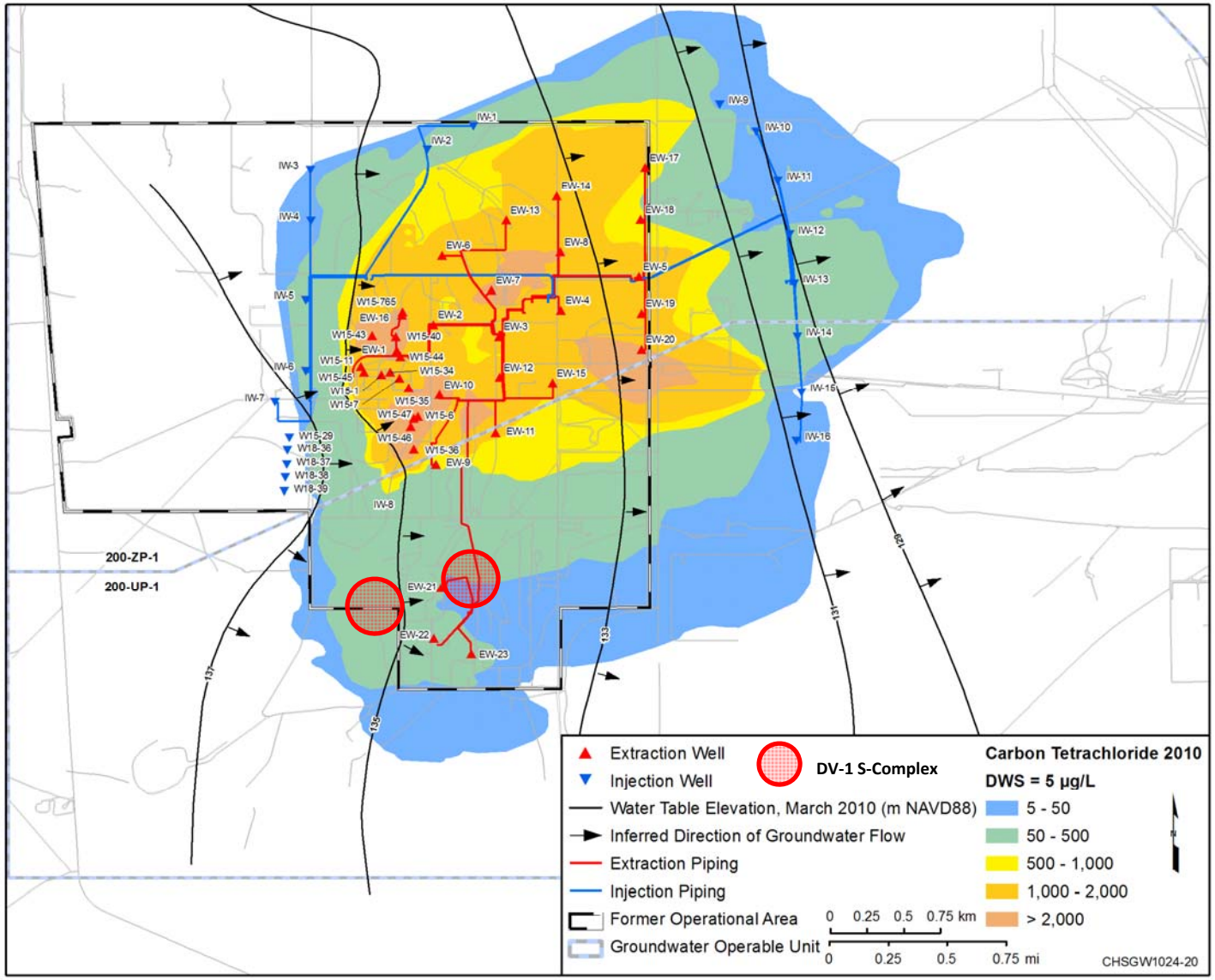

U.S. DEPARTMENT OF ENERGY

Sub-Region 1
[216-S-9 and 216-S-23 Cribs]

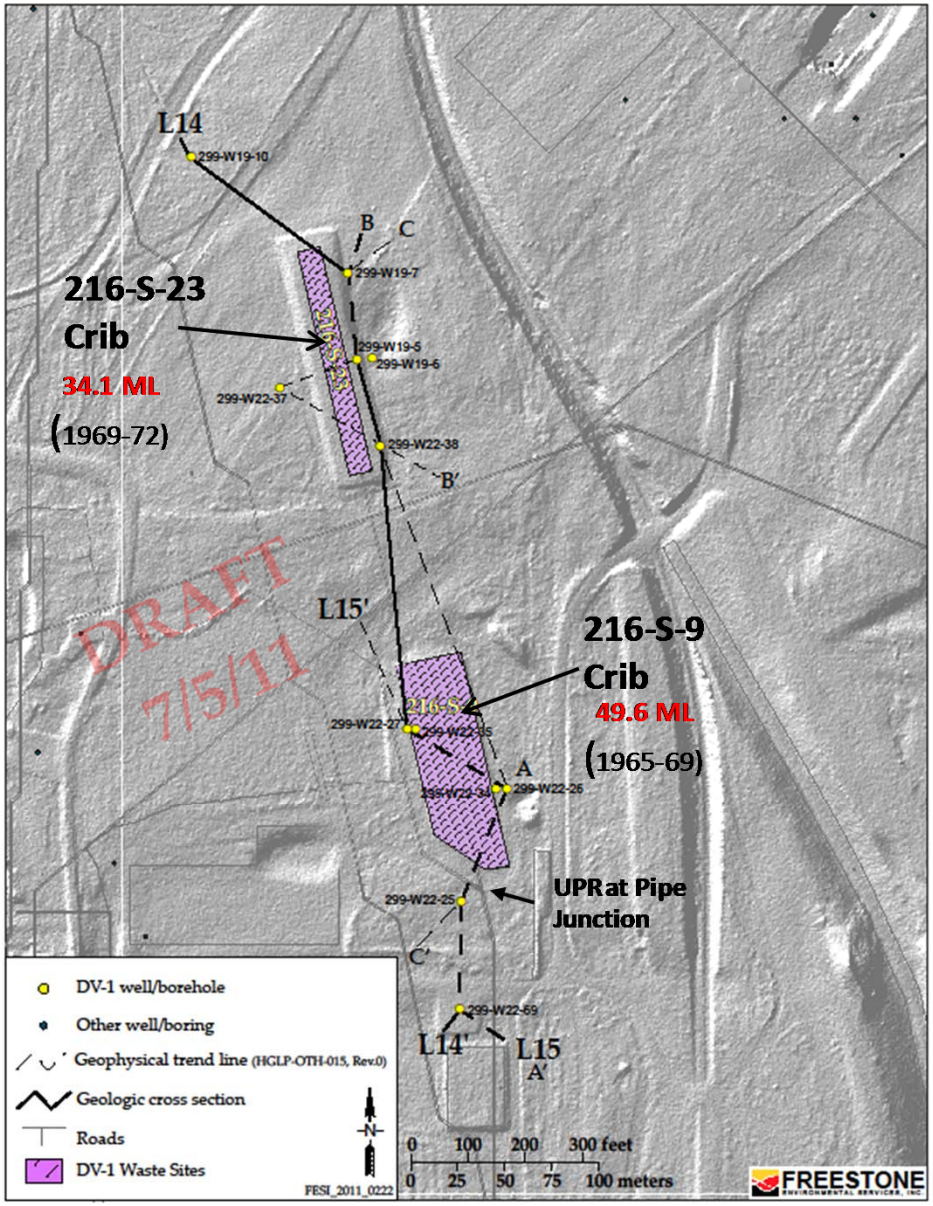

U.S. DEPARTMENT OF ENERGY

Sub-Region 1 Hydrogeology

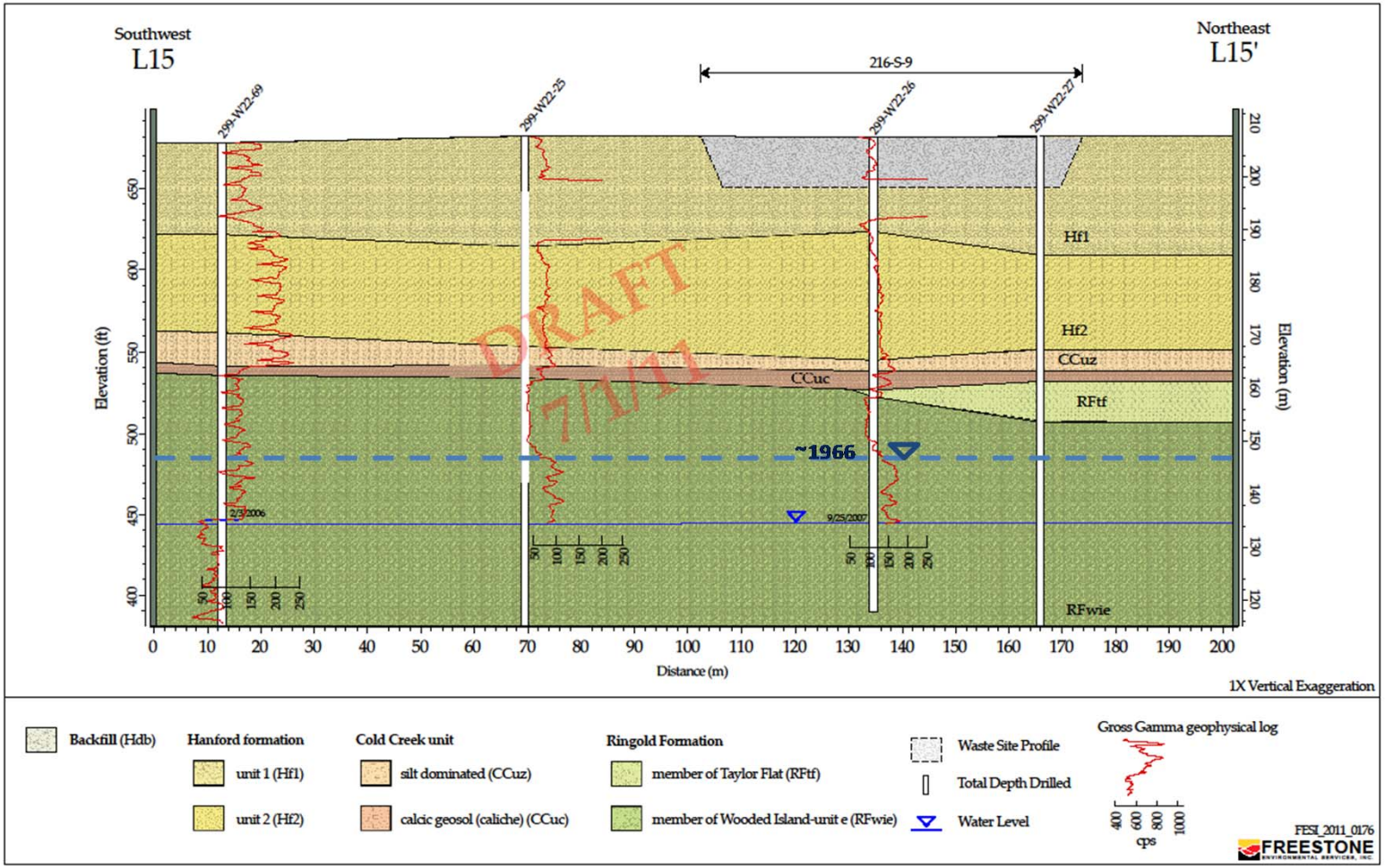

U.S. DEPARTMENT OF ENERGY

SGE Profile at 216-S-9 Crib

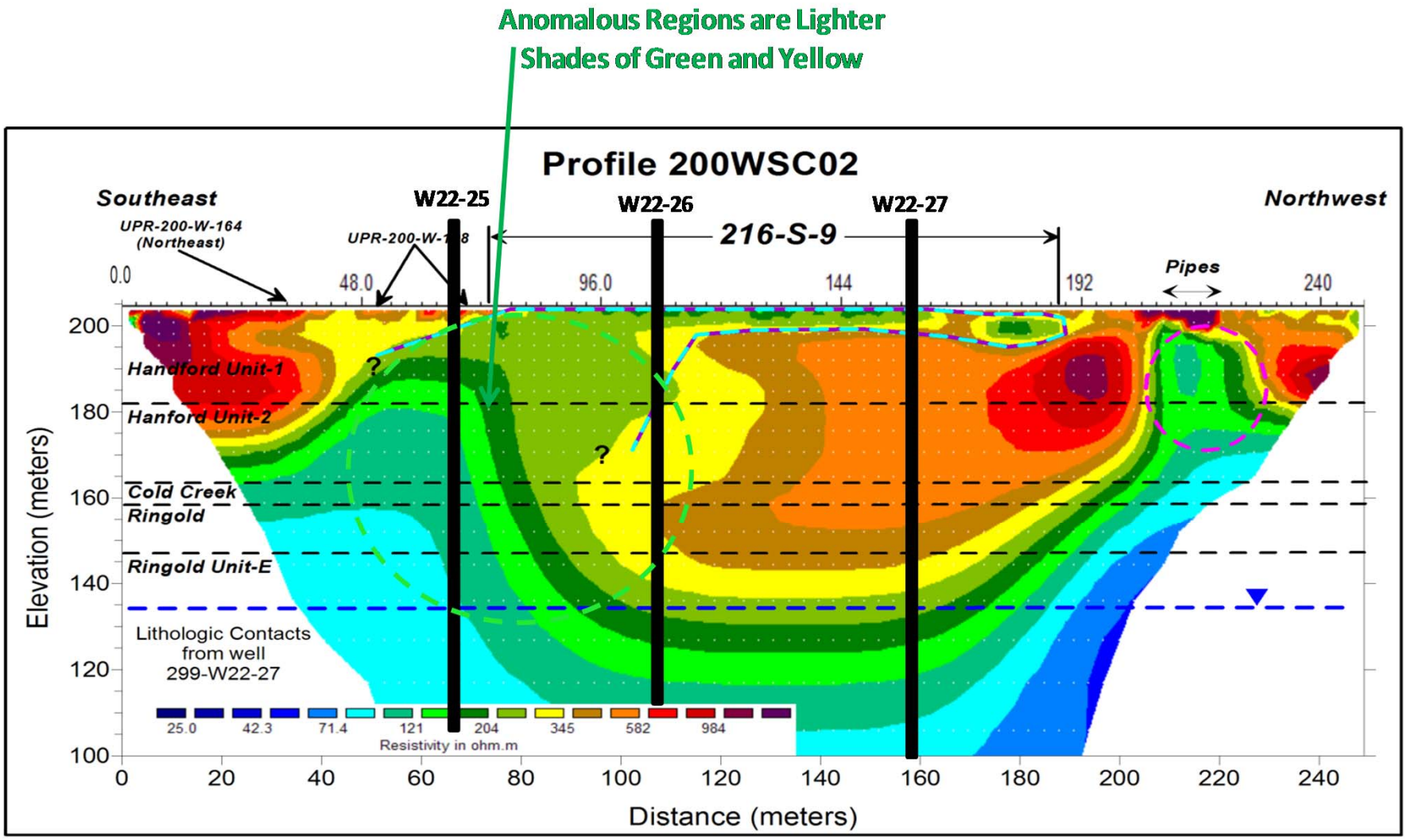

216-S-9 Crib Contaminant Conceptual Model

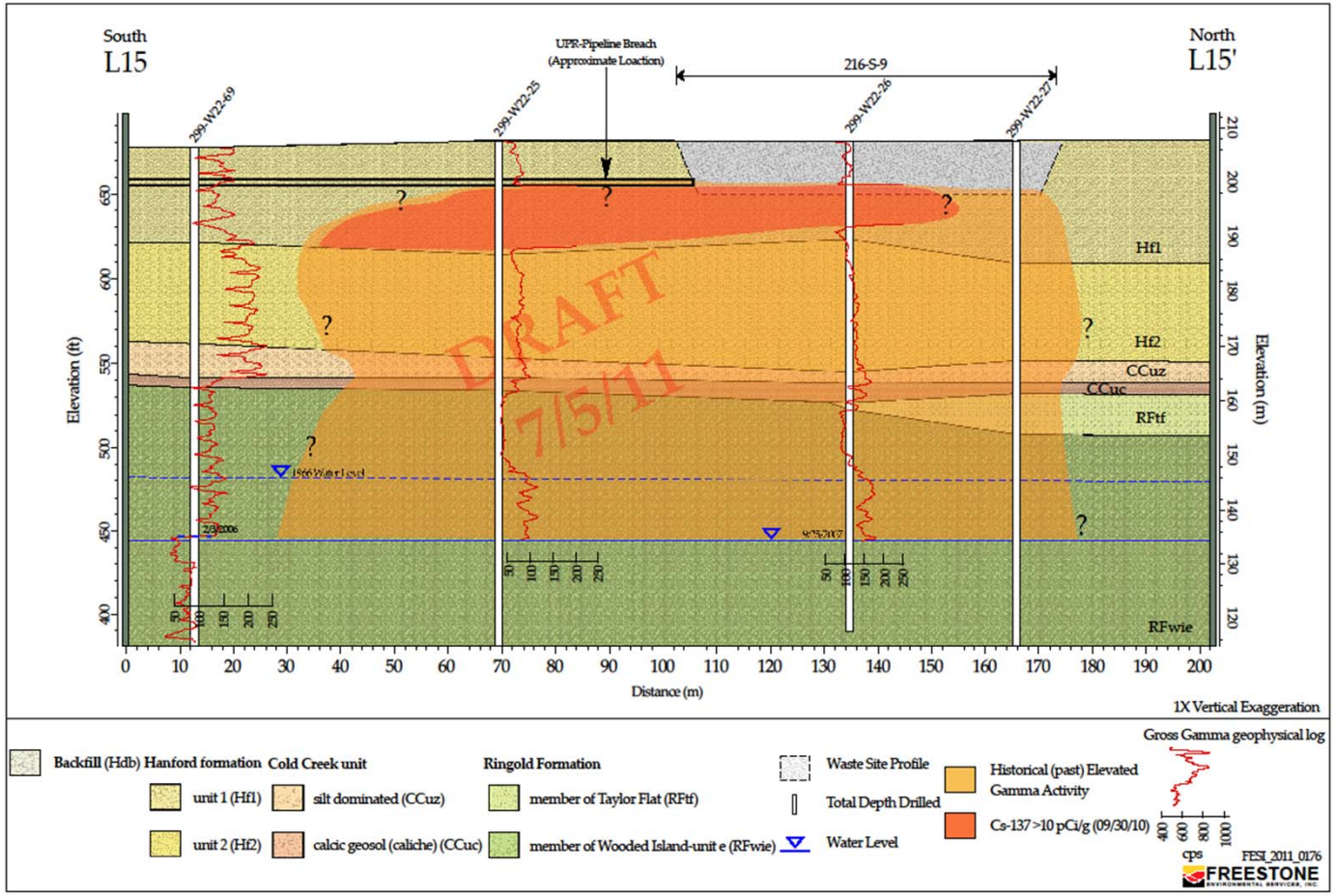

U.S. DEPARTMENT OF ENERGY

Sub-Region 1 Hydrogeology

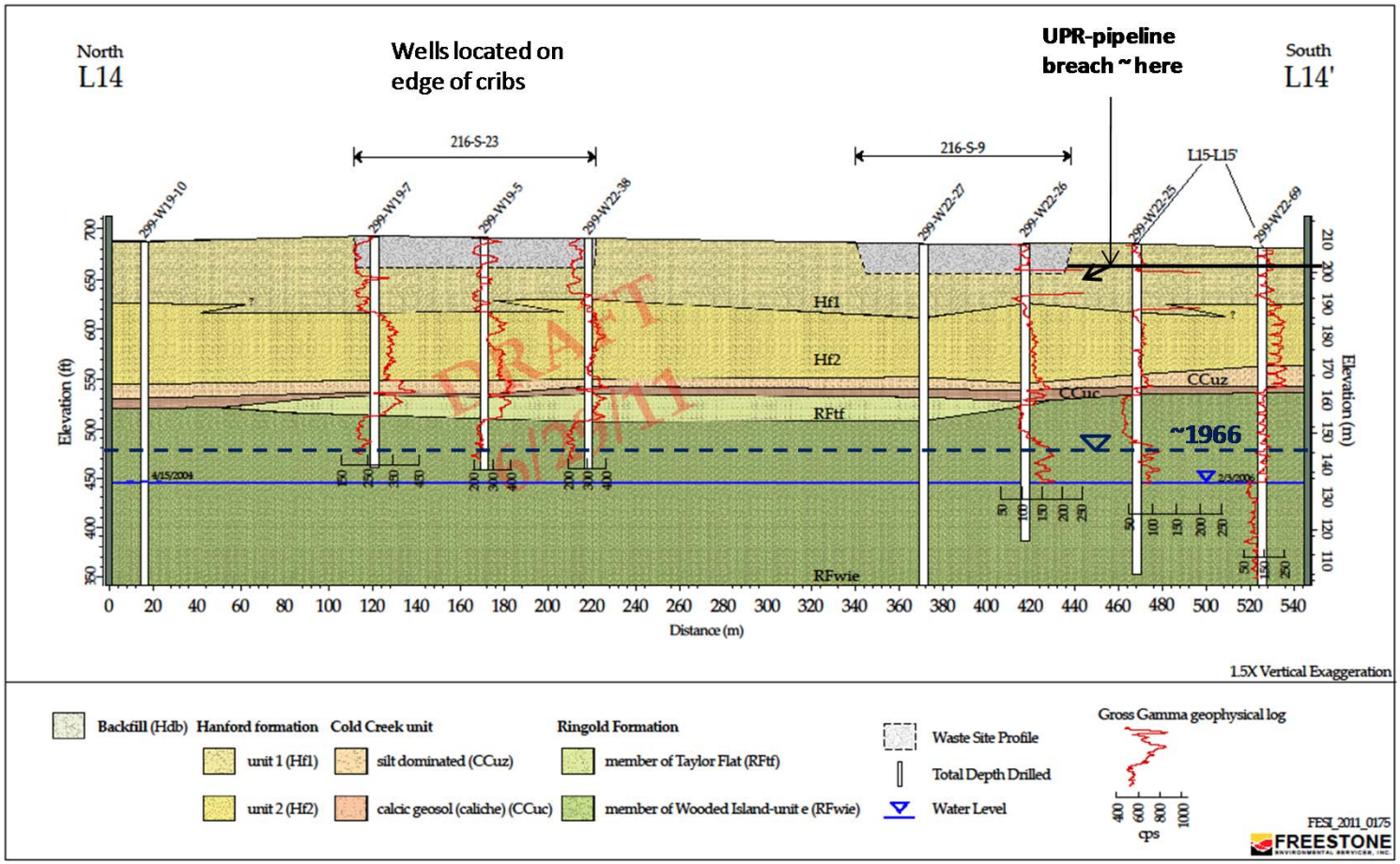

Subregion 1 Contaminant Conceptual Model

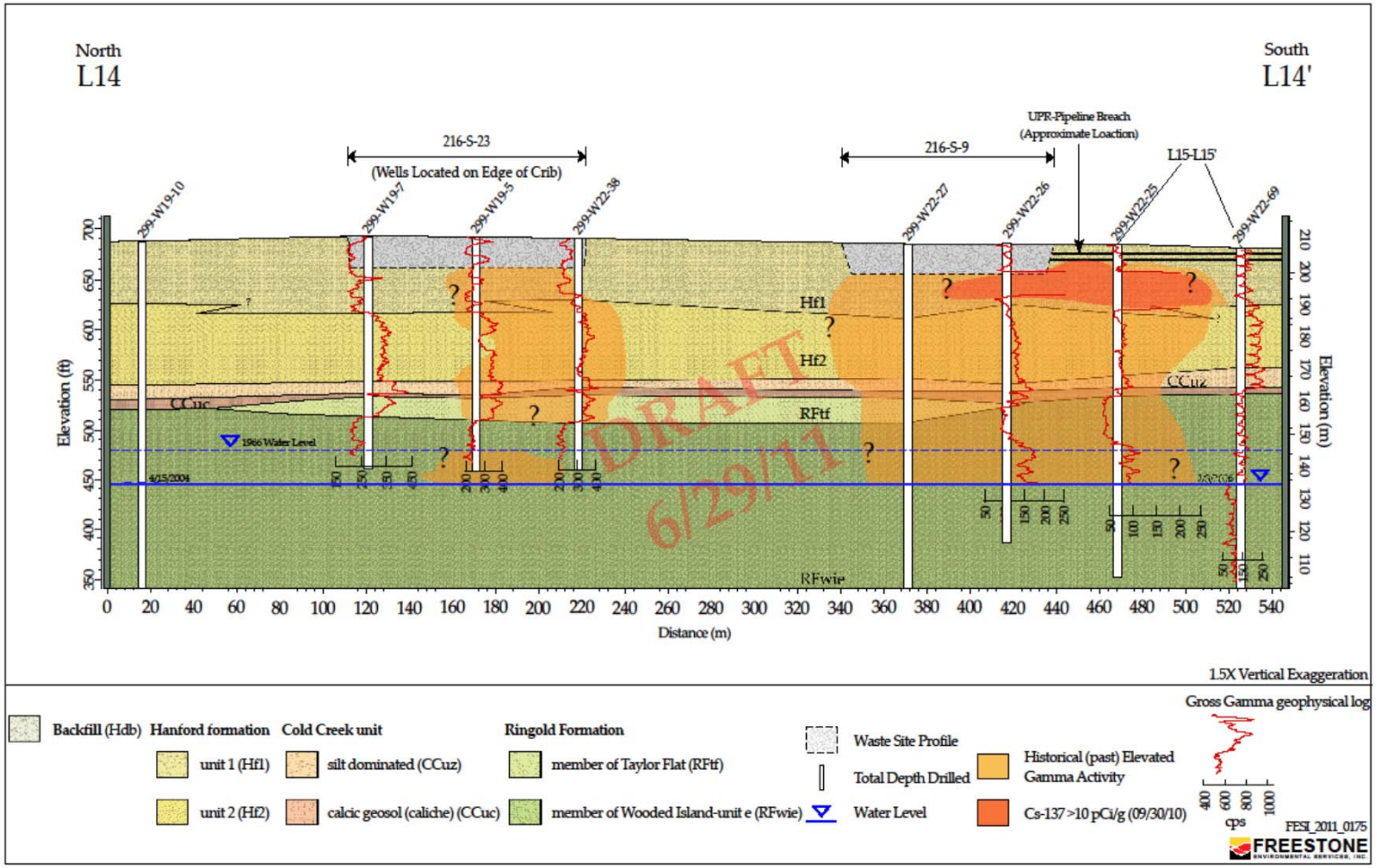

Sub-Region 1
[216-S-9 and 216-S-23 Cribs]

Interpreted Lateral Extent of Contamination

Currently detectable (Cs-137 ≥ 10pCi/g) gamma contamination (less mobile)

Historical (past) detectable gamma contamination (mobile--short half-life; e.g., Ru-106)

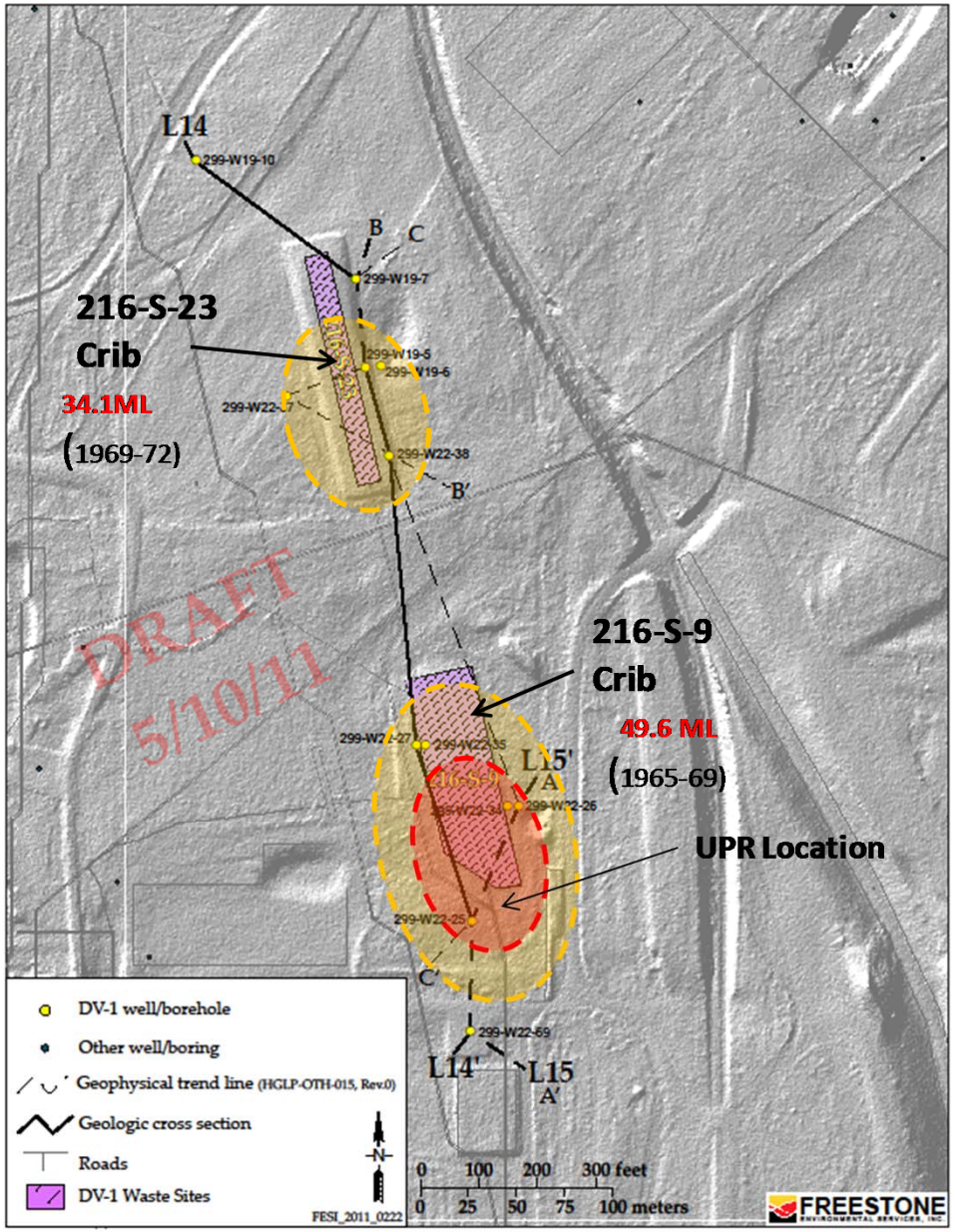

U.S. DEPARTMENT OF ENERGY

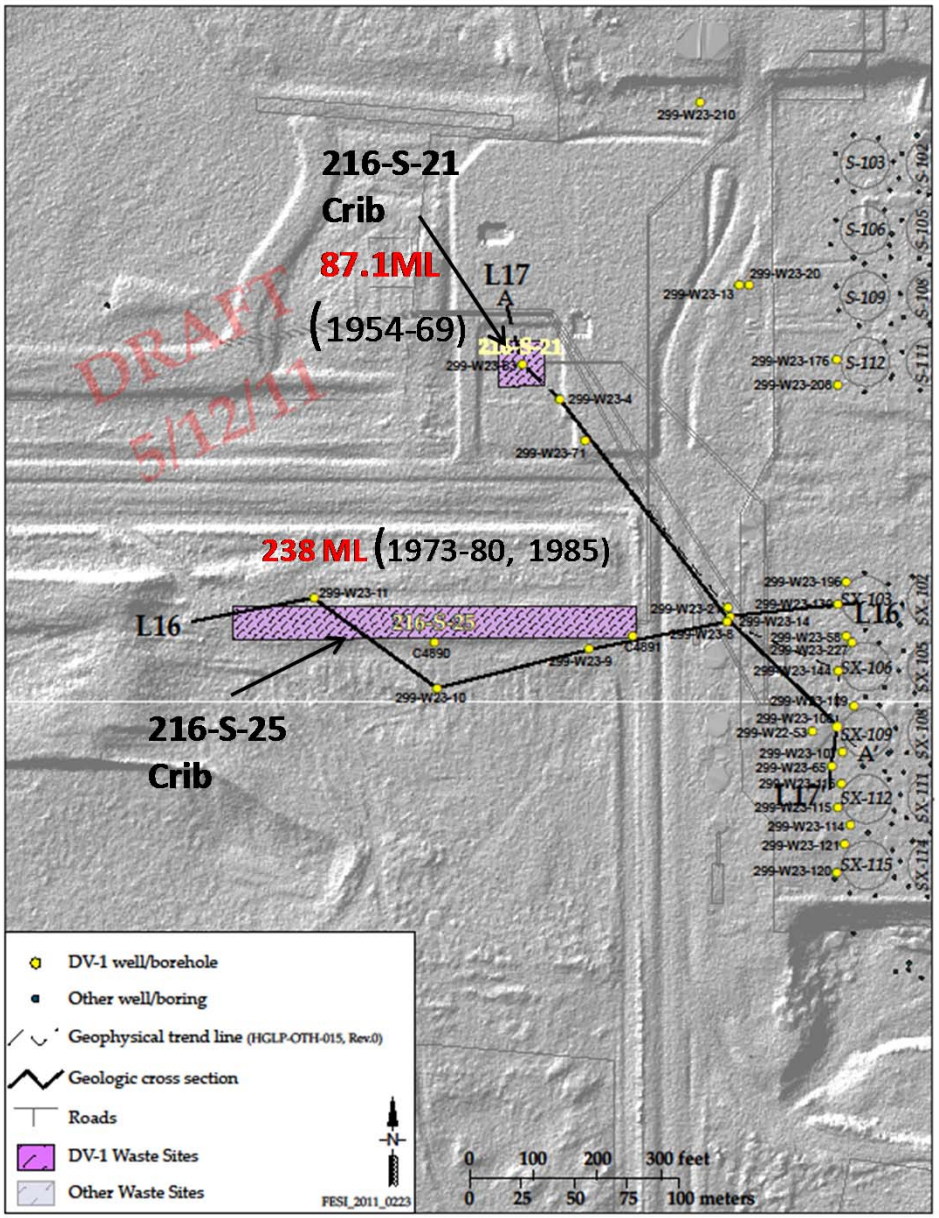

Sub-Region 2

[216-S-21 and 216-S-25 Cribs]

U.S. DEPARTMENT OF ENERGY

Sub-Region 2 Hydrogeology

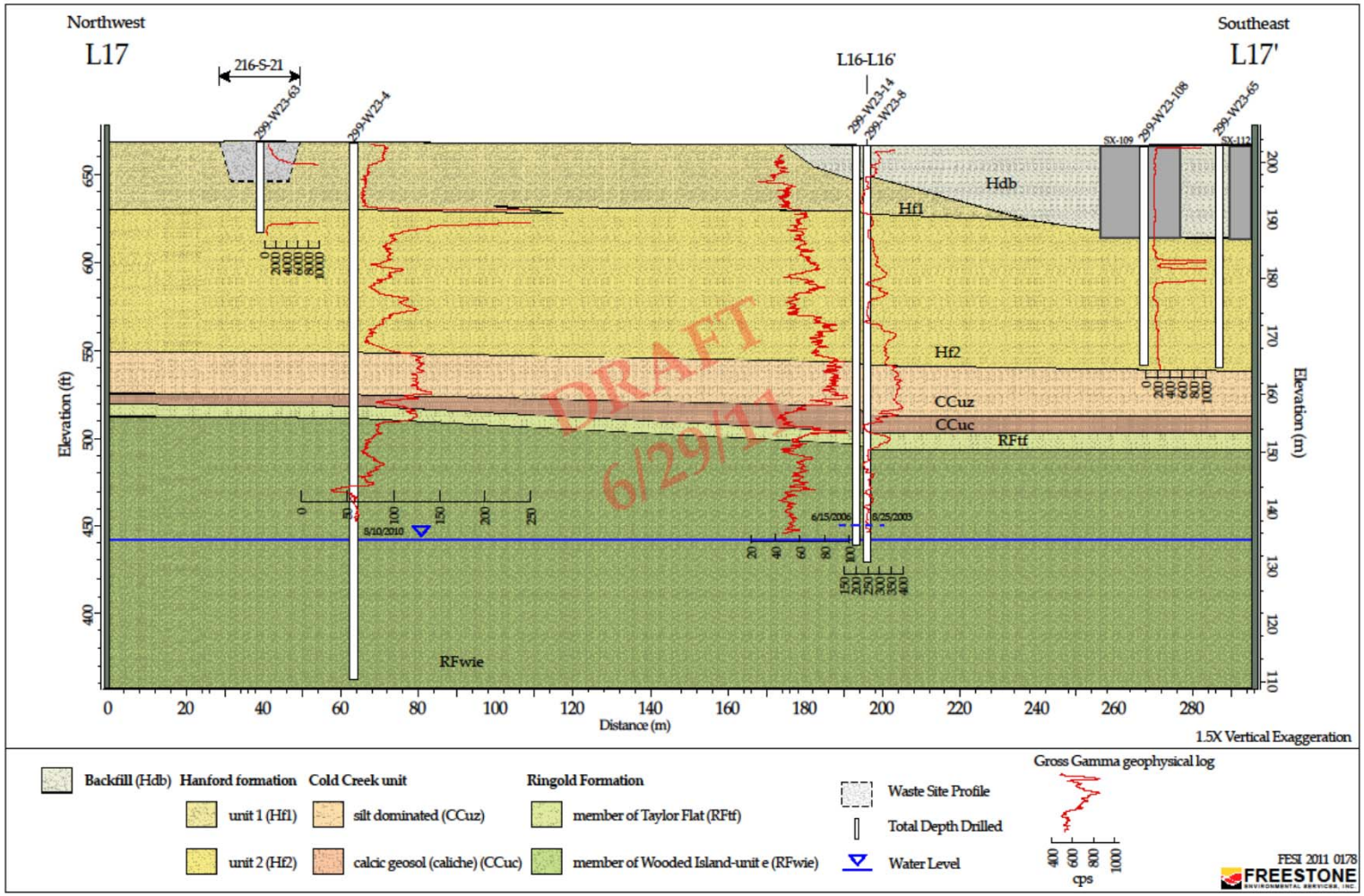

U.S. DEPARTMENT OF ENERGY

216-S-21 Crib Contaminant Conceptual Model

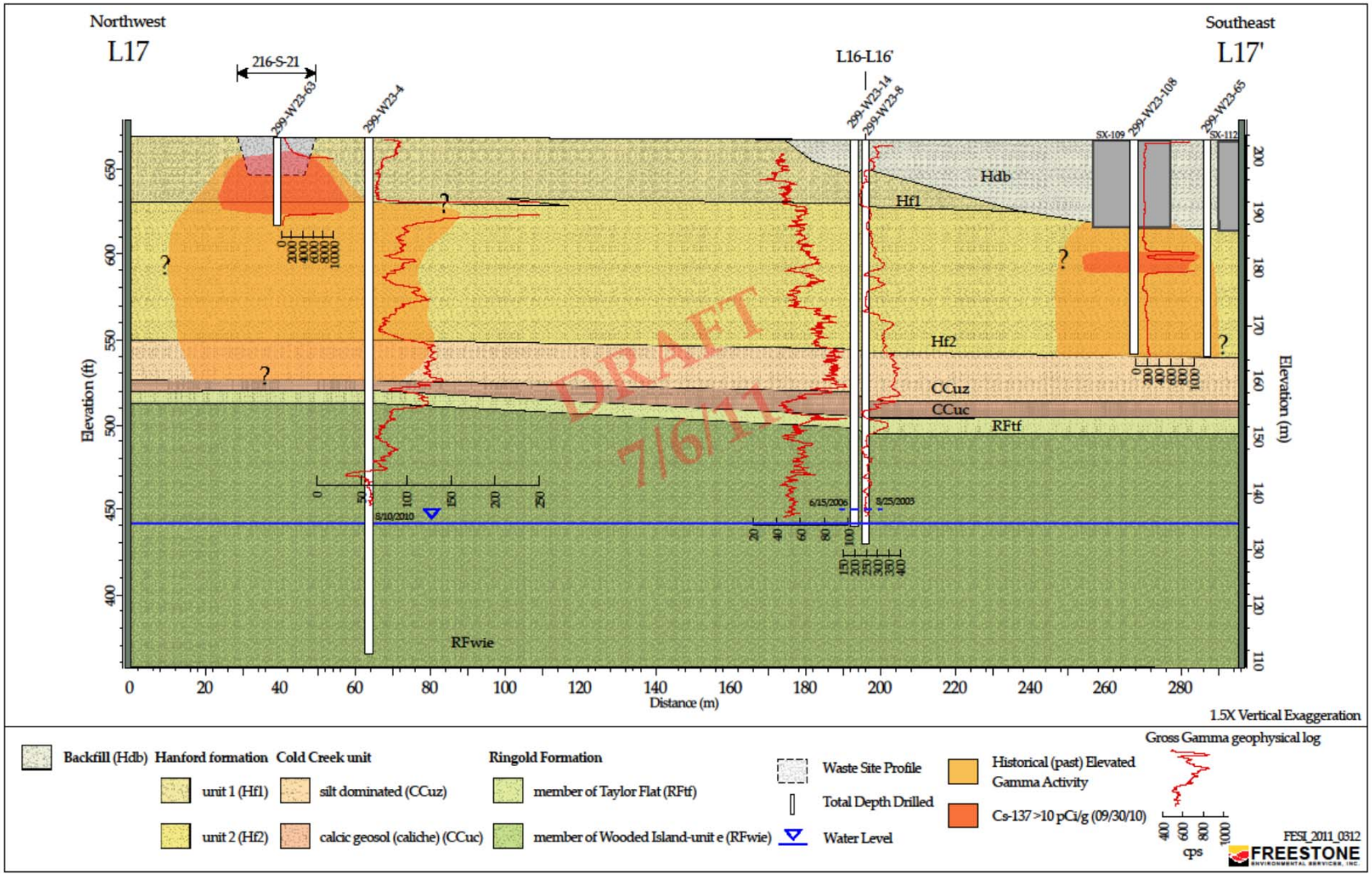

U.S. DEPARTMENT OF ENERGY

Sub-Region 2 Hydrogeology

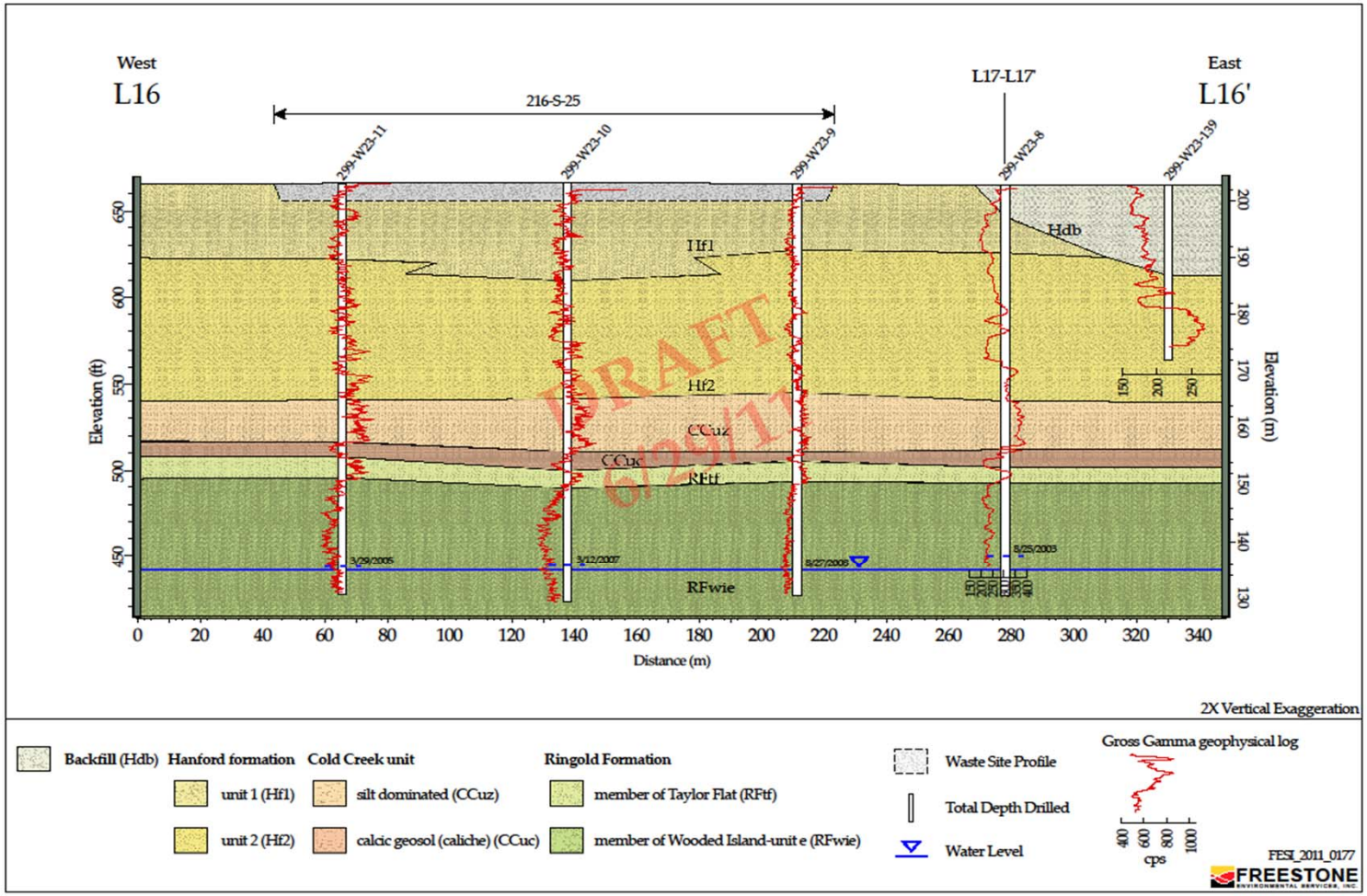

U.S. DEPARTMENT OF ENERGY

Surface Geophysical Profiles Identifying Anomalous Regions Beneath the 216-S-25 Crib

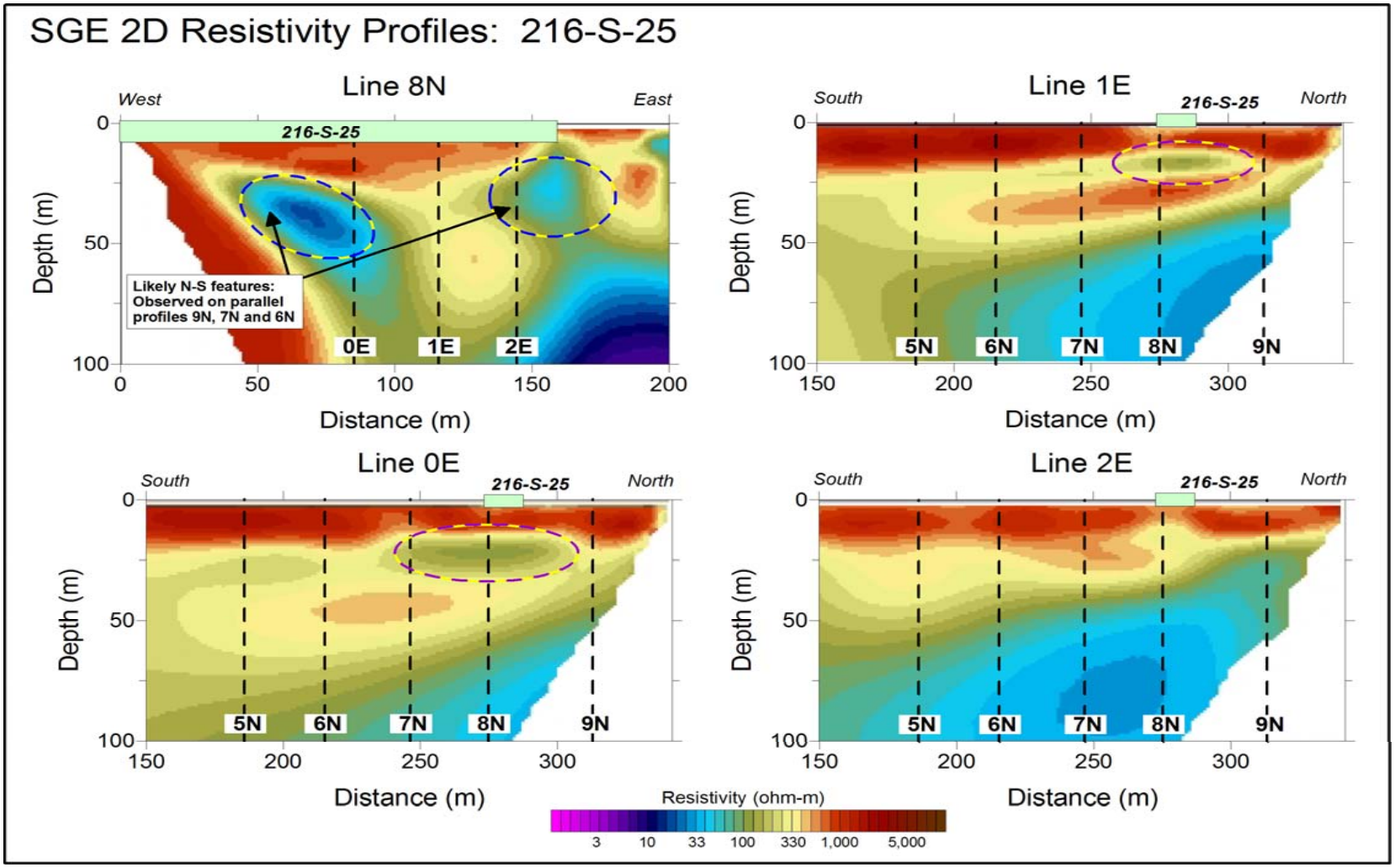

U.S. DEPARTMENT OF ENERGY

216-S-25 Crib Contaminant Conceptual Model

No Gamma Contamination Detected in Wells

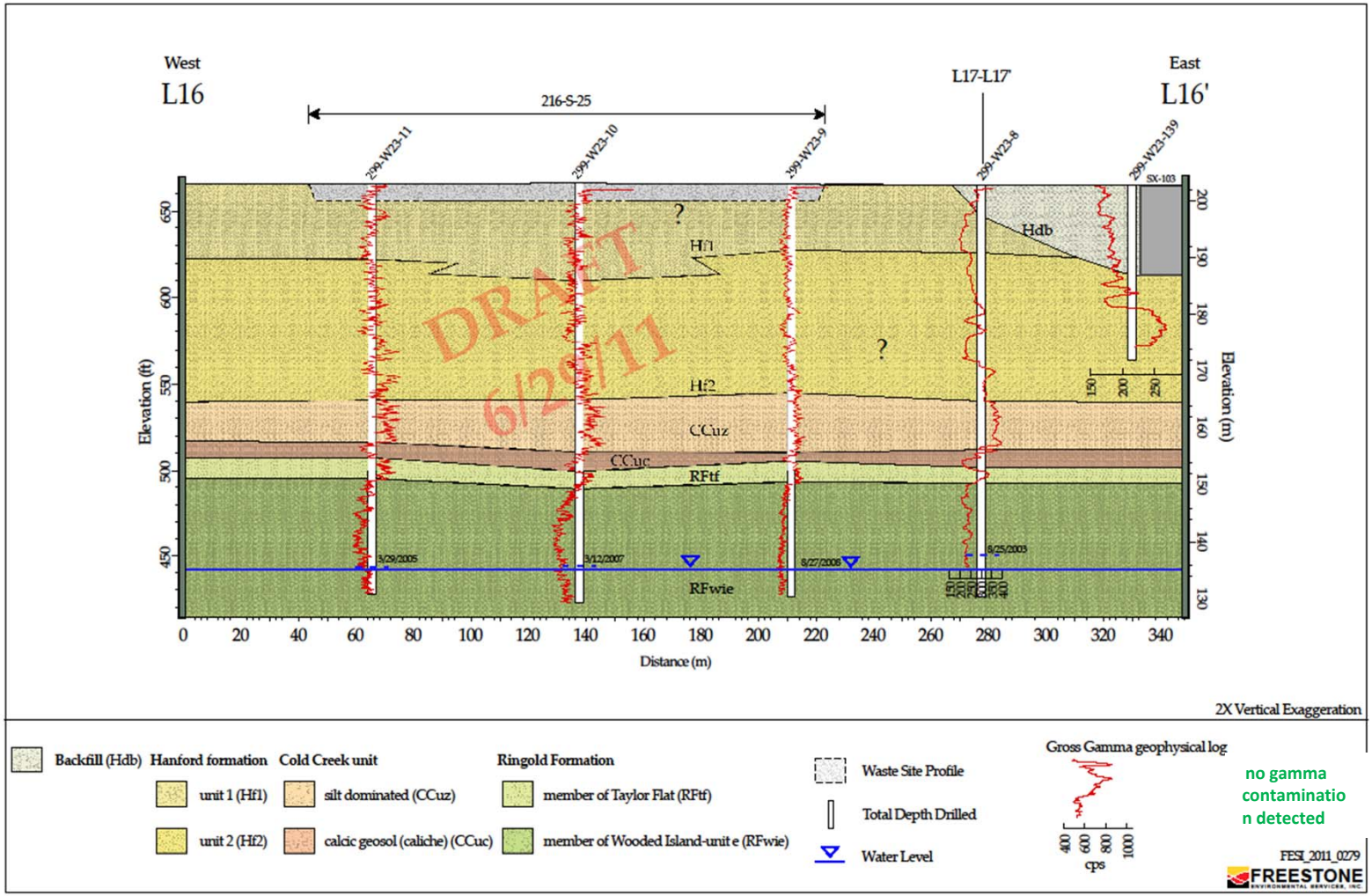

U.S. DEPARTMENT OF ENERGY

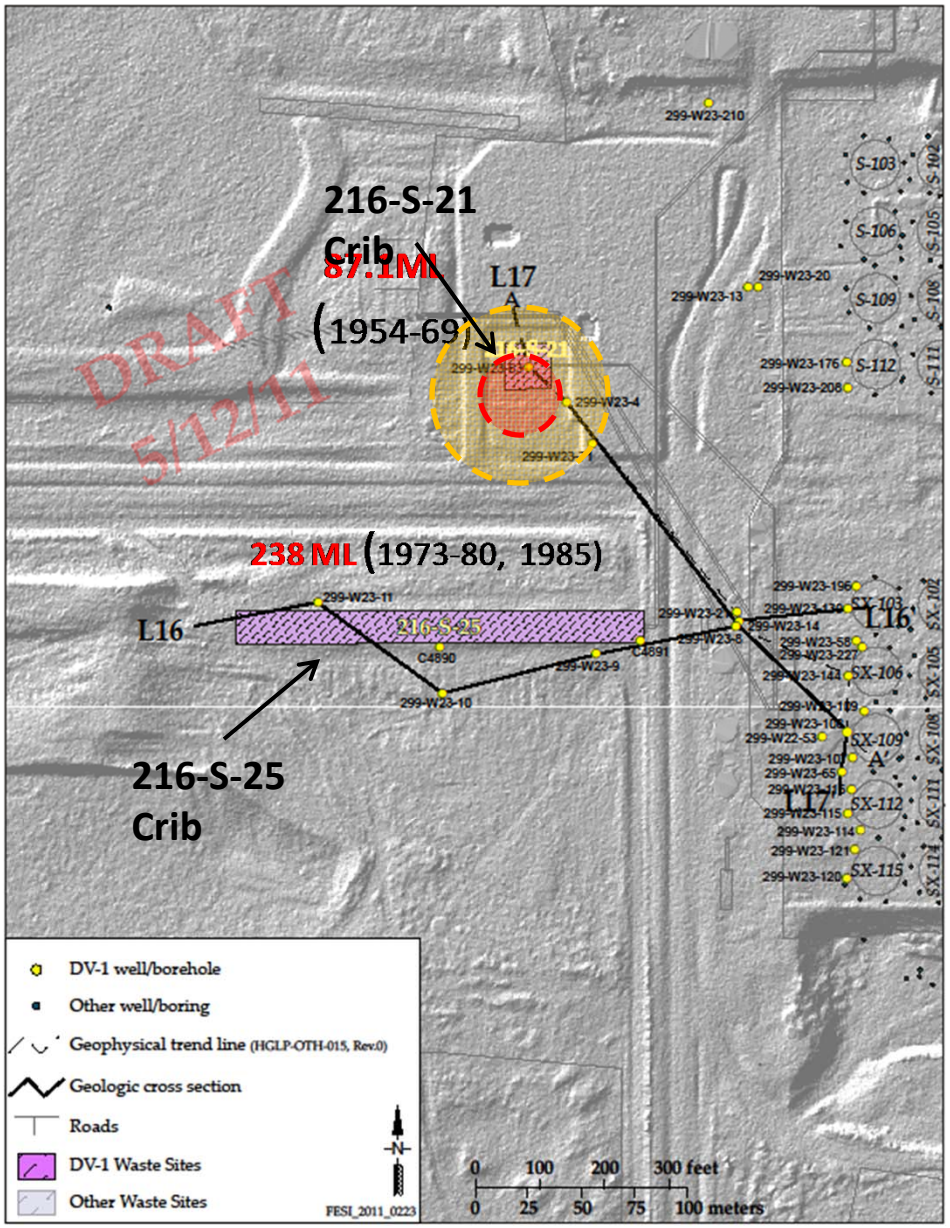

Sub-Region 2

[216-S-21 and 216-S-25 Cribs]

Interpreted Lateral Extent of Contamination

Currently detectable (Cs-137 ≥ 10pCi/g) gamma contamination (less mobile)

Historical (past) detectable gamma contamination (mobile-short half-life; e.g., Ru-106)

U.S. DEPARTMENT OF ENERGY

Supporting Slides

U.S. DEPARTMENT OF ENERGY

Temporal Conceptual Contaminant Migration Laterally and Vertically

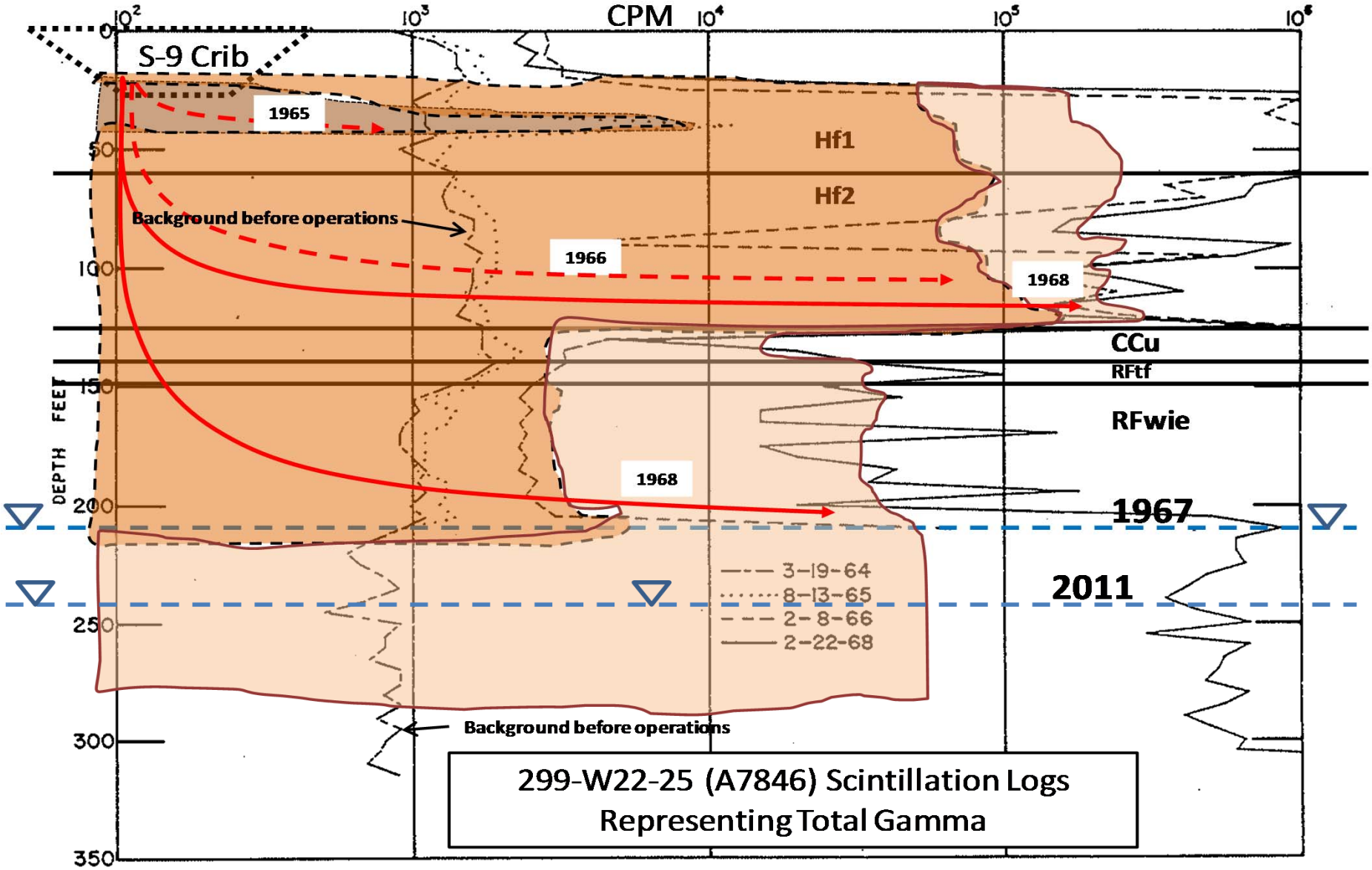

U.S. DEPARTMENT OF ENERGY

216-S-9 Crib Gamma Contaminant Extent

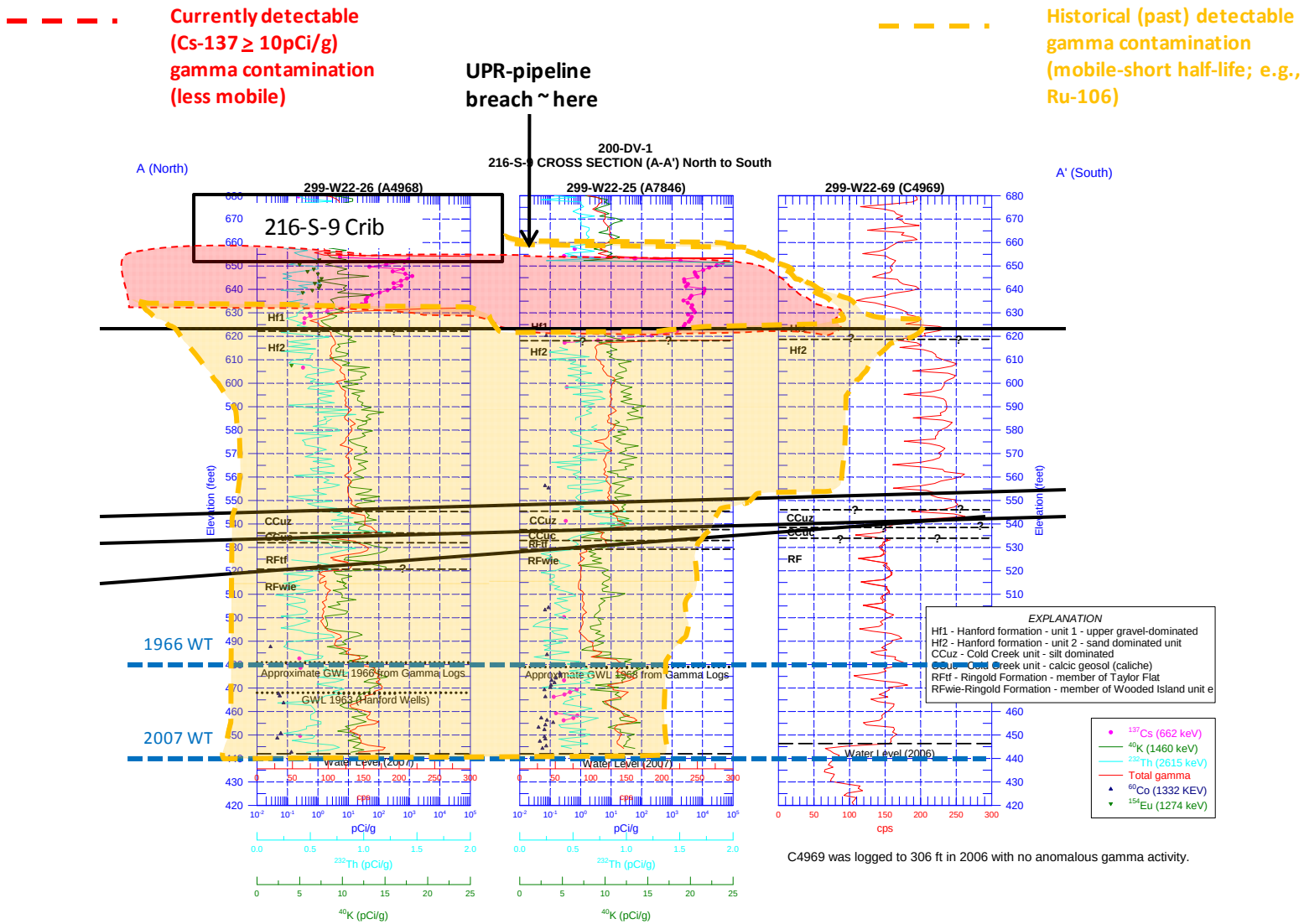

C4969 was logged to 306 ft in 2006 with no anomalous gamma activity.

U.S. DEPARTMENT OF ENERGY

216-S-23 Crib Gamma Contaminant Extent

Historical (past) detectable gamma contamination (mobile-short half-life; e.g., Ru-106)

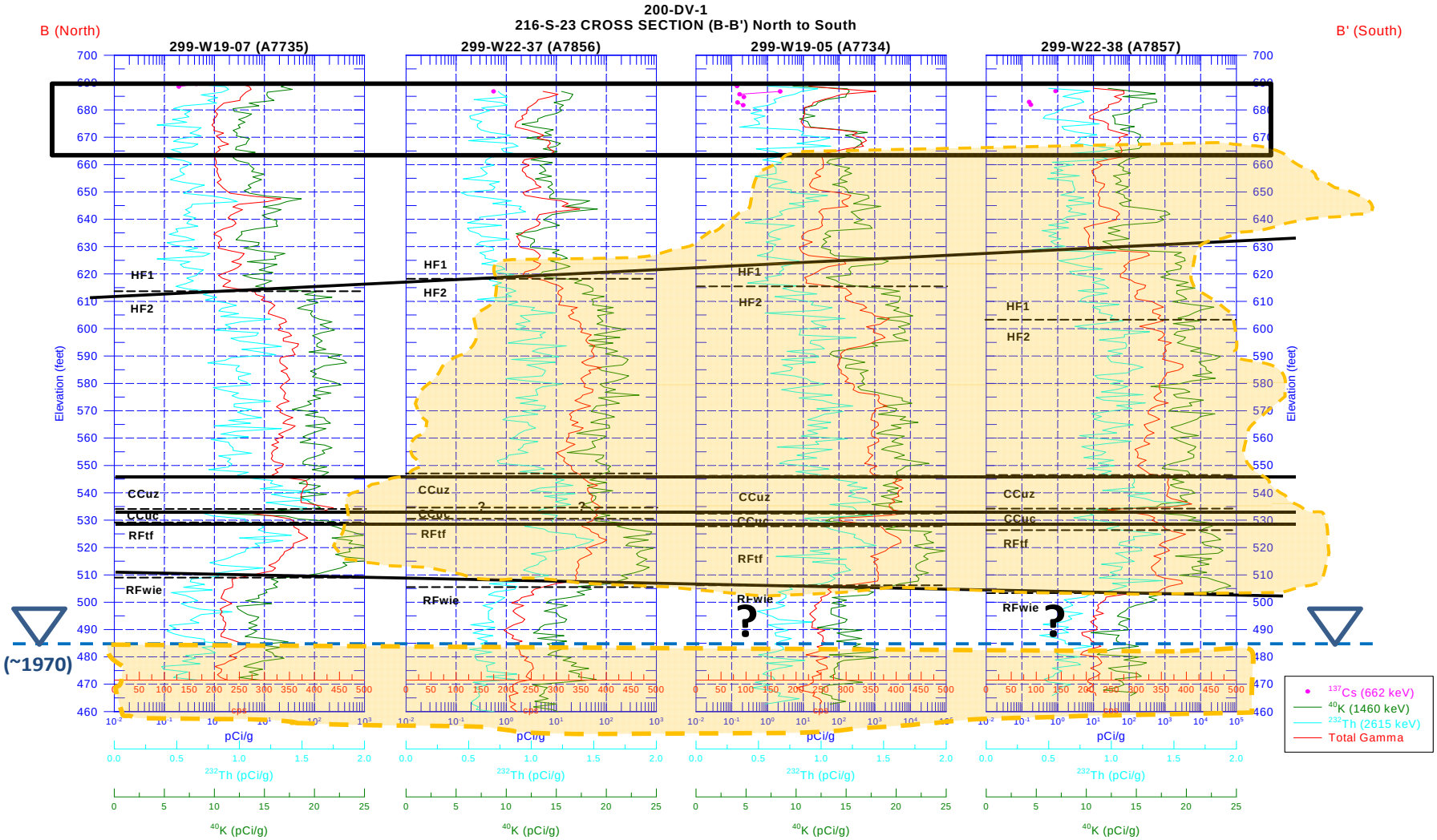

U.S. DEPARTMENT OF ENERGY

S-SX Sub-Region 1 Contaminant Extent

Currently detectable (Cs-137 ≥ 10pCi/g) gamma contamination (less mobile)

Historical (past) detectable gamma contamination (mobile-short half-life; e.g., Ru-106)

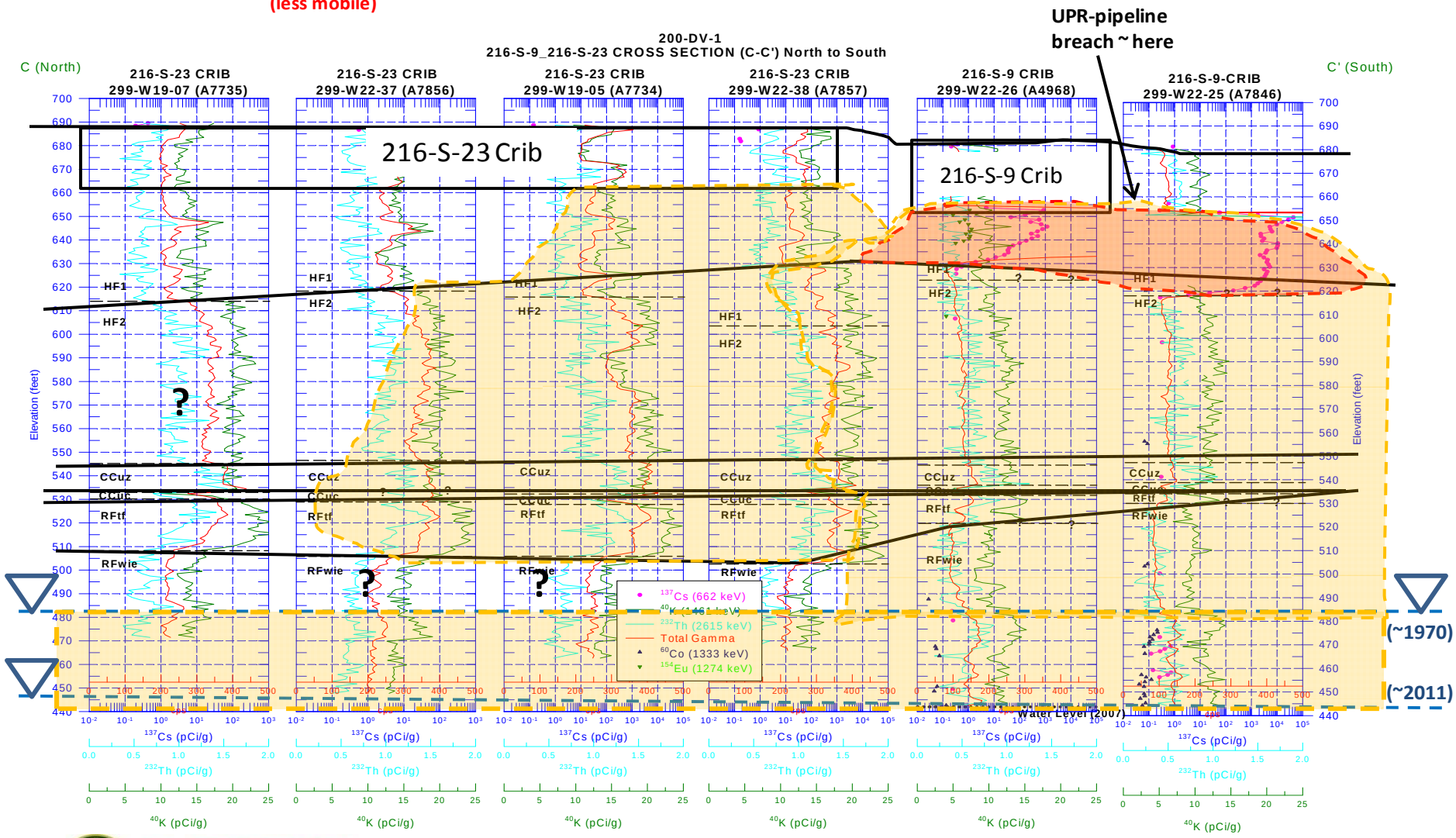

U.S. DEPARTMENT OF ENERGY

Sub-Region 2

[216-S-21 and 216-S-25 Cribs]

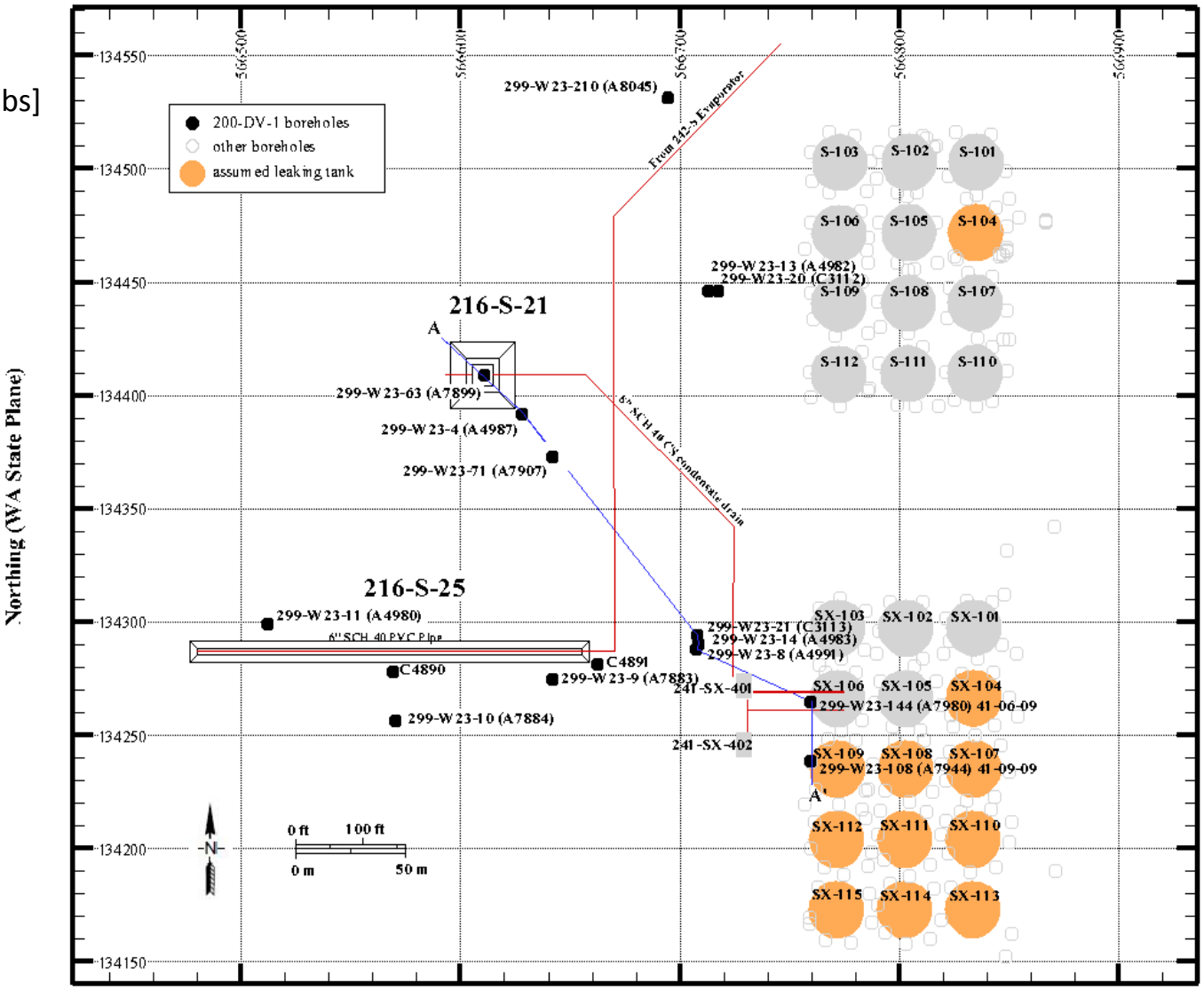

Ref. H-2-44511 Sh. 30 Rev. 6
H-2-44511 Sh. 38 Rev. 7
H-2-44511 Sh. 39 Rev. 2
H-2-44511 Sh. 47 Rev. 3
H-2-39549 Sh. 1 Rev. 3
H-2-46292 Sh. 1 Rev. 1
H-2-44511 Sh. 46 Rev. 6

U.S. DEPARTMENT OF ENERGY

Temporal Changes in Gamma Contamination (Qualitative)

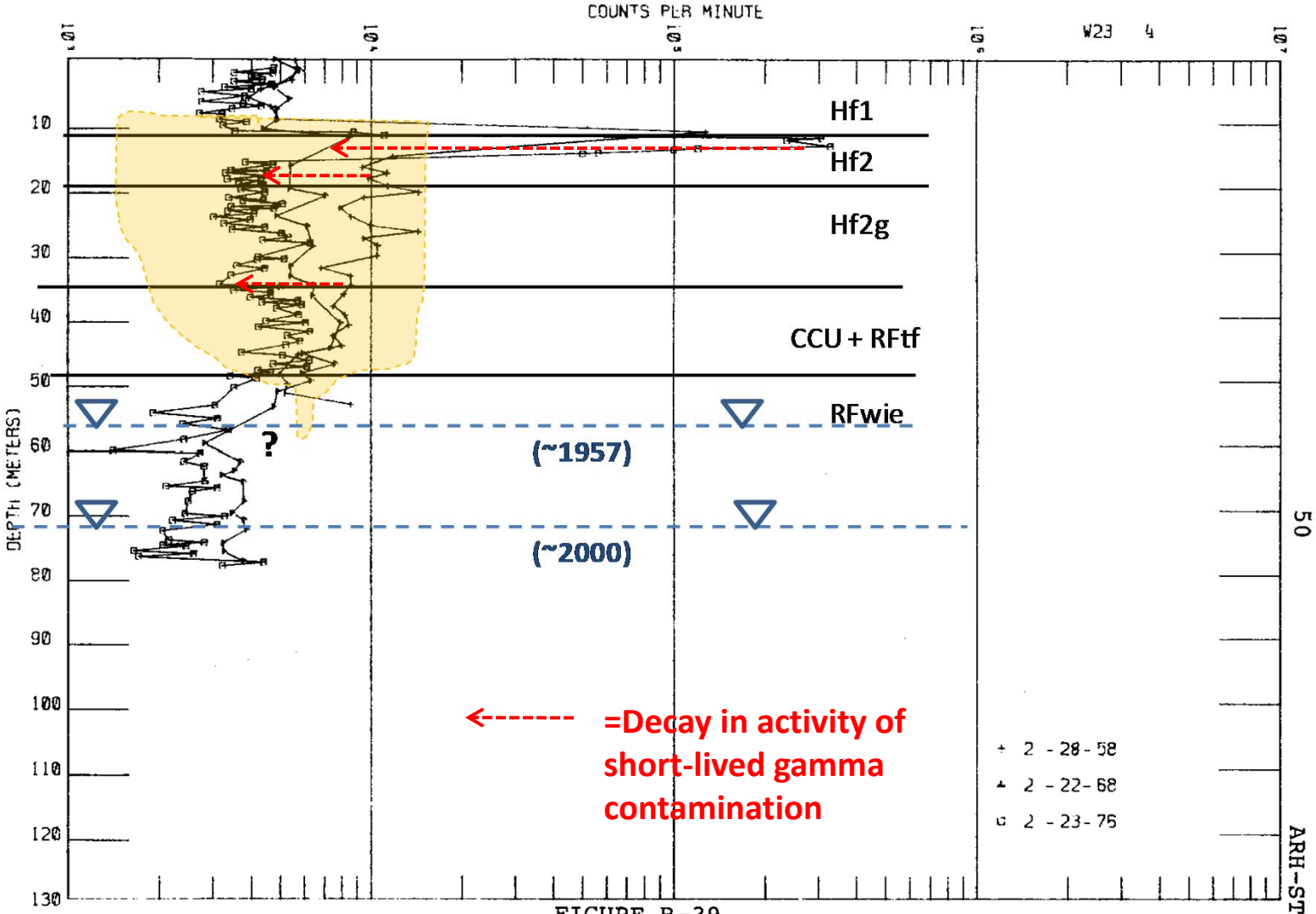

FIGURE B-39

WELL W23-4 SCINTILLATION PROBE PROFILES

U.S. DEPARTMENT OF ENERGY

S-SX Sub-Region 2 Contaminant Conceptual Cross Section

Currently detectable (Cs-137 ≥ 10pCi/g) gamma contamination (less mobile)

Historical (past) detectable gamma contamination (mobile-short half-life; e.g., Ru-106)

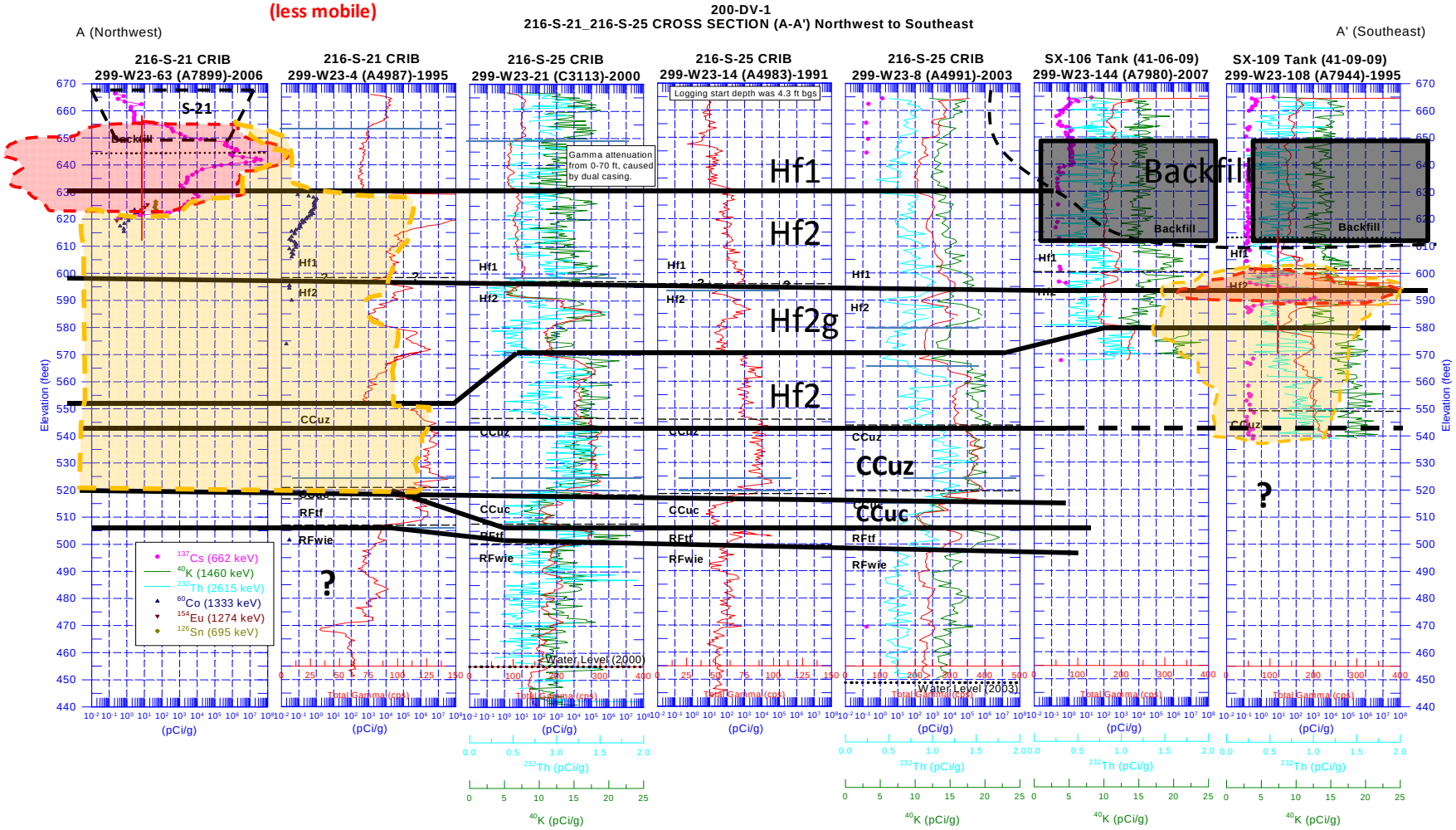

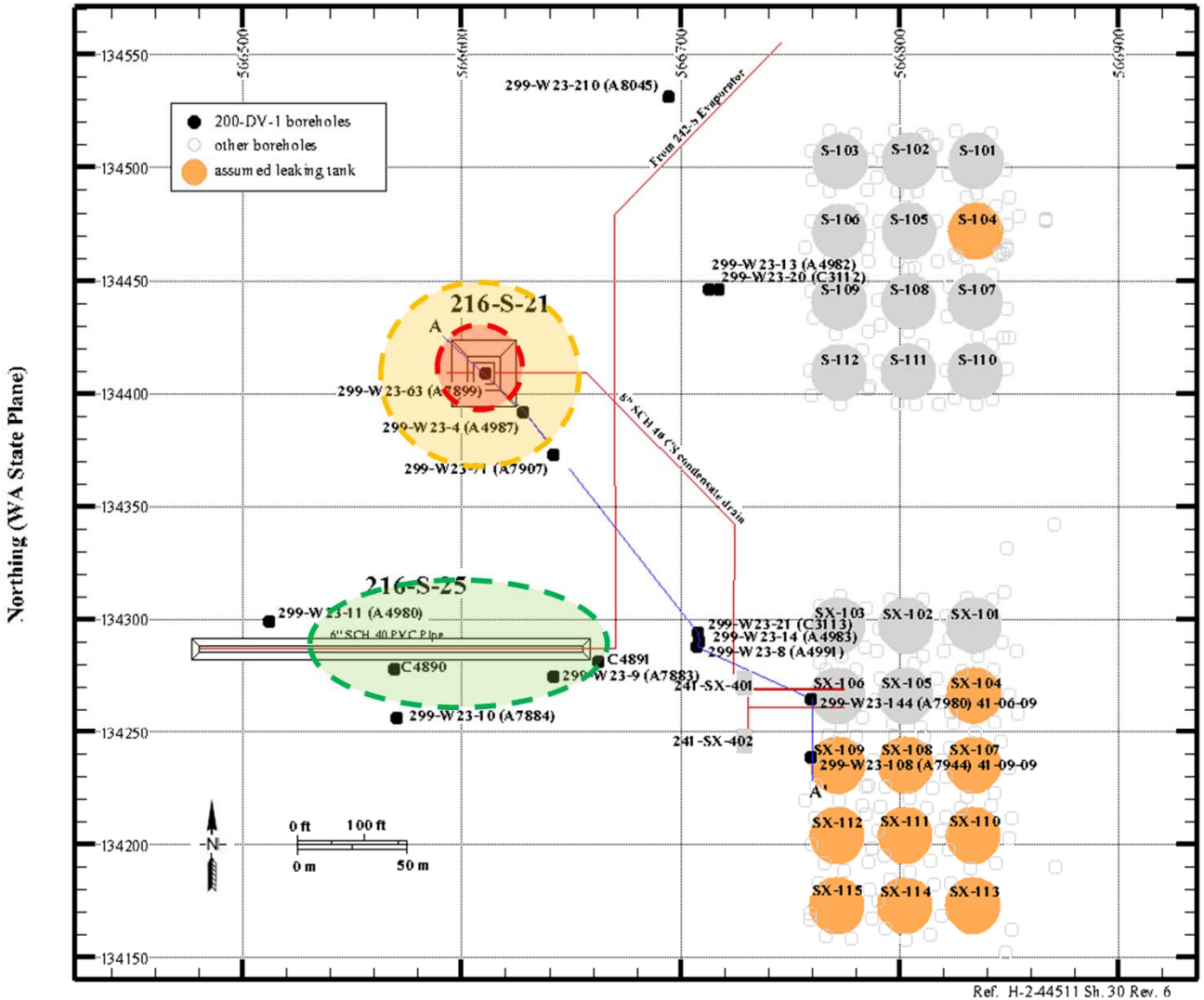

Ref. H-2-44511 Sh. 30 Rev. 6
H-2-44511 Sh. 38 Rev. 7
H-2-44511 Sh. 39 Rev. 2
H-2-44511 Sh. 47 Rev. 3
H-2-39549 Sh. 1 Rev. 3
H-2-46292 Sh. 1 Rev. 1
H-2-44511 Sh. 46 Rev. 6

Sub-Region 2

[216-S-21 and 216-S-25 Cribs]

Interpreted Lateral Extent of Contamination

- Currently detectable (Cs-137 ≥ 10pCi/g) gamma contamination (less mobile)
- Historical (past) detectable gamma contamination (mobile-short half-life; e.g., Ru-106)
- ~SGE Anomalous Extent, no gamma contamination detected

U.S. DEPARTMENT OF ENERGY

200-DV-1 Waste Sites and Regional Contaminant Plumes, 200 West Area

= **Iodine-129**
(DWS=1pCi/L)

= **Uranium**
(DWS=30Ug/L)

= **Technetium-99**
(DWS=900pCi/L)

= **DV-1 Waste Site**

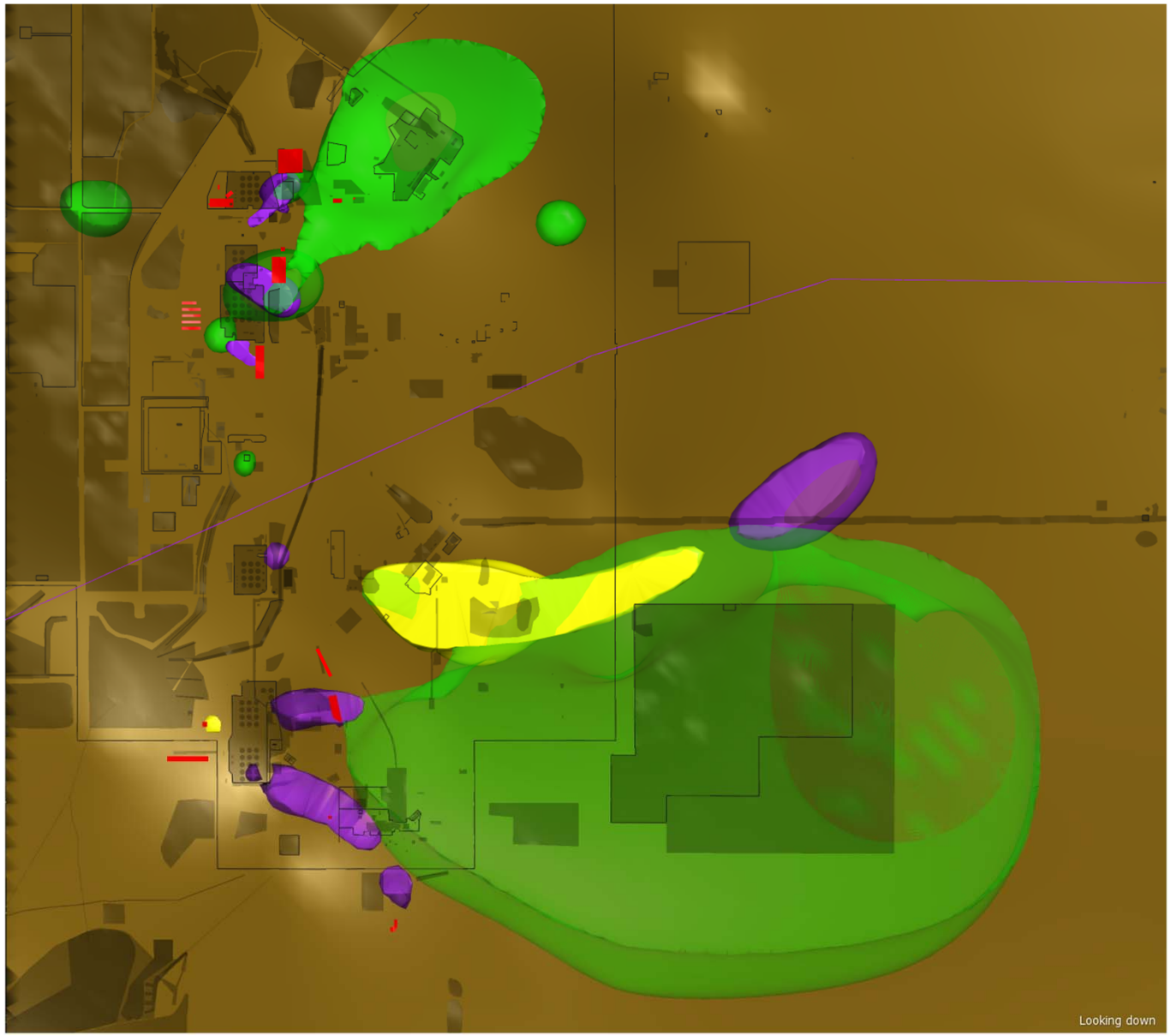

U.S. DEPARTMENT OF ENERGY

299-W19-5 (A7734)

Historical (past) detectable gamma contamination (as total gamma)

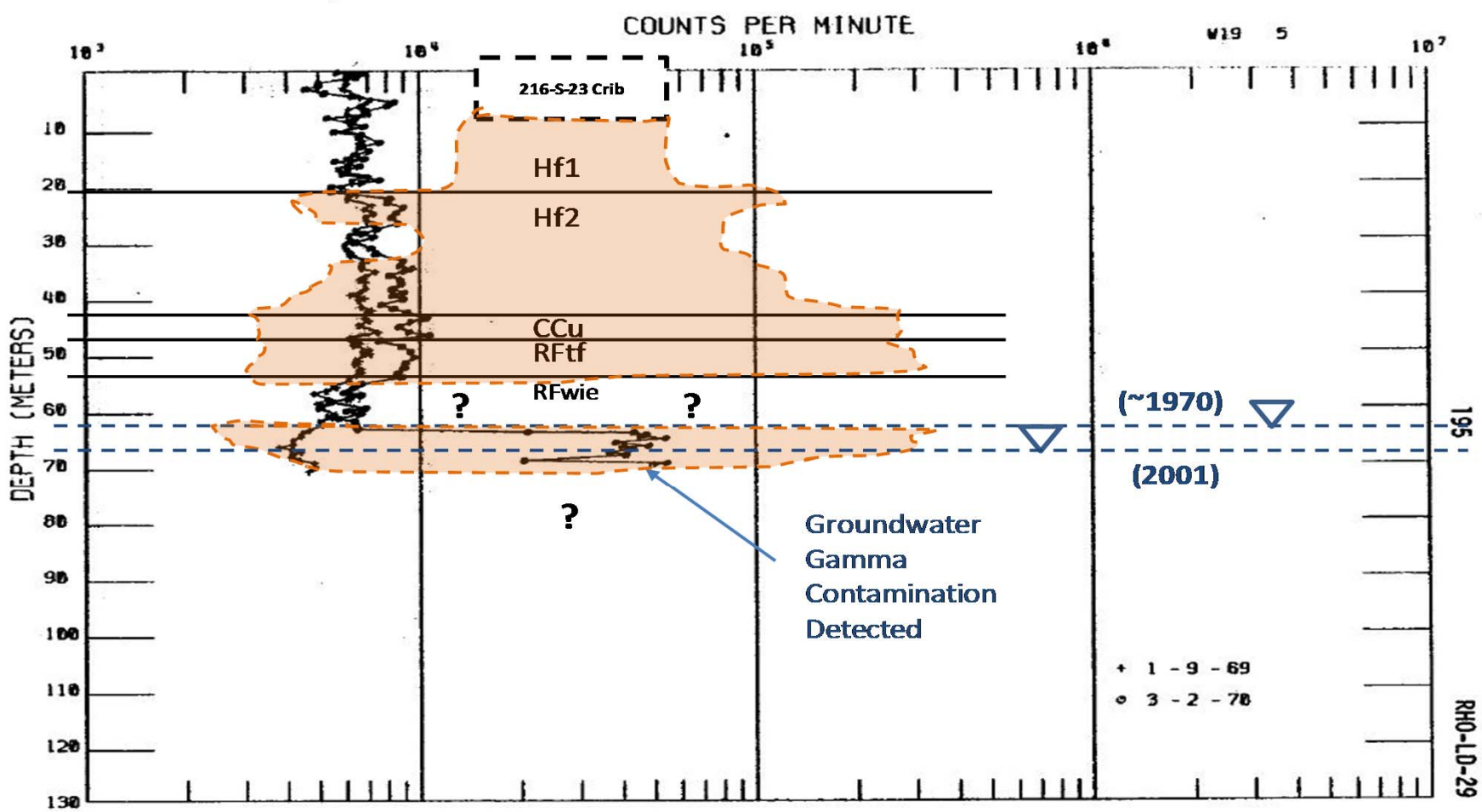

U.S. DEPARTMENT OF ENERGY

299-W19-6 (A4959)

Historical (past) detectable gamma contamination (as total gamma)

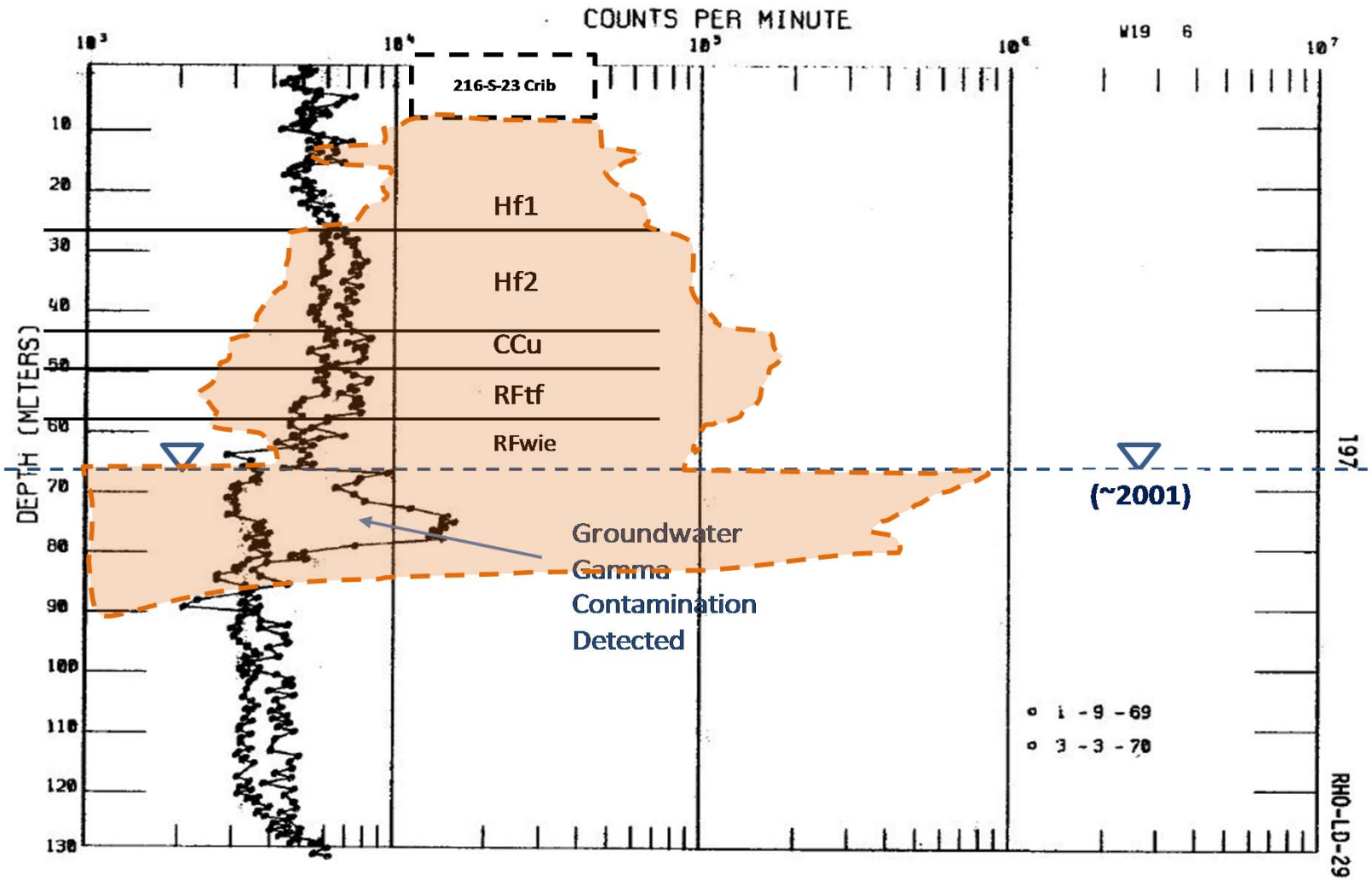

U.S. DEPARTMENT OF ENERGY

S Complex Area
Groundwater Contaminant
Plume Source Determination

	Volume and Inventory % of Total Released to S Complex Area						Residual Waste in VZ Sediments % of Total Released to S Complex Area				
Facility	Vol Disposed	**NO_3**	**U**	**Cr**	**^{129}I**	**^{99}Tc**	**NO_3**	**U**	**Cr**	**^{129}I**	**^{99}Tc**
	(%)	(%)	(%)	(%)	(%)	(%)	(%)	(%)	(%)	(%)	(%)
S-9	**10.79**	**11.47**	**90.3**	0.00	**36.03**	0.30	**11.5**	**90.3**	0.00	**36.0**	0.3
S-23	7.42	0.53	0.00	0.00	0.00	0.00	0.4	0.0	0.00	0.0	0.00
S-SST (S-104)	0.02	6.44	**4.34**	**5.04**	**4.76**	**8.38**	5.8	**3.9**	**4.5**	**4.3**	**7.5**
S-21	**18.97**	0.13	0.03	3.77	0.40	0.61	0.04	0.0	1.2	0.1	0.2
S-25	**62.7**	**61.1**	0.23	**10.35**	0.00	0.00	**12.2**	0.0	**2.1**	0.0	0.0
SX-SST	0.12	**20.29**	**5.07**	**80.9**	**58.8**	**90.7**	**18.3**	**4.6**	**72.8**	**52.9**	**81.6**
Total	100	100	100	100	100	100	48.2	98.9	80.6	93.4	89.7

Notes:

Total for Residual in VZ Sediments does not sum to 100% because some inventory reached groundwater.

Bold % values represent the largest releases or residual inventories for each parameter.

U.S. DEPARTMENT OF ENERGY

Probable Nitrate Groundwater Sources S Complex Area, 200-DV-1 OU

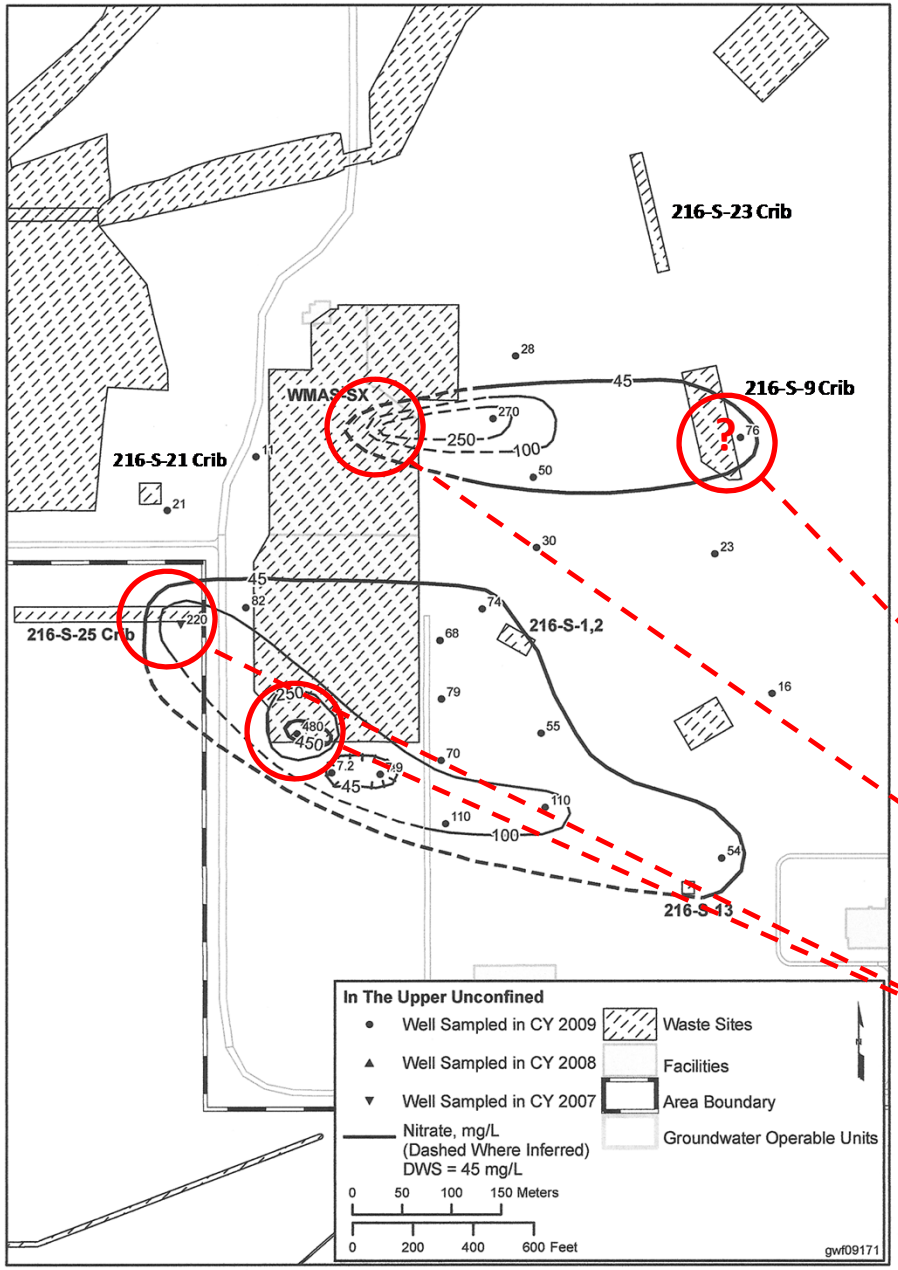

	Volume and Inventory % of Total Released to S Complex Area						Residual Waste in VZ Sediments % of Total Released to S Complex Area				
Facility	Vol Disposed	NO_3	U	Cr	^{129}I	^{99}Tc	NO_3	U	Cr	^{129}I	^{99}Tc
	(%)	(%)	(%)	(%)	(%)	(%)	(%)	(%)	(%)	(%)	(%)
S-9	**10.79**	**11.47**	**90.3**	0.00	**36.03**	0.30	**11.5**	**90.3**	0.00	**36.0**	0.3
S-23	7.42	0.53	0.00	0.00	0.00	0.00	0.4	0.0	0.00	0.0	0.00
S-SST (S-104)	0.02	6.44	**4.34**	**5.04**	**4.76**	**8.38**	5.8	**3.9**	**4.5**	**4.3**	**7.5**
S-21	**18.97**	0.13	0.03	3.77	0.40	0.61	0.04	0.0	1.2	0.1	0.2
S-25	**62.7**	**61.1**	0.23	**10.35**	0.00	0.00	**12.2**	0.0	**2.1**	0.0	0.0
SX-SST	0.12	**20.29**	**5.07**	**80.9**	**58.8**	**90.7**	**18.3**	**4.6**	**72.8**	**52.9**	**81.6**
Total	100	100	100	100	100	100	48.2	98.9	80.6	93.4	89.7

Notes:

Total for Residual in VZ Sediments does not sum to 100% because some inventory reached groundwater.

Bold % values represent the largest releases or residual inventories for each parameter.

U.S. DEPARTMENT OF ENERGY

Probable Chromium Groundwater Sources S Complex Area, 200-DV-1 OU

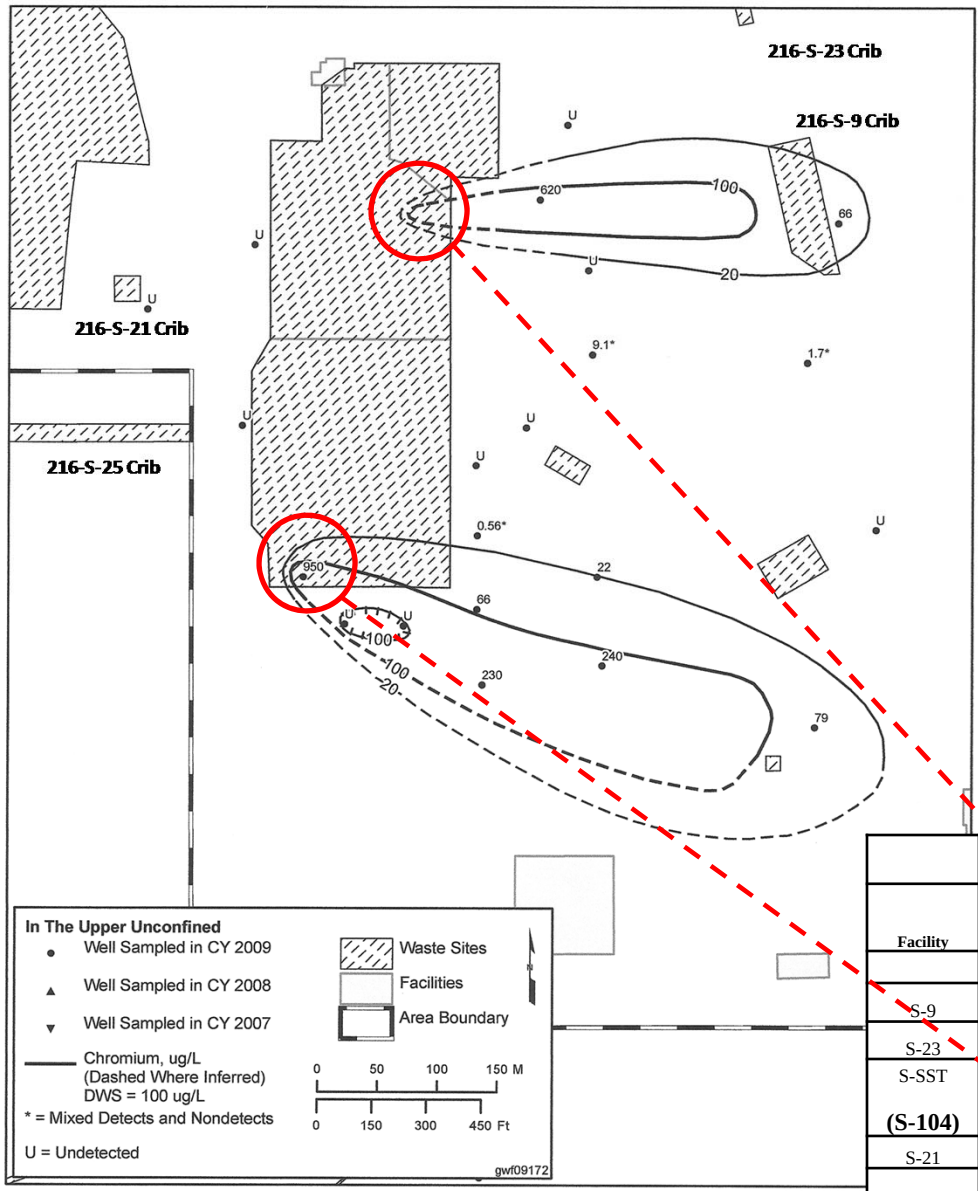

	Volume and Inventory % of Total Released to S Complex Area						Residual Waste in VZ Sediments % of Total Released to S Complex Area				
Facility	Vol Disposed	NO_3	U	Cr	^{129}I	^{99}Tc	NO_3	U	Cr	^{129}I	^{99}Tc
	(%)	(%)	(%)	(%)	(%)	(%)	(%)	(%)	(%)	(%)	(%)
S-9	**10.79**	**11.47**	**90.3**	0.00	**36.03**	0.30	**11.5**	**90.3**	0.00	**36.0**	0.3
S-23	7.42	0.53	0.00	0.00	0.00	0.00	0.4	0.0	0.00	0.0	0.00
S-SST (S-104)	0.02	6.44	**4.34**	**5.04**	**4.76**	**8.38**	5.8	**3.9**	**4.5**	**4.3**	**7.5**
S-21	**18.97**	0.13	0.03	3.77	0.40	0.61	0.04	0.0	1.2	0.1	0.2
S-25	**62.7**	**61.1**	0.23	**10.35**	0.00	0.00	**12.2**	0.0	**2.1**	0.0	0.0
SX-SST	0.12	**20.29**	**5.07**	**80.9**	**58.8**	**90.7**	**18.3**	**4.6**	**72.8**	**52.9**	**81.6**
Total	100	100	100	100	100	100	48.2	98.9	80.6	93.4	89.7

Notes:

Total for Residual in VZ Sediments does not sum to 100% because some inventory reached groundwater.

Bold % values represent the largest releases or residual inventories for each parameter.

U.S. DEPARTMENT OF ENERGY

Probable Iodine-129 Groundwater Sources S Complex Area, 200-DV-1 OU

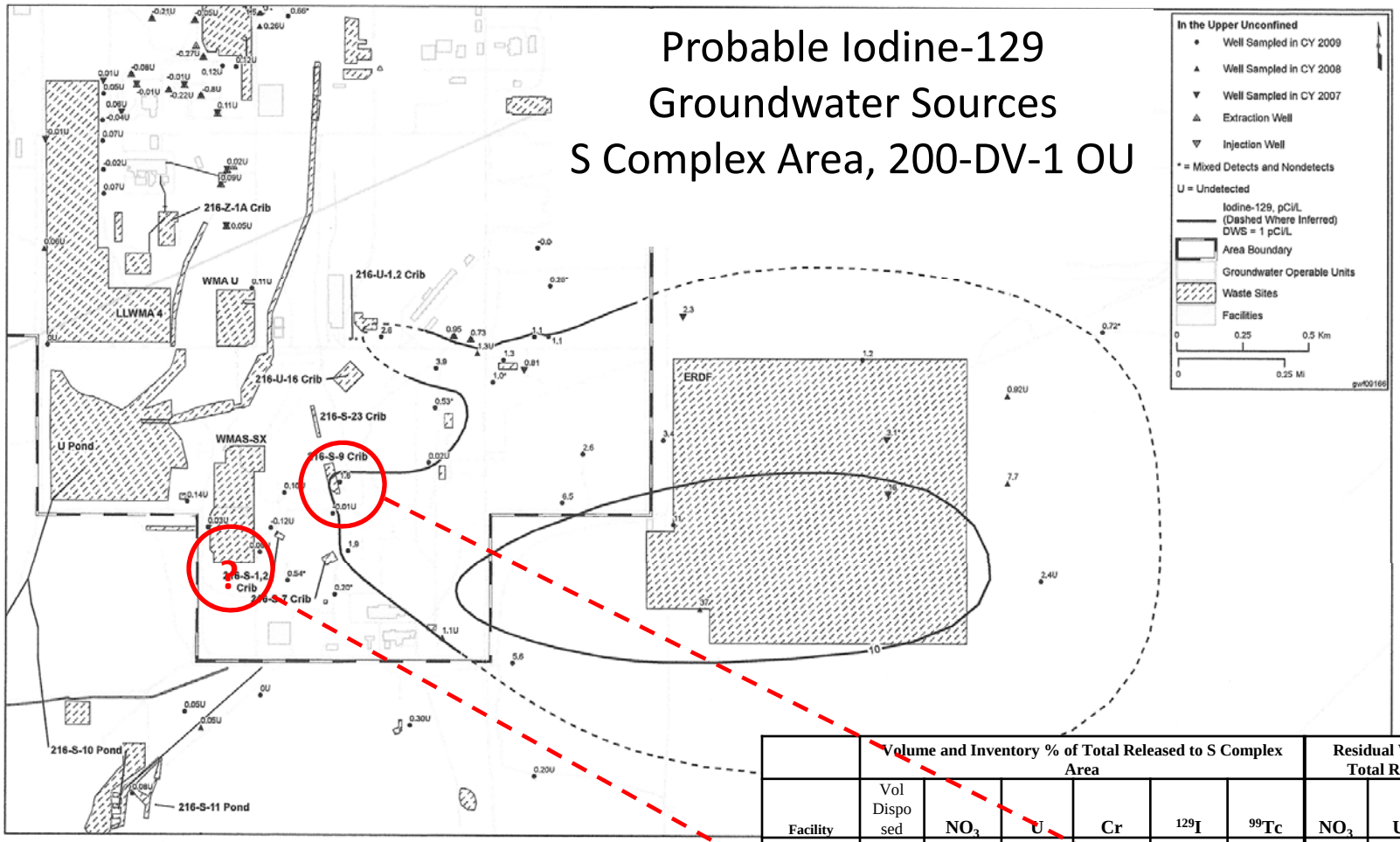

	Volume and Inventory % of Total Released to S Complex Area						Residual Waste in VZ Sediments % of Total Released to S Complex Area				
Facility	Vol Disposed	NO_3	U	Cr	^{129}I	^{99}Tc	NO_3	U	Cr	^{129}I	^{99}Tc
	(%)	(%)	(%)	(%)	(%)	(%)	(%)	(%)	(%)	(%)	(%)
S-9	**10.79**	**11.47**	**90.3**	0.00	**36.03**	0.30	**11.5**	**90.3**	0.00	**36.0**	0.3
S-23	7.42	0.53	0.00	0.00	0.00	0.00	0.4	0.0	0.00	0.0	0.00
S-SST (S-104)	0.02	6.44	**4.34**	**5.04**	**4.76**	**8.38**	5.8	**3.9**	**4.5**	**4.3**	**7.5**
S-21	**18.97**	0.13	0.03	3.77	0.40	0.61	0.04	0.0	1.2	0.1	0.2
S-25	**62.7**	**61.1**	0.23	**10.35**	0.00	0.00	**12.2**	0.0	**2.1**	0.0	0.0
SX-SST	0.12	**20.29**	**5.07**	**80.9**	**58.8**	**90.7**	**18.3**	**4.6**	**72.8**	**52.9**	**81.6**
Total	100	100	100	100	100	100	48.2	98.9	80.6	93.4	89.7

Notes:

Total for Residual in VZ Sediments does not sum to 100% because some inventory reached groundwater.

Bold % values represent the largest releases or residual inventories for each parameter.

U.S. DEPARTMENT OF ENERGY

Probable Technetium-99 Groundwater Sources S Complex Area, 200-DV-1 OU

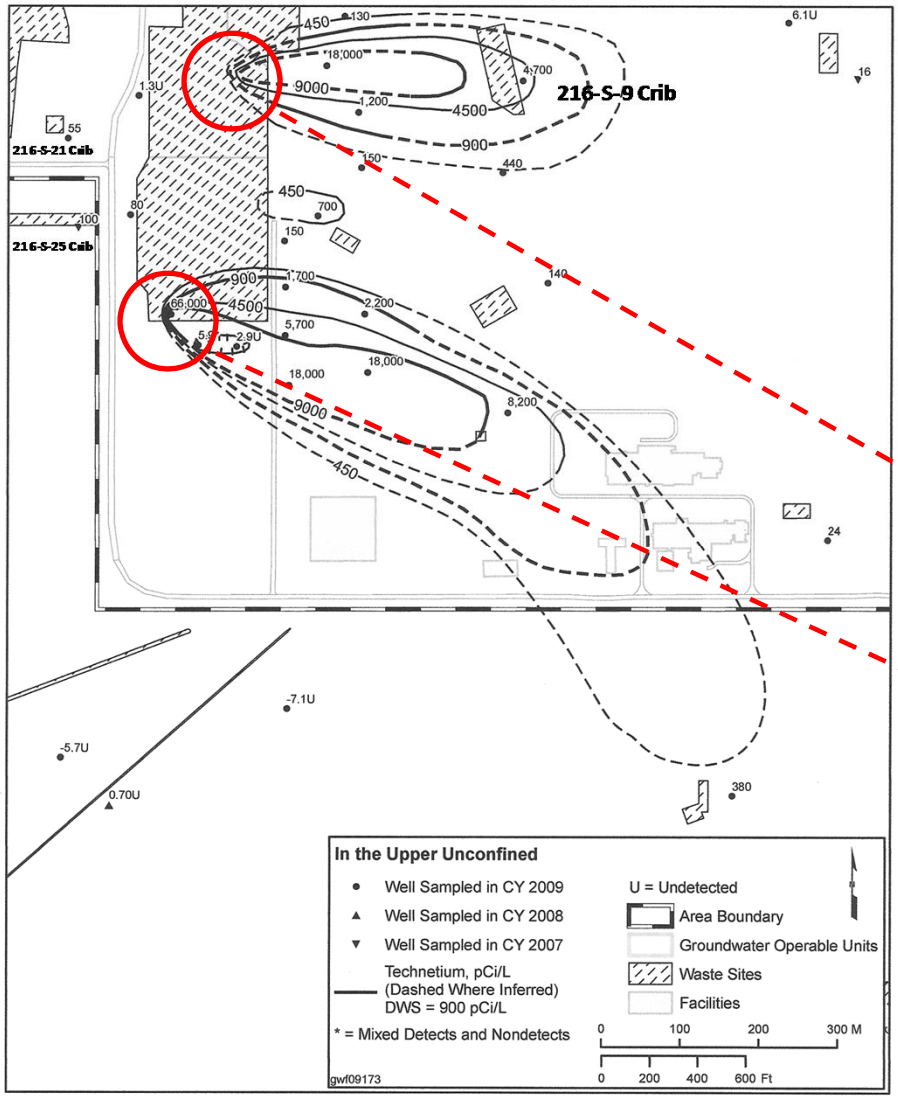

	Volume and Inventory % of Total Released to S Complex Area						Residual Waste in VZ Sediments % of Total Released to S Complex Area				
Facility	Vol Disposed	NO_3	U	Cr	^{129}I	^{99}Tc	NO_3	U	Cr	^{129}I	^{99}Tc
	(%)	(%)	(%)	(%)	(%)	(%)	(%)	(%)	(%)	(%)	(%)
S-9	**10.79**	**11.47**	**90.3**	0.00	**36.03**	0.30	**11.5**	**90.3**	0.00	**36.0**	0.3
S-23	7.42	0.53	0.00	0.00	0.00	0.00	0.4	0.0	0.00	0.0	0.00
S-SST (S-104)	0.02	6.44	**4.34**	**5.04**	**4.76**	**8.38**	5.8	**3.9**	**4.5**	**4.3**	**7.5**
S-21	**18.97**	0.13	0.03	3.77	0.40	0.61	0.04	0.0	1.2	0.1	0.2
S-25	**62.7**	**61.1**	0.23	**10.35**	0.00	0.00	**12.2**	0.0	**2.1**	0.0	0.0
SX-SST	0.12	**20.29**	**5.07**	**80.9**	**58.8**	**90.7**	**18.3**	**4.6**	**72.8**	**52.9**	**81.6**
Total	100	100	100	100	100	100	48.2	98.9	80.6	93.4	89.7

Notes:

Total for Residual in VZ Sediments does not sum to 100% because some inventory reached groundwater.

Bold % values represent the largest releases or residual inventories for each parameter.

U.S. DEPARTMENT OF ENERGY

This page intentionally left blank.